

WCAP-16793-NP
Revision 1

April 2009

Evaluation of Long-Term Cooling Considering Particulate, Fibrous and Chemical Debris in the Recirculating Fluid



WCAP-16793-NP
Revision 1

Evaluation of Long-Term Cooling Considering Particulate, Fibrous and Chemical Debris in the Recirculating Fluid

Timothy S. Andreychek*	Susan L. Baier*
Kevin F. McNamee	William A. Byers
Robert B. Sisk	Kevin J. Barber
David Mitchell	David P. Crane
David J. Fink	Mitchell E. Nissley
Westinghouse Electric Company, LLC	

Gordon Wissinger	Brian G. Lockamon
Heidi Dergel	Paul A. Sherburne
AREVA NP, Inc.	

April 2009

Verified: Paul V. Pyle*
Westinghouse, Systems and Equipment Engineering I

Approved: Timothy D. Croyle*, Manager
Westinghouse, Systems and Equipment Engineering I

This work performed under PWROG Project Number PA-SEE-0312.

***Electronically approved records are authenticated in the Electronic Document Management System.**

Westinghouse Electric Company LLC
P.O. Box 355
Pittsburgh, PA 15230-0355

© 2009 Westinghouse Electric Company LLC
All Rights Reserved

LEGAL NOTICE

This report was prepared as an account of work performed by Westinghouse Electric Company LLC. Neither Westinghouse Electric Company LLC, nor any person acting on its behalf:

- A. Makes any warranty or representation, express or implied including the warranties of fitness for a particular purpose or merchantability, with respect to the accuracy, completeness, or usefulness of the information contained in this report, or that the use of any information, apparatus, method, or process disclosed in this report may not infringe privately owned rights; or
- B. Assumes any liabilities with respect to the use of, or for damages resulting from the use of, any information, apparatus, method, or process disclosed in this report.

COPYRIGHT NOTICE

This report has been prepared by Westinghouse Electric Company LLC and bears a Westinghouse Electric Company copyright notice. As a member of the PWR Owners Group, you are permitted to copy and redistribute all or portions of the report within your organization; however all copies made by you must include the copyright notice in all instances.

DISTRIBUTION NOTICE

This report was prepared for the PWR Owners Group. This Distribution Notice is intended to establish guidance for access to this information. This report (including proprietary and non-proprietary versions) is not to be provided to any individual or organization outside of the PWR Owners Group program participants without prior written approval of the PWR Owners Group Program Management Office. However, prior written approval is not required for program participants to provide copies of Class 3 non-proprietary reports to third parties that are supporting implementation at their plant, and for submittals to the NRC.

**PWR Owners Group
Member Participation* for Project PA-SEE-0312**

Utility Member	Plant Site(s)	Participant	
		Yes	No
AmerenUE	Callaway (W)	X	
American Electric Power	D.C. Cook 1&2 (W)	X	
Arizona Public Service	Palo Verde Unit 1, 2, & 3 (CE)	X	
Constellation Energy Group	Calvert Cliffs 1 & 2 (CE)	X	
Constellation Energy Group	Ginna (W)	X	
Dominion Connecticut	Millstone 2 (CE)	X	
Dominion Connecticut	Millstone 3 (W)	X	
Dominion Kewaunee	Kewaunee (W)	X	
Dominion VA	North Anna 1 & 2, Surry 1 & 2 (W)	X	
Duke Energy	Catawba 1 & 2, McGuire 1 & 2 (W), Oconee 1, 2, 3 (B&W)	X	
Entergy Nuclear Northeast	Indian Point 2 & 3 (W)	X	
Entergy Operations South	Arkansas 2, Waterford 3 (CE), Arkansas 1 (B&W)	X	
Exelon Generation Co. LLC	Braidwood 1 & 2, Byron 1 & 2 (W), TMI 1 (B&W)	X	
FirstEnergy Nuclear Operating Co	Beaver Valley 1 & 2 (W), Davis-Besse (B&W)	X	
Florida Power & Light Group	St. Lucie 1 & 2 (CE)	X	
Florida Power & Light Group	Turkey Point 3 & 4, Seabrook (W)	X	
Nuclear Management Company	Prairie Island 1&2, Pt. Beach 1&2 (W)	X	
Nuclear Management Company	Palisades (CE)	X	
Omaha Public Power District	Fort Calhoun (CE)	X	
Pacific Gas & Electric	Diablo Canyon 1 & 2 (W)	X	
Progress Energy	Robinson 2, Shearon Harris (W), Crystal River 3 (B&W)	X	
PSEG - Nuclear	Salem 1 & 2 (W)	X	
Southern California Edison	SONGS 2 & 3 (CE)	X	
South Carolina Electric & Gas	V.C. Summer (W)	X	
So. Texas Project Nuclear Operating Co.	South Texas Project 1 & 2 (W)	X	
Southern Nuclear Operating Co.	Farley 1 & 2, Vogtle 1 & 2 (W)	X	
Tennessee Valley Authority	Sequoyah 1 & 2, Watts Bar (W)	X	
TXU Power	Comanche Peak 1 & 2 (W)	X	
Wolf Creek Nuclear Operating Co.	Wolf Creek (W)	X	
* Project participants as of the date the final deliverable was completed. On occasion, additional members will join a project. Please contact the PWR Owners Group Program Management Office to verify participation before sending this document to participants not listed above.			

**PWR Owners Group
International Member Participation* for Project PA-SEE-0312**

Utility Member	Plant Site(s)	Participant	
		Yes	No
British Energy	Sizewell B	X	
Electrabel (Belgian Utilities)	Doel 1, 2 & 4, Tihange 1 & 3	X	
Kansai Electric Co., LTD	Mihama 1, Ohi 1 & 2, Takahama 1 (W)	X	
Korea Hydro & Nuclear Power Corp.	Kori 1, 2, 3 & 4 Yonggwang 1 & 2 (W)	X	
Korea Hydro & Nuclear Power Corp.	Yonggwang 3, 4, 5 & 6 Ulchin 3, 4, 5 & 6(CE)	X	
Nuklearna Electramna KRSKO	Krsko (W)	X	
Nordostschweizerische Kraftwerke AG (NOK)	Beznau 1 & 2 (W)	X	
Ringhals AB	Ringhals 2, 3 & 4 (W)	X	
Spanish Utilities	Asco 1 & 2, Vandellos 2, Almaraz 1 & 2 (W)	X	
Taiwan Power Co.	Maanshan 1 & 2 (W)	X	
Electricite de France	54 Units	X	
<p>* This is a list of participants in this project as of the date the final deliverable was completed. On occasion, additional members will join a project. Please contact the PWR Owners Group Program Management Office to verify participation before sending documents to participants not listed above.</p>			

RECORD OF REVISIONS

Revision	Date	Description
0	May 2007	Original
1	April 2009	<p>Rev bars are not included in this document because this revision required a total reorganization of the original document.</p> <p>The text is organized as follows:</p> <p>1 Introduction</p> <ul style="list-style-type: none"> • Section 1.0 from original WCAP <p>2 Long-Term Core Cooling Acceptance Basis</p> <ul style="list-style-type: none"> • Section 3, a few details from Appendix A from original WCAP and applicable RAIs <p>3 Blockage at the Core Inlet</p> <ul style="list-style-type: none"> • Sections 2.1 & 6 from original WCAP, add testing w/ prototypical fuel filters, and applicable RAIs <p>4 Collection of Debris on Fuel Grids</p> <ul style="list-style-type: none"> • Sections 2.2 & 4 from original WCAP, add testing w/ prototypical fuel filters, and applicable RAIs <p>5 Collection of Fibrous Material on Fuel Cladding</p> <ul style="list-style-type: none"> • Section 2.3 from original WCAP and applicable RAIs <p>6 Protective Coating Debris Deposited on Fuel Clad Surfaces</p> <ul style="list-style-type: none"> • Section 2.5 from original WCAP <p>7 Chemical Precipitates and Debris Deposited on Fuel Clad Surfaces</p> <ul style="list-style-type: none"> • Sections 2.4 & 5, and applicable RAIs <p>8 Boric Acid Precipitation</p> <ul style="list-style-type: none"> • Section 2.6 from original WCAP <p>9 Coolant Delivered to the Top of the Core</p> <ul style="list-style-type: none"> • Section 2.7 from original WCAP and applicable RAIs <p>10 Summary</p> <ul style="list-style-type: none"> • Sections 2.8 & 7 from original WCAP and addition of acceptance criteria for fuel debris loading during long-term recirculation from containment sump.

		<p>11 References</p> <p>Appendix A</p> <ul style="list-style-type: none">• Keep and add applicable RAIs <p>Appendix B</p> <ul style="list-style-type: none">• Keep and add applicable RAIs <p>Appendix C</p> <ul style="list-style-type: none">• Keep and add applicable RAIs <p>Appendix D</p> <ul style="list-style-type: none">• Keep and add applicable RAIs <p>Appendix E</p> <ul style="list-style-type: none">• Keep and add applicable RAIs <p>Appendix F</p> <ul style="list-style-type: none">• Keep and add applicable RAIs <p>Appendix G – Description of FA Testing</p> <ul style="list-style-type: none">• New – Add new appendix to describe the fuel assembly testing (in general). The references will provide a hook to the actual test descriptions and data. <p>Appendix H</p> <ul style="list-style-type: none">• New – RAI Set #1 <p>Appendix I</p> <ul style="list-style-type: none">• New – RAI Set #2 <p>Appendix J</p> <ul style="list-style-type: none">• New – RAI Set #3
--	--	--

TABLE OF CONTENTS

LIST OF TABLES	xi
LIST OF FIGURES	xiii
LIST OF ACRONYMS.....	xvii
EXECUTIVE SUMMARY	xix
1 INTRODUCTION	1-1
2 LONG-TERM CORE COOLING ACCEPTANCE BASIS.....	2-1
2.1 INTRODUCTION	2-1
2.2 GSI-191 LONG-TERM CORE COOLING ACCEPTANCE BASES.....	2-1
2.3 SUMMARY	2-2
3 BLOCKAGE AT THE CORE INLET	3-1
3.1 PROTOTYPICAL FUEL ASSEMBLY TESTING	3-1
3.1.1 Available Driving Head.....	3-1
3.1.2 Description of Tests	3-3
3.1.3 Discussion of Test Results	3-3
3.2 WCOBRA/TRAC EVALUATION OF BLOCKAGE AT THE CORE INLET	3-5
3.2.1 Approach	3-5
3.2.2 Selection of Limiting Reactor Vessel Design	3-5
3.2.3 Model Inputs.....	3-6
3.2.4 Results	3-8
3.3 ADDITIONAL WC/T CALCULATIONS.....	3-12
3.3.1 Method Discussion & Input.....	3-12
3.3.2 Results from Flow Area Reduction Runs	3-13
3.3.3 Results from Uniform Loss Coefficient Runs	3-14
3.4 SUMMARY	3-25
4 COLLECTION OF DEBRIS ON FUEL GRIDS.....	4-1
4.1 GENERAL DISCUSSION	4-1
4.2 PROTOTYPICAL FUEL ASSEMBLY TESTING	4-2
4.2.1 Hot Leg Break Collection of Debris on Fuel Grids.....	4-2
4.2.2 Cold Leg Break Collection of Debris on Fuel Grids	4-3
4.2.3 Summary.....	4-3
4.3 CLADDING HEATUP CALCULATIONS	4-4
4.3.1 Clad Heatup Underneath Fuel Grids	4-4
4.3.2 Cladding Heatup between Grids.....	4-7
4.4 SUMMARY	4-9
5 COLLECTION OF FIBROUS MATERIAL ON FUEL CLADDING	5-1
6 PROTECTIVE COATING DEBRIS DEPOSITED ON FUEL CLAD SURFACES	6-1
6.1 INTRODUCTION	6-1
6.2 PROTECTIVE COATINGS BEHAVIOR	6-1
6.3 PREDICTED CLADDING TEMPERATURES AND TEMPERATURE-DRIVE DEBRIS CAPTURE	6-2
6.4 SUMMARY	6-4
7 CHEMICAL PRECIPITATES AND DEBRIS DEPOSITED ON FUEL CLAD SURFACES.....	7-1

7.1	DESCRIPTION OF LOCADM	7-1
7.2	USE OF LOCADM	7-3
7.2.1	Overview	7-3
7.2.2	Summary.....	7-5
8	BORIC ACID PRECIPITATION.....	8-1
9	COOLANT DELIVERED TO THE TOP OF THE CORE.....	9-1
9.1	HOT LEG RECIRCULATION.....	9-1
9.2	UPPER PLENUM INJECTION PLANTS	9-1
9.3	UPPER PLENUM DEBRIS TRANSPORT FOR HOT-LEG BREAK SCENARIO	9-2
9.4	COLLECTION OF DEBRIS ON FUEL	9-2
9.5	TEST FOR UPI-DESIGNED PLANT.....	9-3
10	SUMMARY	10-1
10.1	DISCUSSION	10-1
10.2	GUIDANCE TO LICENSEES CONCERNING EVALUATION OF DEBRIS	10-3
10.2.1	LOCADM.....	10-3
10.2.2	Debris Acceptance Criteria.....	10-4
11	REFERENCES	11-1
APPENDIX A	GSI-191 LTCC ACCEPTANCE BASIS.....	A-1
APPENDIX B	EVALUATION OF BLOCKAGE AT THE CORE INLET	B-1
APPENDIX C	FUEL CLAD HEAT-UP UNDERNEATH GRIDS.....	C-1
APPENDIX D	FUEL CLAD HEAT-UP BETWEEN GRIDS.....	D-1
APPENDIX E	CHEMICAL PRECIPITATION AND SUBSEQUENT IMPACT.....	E-1
APPENDIX F	SUPPORTING SOLUBILITY AND PRECIPITATION CALCULATIONS	F-1
APPENDIX G	DESCRIPTION OF FUEL ASSEMBLY TESTING.....	G-1
APPENDIX H	RAI SET #1 [ML080220258].....	H-1
APPENDIX I	RAI SET #2 [ML080220258].....	I-1
APPENDIX J	RAI SET #3 [ML090680765].....	J-1

LIST OF TABLES

Table 3-1	Core Channel Radial Power Distribution	3-7
Table 4-1	Grid Locations	4-5
Table 4-2	Maximum Clad Temperatures (T_{MAX}).....	4-6
Table 4-3	Clad/Oxide Interface Temperature vs. Chemical Precipitate Thickness.....	4-8
Table 4-4	Clad/Oxide Interface Temperature vs. Chemical Precipitate Thickness.....	4-9
Table 6-1	Precipitate Surface Temperatures vs. Precipitate Thickness.....	6-3
Table 10-1	Acceptance Criteria Debris Limits.....	10-3
Table 10-2	Acceptance Criteria Debris Limits for AREVA TRAPPER Fine Mesh Debris Filter....	10-3
Table B-1	Core Channel Radial Power Distribution	B-3
Table B-2	Subatmospheric Loop Pressure Drop for Containment Pressure=10 psia	B-12
Table B-3	Subatmospheric Loop Pressure Drop for Containment Pressure=12 psia	B-12
Table C-1	General Fuel Rod Dimensions	C-2
Table C-2	Grid Locations	C-2
Table C-3	Fuel Rod Zone Description.....	C-3
Table C-4	Heat Transfer Inputs.....	C-4
Table C-5	Cladding Thermal Properties	C-4
Table C-6	Variable Ranges	C-5
Table C-7	Maximum Clad Temperatures (T_{MAX}).....	C-6
Table D-1	Clad/Oxide Interface Temperature vs. Chemical Precipitate Thickness.....	D-4
Table D-2	Clad/Oxide Interface Temperature vs. Chemical Precipitate Thickness.....	D-5
Table E-1	Example of Relative Power Distributions for Calculating Node Power.....	E-11
Table E-2	Comparison of SKBOR and LOCADM Results.....	E-17
Table E-3	Time dependent inputs for LOCADM example.....	E-22
Table E-3	Time dependent input for LOCADM (continued)	E-23
Table E-4	Materials Input for LOCADM example	E-24
Table E-5.	Density values used in LOCADM example.....	E-25
Table E-6.	Core data input.....	E-26
Table E-7.	Core axial node definition.....	E-26
Table E-8	Core radial node definition	E-26

Table F-1	Input Summary for Solubility Calculations	F-3
Table F-2	Steam Masses Utilized in Solubility Calculation.....	F-4
Table F-3	Calculation Run 1 Results Summary	F-5
Table F-4	Calculation Run 2 Results Summary	F-5
Table F-5	Calculation Run 3 Results Summary	F-6
Table F-6	Calculation Run 4 Results Summary	F-7
Table G-1	Fiber Distribution.....	G-8
Table G-2	Test Matrix for Westinghouse Tests	G-10
Table G-3	Test Matrix for AREVA Tests	G-11
Table G-4	Acceptance Criteria Debris Limits Based on FA Testing.....	G-12
Table G-5	Acceptance Criteria Debris Limits Based on FA Testing.....	G-12

LIST OF FIGURES

Figure 3-1	Plant Transient Power Shape	3-7
Figure 3-2	Case 1 – 82% Core Blockage Modeling Approach.....	3-9
Figure 3-3	Case 2 – 99.4% Core Blockage Modeling Approach.....	3-9
Figure 3-4	Integrated Core Flow vs. Core Boil-off for Case 1 and Case 2	3-10
Figure 3-5	Case 1 and Case 2 Hot Rod Peak Clad Temperature History	3-11
Figure 3-6	Integrated Core Flow vs. Core Boil-off for Channel 13 Flow Reduction 50% Case (Shifted Scale).....	3-15
Figure 3-7	Hot Rod PCT for Channel 13 Flow Reduction 50% Case	3-16
Figure 3-8	Integrated Core Flow vs. Core Boil-off for Channel 13 Flow Reduction 80% Case (Shifted Scale).....	3-17
Figure 3-9	Hot Rod PCT for Channel 13 Flow Reduction 80% Case	3-18
Figure 3-10	Integrated Core Flow versus Core Boil-off for Channel for Uniform $C_D = 50,000$ (Shifted Scale)	3-19
Figure 3-11	Hot Rod PCT for Uniform $C_D = 50,000$	3-20
Figure 3-12	Integrated Core Flow vs. Boil-off for Uniform $C_D = 100,000$ Case (Shifted Scale)	3-21
Figure 3-13	Hot Rod PCT for Uniform $C_D = 100,000$ Case.....	3-22
Figure 3-14	Integrated Core Flow vs. Boil-off for Uniform $C_D = 1,000,000$ Case (Shifted Scale) ..	3-23
Figure 3-15	Hot Rod PCT for Uniform $C_D = 1,000,000$ Case.....	3-24
Figure 4-1	Temperature vs. Deposition Thickness and Thermal Conductivity	4-6
Figure 4-2	Heat Transfer Model (not to scale)	4-7
Figure 4-3	Clad-Oxide Interface Temperature vs. Chemical Precipitate Thickness.....	4-8
Figure A-1	Boil-off Curve for a Westinghouse Four-loop PWR.....	A-5
Figure B-1	Plant Transient Power Shape	B-3
Figure B-2	Plant Vessel Profile	B-4
Figure B-3	Plant Vessel Model Noding Diagram.....	B-5
Figure B-4	Plant Core Channel Modeling.....	B-6
Figure B-5	Plant Loop Model Noding Diagram	B-7
Figure B-6	Case 1 Core Blockage Modeling Approach.....	B-8
Figure B-7	Case 2 Core Blockage Modeling Approach.....	B-9
Figure B-8	Low Power Channel and HA Channel Void Fraction, Case 2 - Unblocked HA Test....	B-10

Figure B-9	Average Core Channel Collapsed Liquid Level for Case 1 and Case 2.....	B-15
Figure B-10	Total Vessel Liquid Mass for Case 1 and Case 2	B-16
Figure B-11	Upper Plenum Global Channel Collapsed Liquid Level for Case 1 and Case 2.....	B-17
Figure B-12	Total Integrated Liquid Flow at the Top of the Core for Case 1 and Case 2 (Positive/Outlet flow represents HA, GT, AVG channels; Negative/Inlet flow represents LP channel)	B-18
Figure B-13	Integrated Core Flow vs. Core Boil-off for Case 1 and Case 2	B-19
Figure B-14	Broken Loop DC Channel Collapsed Liquid Level for Case 1 and Case 2	B-20
Figure B-15	Intact Loop DC Channel Collapsed Liquid Level for Case 1 and Case 2.....	B-21
Figure B-16	Pressurizer Loop DC Channel Collapsed Liquid Level for Case 1 and Case 2	B-22
Figure B-17	Pressurizer Loop Hot Leg Integrated Liquid Flow for Case 1 and Case 2	B-23
Figure B-18	Intact Loop Hot Leg Integrated Liquid Flow for Case 1 and Case 2.....	B-24
Figure B-19	Broken Loop Hot Leg Integrated Liquid Flow for Case 1 and Case 2	B-25
Figure B-20	Case 1 and Case 2 Hot Rod PCT	B-26
Figure B-21	Integrated Core Flow vs. Core Boil-off for Channel 13 Flow Reduction 50%	B-31
Figure B-22	Integrated Core Flow vs. Core Boil-off for Channel 13 Flow Reduction 50% Case (Shifted Scale).....	B-32
Figure B-23	Total Integrated Liquid Flow at the Top of the Core for Channel 13 Flow Reduction 50% Case (Positive/Outlet flow represents HA, GT, AVG channels; Negative/Inlet flow represent LP channel).....	B-33
Figure B-24	Hot Rod PCT for Channel 13 Flow Reduction 50% Case	B-34
Figure B-25	Average Core Channel CLL for Channel 13 Flow Reduction 50% Case	B-35
Figure B-26	Void Fraction at the Exit of the Average Core Channel for Channel 13 Flow Reduction 50% Case	B-36
Figure B-27	Core Pressure Drop for Channel 13 Flow Reduction 50% Case	B-37
Figure B-28	Integrated Core Flow vs. Core Boil-off for Channel 13 Flow Reduction 80% Case....	B-38
Figure B-29	Integrated Core Flow vs. Core Boil-off for Channel 13 Flow Reduction 80% Case (Shifted Scale).....	B-39
Figure B-30	Total Integrated Liquid Flow at the Top of the Core for Channel 13 Flow Reduction 80% Case (Positive/Outlet flow represents HA, GT, AVG channels; Negative/Inlet flow represent LP channel).....	B-40
Figure B-31	Hot Rod PCT for Channel 13 Flow Reduction 80% Case	B-41
Figure B-32	Average Core Channel CLL for Channel 13 Flow Reduction 80% Case	B-42

Figure B-33	Void Fraction at the Exit of the Average Core Channel for Channel 13 Flow Reduction 80% Case	B-43
Figure B-34	Core Pressure Drop for Channel 13 Flow Reduction 80% Case	B-44
Figure B-35	Integrated Core Flow vs. Core Boil-off for Uniform $C_D = 50,000$ Case	B-45
Figure B-36	Integrated Core Flow vs. Core Boil-off for Uniform $C_D = 50,000$ Case (Shifted Scale).....	B-46
Figure B-37	Total Integrated Liquid Flow at the Top of the Core for Uniform $C_D = 50,000$ Case (Positive/Outlet flow represents HA, GT, AVG channels; Negative/Inlet flow represent LP channel).....	B-47
Figure B-38	Hot Rod PCT for Uniform $C_D = 50,000$ Case.....	B-48
Figure B-39	Average Core Channel Collapsed Liquid Level for Uniform $C_D = 50,000$ Case.....	B-49
Figure B-40	Void Fraction at the Exit of the Average Core Channel for Uniform $C_D = 50,000$ Case.....	B-50
Figure B-41	Core Pressure Drop for Uniform $C_D = 50,000$ Case	B-51
Figure B-42	Integrated Core Flow vs. Core Boil-off for Uniform $C_D = 100,000$ Case	B-52
Figure B-43	Integrated Core Flow vs. Boil-off for Uniform $C_D = 100,000$ Case (Shifted Scale)	B-53
Figure B-44	Total Integrated Liquid Flow at the Top of the Core for Uniform $C_D = 100,000$ Case (Positive/Outlet flow represents HA, GT, AVG channels; Negative/Inlet flow represent LP channel).....	B-54
Figure B-45	Hot Rod PCT for Uniform $C_D = 100,000$ Case.....	B-55
Figure B-46	Average Core Channel Collapsed Liquid Level for Uniform $C_D = 100,000$ Case.....	B-56
Figure B-47	Void Fraction at Exit of Average Core Channel for Uniform $C_D = 100,000$ Case	B-57
Figure B-48	Core Pressure Drop for Uniform $C_D = 100,000$ Case	B-58
Figure B-49	Integrated Core Flow vs. Boil-off for Uniform $C_D = 1,000,000$ Case	B-59
Figure B-50	Integrated Core Flow vs. Boil-off for Uniform $C_D = 1,000,000$ Case (Shifted Scale) .	B-60
Figure B-51	Total Integrated Liquid Flow at the Top of the Core for Uniform $C_D = 1,000,000$ Case (Positive/Outlet flow represents HA, GT, AVG channels; Negative/Inlet flow represent LP channel).....	B-61
Figure B-52	Hot Rod PCT for Uniform $C_D = 1,000,000$ Case.....	B-62
Figure B-53	Average Core Channel Collapsed Liquid Level for Uniform $C_D = 1,000,000$ Case.....	B-63
Figure B-54	Void Fraction at Exit of Average Core Channel for Uniform $C_D = 1,000,000$ Case	B-64
Figure B-55	Core Pressure Drop for Uniform $C_D = 1,000,000$ Case	B-65
Figure B-56	Comparison of Reactor Vessel Metal Temperature at Bottom of Fuel; Outside Diameter versus Inside Diameter.....	B-68
Figure B-57	Comparison of Reactor Vessel Metal Temperature at Top of Fuel; Outside Diameter versus Inside Diameter.....	B-69

Figure B-58	Comparison of Fluid Temperature at Top and Bottom of Downcomer	B-70
Figure B-59	Comparison of Fluid Temperature at Top and Bottom of Baffle	B-71
Figure B-60	Comparison of Fluid Temperature in Lower Plenum to Core Inlet	B-72
Figure B-61	Comparison of Fluid Temperature Between Core Inlet and Inside Baffle.....	B-73
Figure B-62	Comparison of Fluid Temperature at Core Outlet and Top Baffle.....	B-74
Figure C-1	Temperature vs. Deposition Thickness and Thermal Conductivity	C-7
Figure D-1	Heat Transfer Model (not to scale)	D-2
Figure D-2	Clad-Oxide Interface Temperature vs. Chemical Precipitate Thickness.....	D-4
Figure E-1	Flow Paths Modeled by LOCADM	E-7
Figure E-2	Deposit Growth Process Assumed by LOCADM When Core is Boiling.....	E-15
Figure E-3	Experimental Fouling Resistance for Calcium Sulfate Deposition (3) Compared to the LOCADM Calculated Fouling Resistance.....	E-19
Figure E-4	Maximum Scale Thickness Values for a PWR with High Fiber and Cal-sil Debris.....	E-27
Figure G-1	Westinghouse Fuel Test Vessel	G-2
Figure G-2	Schematic of Westinghouse Test Loop	G-3
Figure G-3	AREVA Test Loop	G-4
Figure G-4	Schematic of AREVA Test Loop.....	G-5
Figure G-5	Microtherm Scan.....	G-8
Figure G-6	Cal Sil Scan.....	G-9

LIST OF ACRONYMS

B&W	Babcock & Wilcox Co.
B/B	barrel/baffle
BELOCA	best estimate LOCA
BOA	boron-induced offset anomaly
BWST	borated water storage tank
CCFL	counter current flow limitation
CE	Combustion Engineering
CL	cold leg
CLL	collapsed liquid level
CSS	containment spray system
DC	downcomer
dP or ΔP	differential pressure
ECCS	emergency core cooling system
ECR	equivalent clad reacted
FA	fuel assembly
GL	generic letter
GSI	generic safety issue
HA	hot assembly
HL	hot leg
HLSO	hot leg switchover
HPSI	high pressure safety injection
LPSI	low pressure safety injection
LBB	leak before break
LOCA	loss-of-coolant accident
LOADM	LOCA deposition analysis model
LP	lower power
LTCC	long-term core cooling
NRC	Nuclear Regulatory Commission
OD	outer diameter
OEM	original equipment manager
PCT	peak cladding temperature
PWR	pressurized water reactor
PWROG	PWR Owners Group
RAI	request for additional information
RCS	reactor coolant system
RHR	residual heat removal
RV	reactor vessel
RVI	reactor vessel internals
RVVV	reactor vessel vent valves
RWST	refueling water storage tank
SG	steam generator
SIRWT	safety injection and refueling water tank
UP	upper plenum
UPI	upper plenum injection
WC/T	WCOBRA/TRAC

EXECUTIVE SUMMARY

Pressurized water reactor (PWR) containment buildings are designed both to contain radioactive materials releases and to facilitate core cooling in the event of a postulated loss-of-coolant-accident (LOCA). The cooling process requires water discharged from the break and containment spray to be collected in a sump for recirculation by the emergency core cooling system (ECCS) and the containment spray system (CSS). Typically, a containment sump contains one or more screens in series that protect the components of the ECCS from debris that could be washed into the sump. Fibrous debris could form a mat on the screen that would collect particulates, keeping them from being ingested into the ECCS and CSS flow paths. However, as the fiber bed forms, particulates and some fibrous material may be ingested into the ECCS and subsequently, into the reactor coolant system (RCS).

Concerns have been raised about the potential for debris ingested into the ECCS to affect long term core cooling (LTCC) when recirculating coolant from the containment sump. The fuel assembly (FA) bottom nozzles are designed with flow passages that provide coolant flow from the reactor vessel lower plenum into the region of the fuel rods. During operation of the ECCS to recirculate coolant from the containment sump, debris in the recirculating fluid that passes through the sump screen may collect on the bottom surface of the FA bottom nozzle, causing resistance to flow through this path. The collection of sufficient debris on the FA bottom nozzle is postulated to impede flow into the FA and core. Other concerns have been raised with respect to the collection of debris and post accident chemical products within the core itself. Specifically, the debris has been postulated to either form blockages or adhere to the cladding, thereby reducing the ability of the coolant to remove decay heat from the core. Similarly, chemical precipitates have been postulated to plate out on fuel cladding, again resulting in a reduction of the ability of the coolant to remove decay heat from the core.

Guidance provided to the industry in the following documents has been used as the framework for analyses that address these concerns.

- WCAP-16406-P: Section 9.0 (cold leg injection, hot leg injection, fiber, particulates, etc.), including addenda
- NEI 04-07, Volume 1: Section 7.3
- NEI 04-07, Volume 2: Section 7.3
- Draft NRC Staff Review Guidance for Evaluation of Downstream Effects of Debris Ingress into the PWR RCS on Long Term Core Cooling Following a LOCA, dated November 22, 2005.

The Pressurized Water Reactor Owners Group (PWROG) undertook a program to provide additional analyses and information on the effect of debris and chemical products on core cooling for PWRs when the ECCS is realigned to recirculate coolant from the containment sump. The objective of the program was to demonstrate reasonable assurance that sufficient LTCC is achieved for PWRs to satisfy the requirements of 10 CFR 50.46 with debris and chemical products that might be transported to the reactor vessel and core by the coolant recirculating from the containment sump. The debris composition includes particulate and fiber debris, as well as post-accident chemical products. The program was performed such that the results of this program apply to the fleet of PWRs, regardless of the design (Westinghouse, Combustion Engineering [CE], or Babcock & Wilcox [B&W]).

This evaluation considered the design of the PWR, the design of the open-lattice fuel, the design and tested performance of replacement containment sump screens, the tested performance of materials inside containment, and the tested performance of fuel assemblies in the presence of debris. Specific areas addressed in this evaluation include:

- Blockage at the core inlet,
- Collection of debris on fuel grids,
- Collection of fibrous material on fuel cladding,
- Protective coating debris deposited on fuel clad surfaces,
- Production and deposition of chemical precipitants,
- Boric acid precipitation, and
- Coolant delivered from the top of the core.

The following acceptance bases were selected for the evaluation of the topical areas identified above:

1. The maximum clad temperature shall not exceed 800°F.
2. The thickness of the cladding oxide and the fuel deposits should not exceed an average of 0.050 inches in any fuel region.

These acceptance bases were applied after the initial quench of the core and are consistent with the LTCC requirements stated in 10 CFR 50.46 (b)(4) and 10 CFR 50.46 (b)(5). They do not represent, nor are they intended to be, new or additional LTCC requirements. These acceptance bases provide for demonstrating that local temperatures in the core are stable or continuously decreasing and that debris entrained in the cooling water supply will not affect decay heat removal. The 800°F temperature was selected based on autoclave data that demonstrated oxidation and hydrogen pickup to be well behaved at and below the 800°F temperature and the reduction in cladding small. Therefore, there would be minimal reduction in post-LOCA load carrying capability. A discussion of the technical basis for the 800°F temperature is given in Appendix A. The 0.050 inch limit for oxide plus deposits was selected so as to preclude the formation of deposits that would bridge the space between adjacent rods and block flow between fuel channels.

The evaluations performed for the areas identified above provide reasonable assurance of LTCC for all plants. Specifically,

- Adequate flow to remove decay heat will continue to reach the core even with debris from the sump reaching the RCS and core. Plants that operate at the debris loads identified in Section 10 by the FA tests, can state that debris that bypasses the screen will not build an impenetrable blockage at the core inlet. While any debris that collects at the core inlet will provide some resistance to flow, in the extreme case that a large blockage does occur, numerical analyses have demonstrated that core decay heat removal will continue. The details of this evaluation are provided in Section 3.
- Decay heat will continue to be removed even with debris collection at the FA spacer grids. Plants that operate at the debris loads identified in Section 10 by the FA tests, can state that debris that bypasses the screen will not build an impenetrable blockage at the fuel spacer grids. In the

extreme case that a large blockage does occur, numerical and first principle analyses have demonstrated that core decay heat removal will continue. The details of this evaluation are provided in Section 4.

- Fibrous debris, should it enter the core region, will not tightly adhere to the surface of fuel cladding. Thus, fibrous debris will not form a “blanket” on clad surfaces to restrict heat transfer and cause an increase in clad temperature. Therefore, adherence of fibrous debris to the cladding is not plausible and will not adversely affect core cooling. The details of this evaluation are provided in Section 5.
- Protective coating debris, should it enter the core region, will not restrict heat transfer and cause an increase in clad temperature. Therefore, adherence of protective coating debris to the cladding is not plausible and will not adversely affect core cooling. The details of this evaluation are provided in Section 6.
- The chemical effects method developed in WCAP-16530-NP-A was extended to develop a method to predict chemical deposition of fuel cladding. The calculational tool, LOCADM, can be used by each utility to perform a plant-specific evaluation. It is expected that each plant will be able to use this tool to show that decay heat would be removed and acceptable fuel clad temperatures would be maintained. The details of this evaluation are provided in Section 7.
- PWRs use boron as a core reactivity control method and are subject to concerns regarding potential post-LOCA boric acid precipitation in the core. In light of NRC staff and ACRS challenges to the simplified methods commonly used, it has recently become clear that additional insights and new methodologies are needed to answer fundamental questions about boric acid mixing and transport in the RCS and potential precipitation mechanisms that may occur both during the ECCS injection phase and the sump recirculation phase after a LOCA. This will be addressed in a separate PWROG program. This program is discussed in Section 8.
- The PWROG FA test results demonstrated that sufficient flow will reach the core to remove core decay heat. The debris load acceptance criteria developed is bounding and applicable to all PWR plants, including UPI plants. The details of this evaluation are provided in Section 9.

Actions are required of utilities to demonstrate acceptable LTCC with debris and chemical products in the recirculating fluid. Plants will have to perform plant-specific LOCADM evaluations (Section 7 and Appendix E) and prove the plant conditions are bounded by the debris load acceptance criteria (Section 3, 10 and Appendix G). Plants with debris loads above the debris load acceptance criteria may demonstrate adequate LTCC capability through analysis of plant-specific debris loads and/or plant-specific testing.

These actions along with reference to this report provide the basis for demonstrating LTCC will not be compromised following a LOCA as a consequence of debris ingestion to the RCS and core.

1 INTRODUCTION

The scope of Generic Safety Issue 191 (GSI-191) (Reference 1-1) addresses a variety of concerns associated with the operation of the emergency core cooling system (ECCS) and the containment spray system (CSS) in the recirculation mode. These concerns include debris generation associated with a postulated high energy line break, debris transport to the containment sump when the ECCS is realigned to operate in the recirculation mode, and the effects of debris that might pass through the sump screens on downstream components and fuel. In addition to debris resulting from the action of the jet from the postulated pipe break, there is also the potential for generation of chemical products from the reaction of containment materials and coolant that may also be transported to and through the sump screen.

During operation of the ECCS to recirculate coolant from the containment sump, debris in the recirculating fluid that passes through the sump screen may collect on the bottom surface of the fuel assembly (FA) bottom nozzle, causing resistance to flow through this path. The collection of sufficient debris on the FA bottom nozzle is postulated to impede flow into the fuel assemblies and core. Other concerns have been raised with respect to the collection of debris and post accident chemical products within the core itself. Specifically, the debris has been postulated to either form blockages at spacer grids or adhere to the cladding, thereby reducing the ability of the coolant to remove decay heat from the core. Similarly, chemical precipitants have been postulated to plate out on fuel cladding, again resulting in a reduction of the ability of the coolant to remove decay heat from the core.

Guidance provided to the industry in the following documents has been used to provide the framework for analyses that address these concerns.

- WCAP-16406-P-A: Section 9.0 (cold leg injection, hot leg injection, fiber, particulates, etc.) including addenda (Reference 1-2)
- NEI 04 07, Volume 1: Section 7.3 (Reference 1-3)
- NEI 04 07, Volume 2: Section 7.3 (Reference 1-4)
- Draft NRC Staff Review Guidance for Evaluation of Downstream Effects of Debris Ingress into the PWR RCS on Long Term Core Cooling Following a LOCA, dated November 22, 2005. (Reference 1-5)

The Pressurized Water Reactor Owners Group (PWROG) undertook a program to provide additional analyses, test data, and information on the effect of debris and chemical products on core cooling for pressurized water reactors (PWRs) when the ECCS is realigned to recirculate coolant from the containment sump. The objective of the program is to enable each plant to demonstrate that there is reasonable assurance that sufficient long term core cooling (LTCC) is achieved for PWRs to satisfy the requirements of 10 CFR 50.46 with debris and chemical products that are postulated to be transported to the reactor vessel. For the purposes of this work, “long-term core cooling” is defined to be when the ECCS and CSS are realigned to recirculate coolant from the containment sump. The program was performed such that the results of this program apply to the fleet of PWRs, regardless of the design (Westinghouse, Combustion Engineering [CE], or Babcock & Wilcox [B&W]).

2 LONG-TERM CORE COOLING ACCEPTANCE BASIS

2.1 INTRODUCTION

Part of the resolution of GSI-191 involves defining the relevant LTCC bases. This section describes the criteria that will be used in determining GSI-191 acceptance of the debris effects on fuel. These LTCC acceptance criteria are based on the requirements of Title 10 of the Code of Federal Regulations, Part 50.46 (10 CFR 50.46). The criteria are to be used with engineering evaluations that demonstrate acceptable LTCC, once established following the initial recovery of the core post LOCA, is successfully maintained. Successful LTCC is defined as meeting the criteria highlighted in this section. A detailed discussion of the criteria can be found in Appendix A.

2.2 GSI-191 LONG-TERM CORE COOLING ACCEPTANCE BASES

The LTCC acceptance bases defined for GSI-191 are listed below. These acceptance bases are consistent with 10 CFR 50.46 (b)(4) and 10 CFR 50.46 (b)(5) and demonstrate that the local temperatures are stable or continuously decreasing and that debris entrained in the cooling water supply will not affect decay heat removal.

1. Decay Heat Removal/Fuel Clad Oxidation

Maximum cladding temperatures maintained during periods when the core is covered will not exceed a core average clad temperature of 800°F.

Cladding temperatures at or below 800°F maintain the clad within the temperature range where additional corrosion and hydrogen pickup over a 30 day period will not have a significant effect on cladding properties. At temperatures greater than 800°F, there are occurrences of rapid nodular corrosion and higher hydrogen pickup rates that can reduce cladding mechanical performance. Long term autoclave testing has been performed to demonstrate that no significant degradation in cladding mechanical properties would be expected due to a localized hot spot. This information is proprietary to the fuel vendors but could be made available upon request. This testing demonstrated that the increase in oxide thickness and hydrogen loading was limited at temperatures of less than 800°F for periods of 30 days. With limited corrosion and hydrogen pickup, the impact on cladding mechanical performance is not significant. Therefore, no significant degradation in cladding properties would occur due to 30-day exposure at 800°F and there would not be any adverse impact on core coolability. The autoclave results justify a maximum clad temperature 800°F as an LTCC acceptance basis.

2. Deposition Thickness

For current fuel designs, regardless of vendor, the minimum clearance between two adjacent fuel rods, including an allowance for the spacer grid thickness, is greater than 100 mils. Therefore, a 50-mil debris thickness on a single fuel rod is the maximum deposition to preclude touching of the deposition of two adjacent fuel rods with the same deposition. The 50 mil thickness is the maximum acceptable deposition thickness before bridging of adjacent fuel rods by debris is

predicted to occur. The 50 mils of solid precipitation described here include the clad oxide, crud layer and debris deposition.

2.3 SUMMARY

These LTCC bases applicable to GSI-191 have been defined based on the requirements of 10 CFR 50.46 as clarified by the NRC (Reference 2-1). They are summarized as follows:

1. The cladding temperature during recirculation from the containment sump will not exceed 800°F.
2. The deposition of debris and/or chemical precipitates will not exceed 50 mils on any fuel rod.

These bases will facilitate the demonstration of acceptable core cooling following a postulated large break LOCA.

3 BLOCKAGE AT THE CORE INLET

During operation of the ECCS to recirculate coolant from the containment sump, debris in the recirculating fluid that passes through the sump screen may collect on the bottom surface of the FA bottom nozzle, causing resistance to flow through this path. The collection of sufficient debris at this location is postulated to impede flow into the fuel assemblies and core. In order to address this concern, a prototypical FA testing program was initiated to establish limits on the debris mass (particulate, fibrous, and chemical) that could bypass the reactor containment building sump screen and not impede core inlet flow and challenge LTCC.

Additionally, this section provides an overview of WCOBRA/TRAC (WC/T) evaluation, which examines the extreme case of almost complete blockage at the core inlet in order to provide additional assurance that LTCC will not be challenged. This calculation provides additional “defense in depth” assurance that LTCC will be maintained.

3.1 PROTOTYPICAL FUEL ASSEMBLY TESTING

The prototypical FA testing program was designed to establish limits on the debris mass (particulate, fibrous, and chemical) that could bypass the reactor containment building sump screen and not impede core inlet flow and challenge LTCC. An overall test protocol and specific test procedures were developed to ensure that possible thin bed effects were investigated and debris types and characteristics expected in the reactor coolant system (RCS) were represented. Debris loads used in the test were based on sump screen bypass information provided by licensees. A detailed discussion of the test can be found in Appendix G. The following sections summarize the program and pertinent results. The results from these FA tests are discussed in the proprietary test reports (References 3-1 and 3-2).

3.1.1 Available Driving Head

At the time of sump switchover, the core has been fully recovered and the fluid inventory in the RCS is above the top of the core. The core decay heat is being removed by ECCS injection. Core flow is only possible if the manometric balance between the downcomer and the core is sufficient to overcome the flow losses in the reactor vessel (RV) downcomer, RV lower plenum, core, and loops, or reactor vessel vent valves (RVVVs)¹ at the appropriate flow rate.

$$\Delta P_{\text{avail}} = \Delta P_{\text{dz}} - \Delta P_{\text{flow}}$$

where:

ΔP_{avail}	=	Available head to drive flow into the core
ΔP_{dz}	=	Elevation head between downcomer side and core
ΔP_{flow}	=	Flow losses in the RV downcomer, RV lower plenum, core, and loops or RVVVs

-
1. The B&W plant designs have RVVVs that short-circuit the steam path to the break for CL break scenarios. These passive valves provide a path between the RV outlet plenum and the RV upper downcomer region. They open on a small differential pressure and provide a path for steam to vent from the RV upper plenum directly to the break in the CL. Therefore, steam flow through the loops is not expected for B&W-designed plants.

The manometric differences are determined considering plant geometry, system water levels, core void fractions, and flow path resistances. The flow losses are calculated using the following form of the Darcy equation.

$$\Delta P_{\text{flow}} = \frac{k}{A^2} \cdot \frac{\omega^2}{288 \cdot \rho_g \cdot g_c}$$

where:

ΔP_{flow}	=	differential pressure (psid)
k	=	form-loss coefficient
A	=	area upon which the form-loss coefficient is based (ft ²)
ω	=	flow rate (lbm/s)
ρ_g	=	liquid density (lbm/ft ³)
g_c	=	gravitational constant (32.2 lbm-ft/lbf-sec ²)

The driving head at the core inlet is dependent on the break location. In either case, core heatup will not occur until there is sufficient debris accumulation to limit the core flow rate to the point where the fluid is exactly saturated steam at the core exit. Therefore, for either the hot or cold leg break, the calculation of allowed pressure drop for debris should not consider any liquid associated with entrainment or bubbly, frothy flow downstream of the core at the limiting condition.

3.1.1.1 Available Driving Head for Cold Leg Breaks

For postulated cold leg (CL) breaks, the ECCS from each CL runs to the break, ensuring that the downcomer is full to at least the bottom of the CL nozzles. The core level is established by the manometric balance between the downcomer liquid level, the core level, and RCS pressure drop through the loops or RVVVs. The net ECCS flow to the core is only what is required to make up for core boiling to remove the decay heat. Most of the ECCS spills directly out of the break. The flow down stream of the core at recirculation would be two-phase with entrained liquid or a bubbly flow wherein the flow and elevation heads balance the downcomer elevation head to produce a flow rate matching decay heat. As debris builds up, the flow of liquid into the core reduces and the level of liquid downstream of the core lowers or the entrained liquid is not replaced until the critical condition is reached with just sufficient flow to match decay heat with no remaining liquid downstream of the core. This condition is commensurate with the maximum allowed blockage at the core inlet. For these conditions, the available driving head for the CL break is lower than for the hot leg (HL) break. The driving head used for the PWROG FA tests can be found in References 3-1 and 3-2.

3.1.1.2 Available Driving Head for Hot Leg Breaks

For a break in the HL, the ECCS must pass through the core to exit the break. The driving force is the manometric balance between the liquid in the downcomer and the core. Should a debris bed begin to build up in the core, the liquid level will begin to build in the CLs and flow will spill back through the reactor coolant pumps into the pump suction piping, steam generator (SG) inlet plenum, and SG tubes. As the level begins to rise in the SG tubes, the elevation head to drive the flow through the core increases

as well. The driving head reaches its peak when the flow begins to spill over the shortest SG tubes for Westinghouse- and CE-designed plants or reaches the HL spillover elevation for B&W-designed plants. Once the ECCS flow reaches the elevation of the shortest tubes, the flow area of the shortest tubes or HL piping are large enough that no increase in water level to the higher tubes is achieved. This is conservative, as it provides for the minimum static head available. The core mixture level will be at least to the HL nozzle elevation, and the core flow rate will equal the ECCS flow rate. The flow down stream at recirculation would be liquid that has been heated in the core, but not likely boiled, and is being pushed out the break (Appendix J, RAI #14). As debris builds up, the flow of liquid is reduced until boiling initiates and the break flow becomes two-phase. Increased accumulation of debris further slows the flow until the critical condition is reached with just sufficient flow to match decay heat and no liquid downstream of the core. This condition is commensurate with the maximum allowed blockage at the core inlet. The available driving head was calculated based on the conditions in which the core mixture level is postulated to be at the bottom of the HL and the core flow rate equals the ECCS flow rate. The minimum driving head used for the PWROG FA tests can be found in References 3-1 and 3-2.

3.1.2 Description of Tests

The PWROG developed a common test protocol to ensure that testing for all of the PWROG members was consistent among test sites. The protocol is described in Reference 3-3. The test matrix, acceptance criteria, and test procedures were developed based on this protocol. The details of the test program are provided in Appendix G.

3.1.3 Discussion of Test Results

Testing was performed at hot and cold leg break flow rates. These tests demonstrated the following for the bounding debris loads:

- The HL break flow rate (i.e. the highest flow rate) represented the limiting head loss test condition.
- Complete “blockage” of the FA tested was not observed in testing. Coolant flow through the debris collection was maintained.
- Chemical and particulate did not have a significant effect on head loss. Fiber was the greatest driver for increasing head loss at the core inlet.

Plants that have bypass debris loadings that are within the limits of the debris masses tested are bounded by the test. The specific acceptance criteria are listed in Section 10. Several courses or actions have been identified for plants whose debris loads are outside of the limits tested including, but not limited to, reducing problematic debris sources by removing or restraining the affected debris source or plant-specific FA testing.

Specific break locations are further discussed in the following sections.

3.1.3.1 Hot Leg Break Tests

All tests conducted at the HL break flow rates showed a head loss less than that needed to maintain core flow. Therefore, the debris loads tested will not inhibit flow into the core for decay heat removal following a HL break.

3.1.3.2 Cold Leg Break Tests

The debris that reaches the RCS lower plenum and core inlet will be substantially lower than the debris that reaches the core for a HL break. The ECCS flow that reaches the core is only that amount necessary to make up for core boil-off. This boil-off rate is a function of time after trip as a result of the LOCA, the core exit pressure, the amount of subcooling at the core inlet, and decay heat. As time progresses, the decay heat decreases such that the core boil-off rate decreases. Any ECCS flow over and above the boil-off rate is returned to the containment via the break. Once in the sump, the debris may settle or be refiltered through the sump screens before it can return to the RCS.

In order for the debris to transport through the RCS, it must be well-mixed in the ECCS fluid. It is therefore reasonable to assert that the debris is homogeneously mixed with the ECCS fluid such that the fraction of debris that reaches the RV lower plenum is proportional to the fraction of ECCS flow that reaches the RV lower plenum. Based on the assumption that it is well-mixed, and the core to break flow split evaluations, then significantly less debris reaches the RV lower plenum for the CL break than for the HL break. Therefore, the CL tests were conducted with greater than or equal to 50 percent of the fiber that was tested in the HL tests.

The CL test demonstrated that the HL break test results are the bounding condition. Therefore, the acceptance criteria debris loads defined at HL conditions are applicable to the CL break and will not inhibit flow into the core for decay heat removal following a CL break.

3.1.3.3 Impact of Thin Bed on Head Loss

Testing was performed using the NRC March 2008 protocol of adding all particulate debris, then beginning to add the fibrous debris in small quantities so as to provide for the formation of a thin bed (Reference 3-4). All tests followed this guidance, with the NRC staff observing a few of the tests. In all cases, a thin bed was not observed, even with very small quantities of fibrous debris. It was determined that a thin bed was not likely to form at the core inlet.

3.1.3.4 Debris Settling in Lower Plenum

Credit for settling in the lower plenum is not being considered as part of the demonstration of LTCC. However, credit for settling in the lower plenum may be considered, with appropriate and applicable justification, for other issues associated with the closure of GSI-191.

3.1.3.5 Alternate Flow Paths

This testing identifies debris loading limits that preclude the core inlet from becoming fully blocked with debris. Thus, if the core debris loading of plants falls within the limits of the debris loads tested, the core

inlet will not become fully blocked with debris. Therefore, flow paths into the core other than through the core inlet or exit (i.e., alternate flow paths) are not considered in applying the debris mass acceptance criteria and are not credited or utilized in establishing acceptable debris loading conditions for LTCC.

In the event that a plant should choose to credit alternate flow paths for LTCC, the plant would be expected to identify the number, size, flow capability, and potential for blockage of the flow paths the plant is crediting.

3.2 WCOBRA/TRAC EVALUATION OF BLOCKAGE AT THE CORE INLET

To further bolster the assertion that core cooling flow will be maintained, WC/T analyses were performed to demonstrate that adequate flow is provided and redistributed within the core to maintain adequate LTCC. This computer code is used for evaluating best estimate large break LOCA methodology and is described in detail in Reference 3-5. A bounding evaluation was performed, using limiting assumptions, to evaluate the consequences of core inlet blockage on LTCC. The blockage was assumed to deterministically occur and is not representative of actual plant conditions. The objective of the calculation was to demonstrate that, should blockage at the core inlet occur, sufficient liquid could enter the core to remove core decay heat once the plant had switched to sump recirculation with up to 99.4 percent core blockage to assure acceptable cladding temperatures. Presented here is a summary of the evaluation performed. Appendix B contains a more detailed description of the evaluation performed.

3.2.1 Approach

The effects of blockage at the core inlet were simulated by ramping the dimensionless friction factor (C_D) at the core inlet to a large number, simulating a postulated debris buildup that results in a reduction of flow. A modified version of WC/T was created to allow the friction factor at the core inlet to be ramped. Code simulations were performed using standard input for a problem time of 20 minutes. The 20 minute time was taken to be representative of the earliest time of realignment of the ECCS to operate in the recirculation mode. Starting at 20 minutes, the friction factor at the core inlet was ramped to its terminal value over the next 30 seconds. The core inlet flow blockage occurring in 30 seconds from the start of recirculation is not physical and does not represent any plant condition. The postulated core blockage was modeled in this manner to perform a bounding calculation. After the core inlet resistance was ramped to its terminal value of about $C_D = 109$ (which essentially eliminates all flow through the path), the code simulations were run out to 40 minutes to show the flow rate supplied to the core would be sufficient to remove decay heat and maintain a coolable core geometry.

3.2.2 Selection of Limiting Reactor Vessel Design

The core inlet blockage simulations were designed to bound the U.S. PWR fleet. To ensure a bounding calculation, the limiting break type and the limiting vessel design were taken into consideration before selecting a plant model for the simulation.

The selection of the limiting break for modeling purposes combines the conditions from a double-ended CL and a double-ended HL break to create a bounding scenario. During a double-ended CL break, the ECCS will spill into containment, which decreases the driving head of core flow to a minimum. However, the debris that reaches the RCS lower plenum and core inlet for a CL break will be substantially

lower than the debris that reaches the core for a HL break. During a double-ended HL break, no spilling of ECCS occurs. Therefore, an additional driving head from the build-up of liquid level in the downcomer and in the steam generator tubes to the spillover elevation is present. However, the higher flow rates also result in faster debris build-up, and because there is more debris available to accumulate, the HL break represents the conservative case in terms of debris load. To create the worst possible scenario, the limiting break case for modeling purposes will be a modified double-ended CL break, i.e., limiting flow at the core inlet, combined with faster debris build-up time that occurs for a high flow HL break.

Similarly, Westinghouse, CE, and B&W vessel designs were considered and a limiting design was chosen based upon which vessel design would be most limiting with respect to the condition of core inlet flow blockage. Three general Westinghouse vessel designs were considered: designed barrel/baffle (B/B) upflow, converted B/B upflow, and B/B downflow. For Westinghouse designed plants, the most limiting design is downflow plants since the only means for the flow to enter the core is through the lower core plate. As described in Appendix B, this design was also determined to bound both the B&W and CE plants. Thus, a Westinghouse downflow plant was used for this WC/T evaluation.

3.2.3 Model Inputs

A plant with an existing WC/T model, downflow plant configuration, and high core power density is desired for the core blockage simulations. A three-loop downflow model plant rated at 2900 MWt was chosen. The axial power shape used high enthalpy rise peaking factor ($F_{\Delta H} = 1.73$), a skewed to the top power distribution (13 percent axial offset), and a relatively high total peak factor ($F_Q = 2.3$). The top-skewed power shape, shown in Figure 3-1, is limiting compared to base load or bottom skewed power shapes due to the longer time for the quench front to approach the elevations with the highest power and its susceptibility to heatup if the core becomes uncovered due to inlet blockage.

The radial power distributions between the four core channels are listed in Table 3-1. The radial power distribution in the core is flat with the exception of the periphery assemblies and the hot assembly. The hot assembly power is conservatively modeled to a high normalized power of 1.66.

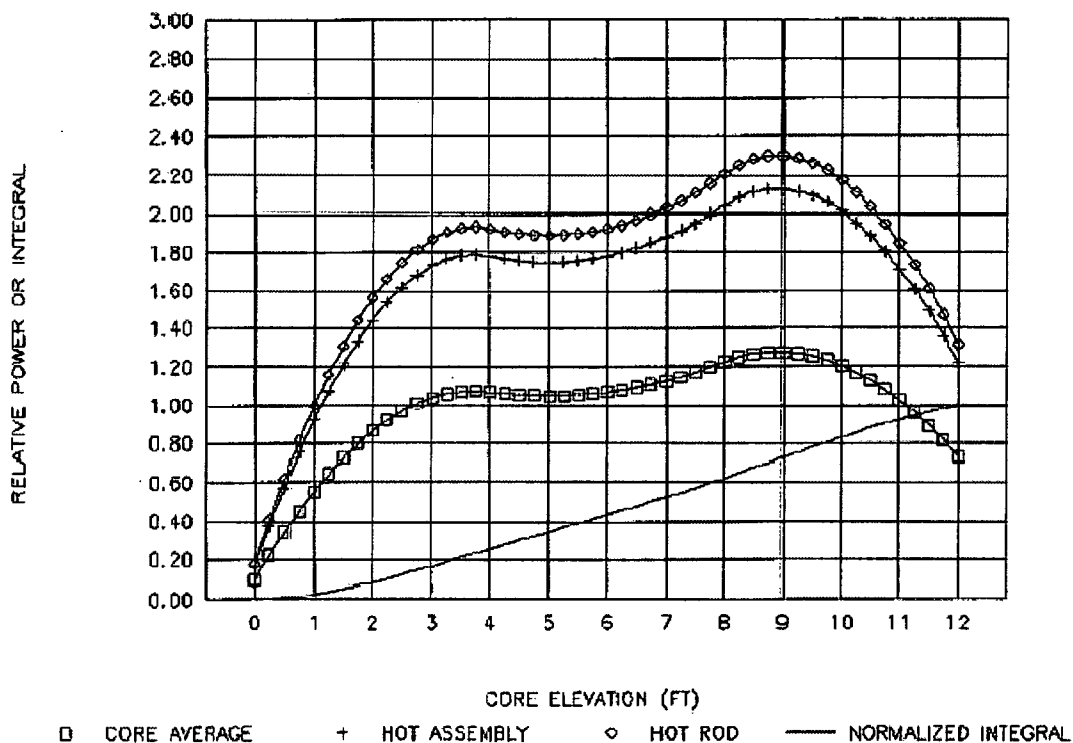


Figure 3-1 Plant Transient Power Shape

Channel Description	Channel Number	Normalized Power	Number of Assemblies
Hot Assembly Channel (HA)	13	1.66	1
Guide Tube Channel (GT)	12	1.17	53
Non-Guide Tube Channel (AVG)	11	1.17	75
Low Power Periphery Channel (LP)	10	0.20	28

Additional information about the plant chosen for the core inlet blockage simulations, including schematics and WC/T nodding diagrams, is provided in Appendix B.

At 20 minutes, in addition to the ramping of the loss coefficient at the core inlet of the model, the ECCS temperature was increased. The increase in the ECCS better simulates the recirculating coolant temperature and is representative of residual heat removal (RHR) heat exchanger outlet temperature following switchover to sump recirculation. The temperature of the injected water was set to be 190°F, which is typical for Westinghouse designs and is expected to bound B&W designs. CE plant designs do not have RHR heat exchangers, and after switchover to recirculation, high pressure safety injection flow is pumped directly from sump to the RCS. As described in Appendix B, the increase in sump ECCS

injection temperature is assessed to be a non-factor in core inlet blockage simulations. Prior to recirculation, termination of extensive downcomer boiling and cooling of vessel internals has already occurred. Therefore, the increase in injection temperature should not lead to boiling and only a small decrease in flow rate supplied to the core will ensue due to the density effects.

3.2.4 Results

Two simulations were run with no changes to the standard noding scheme but with different amounts of core blockage. The first case modeled 82 percent core flow blockage and allowed flow through the periphery fuel assemblies as shown in Figure 3-2. The second case modeled 99.4 percent core flow blockage and allowed flow only through the hot assembly (HA) channel. The cross-sectional core noding schemes for Case 1 and Case 2 are shown in Figure 3-2 and Figure 3-3, respectively.

As shown in Figure 3-4, a comparison between the calculated flow rates for Cases 1 and 2, and the flow rate needed to match core boil-off shows there is ample flow into the core to replace boil-off after the simulated core blockage occurred. Also, as shown in Figure 3-5, the calculated peak clad temperature (PCT) history plot of the hot rod is predicted to occur in traditional early time frame (within ~200 seconds) for a postulated large-break LOCA analysis. Figure 3-5 also shows that after roughly 300 seconds the core is quenched and no significant heatup occurs thereafter. Because no heat up occurs during the sump recirculation phase of the event, the maximum local and core wide oxidation calculations for traditional LOCA analyses are still considered applicable. It is therefore concluded that sufficient liquid can enter the core to remove core decay heat once the plant has switched to sump recirculation with up to 99.4 percent blockage at the core inlet.

The evaluation documented in Appendix B considered the Case 2 modeling approach of leaving the hot assembly unblocked due to core cross-flow. The void fraction in the HA channel was shown to reach higher values, demonstrating that much of the flow exits the HA channel via cross-flow to adjacent lower-power assemblies in the core. It was therefore concluded that there was no non-conservatism in the calculations due to the modeling approach.

The containment back pressure was modeled by a containment pressure vs. time table input for each of the broken loop CL components. The containment backpressures used in both cases were based on the existing pressure vs. time tables used in the best estimate LOCA (BELOCA) analysis. The BELOCA table was extrapolated down to atmospheric pressure and held at atmospheric conditions for the remainder of the simulation. Consistent with the objective of this evaluation, the applicability of this evaluation to sub-atmospheric containments was also evaluated. As stated in Appendix B, it was determined that the sub-atmospheric containment pressure plant designs are bounded by the atmospheric containment simulations performed to examine the effects of core inlet blockage.

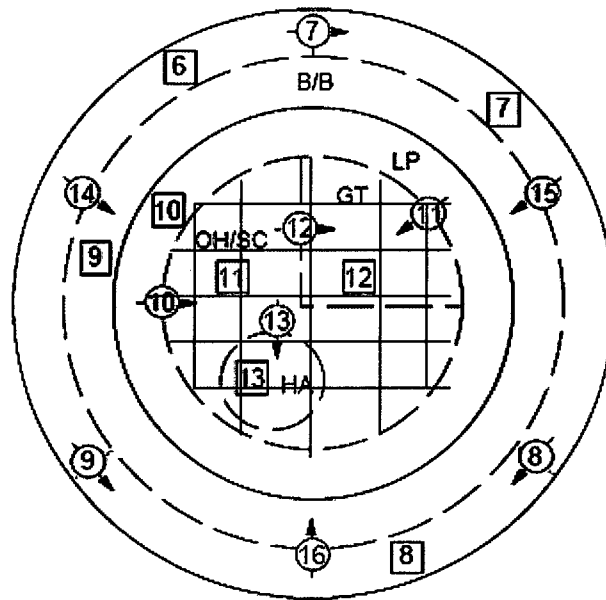


Figure 3-2 Case 1 – 82% Core Blockage Modeling Approach

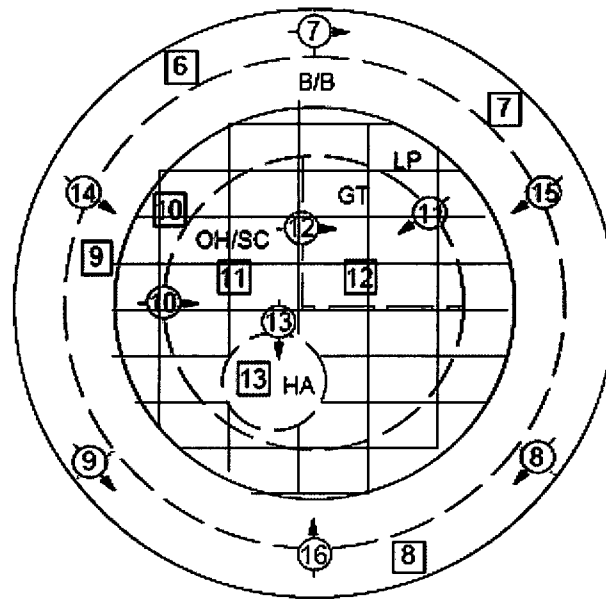
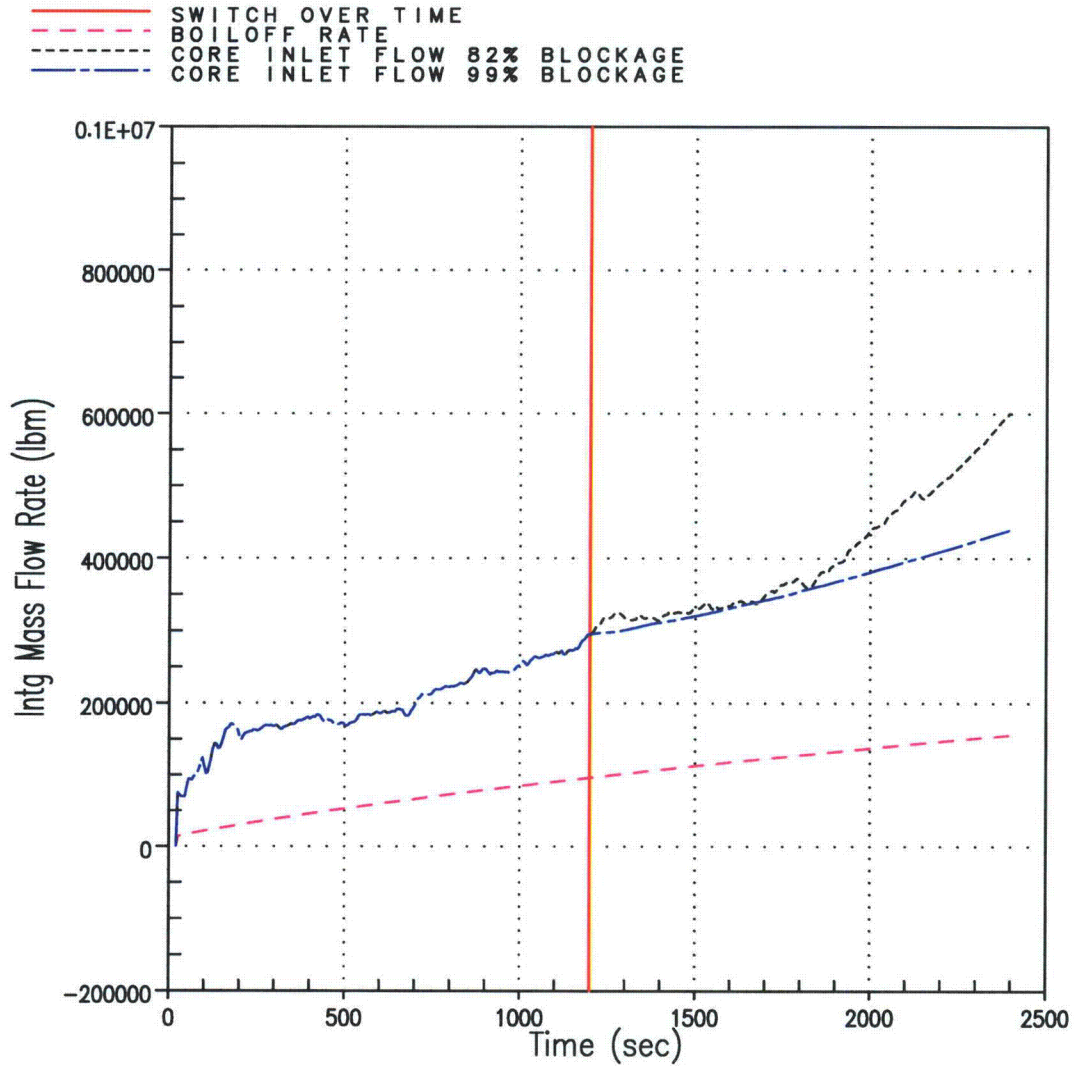


Figure 3-3 Case 2 – 99.4% Core Blockage Modeling Approach

Note: Regions 6, 7, 8, and 9 are the downcomer and downflow B/B regions.



146390733

Figure 3-4 Integrated Core Flow vs. Core Boil-off for Case 1 and Case 2

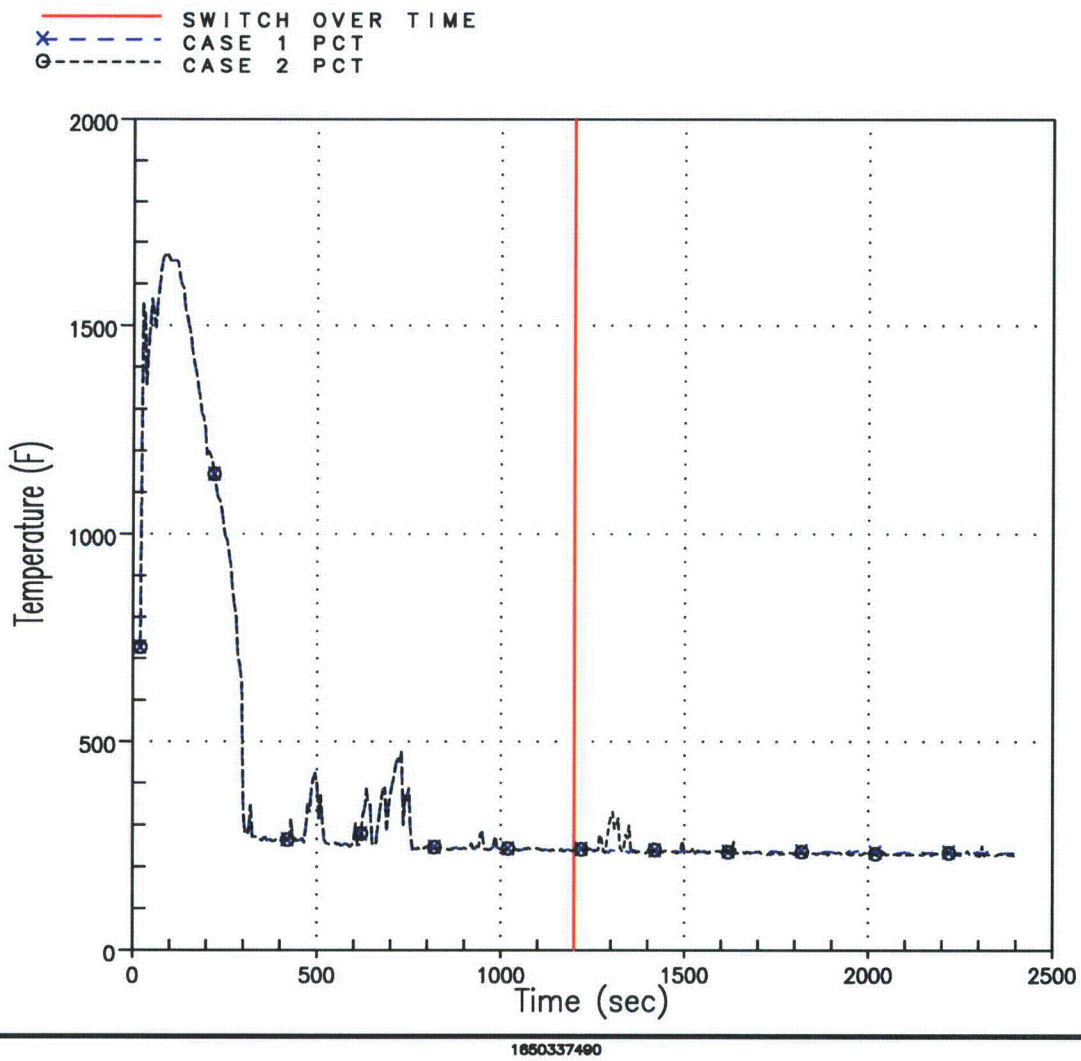


Figure 3-5 Case 1 and Case 2 Hot Rod Peak Clad Temperature History

3.3 ADDITIONAL WC/T CALCULATIONS

Several additional WC/T analyses were performed in support of the effort documented by this report. These WC/T runs were performed at the request of the Advisory Committee for Reactor Safeguards (ACRS) with the purpose of determining the blockage level (either using a reduction in area or increase loss coefficient) that would reduce core flow below that necessary to match coolant boil-off. The detailed documentation for these additional calculations is presented in Appendix B and includes time history plots of the integrated core inlet and exit flow, peak cladding temperature, core collapsed liquid level, core exit void fraction, and core pressure drop for the bounding conditions.

3.3.1 Method Discussion & Input

The base case for the calculation results presented in here is Case 2, or the more restricted flow area case, from Section 3.2. The Darcy equation defines pressure drop as being proportional to the form-loss coefficient and inversely proportional to the flow area squared. Using this principle, two separate approaches were taken to determine the blockage level needed to preclude sufficient flow into the core to provide for LTCC. The first approach considered an area reduction while maintaining the form-loss coefficients. The second approach considered form-loss coefficient increases while maintaining the flow area constant.

- For the first approach, the flow area of the hot channel, Channel 13, was reduced. The input value of the hydraulic loss coefficient, C_D , for the other channels into the core, Channels 10, 11, 12 and 13 remained the same as the base case. To maintain the total core flow area, the adjacent channel (Channel 11, representing an “average channel”) flow area was increased to offset the change in flow area to Channel 13. This change is needed to preserve the total core flow area; however, no flow will enter the core through Channel 11.
- For the second approach, the loss coefficients were increased in increments until boil-off could not be matched.

Areas Used in Reduced Flow Area Approach

The flow area values used in the two flow area reduction cases are as listed below.

Channel 13 50% Flow Reduction Case:

Channel 13 Flow Area	= 23.76 * (0.50)	= 11.88 in ²
Channel 11 Flow Area	= 1782 + 23.76 * (0.50)	= 1794. in ²

Channel 13 80% Flow Reduction Case:

Channel 13 Flow Area	= 23.76 * (0.20)	= 4.752 in ²
Channel 11 Flow Area	= 1782 + 23.76 * (0.80)	= 1801. in ²

Due to time constraints, the transient run time was reduced from 2400 seconds to 1500 seconds for the calculations that were performed. The transient calculation time of 1500 seconds is sufficient to demonstrate whether the reduction in core flow would be sufficient to match boil-off.

C_D Values used in Increased Loss Coefficient Approach

In order to determine the blockage level that would reduce core flow below that necessary to match coolant boil-off, the inlet core loss coefficients were increased in increments until boil-off could not be matched. The computer calculations made include uniform loss coefficients of 50,000, 100,000, and 1,000,000. The only changes required for these runs were updates to the variables used to activate the dimensionless loss coefficient ramp logic. For these cases, the C_D input value was changed from 10^9 to desired C_D value to reduce flow through peripheral channels, the average channels and the hot assembly channel instead of block flow. Also, the feature to allow the C_D value of all core inlet channels to vary as a function of time was enabled.

Three runs were made; $C_D = 50,000$, $C_D = 100,000$ and $C_D = 1,000,000$. The increase in C_D values to the desired values was accomplished over a 30 second time interval. The ramp up started at the time of switchover from injection from the BWST/RWST to recirculation from the sump, transient time $t = 1200$ seconds and was completed at transient time $t = 1230$ seconds.

Again, due to time constraints, the transient run time was reduced from 2400 seconds to 1500 seconds for the calculations that were performed. The transient calculation time of 1500 seconds is sufficient to demonstrate whether the reduction in core flow would be sufficient to match boil-off.

3.3.2 Results from Flow Area Reduction Runs

The first flow reduction run performed reduced the hot channel (Channel 13) flow area of Case 2 by 50%, which yields a total core inlet flow reduction of 99.7% compared to an unblocked core. Figure 3-4 shows a comparison of the integrated core inlet flow and the core boil-off rate, starting at 1200 seconds, the time that switchover from injection to recirculation from the containment sump is simulated. As shown, even with the increase in core blockage, the flow that enters the core is still in excess of the boil-off rate. The Peak Cladding Temperature (PCT) is shown in Figure 3-5. There are no significant PCT excursions after the core blockage is simulated.

The next flow reduction run performed reduced the hot channel (Channel 13) flow area by 80%, which yields a total core inlet flow area reduction of 99.9%. Figures 3-6 shows a comparison of the integrated core inlet flow and boil-off rate, again starting at 1200 seconds. For this increase in core blockage, the flow that enters the core can not match the boil-off rate. In addition, Figure 3-7 shows that the PCT increases for the remainder of the calculation.

These results indicate that a total core inlet area reduction of up to as much as 99.7% will still allow sufficient flow into the core to provide for removal of decay heat and assure LTCC.

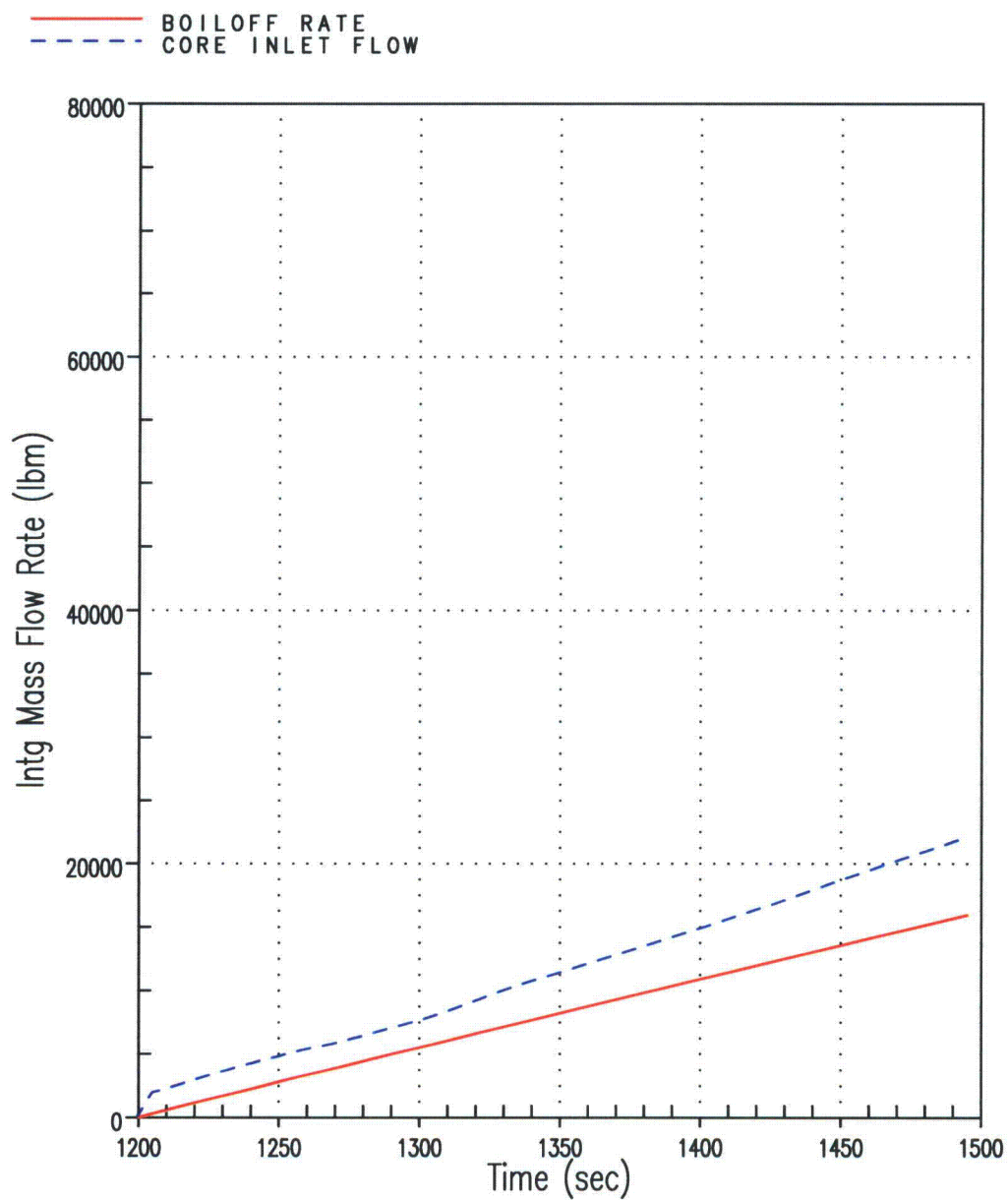
3.3.3 Results from Uniform Loss Coefficient Runs

The first uniform loss coefficient run performed applied a uniform C_D of 50,000 at the core inlet. Figures 3-8 shows a comparison of the integrated core inlet flow and boil-off rate, again starting at the time of switchover from injection to recirculation from the sump. As shown, even with the increase of the loss coefficient at the inlet, the flow that enters the core is still in excess of the boil-off rate. (Note that the integrated mass flow behavior shown between time $t = 1200$ seconds and time $t = 1250$ seconds of Figure 3-8 is the result of the 30 second ramp-up of the hydraulic loss coefficient, C_D , to 50,000 that is initiated in the calculations at time $t = 1200$ seconds.) The PCT is shown in Figure 3-9. There are no significant PCT excursions after the core inlet loss coefficient is increased.

The second uniform loss coefficient run performed applied a uniform C_D of 100,000 at the core inlet. Figure 3-10 shows a comparison of the integrated core inlet flow and boil-off rate. As shown, even with the further increase of the loss coefficient at the inlet, the flow that enters the core is still in excess of the boil-off rate. (Note that the integrated mass flow rate of Figure B-43 shows a similar behavior as was shown in Figure B-36. Again, this is due to the 30 second ramp-up of the hydraulic loss coefficient, C_D , to 100,000 that is initiated in the calculations at time $t = 1200$ seconds, but extends the behavior over a slightly longer period of time.) The PCT is shown in Figure 3-11. There are no significant PCT excursions after the core inlet loss coefficient is increased.

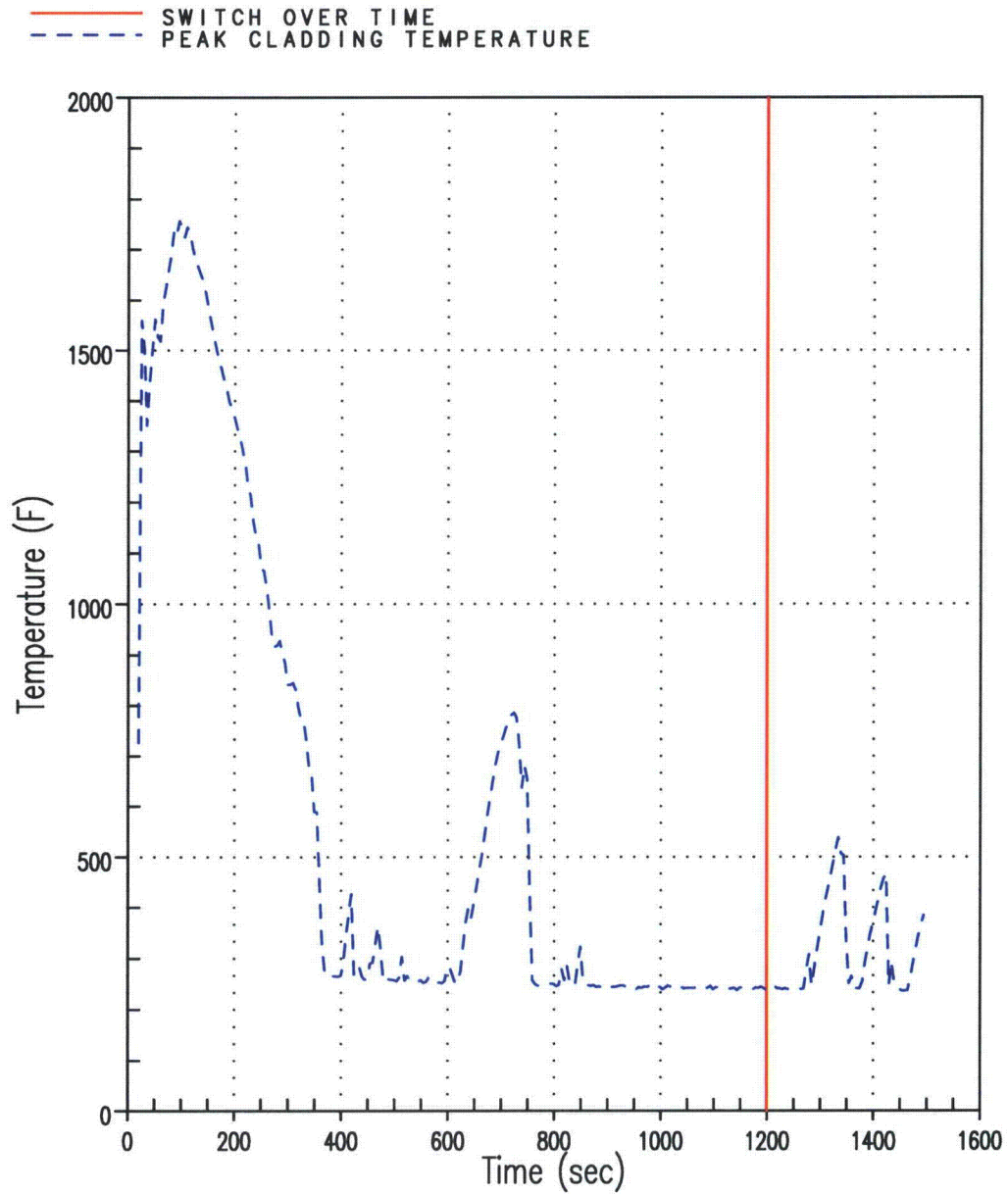
The next uniform loss coefficient run performed applied a uniform C_D of 1,000,000 at the core inlet. Figures 3-12 shows a comparison of the integrated core inlet flow and boil-off rate. With the increased resistance to flow into the core specified for this case, the flow that enters the core can not match the boil-off rate. As a consequence, as shown in Figure 3-13, the PCT increases until the end of the transient calculation.

The results indicate that an increase in the form loss coefficient at the core inlet of up to $C_D = 100,000$ for the limiting plant and fuel load design will allow for sufficient flow into the core to remove decay heat and provide for LTCC.



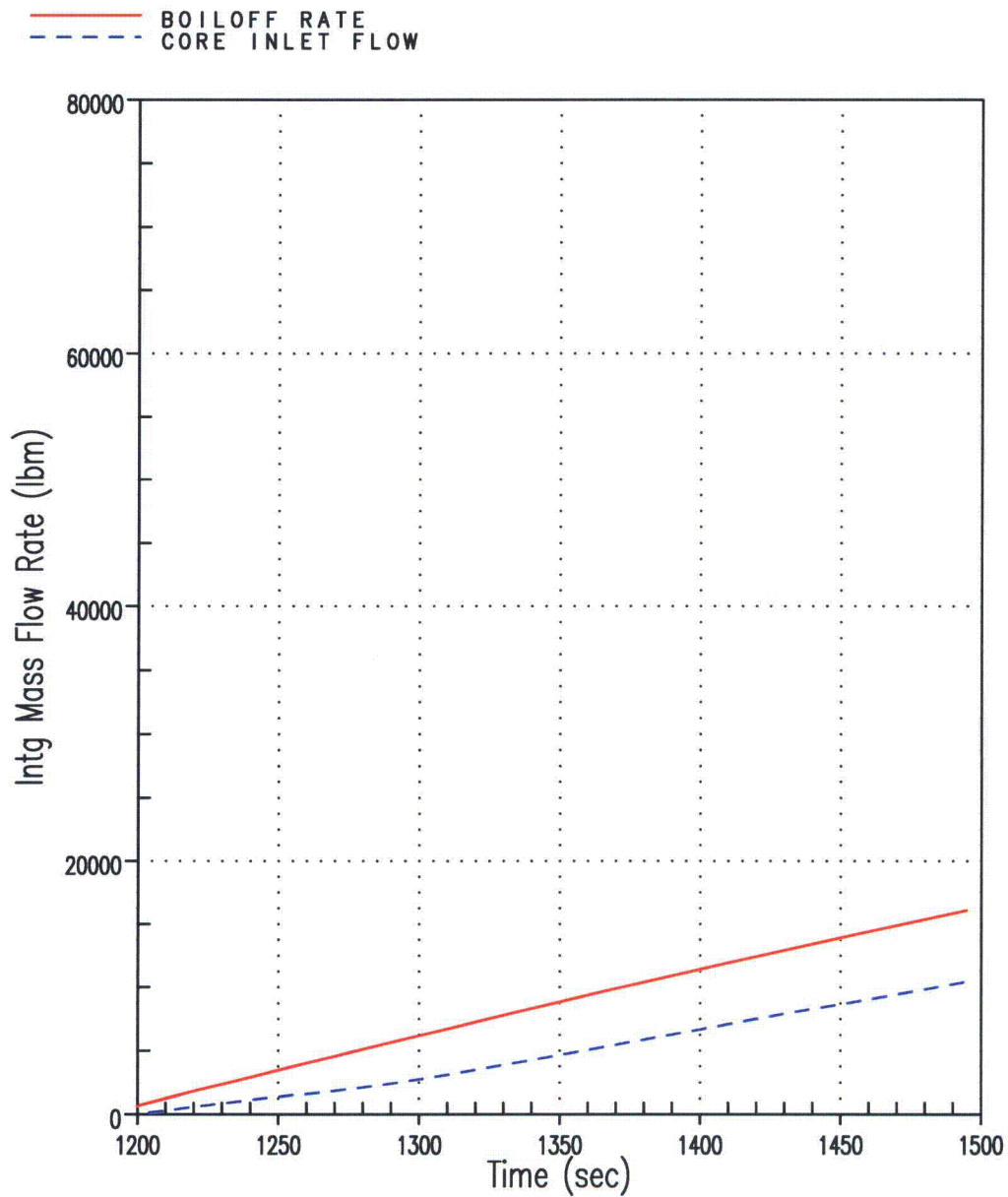
409461908

Figure 3-6 Integrated Core Flow vs. Core Boil-off for Channel 13 Flow Reduction 50% Case (Shifted Scale)



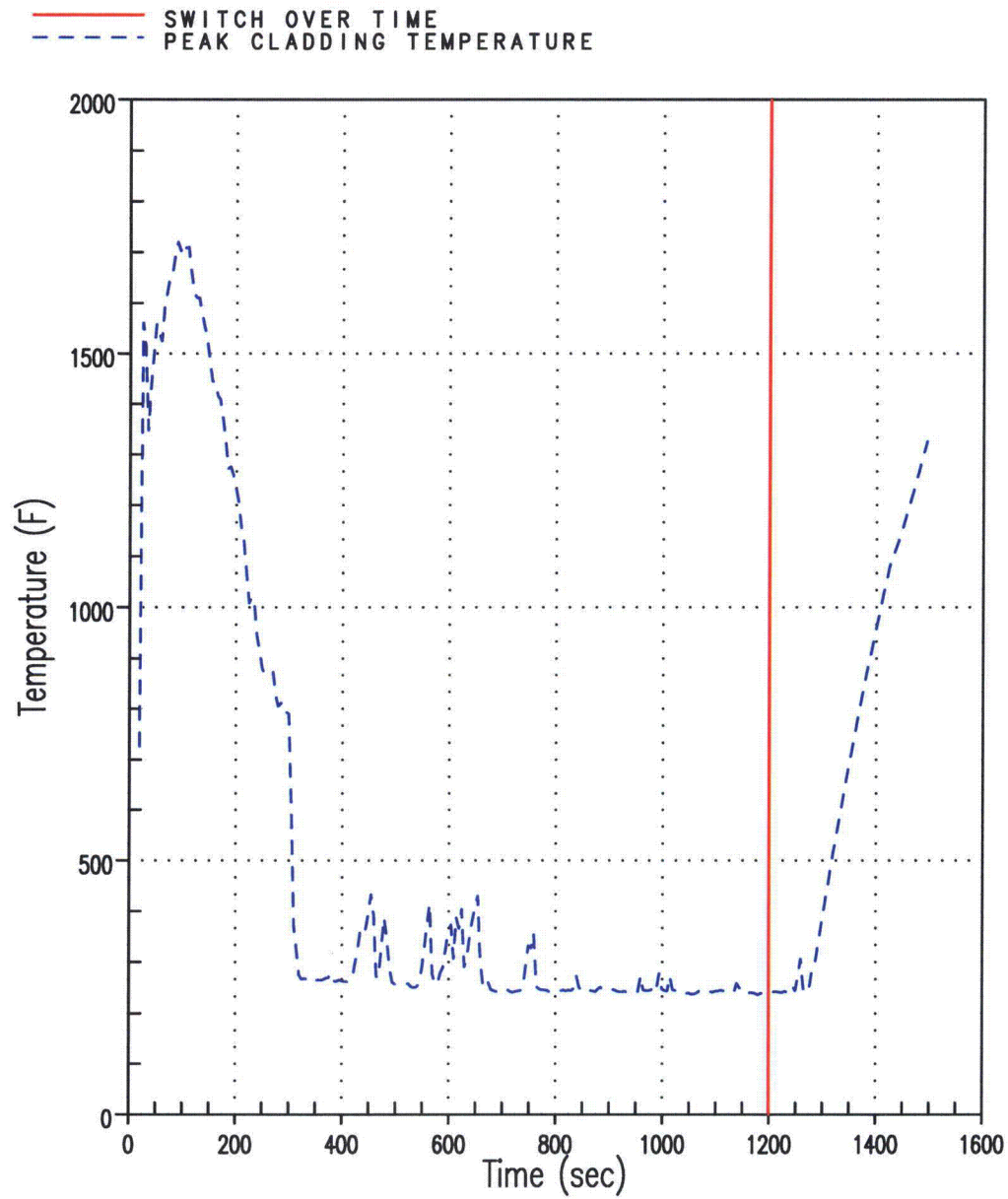
188413088

Figure 3-7 Hot Rod PCT for Channel 13 Flow Reduction 50% Case



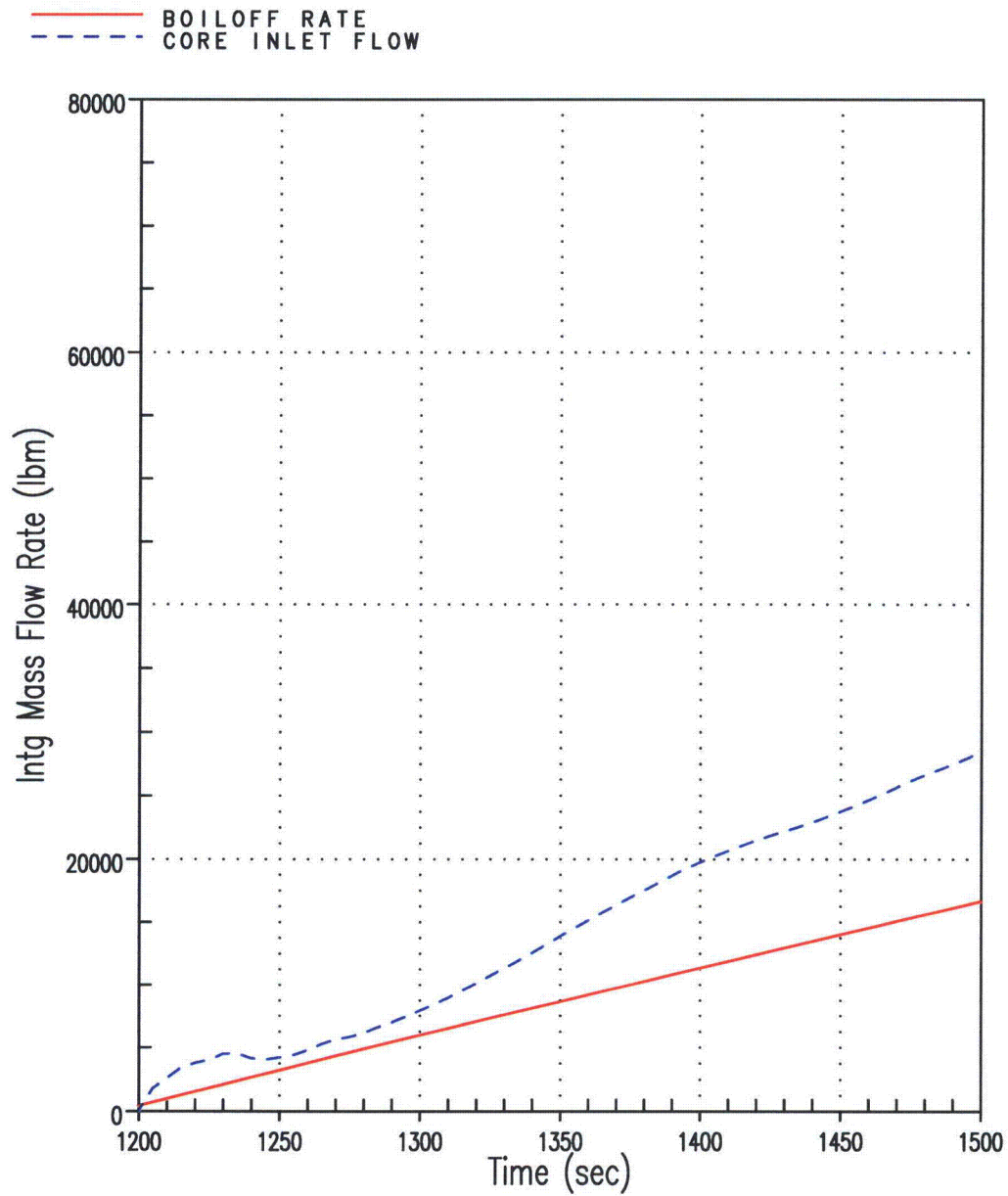
441943533

Figure 3-8 Integrated Core Flow vs. Core Boil-off for Channel 13 Flow Reduction 80% Case (Shifted Scale)



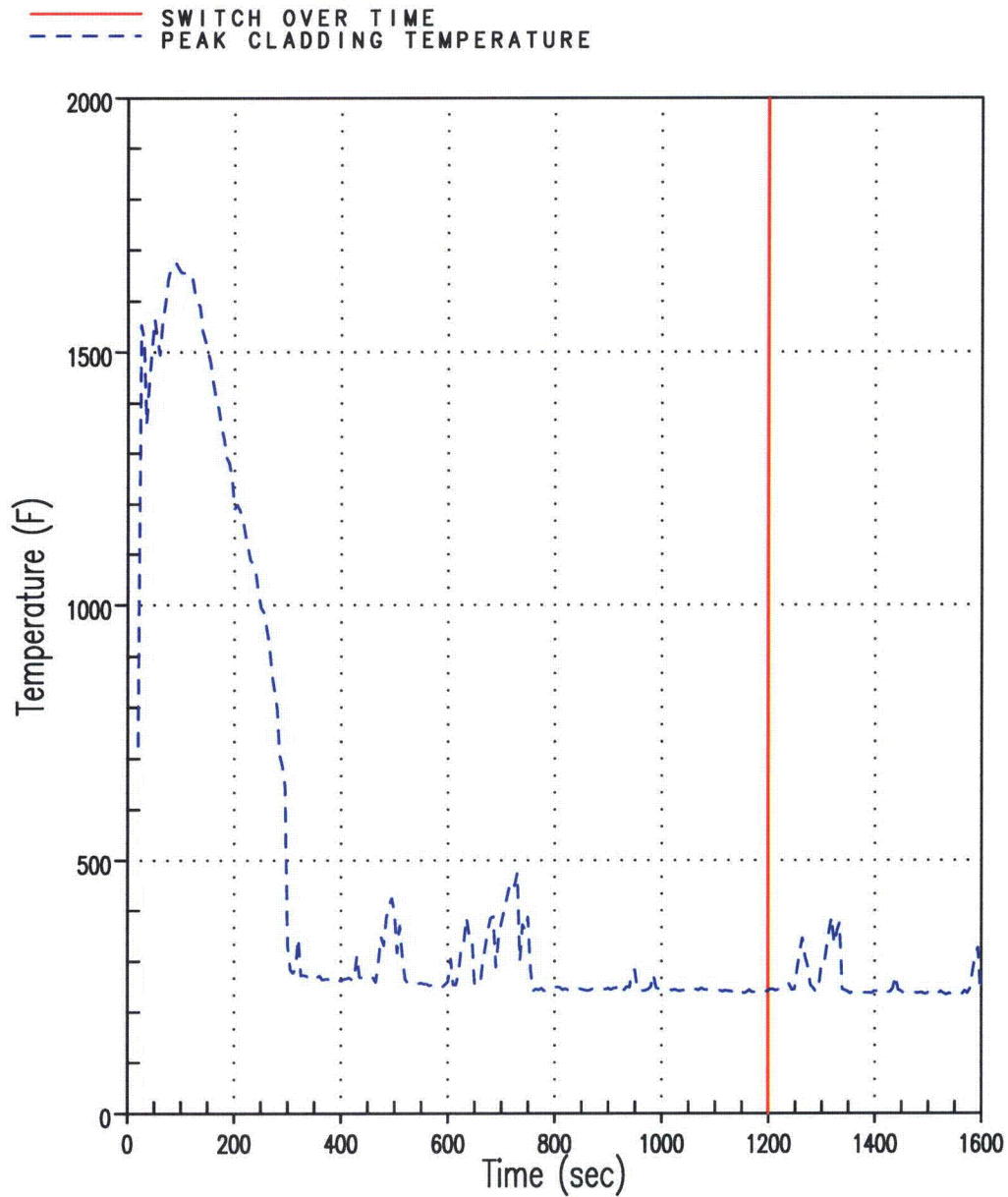
858292612

Figure 3-9 Hot Rod PCT for Channel 13 Flow Reduction 80% Case



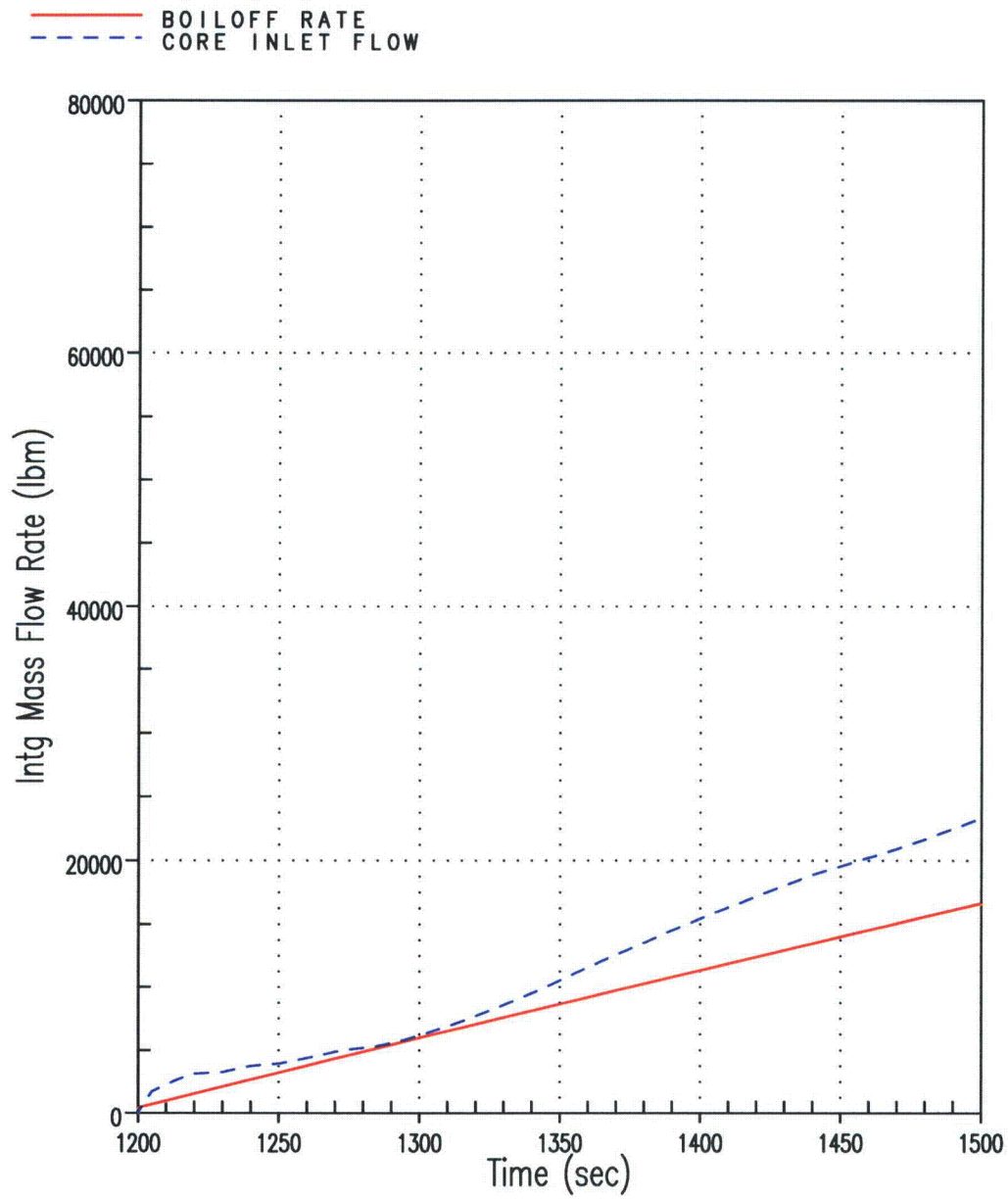
221025277

Figure 3-10 Integrated Core Flow versus Core Boil-off for Channel for Uniform $C_D = 50,000$ (Shifted Scale)



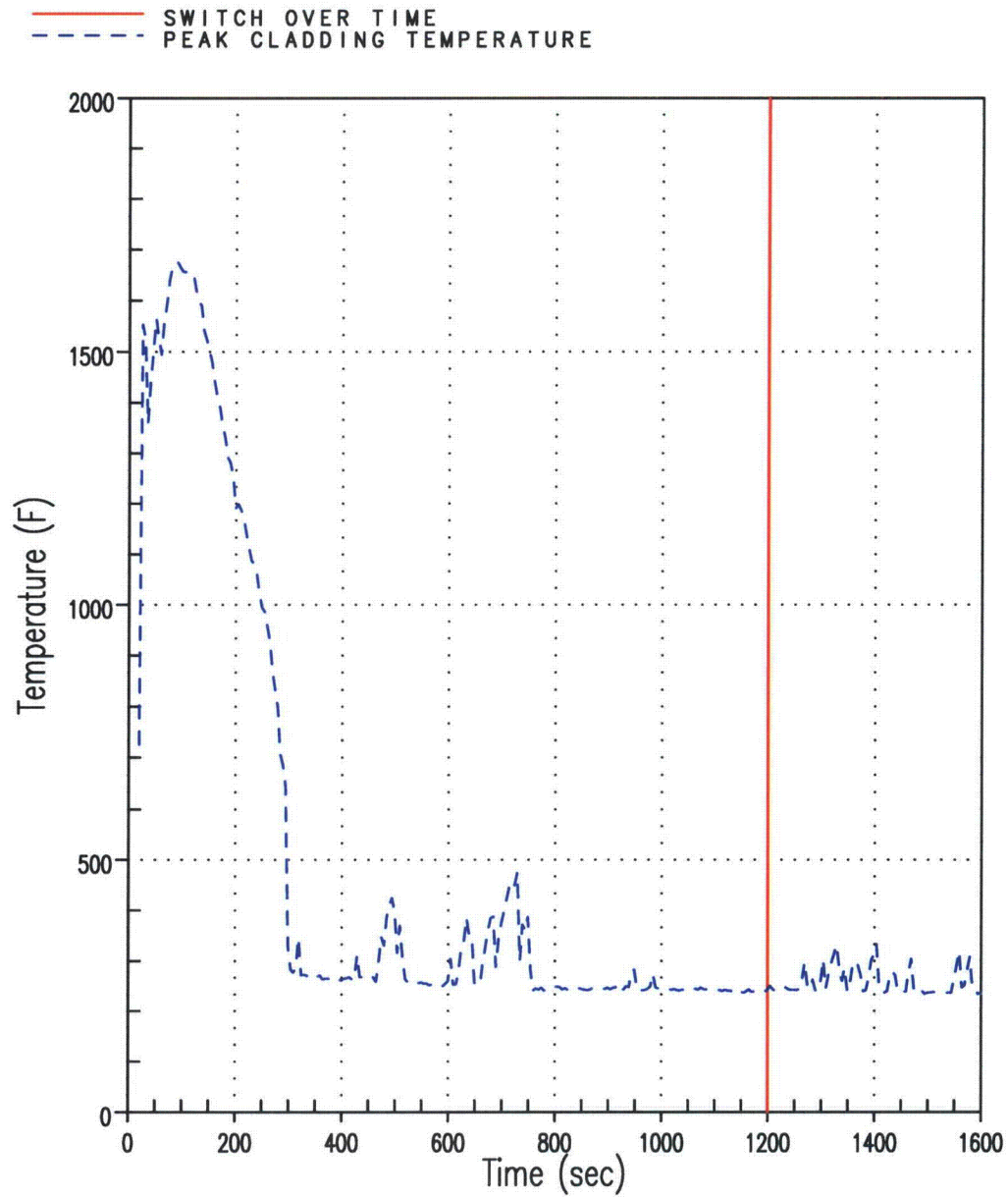
1912580083

Figure 3-11 Hot Rod PCT for Uniform $C_D = 50,000$



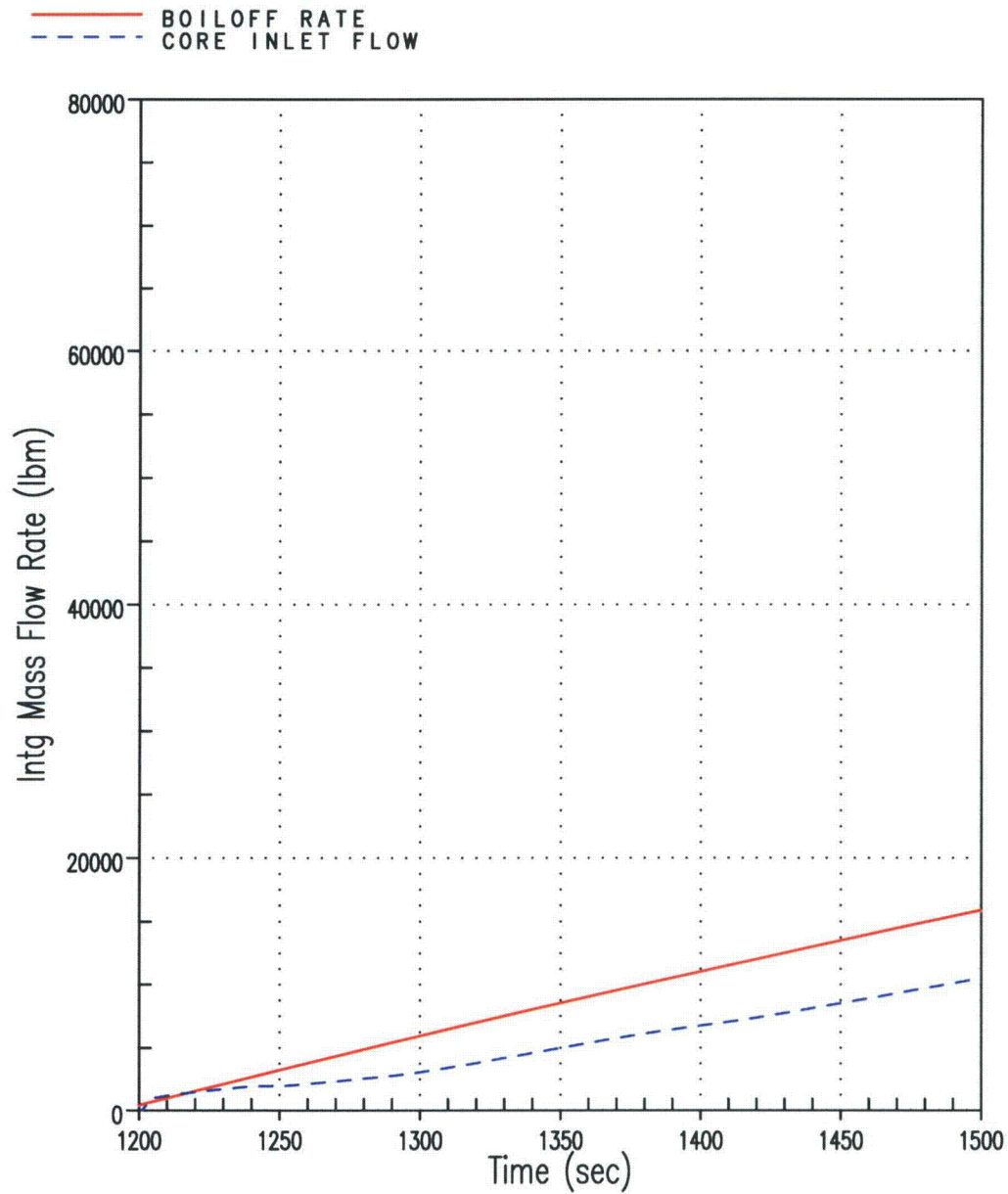
913425722

Figure 3-12 Integrated Core Flow vs. Boil-off for Uniform $C_D = 100,000$ Case (Shifted Scale)



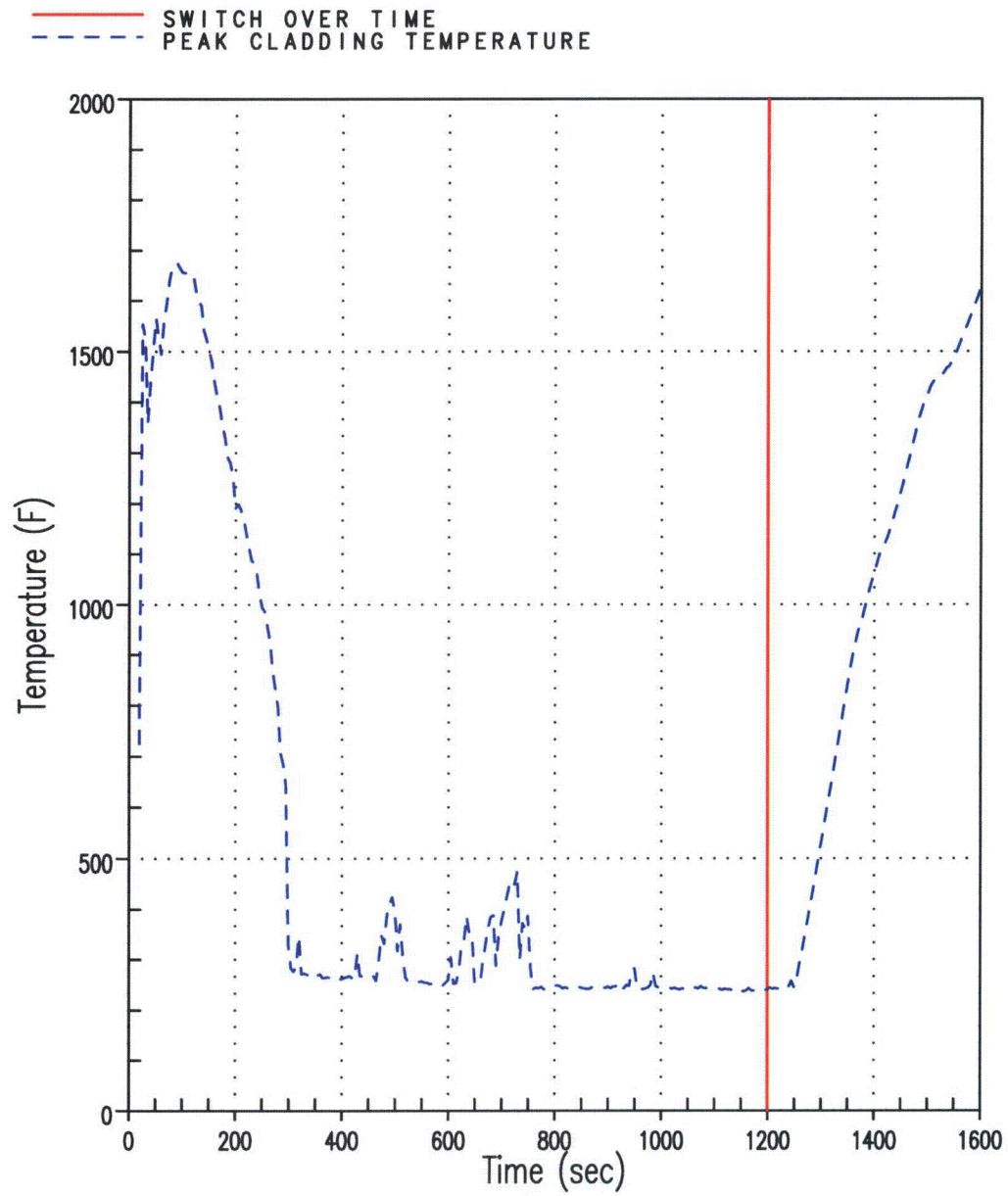
2013607248

Figure 3-13 Hot Rod PCT for Uniform $C_D = 100,000$ Case



1628827304

Figure 3-14 Integrated Core Flow vs. Boil-off for Uniform $C_D = 1,000,000$ Case (Shifted Scale)



566588943

Figure 3-15 Hot Rod PCT for Uniform $C_D = 1,000,000$ Case

3.4 SUMMARY

The FA testing program demonstrated that, at the debris load acceptance criteria, no potential blockage is expected that restricts flow into or through the core such that removal of decay heat and maintaining of decay heat is compromised. Therefore, plants that have bypass debris loadings that are within the limits of the debris masses tested are bounded by the test. The specific acceptance criteria are listed in Section 10.

In addition to the FA testing program, WC/T examined the cases of 82% and 99.4% blockage of the core inlet flow area. Additional sensitivity calculations performed with WC/T demonstrate there is margin in these two cases. While the blockage simulated by these calculations will not occur with the FA debris loadings used in the FA testing, these WC/T calculations provide additional assurance that LTCC will not be compromised. It was concluded that sufficient liquid can enter the core to remove core decay heat once the plant has switched to sump recirculation with up to 99.4 percent blockage at the core inlet.

4 COLLECTION OF DEBRIS ON FUEL GRIDS

Debris that does not collect at the core inlet will pass through the FA bottom nozzle and enter the core region. It is possible that this debris may lodge in some of the smaller clearances in the fuel grids. Three supporting analyses are presented in this section to demonstrate that blockage at spacer grids will not impede LTCC. First, a general discussion of debris build up is presented along with an evaluation of the effect on LTCC. Second, the FA test data is reviewed. Finally, ANSYS® and first principle calculations are presented to demonstrate that the fuel rod will continue to be cooled even for extreme cases with significant blockages around the fuel grids.

4.1 GENERAL DISCUSSION

Each FA has a number of spacer grids. These grids are designed to support the fuel rods. Following a LOCA, they provide the most likely location for debris accumulation within the core region. Spacer grid designs commonly used have hard and soft stops, which are small “springs” in the middle of the grids. These “springs” and the leading edge of the grids are the most likely locations for debris to build up, although flow diversion will limit the buildup at this location

The size of particulate debris that may pass through the replacement sump screens is dependent upon the hole size of the replacement sump screen. This dimension is 0.11 in. or less. The maximum debris size that may be passed by sump screens is of the magnitude of the maximum clearance between fuel rods and grid. Smaller particulate and fibrous debris of the order of 0.04 in. is smaller than the clearance about the “springs” and will readily pass through the grid structures.

The design of a fuel grid allows for cross flow through the grid between adjacent fuel rods. That is, the stops are punched out of the grid such that a flow path exists from one fuel rod to the next near the middle of the spacer grid. This will limit both the extent of the debris build up and its consequences. Should debris collect and form a resistance to the flow of coolant along the fuel rod, both coolant and debris carried by the coolant will be diverted to adjacent “cleaner” locations. A similar phenomenon will occur for fuel designs without hard or soft stops, albeit at the leading edge of the grid. As debris builds up at the leading edge, the flow will divert around it to open channels, limiting the debris build up.

Debris that does collect will have some packing factor that will allow “weeping” flow through debris buildup to cool the cladding. Complete compaction of the debris will not occur and the packing density of the debris is limited to less than unity or perfect compaction. From Reference 4-3, the packing will most likely be less than ~60 percent. Thus, any debris buildup will not become impenetrable. Boiling in the area of the blockage will occur with less than a 10 to 15°F increase in the clad temperature over the adjacent coolant temperature. Even a small amount of fluid flow through the debris bed will provide sufficient heat removal via convection to maintain the fuel rod a few degrees below the liquid saturation temperature.

This general discussion provides solid arguments for asserting that blockages at the spacer grids will not adversely affect LTCC. Additional arguments and analyses are further developed in the following sections.

4.2 PROTOTYPICAL FUEL ASSEMBLY TESTING

The PWROG sponsored a test program to justify acceptance criteria for the mass of debris that can be deposited at the core entrance and not impede LTCC flows to the core. By testing a prototypical FA with spacer grids, additional information was obtained regarding the buildup of debris at the spacer grids. A detailed discussion of the test can be found in Appendix G. The results from these FA tests are discussed in the proprietary test reports (References 4-1 and 4-2).

During the FA tests, debris was observed to accumulate at spacer grids. In some cases the accumulation seemed to be extensive. However, a review of the test data indicated that coolant continued to pass through the debris bed, verifying the “weeping” flow postulated in Section 4.1. Furthermore, the blockage at the spacer grids observed during the testing is conservative as discussed in the following sections.

4.2.1 Hot Leg Break Collection of Debris on Fuel Grids

During the FA tests, debris was observed to accumulate at spacer grids during tests performed at the HL break flow rates. While some buildup is expected, the observations from the tests represent an upper bound of the debris accumulation because of the following conservatisms in the testing process.

- Following a HL break, the ECCS volume must pass through the core to reach the break. Once the debris-laden fluid exits the break, it is returned to the sump where it can settle or at least be filtered again before it can return to the RCS. As the debris bed builds up on the sump strainer, less debris reaches the RCS. In the test loop, the debris-laden water was continuously circulated without filtration, allowing the debris multiple opportunities to be captured on the fuel filter or spacer grid.
- While the entire ECCS volume must pass through the core to reach the break, core boiling may not be suppressed following a HL break. This is more likely if one train of ECCS is lost to a failure. With boiling, additional turbulence is present in the core region, which will tend to remove debris from the spacer grids and confine blockages to isolated regions. Boiling was not simulated in the test loop.
- The FA tests were conducted with fewer spacer grids than would be present in an operating plant. The additional spacer grids provide more locations for debris to accumulate. The result is that the debris will be distributed among more spacer grids than in the FA tests.
- Following a LOCA, rod and assembly bow will occur as a result of the thermal transient on the fuel rods. As a consequence, flow channels between fuel assemblies will become larger in some locations and smaller in others. These channels will allow flow around blockages at spacer grids, should they form. Rod and assembly bowing were not modeled in the test loop.

Based on these conservatisms, it is reasonable to state that the debris buildup observed during the tests that simulated a HL break is not prototypical but represents an upper bound on the possible blockage. That is, the debris accumulation at any given spacer grid following a LOCA will be less than that witnessed in the PWROG FA tests.

4.2.2 Cold Leg Break Collection of Debris on Fuel Grids

During the FA tests, debris was observed to accumulate at spacer grids during tests performed at the CL break flow rates. While some buildup is expected, the observations from the tests represent an upper bound of the debris accumulation because of the following conservatisms in the testing process.

- The net ECCS flow into the core region is only the amount required to make up for core boiling. Excess ECCS flow runs back out the break and it carries debris because it is well mixed and distributed within the fluid. For B&W- and Westinghouse-designed plants, only 5 to 10 percent of the debris will reach the core. For CE-designed plants, less than 50 percent of the debris will reach the core. Consequently, less than half of the debris that reaches the RCS with the ECCS flow will reach the RV lower plenum or core region. The amount of debris simulated in the PWROG test program was larger than the amount of debris expected to reach the core.
- The FA tests were conducted with fewer spacer grids than would be present in an operating plant. In the plant, the core flow will be multidimensional. Boiling at high-power locations will push liquid and steam to the top of the core where the steam will escape. The liquid will flow down the lower power regions of the core. This results in a vigorously mixed boiling pot of liquid that will continuously move any debris that is not trapped. The additional spacer grids will provide additional locations for debris to accumulate. The result is that there will not be coplanar blockage of the core that could lead to unacceptable core cooling. There may be unique flow patterns related to potential local debris formation but core cooling is maintained. Any local blockages will not result in significant fuel pin heatup because they will be well dispersed in regions with limited size.
- Following a LOCA, rod and assembly bow will occur as a result of the thermal transient on the fuel rods. As a consequence, flow channels between FAs will become larger in some locations and smaller in others. These channels will allow flow around blockages at spacer grids, should they form. Rod and assembly bowing were not modeled in the test loop.

Based on these conservatisms, it is reasonable to state that the debris buildup seen at the top spacer grids during the tests is not prototypical for a CL break. Instead, the debris buildup at spacer grids will be considerably lower than the debris buildup at spacer grids seen in the test with a low likelihood of extensive blockages at any one spacer grid. While debris may accumulate at these locations, the blockage will be localized and not extend across the core. Therefore, the pressure drop at the intermediate spacer grids for a CL break will be much less than that observed in the tests.

4.2.3 Summary

For each test, debris was seen to accumulate at the spacer grids. While some buildup is expected, the observations from the tests represent an upper bound of the debris accumulation as discussed in the previous sections. Further, these buildups, as extensive as some of them were, did not form an impenetrable blockage to flow. Therefore, “weeping” flow was confirmed such that flow continued near the fuel rod such that decay heat could continue to be removed.

Additionally, the PWROG FA tests were performed to define the limits on the mass of debris that may bypass the sump screen and still provide for a sufficient flow pressure drop across the FA such that sufficient flow is provided to assure LTCC requirements are satisfied. Plants that have bypass debris loadings that are within the limits of the debris masses tested are able to meet the LTCC requirements. Further, the blockages that do occur can be treated as localized blockages

4.3 CLADDING HEATUP CALCULATIONS

4.3.1 Clad Heatup Underneath Fuel Grids

In an extreme case, it has been postulated that the volume between the fuel rod and spacer grid could completely fill with debris. An evaluation was performed to determine the cladding surface temperature of a fuel rod within a fuel grid when the rod is plated with debris in a post LOCA recirculation environment. A parametric study was performed to show the effects on the maximum temperature of the fuel rod underneath a grid strap caused by varying debris thickness and the thermal conductivity of the debris. The following sections summarize this analysis. Appendix C contains a detailed discussion of this calculation, including a discussion of assumptions and boundary conditions.

4.3.1.1 Method Discussion

An ANSYS® finite element model of a single fuel rod was created to predict fuel cladding heat up within a spacer grid. The model was cut down to a “1 quarter pie piece.” This allowed for the preservation of symmetry of the fuel rod.

To conservatively model convection from the fuel rod surface, the clad was divided into 20 zones. No convection was assumed to occur at the planes of symmetry. A mesh size of 0.05 in. was used for the model.

A constant heat flux was assigned to the entire inner surface of the cladding, and convection heat transfer, with a constant convection coefficient, assigned to the entire outer surface of the rod assembly. Four values were used to parametrically simulate the range of thermal conductivities for the postulated deposition on the fuel clad surface. The thermal conductivity values were 0.1, 0.3, 0.5, and

$0.9 \left(\frac{\text{BTU}}{\text{hr} \cdot \text{ft} \cdot ^\circ\text{F}} \right)$. These thermal conductivities were applied to a range of deposition thicknesses ranging from 5 mils to 50 mils.

4.3.1.2 Fuel Rod Model

The ANSYS model simulated a 12 ft., 0.36-in. diameter fuel rod. The cladding thickness was 0.0225 in. Spacer grids were modeled as 2.25 in. for the large grids, and 0.475 in. for the smaller grids. Table 4-1 lists the elevations of the fuel grids, relative to the bottom of the fuel.

Table 4-1 Grid Locations	
Grid Type	Elevation from Base (in)
Standard	24.57
Standard	45.07
Standard	65.67
Mixing Vane	76.77
Standard	86.17
Mixing Vane	97.37
Standard	106.77
Mixing Vane	117.87
Standard	127.27

The material thermal properties for the cladding material were also taken from the WC/T model described in Appendix B. Table C-5 of Appendix C contains the specific values used for this model.

4.3.1.3 Results

The calculated maximum clad temperatures are summarized in Table 4-2 and are shown graphically in Figure 4-1.

The calculated maximum clad temperatures calculated with this model all occur within the spacer grid. Assuming the minimum thermal conductivity of the debris collected in the grid and assuming a debris thickness of 50 mils, a maximum cladding temperature behind a grid of 474°F is calculated. This calculated temperature is well below the 800°F LTCC acceptance basis identified in Appendix A. Thus, the clad surface temperature acceptance basis of 800°F identified in Appendix A is satisfied.

The temperatures calculated with this model are conservatively high. The calculation assumed no flow through the debris in the grid. As observed in the PWROG testing, in the presence of debris, flow continued through the debris buildup. Thus, some coolant flow is expected to pass through the debris buildup within the spacer grid, cooling the clad surface. Not accounting for this flow through the debris, captured between the grid and the fuel rod, provides for a conservatively large cladding temperature.

Debris Thickness (mils)	Debris Thermal Conductivity $\left(\frac{BTU}{hr * ft * ^\circ F}\right)$			
	0.1	0.3	0.5	0.9
	T_{MAX}	T_{MAX}	T_{MAX}	T_{MAX}
0	260°F	260°F	260°F	260°F
5	—	269°F	266°F	264°F
10	305°F	277°F	271°F	266°F
15	—	284°F	275°F	269°F
20	—	291°F	280°F	271°F
25	—	297°F	284°F	274°F
30	386°F	303°F	288°F	276°F
35	—	310°F	291°F	278°F
40	—	316°F	295°F	281°F
45	—	322°F	299°F	283°F
50	474°F	327°F	302°F	285°F

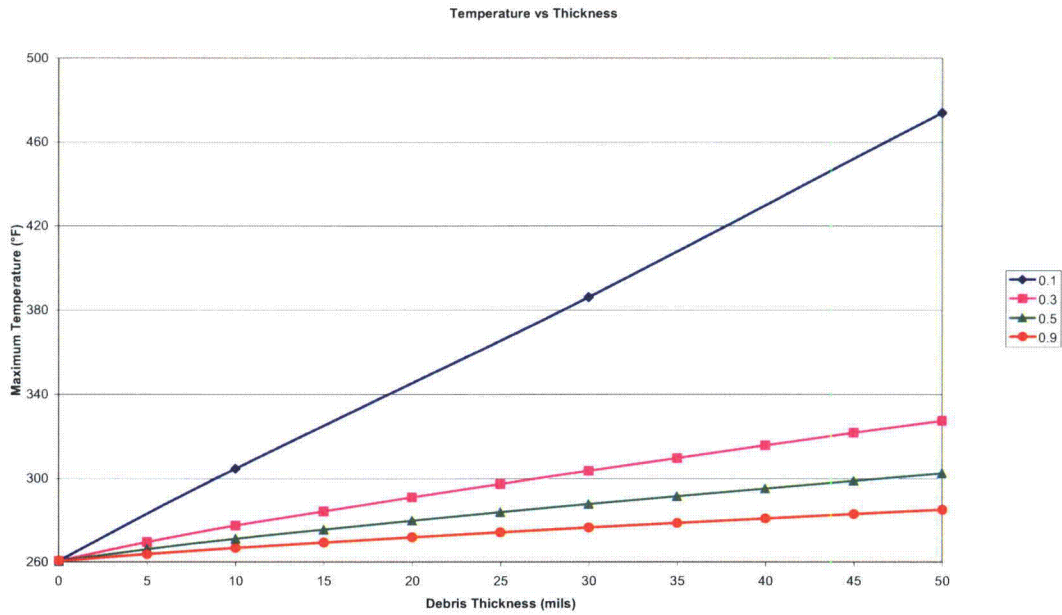


Figure 4-1 Temperature vs. Deposition Thickness and Thermal Conductivity

4.3.2 Cladding Heatup between Grids

The purpose of this analysis was to determine the cladding temperature of a fuel rod between spacer grids with debris deposited on the clad surface in a post-LOCA recirculation environment. While this section discusses blockages at spacer grids, this analysis provides additional information on core cooling when the debris accumulation is allowed to occur without the spacer grid impeding the buildup. A parametric study was performed to show the effects on the maximum temperature of the fuel rod due to deposited debris by varying debris thickness and thermal conductivity. The following sections summarize this analysis. A detailed discussion of the methodology can be found in Appendix D.

4.3.2.1 Methodology

This analysis considered the cladding as being surrounded by concentric layers of oxide, crud, and chemical precipitate, with no gaps between them. The source of heat was decay heat in a post-LOCA environment, and the section of rod analyzed was assumed to be fully exposed to a two-phase liquid/vapor environment in the core. This analysis used the generic resistance form of the heat transfer equation, for a radial coordinate system. A figure of the model is included in Figure 4-2.

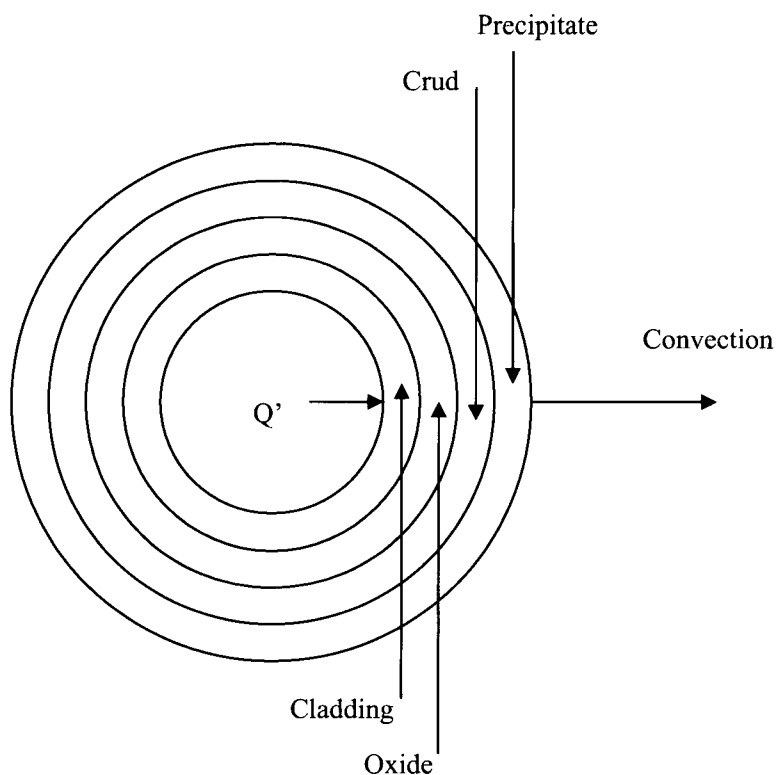


Figure 4-2 Heat Transfer Model (not to scale)

4.3.2.2 Results

Table 4-3 lists the clad/oxide interface temperatures for each of the analyzed cases.

In all cases, the maximum clad surface temperatures calculated between fuel grids under conservatively applied LTCC conditions were less than 560°F. Thus, the clad surface temperature acceptance basis of 800°F is satisfied for debris thickness of up to 50 mils.

Chemical Precipitate Thickness (mils)	$k_{\text{precipitate}}$ BTU/hr-ft-°F			
	0.1	0.3	0.5	0.9
0	273°F	273°F	273°F	273°F
10	336°F	293°F	285°F	279°F
20	396°F	313°F	296°F	286°F
30	453°F	331°F	308°F	291°F
40	508°F	350°F	318°F	297°F
50	560°F	367°F	328°F	302°F

Figure 4-3 plots the clad/oxide interface temperature as a function of chemical precipitate thickness for four values of precipitate thermal conductivity.

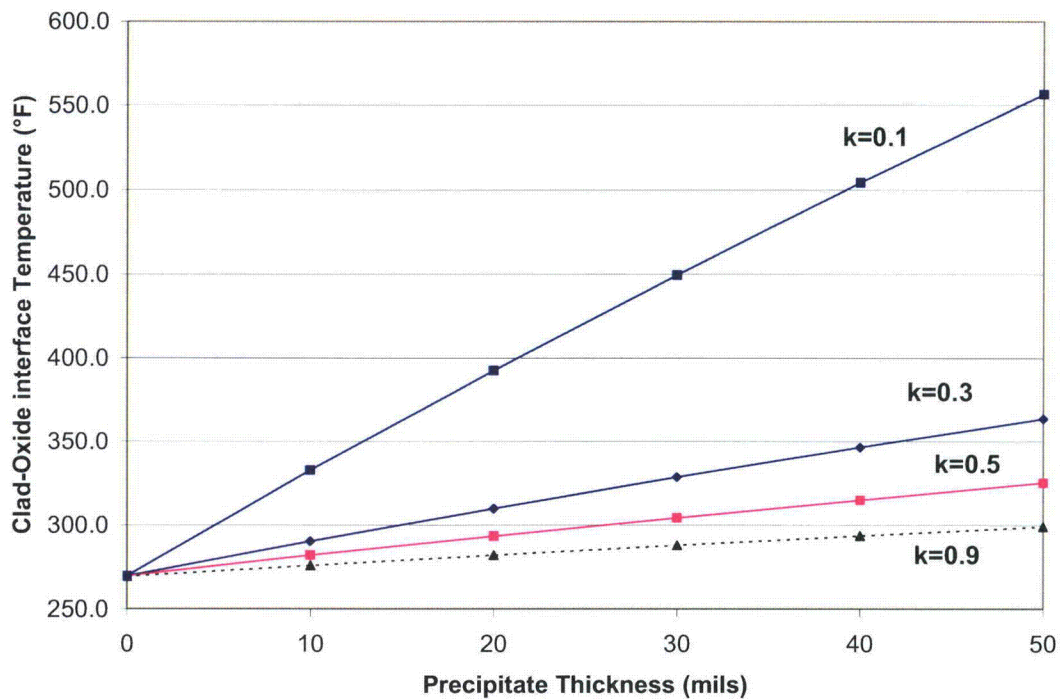


Figure 4-3 Clad-Oxide Interface Temperature vs. Chemical Precipitate Thickness

4.3.2.3 Sensitivity Calculations for Other PWR Fuel Designs

The fuel rod diameter used in the calculations 0.36 in. To demonstrate the applicability of these results to all PWR fuel designs, two sets of sensitivity calculations were performed using the following fuel rod specifications:

- 0.42 in. outer diameter (OD) fuel rod at 0.388 kW/ft power value
- 0.416 in. OD fuel rod at 0.383 kW/ft power value

These two cases, along with the calculations for the 0.360 in. fuel rod, are expected to bound all PWR fuel types.

Table 4-4 lists the clad/oxide interface temperatures for these two sensitivity calculations. The calculations used a bounding low value for thermal conductivity of precipitate.

Chemical Precipitate Thickness (mils)	$k_{\text{precipitate}} = 0.1 \text{ BTU/hr-ft-}^\circ\text{F}$	
	0.422" OD rod	0.416" OD rod
0	284°F	284°F
10	377°F	377°F
20	466°F	466°F
30	552°F	552°F
40	634°F	634°F
50	714°F	713°F

4.4 SUMMARY

Debris that does not collect at the core inlet will pass through the FA bottom nozzle and enter the core region. It is possible that this debris may lodge in some of the smaller clearances in the spacer grids. The debris buildup at these locations will not impede LTCC, because the extent of the buildup is limited by the spacer grid design and debris that does collect will have some packing factor that will allow "weeping" flow through the resulting debris bed.

While FA testing demonstrated that debris did collect at the spacer grids, these observations represent an upper bound of the debris accumulation because of conservatism in the testing process. Instead, the debris buildup at spacer grids in an operating plant will be considerably lower with a low likelihood of blockages at any singular spacer grid. The blockages that do occur can be treated as localized blockages. Further, a review of the test data indicated that coolant continued to pass through the debris bed, verifying the "weeping" flow asserted above.

For localized blockages, the maximum surface temperature calculated for cladding between two grids, using conservative boundary conditions representative of those during recirculation from the containment sump following a postulated LOCA is less than 800°F. For the 0.360 in. diameter fuel rod, the maximum temperature with 50 mils of precipitate on the clad OD is calculated to be less than 560°F. For the 0.416 in. or 0.422 in. rods, the maximum temperature with 50 mils of precipitate on the clad OD is calculated to be less than 715°F.

These temperatures are conservatively large, as they assume a decay heat level at the time of ECCS switchover to recirculation from the containment sump (20 minutes after initiation of the transient). At this time in the transient, there has been no time to build a layer of precipitate. Chemical products have had little time to form and the concentrations are therefore low, and coolant from the sump is just being introduced into the RV by the ECCS. As decay heat continues to decrease, the calculated clad surface temperatures for a specific thickness of precipitate would also decrease.

Therefore, plants that have bypass debris loadings that are within the limits of the debris masses tested will not impede LTCC by collecting on the fuel grids. The specific acceptance criteria are listed in Section 10.

5 COLLECTION OF FIBROUS MATERIAL ON FUEL CLADDING

It has been postulated that debris that reaches the core can adhere to the cladding surface. Adherence of fibrous debris is discussed here.

Testing was performed to assess the collection of fibrous debris on fuel cladding surfaces. The results are discussed and evaluated in NEA/CNSI/R (95)11 (Reference 5-1). The following observations were recorded:

1. From Section 5.4.2.1 of the report, there was little adherence noted of fibrous material to clad surfaces, and the material that did adhere was loose and easily removed. What was observed to adhere to clad surfaces was the binder used to make fiberglass. This binder, however, was observed to carry with it very limited fibrous debris. The report noted that much of the binder is quickly driven off of the fiberglass due to the heat associated with normal operating conditions. These observations were determined to be applicable to both NUKON and Knauf ET Panel.
2. Section 5.4.2.3 of the report provided observations regarding fibrous collection of fuel grids. It was noted that fibrous debris will collect on grids, but that a pure fibrous bed is porous and water will pass through a pure fiber bed.

These test results indicate that fibrous debris, should it enter the core region, will not tightly adhere to the surface of fuel cladding. Thus, fibrous debris will not form a "blanket" on clad surfaces to restrict heat transfer and cause an increase in clad temperature. Therefore, adherence of fibrous debris to the cladding is not plausible and will not adversely affect core cooling.

6 PROTECTIVE COATING DEBRIS DEPOSITED ON FUEL CLAD SURFACES

6.1 INTRODUCTION

A concern has been raised regarding the melting of material, particularly protective coatings (paint) that may have been either deposited directly on cladding surfaces, or collected within fuel grids or behind debris beds within the fuel grids. This section discusses both of these occurrences for protective coatings.

6.2 PROTECTIVE COATINGS BEHAVIOR

Protective coatings used inside a PWR containment building may generally be grouped into three categories:

1. Zinc-rich primers
2. Epoxies – either applied directly to the surface of a substrate or to a primer or surfacer that has already been applied to a substrate
3. Non-epoxies – typically applied to small equipment by original equipment manufacturers (OEM's)

The potential for each of these categories of coatings to challenge LTCC is evaluated.

Zinc-rich primers may release elemental zinc to the post-LOCA sump in a powder-like form. The PWROG chemical effects test program described in WCAP-16530-NP-A (Reference 6-1) has demonstrated that, in general, there is very little zinc reaction with the post-accident sump fluid chemistry. Therefore, zinc-rich primers are evaluated to have negligible affect on post-LOCA chemical precipitant production. If zinc powder were carried into the core and deposited directly onto fuel cladding surfaces or collected within fuel grids, the powder would behave materially and thermally as zinc. The thermal conductivity for zinc is relatively high (approximately 65 Btu/hr-ft-°F). Thus, zinc powder, if it were to be deposited directly onto fuel cladding surfaces or collected behind fuel grids, would not act to insulate the clad surface. Therefore, zinc from zinc-rich primers is not a concern for and does not present a challenge to LTCC.

The non-epoxy coatings are alkyds, urethanes, and acrylics. The amount of these coatings inside containment is generally limited to selected OEM-supplied equipment, such as electrical junction boxes, and represents a small amount of material of the order of a few thousand square feet or less. Thus, these coatings do not represent a significant debris load in the sump. Furthermore, these coatings are, as a class, chemically benign and do not react to the post-LOCA sump fluid. In the case of alkyds, the coating would break down into oligomeric carboxylate salts and glycol. The oligomeric carboxylate salts would tend to inhibit the formation of precipitates. However, since the amount of alkyds inside containments is small, and the salts are expected to be altered by radiolysis, no credit is taken for their presence inside containment. For these reasons, these non-epoxy coatings are evaluated to have a negligible effect on post-LOCA chemical precipitant production and therefore, are not a concern with respect to LTCC.

Most PWR containment buildings have a significant amount of epoxy coatings. Epoxy coatings will retain their structural integrity at temperatures up to about 350°F. When immersed in fluids at temperatures less than 350°F, epoxy coating debris is not sticky or tacky and has no propensity to adhere to the surface of fuel cladding. Therefore, these coatings will not, on their own, attach themselves to cladding.

Testing of epoxy coating systems in both acidic and basic solutions has demonstrated that epoxy coating systems are chemically inert and contribute only a small amount of leachate. From the response to RAI#2 of Section D to Reference 6-1, the total maximum contribution of leachates from epoxy coatings was conservatively estimated to result in a concentration in the recirculating coolant of less than 16 ppb (parts per billion) for a Westinghouse large four-loop PWR. This value was calculated using the conservative assumption that all leachable material from submerged coatings goes into solution. Considering the small amount of leachates released by epoxy coatings, even under the most conservative assumption that all leachates are released to the sump fluid inventory, epoxy coatings are evaluated to be chemically inert in the post-LOCA chemical environment and therefore have a negligible effect on post-LOCA precipitant production. Thus, epoxy coatings are evaluated to not present a concern with respect to LTCC.

To summarize, protective coatings are generally considered to have minimal impact on the post-LOCA chemistry of the containment sump due to either the small amount of material (non-epoxies) or the demonstrated chemical inertness of the coating itself (zinc-rich primers and epoxy coatings).

6.3 PREDICTED CLADDING TEMPERATURES AND TEMPERATURE-DRIVE DEBRIS CAPTURE

The WC/T calculations presented in Section 3 and Appendix B simulate the postulated LOCA transient starting with the initial blowdown and extending into the LTCC portion of the event where coolant is recirculated from the containment building sump. Two base case simulations are reported: a case with 82 percent of the core inlet blocked, and a second case with 99.4 percent of the core inlet blocked. In both cases, recirculation from the containment sump is initiated at 1200 seconds (20 minutes). The maximum cladding temperatures calculated for anywhere on the cladding are shown in Figure 3-5.

The temperature history plot of Figure 3-5 demonstrates several important behaviors associated with post-LOCA LTCC and the potential for collecting and melting coatings debris. The predicted clad surface temperature history is evaluated relative to a 350°F temperature value, which is the value at which epoxy coatings begin to lose their structural integrity and become pliable and possibly tacky.

1. Prior to 1200 seconds into the transient, coolant is drawn from the refueling water storage tank (RWST).
2. By 1200 seconds into the transient, the time that recirculation from the containment sump is initiated, the maximum cladding temperatures in the core are about 260°F.
3. After 1200 seconds into the transient, the maximum temperature of either the cladding directly exposed to the recirculating coolant, or the precipitate surface directly exposed to the recirculating coolant, is calculated to be less than 275°F. This temperature is well below the 350°F value at which epoxy coatings begin to be affected by temperature.

During the initial recovery period, and before beginning to recirculate coolant from the sump, all flow to the core originates from the accumulators, the RWST, or the borated water storage tank (BWST). Since there is no coatings debris in the RWST or BWST fluid inventory, no coatings debris is introduced to the fuel while coolant is provided by the accumulators or drawn from the RWST or BWST. By the time that the RWST or BWST inventory is depleted, the core is “recovered” with clad temperatures well below the 350°F temperature at which epoxy coatings are affected by temperature. Figure 3-5 demonstrates that, even with 99.4 percent of the fuel entrance blocked, sufficient water is provided to maintain cladding temperatures at about 250°F.

Additional WC/T sensitivity calculations, described in Section B.5 of Appendix B, were performed for the purpose of determining the amount of blockage necessary to reduce core flow below that necessary to match core boil-off. These calculations represent extreme conditions that are precluded by a plant maintaining the debris loading on the fuel within the limits identified in References 6-2 and 6-3. Therefore, the results of those WC/T sensitivity calculations described in Section B.5 do not apply to the discussion on coatings presented here.

Parametric cladding heat-up calculations described in Appendix D were performed for both a blocked grid and for a debris-covered fuel rod. These parametric calculations show that for a precipitate with a sufficiently small value for thermal conductivity and a sufficiently large value of deposited thickness, clad surface temperatures in excess of 350°F may be predicted. However, these same calculations also demonstrate that the temperature of the precipitate surface at the boundary of the coolant, where coatings debris might be expected to collect should they become sticky or tacky, is within about 15°F of the adjacent coolant temperature at the time of switchover. From the fuel rod heat-up calculations described in Appendix B, the surface temperature of the precipitate surface is calculated to be less than 270°F at the time of switchover. The results of these calculations are summarized in Table 6-1. Surface temperatures in the range of 270°F are sufficiently cool so that the material properties of the epoxy coatings will not be affected.

Coolant Temperature, T_{∞} (°F)	Precipitate Thickness (mils)	Maximum Precipitate OD Surface Temperature (°F)
250	0	268
250	10	267
250	20	266
250	30	266
250	40	265
250	50	264

Thus, due to the low surface temperatures of either the cladding material before precipitates might collect on the clad surface, or the surface of the precipitate deposited on fuel cladding, the potential for collection, retaining, and melting protective coatings on cladding surfaces or within fuel grids during the LTCC phase of a postulated LOCA is not considered credible.

6.4 SUMMARY

There are three general categories of protective coatings used inside a PWR containment building: zinc-rich primers, epoxy coatings, and non-epoxy coatings. These three categories of coatings have been evaluated to have negligible effect on the generation of precipitate.

1. The amount of non-epoxy coatings used inside a PWR containment building is small and therefore, has negligible contribution to post-LOCA PWR chemistry effects.
2. PWROG testing (Reference 6-1) has demonstrated that zinc contributes little to the generation of corrosion products post-LOCA and therefore, zinc-rich primers have negligible contribution to post-LOCA PWR chemistry effects.
3. Chemical resistance testing has demonstrated that epoxy coating systems are chemically inert and contribute only a small amount of leachate to the recirculating coolant and therefore, epoxy coatings are evaluated to have negligible contribution to post-LOCA PWR chemistry effects (response to RAI#2 in Section D of Reference 6-1).

Furthermore, conservative calculations of clad temperatures with deposited precipitate on the cladding surface demonstrate that, for the expected range of deposited precipitate, the precipitate surface temperatures are predicted to remain well below the value that would result in the melting of epoxy coatings debris that may be transported to the core region.

Therefore, protective coatings debris is evaluated to have a negligible effect on the post-LOCA chemistry of a PWR and on post-LOCA LTCC. Also, protective coatings debris has been evaluated to have negligible effect on post LOCA LTCC.

7 CHEMICAL PRECIPITATES AND DEBRIS DEPOSITED ON FUEL CLAD SURFACES

After a LOCA, the chemical makeup of the containment sump and core provides the potential for chemical interactions that may lead to precipitate formation and plate-out on the fuel rods. Consequently, core cooling may be compromised. A method to calculate the amount of these chemical products that might be generated was developed in WCAP-16530-NP-A (Reference 7-1). Additional work was performed by the PWROG to address excessive margins in the calculations through the use of plant-specific inputs to the calculations. These plant-specific inputs include, but are not limited to plant-specific initial pH values, plant-specific sump fluid temperature histories, and plant-specific alloys of reactant materials.

The chemical precipitates that may form may be transported to the core and influence the pressure drop of debris accumulation at the core inlet or spacer grids. This effect on LTCC is addressed in Section 3 and 4 and Appendix G.

Chemicals may also deposit on the hot fuel rods and possibly insulate them and inhibit decay heat removal. The method developed in WCAP-16530-NP-A (Reference 7-1) was extended to predict chemical deposition on fuel cladding due to the transport of debris and chemical products into the RCS and the core region by the coolant recirculated from the containment sump. The new method is called the LOCA deposition model (LOCADM).

7.1 DESCRIPTION OF LOCADM

LOCADM is a calculation tool that can be used to conservatively predict the build-up of chemical deposits on fuel cladding after a LOCA. The source of the chemical products is the interaction of the fluid inventory in the reactor containment building sump with debris and other materials exposed to and submerged in the sump fluid or containment spray fluid. LOCADM predicts both the deposit thickness and cladding surface temperature as a function of time at a number of core locations or "nodes." The deposit thickness and maximum surface temperature within the core are listed in the output for each time period so that the user can compare these values to the acceptance basis for long term cooling.

A complete description and qualification of LOCADM is presented in Appendix E. A summary is provided here.

The chemical inputs into LOCADM are the volumes of different debris sources such as fiberglass and calcium silicate (cal-sil) insulation. The surface areas of uncoated concrete, aluminum submerged in the sump, and aluminum exposed to spray are also required. The sump and spray pH are specified as a function of time, as are the inputs of sodium hydroxide, trisodium phosphate, sodium tetraborate, lithium hydroxide and boric acid as appropriate.

Chemical product transport into the core is assumed to occur by the following process:

1. Containment materials corrode or dissolve, forming solvated molecules and ions.

2. Some of the dissolved material precipitates, but the precipitates remain in solution as small particles that do not settle.
3. The dissolved material and suspended particles pass through the sump screen and into the core during recirculation. For the purpose of adding conservatism, it is assumed that none of the precipitates are retained by the sump screen or any other non-fuel surfaces.

Note that the transport of small fibers that do not dissolve but are small enough to be transported through the sump screen and into the core is not considered explicitly in LOCADM. The quantity of transported fines is expected to be small compared to both the total amount of debris and the amount of debris that dissolves or corrodes. Fiber can be accounted for in LOCADM in cases where it is significant by use of a “bump-up factor” applied to the initial debris inputs. The bump-up factor is set such that total mass of deposits on the core after 30 days is increased by the best estimate of the mass of the fiber that bypasses the sump screen.

Coolant flow rates into the reactor mixing volume as a function of time must be provided by the user and are obtained from a plant’s safety analysis for LTCC. The relative amounts of steam and liquid flow out of the reactor mixing volume are calculated by LOCADM. The core input is generalized. The coolant flow could be coming from the CL, the HL, or from upper plenum injection. Various operational modes are accounted for by varying the rate of flow into the mixing volume and the source of the flow (safety injection or recirculated coolant.) Values for generically applicable mixing volumes have been identified and will be provided to users. The temperature of the sump and reactor coolant as a function of time must also be entered by the user.

Within the mixing volume, the coolant is assumed to be perfectly mixed. Coolant chemical products entering the reactor are distributed evenly between all core nodes before deposition calculations are performed. The entire mixing volume is also assumed to be at the same temperature. Pressure is determined by the upper plenum pressure and the hydrostatic pressure at different elevations in the core. No attempt was made to model flow within the mixing volume and variations in that flow that might be caused by grids and flow obstructions. Since flow was not modeled, a heat transfer coefficient of $400 \text{ W/m}^2\text{-}^\circ\text{K}$ ($70 \text{ BTU/ft}^2 \text{ }^\circ\text{F}$) was assumed for transfer of heat between bulk coolant with the fuel channels and the surface of the deposits since this is a typical heat transfer coefficient for convective flow within natural circulation systems.

LOCADM deposits chemical products that are dissolved or suspended in solution throughout the core in proportion to the amount of boiling in each core node. It is assumed that deposition rate is equal to the steaming rate multiplied by the chemical product concentration at each node. If there is no boiling, the chemical products are distributed according to heat flux, at an empirically derived rate that is $1/80^{\text{th}}$ of the deposition that would have occurred if all of the heat had gone into the boiling process.

The deposition algorithm does not rely on solubility or any other chemical characteristics of the chemical products to determine the deposition rate. All chemical material that is transported to the fuel surface by boiling is assumed to deposit. LOCADM uses a default deposit thermal conductivity for the deposited material of $0.1 \text{ Btu/(hr-ft-}^\circ\text{F)}$, which is low enough to bound expected core deposits. Likewise, the default deposit density is low enough (e.g., 35 lbm Ca/ft^2) to bound expected deposits including those that incorporate absorbed boron or boron bonded to chemical product elements. Consistent with current

licensing basis calculations for PWRs that demonstrate that the boric acid concentration in the core is limited to values below the solubility limit, the LOCADM does not precipitate boric acid. The same is true for sodium phosphate, sodium borates, and sodium hydroxide, which are also highly soluble.

The core nodding within LOCADM can be adjusted by the user. Appendix E provides guidance to the LOCADM user for node selection for different types of cores.

LOCADM runs within Microsoft EXCEL® and should be easy to use for those familiar with EXCEL. The first sheet of the workbook instructs the user on how to enter the chemical and flow inputs into worksheets in tabular form. A macro written in Visual Basic for Applications is then run. The macro reads the input, looks for input errors, calculates core conditions in one second intervals, and then outputs the results within the same workbook.

7.2 USE OF LOCADM

Each plant must perform a LOCADM analysis in order to demonstrate the plant is operating within the acceptance criteria defined in Section 2. This section provides a brief overview of how to perform a LOCADM calculation. Appendix E and references 7-2, 7-3, 7-4 and 7-5 must be consulted for additional guidance.

7.2.1 Overview

7.2.1.1 Inputs

There are 5 input worksheets: 1) Time Input, 2) Materials Input, 3) Materials Conversion, 4) Core Data Input and 5) Switches.

Time Input

The Time Input worksheet contains inputs for time, pH, temperature, flows, pressure and the LOCA mode. Generally, higher pH and temperature values are conservative. Spray pH values should not be entered after the containment spray is terminated. The guidance in Reference 7-4 should be followed when addressing the flow data. The pressure column contains an equation to calculate the saturation pressure of the RV coolant temperature. Reference 7-4 also provides guidance for pressure inputs.

The LOCA mode is defined specifically for LOCADM and reflects the times at which changes take place in the ECCS operations. The modes are defined as follows:

- Mode 1: Blowdown/Refill phase (blowdown of water from RCS immediately after the LOCA and refill from accumulators and RWST).
- Mode 2: After reactor vessel refill but before recirculation begins.
- Mode 3: Recirculation from the sump (assumed water is injected into the CL.)
- Mode 4: HL injection (still recirculating water from the sump and injecting into HL.)

Materials Input

The Materials Input worksheet contains the masses of debris that would be present in the post-LOCA sump that could create deposits. These inputs are relatively straightforward but care must be taken to ensure the units are consistent. The other inputs in this worksheet are the initial sump liquid volume and the initial RV liquid mass.

The initial sump liquid volume must equal the volume of water present in the sump at the start of recirculation (after blowdown and refill have occurred) if the Pre-Filled Sump Option, described in Appendix E, is being used. If the Pre-Filled Sump Option is not being used, this value is zero. It is good practice to run two analyses, one with a minimum sump volume and the other with a maximum sump volume to ensure the most conservative volume is being used.

Refer to Reference 7-2 for the recommended initial RV liquid mass. These values are based upon plant design.

Materials Conversion

The Materials Conversion worksheet is used to convert the inputs from the Materials Input worksheet to masses in kilograms. Densities in this worksheet are typical but any density can be changed to reflect plant-specific conditions.

Core Data Input

The Core Data Input worksheet contains data about the reactor core. Values for the majority of the variables can be obtained from Appendix E and References 7-2, 7-3, 7-4, and 7-5. The plant fuel vendor must be consulted to assure appropriate inputs for the core peaking.

Switches

This worksheet can be used to impose certain additional criteria on the analysis. In most cases, the guidance is to retain the default inputs.

7.2.1.2 Outputs

The results of the LOCADM analysis are provided in three worksheets: 1) Out, 2) Releases by Material and 3) Scale Thickness. The Out worksheet contains the majority of the results of the LOCADM analysis. It is a good practice to make sure the final out mass is equal to the input mass plus the total mass of all materials released into the sump water (this mass is the sum of materials in the 'Releases by Material' worksheet). Care with units needs to be taken when performing this calculation.

The acceptance criteria results are found in the 'Maximum LOCA scale thickness' and 'Fuel Cladding Temp at Max Thickness' columns of the Out worksheet. Additional calculations are required in order to calculate the total deposition on the fuel rod:

- The total deposition is comprised of crud, oxide and the LOCA scale.

- Maximum LOCA Scale Thickness: The last value in the 'Maximum LOCA scale thickness' column.
- Crud Thickness: Assumed to be 140 microns.
- Oxide Thickness: Assumed to be 152 microns
- Add these three values (in microns) and convert to mils (25.4 microns per 1 mil).
- Compare this value to the acceptance criteria of 50 mils

7.2.1.3 Additional Steps

Aluminum Release Rate

In order to provide more appropriate levels of aluminum release for the LOCADM analysis in the initial days following a LOCA, licensees shall apply a factor of two to the aluminum release. The recommended procedure for modifying the aluminum release rate is described in Reference 7-5.

Bump-Up Factor

LOCADM does not contain an input for debris which bypasses the sump screen and is available for deposition in the core. Only material released from corrosion or dissolution processes is considered. However, some debris fines may bypass the sump screen and enter the core area where it could be deposited. A quantitative estimate of the effect of the fiber on deposit thickness and fuel temperature can be accounted for in LOCADM by use of a "bump-up factor" applied to the initial debris inputs. The bump-up factor is set such that total release of chemical products after 30 days is increased by the best estimate of the mass of the fiber that bypasses the sump screen. This allows the bypassed material to be deposited in the same manner as a chemical reaction product. The recommended procedure for including fiber bypass in the LOCADM deposition calculations is illustrated in Reference 7-4.

7.2.2 Summary

The methodology presented here is intended to provide a plant specific method to evaluate core deposition, which meets the NRC requirements for predicting post LOCA deposit formation on the core. The recommended modeling approach assumes that all material transported to the fuel surface by boiling will deposit. This conservative approach diminishes the importance of impurity chemical or radiochemical reactions since these reactions could not increase the amount of core deposition beyond what was already measured. Organic coating materials are not expected to experience radiation levels which would cause degradation and subsequent transfer onto heat transfer surfaces. Also, it is expected that most plants using this methodology will be able to demonstrate acceptable LTCC in the presence of core deposits.

8 BORIC ACID PRECIPITATION

All three US PWR designs (B&W, CE, or Westinghouse) use boron as a core reactivity control method and are subject to concerns regarding potential post LOCA boric acid precipitation in the core. All three plant designs have procedures that instruct the operators to realign the ECCS to prevent the core region boric acid concentration from reaching the precipitation point. The common approach for demonstrating adequate boric acid dilution in a post LOCA scenario includes the use of simplified methods with conservative boundary conditions and assumptions. These simplified methods are used with limiting scenarios in calculations to show that boric acid precipitation will not occur or to determine the time at which appropriate operator action must be taken to initiate an active boric acid dilution flow path. In light of NRC staff and ACRS challenges to the simplified methods commonly used, it has recently become clear that additional insights and new methodologies are needed to answer fundamental questions about boric acid mixing and transport in the RCS and potential precipitation mechanisms that may occur both during the ECCS injection phase and the sump recirculation phase after a LOCA. In response to this need, the PWROG is currently funding a program to define, develop and obtain NRC approval of post LOCA-boric acid precipitation analysis scenarios, assumptions and acceptance criteria and resultant methodologies that demonstrate that adequate post-LOCA LTCC.

9 COOLANT DELIVERED TO THE TOP OF THE CORE

There are two scenarios by which coolant can be delivered to the top of the core.

1. For a break in the CL piping, plants may introduce recirculating coolant into HLs to act as flushing flows to mitigate the potential for boric acid precipitation.
2. The ECCS for Westinghouse two-loop PWRs provide for the delivery of coolant directly to the upper plenum through injection nozzles in the RV upper plenum (Upper Plenum Injection or UPI). This flow path is established at the initiation of the ECCS actuation and is maintained throughout plant recovery.

When the ECCS is recirculating coolant from the containment sump, debris in the recirculating coolant can flow into the core.

9.1 HOT LEG RECIRCULATION

HL recirculation is typically initiated several hours after the postulated large LOCA. At this time, the containment sump inventory typically has been recirculated through the ECCS and RCS several times. This provides for particulate and fibrous debris generated by the initial break and carried in the recirculating coolant to be depleted either by capture on the sump screen, or by settle-out in the containment sump or in low-flow locations of the ECCS RV flow path such as the RV lower plenum. Thus, the amount of particulates and fibrous debris in the recirculating flow at the time of initiation of HL recirculation is small. Examples of debris depletion are given in WCAP-16406-P-A (Reference 9-3).

9.2 UPPER PLENUM INJECTION PLANTS

The ECCS for Westinghouse two-loop PWRs provide for the delivery of coolant directly to the upper plenum through injection nozzles in the RV UPI. This flow path is established at the initiation of the ECCS actuation and is maintained throughout plant recovery. This flow path may provide for the delivery of debris in the recirculating coolant from the initiation of recirculation from the containment sump.

The sump screen will limit both the size and the amount of the particulate and fibrous debris to the reactor.

1. For a HL break, upon switchover from injection from the RWST, coolant flow to the core is through the UPI ports with all CL flow initially secured. The amount of debris that reaches the core depends on the flow patterns in the upper plenum and is discussed in detail in Section 9.3.
2. For a CL break, the debris introduced by the UPI flow to the RV will flow into the core.

9.3 UPPER PLENUM DEBRIS TRANSPORT FOR HOT-LEG BREAK SCENARIO

ECCS that enters the upper plenum following a HL break for UPI plants can either enter the core or exit the break. There is some flow to the core to make up for steam produced by the decay heat removal process. However, the majority of the flow will exit the break. This assertion is supported by the following discussion.

The UPI nozzle for a Westinghouse 2-loop PWR has an inside diameter of about 4 inches. These nozzles are located approximately 180° opposite of each other. Assuming a minimum total UPI flow of 1200 gpm and an equal flow distribution between the two UPI nozzles, the flow rate through each nozzle is 600 gpm or approximately 1.34 ft³/sec. Thus, the minimum velocity of the UPI flow through each UPI nozzle is calculated to be approximately 15.3 ft/sec. At these jet velocities, the upper plenum coolant inventory is not stagnant. Rather, the UPI jet flow, in conjunction with impingement of the jets on upper internals structures, generates turbulent mixing of the UPI flow with the coolant inventory in the upper plenum.

The volume between the top of the active fuel and the bottom of the HL for a Westinghouse two-loop PWR is about 190 ft³. For a UPI flow of 1200 gpm, the equivalent volumetric flow is about 2.68 ft³/sec. Neglecting any water level above the bottom of the HL, which would be small for a double-ended guillotine HL break, and assuming a constant volume of water in the upper plenum, approximately 71 seconds are required to “turn over” the entire fluid inventory of the upper plenum. This quick turn-over time further supports that the upper plenum is well mixed by the UPI flow.

The turbulent mixing of the upper portion of the core will result in a situation where debris that enters the upper plenum with the coolant will either be kept in suspension and expelled through the HL piping, or will be deposited over a broad area of the core.

9.4 COLLECTION OF DEBRIS ON FUEL

Considering the above, the debris that may be captured on fuel features such as mixing vanes, fuel grids and on debris capturing features at the bottom of the fuel is limited. The collection of debris by these features will also occur over time; that is, the formation of a debris bed will take time to develop. As noted in Section 4.1, the debris that is collected will have some packing factor that will allow “weeping” flow through particulate debris buildup and into the core. That is, complete compaction of the debris will not occur and the packing density of the debris is limited to less than unity or perfect compaction. Again, from Reference 9-1, the packing will most likely be less than ~60 percent. This will allow for coolant to pass through a debris bed that might form.

The 60% packing factor can be conservatively thought of as a 60% blockage of the core. This would present a bounding or maximum resistance to flow through the debris bed. The \overline{WC}/T evaluations described in Section 3.2 demonstrate that adequate flow is maintained with a deterministically assigned blockage of 82% to provide for LTCC. Thus, conservatively taking the 60% packing factor to be representative of a 60% blockage, adequate LTCC will be provided for.

Westinghouse 2-loop plants with UPI do not maintain flow into CLs once the switchover of the ECCS from injecting from the RWST to recirculating coolant from the reactor containment building sump is accomplished; the recirculating flow is ducted to the RV through the UPI penetrations in the reactor upper

plenum. For CL breaks, coolant is introduced into the RV from the UPI nozzles and flows down through the core and out the break. If blockage due to the accumulation of debris were to occur, it would occur at the top of the fuel. As was the case with bottom-up flooding of the core, and as demonstrated in the data presented in Section 3.1, a complete blockage is not expected of plants that are within the debris load acceptance criteria. This was demonstrated by testing as described in Section 9.5.

As described in Section 9.3, the turbulent mixing of the upper portion of the core will cause the debris that enters the upper plenum with the coolant to either be kept in suspension and expelled through the HL piping (for a HL break scenario), or will be deposited over a broad area of the core. Should the fiber collect preferentially at grid locations, the analysis performed in Appendix D of this report applies to UPI plants and this analysis demonstrates that adequate cooling in such locations will be maintained. The testing described in Section 9.5 demonstrates sufficient flow will be maintained with debris in the fluid delivered to a FA that LTCC is not challenged. Thus, in case of either a HL or a CL break, the formation of a debris bed on the bottom of the fuel is not considered credible.

If the coolant flow is sufficiently restricted through a debris bed that clad temperatures increase to about 15°F to 20°F above the coolant temperature, the coolant would begin to boil. The steam formed would be about 40 to 50 times the volume of the water, and would cause the debris bed to be displaced, allowing for coolant to flow to and cool the cladding surface. This process would provide for cooling of the clad.

The conservative clad heat-up calculations documented in Appendix D demonstrate that acceptably low clad temperatures are calculated with as much as 50 mils of solid precipitate applied to the outside surface of a fuel rod. These calculations provide further assurance that, with weeping flow through a debris bed collected on fuel elements, LTCC for UPI plants will be maintained.

The evaluation of effect of chemicals dissolved in the UPI flow for a HL break are performed on a plant-specific basis using the LOCADM calculation tool described in Section 7 and Appendix E. To account for deposition on fuel cladding in the core, a bump-up factor is used in the LOCADM calculation to deposit fiber material according to the core boiling and heat flux distribution.

9.5 TEST FOR UPI-DESIGNED PLANT

The purpose of the UPI test was to perform testing to justify the applicability of the debris load acceptance criteria defined by HL break conditions to UPI-designed plants. To simulate the limiting break, the UPI CL break (analogous to the previously discussed HL break) was tested. This test was conducted with the maximum debris loads that were tested in the Westinghouse HL test. The pressure drop was well below what is required to maintain core flow for UPI plants. Therefore, the test results demonstrated that sufficient flow will reach the core to remove core decay heat and the acceptance criteria developed at HL conditions is bounding and applicable to UPI plants. Appendix G and Reference 9-2 contain additional information about the UPI test and the applicability of the debris acceptance criteria to UPI plants.

10 SUMMARY

10.1 DISCUSSION

PWR containment buildings are designed to facilitate core cooling during a postulated LOCA event. In some LOCA scenarios, the cooling process requires water discharged from the break, ECCS, and CSS to be collected in a sump for recirculation by these systems. The discharged coolant water in the sump will contain chemical impurities and debris as the result of interaction with containment materials.

There has been concern that following a LOCA, the chemical precipitate, fibrous and particulate debris within the sump could collect on the sump screen and block the flow of cooling water into the core. There is also concern about the effects of the debris that passes through the sump screen. This debris could be ingested into the ECCS and flow into the RCS.

The PWROG sponsored a program to analyze the effects of debris and precipitates on core cooling for PWRs when the ECCS is realigned to recirculate coolant from the containment sump. The intent was to demonstrate adequate heat-removal capability for all plant scenarios. Additionally, the PWROG initiated prototypical FA testing to establish limits on the debris mass (particulate, fibrous, and chemical) that could bypass the reactor containment building sump screen. These debris limits will not cause unacceptable head loss that would impede core inlet flow and challenge LTCC. These limits will be referred to as the debris load acceptance criteria and are intended to demonstrate that adequate flow for long-term decay heat removal exists at these levels.

This evaluation considered the design of the PWR, the design of the open-lattice fuel, the design and tested performance of replacement containment sump screens, the tested performance of materials inside containment, and the tested performance of fuel assemblies in the presence of debris. Specific areas addressed in this evaluation included:

- Blockage at the core inlet,
- Collection of debris on fuel grids,
- Collection of fibrous material on fuel cladding,
- Protective coating debris deposited on fuel clad surfaces,
- Production and deposition of chemical precipitants,
- Boric acid precipitation, and
- Coolant delivered from the top of the core.

The following acceptance criteria were selected for the evaluation of the topical areas identified above:

1. The maximum clad temperature shall not exceed 800°F.
2. The thickness of the cladding oxide and the fuel deposits should not exceed an average of 0.050 inches in any fuel region.

These acceptance bases were applied after the initial quench of the core and are consistent with the LTCC requirements stated in 10 CFR 50.46 (b)(4) and 10 CFR 50.46 (b)(5). They do not represent, nor are they intended to be, new or additional LTCC requirements. These acceptance bases provide for demonstrating that local temperatures in the core are stable or continuously decreasing and that debris entrained in the cooling water supply will not affect decay heat removal.

The evaluations performed for the areas identified above provide reasonable assurance of LTCC for all plants. Specifically,

- Adequate flow to remove decay heat will continue to reach the core even with debris from the sump reaching the RCS and core. Plants that operate at the debris loads identified in Tables 10-1 (and 10-2, if applicable), can state that debris that bypasses the screen will not build an impenetrable blockage at the core inlet. While any debris that collects at the core inlet will provide some resistance to flow, in the extreme case that a large blockage does occur, numerical analyses have demonstrated that core decay heat removal will continue. The details supporting this evaluation are provided in Section 3.
- Decay heat will continue to be removed even with debris collection at the FA spacer grids. Plants that operate at the debris loads identified in Tables 10-1 (and 10-2, if applicable), can state that debris that bypasses the screen will not build an impenetrable blockage at the fuel spacer grids. In the extreme case that a large blockage does occur, numerical and first principle analyses have demonstrated that core decay heat removal will continue. The details supporting this evaluation are provided in Section 4.
- Fibrous debris, should it enter the core region, will not tightly adhere to the surface of fuel cladding. Thus, fibrous debris will not form a “blanket” on clad surfaces to restrict heat transfer and cause an increase in clad temperature. Therefore, adherence of fibrous debris to the cladding is not plausible and will not adversely affect core cooling. The details supporting this evaluation are provided in Section 5.
- Protective coating debris, should it enter the core region, will not restrict heat transfer and cause an increase in clad temperature. Therefore, adherence of protective coating debris to the cladding is not plausible and will not adversely affect core cooling. The details supporting this evaluation are provided in Section 6.
- The chemical effects method developed in WCAP-16530-NP-A was extended to develop a method to predict chemical deposition of fuel cladding. The calculational tool, LOCADM, will be used by each utility to perform a plant-specific evaluation. It is expected that each plant will be able to use this tool to show that decay heat would be removed and acceptable fuel clad temperatures would be maintained. The details for using LOCADM are provided in Section 7 and Appendix E.
- The commonly used approach for demonstrating adequate boric acid dilution in a post-LOCA scenario includes the use of simplified methods with conservative boundary conditions and assumptions. In light of NRC staff and ACRS challenges to the simplified methods commonly used, it has recently become clear that additional insights and new methodologies are needed to answer fundamental questions about boric acid mixing and transport in the RCS and potential precipitation mechanisms that may occur both during the ECCS injection phase and the sump recirculation phase after a LOCA. This will be addressed in a separate PWROG program. This program is discussed in Section 8.
- The PWROG FA test results demonstrated that sufficient flow will reach the core to remove core decay heat. UPI plants that operate at the debris loads identified in Tables 10-1, can state that

debris that bypasses the screen will not build an impenetrable blockage within the core region. The details supporting this evaluation are provided in Section 9.

Debris Type	Debris Load per Fuel Assembly ^(Note 1)
Fiber	< 0.33 lb
Particulate	< 29 lb
Chemical	< 13 lb
Calcium silicate	< 6 lb
Microporous Insulation	< 3.2 lb

Note 1: These are generic acceptance criteria. Please refer to the fuel vendor proprietary test reports for vendor-specific data.

For fuel designs that incorporate the AREVA TRAPPER fine mesh debris filter, the following debris limits apply:

Debris Type	Debris Load per Fuel Assembly
Fiber	< 0.24 lb
Particulate	< 29 lb
Chemical	< 13 lb
Calcium silicate	< 6 lb
Microporous Insulation	< 1.2 lb

10.2 GUIDANCE TO LICENSEES CONCERNING EVALUATION OF DEBRIS

Actions are required of utilities to prove acceptable LTCC with debris and chemical products in the recirculating fluid. Plants will have to perform plant-specific LOCADM evaluations and prove the plant conditions are bounded by the debris load acceptance criteria. These actions along with reference to this report provide the basis for demonstrating that LTCC will not be compromised following a LOCA as a consequence of debris ingestion to the RCS and core.

10.2.1 LOCADM

Plants will have to perform a LOCADM evaluation (Section 7 and Appendix E) based on plant-specific debris inputs and prove they are within the acceptance criteria.

10.2.2 Debris Acceptance Criteria

Debris loads used in the FA test program were based on sump screen bypass information provided by licensees. The FA testing was reported in proprietary submittals that support this document. The results from these FA tests are discussed in the proprietary test reports (References 10-1 and 10-2).

As part of the effort to invoke this WCAP in the plant licensing basis, each plant will compare their plant-specific debris load against the FA debris masses tested. Plants that have bypass debris loadings that are within the limits of the debris masses tested are bounded by the test. Plants will also have to demonstrate that the available driving head (for both hot and cold leg breaks) is equal to or greater than the limits adhered to in this test program.

Several courses of action have been identified for plants whose debris loads are outside of the limits tested. These actions include, but not limited to, reduction of problematic debris sources by removing or restraining the affected debris source, plant-specific FA testing, or engineering evaluations. Engineering evaluations could be applicable to plants that have one debris source that is slightly higher than the acceptance criteria but all other debris sources are significantly lower than the recommended limits. These evaluations can also be used for plants that have different fuel filters, greater driving head, among other variables.

11 REFERENCES

Section 1

- 1-1 Generic Safety Issue 191 (GSI-191), "Assessment of Debris Accumulation on Pressurized Water Reactor (PWR) Sump Performance."
- 1-2 WCAP-16406-P-A, Revision 1, "Evaluation of Downstream Sump Debris Effects in Support of GSI-191," March 2008.
- 1-3 NEI 04-07, Volume 1, Revision 0, "Pressurized Water Reactor Sump Performance Evaluation Methodology," December 2004.
- 1-4 NEI 04-07, Volume 2, Revision 0, "Pressurized Water Reactor Sump Performance Evaluation Methodology, 'Safety Evaluation by the Office of Nuclear Reactor Regulation Related to NRC Generic Letter 2004-02, Revision 0, December 6, 2004'," December 2004.
- 1-5 Letter from John Hannon, "Draft NRC Staff Review Guidance for Evaluation of Downstream Effects of Debris Ingress into the PWR RCS on Long Term Core Cooling Following a LOCA," November 22, 2005. [ML053000103]

Section 2

- 2-1 LTR-NRC-06-46, "Requested NRC Action from Meeting with Westinghouse on April 12, 2006; Acceptance Criteria for Long-Term Core Cooling following Quenching and Reflooding of the Core; PWR Containment Sump Downstream Effects Resolution of GSI-191," dated July 14, 2006.

Section 3

- 3-1 AREVA Document 51-9102685-000, "GSI-191 FA Test Report for PWROG," March 2009. [Proprietary to AREVA fuel customers.]
- 3-2 WCAP-17057-P, "GSI-191 Fuel Assembly Test Report for PWROG," March 2009. [Proprietary to Westinghouse fuel customers.]
- 3-3 LTR-SEE-I-09-34, "Transmittal of PWROG Fuel Assembly Debris Capture and Head Loss Protocol to PWROG Members," March 2009.
- 3-4 Revised Guidance for Review of Final Licensee Responses to Generic Letter 2004-02, "Potential Impact of Debris Blockages on Emergency Recirculation During Design Basis Accidents at Pressurized Water Reactors," March 2008. [ML080230112]
- 3-5 WCAP-12945-P-A, Volume 1, Revision 2, and Volumes 2 through 5, Revision 1. "Code Qualification Document for Best Estimate LOCA Analysis," Bajorek, S.M., et. Al., 1998.

Section 4

- 4-1 AREVA Document 51-9102685-000, "GSI-191 FA Test Report for PWROG," March 2009. [Proprietary to AREVA fuel customers.]
- 4-2 WCAP-17057-P, "GSI-191 Fuel Assembly Test Report for PWROG," March 2009. [Proprietary to Westinghouse fuel customers.]
- 4-3 Richard A. Williams et. al, "Predicting Packing Characteristics of Particles of Arbitrary Shapes," KONA No. 22, Osaka, Japan, 2004.

Section 5

- 5-1 NEA/CSNI/R (95)11, "Knowledge Base for Emergency Core Cooling System Recirculation Reliability," February 1996.

Section 6

- 6-1 WCAP-16530-NP-A, Revision 0, "Evaluation of Post-Accident Chemical Effects in Containment Sump Fluids to Support GSI-191," March 2008.
- 6-2 AREVA Document 51-9102685-000, "GSI-191 FA Test Report for PWROG," March 2009. [Proprietary to AREVA fuel customers.]
- 6-3 WCAP-17057-P, "GSI-191 Fuel Assembly Test Report for PWROG," March 2009. [Proprietary to Westinghouse fuel customers.]

Section 7

- 7-1 WCAP-16530-NP-A, Revision 0, "Evaluation of Post-Accident Chemical Effects in Containment Sump Fluids to Support GSI-191," March 2008.
- 7-2 OG-07-419, "Transmittal of LOCADM Software in Support of WCAP-16793-P, 'Evaluation of Long-Term Cooling Associated with Sump Debris Effects' (PA-SEE-0312)," September 2007.
- 7-3 OG-07-477, "Responses to the NRC Request for Additional Information (RAI) on WCAP-16793-NP, 'Evaluation of Long-Term Cooling Considering Particulate, Fibrous and Chemical Debris in the Recirculating Fluid' (PA-SEE-0312)," October 2007.
- 7-4 OG-07-534, "Transmittal of Additional Guidance for Modeling Post-LOCA Core Deposition with LOCADM Document for WCAP-16793-NP (PA-SEE-0312)," December 2007.
- 7-5 OG-08-64, "Transmittal of LTR-SEE-I-08-30, 'Additional Guidance for LOCADM for Modification to Aluminum Release' for Westinghouse Topical Report WCAP-16793-NP, 'Evaluation of Long Term Cooling Considering Particulate, Fibrous and Chemical Debris in the Recirculating Fluid' (PA-SEE-0312)," January 2008.

Section 9

- 9-1 Richard A. Williams et. al, "Predicting Packing Characteristics of Particles of Arbitrary Shapes," KONA No. 22, Osaka, Japan, 2004.
- 9-2 WCAP-17057-P, "GSI-191 Fuel Assembly Test Report for PWROG," March 2009. [Proprietary to Westinghouse fuel customers.]
- 9-3 WCAP-16406-P-A, Revision 1, "Evaluation of Downstream Sump Debris Effects in Support of GSI-191," March 2008.

Section 10

- 10-1 AREVA Document 51-9102685-000, "GSI-191 FA Test Report for PWROG," March 2009. [Proprietary to AREVA fuel customers.]
- 10-2 WCAP-17057-P, "GSI-191 Fuel Assembly Test Report for PWROG," March 2009. [Proprietary to Westinghouse fuel customers.]

APPENDIX A GSI-191 LTCC ACCEPTANCE BASIS

A.1 INTRODUCTION

The PWROG is leading an industry effort to resolve the issues associated with GSI-191 as they pertain to the core. Part of that resolution involves defining the relevant LTCC bases. This appendix describes the acceptance criteria that will be used in determining GSI-191 acceptance of the debris effects on fuel. These LTCC acceptance criteria are based on the requirements of Title 10 of the Code of Federal Regulations, Part 50.46 (10 CFR 50.46). The criteria are to be used with engineering evaluations that demonstrate acceptable LTCC, once established following the initial recovery of the core post-LOCA, is successfully maintained. Successful LTCC is defined as meeting the criteria defined in this appendix.

A.2 REQUEST FOR LONG-TERM CORE COOLING REQUIREMENT CLARIFICATION

On April 12, 2006, NRC staff met with representatives from industry and Westinghouse to discuss acceptance criteria for nuclear plant licensees to employ for evaluating potential effects of debris that may be ingested into the RV following the transition to sump recirculation following a postulated large-break LOCA. The purpose of the criteria is to assist licensees in addressing issues associated with GSI-191 PWR sump performance.

By letter dated July 14, 2006, Westinghouse requested the NRC clarify its LTCC requirements under 10 CFR 50.46 (Reference A-1). The requests were specified as follows:

1. It is requested that NRC provide clarification of the requirements and acceptance criteria for LTCC once the core has quenched and reflooded. This clarification will be used by PWROG in developing the GSI-191 debris ingestion evaluation method for reactor fuel.
2. The standard mission time employed for GSI-191 is 30 days. This mission time may not be appropriate for evaluation of nuclear fuel issues. The NRC staff is requested to provide clarification on this requirement and how it applies to evaluation of debris ingestion effects on reactor fuel. The PWROG will use this clarification in developing the GSI-191 debris ingestion evaluation method for reactor fuel.

By letter dated August 16, 2006, the NRC responded to the request for clarification (Reference A-2). The NRC letter provides the basis for defining LTCC requirements that may be used to address issues associated with GSI-191.

A.3 NRC CLARIFICATION OF LONG-TERM CORE COOLING REQUIREMENTS

With respect to Item 1, the NRC response identified that the 10 CFR 50.46 rule was constructed in two parts as follows:

The first part governs the performance of the emergency core cooling system (ECCS) during the initial phases of blow down, quench and re flood. During this period, the ECCS is injecting water from the refueling water storage tank (RWST) into the reactor in an effort to ensure that fuel damage is minimized. The criteria used to conclude that fuel damage is minimized are the temperature criteria for the cladding and the oxidation and hydrogen generation values.

The rule then establishes a criterion for long term cooling during any recirculation phase (whether natural or forced recirculation). The acceptance criterion is simply that the calculated core temperature shall be maintained at an acceptably low value and decay heat shall be removed for the extended period of time required by the long lived radioactivity remaining in the core.

The NRC staff has typically considered the criteria in paragraph (b)(5) to be satisfied when the fuel in the core is quenched, the switch from injection to recirculation phases is complete, and the recirculation flow is large enough to match the boil-off rate. The staff is concerned about the potential for loss of long term cooling capability from chemical effects (boron precipitation) or physical effects (debris). For example, the staff's standard position is that a core flushing flow path should be established well before boron concentrations reach the precipitation limit (Ref. Information Notice 93 66). Similarly, analysis should demonstrate that no significant increase in calculated peak clad temperature (PCT) occurs by demonstrating that the bulk temperature at the core exit is maintained essentially constant at the temperature achieved at the initiation of recirculation or is continuing to decrease. The following paragraph provides further qualification of the NRC concerns with respect to increases in fuel temperature during the recirculation phase.

While the current staff position is conservative with respect to protection of the fuel, other options may be available that provide protection of the fuel, assure a coolable geometry, and could be used to demonstrate compliance with paragraph (b)(5). The staff notes that fuel qualification testing has been restricted to heating the fuel cladding to the regulatory limit and then quenching the material to examine the ductility and strength remaining. The staff is not aware of any testing done to examine the subsequent reheating of fuel to the 10 CFR 50.46 limit with a subsequent second quench (either slow or fast). Situations showing a localized moderate (on the order of 100-200 degrees C) PCT increase could be considered as acceptably low if properly justified. The staff would expect any such justifications to consider degradation of the cladding oxide layer, hydrogen embrittlement of the cladding, and accumulated diffusion of oxygen within the cladding microstructure. Duration of time at elevated temperature and peak temperature experienced by the clad should also be limited and justified. The staff would expect the justifications to be supported by test data, where possible.

- The submitted information would form the basis for any determination that the calculated core temperatures remain acceptably low as required by the rule. The second clause of 10 CFR 50.46(b)(5), "decay heat removed for the extended period of time required by the long lived radioactivity remaining in the core" was not identified as an issue needing clarification in Westinghouse letter LTR-NRC-06-46, or at the meeting with Westinghouse on April 12, 2006. The Westinghouse representatives in attendance at the meeting agreed with the staff on the definition of this clause and had no questions on its meaning. Based on this, the staff expects that this clause needs no further clarification.

With respect to Item 2, the NRC response notes the following;

For GSI-191, the 30-day criterion was originally intended for evaluation of operability of equipment. For analysis of core cooling following debris ingestion into the RV, the staff believes that an adequate post-LOCA evaluation duration would be demonstrated when bulk and local temperatures are shown to be stable or continuously decreasing with the additional assurance that any debris entrained in the cooling water supply would not be capable of affecting the stable heat removal mechanism due to sump screen clogging or downstream effects.

A.4 GSI-191 LONG-TERM CORE COOLING ACCEPTANCE BASES

The LTCC acceptance bases defined for GSI-191 are listed below. These acceptance bases are applied after the initial quench of the core and consistent with the LTCC requirements stated in 10 CFR 50.46 (b)(4) and 10 CFR 50.46 (b)(5). They do not represent, nor are they intended to be new or additional LTCC requirements. These acceptance bases provide for demonstrating that local temperatures in the core are stable or continuously decreasing and that debris entrained in the cooling water supply will not affect decay heat removal.

- **Decay Heat Removal/Fuel Clad Oxidation**

Maximum cladding temperatures maintained during periods when the core is covered will not exceed a core average clad temperature of 800°F.

Cladding temperatures at or below 800°F maintain the clad within the temperature range where additional corrosion and hydrogen pickup over a 30 day period will not have a significant effect on cladding properties. At temperatures greater than 800°F, there are occurrences of rapid nodular corrosion and higher hydrogen pickup rates that can reduce cladding mechanical performance. Long-term autoclave testing has been performed to demonstrate that no significant degradation in cladding mechanical properties would be expected due to a localized hot spot. This information is proprietary to the fuel vendors but could be made available upon request. This testing demonstrated that the increase in oxide thickness and hydrogen loading was limited at temperatures of less than 800°F for periods of 30 days. With limited corrosion and hydrogen pickup, the impact on cladding mechanical performance is not significant. Therefore no significant degradation in cladding properties would occur due to 30-day exposure at 800°F, and there would not be any adverse impact on core coolability. Based on the autoclave results, the data is sufficient to justify a maximum clad temperature of 800°F as an LTCC acceptance basis.

- **Deposition Thickness**

For current fuel designs, regardless of vendor, the minimum clearance between two adjacent fuel rods, including an allowance for the spacer grid thickness, is greater than 100 mils. Therefore, a 50-mil debris thickness on a single fuel rod is maximum deposition to preclude touching of the deposition of two adjacent fuel rods with the same deposition. The 50 mil thickness is the maximum acceptable deposition thickness before bridging of adjacent fuel rods by debris is predicted to occur.

A.5 DISCUSSION

Decay Heat Removal and Required Coolant Flow

LOCA ECCS analyses consider the LOCA transient behavior to the point in time at which fuel temperatures are decreasing, the mixture level in the core is rising, and the peak clad temperature has been captured. At the start of sump recirculation, the core has been quenched and is covered by a two-phase liquid/steam mixture and/or single phase liquid. After the start of sump recirculation, LTCC is demonstrated by showing that there is sufficient flow to replace core boil-off, thus keeping the core covered and preventing additional fuel clad heat-up.

For some post-LOCA scenarios, precipitation of boric acid in the core region is prevented by core flow above the core boil-off rate. In these cases, the required core flow to provide for boric acid dilution is usually represented as a multiplier on core flow.

Flow rates required to match boil-off become small quickly following the postulated event. The required flow rate to match boil-off for a large Westinghouse four-loop PWR is taken from the emergency operating procedures (EOP) and shown in Figure A-1. While the actual values are dependent on the initial core power level, these values are representative of the PWR fleet. Within four hours following a postulated LOCA, the required flow to match boil-off is about 250 gallons per minute. At 10 hours, the flow required to match boil-off is about 200 gallons per minute, and at 30 hours, the flow required to match boil-off is about 150 gallons per minute.

The PWROG has used multiple methods to demonstrate that the minimal flow required to remove core decay can be maintained. Testing of a FA in the presence of debris has established the maximum mass of fiber, particulate, and chemical precipitates that would not cause total blockage of the flow into the FA (References A-3 and A-4). Analyses with large system codes (Section 3 and 4) show that substantial blockage at the core inlet can be tolerated and still maintain the necessary flow rate to maintain acceptable low fuel cladding temperatures.

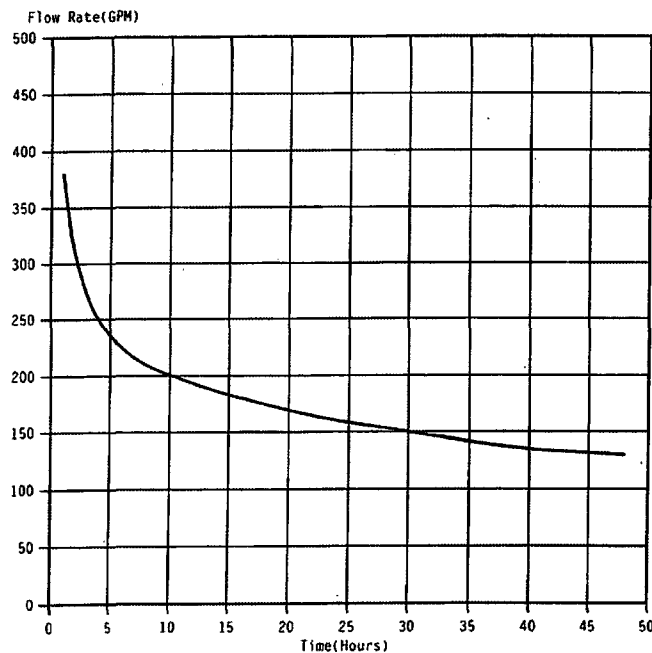


Figure A-1 Boil-off Curve for a Westinghouse Four-loop PWR

Spacing Between Fuel Rods

The minimum clearance between two adjacent fuel rods, including an allowance for the spacer grid thickness, is greater than 100 mils. Therefore, a 50-mil debris thickness on a single fuel rod is maximum deposition to preclude touching of the deposition of two adjacent fuel rods with the same deposition. The 50 mil thickness is the maximum acceptable deposition thickness before bridging of adjacent fuel rods by debris is predicted to occur. The 50 mils of solid precipitation described here include the clad oxide, crud layer and debris deposition.

The example chemical product deposition calculation documented in Appendix E was performed with inputs intended to maximize chemical deposition. That deposition calculated for the sample case was less than 30 mils. Thus, although the chemical deposition of fuel is a plant-specific calculation, plants are not expected to calculate deposition thicknesses in excess of 30 mils.

The formation of a chemical deposition layer followed by the collection of fibrous debris in the remaining open channel will not challenge the cooling of the clad. As was shown in the response to RAI #15, Appendix H, the effective thermal conductivity of a fibrous debris bed is at least 5 times greater than the minimum thermal conductivity of 0.1 Btu/(hr-ft-°F) used in the cladding heat up calculations in Appendix D and with LOCADM in Appendix E.

Thus, for chemical deposition, the range of cladding heat up calculations between spacer grids considering up to a 50 mil buildup presented in Tables D-1 and D-2 of Appendix D are bounding. The maximum calculated clad temperature listed in these tables for up to 50 mils of deposition is below 800°F.

Therefore, a maximum debris layer buildup of 50 mils is an appropriate acceptance criterion for the span between grids.

Spacing Between Fuel Rods and Grids

For current fuel designs, the minimum clearance between the cladding and the spacer grid is about 40 mils. This occurs where the springs and dimples of the grid contact the fuel rod. The maximum clearance between the cladding and the spacer grid occurs along the diagonal of the of a grid cell and is about 110 mils. Thus, if a spacer grid were to become completely filled by either a fibrous debris bed or a chemical deposition, the radial thickness of the debris on the clad would vary from about 40 mils to about 110 mils about the circumference of a fuel rod.

Calculations documented in Appendix C assess the clad temperature under a debris bed in a single spacer grid/fuel rod configuration. The results of these calculations are summarized in Table C-7 of Appendix C. To use these results to assess a maximum clad temperature under worst case debris or chemical deposition under a spacer grid/fuel rod configuration, the following assumptions are made:

- A uniform debris layer thickness of 110 mils is assumed on the cladding.
- The debris layer is assigned the conservative effective thermal conductivity for a fibrous debris bed or chemical deposition layer of 0.1 Btu/(hr-ft-°F).

Under these limiting assumptions, the clad temperature is estimated to be less than 738°F by extrapolating the calculated clad temperatures listed in Table C-7 for the effective thermal conductivity of 0.1 Btu/(hr-ft-°F). This temperature value is an extremely conservative estimate of the clad temperature under worst case debris or chemical deposition beneath a spacer grid/fuel rod configuration for the following reasons:

- A conservatively small value of conduction through the debris bed is used. (As was shown in the response to RAI #15, Appendix H, the effective thermal conductivity of a fibrous debris bed is at least 5 times greater than the minimum thermal conductivity of 0.1 Btu/(hr-ft-°F) used in the cladding heat up calculations in Appendix C and with LOCADM in Appendix E.)
- The calculation does not account for circumferential heat transfer about the debris bed which would form in the spacer grid between the dimples and springs and the corners of the spacer grid.
- In the case of a fibrous debris bed, convection of heat by the flow of coolant through the debris bed is neglected (The ability of coolant to pass through a fibrous and particulate debris bed under PWR LTCC flow conditions was demonstrated in the response by testing).

The formation of a deposition, either fibrous or chemical, under a clad and followed by the collection of fibrous debris in the remaining open channel will not challenge the cooling of the clad.

Based on observations from testing of fibrous debris collection on debris capturing grids, a complete blockage of a spacer grid with fibrous and particulate debris will not occur for the limits of fibrous debris ingestion reported in Section 10. The test data shows that, for the allowed fibrous, particulate, and chemical precipitate debris loads, flow through the resulting debris bed is maintained.

Industry Experience with At-Power Clad Oxidation

As noted previously, long-term autoclave testing has been performed to demonstrate that no significant degradation in cladding mechanical properties would be expected due to a localized hot spot. This testing demonstrated that the increase in oxide thickness and hydrogen loading was limited at temperatures of less than 800°F for periods of 30 days. It is noted that there was an at-power experience at the Calvert Cliffs Nuclear Power Plant during the late 1970's in which clad temperatures increased to 800°F so that operation for several weeks caused the oxide layer to build on the cladding. This at-power operating experience is not applicable to the post-LOCA LTCC conditions the acceptance basis addresses as discussed below.

- The core conditions that resulted in the clad oxidation at Calvert Cliffs during the late 1970's would not exist in the core post-LOCA. At-power clad corrosion is driven by temperature, fast neutron flux, and thermal feedback through an oxide layer. During long term cooling post-LOCA, the fast neutron flux is negligible and the heat flux is low. Thus, for post-LOCA conditions, only the temperature is directly applicable to corrosion and autoclave data is more representative of the temperature-driven corrosion that would be experienced by cladding. Evaluation of autoclave data for cladding at temperatures of 800°F and below shows only small increases in the corrosion thickness and hydrogen loading compared to the post-LOCA transient conditions immediately following the postulated break that occur prior to long-term cooling.
- Local increases in corrosion due to local hot spots will not impact long term cooling. The impact of corrosion on the clad material properties is small and the heat load continues to decrease with time. The 17 percent equivalent clad reacted (ECR) criteria apply to the LOCA event only. If the local conditions immediately post-LOCA were close to the 17 percent ECR limit (pre-transient corrosion and transient ECR), then the small amount of additional corrosion from a hot spot which resulted in approaching 800°F for 30 days could reach or marginally exceed 17 percent ECR. However, based on the sample deposition calculation, the conservative core blockage calculations and the parametric clad heat-up calculations presented in Section 4, cladding temperatures approaching 800°F for post-LOCA LTCC are not expected.
- Also, the peak ECR region on the rod is not expected to be the same region where a local hot spot would occur. Local hot spots would be expected to occur lower in the core and at or just below a spacer grid. Pre-transient corrosion is suppressed at the spacer grid locations.
- In addition, much of the reduction in ductility from high temperature oxidation (> 1832°F) is due to oxygen diffusion ahead of the oxide layer. At temperatures of < 930°F, there is no observation of oxygen diffusion ahead of the oxide layer.

In summary, the PWR industry at-power experience with cladding oxidation is not applicable to the post-LOCA LTCC environment.

Impacts of Local Hot Spots

The ingestion of debris through the sump screens and the potential chemical effects from the generation of chemical by-products from the reaction of containment material and coolant following a LOCA create

the possibility of local “hot spots” occurring in the reactor core. Based on the designs and flow hole sizes of the replacement sump screens, and test data obtained using those designs, the passing of debris in sufficient quantity or size to result in a hot spot is considered small and will not challenge overall LTCC of the fuel. However, the consequences of the formation of hot spots should be evaluated.

Local “hot spots” could occur as a result of debris catching and accumulating on the various nozzles and grids of an FA or by chemical by-products plating out on parts of the fuel. The potential effects of these local “hot spots” can be assessed against the ECCS criteria (10 CFR 50.46) and for their potential impact on the health and safety of the public above those considered for a LOCA.

The current regulatory criteria for LTCC is identified in 10 CFR 50.46 (b)(5), “Long-term cooling. After any calculated successful initial operation of the ECCS, the calculated core temperature shall be maintained at an acceptably low value and decay heat shall be removed for the extended period of time required by the long-lived radioactivity remaining in the core.”

- “...temperature shall be maintained at an acceptably low value” is interpreted to mean less than 800°F (427°C). (Note: A value of 800°F is cited as the maximum acceptable clad temperature to be consistent with the acceptance basis presented in Section A.4, GSI-191 LTCC Acceptance Basis.)
- “...extended period of time” is interpreted to mean showing that the local temperatures are stable or continuously decreasing and that debris entrained in the cooling water supply will not affect decay heat removal.

As noted previously, based on the testing of replacement sump screens, the passing of debris in sufficient quantity or size to result in a hot spot is considered small and will not challenge overall LTCC of the fuel. However, assuming a “hot spot” occurs during LTCC following a LOCA, the following should be considered:

- For dose considerations, all fuel is considered to have failed. Therefore, “hot spots” do not contribute additional dose.
- Given a sustainable quench and the replacement of boil-off, any fuel cladding “hot spot” would remain underwater.
- Transitioning the ECCS from a clean water source to recirculation from the reactor containment building sump is addressed under the current licensing basis of PWRs. It is also noted that, during HL switchover or, for B&W plants, the establishment of a core flushing flow, there is no interruption of coolant to the core. Therefore, there is no clad heat-up transient during this operation.

Once the transition of the ECCS from a clean water source to recirculation of coolant from the reactor containment building sump has occurred, there is no interruption (termination) of coolant flow to the core due to system realignments such as initiation of HL recirculation. For plants that have a reduction in flow associated with systems realignments, the supplied flow remains above the core boil-off rate and will not result in a reheat of the cladding. Therefore, for long term

cooling, the appropriate acceptance basis for clad temperature is 800°F. This acceptance basis is based on the results of long term autoclave testing that used clean water at temperatures up to about 700°F, and steam at temperatures ranging from 700°F to 900°F.

- A coolable core geometry must be maintained during LTCC.
- The fuel will not be reused.

The source of heat post-LOCA is from decay heat in the fuel rod. This source is limited to the fuel in the rod and decreases with time. “Hot spots” can arise only if the local flow is severely restricted. Local temperature increases would be mitigated by the boil off in the region. Also, the grids act as a radiator and there will be conductive heat removal axially along the fuel rod. If quench is sustained and the boil-off is replaced, the ability of the “hot spot” to obtain significant temperatures (approaching 2200°F (1204°C)) is severely limited.

However, should localized temperatures at a “hot spot” reach sufficient levels to further degrade or damage the fuel cladding, the impact of the temperature increase on LTCC is minimal. Since all rods are assumed to have failed during the LOCA, no additional impact to dose is expected. In addition, if a buildup of chemical deposits or debris were to form such that the buildup would cause an increase in cladding temperature, there are two possible outcomes:

1. The deposit goes back into solution as the cladding temperature increases and the “hot spot” is subsequently cooled.
2. The deposit is fixed and remains on the surface (it does not go back into solution) and the “hot spot” remains.

For the first case, the “hot spot” is self-limiting. For the second case, if the temperature at the “hot spot” were to increase to a level that damage to the fuel cladding would result, the remainder of the fuel rods, fuel skeleton, and other fuel assemblies, would serve to contain the fuel and maintain structural spacing to provide geometry for LTCC. Thus, the fixed deposit would not further impact the coolability of the fuel.

The ability to maintain an average fuel clad temperature below 2200°F during LTCC can be demonstrated. Regardless of the actual temperatures obtained at a localized “hot spot” and the localized damage to fuel cladding during LTCC, the requirements of 10 CFR50.46 will continue to be met.

To summarize, given that the fuel will not be reused following a LOCA, localized “hot spots” during LTCC do not increase the risk to the health and safety of the public and does not jeopardize core coolability as long as the core remains covered and boil-off is replaced.

Impacts of Boric Acid Concentration

The impacts of boric acid concentration will be addressed in a separate PWROG program.

A.6 SUMMARY

The LTCC criteria identified here and proposed for use to address GSI-191 are consistent with the requirements of 10 CFR 50.46. Furthermore, the criteria are conservative and, when used in conjunction with engineering calculations performed considering GSI-191 concerns, provide reasonable assurance that LTCC is successfully maintained.

LTCC bases applicable to GSI-191 have been defined based on the clarification offered by the NRC (Reference A-2). They are summarized as follows:

1. The cladding temperature during recirculation from the containment sump will not exceed 800 F.
2. The deposition of debris and/or chemical precipitates will not exceed 50 mils on any fuel rod.

Properly applied, these bases will facilitate the demonstration of acceptable core cooling following a postulated large break LOCA.

A.7 REFERENCES

- A-1 LTR-NRC-06-46, "Requested NRC Action from Meeting with Westinghouse on April 12, 2006; Acceptance Criteria for Long-Term Core Cooling following Quenching and Reflooding of the Core; PWR Containment Sump Downstream Effects Resolution of GSI-191," July 14, 2006.
- A-2 Nuclear Regulatory Commission Response to Westinghouse Letter LTR-NRC-06-46 Dated July 14, 2006, Regarding Pressurized Water Reactor (PWR) Containment Sump Downstream Effects," August 16, 2006, ADAMS No. ML0620704511.
- A-3 AREVA Document 51-9102685-000, "GSI-191 FA Test Report for PWROG," March 2009.
- A-4 WCAP-17057-P, "GSI-191 Fuel Assembly Test Report for PWROG," March 2009.

APPENDIX B EVALUATION OF BLOCKAGE AT THE CORE INLET

B.1 OBJECTIVE

The purpose of this task is to demonstrate that sufficient LTCC is achieved to satisfy the requirements of 10 CFR 50.46 considering the effects of debris ingested into the RCS and core during post-accident operation when safety systems are realigned to recirculate inventory from the containment sump. The flow at the core inlet could be suppressed due to the build-up of sump debris at the lower core plate and bottom nozzle. To show LTCC would be maintained in this situation WC/T simulations were run blocking the inlet at the core entrance with an increased k-factor. This calculation provides additional “defense in depth” to the FA testing to assure that LTCC will be maintained.

B.2 APPROACH

To evaluate the effects of blockage at the core inlet, the dimensionless friction factor (C_D) was ramped at the core inlet to simulate blockage due to debris buildup. A modified version of WC/T was created to allow the ramping of the friction factor at the core inlet. Code simulations were run to the beginning of recirculation (conservatively assumed to be 20 minutes) at which point the ramping of the friction factor took place over 30 seconds. Note that the core inlet flow blockage occurring in 30 seconds from the start of recirculation is non-physical and was modeled in such a manner to perform a bounding calculation. After the core inlet resistance was increased, the code simulations were run out to 40 minutes to show the flow rate supplied to the core would be sufficient to remove decay heat and maintain LTCC.

B.3 MODEL DESCRIPTION AND ASSUMPTIONS

The core inlet blockage simulations were meant to bound the U.S. PWR fleet. To ensure a bounding calculation, the limiting break type and the limiting vessel design were taken into consideration before selecting a plant model for the simulation.

B.3.1 Plant Type Selection Criteria

The selection of the limiting break combines the conditions from a double-ended CL and a double-ended HL break to create a bounding scenario. During a double-ended CL break, the ECCS will spill into containment, decreasing the driving head of core flow to a minimum. However, because of the low flow rate, a slow debris build-up at the core inlet ensues, which is non-limiting. During a double-ended HL break no spilling of ECCS occurs, therefore an additional driving head from the build-up of liquid level in the downcomer and in the steam generator tubes to the spillover elevation is present. However, the higher flow rates also result in faster debris build-up. To create the worst possible scenario, the limiting break case will be a double-ended CL break (i.e., limiting driving head at the core inlet) combined with faster debris build-up time that occurs for a high flow HL break.

The limiting vessel design was chosen based upon which core design would be most limiting under the condition of core inlet flow blockage. Three general vessel designs were considered: designed B/B upflow, converted B/B upflow, and B/B downflow. Designed B/B upflow is the least limiting due to the

numerous large pressure relief holes in the baffle wall. The relief holes allow flow to bypass a blocked core inlet but still enter the core. Converted upflow plants are considered more limiting than designed upflow plants due to the absence of the pressure relief holes, such that only limited bypass flow may enter near the top of the core. The most limiting design is downflow plants since the only means for the flow to enter the core is through the lower core plate.

Other PWR vessel designs were considered including B&W and CE designs. B&W plants are similar to the Westinghouse upflow design with the numerous pressure relief holes in the baffle wall. Therefore, the design is non-limiting with respect to core inlet flow. Other differences in the B&W design, such as the RVVV, were concluded to have no impact on this issue. CE plants are similar to the Westinghouse converted upflow plant in that they have no pressure relief holes, but limited flow may enter near the top of the core. Therefore the design is non-limiting with respect to core inlet flow. CE plant designs lack RHR heat exchangers, and after switchover to recirculation high pressure safety injection flow goes directly from sump to the RCS. The higher ECCS injection temperature is considered to have a small effect on core inlet blockage simulations. Prior to recirculation, termination of extensive downcomer boiling and cooling of vessel internals has already occurred. Therefore, the increase in injection temperature should not lead to boiling and only a small decrease in flow rate supplied to the core will result.

Therefore, it is concluded that the Westinghouse downflow design is bounding for this analysis.

B.3.2 Description of and Basis for Model Inputs

A plant with an existing WC/T model, downflow plant configuration, and high core power density is desired for the core blockage simulations. A three-loop downflow model plant rated at 2900 MWt was chosen. The power shape of the plant's BELOCA reference transient used for these simulations is shown in Figure B-1.

The axial power shape uses a high enthalpy rise peaking factor ($F_{\Delta H} = 1.73$), a skewed to the top power distribution (13 percent axial offset), and a relatively high total peak factor ($F_Q = 2.3$). The top-skewed power shape shown in Figure B-1 is limiting compared to base load or bottom skewed power shapes due to the longer time for the quench front to approach the elevations with the highest power, and its susceptibility to heatup if the core becomes uncovered due to inlet blockage. The total peaking factor is on the order of 20 percent higher than a normal base load power shape would exhibit. F_Q higher than 2.3 will only occur in rare transient conditions, where such an F_Q would be temporary and not indicative of the long-term axial decay heat power distribution of interest for LTCC. Therefore, the inputs represent reasonably bounding values for the PWR fleet.

The radial power distributions for the four core channels shown in Figure B-3 are displayed in Table B-1.

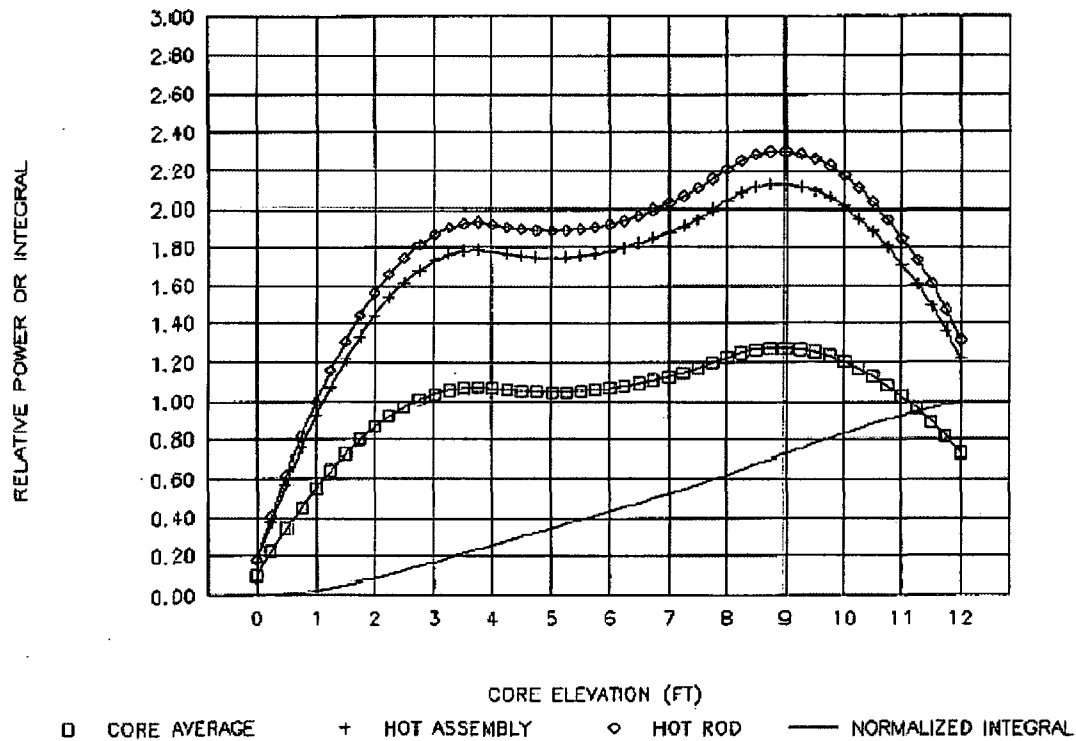


Figure B-1 Plant Transient Power Shape

Table B-1 Core Channel Radial Power Distribution			
Channel Description	Channel Number	Normalized Power	Number of Assemblies
Hot Assembly Channel (HA)	13	1.66	1
Guide Tube Channel (GT)	12	1.17	53
Non-Guide Tube Channel (AVG)	11	1.17	75
Low Power Periphery Channel (LP)	10	0.20	28

The radial power distribution in the core is flat other than in the periphery assemblies and the hot assembly. The hot assembly power is conservatively modeled to a high normalized power of 1.66.

Additional information on the plant chosen for the core inlet blockage simulations is given in the schematics and nodding diagrams shown in Figures B-2 through B-5.

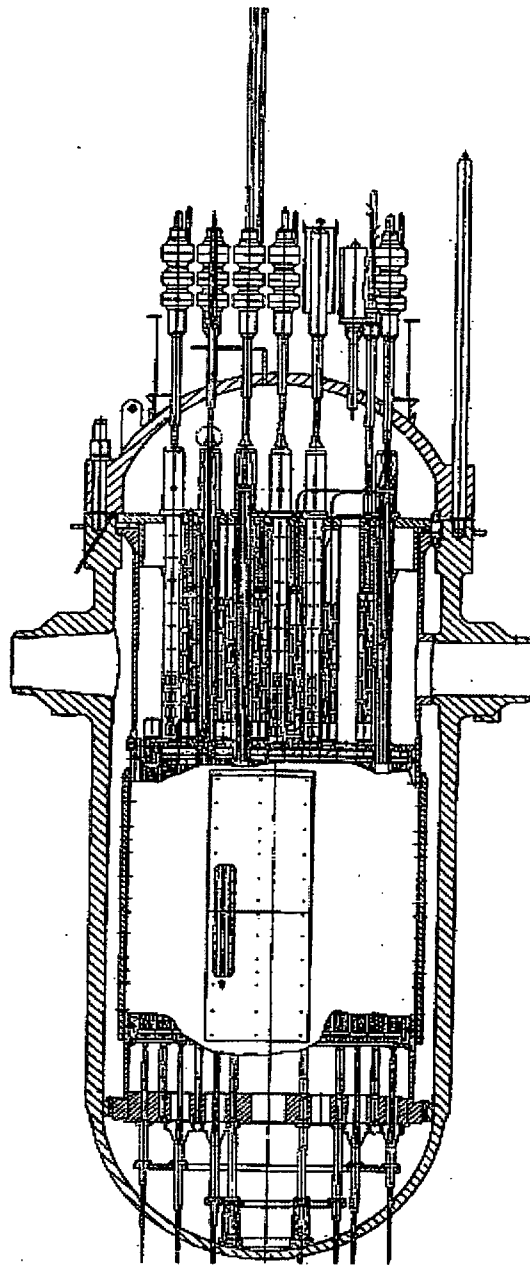


Figure B-2 Plant Vessel Profile

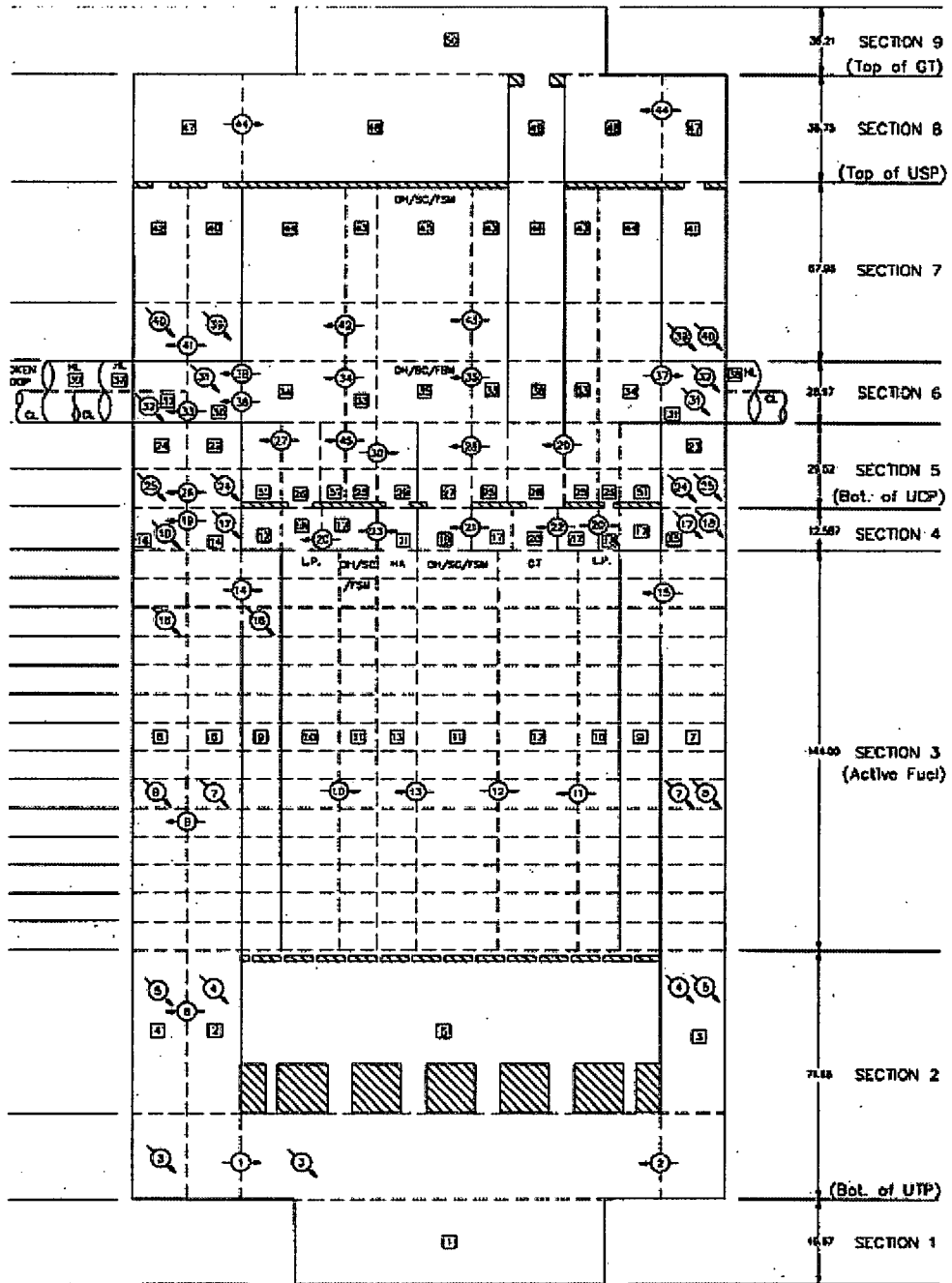
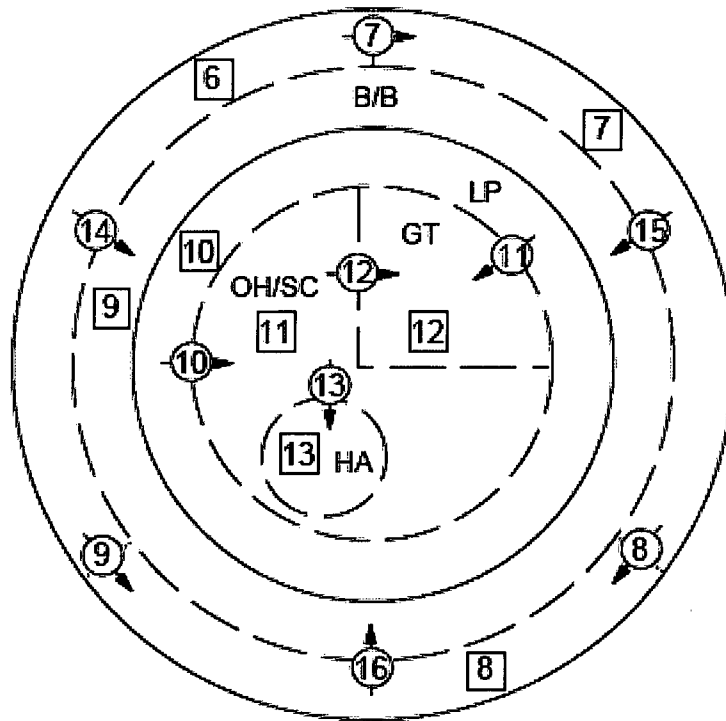


Figure B-3 Plant Vessel Model Noding Diagram



□ - channel
♂ - gap

Figure B-4 Plant Core Channel Modeling

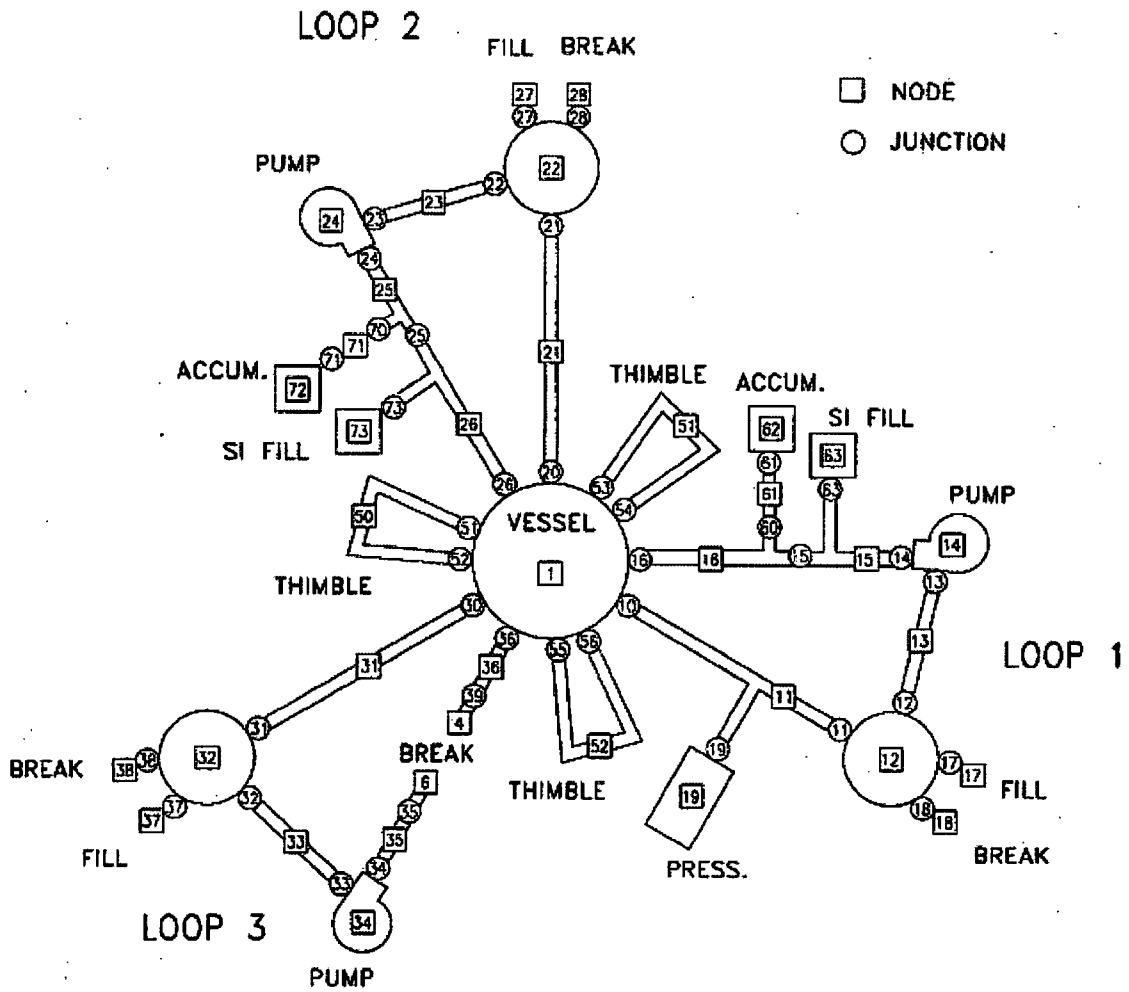


Figure B-5 Plant Loop Model Noding Diagram

The modified WC/T code version and the plant model shown in Figure B-3 were used to study the effects of core blockage on LTCC. The calculations modeled the ramp-up of the dimensionless loss coefficient (C_D) at the core inlet and the increase of the temperature of the ECCS injection water at 20 minutes, which is the modeled beginning of sump recirculation. It should be noted that the increase in the value of C_D , simulating the debris build-up over 30 seconds, is non-physical and was modeled to occur over such a short time period to perform a bounding calculation. The increase in the injection temperature represents a representative RHR heat exchanger outlet temperature following switchover to sump recirculation. The temperature of the injected water was set to be 190°F, which is typical for Westinghouse designs and is expected to bound B&W plant designs. While CE plants may have slightly higher temperatures, the effect on the transient will be minimal. Following preliminary test calculations, it was decided to ramp C_D to extremely large values to completely block the chosen core channels to simulate a percentage of core blockage.

Initially, two simulations were run with no changes to the standard noding but with different amounts of simulated core blockage,. The first case modeled 82% core flow blockage by ramping the value for C_D up to 10^9 in all core channels except for the Lower Power (LP) periphery channel (representing 28 of 157 assemblies). Figure B-6 displays the core channel modeling used for Case 1. Channels 11, 12, and 13 are crossed out to represent total blockage at the inlet of the channels. For this modeling approach flow will only enter the core through channel 10.

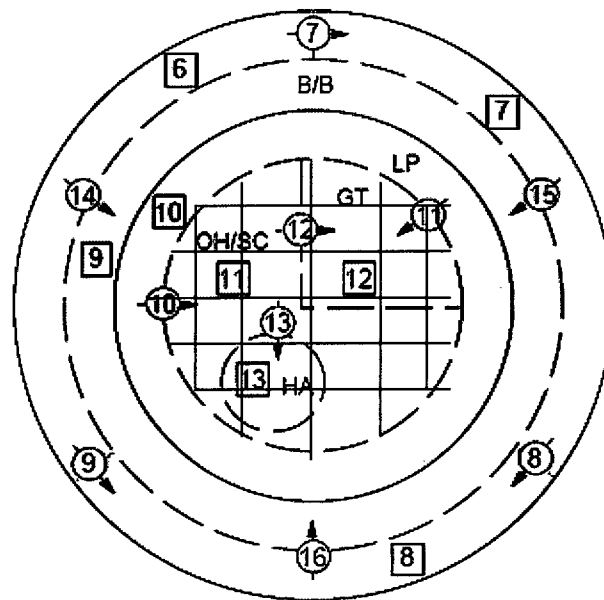


Figure B-6 Case 1 Core Blockage Modeling Approach

The second case modeled 99.4% core flow blockage by ramping the value for C_D up to 10^9 in all core channels except for the Hot Assembly (HA) channel. Figure B-7 displays the core channel modeling used for Case 2. Channels 10, 11, and 12 are crossed out to represent total blockage at the inlet of the channels. For this modeling approach flow will only enter the core through channel 13.

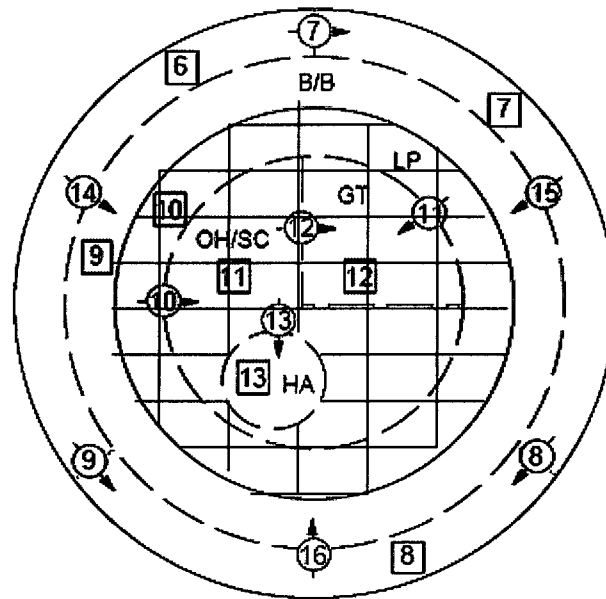


Figure B-7 Case 2 Core Blockage Modeling Approach

The Case 2 modeling approach of leaving the hot assembly unblocked is justified as acceptable due to core cross-flow. The top-skewed power shape used in the simulations creates limiting core conditions in the top half of the core. The flow supplied to the core distributes throughout the core channels, and by the higher power elevations, the flow will be well allocated to all the core channels. This statement can be supported by examining the void fraction of the LP periphery channel and the HA channel. Figure B-8 plots the LP void fraction and the HA void fraction from 2000 to 2400 seconds, near the top of the core. The figure shows the void fraction in the HA channel reaching higher values, demonstrating much of the flow exits the HA channel via cross-flow through the core and suggesting no non-conservatism due to the modeling approach.

The containment back pressure was modeled by a containment pressure vs. time table input for each of the broken loop CL break components. The containment backpressures used in both cases were based on the existing pressure vs. time tables used in the BELOCA analysis. The BELOCA table was extrapolated down to atmospheric pressure and held there. As a result, the containment pressure is assumed to be at atmospheric conditions by switchover to sump recirculation.

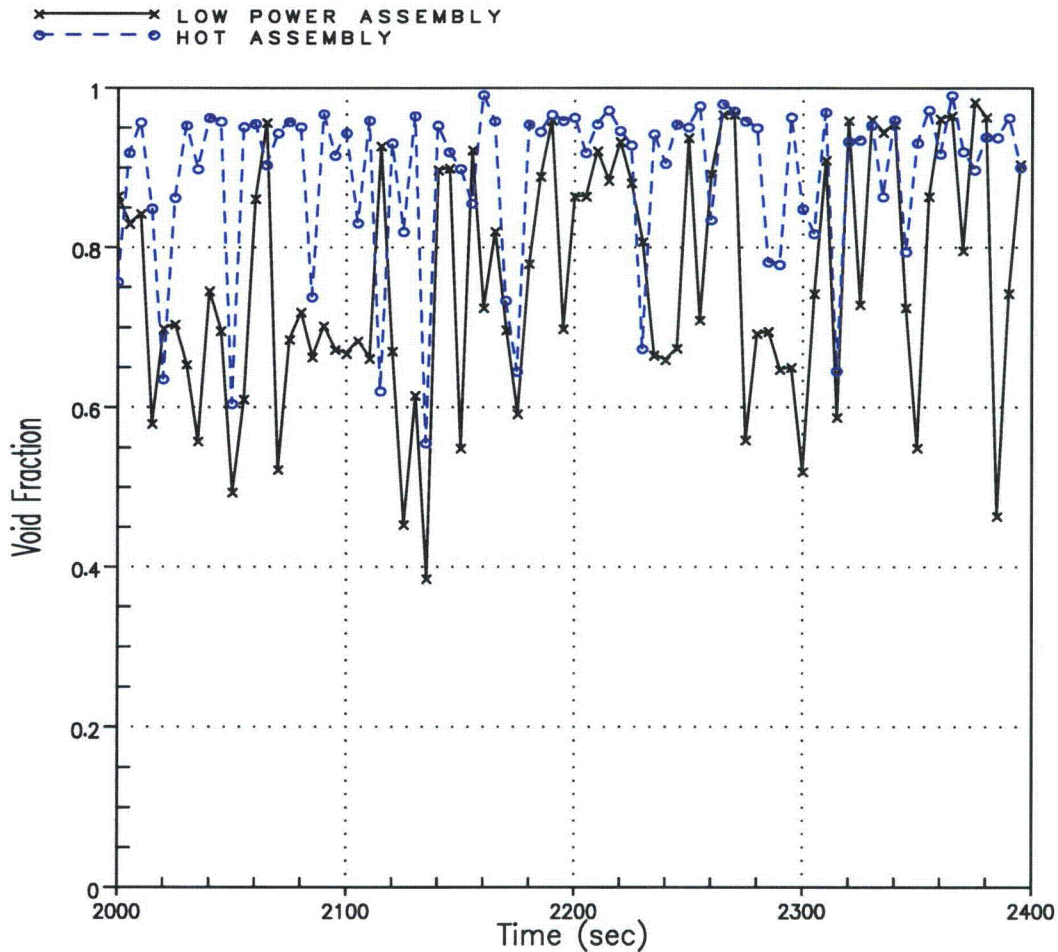


Figure B-8 Low Power Channel and HA Channel Void Fraction, Case 2 - Unblocked HA Test

The additional effects of sub-atmospheric containment plants on the transient have been considered to show the calculations performed apply to the entire US PWR fleet. The containment pressure and pressure drop through the RCS loops have a direct affect on the boil-off rate for a postulated CL break. The decrease in the containment pressure for a subatmospheric plant could cause an increase in loop pressure drop, which could lead to higher core exit pressures and higher boil-off rates. The increased core exit pressure corresponds to higher boil-off rates through the inversely proportional relationship between the boil-off rate ($\omega_{boiloff}$) and the latent heat of vaporization, i.e.,

$$\omega_{boiloff} = \frac{Q_{DH}}{h_{fg}} \quad (B-1)$$

The relationship between the pressure drop and the containment break pressure, i.e., steam density, is shown in Darcy's equation.

$$\Delta P_{\text{loop}} = \frac{k}{A^2} \frac{\omega_{\text{boiloff}}^2}{288 \cdot \rho_g \cdot g_c} \quad (\text{B-2})$$

Hand calculations were performed to estimate the loop pressure drop using subatmospheric containment pressures to examine whether the core exit pressure would increase. The hand calculations compared the ratio of the loop pressure drop between atmospheric and subatmospheric containment conditions. Combining Equations (B-1) and (B-2) to create a pressure drop ratio yields,

$$\frac{\Delta P_{\text{sub}}}{\Delta P_{\text{dry}}} = \left(\frac{h_{\text{fg_dry}}}{h_{\text{fg_sub}}} \right)^2 \left(\frac{\rho_{\text{g_dry}}}{\rho_{\text{g_sub}}} \right) \quad (\text{B-3})$$

Loop pressure drop values were taken from calculations performed for atmospheric containment simulations. The largest loop pressure drop after switchover to sump recirculation was found to be approximately be $(18.0-14.7) = 3.3$ psia. First, assuming the pressure drop (ΔP) would be the same for the subatmospheric containment conditions, iterative calculations were performed to calculate the loop pressure drop for subatmospheric containment conditions. The calculation was performed twice using containment pressures of 10 psia and 12 psia to address potential non-linearity of the density changes in the pressure range of interest. The calculations found that the loop ΔP would increase, however, the core exit pressure would be lower (tables representing the values used in the final iterations are shown in Tables B-2 and B-3 below). Therefore, the subatmospheric containment pressure plant designs are bounded by the atmospheric containment simulations performed to examine the effects of core inlet blockage.

The core inlet blockage simulations were performed using 'typical' Westinghouse RHR heat exchanger outlet temperature for sump ECCS injection (190°F). It has been acknowledged that CE plant designs do not have RHR heat exchangers, and after switchover to recirculation High Pressure Safety Injection flow goes directly from sump to the RCS. The increase in sump ECCS injection temperature is assessed to be a non-factor in core inlet blockage simulations. The flow rate required to replace boil-off at 20 minutes is less than 60 lbm/sec. The highest injection temperature of concern is estimated to be 250°F, i.e., an increase of 60°F. Prior to recirculation, termination of extensive downcomer boiling and cooling of vessel internals has already occurred, therefore the increase in injection temperature should not lead to boiling and only a small decrease in flow rate supplied to the core will ensue due to the density effects. It is therefore assessed that an increase of 60°F to the ECCS injection should not affect core inlet blockage simulations.

Table B-2 Subatmospheric Loop Pressure Drop for Containment Pressure=10 psia					
Second Iteration					
Pressure (psia)	Density (lbm/ft³)	Enthalpy (Btu/lbm)	Density (lbm/ft³)	Enthalpy (Btu/lbm)	h_{fg} (Btu/lbm)
Sub cont.					
14.4	59.854	179.25	0.036607	1150.7	971.45
10	60.281	161.36	0.026027	1143.8	982.44
average	60.0675	170.305	0.031317	1147.25	976.945
Dry					
18	59.565	190.79	0.045103	1154.9	964.11
14.7	59.829	180.3	0.03732	1151	970.7
average	59.697	185.545	0.041212	1152.95	967.405
Pressure Ratio					
1.290371					
New P core (psia)		Sub-atm DP (psia)			
14.3		4.3			
New P core less than 18 psia					

Table B-3 Subatmospheric Loop Pressure Drop for Containment Pressure=12 psia					
Second Iteration					
Pressure (psia)	Density (lbm/ft³)	Enthalpy (Btu/lbm)	Density (lbm/ft³)	Enthalpy (Btu/lbm)	h_{fg} (Btu/lbm)
Sub cont.					
15.9	59.729	184.32	0.040162	1152.5	968.18
12	60.074	170.16	0.030868	1147.2	977.04
average	59.9015	177.24	0.035515	1149.85	972.61
Dry					
18	59.565	190.79	0.045103	1154.9	964.11
14.7	59.829	180.3	0.03732	1151	970.7
average	59.697	185.545	0.041212	1152.95	967.405
Pressure Ratio					
1.14801					
New P core (psia)		Sub-atm DP (psia)			
15.8		3.8			
New P core less than 18 psia					

(Note: All properties used in Table B-2 and Table B-3 were taken from NIST Thermophysical Properties of Fluid (Reference B-1). Pressure drop ratios evaluated using average properties of core exit and containment pressures)

B.3.3 Assessment of Blockage at Core Inlet

This section discusses the results of the core inlet blockage $\underline{WC/T}$ simulations. The effects of core blockage on PCT and rod quench are examined through examination of hydraulic results.

The flow distribution results were examined to determine if the flow through channels where the resistance was ramped was indeed blocked and if the flow from the blocked channels enters the unblocked channel, i.e., where the blocked core channel flow was diverted. The C_D ramp of 10^9 at sump switchover time completely blocks all flow into the blocked channels as expected. Also, a large increase in the flow into the unblocked channels occurs at switchover time due to the flow diversion from the blocked channels.

Next, the core inventory is examined. Figure B-9 displays the collapsed liquid level of an average assembly core channel (channel 11 on Figure B-3). The figure shows a slight increase in the collapsed liquid level occurring after the core is blocked for both Case 1 and Case 2. Similar to the core collapsed liquid level, the total vessel liquid mass plotted in Figure B-10 shows that the vessel continues to increase in liquid mass even after the core channels are blocked. The increase in the core liquid mass can be attributed to the flow supplied to the core being in excess of the boil-off rate or from liquid inventory in the UP entering the core. The UP global channel (area above upper core plate) collapsed liquid level plotted in Figure B-11 shows UP inventory is available, however, countercurrent flow limitation (CCFL) at the upper elevations of the core may restrict the UP inventory from entering the core region. Predicted flow results are difficult to assess due to oscillations. In order to clearly present the results, the flow figures plot the integral of the flow rates and examine the slopes of the figures to draw conclusions. Figure B-12 plots the integral of liquid flow rate at the exit of the core. The core outlet flow represents the HA, AVG, and GT core channels and the core inlet flow represents the LP core channel. The lower vapor velocity in the LP channel allows the liquid from the UP to drain into the core increasing the core liquid mass, aiding LTCC.

Whether the increase in core liquid inventory is also aided by the flow supplied at the core inlet can be identified by a comparison between the total core flow and the flow rate needed to match core boil-off. The flow rate to match the core boil-off rate was calculated by dividing the core power by the core average h_{fg} . Figure B-13 compares the integrated inlet flow rate vs. the integrated boil-off rate. The figure shows the flow supplied to the core is larger than the boil-off rate after the time that switchover to recirculate from the containment sump has occurred for both cases. The increase in core liquid mass can therefore be partially attributed to the inlet flow.

The different inlet flow between Case 1 and Case 2 shown in Figure B-13 can be explained due to the difference in the resistance at the core inlet. The resistance ramp, which simulates debris build up, effectively decreases the core inlet flow and causes the core liquid inventory to increase at a lower rate. The core inlet flow rate is governed by the driving head in the downcomer and the amount of flow resistance. The collapsed liquid level (CLL) for each downcomer (DC) channel is plotted in Figure B-14 through B-16. In Case 2, the DC CLL increases well before the DC CCL calculated for Case 1. The increase in the downcomer CLL for Case 2 is calculated to occur due to the large resistance at the core inlet.

In Case 1, the DC CLL increases at a slower rate than Case 2. Although the resistance is ramped in Case 1 to block 82% of the core flow area, significant flow is still able to enter the core without the additional build-up of driving head in the downcomer. The higher core inlet flow rate for Case 1 shown in Figure B-13 increases the UP liquid inventory and eventually increases the liquid flow rate in the loops. The integral of the HL liquid flow rates for each loop are compared in Figures B-17 through B-19. The increased loop liquid flow in Case 1 allows for some liquid inventory to flow through the steam generators and eventually make it back into the downcomer, increasing the downcomer liquid level starting around 1600 seconds (as shown in Figures B-14 through B-16) and increasing the driving head. The build up of driving head explains the increase in the core inlet flow rate for Case 1 shown in Figure B-13.

Finally, the PCT of the hot rod is examined. The hot rod PCT vs. time is displayed in Figure B-20. WC/T predicts the PCT to occur for both cases within the traditional LOCA analysis space. After roughly 300 seconds the core is quenched and no significant heatup occurs thereafter. Because no late heat up occurs, the local maximum and core-wide oxidation calculations for traditional LOCA analyses are still considered applicable. It is concluded that sufficient liquid can enter the core to remove core decay heat once the plant has switched to sump recirculation with up to 99.4% core blockage.

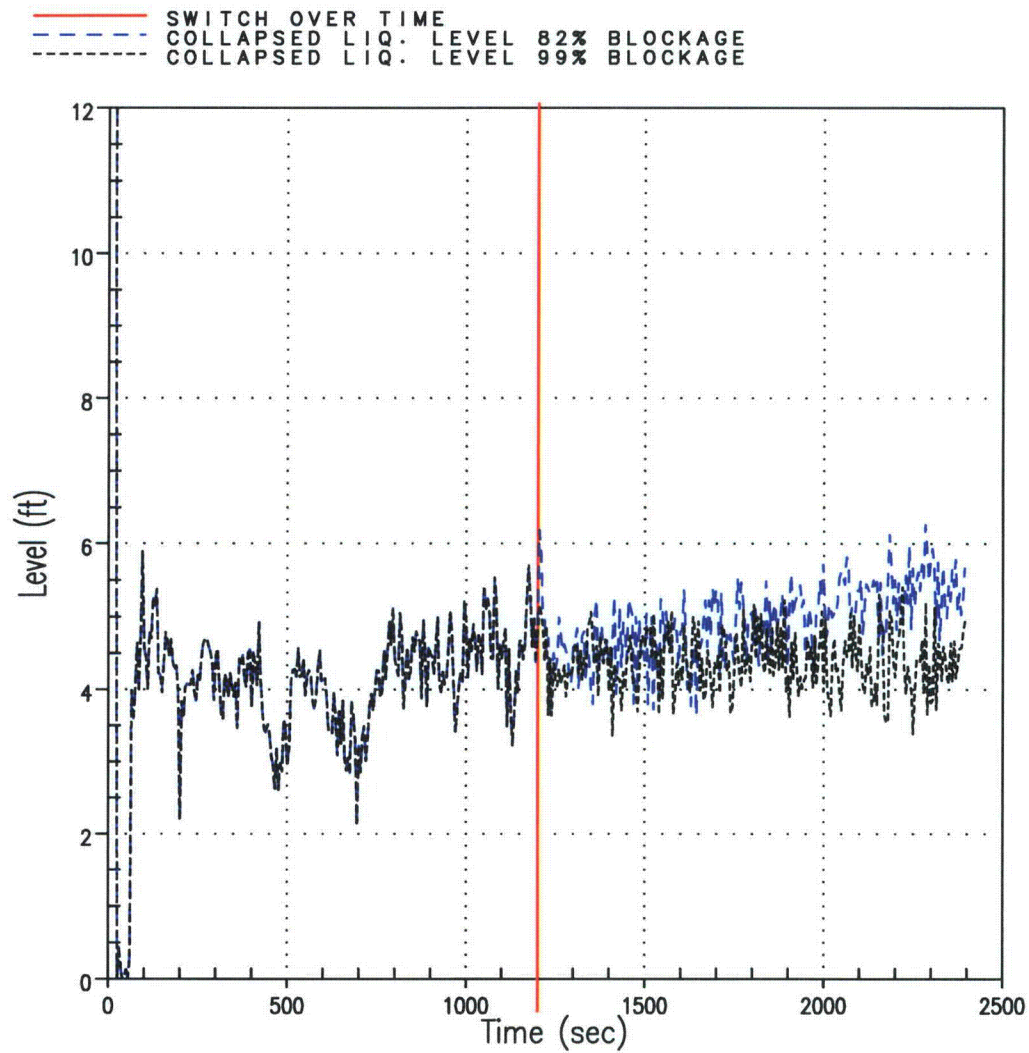


Figure B-9 Average Core Channel Collapsed Liquid Level for Case 1 and Case 2

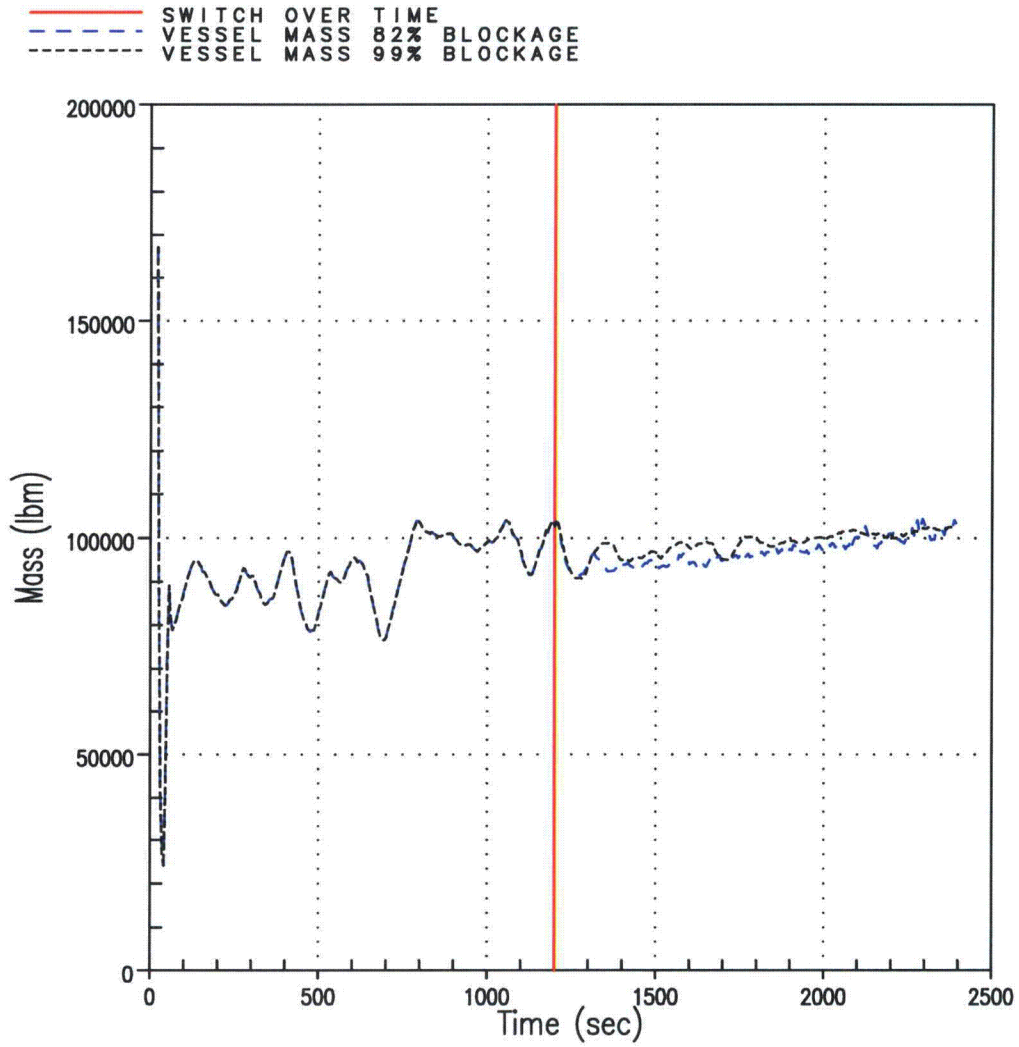


Figure B-10 Total Vessel Liquid Mass for Case 1 and Case 2

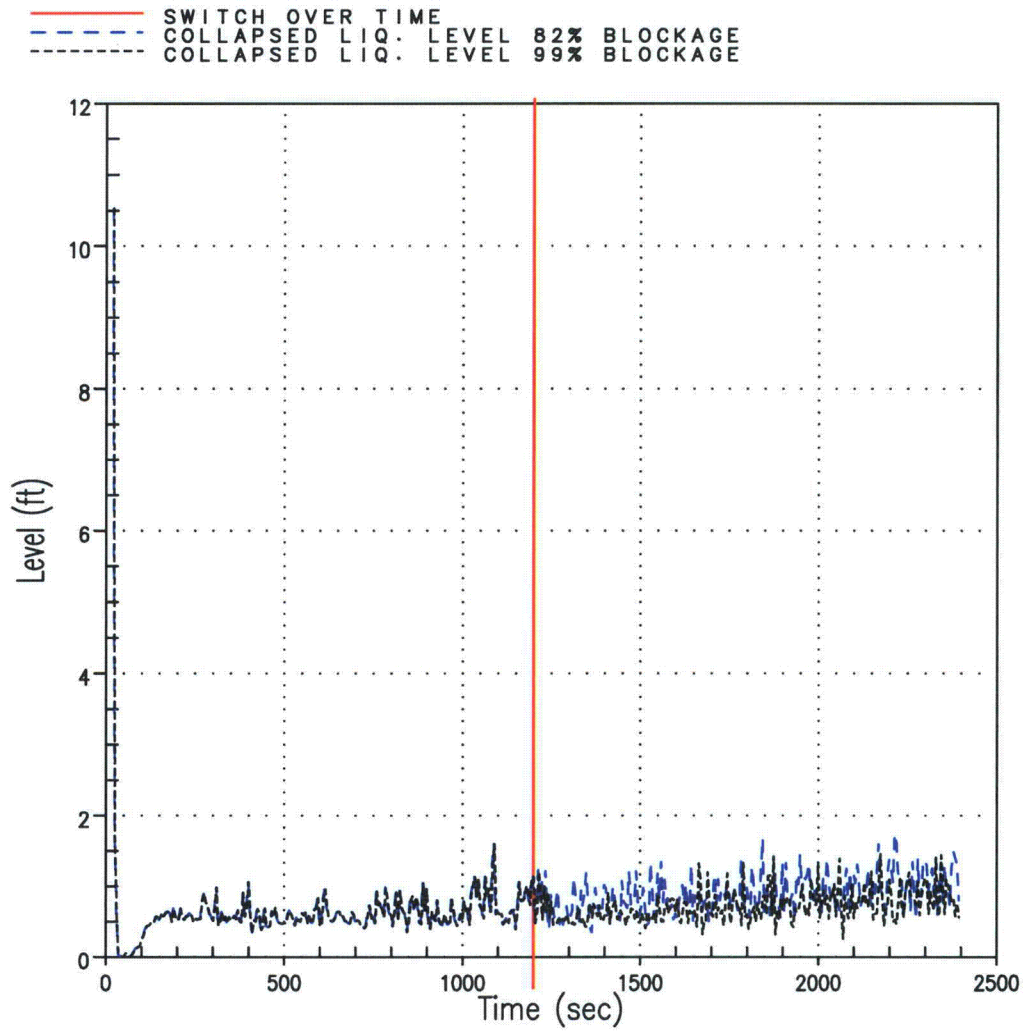


Figure B-11 Upper Plenum Global Channel Collapsed Liquid Level for Case 1 and Case 2

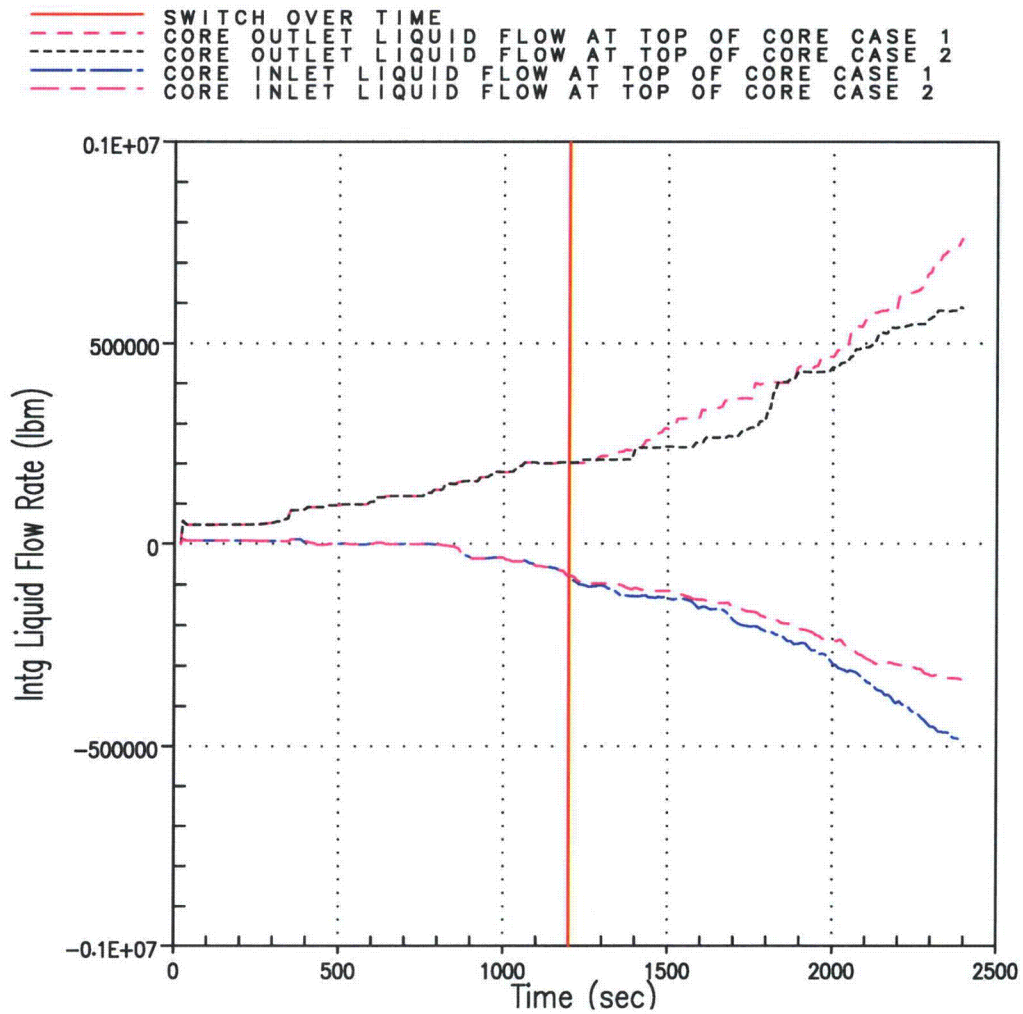


Figure B-12 Total Integrated Liquid Flow at the Top of the Core for Case 1 and Case 2
(Positive/Outlet flow represents HA, GT, AVG channels; Negative/Inlet flow represents LP channel)

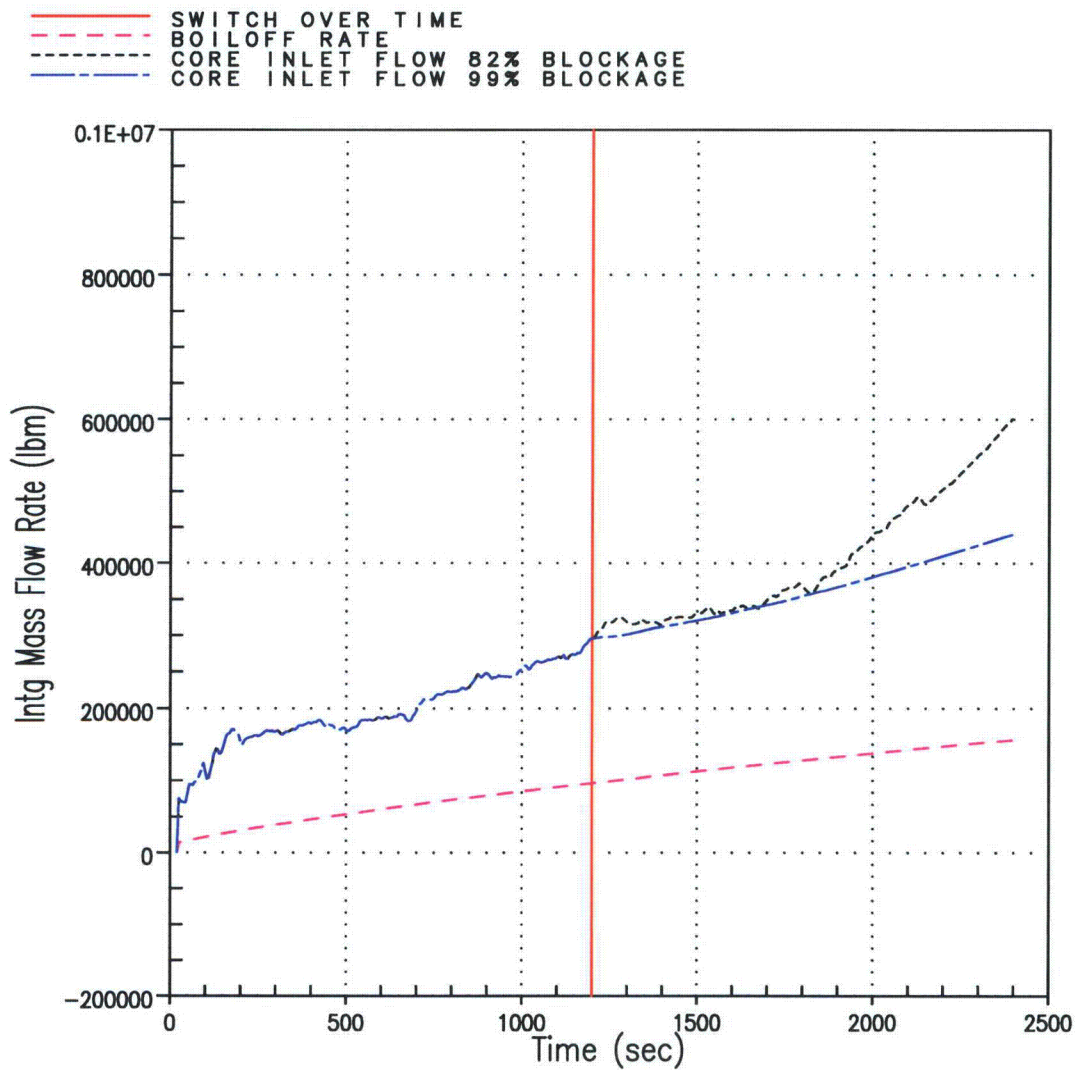


Figure B-13 Integrated Core Flow vs. Core Boil-off for Case 1 and Case 2

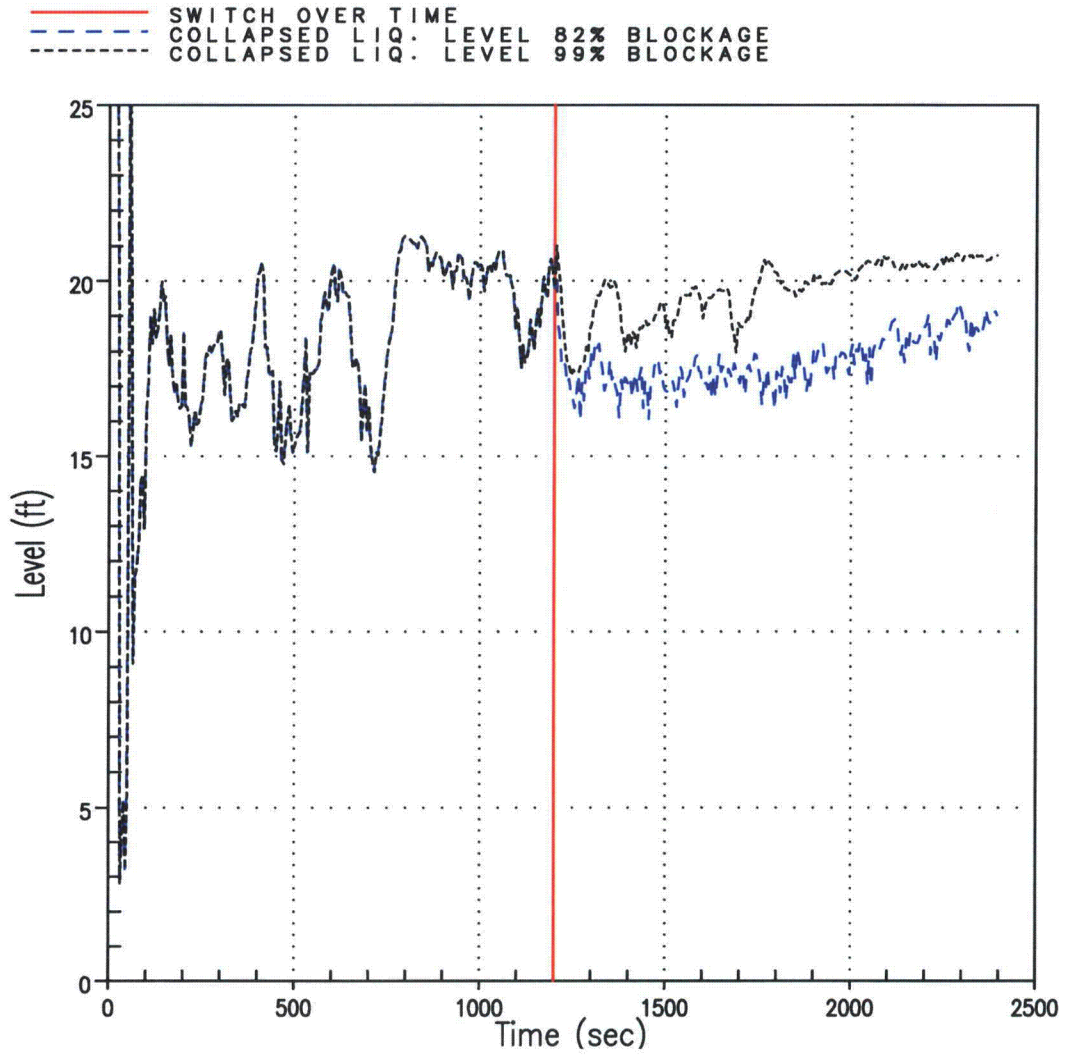


Figure B-14 Broken Loop DC Channel Collapsed Liquid Level for Case 1 and Case 2

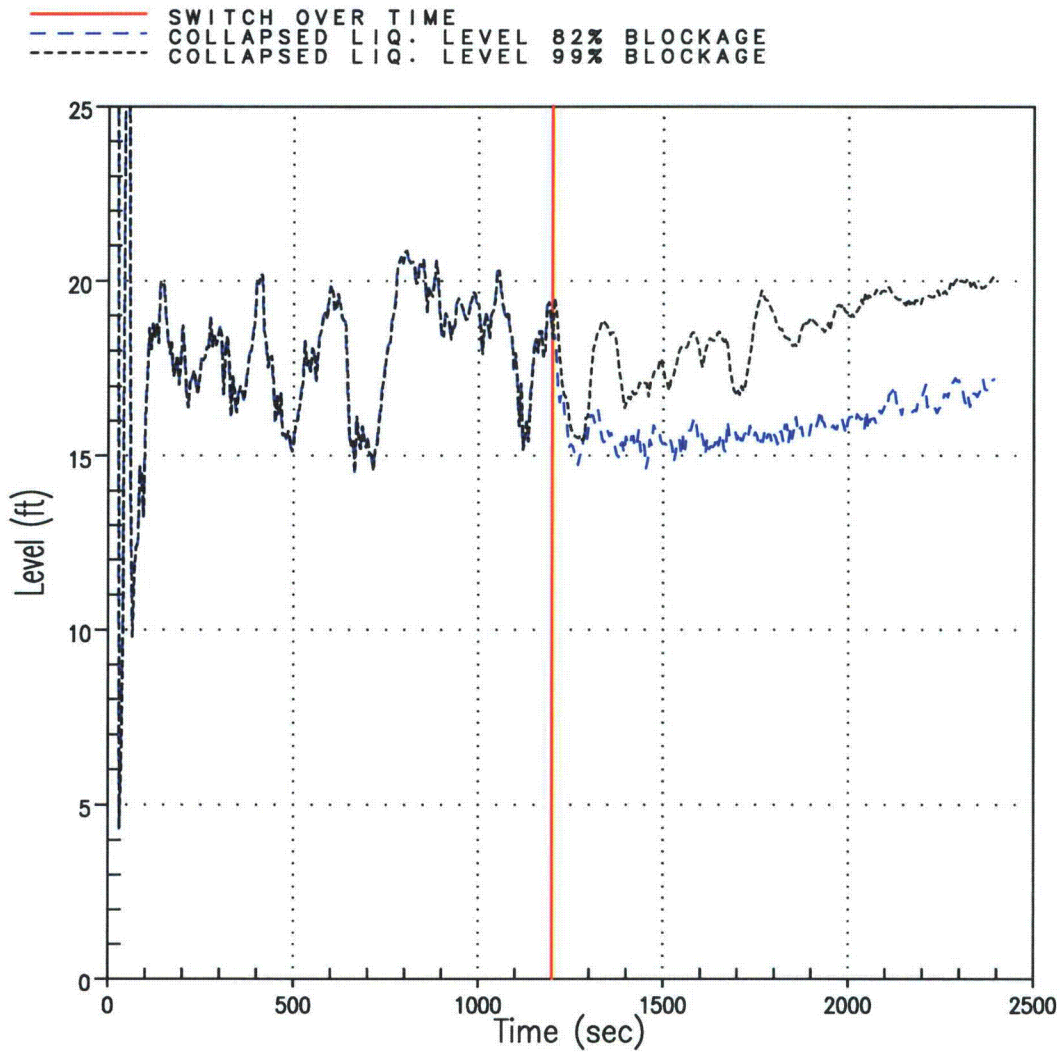


Figure B-15 Intact Loop DC Channel Collapsed Liquid Level for Case 1 and Case 2

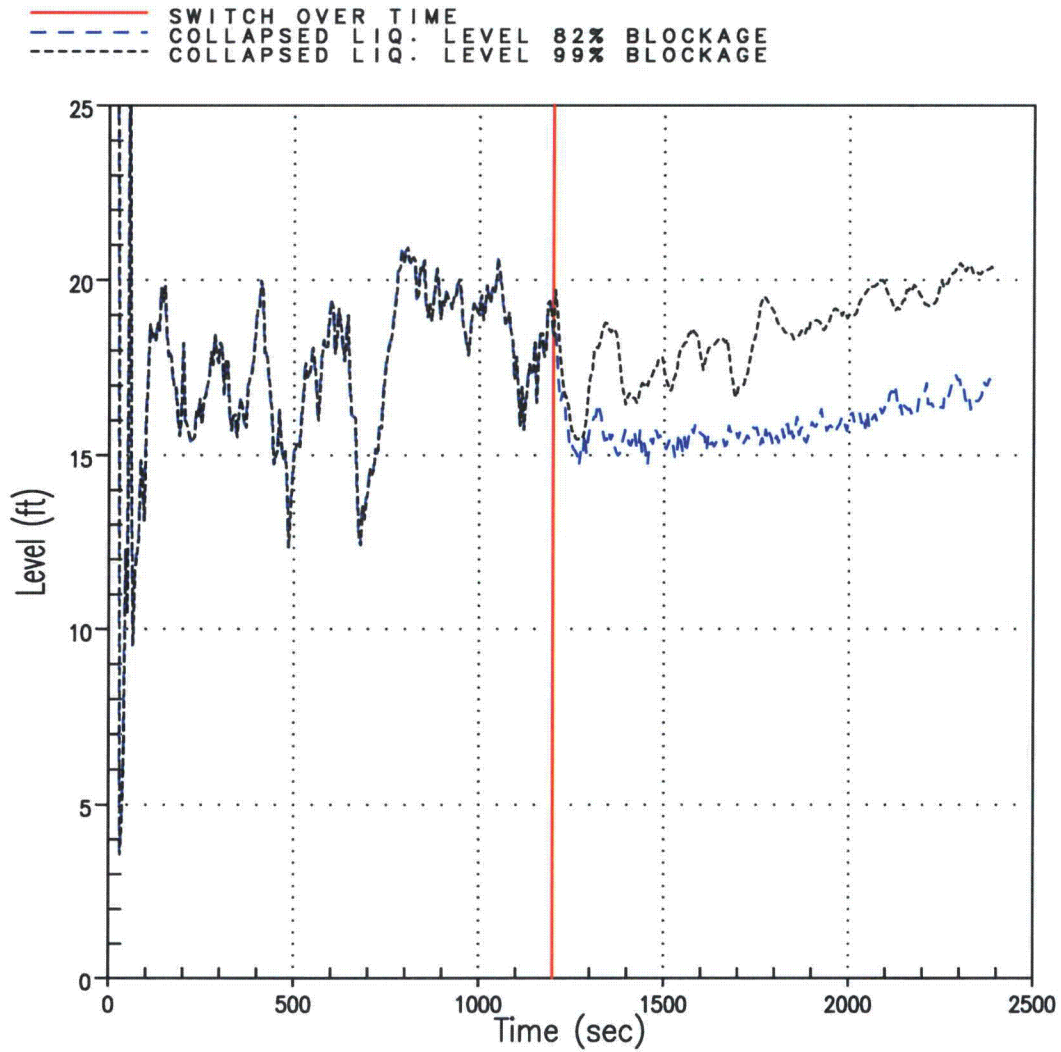


Figure B-16 Pressurizer Loop DC Channel Collapsed Liquid Level for Case 1 and Case 2

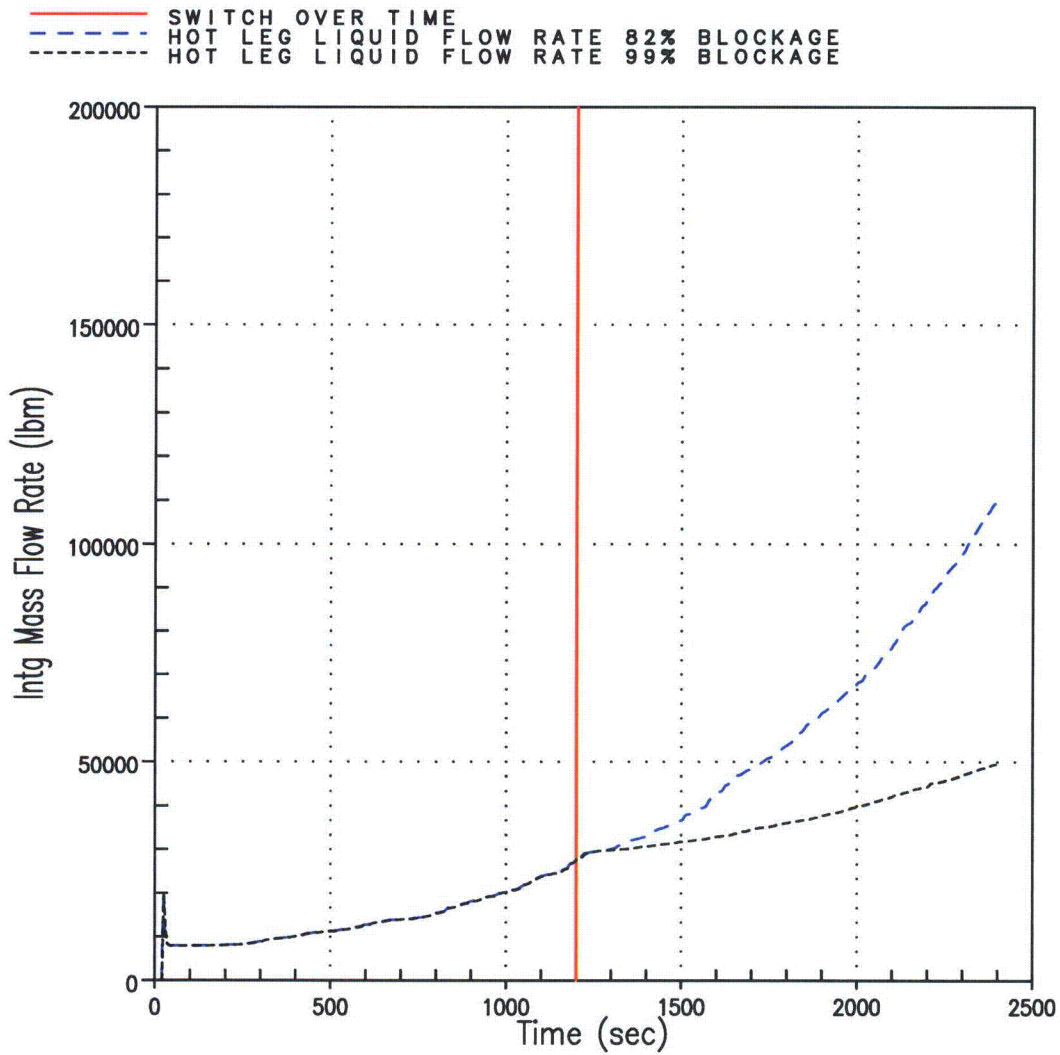


Figure B-17 Pressurizer Loop Hot Leg Integrated Liquid Flow for Case 1 and Case 2

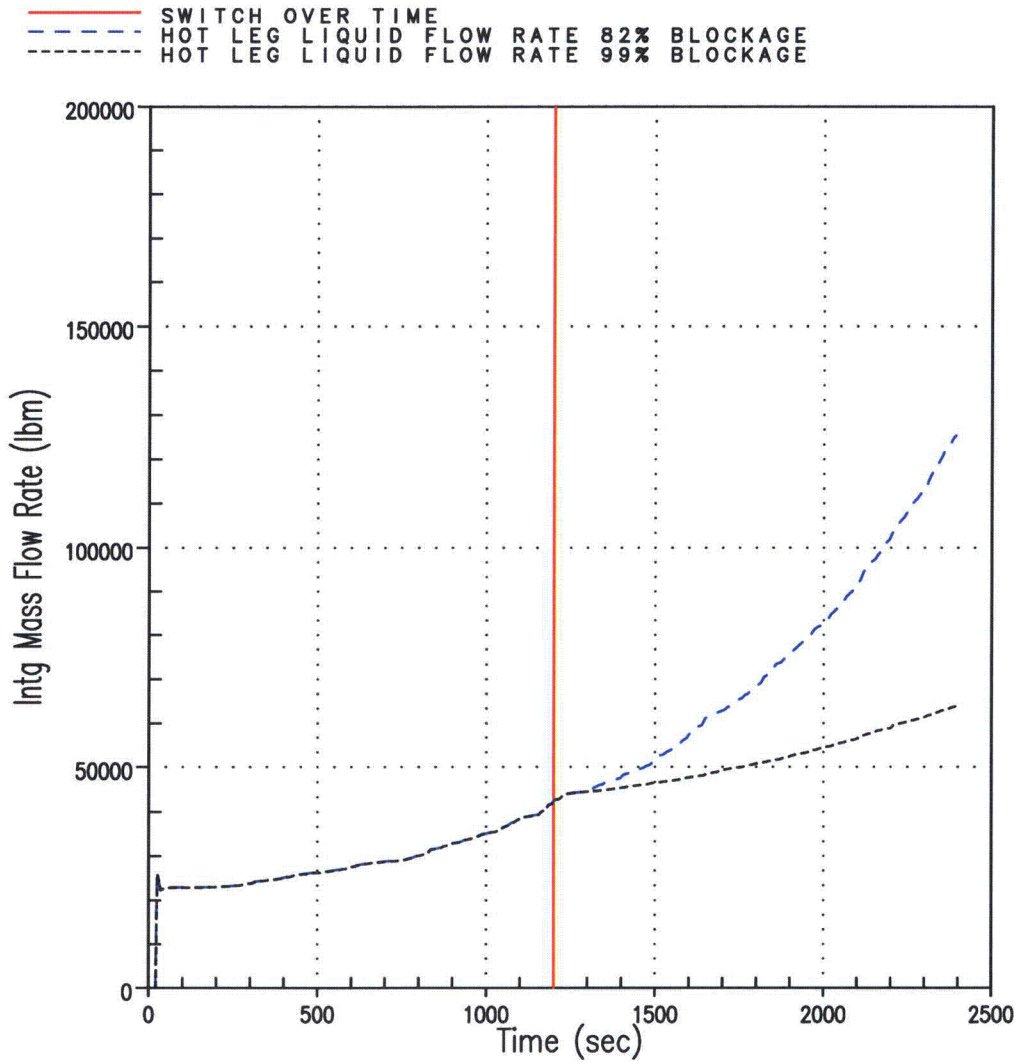


Figure B-18 Intact Loop Hot Leg Integrated Liquid Flow for Case 1 and Case 2

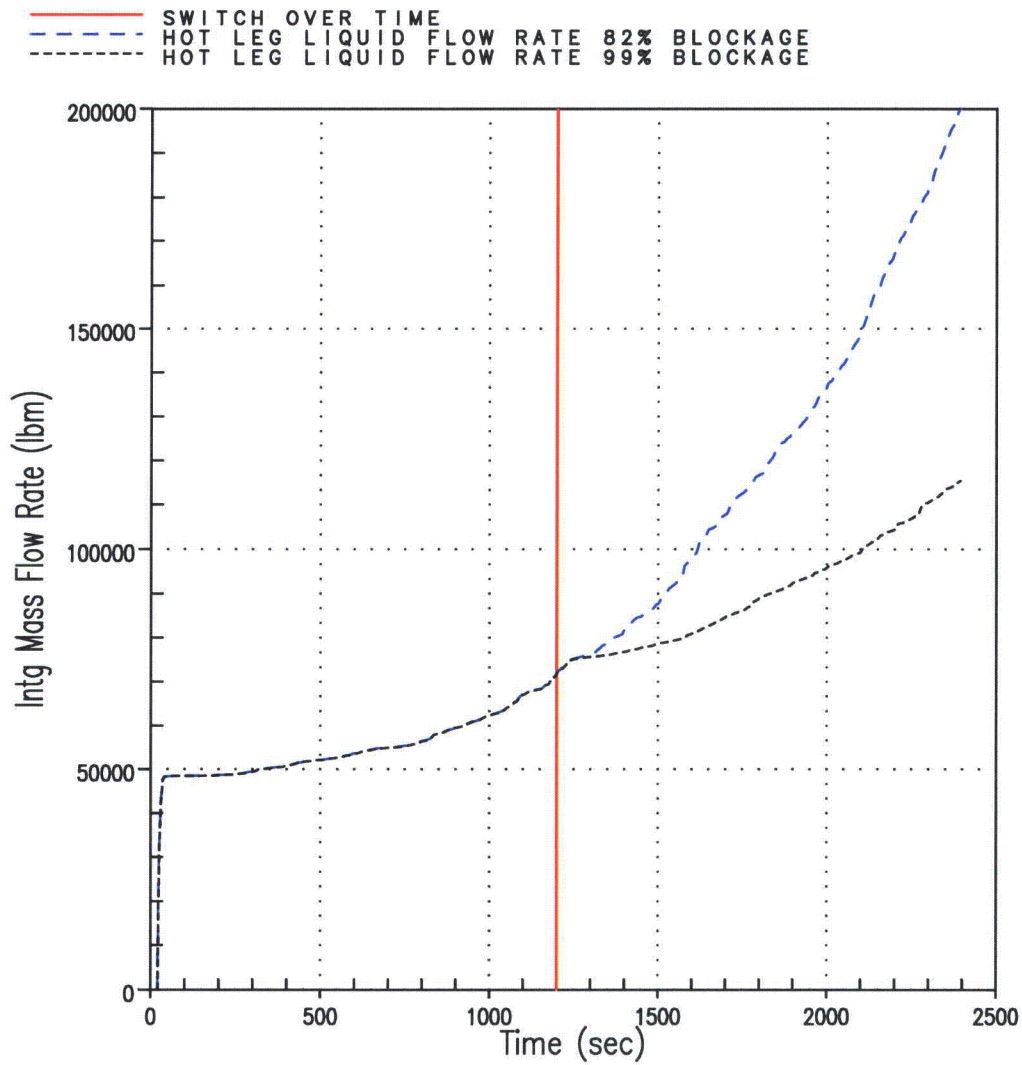


Figure B-19 Broken Loop Hot Leg Integrated Liquid Flow for Case 1 and Case 2

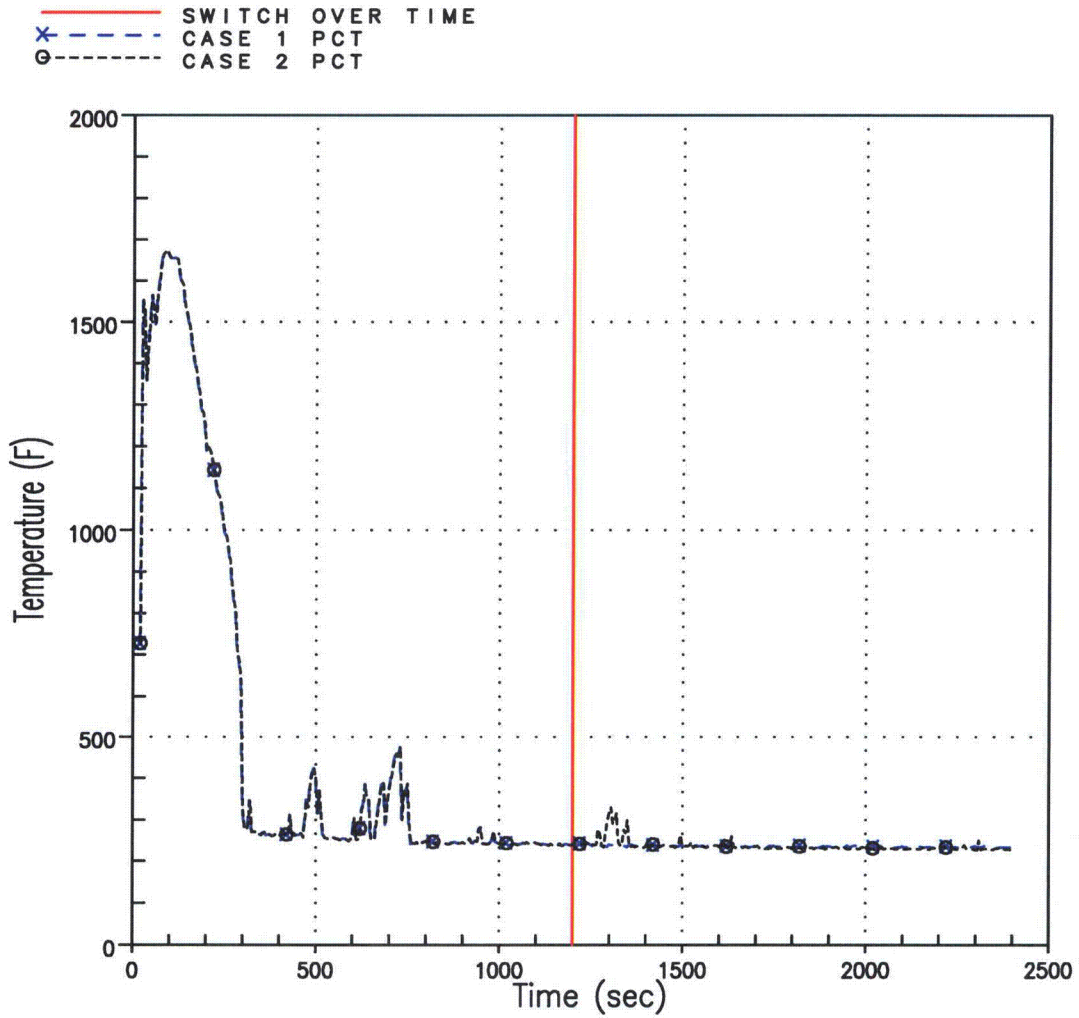


Figure B-20 Case 1 and Case 2 Hot Rod PCT

B.4 SUMMARY

The effects of 82% and 99.4% blockage of the core inlet flow area were examined using $\underline{WC/T}$. A comparison between the calculated rates and the flow rate needed to match core boil-off showed ample flow in the core to replace boil-off after core blockage occurred. Also, the PCT plot of the hot rod shows the PCT occurs in traditional LOCA analysis space and after roughly 300 seconds the core is quenched and no significant heatup occurs thereafter. Because no late heat up occurs, the maximum local and core-wide oxidation calculations for traditional analyses are still considered applicable. It is concluded that sufficient liquid can enter the core to remove core decay heat once the plant has switched to sump recirculation with up to 99.4% core blockage.

B.5 ADDITIONAL $\underline{WC/T}$ CALCULATIONS

Several additional $\underline{WC/T}$ analyses were performed in support of the effort documented by this report. These $\underline{WC/T}$ runs were performed at the request of the ACRS with the purpose of determining the blockage level (either using a reduction in area or increase loss coefficient) that would reduce core flow below that necessary to match coolant boil-off. The documentation for these additional calculations include figures of the integrated core inlet and exit flow, peak cladding temperature, core collapsed liquid level, core exit void fraction, and core pressure drop for the bounding conditions.

B.5.1 Method Discussion & Input

Two $\underline{WC/T}$ runs made in support of WCAP-16793-NP are described in Section B-3. These analyses demonstrated that up to 99.4% of the core inlet could be blocked and still maintain sufficient flow to reach the core to remove core decay heat. In order to assess the blockage level that would reduce core flow below that necessary to match coolant boil-off, modifications were made to the flow area and loss coefficient input values used in the original runs and the calculations repeated.

The base case for the calculation results presented in this section is Case 2, or the more restricted flow area case, from Section B-3. The Darcy equation defines pressure drop as being proportional to the form-loss coefficient and inversely proportional to the flow area squared. Using this principle, two separate approaches were taken to determine the blockage level needed to preclude sufficient flow into the core to provide for LTCC. The first approach considered an area reduction while maintaining the form-loss coefficients. The second approach considered form-loss coefficient increases while maintaining the flow area constant.

- For the first approach, the flow area of the hot channel, Channel 13 (see Figure B-7), was reduced. The input value of the hydraulic loss coefficient, C_D , for the other channels into the core, Channels 10, 11, 12 and 13 remained the same as the base case. As discussed, for this modeling approach, flow will only enter the core through the hot channel (Channel 13). To maintain the total core flow area, the adjacent channel (Channel 11, representing an “average channel”) flow area was increased to offset the change in flow area to Channel 13. This change is needed to preserve the total core flow area; however, no flow will enter the core through Channel 11. These cases are discussed in Section B.3.2.

For the second approach, the loss coefficients of the hot channel, Channel 13 (see Figure B-7), were increased in increments until the flow rate into the core was less than the core boil-off rate. These case are discussed in Section B.3.3..

B.5.2 Areas used in Reduced Flow Area Approach

The flow area values used in the two flow area reduction cases are as listed below.

Channel 13 50% Flow Reduction Case:

Channel 13 Flow Area	= 23.76 * (0.50)	= 11.88 in ²
Channel 11 Flow Area	= 1782 + 23.76 * (0.50)	= 1794. in ²

Channel 13 80% Flow Reduction Case:

Channel 13 Flow Area	= 23.76 * (0.20)	= 4.752 in ²
Channel 11 Flow Area	= 1782 + 23.76 * (0.80)	= 1801. in ²

Due to time constraints, the transient run time was reduced from 2400 seconds to 1500 seconds for the calculations that were performed. The transient calculation time of 1500 seconds is sufficient to demonstrate whether the reduction in core flow would be sufficient to match boil-off.

B.5.3 C_D Values used in Increased Loss Coefficient Approach

In order to determine the blockage level that would reduce core flow below that necessary to match coolant boil-off, the inlet core loss coefficients were increased in increments until boil-off could not be matched. The computer calculations made include uniform loss coefficients of 50,000, 100,000, and 1,000,000. The only changes required for these runs were updates to the variables used to activate the dimensionless loss coefficient ramp logic. For these cases, the C_D input value was changed from 10⁹ to desired C_D value to reduce flow through peripheral channels, the average channels and the hot assembly channel instead of block flow. Also, the feature to allow the C_D value of all core inlet channels to vary as a function of time was enabled.

Three runs were made; C_D = 50,000, C_D = 100,000 and C_D = 1,000,000. The increase in C_D values to the desired values was accomplished over a 30 second time interval. The ramp up started at the time of switchover from injection from the BWST/RWST to recirculation from the sump, transient time t = 1200 seconds and was completed at transient time t = 1230 seconds.

Again, due to time constraints, the transient run time was reduced from 2400 seconds to 1500 seconds for the calculations that were performed. The transient calculation time of 1500 seconds is sufficient to demonstrate whether the reduction in core flow would be sufficient to match boil-off..

B.5.4 Results from Flow Area Reduction Runs

The first flow reduction run performed reduced the hot channel (Channel 13) flow area by 50%, which yields a total core inlet flow reduction of 99.7% compared to an unblocked core. The plots for this case are shown in Figures B-21 through B-27. Figures B-21 and B-22 show comparisons of the integrated core inlet flow and the core boil-off rate. As shown, even with the increase in core blockage, the flow

that enters the core is still in excess of the boil-off rate. Figure B-23 displays the integrated liquid flow at the core exit. The figure illustrates that, although liquid in excess of that needed to keep the core quenched enters the core, every little liquid flow is present at the core exit after the blockage occurs. The Peak Cladding Temperature (PCT) is shown in Figure B-24. There are no significant PCT excursions after the core is blocked. Figure B-25 displays the collapsed liquid level of the average assembly core channel (Channel 11 of Figure B-7). The figure shows that the collapsed liquid level drops slightly at the time blockage occurs, however, the liquid level continues to increase even after the blockage to the hot channel (Channel 13) is fully implemented at 1230 seconds. The void fraction at the core exit shown in Figure B-26 again illustrates that liquid is present at the top of the core which shows the flow that enters the core after blockage occurs is still in excess of the boil-off rate. The core pressure drop is displayed in Figure B-27. The figure displays an increased pressure drop of roughly 2 psi as blockage at the core inlet is increased. As the conditions in the Reactor Coolant System (RCS) adjust to increase in core blockage, it is noticed that the core pressure drop fluctuates consistent with the core liquid level.

The next flow reduction run performed reduced the hot channel (Channel 13) flow area by 80%, which yields a total core inlet flow area reduction of 99.9%. The plots for this case are shown in Figures B-28 through B-34. Figures B-28 and B-29 show comparisons of the integrated core inlet flow and boil-off rate. As shown, with the increase in core blockage, the flow that enters the core cannot match the boil-off rate. Since all the liquid entering the core at the inlet is boiled-off, there is no liquid flow at the core exit (as shown in Figure B-30). In addition, Figure B-31 shows that the PCT increases until the end of the transient once the core liquid level, shown in Figure B-32, is reduced to a level that the core becomes unquenched. Continuing with the trend discussed above, the void fraction at the core exit (Figure B-33) shows that only vapor is present. The core pressure drop is displayed in Figure B-34. The figure displays a pressure drop of roughly 4 psi at the core inlet as a result of the blockage at the core inlet.

These results indicate that a total core inlet area reduction of up to as much as 99.7% will still allow sufficient flow into the core to provide for removal of decay heat and assure LTCC.

B.5.5 Results from Uniform Loss Coefficient Runs:

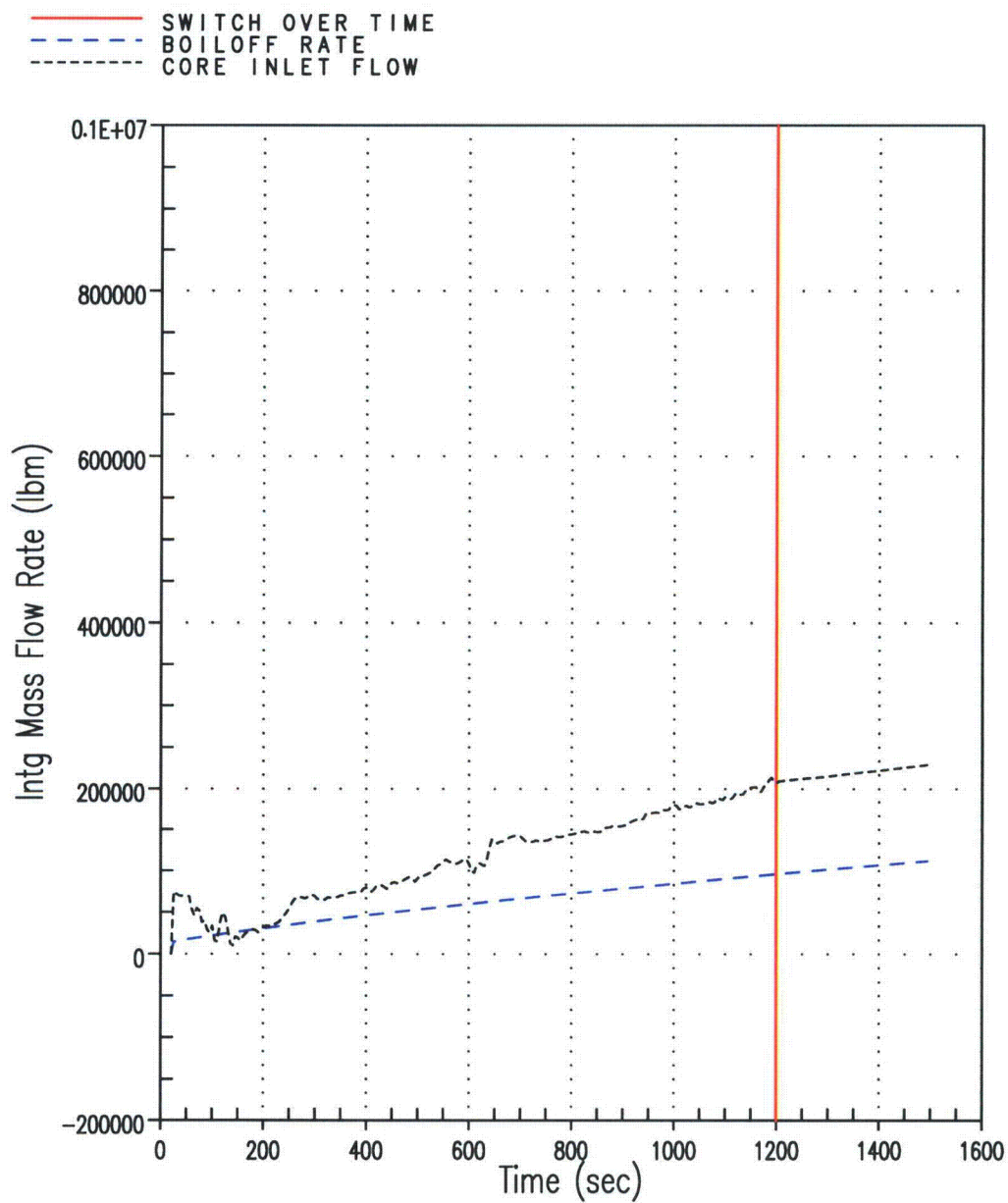
The first uniform loss coefficient run performed applied a uniform C_D of 50,000 at the core inlet. The plots for this case are shown in Figures B-35 through B-41. Figures B-35 and B-36 show comparisons of the integrated core inlet flow and boil-off rate. As shown, even with the increase of the loss coefficient at the inlet, the flow that enters the core is still in excess of the boil-off rate. (Note that the integrated mass flow behavior shown between time $t = 1200$ seconds and time $t = 1250$ seconds of Figure B-36 is the result of the 30 second ramp-up of the hydraulic loss coefficient, C_D , to 50,000 that is initiated in the calculations at time $t = 1200$ seconds.) Figure B-37 displays the integrated liquid flow at the core exit. The figure displays that liquid in excess of that needed to keep the core quenched enters the core and that liquid flow is present at the top of the core even after the increase of the loss coefficient at the inlet. The PCT is shown in Figure B-38. There are no significant PCT excursions after the core inlet loss coefficient is increased. Figure B-39 displays the collapsed liquid level of the average assembly core channel (Channel 11 of Figure B-7). The figure shows that the collapsed liquid level drops slightly at the time blockage occurs, however, the liquid is maintained even after the increase in the loss coefficient at the inlet. The void fraction at the core exit shown in Figure B-40 again illustrates that liquid is present at the top of the core which shows the flow that enters the core after the increase of the loss coefficient occurs is still in excess of the boil-off rate. The core pressure drop is displayed in Figure B-41. The figure

displays an increased pressure drop of roughly 2 psi as blockage at the core inlet is increased. As the conditions in the Reactor Coolant System (RCS) adjust to increase in core blockage, it is noticed that the core pressure drop fluctuates consistent with the core liquid level.

The second uniform loss coefficient run performed applied a uniform C_D of 100,000 at the core inlet. The plots for this case are shown in Figures B-42 through B-48. Figures B-42 and B-43 show comparisons of the integrated core inlet flow and boil-off rate. As shown, even with the further increase of the loss coefficient at the inlet, the flow that enters the core is still in excess of the boil-off rate. (Note that the integrated mass flow rate of Figure B-43 shows a similar behavior as was shown in Figure B-36. Again, this is due to the 30 second ramp-up of the hydraulic loss coefficient, C_D , to 100,000 that is initiated in the calculations at time $t = 1200$ seconds, but extends the behavior over a slightly longer period of time.) Figure B-44 displays the integrated liquid flow at the core exit. The figure displays that liquid in excess of that needed to keep the core quenched enters the core and that some liquid flow is still present at the top of the core even after the increase of the loss coefficient at the inlet. The PCT is shown in Figure B-45. There are no significant PCT excursions after the core inlet loss coefficient is increased. Figure B-46 displays the collapsed liquid level of the average assembly core channel (Channel 11 of Figure B-7). The figure shows that the collapsed liquid level drops slightly at time blockage occurs, however, the liquid level recovers even after the increase in the loss coefficient at the inlet. The void fraction at the core exit shown in Figure B-47 again illustrates that liquid is present at the top of the core which shows the flow that enters the core after the increase of the loss coefficient occurs is still in excess of the boil-off rate. The core pressure drop is displayed in Figure B-48. The figure displays an increased pressure drop of roughly 2 psi as blockage at the core inlet is increased. As the conditions in the RCS adjust to increase in core blockage, it is noticed that the core pressure drop fluctuates consistent with the core liquid level.

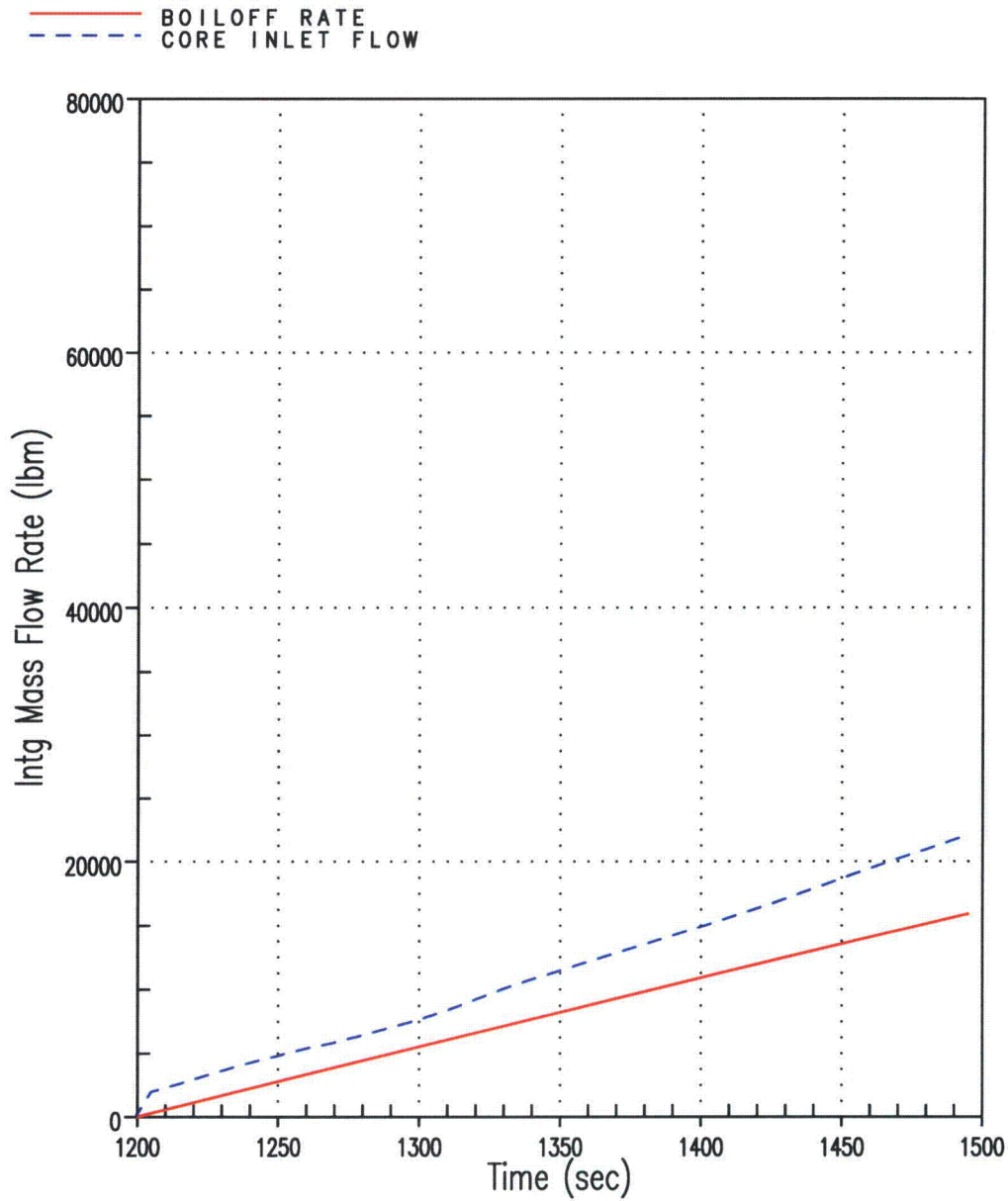
The next uniform loss coefficient run performed applied a uniform C_D of 1,000,000 at the core inlet. The plots for this case are shown in Figures B-49 through B-55. Figures B-49 and B-50 show comparisons of the integrated core inlet flow and boil-off rate. As shown, with the increase in core blockage, the flow that enters the core can not match the boil-off rate. Since all the liquid entering the core at the inlet is boiled-off, there is no liquid flow at the core exit (as shown in Figure B-51). In addition, it is displayed in Figure B-52 that the PCT increases until the end of the transient once the core liquid level, shown in Figure B-53, is reduced to a level that the core becomes unquenched. Continuing with the trend discussed above, the void fraction at the core exit (Figure B-54) shows that only vapor is present. The core pressure drop is displayed in Figure B-55. The figure displays an increased pressure drop of roughly 4 psi as blockage at the core inlet is increased and the core liquid level begins to stabilize.

The results indicate that an increase in the form loss coefficient at the core inlet of up to $C_D = 100,000$ for the limiting plant and fuel load design will allow for sufficient flow into the core to remove decay heat and provide for LTCC.



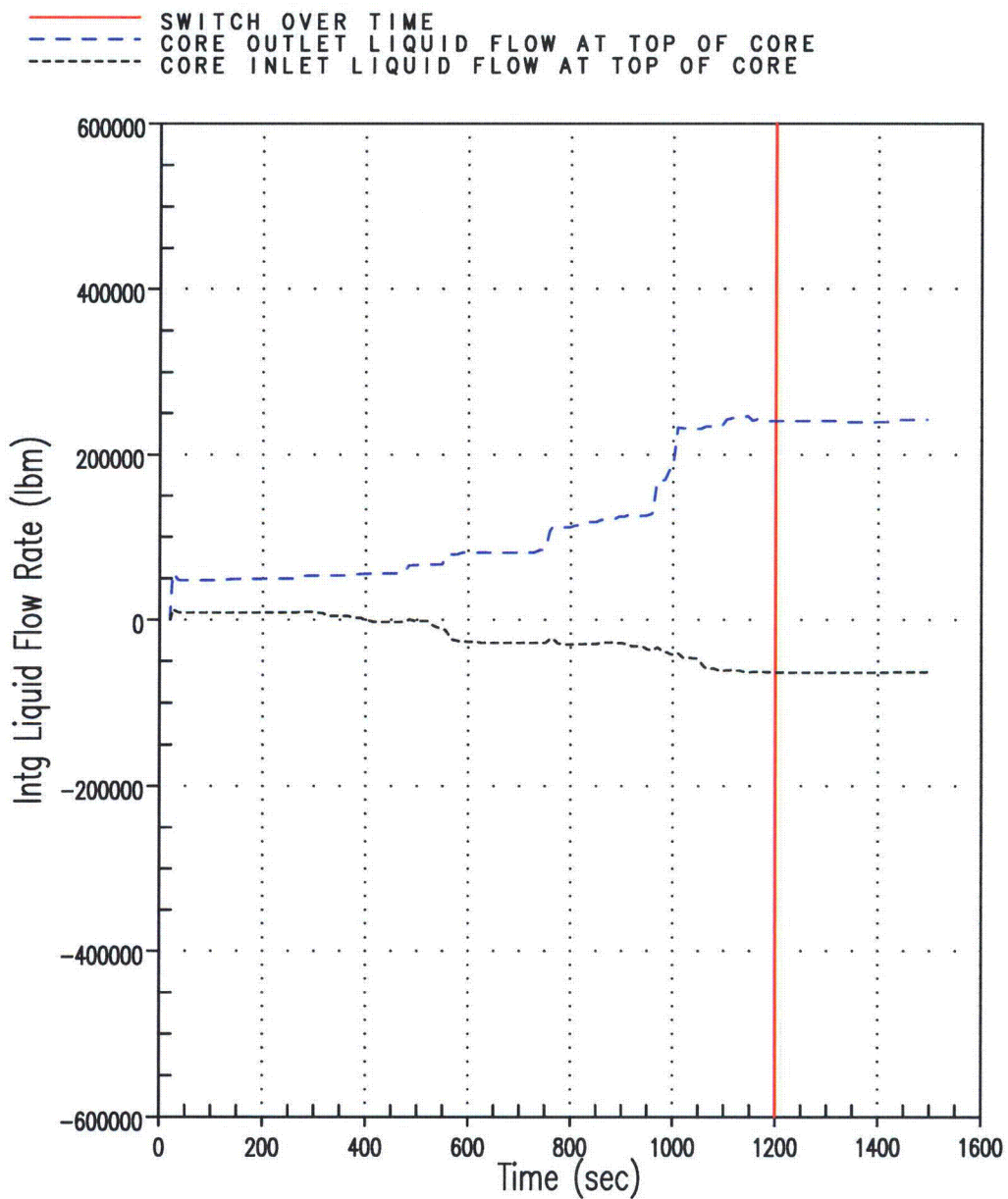
409461908

Figure B-21 Integrated Core Flow vs. Core Boil-off for Channel 13 Flow Reduction 50%



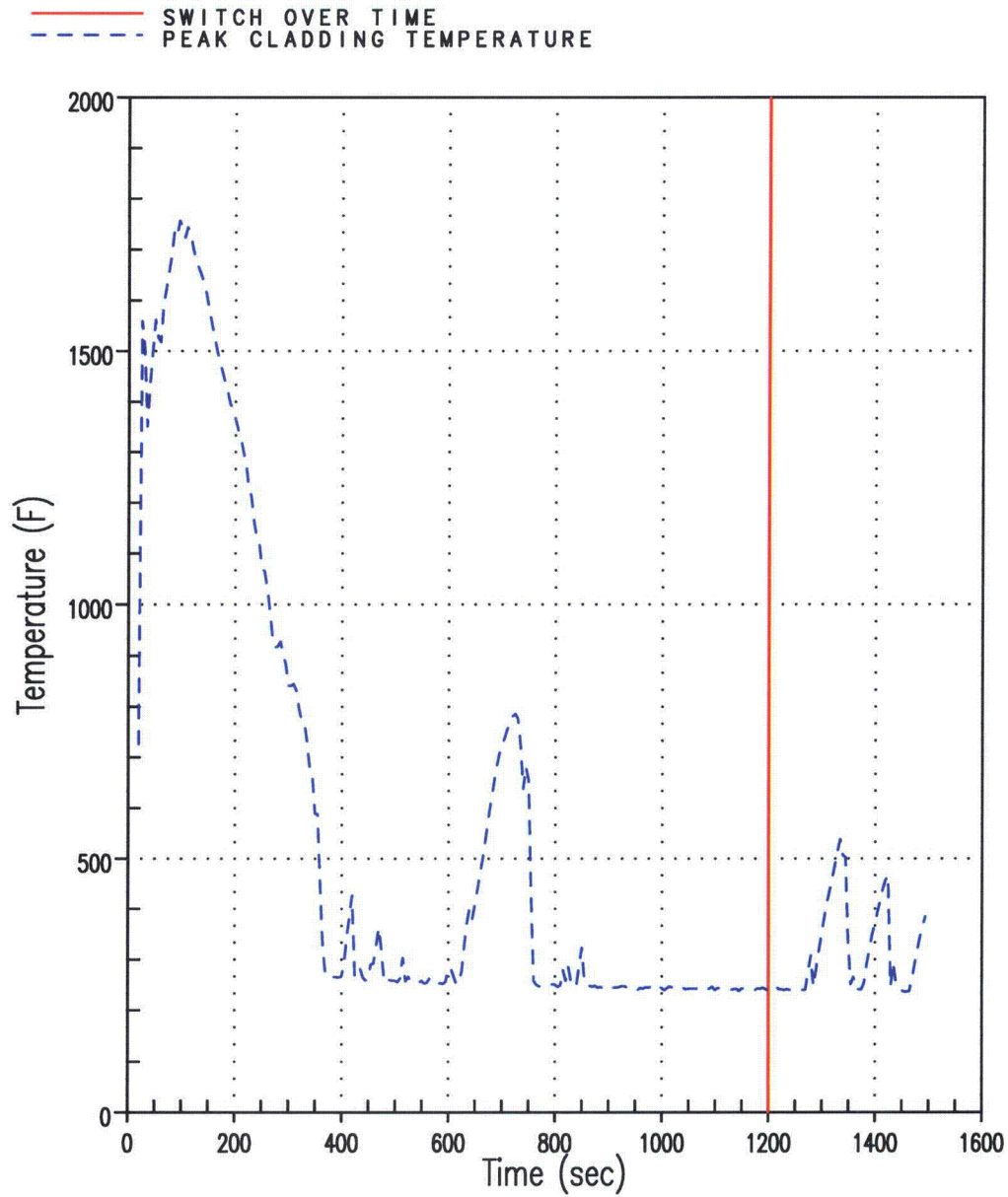
409461908

Figure B-22 Integrated Core Flow vs. Core Boil-off for Channel 13 Flow Reduction 50% Case (Shifted Scale)



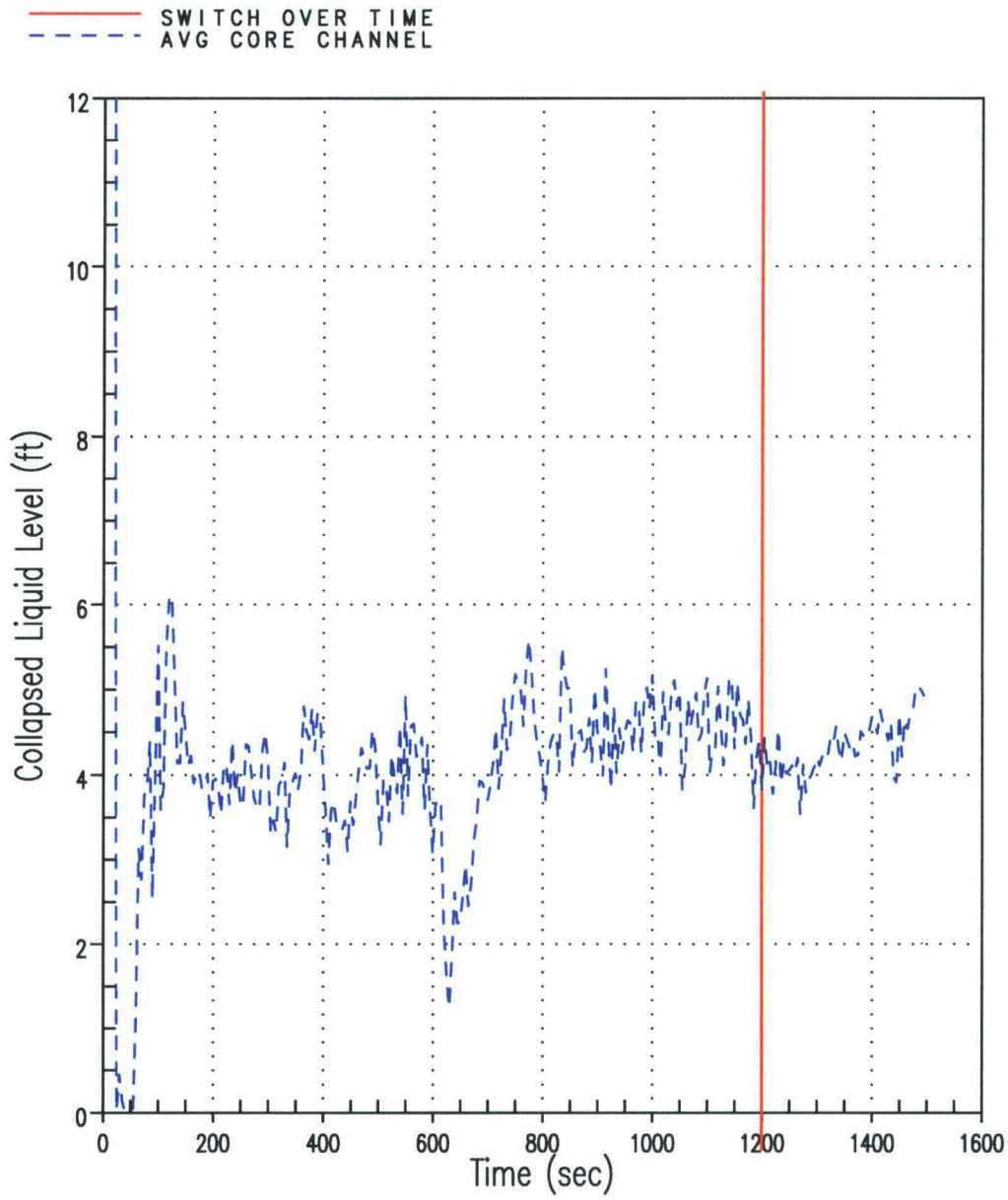
512214912

Figure B-23 Total Integrated Liquid Flow at the Top of the Core for Channel 13 Flow Reduction 50% Case (Positive/Outlet flow represents HA, GT, AVG channels; Negative/Inlet flow represent LP channel)



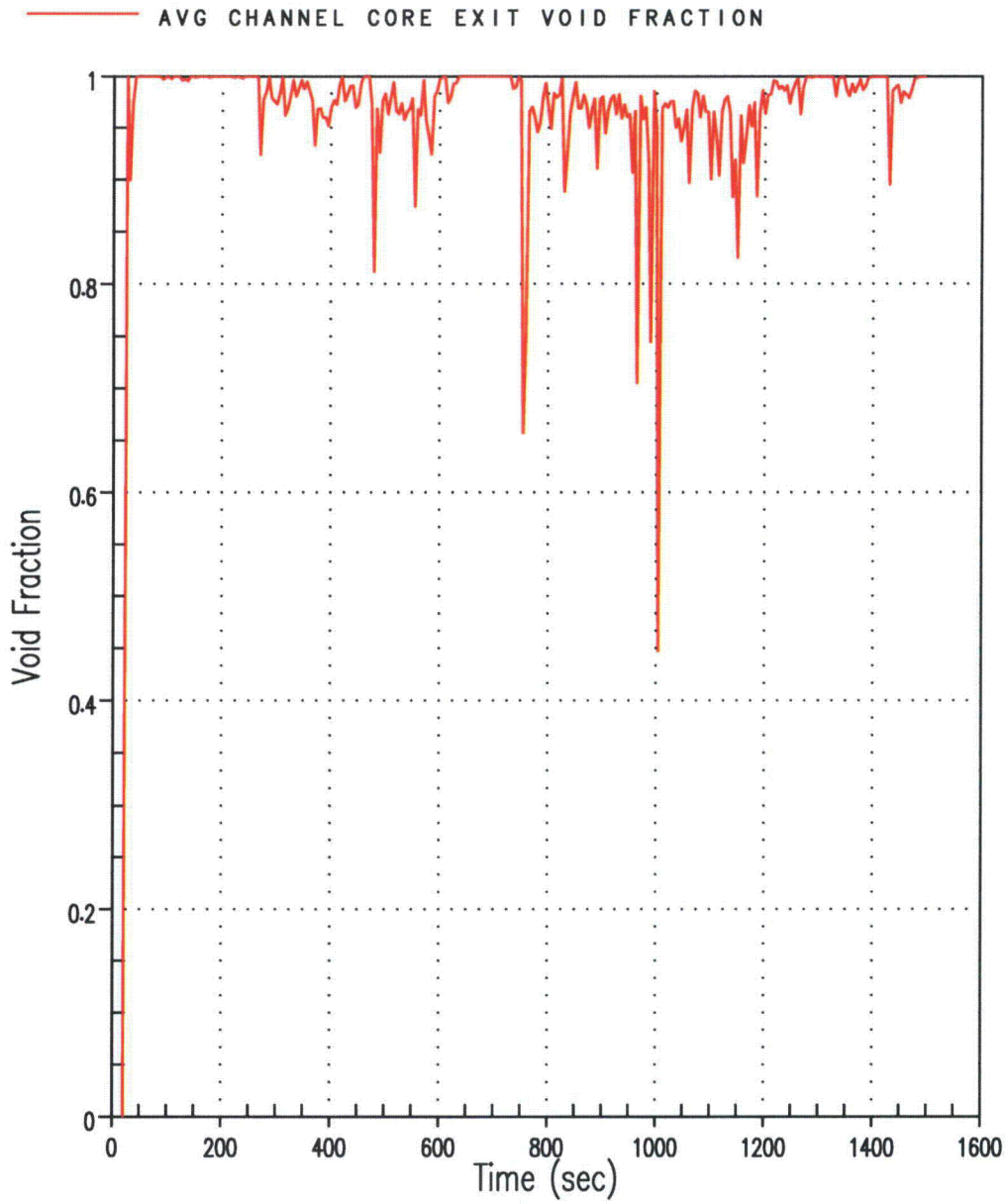
188413088

Figure B-24 Hot Rod PCT for Channel 13 Flow Reduction 50% Case



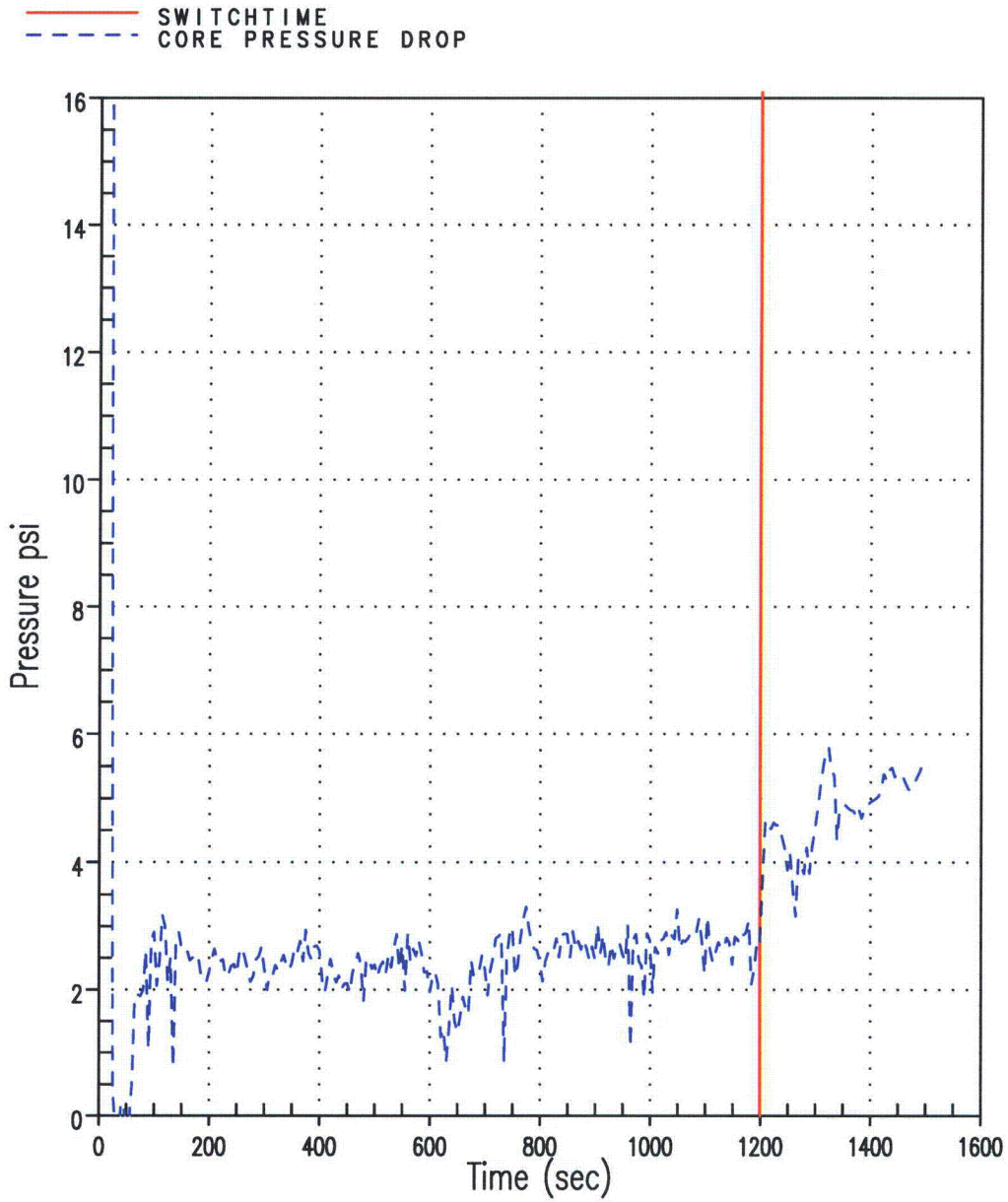
1075481719

Figure B-25 Average Core Channel CLL for Channel 13 Flow Reduction 50% Case



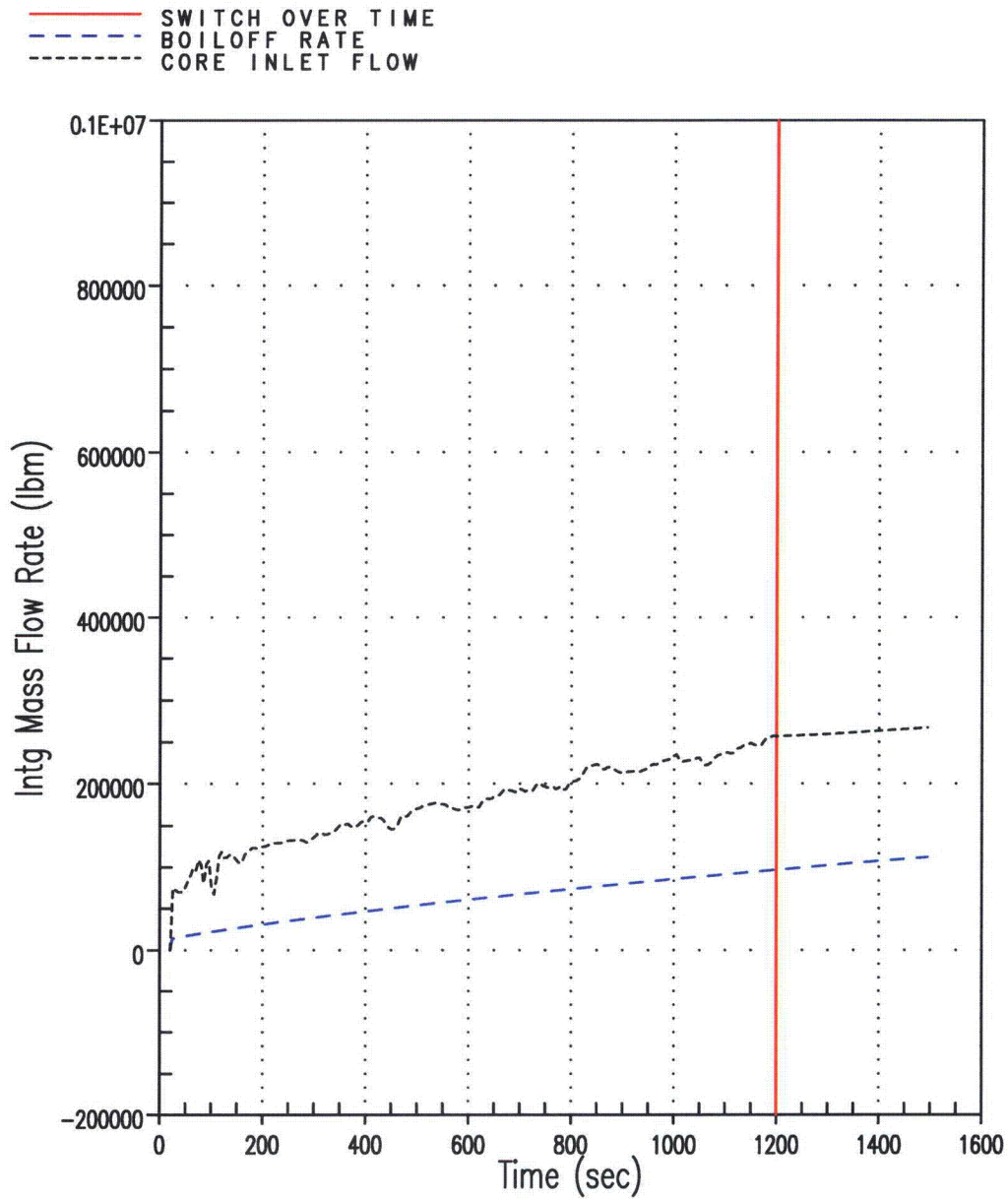
1951861530

Figure B-26 Void Fraction at the Exit of the Average Core Channel for Channel 13 Flow Reduction 50% Case



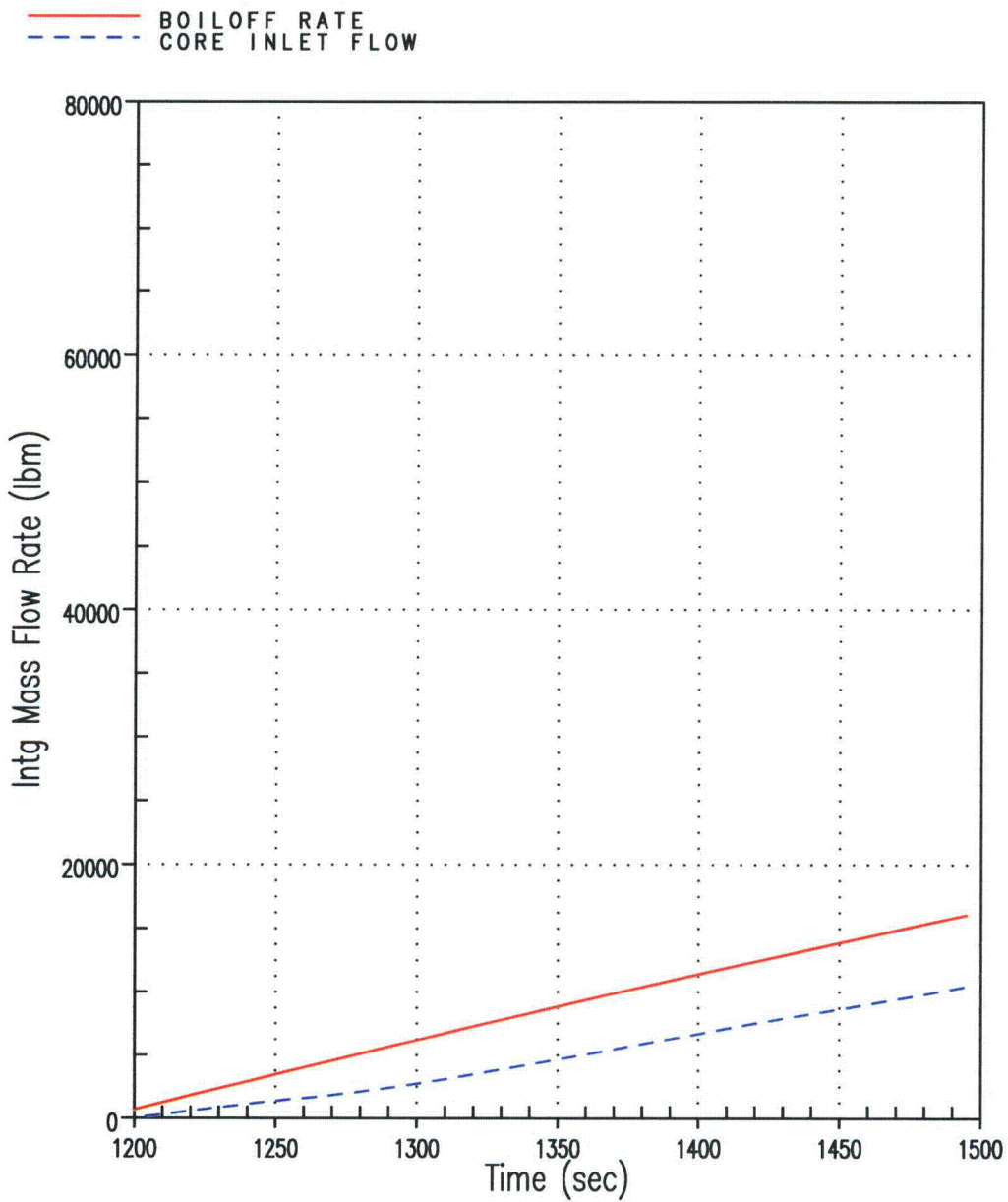
1566769324

Figure B-27 Core Pressure Drop for Channel 13 Flow Reduction 50% Case



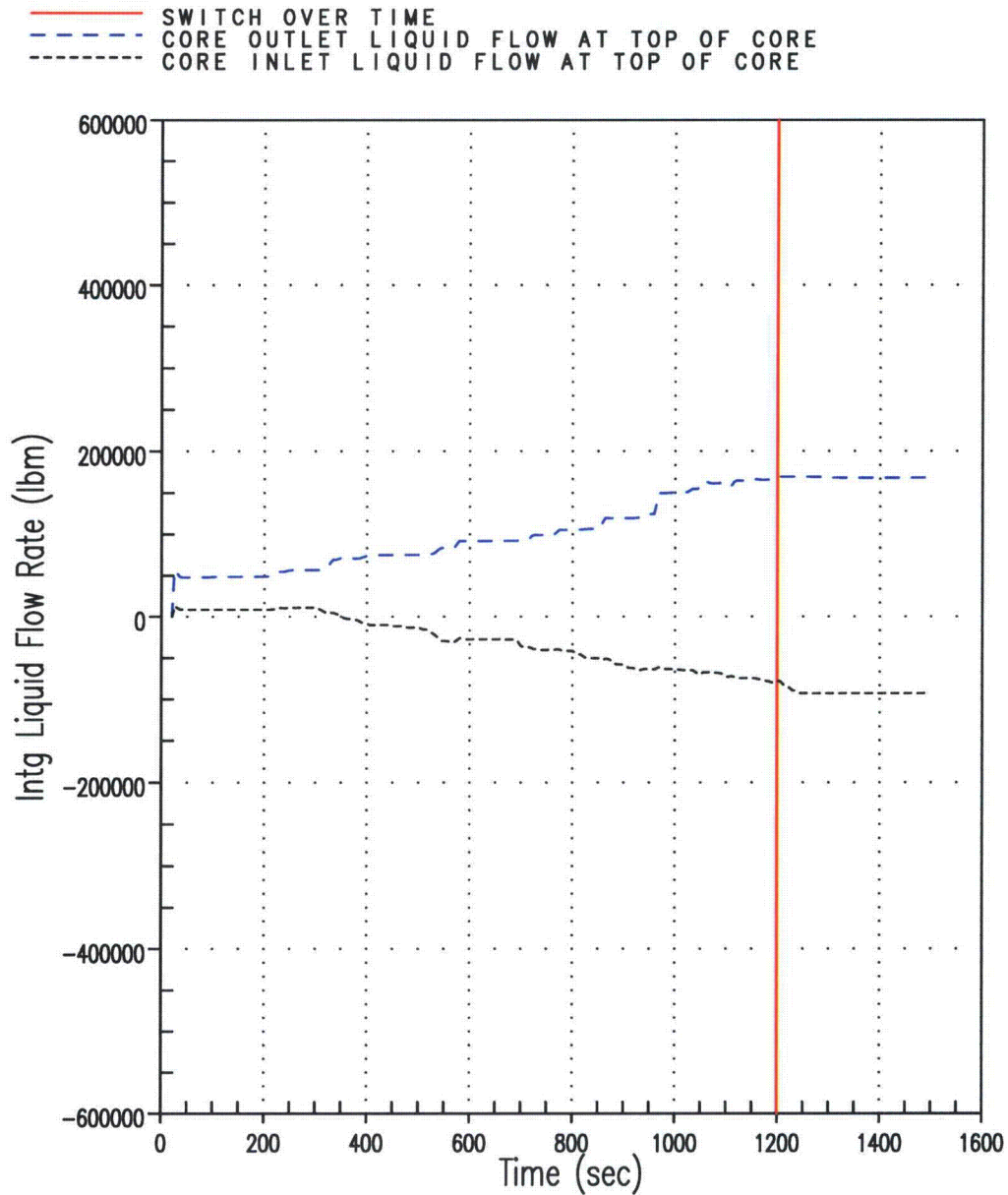
441943533

Figure B-28 Integrated Core Flow vs. Core Boil-off for Channel 13 Flow Reduction 80% Case



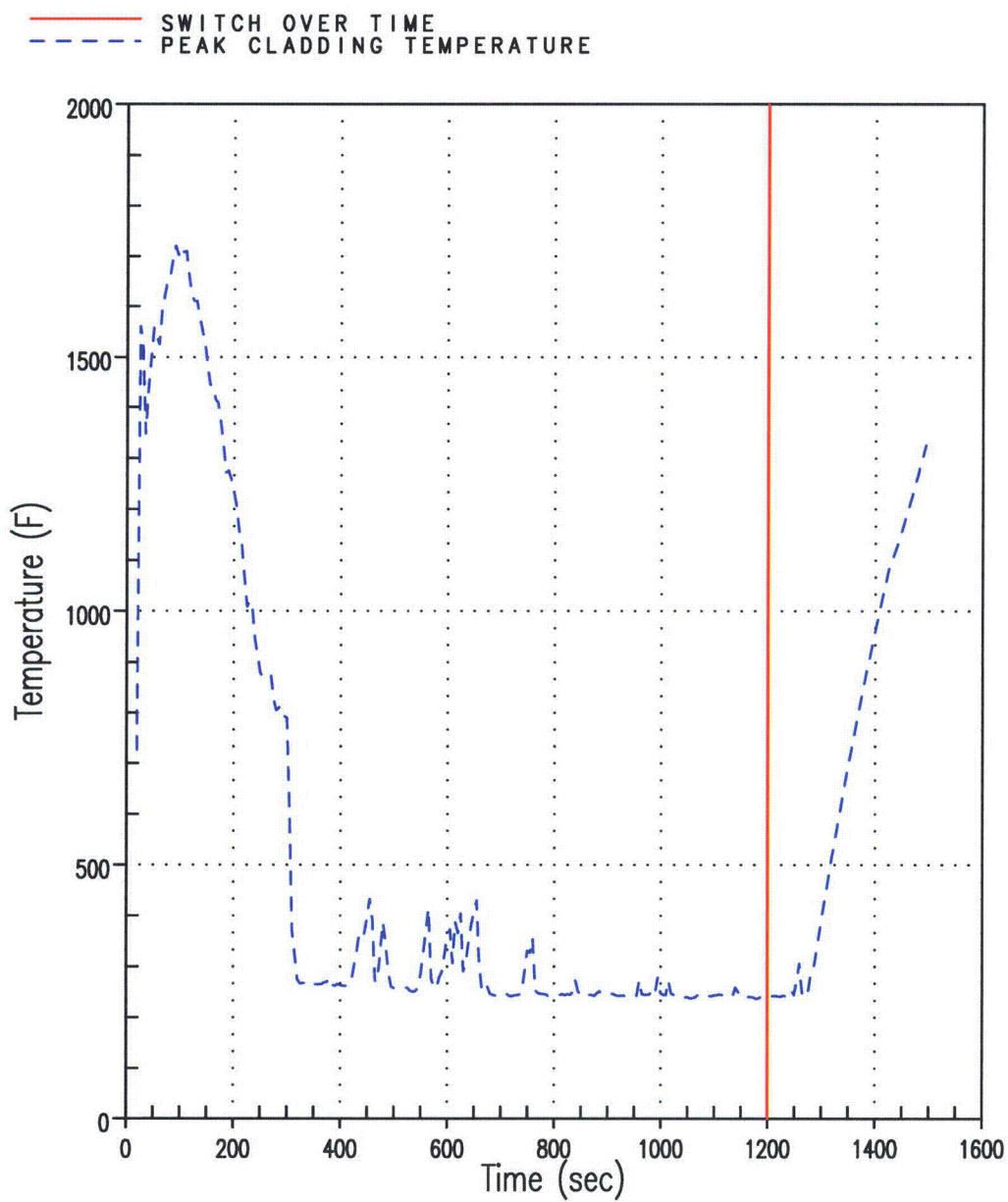
441843533

Figure B-29 Integrated Core Flow vs. Core Boil-off for Channel 13 Flow Reduction 80% Case (Shifted Scale)



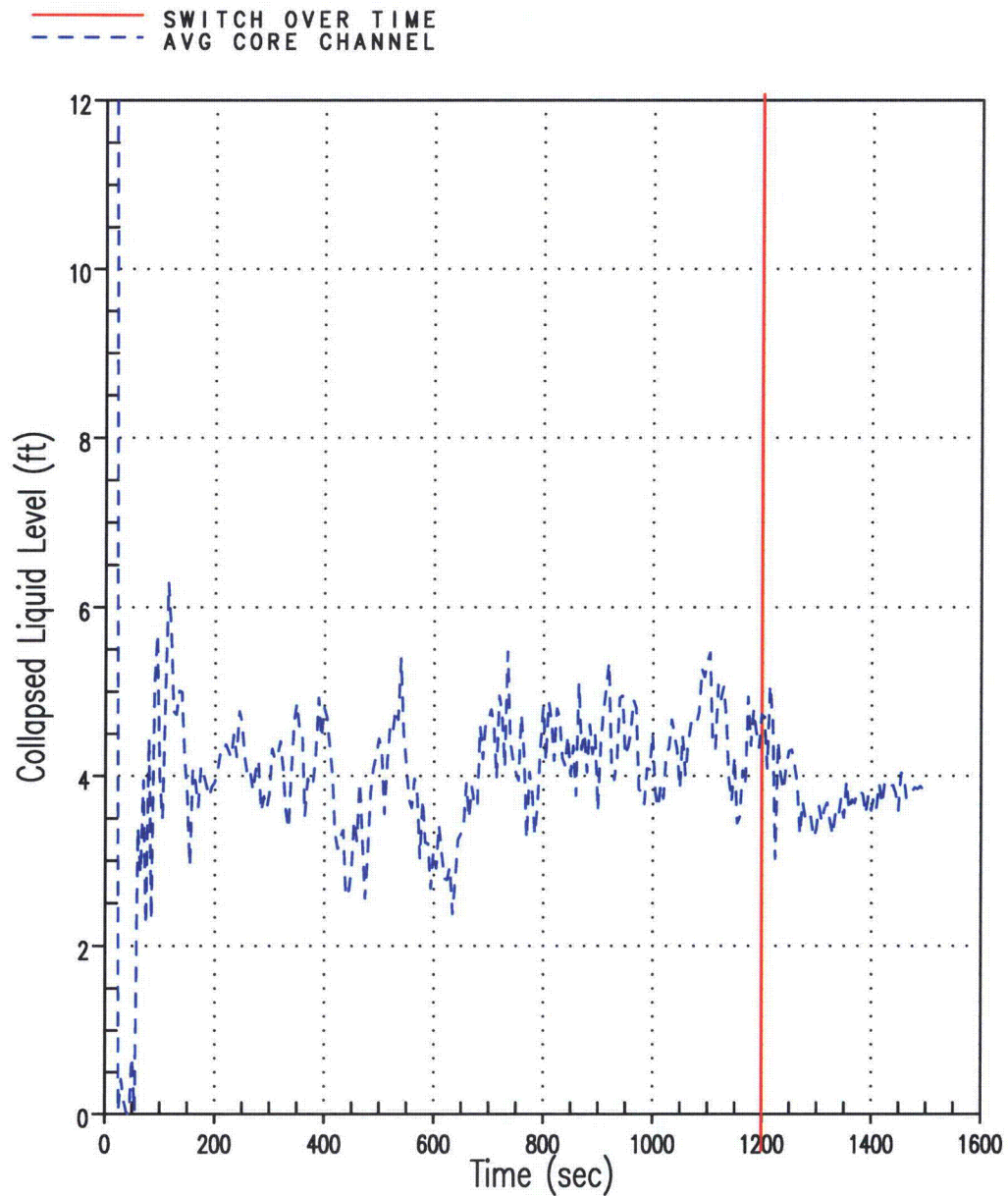
289992098

Figure B-30 Total Integrated Liquid Flow at the Top of the Core for Channel 13 Flow Reduction 80% Case (Positive/Outlet flow represents HA, GT, AVG channels; Negative/Inlet flow represent LP channel)



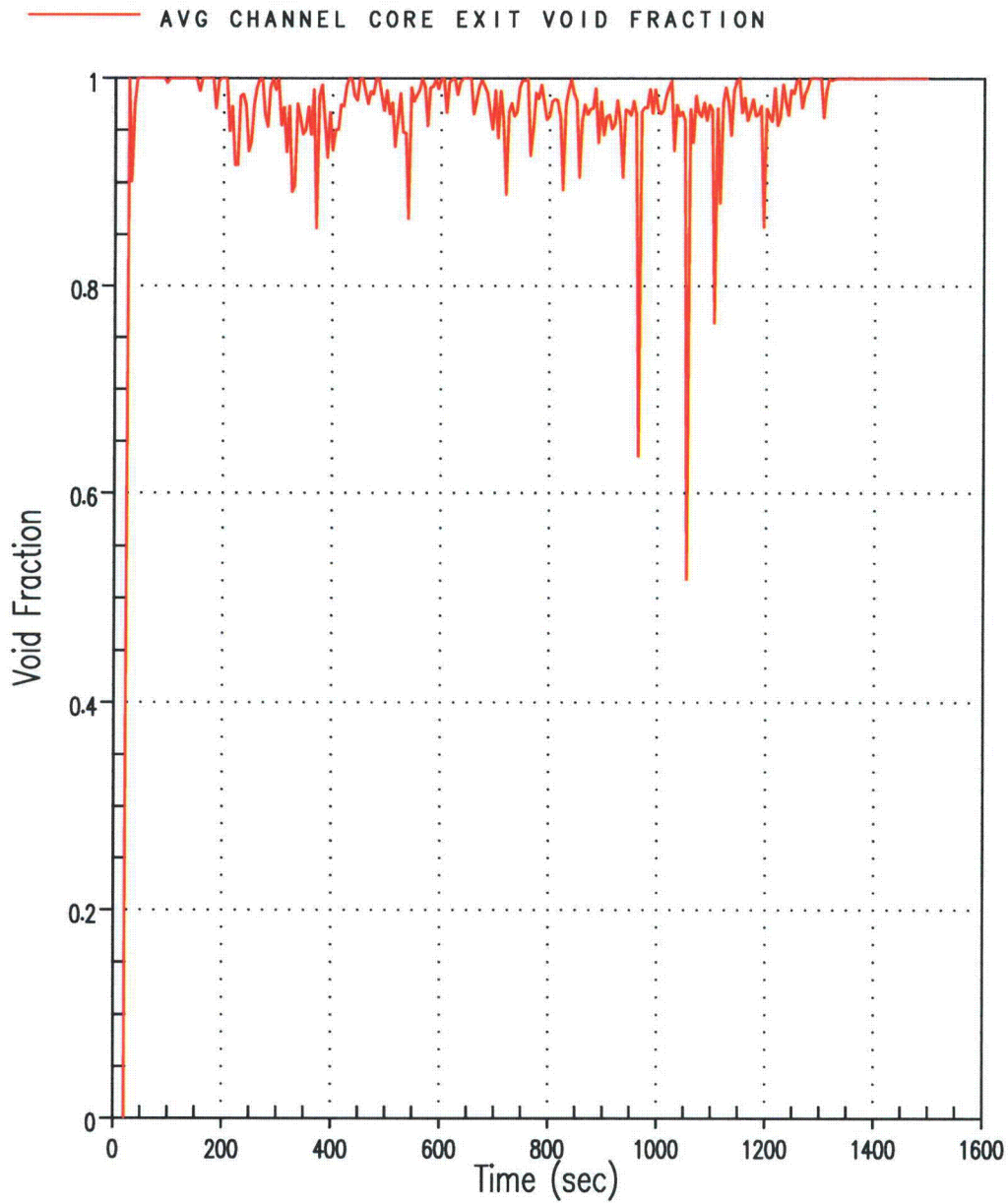
858292612

Figure B-31 Hot Rod PCT for Channel 13 Flow Reduction 80% Case



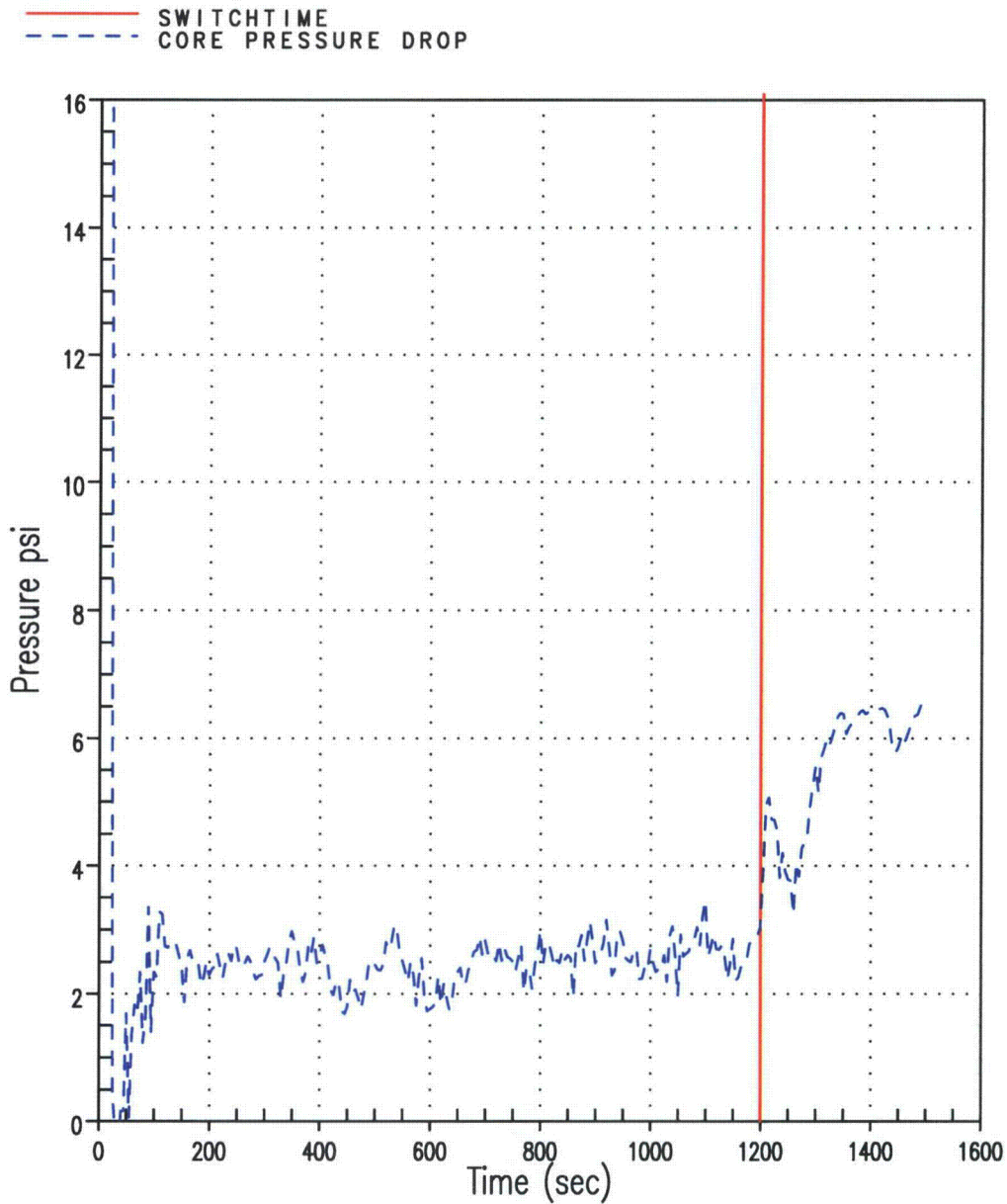
2061668183

Figure B-32 Average Core Channel CLL for Channel 13 Flow Reduction 80% Case



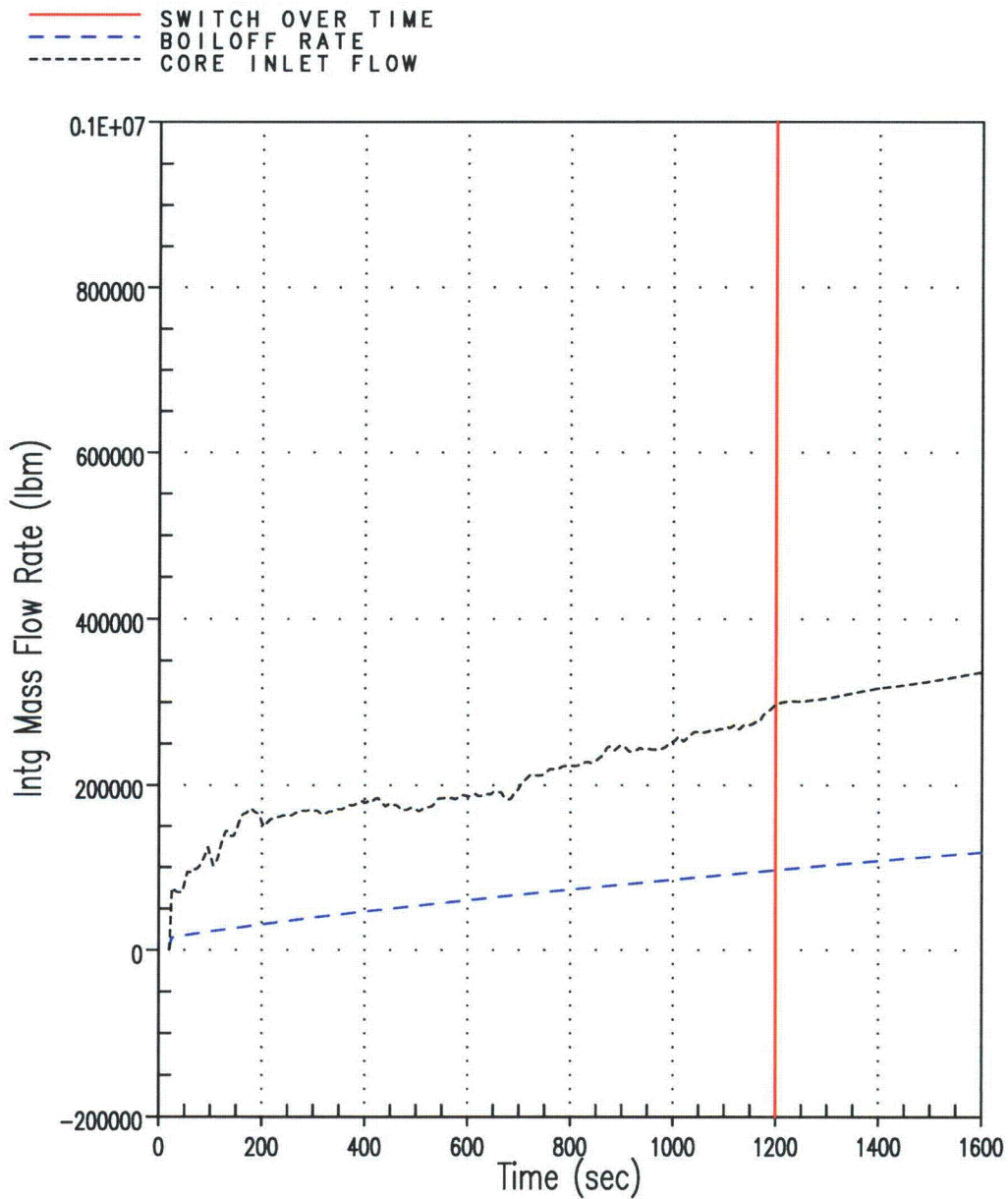
1066716945

Figure B-33 Void Fraction at the Exit of the Average Core Channel for Channel 13 Flow Reduction 80% Case



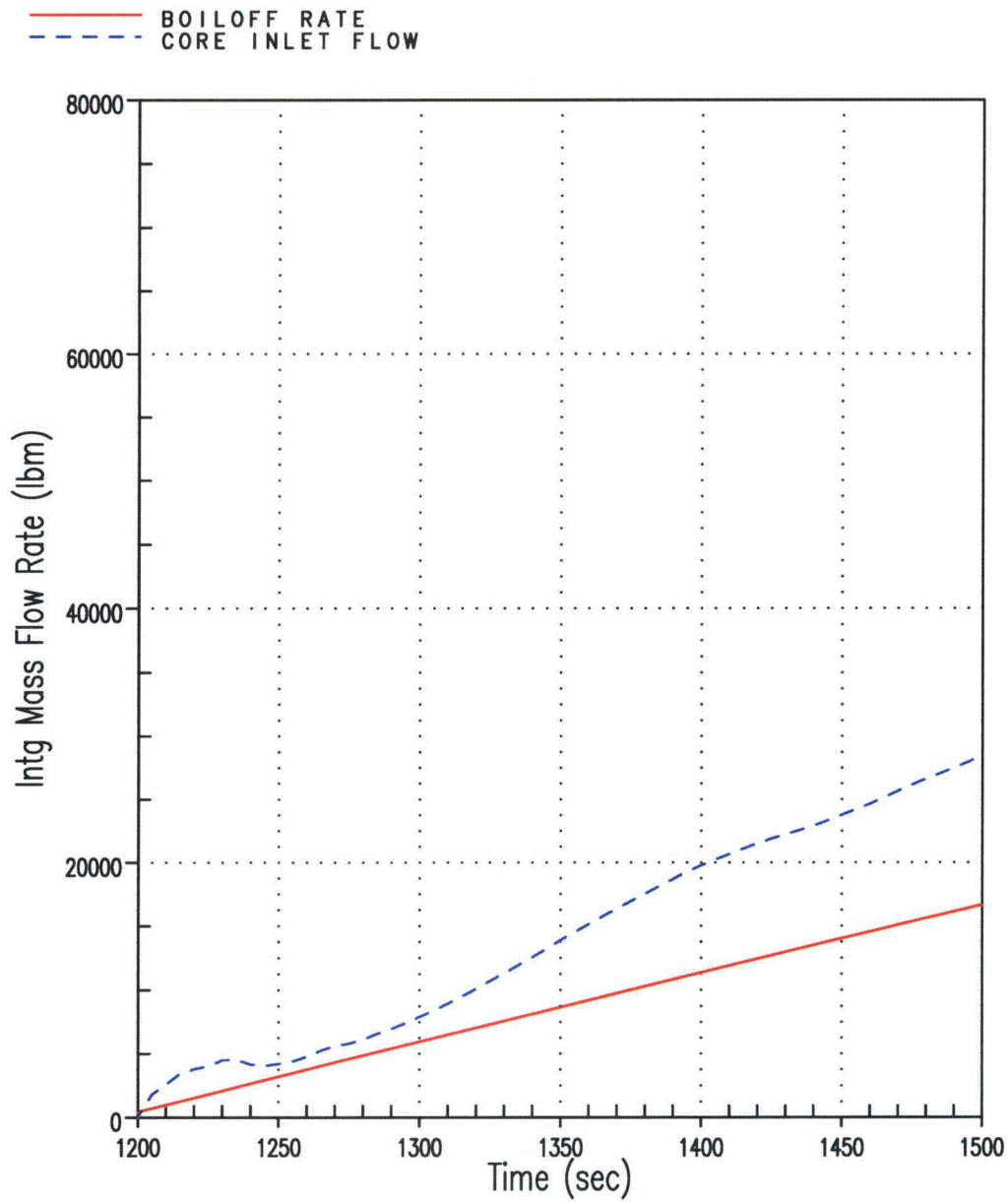
301250483

Figure B-34 Core Pressure Drop for Channel 13 Flow Reduction 80% Case



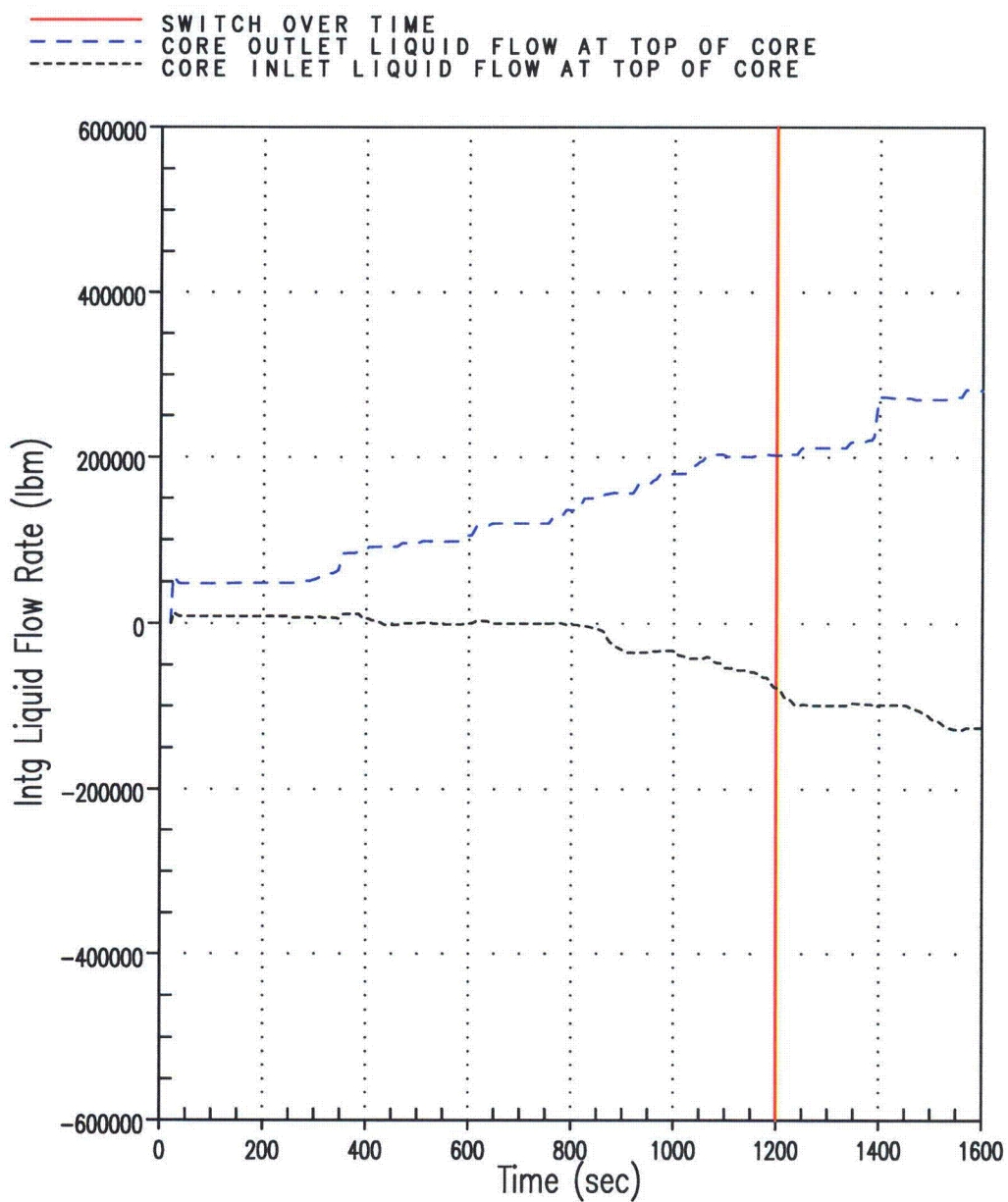
221025277

Figure B-35 Integrated Core Flow vs. Core Boil-off for Uniform $C_D = 50,000$ Case



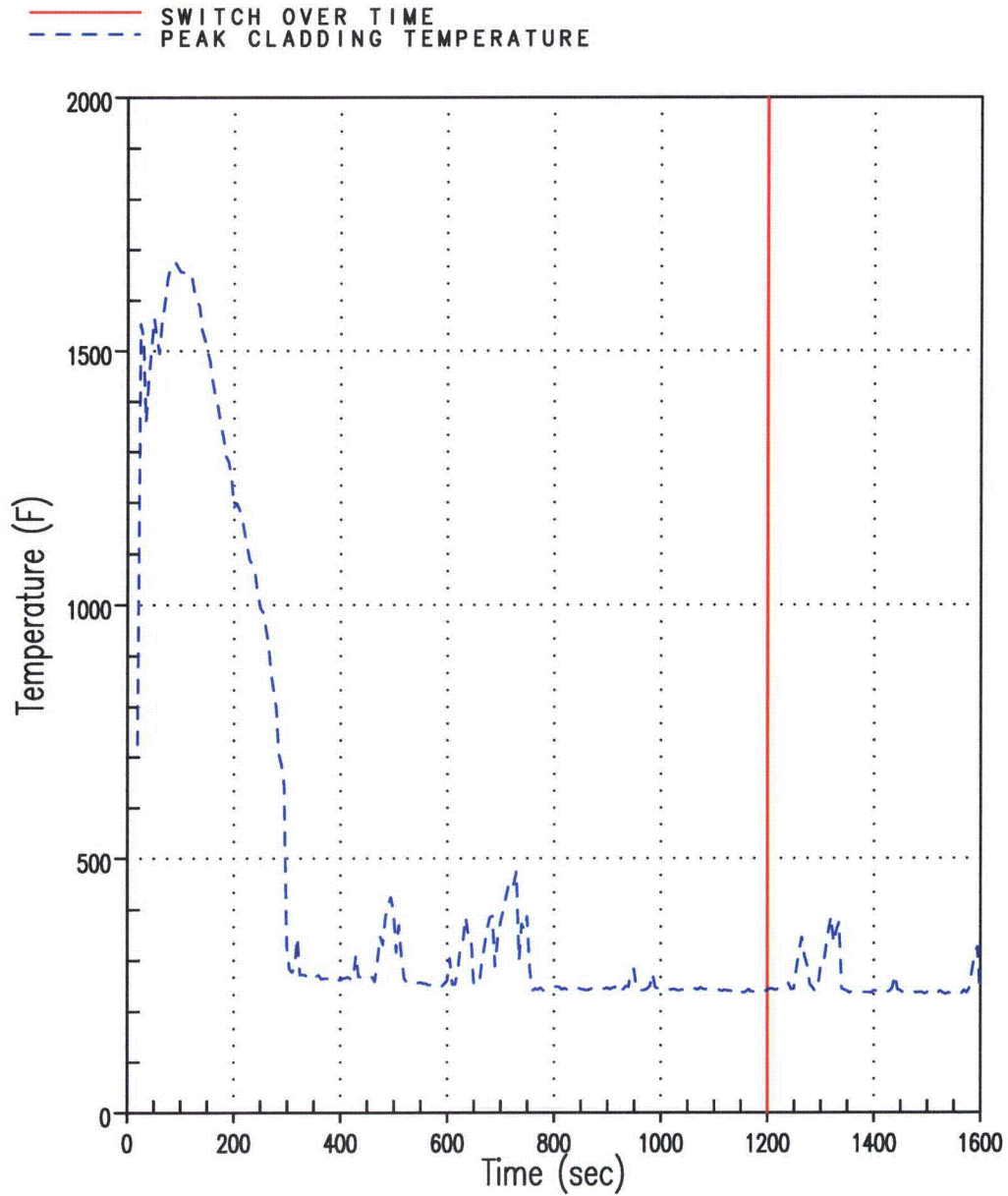
221025277

Figure B-36 Integrated Core Flow vs. Core Boil-off for Uniform $C_D = 50,000$ Case (Shifted Scale)



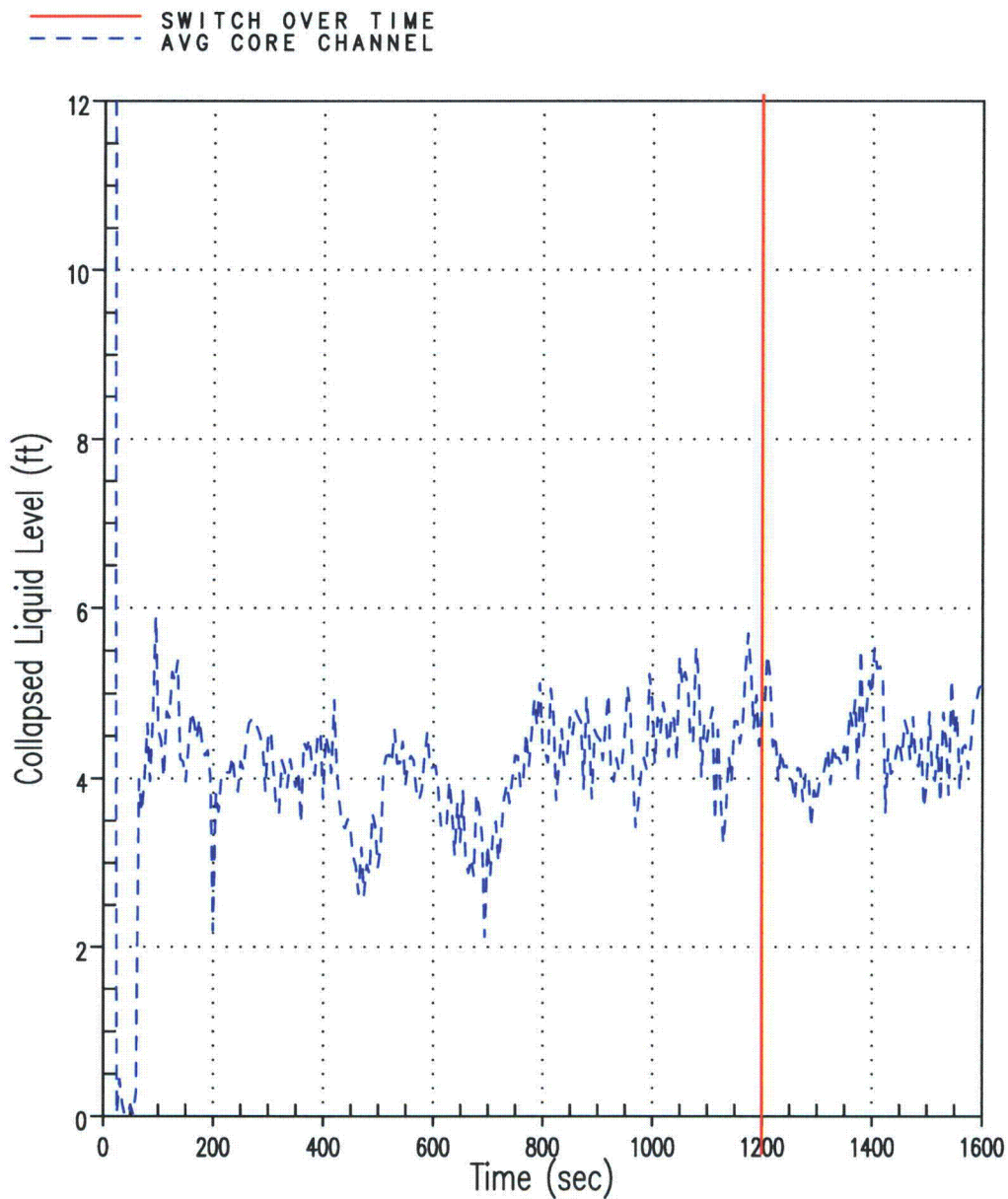
1745042723

Figure B-37 Total Integrated Liquid Flow at the Top of the Core for Uniform $C_D = 50,000$ Case (Positive/Outlet flow represents HA, GT, AVG channels; Negative/Inlet flow represent LP channel)



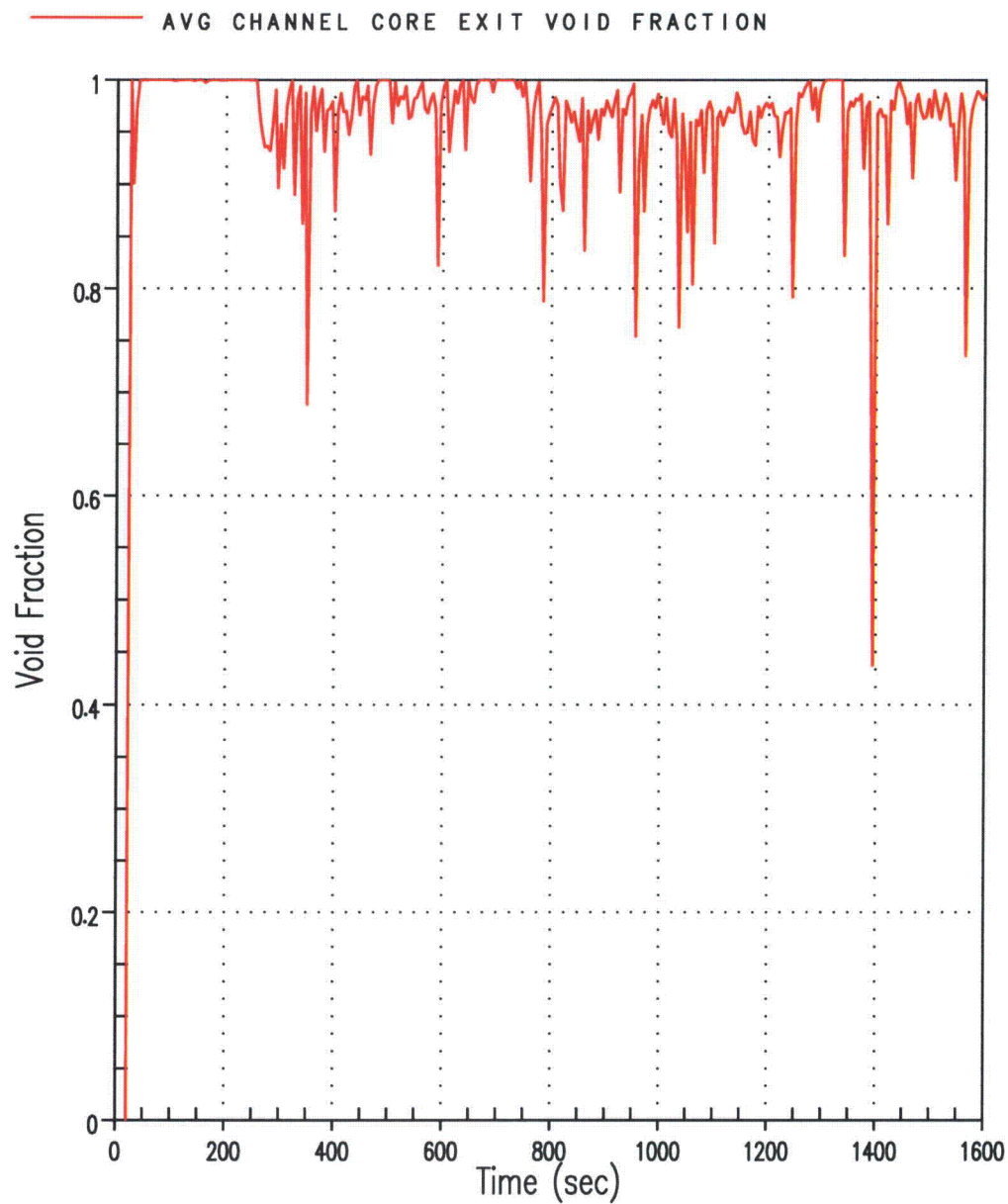
1912580093

Figure B-38 Hot Rod PCT for Uniform $C_D = 50,000$ Case



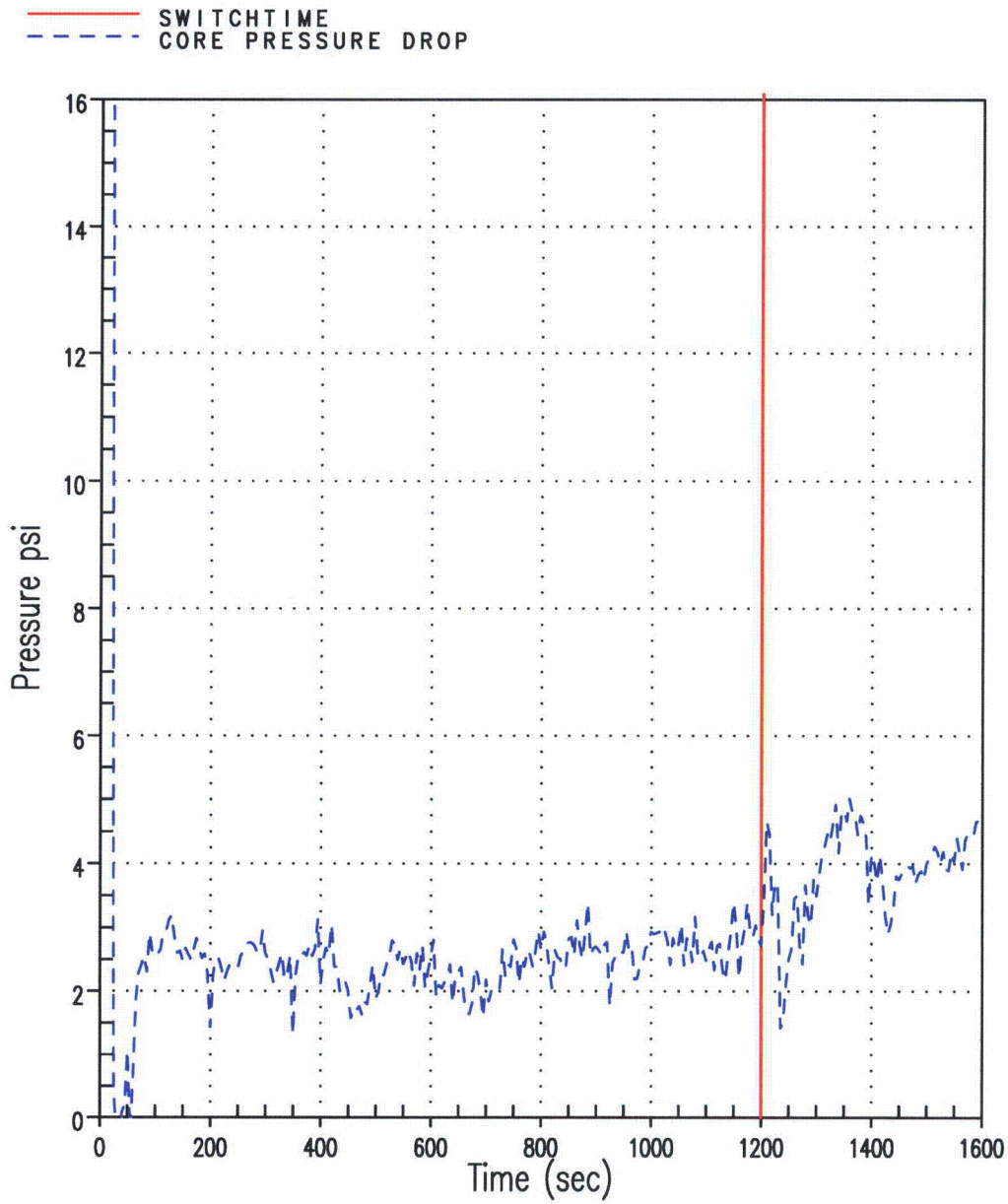
428299048

Figure B-39 Average Core Channel Collapsed Liquid Level for Uniform $C_D = 50,000$ Case



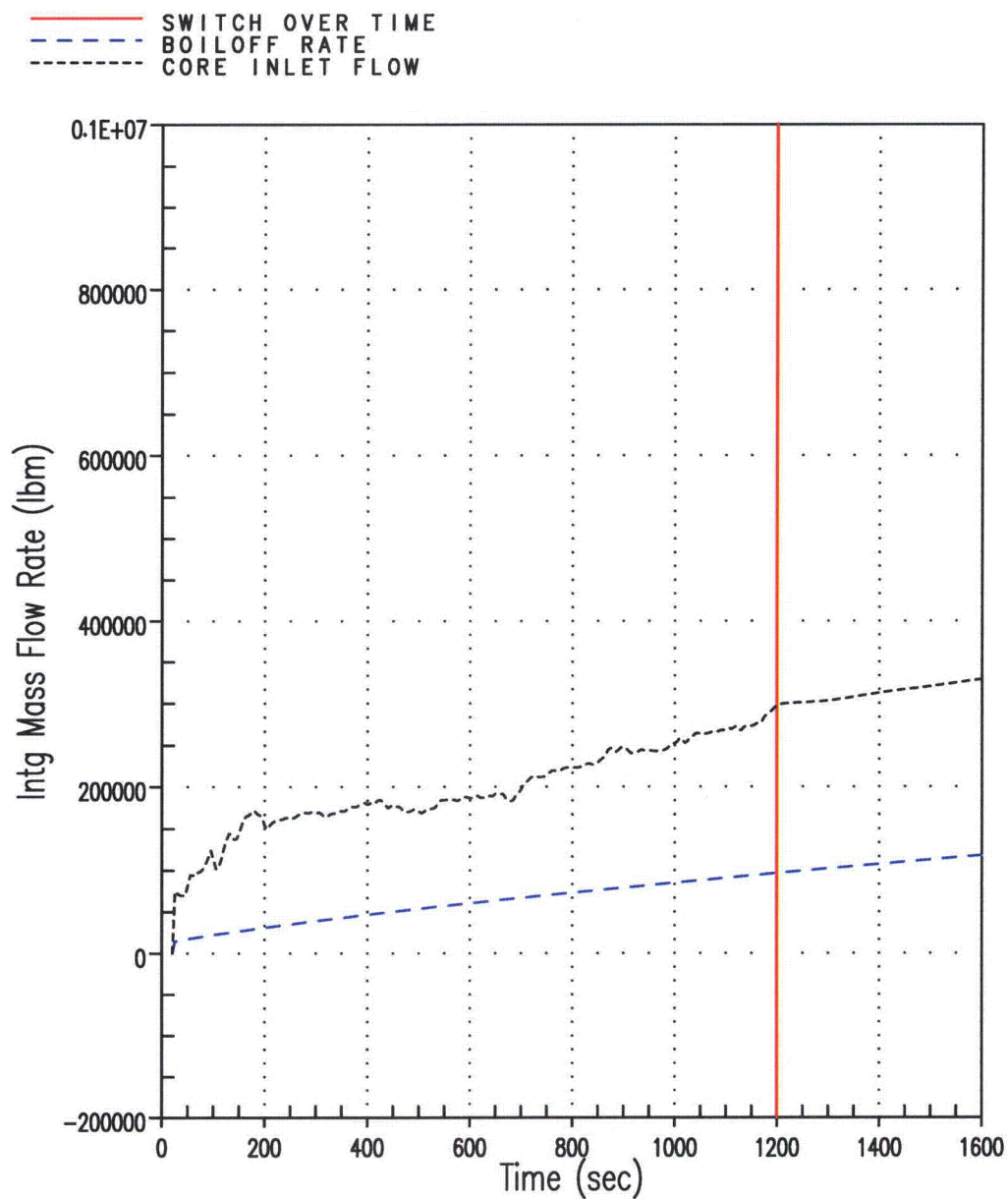
354120819

Figure B-40 Void Fraction at the Exit of the Average Core Channel for Uniform $C_D = 50,000$ Case



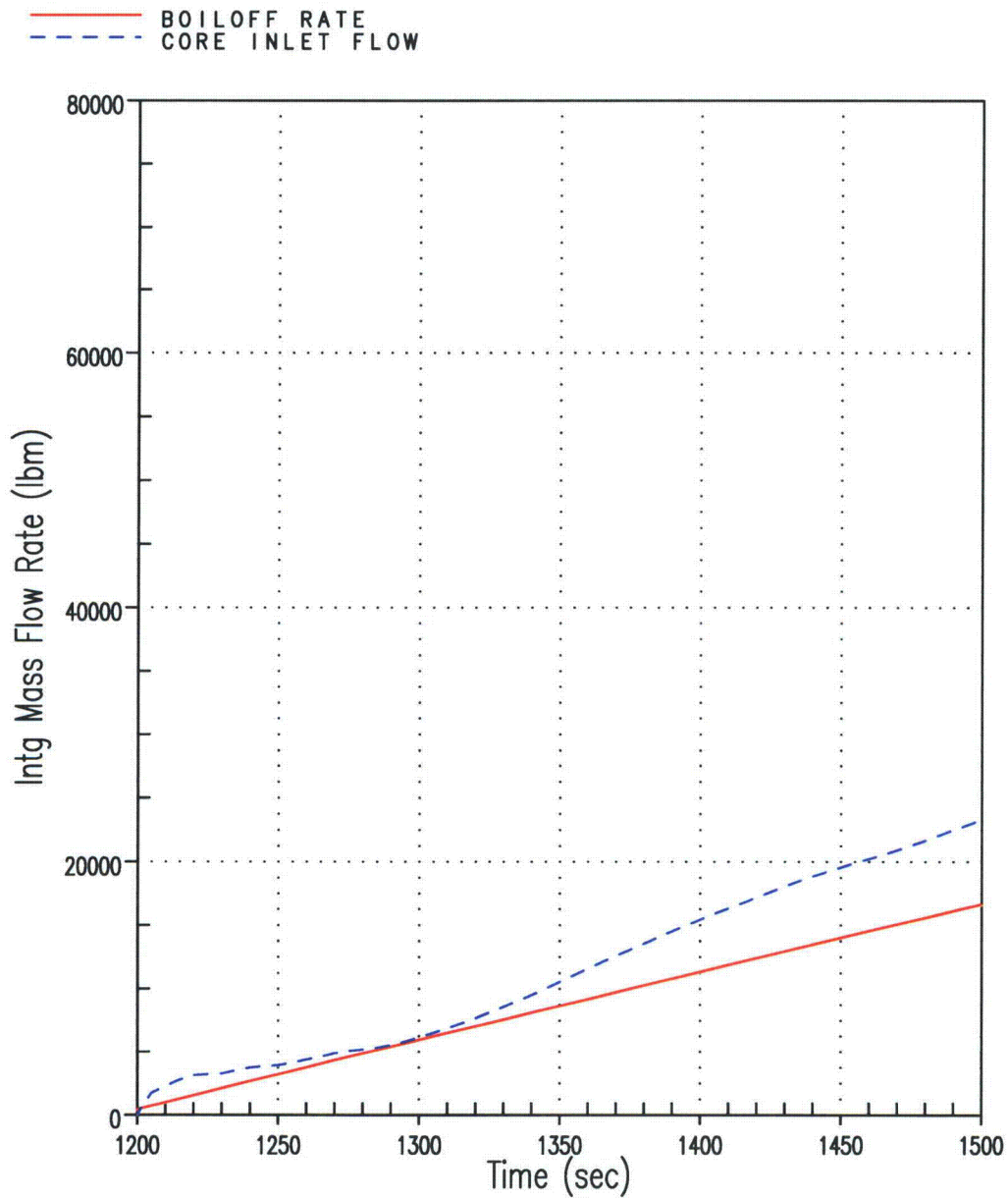
321274172

Figure B-41 Core Pressure Drop for Uniform $C_D = 50,000$ Case



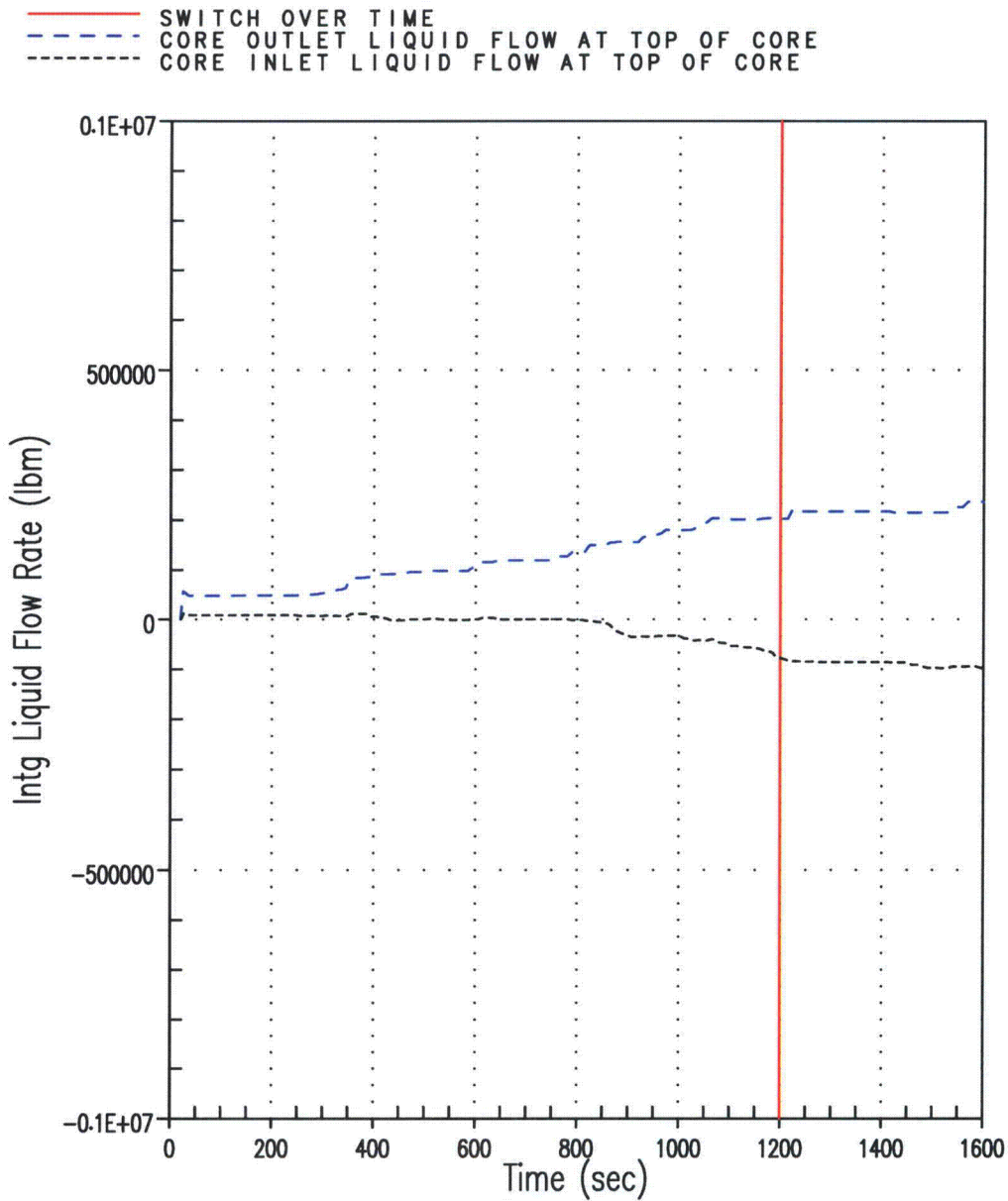
913425722

Figure B-42 Integrated Core Flow vs. Core Boil-off for Uniform $C_D = 100,000$ Case



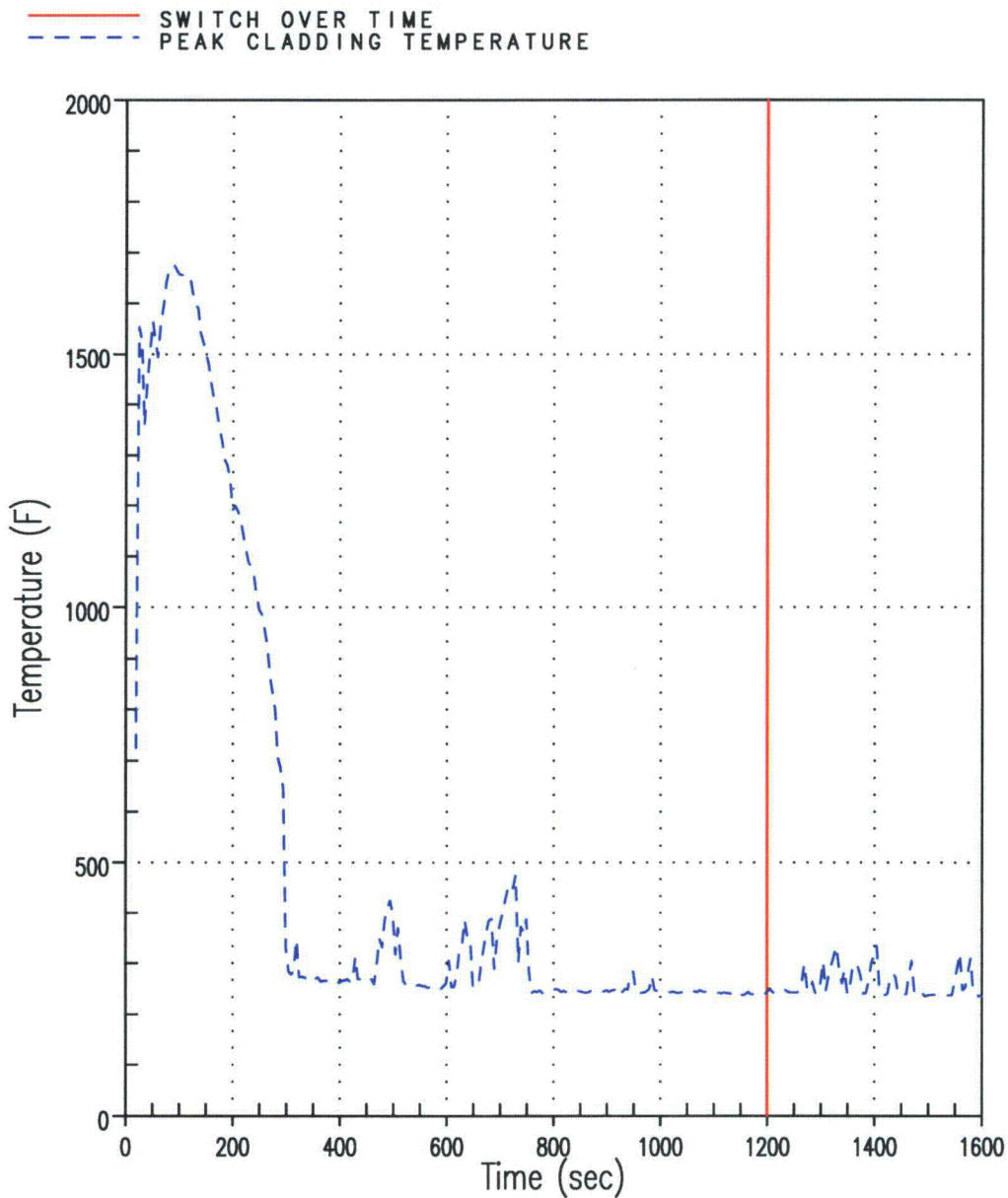
913425722

Figure B-43 Integrated Core Flow vs. Boil-off for Uniform $C_D = 100,000$ Case (Shifted Scale)



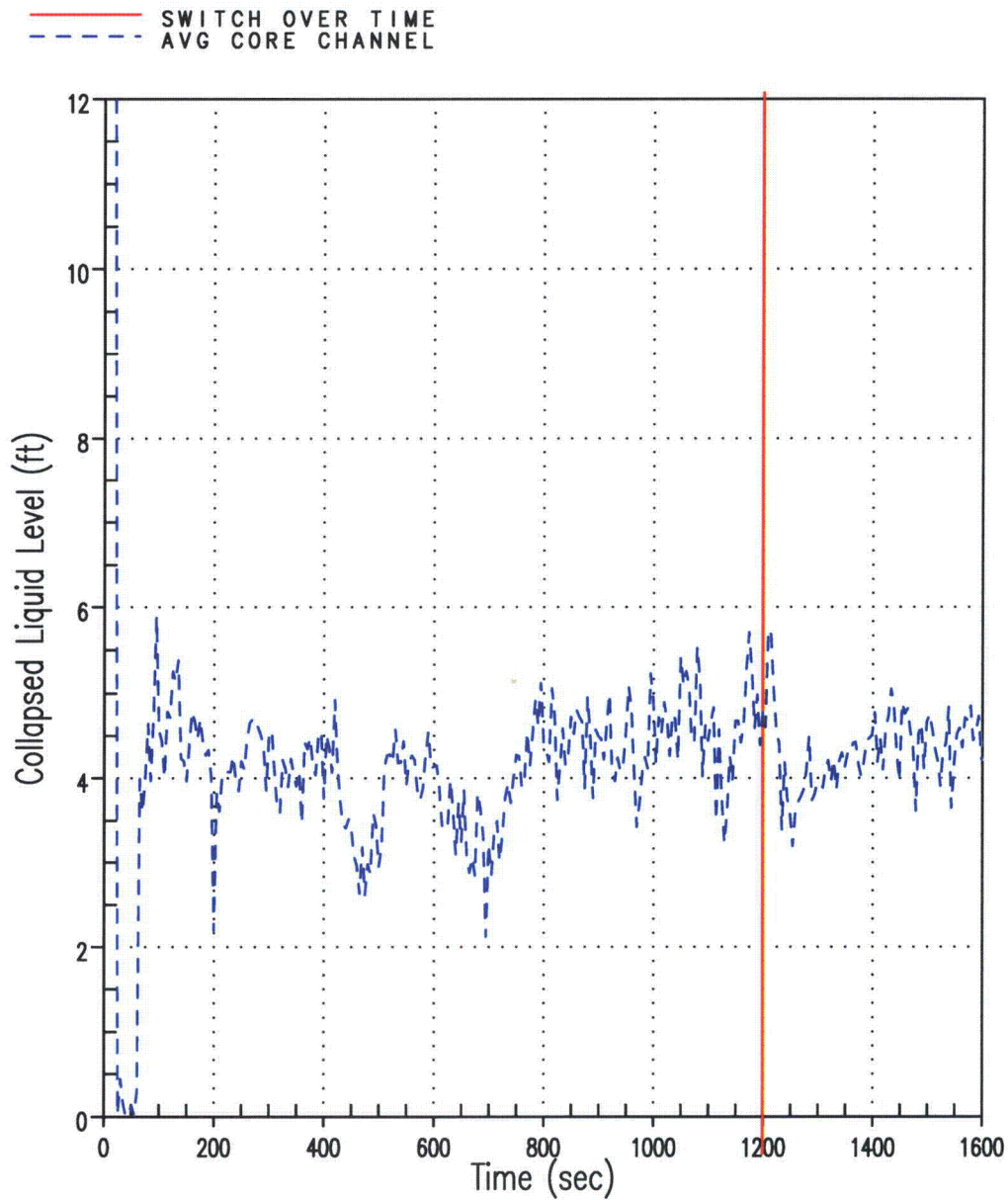
1072306012

Figure B-44 Total Integrated Liquid Flow at the Top of the Core for Uniform $C_D = 100,000$ Case (Positive/Outlet flow represents HA, GT, AVG channels; Negative/Inlet flow represent LP channel)



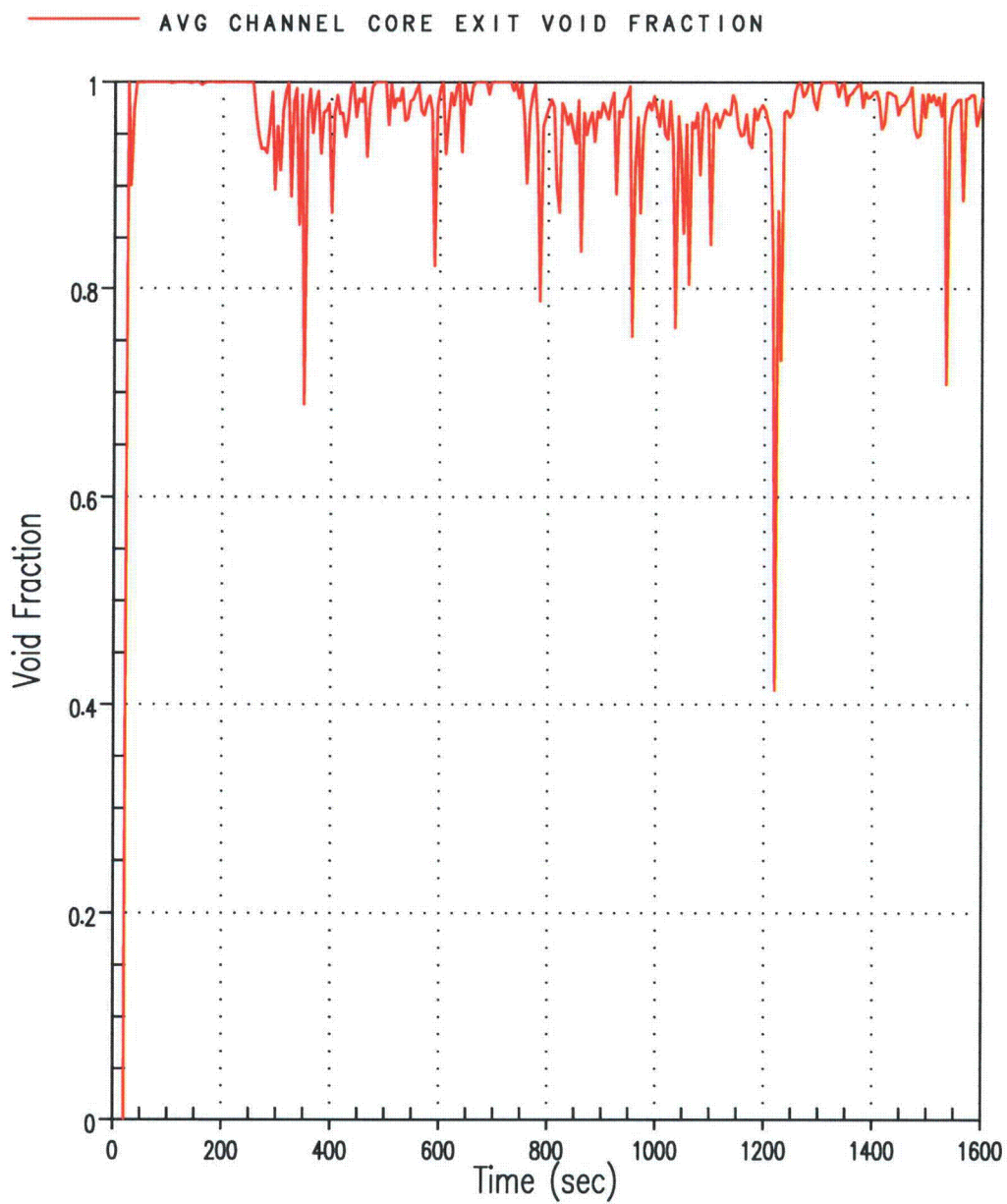
2013807248

Figure B-45 Hot Rod PCT for Uniform $C_D = 100,000$ Case



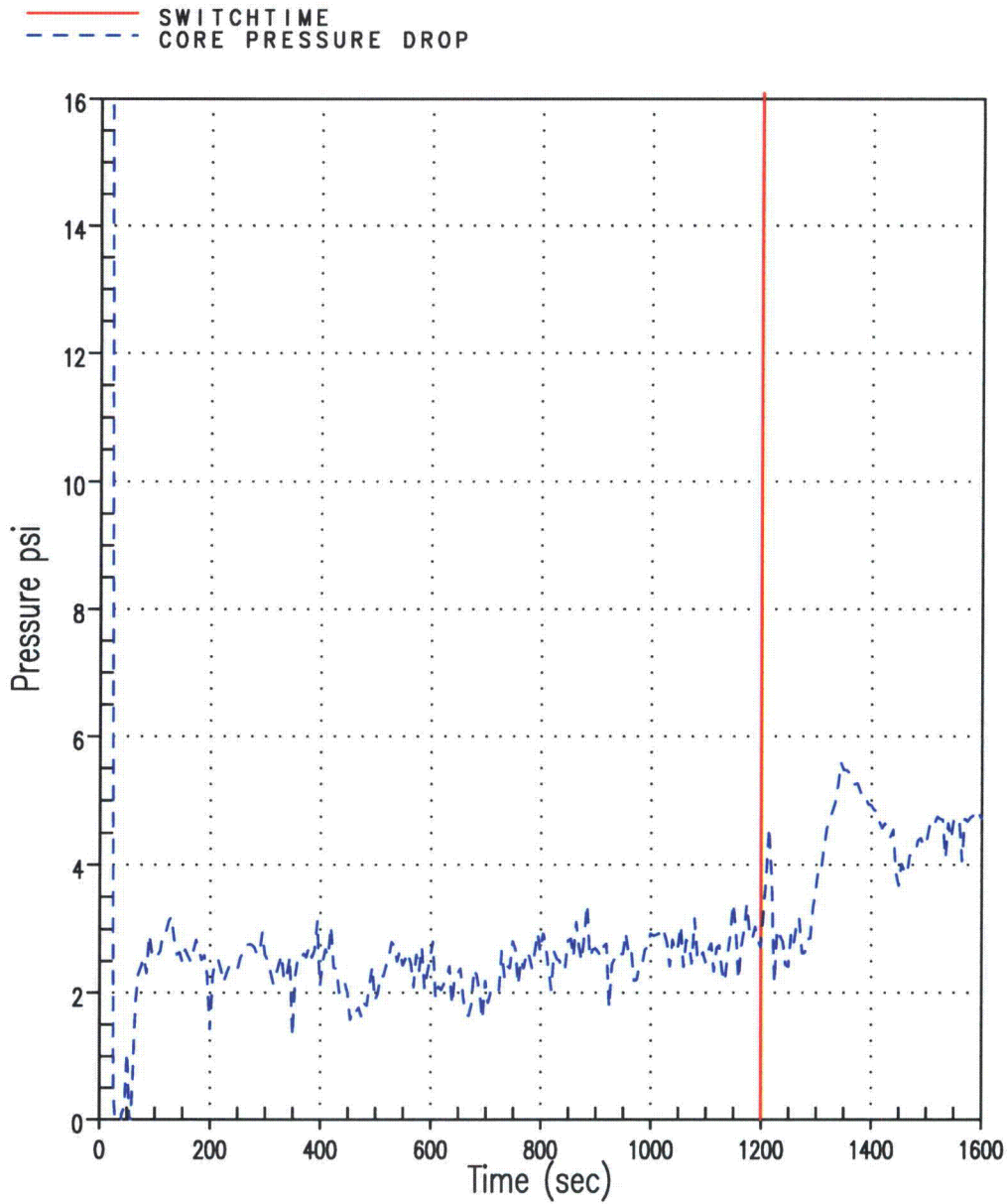
1470404378

Figure B-46 Average Core Channel Collapsed Liquid Level for Uniform $C_D = 100,000$ Case



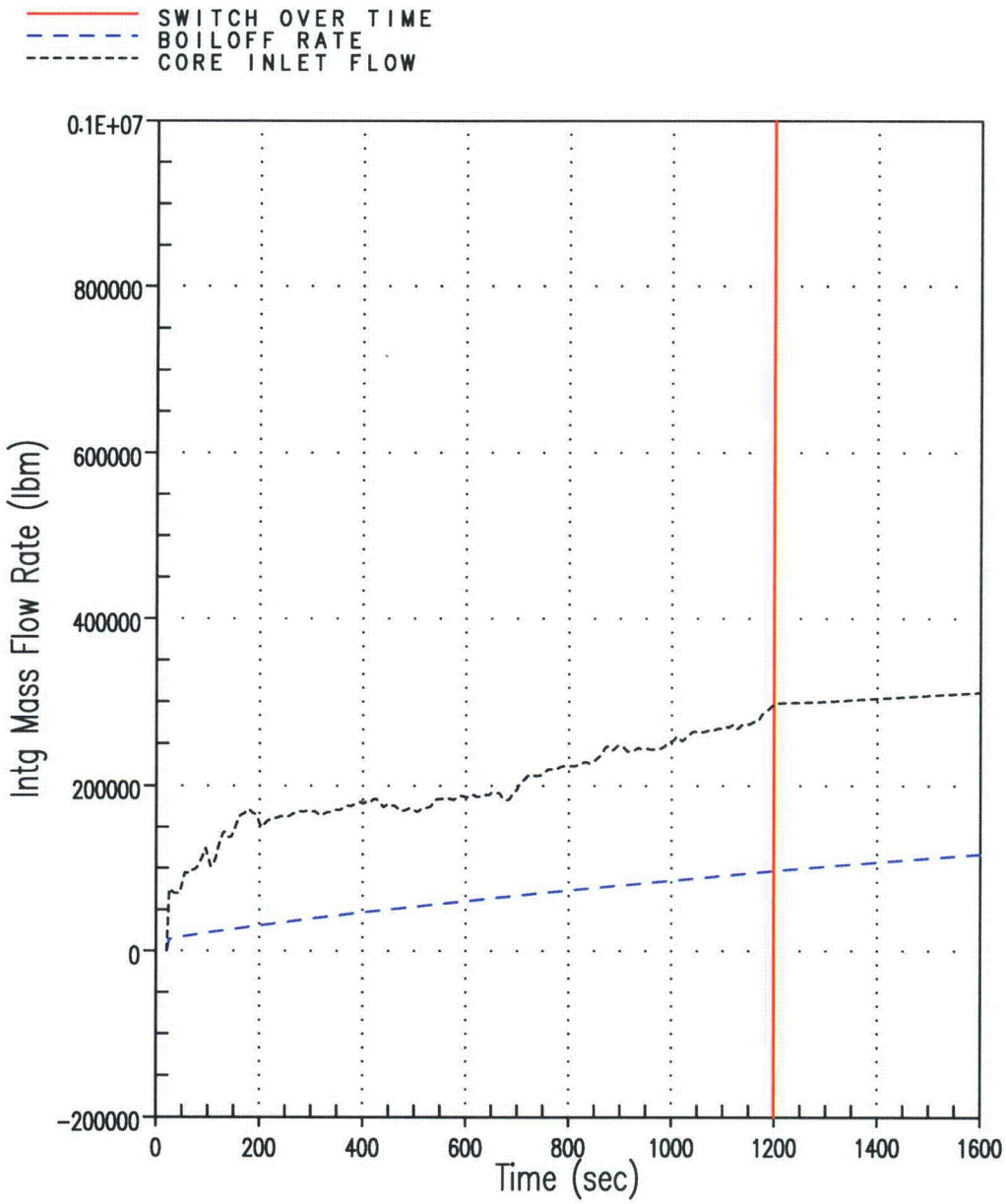
747525079

Figure B-47 Void Fraction at Exit of Average Core Channel for Uniform $C_D = 100,000$ Case



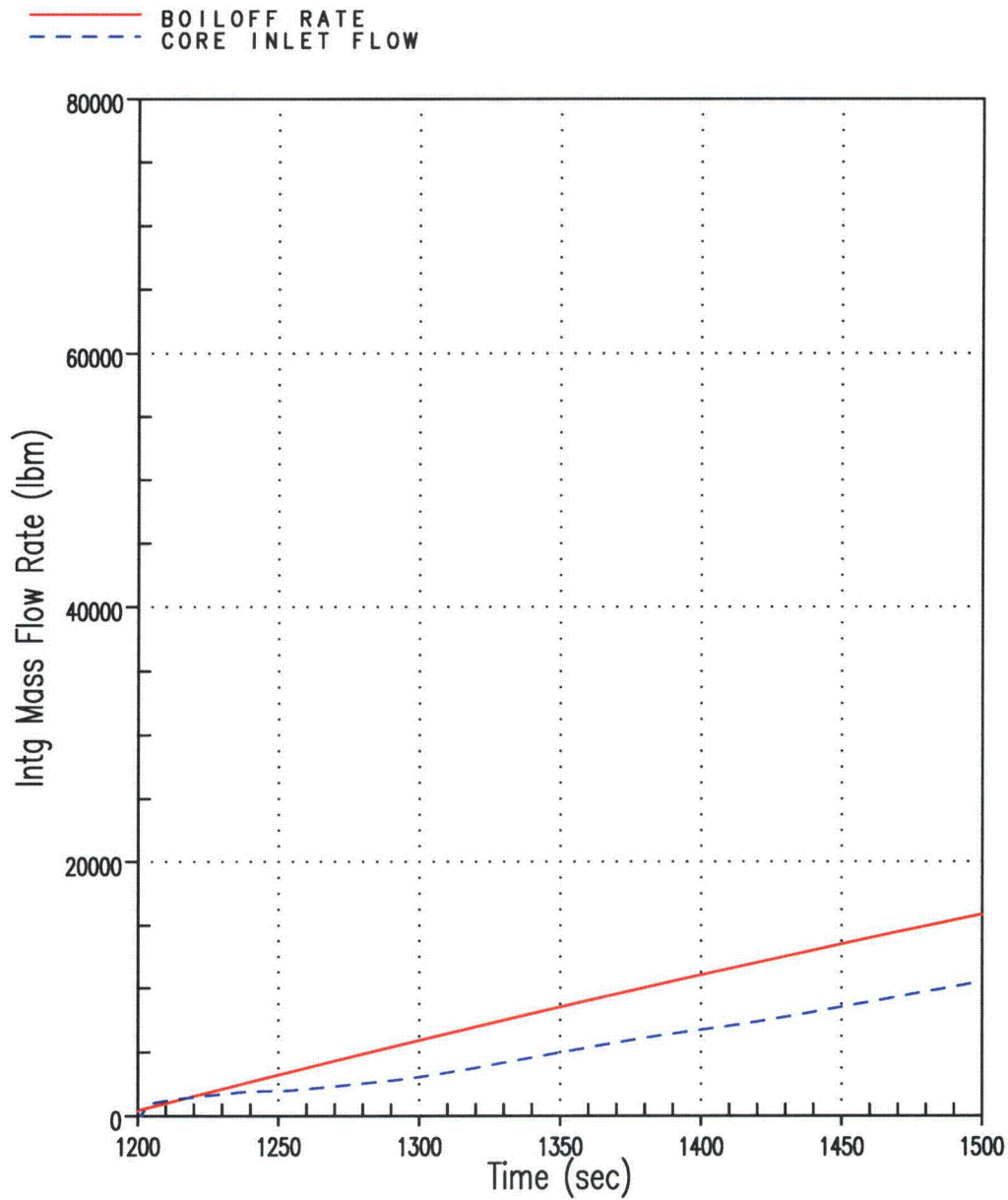
1552950110

Figure B-48 Core Pressure Drop for Uniform $C_D = 100,000$ Case



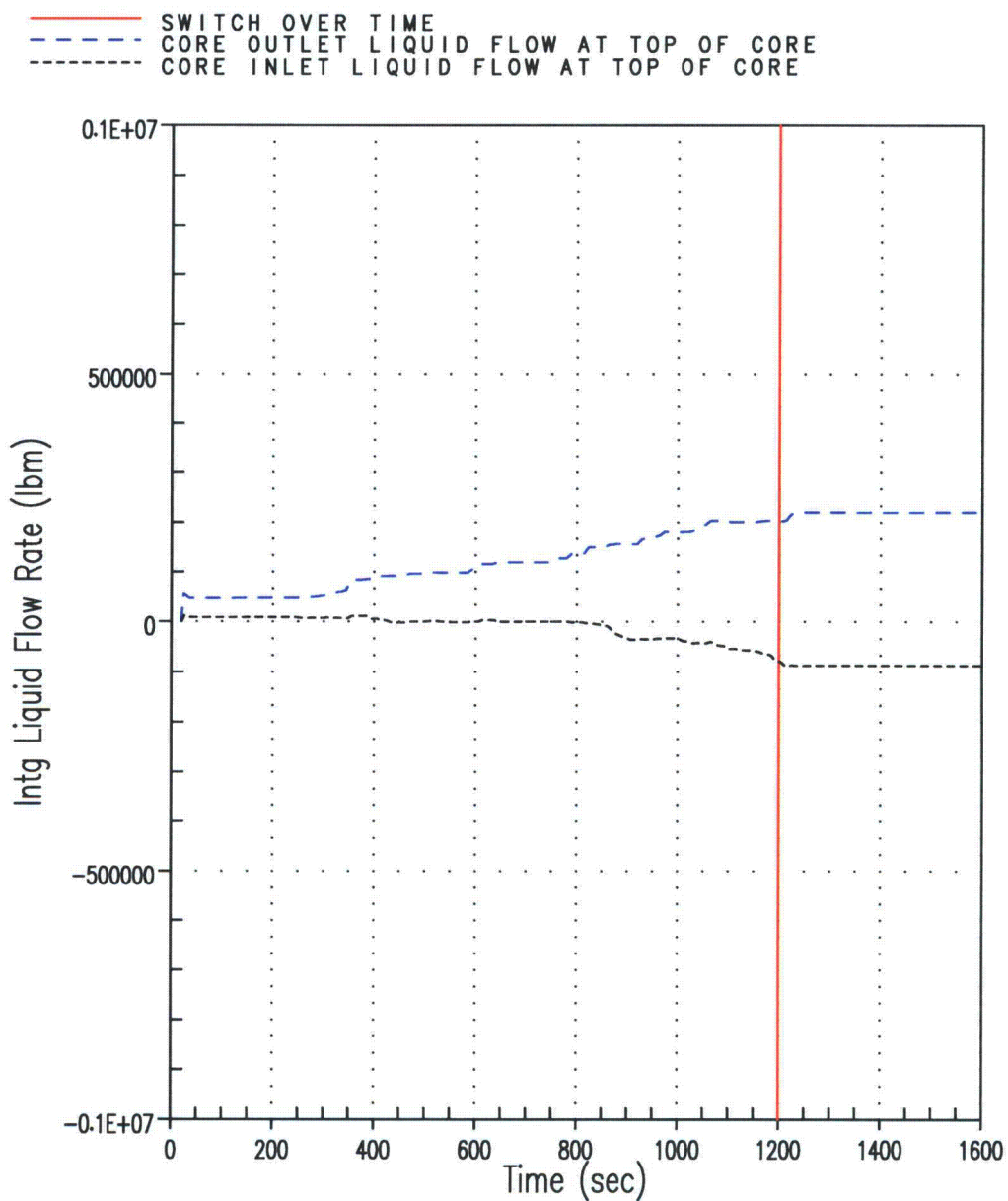
1628827304

Figure B-49 Integrated Core Flow vs. Boil-off for Uniform $C_D = 1,000,000$ Case



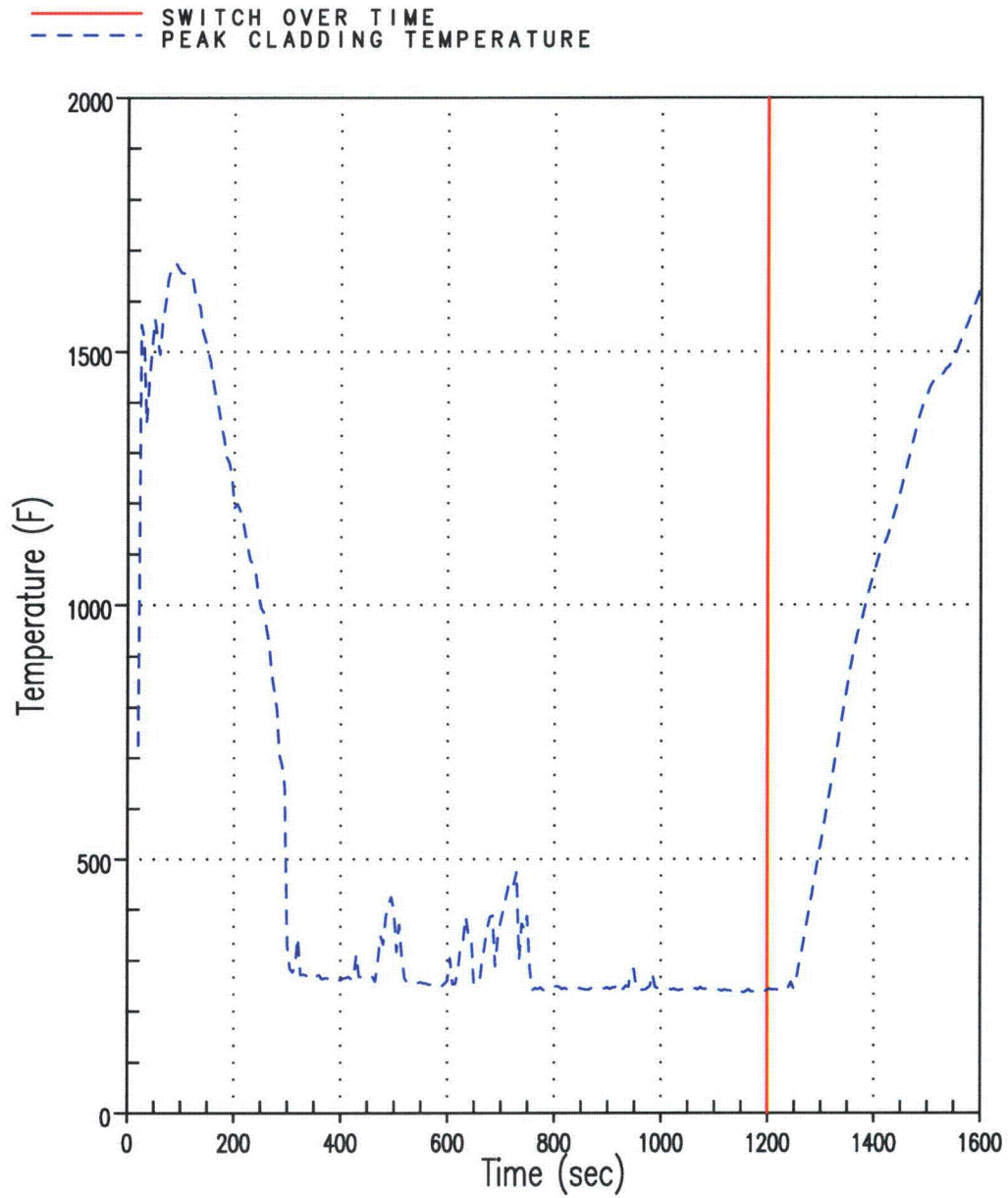
1628627304

Figure B-50 Integrated Core Flow vs. Boil-off for Uniform $C_D = 1,000,000$ Case (Shifted Scale)



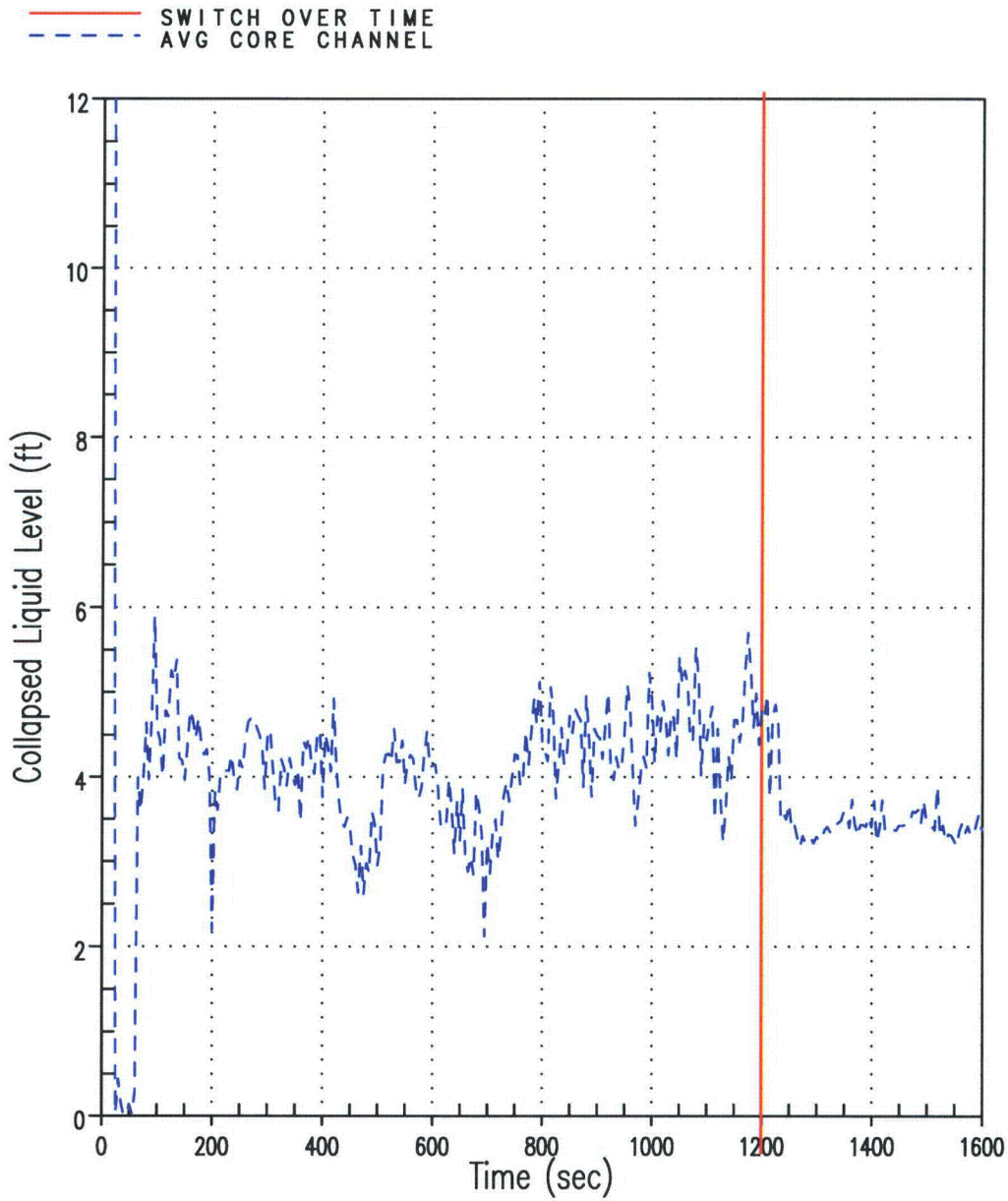
973451765

Figure B-51 Total Integrated Liquid Flow at the Top of the Core for Uniform $C_D = 1,000,000$ Case (Positive/Outlet flow represents HA, GT, AVG channels; Negative/Inlet flow represent LP channel)



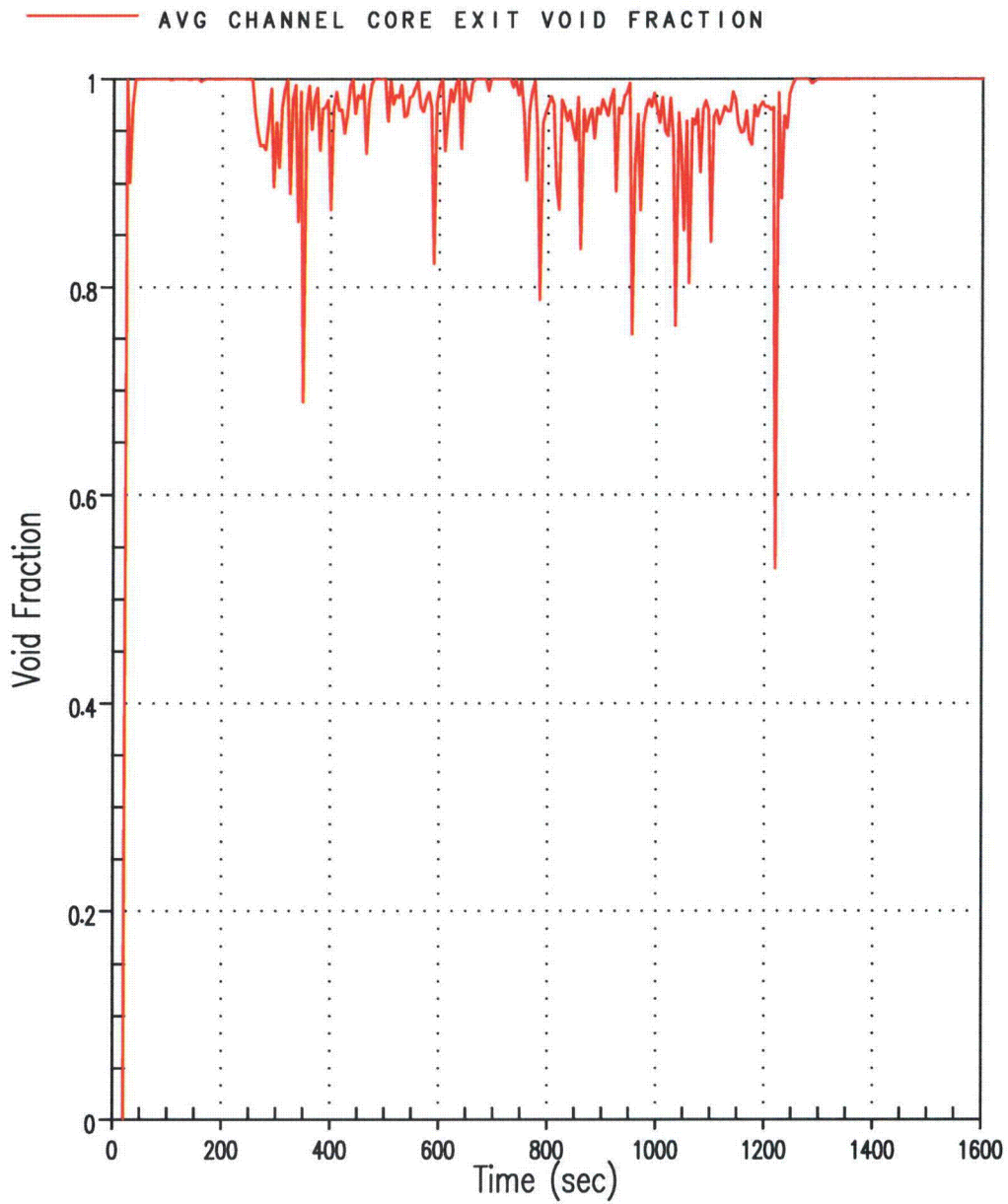
566586943

Figure B-52 Hot Rod PCT for Uniform $C_D = 1,000,000$ Case



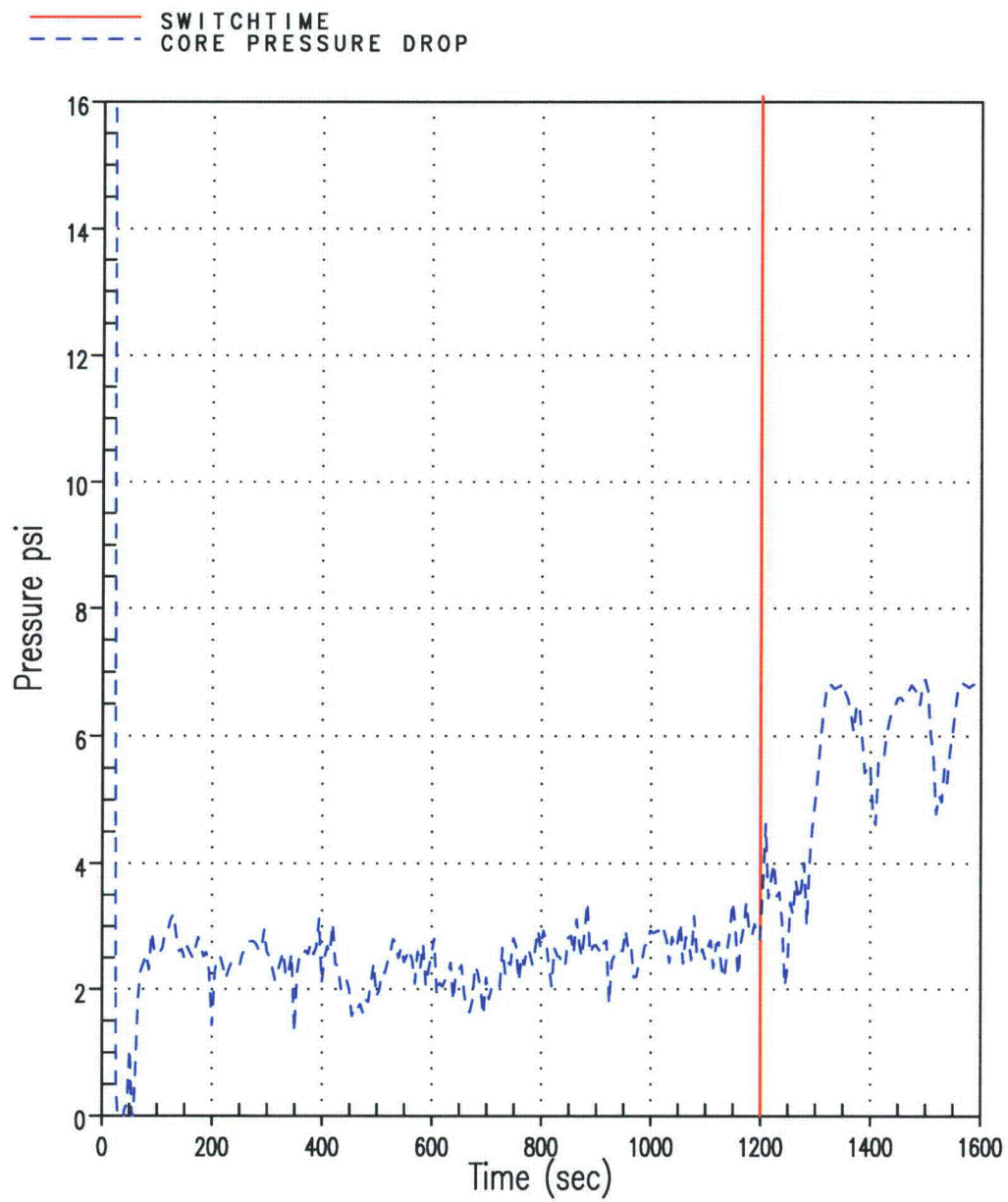
403478450

Figure B-53 Average Core Channel Collapsed Liquid Level for Uniform $C_D = 1,000,000$ Case



1414870568

Figure B-54 Void Fraction at Exit of Average Core Channel for Uniform $C_D = 1,000,000$ Case



1923232683

Figure B-55 Core Pressure Drop for Uniform $C_D = 1,000,000$ Case

B.6 EFFECT OF THICK METAL STORED ENERGY ON COOLANT TEMPERATURE

The WC/T calculations were also used to evaluate the potential for ECCS coolant to absorb thermal energy from the thick metal reactor vessel components during recirculation of coolant from the containment building sump. This was done to assess the potential effect of changes on the recirculating coolant temperature on solubility limits of post-accident chemical products.

The thermal energy stored in the thick RV shell and the RV B/B is small, as demonstrated in the following discussion, and has no more than about a 5°F influence on the coolant temperature from the time it enters the RV until it enters the core inlet. This temperature rise in the RV is small and has results in no more than about a 5% change in solubility of aluminum-based and calcium-based precipitates. This change has no effect on the potential for chemical precipitates to form in the vessel as a result of these phenomena.

The postulated CL break was chosen as this is the bounding case for heat-up of the coolant as it passes by the thick metal components of the RV. The low flow-rates associated with a CL break (matching boil-off) provide the greatest residence time of the fluid next to the metal structures, allowing for the maximum heat-up of the coolant. A postulated HL break, while having a larger velocity, also has a reduced residence time in the RV, minimizing the opportunity for coolant heat-up.

At the time that the ECCS is realigned to draw suction from the reactor containment building sump from the BWST/RWST, the heat transfer process between the thick metal components of the RV and the ECCS fluid in the RV is conduction limited. Under these conditions, there is little increase in temperature of the ECCS fluid as it passes by the thick-metal RV components and enters into the reactor core. The time history plots prepared from the WC/T calculations reported in Section B-3, confirm that this is conduction-limited heat transfer process, and that there is minimal temperature change of the coolant as it enters the RV and flows to the core.

Figure B-56, Comparison of Reactor Vessel Metal Temperature at Bottom of Fuel; Outside Diameter versus Inside Diameter, and Figure B-57, Comparison of Reactor Vessel Metal Temperature at Top of Fuel; Outside Diameter versus Inside Diameter, are time history plots of the temperature of the inner and outer RV metal nodes of the WC/T calculations for a postulated CL break. From Figures B-56 and B-57, it is noted that the temperature of the inner RV metal node at the top and bottom of the core is relatively unchanged over the 300 seconds following switchover from BWST/RWS injection to recirculation from the reactor containment building sump. Over this same time period, the outer RV node is predicted to drop by about 30°F. These figures demonstrate that the heat transfer process is conduction limited.

Figure B-58, Comparison of Fluid Temperature at Top and Bottom of Downcomer, shows that there no more than about 5°F temperature gain in the coolant as it passes from the top to the bottom of the downcomer. Likewise, Figure B-59, Comparison of Fluid Temperature at Top and Bottom of Baffle, shows a similar behavior. It is noted that the initial 10°F temperature difference diminishes to about a 5°F temperature difference within about 150 seconds of switchover from BWST/RWST injection to recirculation from the reactor containment building sump. Figure B-60, Comparison of Fluid Temperature in Lower Plenum to Core Inlet, shows that the coolant at the core entrance is calculated to be generally slightly warmer but within about 5°F of the coolant in the RV lower plenum. Figures B-61 and B-62, Comparison of Fluid Temperature Between Core Inlet and Inside Baffle, and Comparison of Fluid

Temperature Between Core Outlet and Inside Baffle, respectively, shows the calculated fluid temperatures at the core inlet and core outlet to be within less than about 5°F of each other throughout the calculation time period. More importantly, over the last 100 seconds of the calculation period, comparisons show almost no temperature difference between the fluid in the core and in the baffle.

Based on these comparisons for a postulated CL break, it is concluded that the thermal energy stored in the thick RV shell and the RV baffle/barrel has no more than about a 5°F influence on the coolant temperature from the time it enters the RV until it enters the core inlet for either the CL or HL break scenarios. This conclusion is applicable to all plants, as is demonstrated by considering the Biot number, N_{Bi} , for this scenario. The Biot number is the ratio of surface conductance to internal conduction of a solid;

$$N_{Bi} = \frac{H \times L}{k}$$

where:

H = Surface heat transfer coefficient

L = Thickness of the solid

k = Thermal conductivity of the solid

At the time of initiation of recirculation from the reactor containment building sump, there is no boiling in the downcomer and the convective heat transfer coefficient between the thick metal and the coolant is

dependent upon local flow rate and is evaluated to between less than $3 \frac{Btu}{hr - ft^2 - ^\circ F}$ for a postulated HL

break. The thickness of a RV is about 8 inches. For evaluating a Biot Number, one-half of the thickness or 4 inches (0.33 ft.) will be used. The thermal conductivity of mild (carbon) steel is about

$28 \frac{Btu}{hr - ft - ^\circ F}$. Thus, the Biot Number for this scenario would be;

$$N_{Bi} \leq 0.036$$

The above calculation demonstrates that the dominate resistance to heat transfer from the RV thick metal during recirculation is due to the convective resistance between the RV surface and the fluid.

The stainless steel cladding on the inside of the RV was ignored for this evaluation. Stainless steel is about 1/3 as conductive as mild (carbon) steel. Although the cladding is thin, inclusion of this material in the evaluation of a Biot Number would further favor the convection limited process.

The fluid temperature rise of $\leq 5^\circ F$ predicted by WC/T calculations for a postulated CL break is small in comparison to that needed to change solubility limits and is evaluated to have no affect on the solubility of aluminum-based precipitates, the solubility of calcium-based precipitates and the potential for chemical precipitates to form in the vessel as a result of the release of stored thermal energy from thick-metal components of the RV.

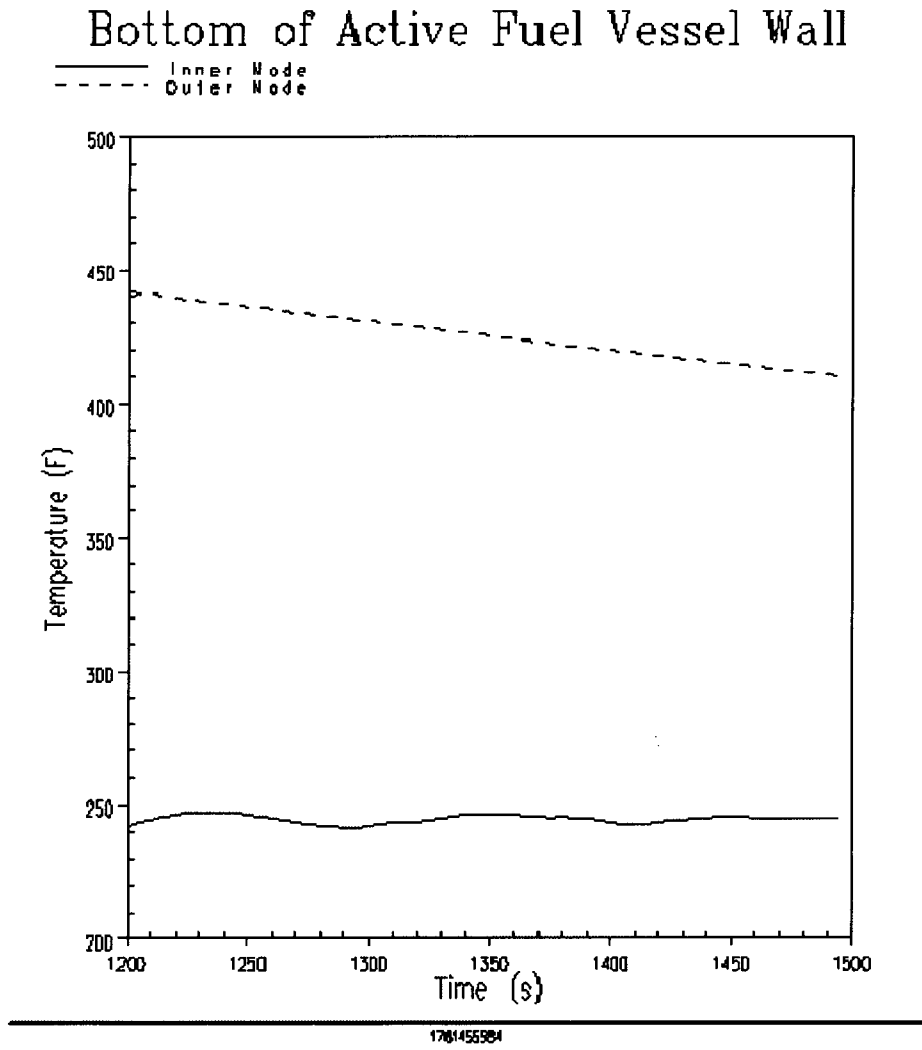


Figure B-56 Comparison of Reactor Vessel Metal Temperature at Bottom of Fuel; Outside Diameter versus Inside Diameter

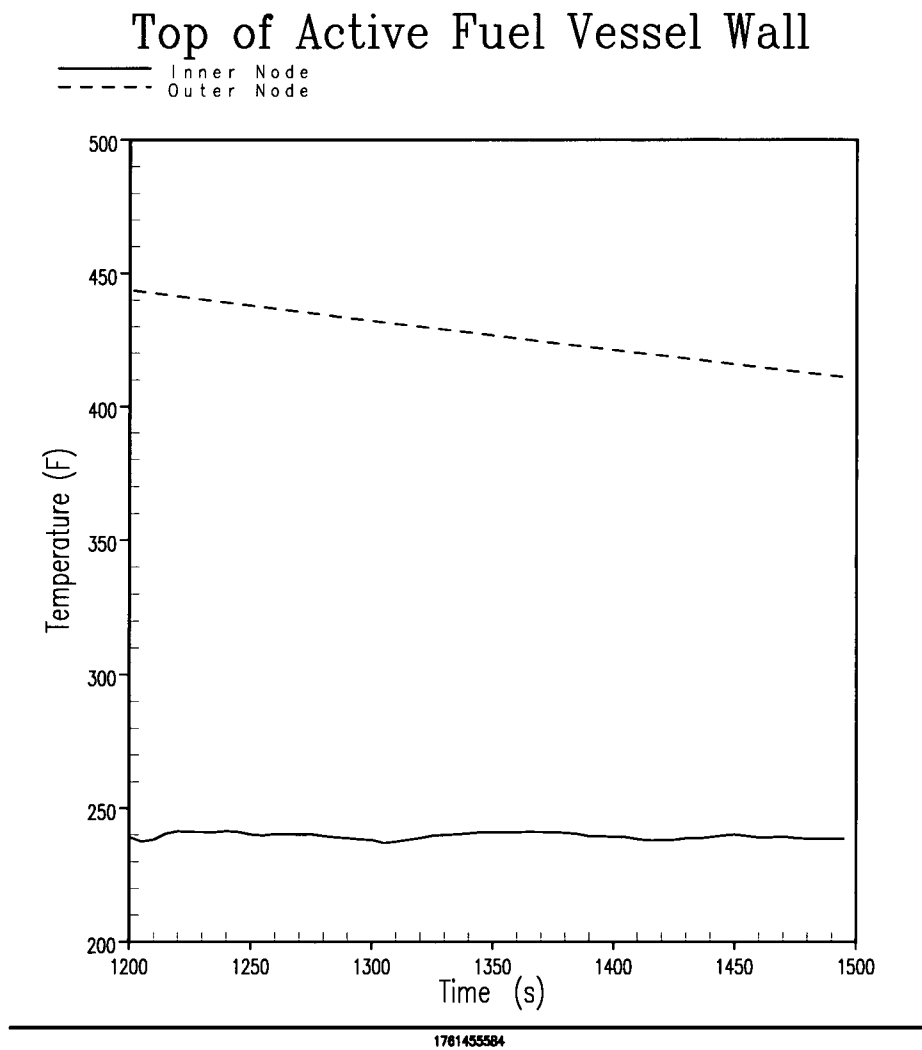


Figure B-57 Comparison of Reactor Vessel Metal Temperature at Top of Fuel; Outside Diameter versus Inside Diameter

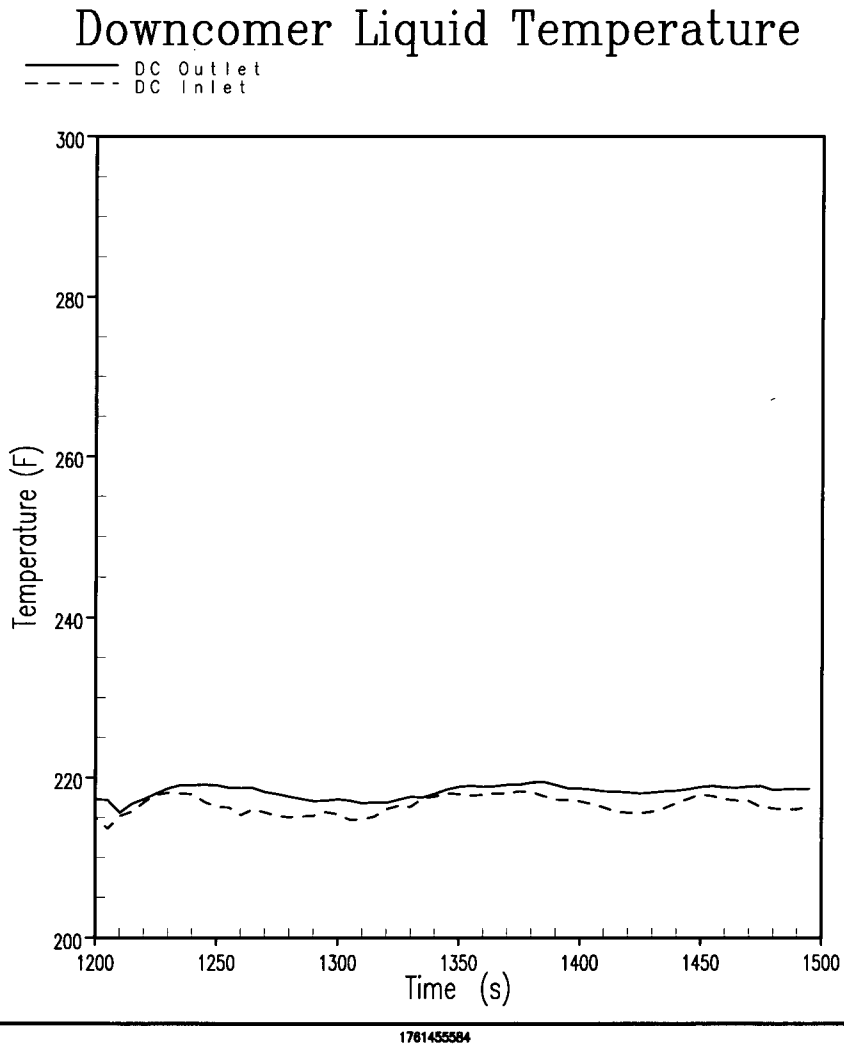
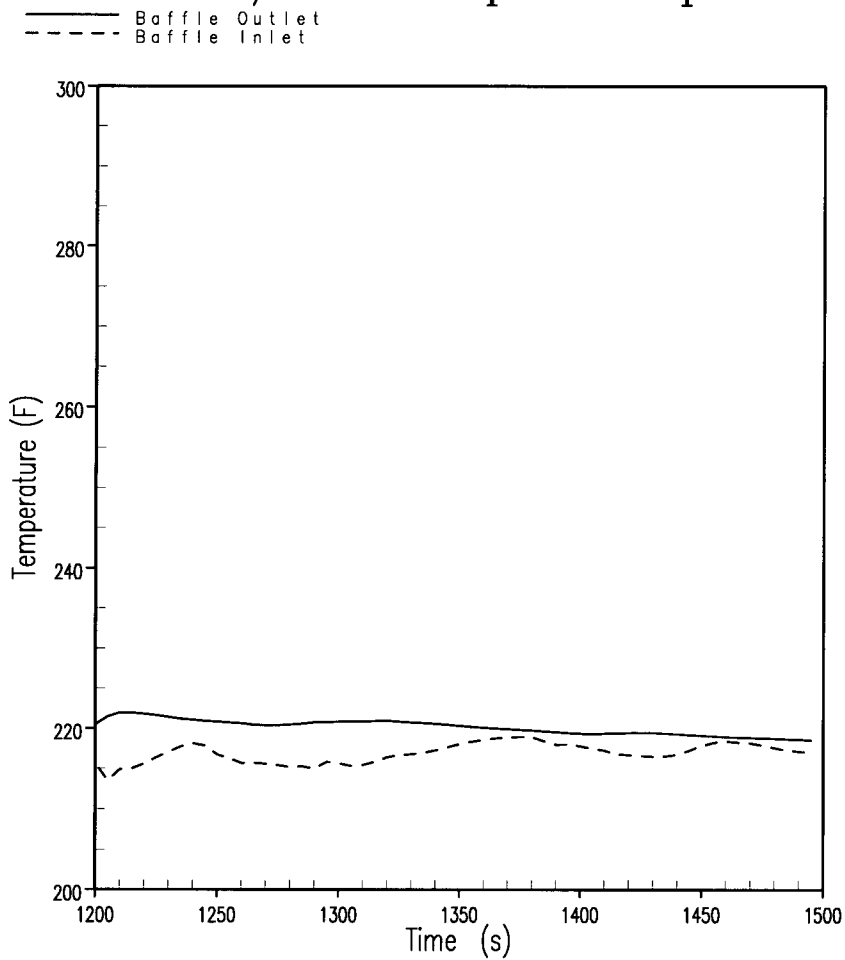


Figure B-58 Comparison of Fluid Temperature at Top and Bottom of Downcomer

Baffle Inlet/Outlet Liquid Temperature

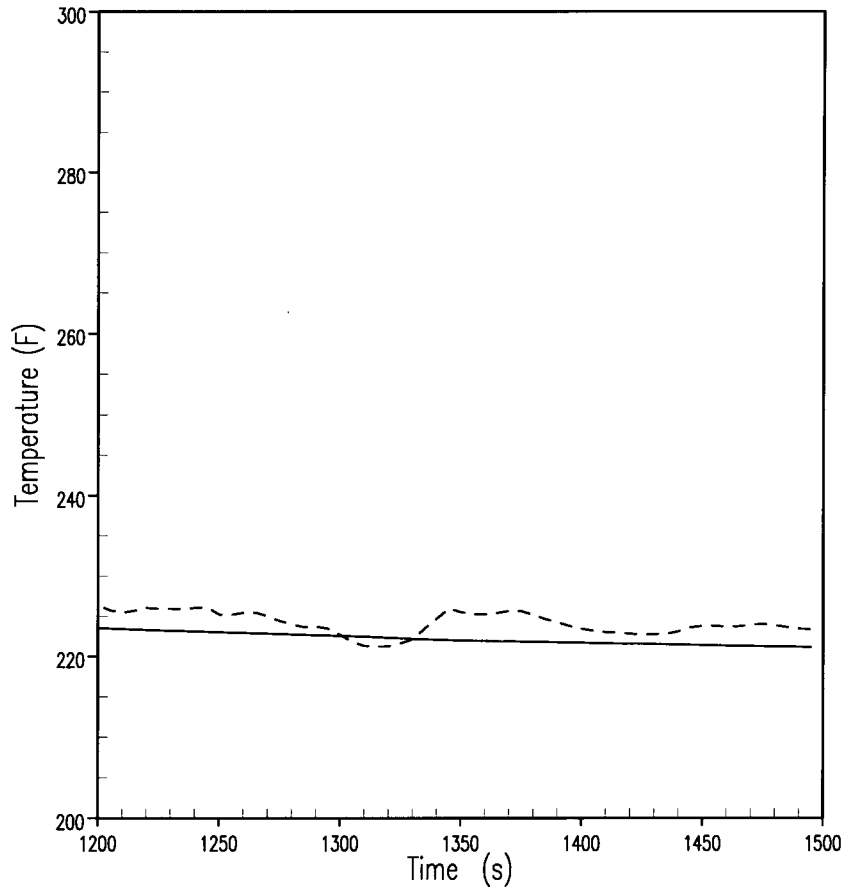


1781455584

Figure B-59 Comparison of Fluid Temperature at Top and Bottom of Baffle

Lower Plenum to Core Liquid Temperature

— Lower Plenum
- - - Bottom of Core



1761455584

Figure B-60 Comparison of Fluid Temperature in Lower Plenum to Core Inlet

Core Inlet Elevation Baffel Plate

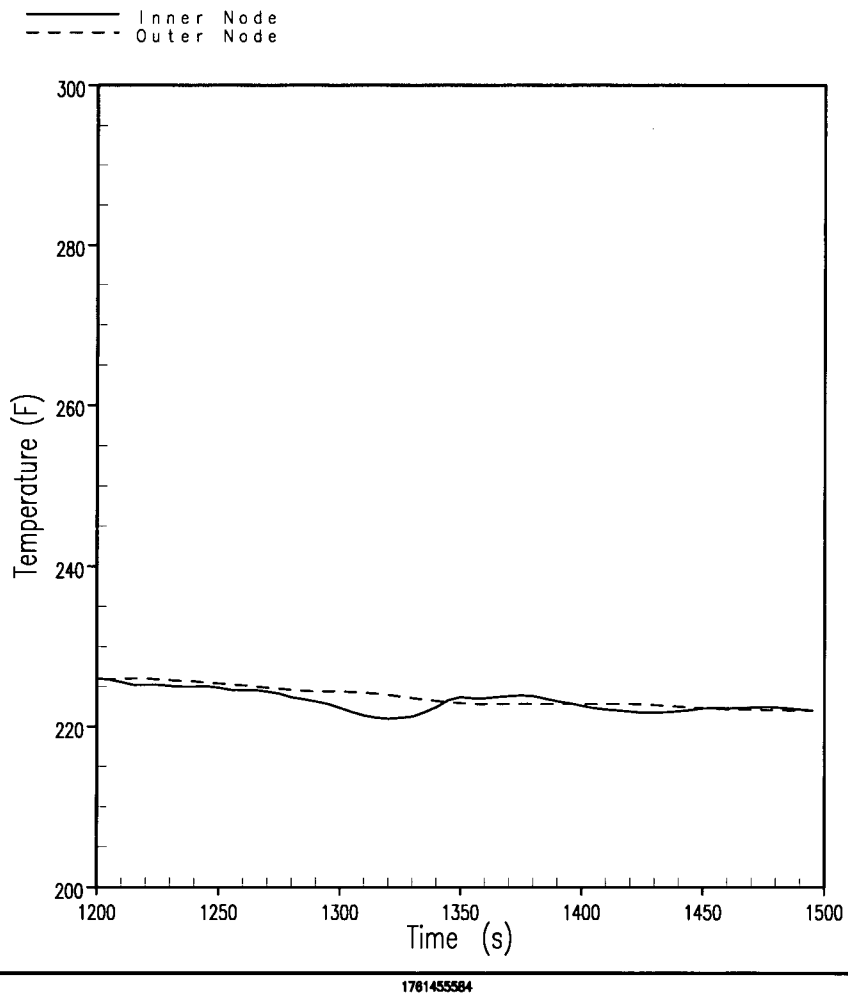
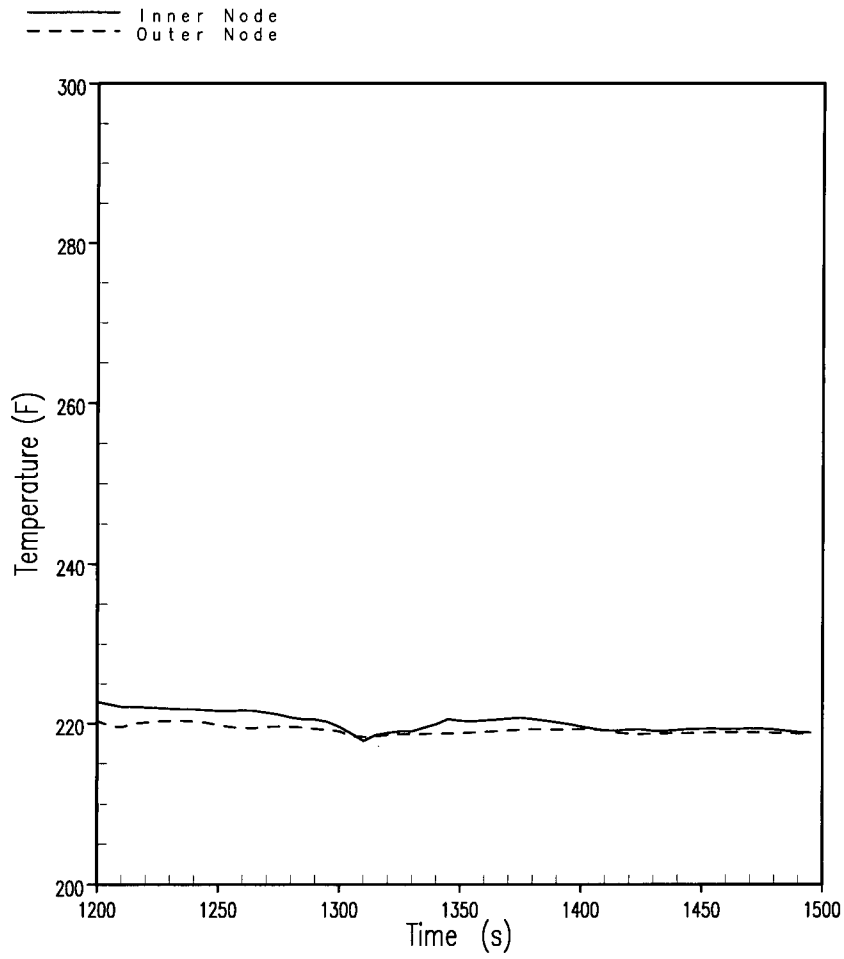


Figure B-61 Comparison of Fluid Temperature Between Core Inlet and Inside Baffle

Core Outlet Elevation Baffel Plate



1761455584

Figure B-62 Comparison of Fluid Temperature at Core Outlet and Top Baffle

B.7 REFERENCES

- B-1. Thermophysical Properties of Fluid Systems, <http://webbook.nist.gov/chemistry/fluid/>, April 11, 2007.

APPENDIX C

FUEL CLAD HEAT-UP UNDERNEATH GRIDS

C.1 INTRODUCTION

In an extreme case, it has been postulated that the volume between the fuel rod and spacer grid could completely fill with debris. An evaluation was performed to determine the cladding surface temperature of a fuel rod within a fuel grid when the rod is plated with debris in a post-LOCA recirculation environment. A parametric study was performed to show the effects on the maximum temperature of the fuel rod within the spacer grid caused by varying debris thickness and the thermal conductivity of the debris. A detailed discussion of this calculation, including a discussion of assumptions and boundary conditions, is presented here.

C.2 ANSYS DISCUSSION

The ANSYS mechanical software was used for the cladding heat up behind fuel grids. This software is in common use internationally to solve a wide range of mechanical engineering problems. The use of the thermal analysis capability for this model is in accordance and consistent with standard industry practices for ANSYS mechanical software and other similar engineering problem solving software.

The ANSYS mechanical software offers a comprehensive product solution for structural linear/nonlinear and dynamics analysis. The product offers a complete set of elements behavior, material models, and equation solvers for a wide range of engineering problems. In addition, ANSYS offers thermal analysis and coupled-physics capabilities involving acoustic, piezoelectric, thermal-structural, and thermal-electric analysis. For the cladding heat up calculations, only the thermal solution capabilities of the ANSYS mechanical software were used.

C.3 METHOD

A model of a single fuel rod was created in Solidworks® and imported into ANSYS. The model was cut down to a “1 quarter pie piece” in order to reduce the size of the model to be analyzed, while maintaining symmetry. In order to conservatively model the convection, the clad was divided into 20 zones. To preserve accuracy of this model, no convection was assumed to occur at the planes of symmetry. This was done to ensure that the convection was modeled only on the outer surface of the fuel rod assembly, and not on the surface of the cladding under the grids and the debris. A similar technique of dividing one large portion of the modeled fuel rod into multiple smaller segments was used to simulate the layers of debris in the runs using a thin debris layer (10 mils and under) in order to allow ANSYS to more easily generate a mesh. Once in ANSYS, all bodies in the model were meshed using a refined mesh size of 0.05, in order to create a finer mesh while still allowing the program to complete the analysis in a reasonable amount of time.

After the mesh was generated, a constant heat flux was set on the entire inner surface of the cladding, and convection heat transfer, with a constant convection coefficient set on the entire outer surface of the rod assembly. The mission time as defined in WCAP-16406-P-A (Reference C-1) is 30 days. In order to allow ANSYS to accurately model the simulation, the minimum time step was set to 10 seconds, but the

maximum time step was set to 400 hours. This allowed the simulation to speed up after steady state conditions had been reached, but still ensured that the final conditions had been achieved, without having to perform multiple runs for each scenario. Each model, with the exception of the clean rod, was run four times to collect data for debris thermal conductivities of 0.3, 0.5, and 0.9 $\left(\frac{\text{BTU}}{\text{hr} \cdot \text{ft} \cdot ^\circ\text{F}}\right)$. A new model was also generated for each debris thickness, from 5 to 50 mils.

C.4 MODEL INPUTS

The values in the Tables C-1 through C-4 are taken from the WC/T model described in Appendix B, thus providing for consistency between this calculation and the core inlet blockage calculation. Table C-1 summarizes the physical dimensions of the fuel rod model. Table C-2 lists the location of the standard and mixing vane grids modeled in this calculation. Table C-3 identifies the location of spacer and mixing vane grids along the length of the fuel rod.

Dimension	Value
Outer Cladding Diameter (in)	0.36
Cladding Thickness (in)	0.0225
Rod Length (in)	144
Grid Thickness (in)	0.018
Large Grid Length (in)	2.25
Small Grid Length (in)	0.475

Grid Type	Elevation from Base (in)
Large	24.57
Large	45.07
Large	65.67
Small	76.77
Large	86.17
Small	97.37
Large	106.77
Small	117.87
Large	127.27

Zone	Begin (in)	End (in)	Description	Debris
1	0.000	24.570	Clad – 1	No
2	24.570	26.820	Large Grid – 1	No
3	26.820	45.070	Clad – 2	No
4	45.070	47.320	Large Grid - 2	No
5	47.320	65.670	Clad – 3	No
6	65.670	67.920	Large Grid – 3	No
7	67.920	76.770	Clad – 4	No
8	76.770	77.245	Small Grid – 1	No
9	77.245	86.170	Clad – 5	No
10	86.170	88.420	Large Grid – 4	No
11	88.420	96.000	Clad – 6a *	No
12	96.000	97.370	Clad – 6b *	Yes
13	97.370	97.845	Small Grid – 2	Yes
14	97.845	106.770	Clad – 7	Yes
15	106.770	109.020	Large Grid – 5	Yes
16	109.020	117.870	Clad – 8	Yes
17	117.870	118.345	Small Grid – 3	Yes
18	118.345	127.270	Clad – 9	Yes
19	127.270	129.520	Large Grid – 6	Yes
20	129.520	144.000	Clad – 10	Yes

* The clad modeled in Section 6 was segregated into two parts, Zone 11 and Zone 12. This was done to provide for the simulation of oxide, crud and/or chemical product deposition over the fuel rod elevation extending from 96.000 in. to 144.000 in. Therefore, Zone 12 is modeled with a layer of material (oxide, crud, and/or chemical product deposition), while Zone 11 is modeled as a clean-surface fuel rod.

Table C 4 lists the average values of the thermal hydraulic boundary conditions used for the single fuel rod heat-up calculations. These values were taken from the WC/T output for the LOCA simulation at 1200 seconds after the initiation of the transient from Appendix B; the time of switchover from injection from the RWST to recirculation from the containment sump. The values listed in the table are averages of the values taken at multiple points along the surface of the fuel rod surface. Table C-5 lists the thermal properties of the cladding material modeled in the WC/T analysis and were used for the fuel rod heat-up calculation described in this appendix. Table C-6 lists the range of values for the two input parameters that were varied for the calculations described in this appendix.

Input	Value
Liquid Heat Transfer Coefficient $\left(\frac{\text{BTU}}{\text{hr} * \text{ft} * ^\circ\text{F}} \right)$	638.32
Vapor Heat Transfer Coefficient $\left(\frac{\text{BTU}}{\text{hr} * \text{ft} * ^\circ\text{F}} \right)$	17.30
Ambient Liquid Temperature ($^\circ\text{F}$)	194.02
Ambient Vapor Temperature ($^\circ\text{F}$)	224.95
Heat Flux, Outer Cladding Surface $\left(\frac{\text{BTU}}{\text{hr} * \text{ft}^2} \right)$	6508.93

Temp ($^\circ\text{F}$)	k $\left(\frac{\text{BTU}}{\text{hr} * \text{ft} * ^\circ\text{F}} \right)$	Cp $\left(\frac{\text{BTU}}{\text{lb}_M * ^\circ\text{F}} \right)$
200	7.984	0.07044
250	8.129	0.07183
300	8.274	0.07276
350	8.419	0.07356
400	8.564	0.07436
450	8.709	0.07516
500	8.854	0.07596
550	8.999	0.07676
600	9.144	0.07756
650	9.289	0.07836
700	9.434	0.07914
750	9.595	0.07979
800	9.860	0.08044
850	10.13	0.08109
900	10.39	0.08174
950	10.65	0.08239
1000	10.92	0.08303

Table C-6 Variable Ranges		
Property	Lower Value	Upper Value
Debris Thermal Conductivity $\left(\frac{\text{BTU}}{\text{hr} \cdot \text{ft} \cdot ^\circ\text{F}}\right)$	0.1	0.9
Debris Thickness (mils)	0	50

The accepted EPRI value for crud thermal conductivity according to EPRI Project document, “Boron-induced Offset Anomaly (BOA) Risk Assessment Tool” is $0.5 \left(\frac{\text{BTU}}{\text{hr} \cdot \text{ft} \cdot ^\circ\text{F}}\right)$. In order to perform a sensitivity study, values of 0.1, 0.3 and $0.9 \left(\frac{\text{BTU}}{\text{hr} \cdot \text{ft} \cdot ^\circ\text{F}}\right)$ were also analyzed. The crud thickness is modeled up to a maximum value of 50 mils as this bounds what the operating plants would be expected to experience.

C.5 ASSUMPTIONS

- The top third of the fuel rod (4 ft) was assumed to be covered in a layer of debris, the bottom two thirds (8 ft) was assumed to remain clean throughout the event.
- All debris that reaches the fuel rod was evenly distributed over the affected area, and was modeled with uniform thermal properties.
- The heat generated by the fuel pellets was modeled as a constant heat flux exerted on the entire inner surface of the cladding (but was based on an outer heat flux value). This assumption was made to simplify the model by removing the fuel pellets and the gap, while maintaining thermal accuracy.
- The cladding material type did not factor into this evaluation, since the value was ultimately based on the heat flux at the cladding surface.
- No convection occurred under the grids in the fuel rod assembly. This assumption was made to maintain conservatism, as the actual value will be less than the value on the surface of the assembly, but the exact value is unknown.
- Grids were assumed to have the same thermal properties as cladding.
- Debris was assumed to have the same thermal properties as crud. The accepted EPRI Value for the crud thermal conductivity was $0.5 \left(\frac{\text{BTU}}{\text{hr} \cdot \text{ft} \cdot ^\circ\text{F}}\right)$.

C.6 RESULTS

The calculated maximum clad temperatures are summarized in Table C-7 and are shown graphically in Figure C-1.

Table C-7 Maximum Clad Temperatures (T_{MAX})				
Debris Thickness (mils)	Debris Thermal Conductivity $\left(\frac{\text{BTU}}{\text{hr} \cdot \text{ft} \cdot ^\circ\text{F}}\right)$			
	0.1	0.3	0.5	0.9
	T_{MAX}	T_{MAX}	T_{MAX}	T_{MAX}
0	260°F	260°F	260°F	260°F
5	—	269°F	266°F	264°F
10	305°F	277°F	271°F	266°F
15	—	284°F	275°F	269°F
20	—	291°F	280°F	271°F
25	—	297°F	284°F	274°F
30	386°F	303°F	288°F	276°F
35	—	310°F	291°F	278°F
40	—	316°F	295°F	281°F
45	—	322°F	299°F	283°F
50	474°F	327°F	302°F	285°F

The calculated maximum clad temperatures all occur under a grid on the upper section of the fuel rod assembly. Assuming the minimum thermal conductivity of the debris collected in the grid and assuming a debris thickness of 50 mils, a maximum cladding temperature behind a grid of 474°F is calculated. This calculated temperature is well below the 800°F LTCC acceptance basis identified in Appendix A. Thus, the clad surface temperature acceptance basis of 800°F identified in Appendix A is satisfied.

The temperatures calculated with this model are conservative. The calculation assumed no flow through the grid. Thus, some coolant flow is expected to pass through the grid, cooling the clad surface. Not accounting for flow through the debris captured between the grid and the clad provides for the calculation of a conservatively high clad surface temperature.

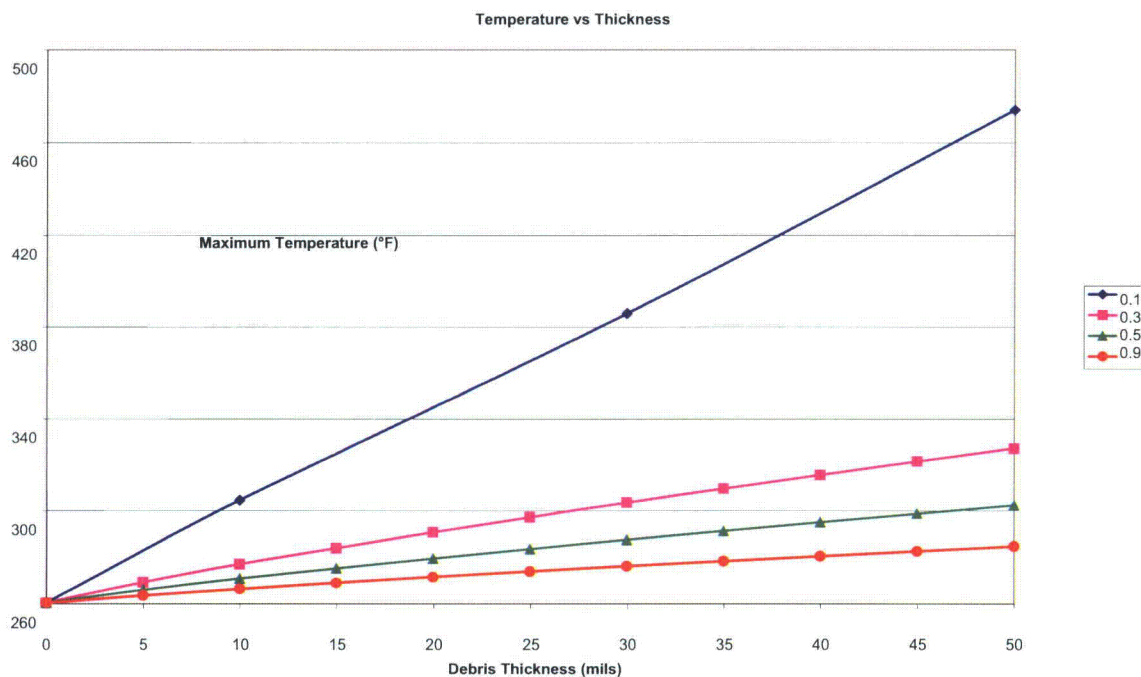


Figure C-1 Temperature vs. Deposition Thickness and Thermal Conductivity

Comparing these results to those of Appendix D, the corresponding Appendix D temperatures are approximately 15°F to 86°F hotter. The reason for this is that the Appendix D analysis used a bulk fluid temperature that was 25°F hotter, and a heat flux that was 25 percent larger, and considered oxide and crud layers, each 100 microns (4 mils) thick, in addition to a 50 mil layer of precipitate. These additional layers also contributed several °F to the temperature increase predicted by the calculations described in Appendix D.

C.7 REFERENCES

- C-1 WCAP-16406-P-A, Revision 1, "Evaluation of Downstream Sump Debris Effects in Support of GSI-191," March 2008.

APPENDIX D

FUEL CLAD HEAT-UP BETWEEN GRIDS

D.1 INTRODUCTION

In an extreme case, it has been postulated that debris could adhere to the fuel rods and impede decay heat removal. A parametric study was performed to show the effects on the maximum temperature of the fuel rod due to deposited debris by varying debris thickness and the thermal conductivity of the debris. A detailed discussion of this calculation, including a discussion of assumptions and boundary conditions, is presented here.

D.2 DESCRIPTION

This appendix provides an engineering analysis of the heat transfer behavior associated with fuel cladding that has a coating or layering of oxide, crud, and debris precipitate. Boundary conditions are decay heat of the fuel and two phase thermal hydraulic conditions associated with the core in a post LOCA environment.

The acceptance criterion used was the 800°F value identified in Appendix A. The temperature at the oxide/clad interface was compared to the acceptance criterion; this location represented the OD surface of the cladding. As noted in Appendix A, this temperature was chosen as autoclave testing has demonstrated that it is a value below which excessive cladding oxidation and hydrogen embrittlement has been demonstrated to not to occur.

D.3 METHODOLOGY

This analysis considered the cladding as being surrounded by concentric layers of oxide, crud, and chemical precipitate, with no gaps between them. The source of heat was decay heat in a post-LOCA environment, and the section of rod analyzed was assumed to be fully exposed to a two-phase liquid/vapor environment in the core. This analysis used the generic resistance form of the heat transfer equation, for a radial coordinate system.

Figure D-1 provides a graphical depiction of the analysis model.

D.4 INPUTS/ASSUMPTIONS

- This analysis only considered heat conduction in the radial direction. No axial heat conduction was assumed to occur.
- This analysis did not assume the presence of any grid components.
- The fuel rod power value was assumed to be a constant value of 0.226 kW/ft. This is a reasonable value for the peak power level at 20 minutes post-LOCA.

- The fuel cladding outside diameter was assumed to be 0.360 in. (a typical value for Westinghouse fuel).
- The cladding material type does not factor into this evaluation, since the calculation uses the heat flux at the cladding/oxide interface.
- The total convective heat transfer coefficient was assumed to be a constant value of 650 BTU/hr-ft²-°F. This is a reasonable value at 20 minutes post-LOCA.
- The assumed conductive heat transfer coefficients were:
 - Oxide – Constant value of 1.27 BTU/hr-ft-°F (based on accepted PWR industry experience).
 - Crud – Constant value of 0.3 BTU/hr-ft-°F (based on accepted EPRI Value).
 - Debris Precipitate – Analysis cases considered are 0.1, 0.3, 0.5, and 0.9 BTU/hr-ft-°F.

The values of thermal conductivity represent bounding values for a silicate precipitate (0.1 BTU/hr-ft-°F), a bounding value for a calcium-based precipitate (0.3 BTU/hr-ft-°F), a value for crud reported by EPRI (0.5 BTU/hr-ft-°F), and enhanced heat transfer through a highly conductive and porous medium (0.9 BTU/hr-ft-°F).

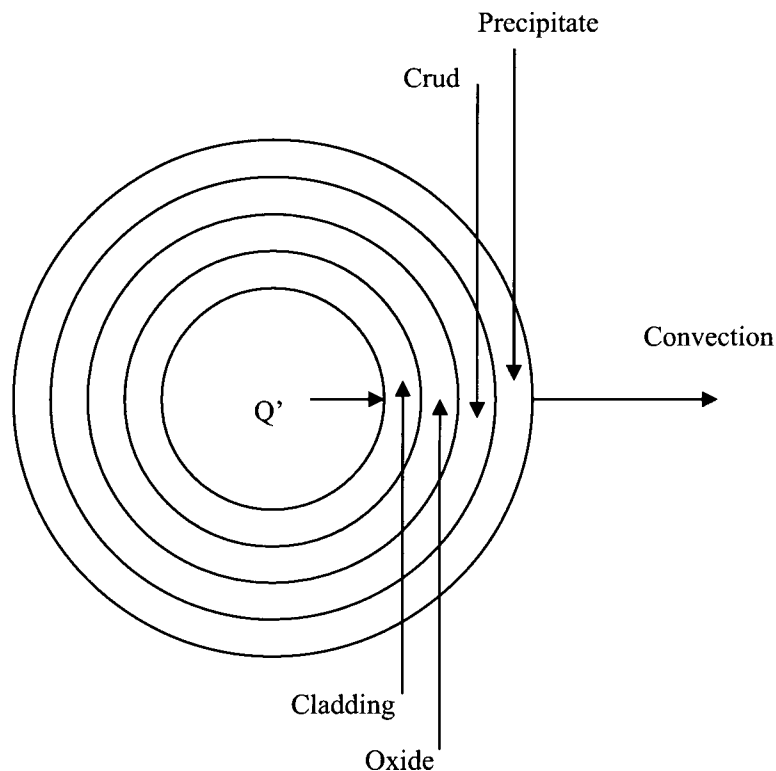


Figure D-1 Heat Transfer Model (not to scale)

- The thickness of each material was assumed to remain uniform around the circumference of the fuel rod:
 - Oxide – Constant value of 100 microns (0.004 in) (based on upper bound of PWR industry experience).
 - Crud – Constant value of 100 microns (0.004 in) (based on upper bound of PWR industry experience).
 - Debris Precipitate – Analysis cases varied from 0 to 50 mils (0.05 in) in 10 mil increments.

- No contact resistance was assumed to exist between material layers. The term ‘contact resistance’ refers to the resistance to the transmission of heat across the boundary of two adjacent solids. This resistance to heat flow is due to gases or vacant spaces between the two solids.

The development of the oxide layer and the deposition of the crud layer on the oxide, both which occur at power operations, are gradual and occur over time. The oxide provides nucleation sites for the deposition of the crud and the crud adheres to the outer oxide layer. The thermal conductivity of both the clad oxide layer and the crud already account for the morphology of their formation, including gases or vacant spacers. Since the crud adheres to the outer clad oxide layer by attaching itself to surface irregularities in the oxide layer, additional surface resistance was evaluated and found not to be appropriate during long-term core.

Similarly, the deposition of the debris layer on the crud surface is also gradual and occurs over time. The deposition on and adhesion to the surface of the crud layer is evaluated to be similar to that of the crud onto the clad oxide layer. Considering that a conservatively small thermal conductivity value for the debris deposition of 0.1 Btu/(hr-ft-°F) is used for the parametric study, the use of a contact resistance is evaluated to be both inappropriate and overly conservative.

- The bulk fluid temperature (T_{∞}) was assumed to be 250°F. This is a reasonable and expected value for the post-LOCA fluid temperature within the core.

D.5 RESULTS (TABLE/FIGURE)

Table D-1 lists the clad/oxide interface temperatures for each of the four values of precipitate thermal conductivity analyzed.

Chemical Precipitate Thickness (mils)	$k_{\text{precipitate}}$ BTU/hr-ft-°F			
	0.1	0.3	0.5	0.9
0	273°F	273°F	273°F	273°F
10	336°F	293°F	285°F	279°F
20	396°F	313°F	296°F	286°F
30	453°F	331°F	308°F	291°F
40	508°F	350°F	318°F	297°F
50	560°F	367°F	328°F	302°F

Figure D-2 plots the clad/oxide interface temperature as a function of chemical precipitate thickness for four values of precipitate thermal conductivity.

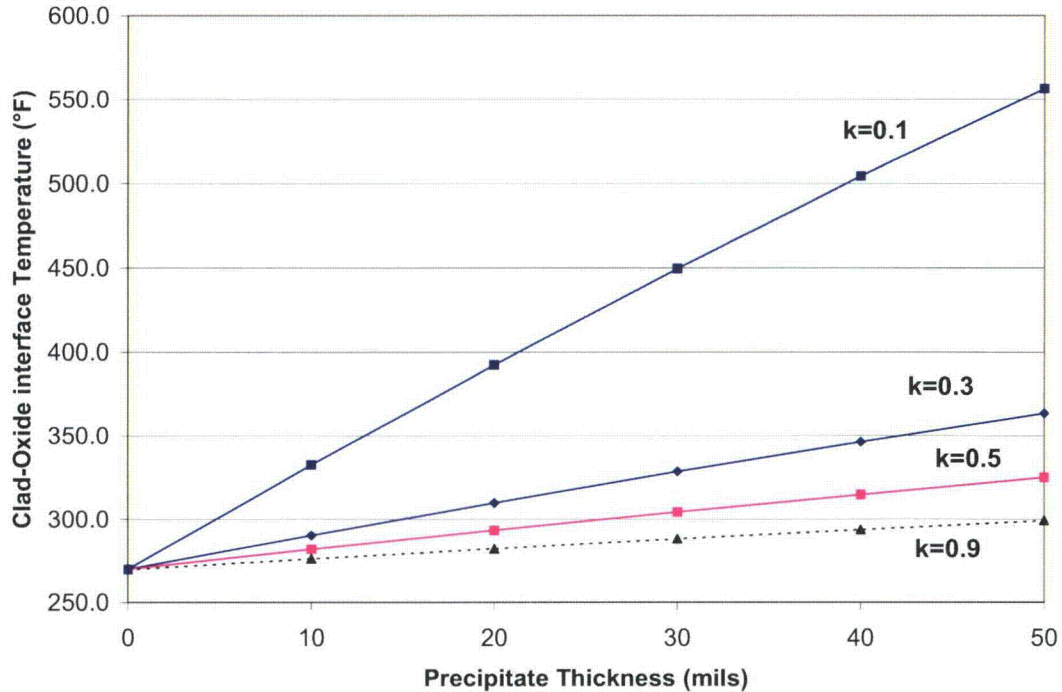


Figure D-2 Clad-Oxide Interface Temperature vs. Chemical Precipitate Thickness

D.6 SENSITIVITY CALCULATIONS FOR OTHER PWR FUEL DESIGNS

The fuel rod diameter used in the calculations listed in Table D-1 was 0.36 in. To demonstrate the applicability of these results to all PWR fuel designs, two sets of sensitivity calculations were performed using the following fuel rod specifications:

- 0.422 in. OD fuel rod at 0.388 kW/ft power value
- 0.416 in. OD fuel rod at 0.383 kW/ft power value

These two cases, along with the calculations for the 0.360 in. fuel rod, are expected to bound all PWR fuel types.

Table D-2 lists the clad/oxide interface temperatures for these two sensitivity calculations.

Chemical Precipitate Thickness (mils)	$k_{\text{precipitate}} = 0.1 \text{ BTU/hr-ft-}^\circ\text{F}$	
	0.422" OD rod	0.416" OD rod
0	283.6°F	283.6°F
10	377.0°F	376.9°F
20	466.4°F	466.2°F
30	552.1°F	551.9°F
40	634.5°F	634.1°F
50	713.8°F	713.2°F

D.7 SUMMARY

In all cases, the maximum surface temperature calculated for cladding between two grids, using conservative boundary conditions representative of those during recirculation from the containment sump following a postulated LOCA, is less than 800°F. For the 0.360 in. diameter fuel rod, the maximum temperature with 50 mils of precipitate on the clad OD is calculated to be less than 560°F. For the 0.416 in. or 0.422 in. rods, the maximum temperature with 50 mils of precipitate on the clad OD is calculated to be less than 715°F. Thus, all current PWR fuel designs satisfy the 800°F acceptance basis defined in Appendix A.

It is interesting to note that, assuming about a 10 mil precipitate layer (see the sample calculations of precipitate given in Appendix E) for the thicker fuel rods, the maximum clad temperature is calculated to be about 377°F. Thus, for a realistic thickness of precipitate, fuel surface temperatures are expected to be below 400°F.

It is also noted that these temperatures are conservatively large, as they assume a constant decay heat level at the time of ECCS switchover to recirculation from the containment sump (20 minutes after initiation of the transient). At this time in the transient, there has been no time to build a layer of precipitate. Chemical products have had little time to form and the concentrations are therefore low, and coolant from the sump is just being introduced into the RV by the ECCS. As decay heat continues to decrease, the calculated clad surface temperatures for a specific thickness of precipitate would also decrease.

Comparing these results of Table D-1 to those of Appendix C, the corresponding temperatures in the Appendix D calculations are approximately 15°F-86°F hotter. The reason for this is that the Appendix D analysis used a bulk fluid temperature that was 25°F hotter than that used for the calculations of Appendix C and a heat flux that was 25 percent larger. In addition, Appendix D considered oxide and crud layers, each 100 microns (4 mils) thick, in addition to a 50 mil layer of precipitate. These additional layers also contributed to the slightly higher calculated fuel clad surface temperature increase.

APPENDIX E

CHEMICAL PRECIPITATION AND SUBSEQUENT IMPACT

E.1 OBJECTIVE

The purpose of this evaluation is to predict the growth of fuel cladding deposits from coolant impurities after a LOCA.

E.2 INTRODUCTION

PWR containment buildings are designed to facilitate core cooling in the event of a LOCA. In some LOCA scenarios, the cooling process requires water discharged from the break and containment spray to be collected in a sump for recirculation by the ECCS and CSS. The water in the sump will contain chemical impurities and debris as the result of the interaction of the discharged coolant with containment materials. Major classes of debris and chemical impurities include:

1. Insulation
2. Ablated structural materials, such as concrete
3. Small particulates from corrosion of system materials
4. Dissolved corrosion products

In addition, the sump water will contain chemicals that are intentionally added for post-LOCA pH, corrosion, and reactivity control:

1. Buffering agents, such as:
 - a. Sodium hydroxide (NaOH)
 - b. Trisodium phosphate (TSP)
 - c. Sodium tetraborate (NaTB)
2. Boric acid
3. Lithium Hydroxide

Boric acid is always added for reactivity control. It is usually combined with only one of the three alkaline materials (NaOH, TSP, or NaTB) to adjust the pH of the coolant. This is done to promote iodine retention and to reduce stress corrosion cracking. Small amounts of lithium hydroxide also will be found in the coolant, since it is used for pH control during normal operation of the plant.

There has been much concern recently that fibrous and particulate debris within the sump after a LOCA could collect on the sump screen and block the flow of cooling water into the core. There is also a concern that debris could collect at other locations within the ECCS such as the FA grids. The NRC identified its concern regarding maintaining adequate LTCC in GSI-191 (Reference E-1). Generic Letter (GL) 2004-02 (Reference E-2), issued in September 2004, identified actions that utilities must take to address the sump blockage issue. The NRC's position is that plants must be able to demonstrate that

debris transported to the sump screen after a LOCA will not lead to unacceptable head loss for the recirculation pumps, will not impede flow through the ECCS and CSS, and will not adversely affect the long-term operation of either the ECCS or the CSS.

To demonstrate acceptable ECCS and CSS performance, licensees must be able to account for chemical reactions within the coolant that could alter flow through the sump screen or lead to deposition of material within the core.

Westinghouse previously developed a method for predicting post-LOCA chemical reactions and the formation of material that could block sump screens in WCAP-16530-NP-A (Reference E-3). This methodology has been reviewed by the NRC, and the industry has been using it as a basis for demonstrating adequate sump screen performance in plant-specific sump screen testing.

Post-LOCA chemical reactions can also occur in the core. Aside from precipitates adding to the head loss in the core (which is addressed in the FA testing in Appendix G), there is a concern that chemical plate-out on the hot fuel cladding can impede the heat removal from the fuel rods. The NRC issued specific guidance for responding to this concern to the industry at the GSI-191 Resolution Status Meeting of February 7, 2007 (Reference E-4). The NRC asked that submittals intended to demonstrate the viability of LTCC meet the following requirements specific to chemical effects concerns:

1. The methods must be flexible enough to include different ECCS and RCS designs
2. Chemical concentration effects due to long-term boiling should be assessed
3. The plate-out of deposits on the fuel rods should be considered
4. The effect of deposits on heat transfer should be estimated

LOCADM was developed to enable plants to address the above concerns when documenting the viability of long term cooling with respect to the fuel.

E.3 OVERVIEW OF LOCADM

LOCADM is a calculational tool that can be used to conservatively predict the build-up of chemical deposits on fuel cladding after a LOCA. The source of the chemical products is the interaction of the fluid inventory in the reactor containment building sump with debris and other materials exposed to and submerged in the sump fluid or containment spray fluid. LOCADM predicts both the deposit thickness and cladding surface temperature as a function of time at a number of core locations or "nodes." The deposit thickness and maximum surface temperature within the core are listed in the output for each time period so that the user can compare these values to the acceptance basis for long term cooling.

The chemical inputs into LOCADM are the volumes of different debris sources such as fiberglass and calcium silicate (cal-sil) insulation. The surface areas of uncoated concrete, aluminum submerged in the sump, and aluminum exposed to spray are also required. The sump and spray pH are specified as a function of time, as are the inputs of sodium hydroxide, trisodium phosphate, sodium tetraborate, lithium hydroxide, and boric acid.

Chemical product transport into the core is assumed to occur by the following process:

- Containment materials corrode or dissolve, forming solvated molecules and ions.
- Some of the dissolved material precipitates, but the precipitates remain in solution as small particles that do not settle.
- The dissolved material and suspended particles pass through the sump screen and into the core during recirculation. For the purpose of adding conservatism, it is assumed that none of the precipitates are retained by the sump screen or any other non-fuel surfaces.

Note that the transport of small fibers that do not dissolve but are small enough to be transported through the sump screen and into the core is not considered explicitly in LOCADM. The quantity of transported fines is expected to be small compared to both the total amount of debris and the amount of debris that dissolves or corrodes. Fiber can be accounted for in LOCADM in cases where it is significant by use of a “bump-up factor” applied to the initial debris inputs. The bump-up factor is set such that total mass of deposits on the core after 30 days is increased by the best estimate of the mass of the fiber that bypasses the sump screen. Guidance on using the bump-up factor is provided in Section E.9.3.3.

Coolant flow rates into the reactor mixing volume as a function of time must be provided by the user and are obtained from a plant’s safety analysis for long term core-cooling. The relative amounts of steam and liquid flow out reactor mixing volume are calculated by LOCADM. The core input is generalized. The coolant flow could be coming from the CL, the HL, or from UPI. Various operational modes are accounted for by varying the rate of flow into the mixing volume and the source of the flow (safety injection or recirculated coolant). Values for generically applicable mixing volumes have been identified and will be provided to users (Reference E-7). The temperature of the sump and reactor coolant as a function of time must also be entered by the user.

Within the mixing volume, the coolant is assumed to be perfectly mixed. Coolant chemical products entering the reactor are distributed evenly between all core nodes before deposition calculations are performed. The entire mixing volume is also assumed to be at the same temperature. Pressure is determined by the upper plenum pressure and the hydrostatic pressure at different elevations in the core. No attempt was made to model flow within the mixing volume and variations in that flow that might be caused by grids and flow obstructions. Since flow was not modeled, a heat transfer coefficient of $400 \text{ W/m}^2\text{-}^\circ\text{K}$ ($70 \text{ BTU/ft}^2 \text{ }^\circ\text{F}$) was assumed for transfer of heat between bulk coolant with the fuel channels and the surface of the deposits since this is a typical heat transfer coefficient for convective flow within natural circulation systems.

LOCADM deposits chemical products that are dissolved or suspended in solution throughout the core in proportion to the amount of boiling in each core node. It is assumed that deposition rate is equal to the steaming rate times the chemical product concentration at each node. If there is no boiling, the chemical products are distributed according to heat flux, at an empirically derived rate that is $1/80^{\text{th}}$ of the deposition that would have occurred if all of the heat had gone into the boiling process.

The deposition algorithm does not rely on solubility or any other chemical characteristics of the chemical products to determine the deposition rate. All chemical material that is transported to the fuel surface by boiling is assumed to deposit. LOCADM uses a default deposit thermal conductivity for the deposited material of $0.1 \text{ Btu/(hr-ft-}^\circ\text{F)}$, which is low enough to bound expected core deposits. Likewise, the

default deposit density is low enough (e.g. 35 lbm Ca/ft²) to bound expected deposits including those that incorporate adsorbed boron or boron bonded to chemical product elements. Consistent with current licensing basis calculations for PWRs that demonstrate that the boric acid concentration in the core is limited to values below the solubility limit, the LOCADM does not precipitate boric acid. The same is true for sodium phosphate, sodium borates and sodium hydroxide, which are also highly soluble.

The core nodding within LOCADM can be adjusted by the user. Section E.7 provides guidance to the LOCADM user for node selection for different types of cores.

LOCADM runs within Microsoft EXCEL and should be easy to use for those familiar with EXCEL. The first sheet of the workbook instructs the user on how to enter the chemical and flow inputs into worksheets in tabular form. A macro written in Visual Basic for Applications is then run. The macro reads the input, looks for input errors, calculates core conditions in one second intervals, and then outputs the results within the same workbook.

E.4 DISCUSSION OF MAJOR ASSUMPTIONS

The deposition method makes several assumptions that are conservative and, as a result, the predictions of deposit thickness and fuel surface temperature should be considered to be bounding rather than best estimate for the following reasons.

1. The calculations assume an increase in deposit volume (or indirectly, mass) during precipitation due to the incorporation of species, such as the waters of hydration or boric acid. However, specific compounds are not assumed. This is done by specifying a deposit density that is sufficiently low to bound possible hydrates and adsorbed species (e.g. 35 lbm Ca/ft²).
2. Deposits, once formed, will not be thinned by flow attrition or by dissolution.
3. No deposition takes place apart from the fuel heat transfer surfaces. A best estimate approach would have accounted for deposition on non-fuel surfaces such as the RHR heat exchangers and surfaces in containment, resulting in thinner core deposits.
4. The mass balance approach for determining material transport around the ECCS does not take into account any moisture carry-over in the steam exiting the RV. Experimental measurements simulating the post-LOCA environment indicate that concentration of non-volatile material within the RV will be considerably reduced if moisture carryover is included in the estimation. Not including boron in the moisture carryover is conservative but non-realistic.
5. The effect of boiling point elevation due to the concentration of solutes is not currently modeled. This simplification will result in an over-prediction of boiling in the core and thus any error introduced by the simplification will be in the conservative direction.
6. Only species that have dissolved into solution or species that have dissolved and then precipitated into suspended particles are considered. The transport of large debris particles from containment and re-deposition of debris from fuel failures have not been included. Larger debris will either settle or will be physically retained on the sump screen, the FA fuel filters, or other locations

where flow is restricted. This mode of blockage has been addressed in other sections of this report.

7. All impurities transported into a deposit by boiling will be deposited at a rate that is equal to the steaming rate multiplied by the coolant impurity concentration. When the temperature at the oxide/deposit interface is below the boiling point, deposition is assumed to occur via convective deposition rather than by boiling. The non-boiling rate of deposit build-up is proportional to heat flux and is $1/80^{\text{th}}$ of that of boiling deposition at the same heat flux. This ratio is based on empirical data for mixed calcium salts under boiling and non-boiling conditions (Reference E-13).
8. The deposition of impurities on the fuel clad surface is assumed to be distributed according to the core power distribution.

E.5 DEBRIS DISSOLUTION AND CORROSION RATES

The chemical reactions of most concern for core deposition are those that release material into solution in a form where it can bypass the sump screen, collect in the RV, and precipitate on heated fuel cladding surfaces. The chemical reactions leading to the generation of such transportable material follow:

1. Corrosion or dissolution of system materials to directly produce a hydrous corrosion product that does not settle.
2. Corrosion or dissolution of system materials to produce dissolved material that later forms precipitates on the fuel due to temperature change and/or pH change.
3. Corrosion or dissolution of system materials followed by chemical reactions with other coolant chemicals to produce hydrous precipitates that do not settle.

Corrosion or dissolution of system materials is a first step that is common to all of the reactions. Any assessment of precipitation or deposition reactions within the post-LOCA environment must be able to estimate the dissolution behavior of containment materials.

A method to estimate the dissolution of containment materials has previously been developed and has been documented in WCAP-16530-NP-A (Reference E-3). The same equations and methods were used in the LOCADM model to estimate the release of calcium, aluminum, and silicon from containment materials.

The dissolution model in WCAP-16530-NP-A was developed using a database of containment material dissolution information that was generated as part of a previous PWROG project performed to support closure of GSI-191. The bench test data were collected specifically to facilitate the development of the dissolution model. The development of the dissolution model is described in WCAP-16530-NP-A.

The containment materials that were tested in WCAP-16530-NP-A are listed below:

1. Aluminum
2. Concrete (Calcium Silicates)
3. CalSil (Calcium Silicates)
4. Nukon Fiberglass (E-Glass, Calcium Aluminum Silicate)
5. High Density Fiberglass (E-Glass, Calcium Aluminum Silicate)
6. Mineral Wool (Magnesium, Calcium, Aluminum Silicate with Iron Oxide)
7. MIN-K (Amorphous Silica + E-Glass)
8. Fiber Frax Durablanket (Aluminum Silicate)
9. Interam (Polymer Filled Aluminum Silicate Fiber with Aluminum Backing)
10. Carbon Steel (Iron)
11. Galvanized Steel (Zinc Coated Iron)

The deposition model includes all of these materials, with the exceptions of carbon steel and galvanized steel, since the releases from these materials were low.

The chemical effects dissolution model has been coupled with the deposition model so that the two processes interact. Deposition in the core will increase the dissolution of material in the sump due to the removal of dissolved material from the sump solution. Dissolution of material in the sump will increase deposition rates in the core. LOCADM also assumes that the fluid in the sump and reactor are well mixed, and the dissolution of calcium, aluminum or silicon from one material will inhibit the dissolution of calcium, aluminum or silicon from another material by the common ion effect. Specific interactions, such as corrosion inhibition of aluminum by silicates or phosphates have not been included. Such interactions would reduce the amounts of material available for deposition on the core, but they have been ignored to add conservatism to the predictions.

E.6 TRANSPORT OF COOLANT, DISSOLVED SPECIES AND SUSPENDED SOLIDS WITHIN THE ECCS

The flow paths considered in this model are shown in Figure E-1.

Flows within the ECCS transport material primarily between two different coolant inventories: the sump and the RV. It is assumed that the mass of any liquid in the piping or vapor in the steam phase is negligible compared to the sump and RV masses. Coolant with impurities is moved into and out of the RV or sump.

Two other coolant inventories are considered early in the LOCA, the RWST or BWST and the sodium hydroxide spray additive tank (NaOH). The liquid masses available in these tanks is not specified in the LOCADM input, but implied by the flow rates and flow times from each tank.

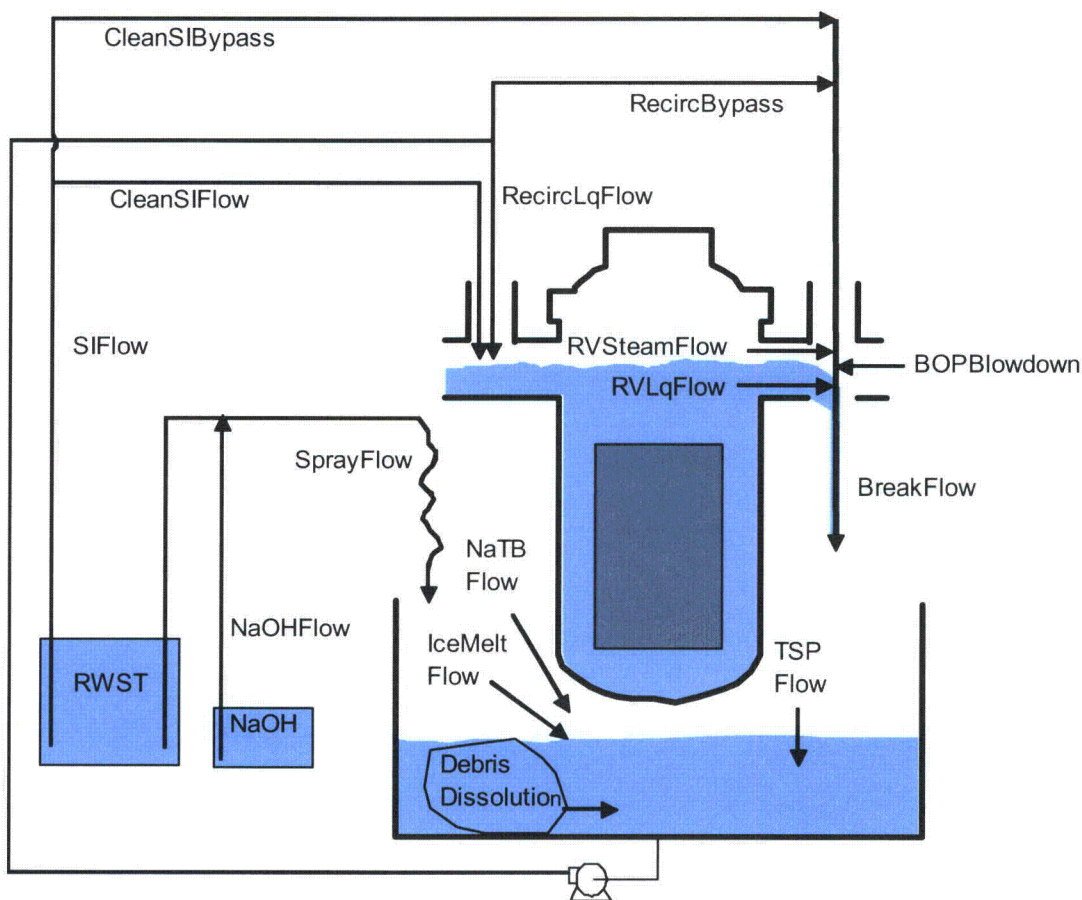


Figure E-1 Flow Paths Modeled by LOCADM

The mass inventory in the sump (SumpLqMass) is specified initially and is increased by the coolant mass flow from the break (BreakFlow) and the water flow from ice melt (IceMeltFlow) as well as the spray flow (Sprayflow). Mass is also added to the sump mass inventory by dissolution of TSP (trisodium phosphate), dissolution of NaTB (sodium tetraborate) and debris. It is decreased by the recirculation flow out of the sump. It should be noted that the IceMeltFlow input includes only water from ice melt. The NaTB flow is specified separately to accommodate plants that have NaTB input from baskets in containment.

The spray flow has two components, liquid from the RWST or BWST and a flow of sodium hydroxide solution (NaOHFlow) from the sodium hydroxide addition tank.

The break flow is divided into five different components: the blowdown from the balance-of-plant (BOPBlowdown), the RV liquid effluent (RVLqFlow), the steam exiting the RV (RVSteamFlow), the recirculated injection flow that bypasses the reactor (RecircBypass), and the safety injection flow from the RWST or BWST that bypasses the reactor (CleanSIBypass).

Inputs to the RV are the safety injection flows from the RWST or BWST (CleanSIFlow) and the recirculated coolant safety injection flow (RecircLqFlow).

The initial RV coolant mass (RVLqMass) is an input to the calculations as is the initial mass of fluid in the sump (SumpLqMass).

When the ECCS is in the recirculation mode, the recirculation flow may either enter the RV and mix with its contents (RecircLqFlow) or may bypass the reactor and flow out of the break (RecircBypass).

The mass inventories of the pH adjustment chemicals as well as the impurities calcium, aluminum, and silicon are maintained and adjusted every time step. From the mass inventories, concentrations are calculated and the concentrations are then used with various flows to determine the mass transport. The concentration is calculated in ppm as illustrated in Equation E-1.

$$C_x = (m_x / m_T) * 1,000,000 \quad (E-1)$$

where:

C_x = concentration of species x in ppm.

m_x is the mass of species x in the coolant inventory (e.g., kilograms Ca in the sump)

m_T is the total mass of liquid, dissolved and suspended material in the inventory

The mass flow of species x is then:

$$\text{MassFlow}_x = (C_x * \text{Flowrate} * dt) / 1,000,000 \quad (E-2)$$

where:

MassFlow_x is the mass flow in kg during the time interval

Flowrate is the total flowrate in kg/s (e.g., RecircLqFlow)

dt is the time interval in seconds = 1 second

The steam flow from the RV (RVSteamFlow) is calculated for each time step as shown below:

$$\text{RVSteamFlow} = P_o * P/P_o * dt / h_{fg} \quad (E-3)$$

where:

P_o	=	100 percent full core power before break (Watts thermal)
P/P_o	=	core power fraction at beginning of the time step (Appendix K)
dt	=	time step = 1 second
h_{fg}	=	standard enthalpy of vaporization (Joules/kg)

The standard enthalpy of vaporization (h_{fg}) for water was used in LOCADM. A formula was used to calculate this value as a function of temperature. The function produces a value near 2250 kJ/kg near 212°F. The standard enthalpy of vaporization for water is a good approximation except for the most

concentrated boric acid solution, and then the water will produce conservative results. The steam flow is set to zero whenever the temperature of the RV liquid falls below the boiling point by more than 1 degree Celsius. No correction is made for lower plenum subcooling, for the purpose of conservatism. The coolant within the RV is all assumed to be at the same temperature.

The mass of liquid in the sump at the end of a time step (SumpLqMass_e) in kilograms is determined by adding all of the mass inflows and subtracting all of the mass outflows from the sump liquid mass at the beginning of the time step (SumpLqMass_i).

$$\text{SumpLqMass}_e = \text{SumpLqMass}_i + (\text{IceMeltRate} + \text{NaTBFlow} + \text{TSPFlow} + \text{Breakflow} + \text{SprayFlow} - \text{RecircBypass} - \text{RecircLqFlow}) * dt \quad (\text{E-4})$$

The flowrate of recirculating coolant bypassing the reactor (RecircBypass) is obtained from mass balance considerations:

$$\text{RecircBypass} = \text{Breakflow} - \text{BOPBlowdown} - \text{RecircLqFlow} - \text{CleanSIFlow} - \text{CleanSIBypass} \quad (\text{E-5})$$

The above equation only holds when the RV has refilled and the inflow equals the outflow. This should be the case anytime there is recirculation flow. The recirculating coolant flow bypassing the reactor is of course zero before recirculation starts.

The mass flowrate of liquid exiting the RV is calculated according to Equation E-6, which was obtained by assuming the mass balance:

$$\text{RVLqFlow} = \text{Breakflow} - \text{BOPBlowdown} - \text{CleanSIBypass} - \text{RecircBypass} - \text{RVSteamFlow} \quad (\text{E-6})$$

E.7 MODELING OF THE CORE

The deposition model divides the core into user defined nodes that differ in location and relative decay power. The node is identified by region number and by axial location number. The software allows for as many as 200 regions and each region can correspond to a single assembly, a traditional fuel region having a particular enrichment and burn-up, or a group of rods, all with similar powers in different assemblies. The axial location numbers refer to the axial location of a node with lower numbers corresponding to higher elevations in the core. As many as 10 axial elevations can be defined, so the core may have as many as 2000 nodes. The axial divisions are assumed to span the fuel pellet stack and to divide it into nodes of equal height. For instance, a 12 foot high pellet stack might be divided into 3 axial nodes each 4 feet in height.

A number of parameters are associated with each node. The nodal parameters are decay power, fuel surface area (or number of rods), initial zirconium oxide thickness, initial crud thickness, and average depth within the core. These values are input as relative values. For instance, each region has a relative power and the weighted average of all relative powers must be 1.0. The weighting is done by number of rods in each region. Likewise, a relative power is associated with each axial location, and the average power of all axial locations will equal 1.0. To obtain the relative power of a particular node, the region

relative power is multiplied by the axial relative power. To get the total decay power for a particular node, the core decay power is multiplied by node area fraction and then by the region relative power and the axial relative power. The deposition predicted to occur in the core is distributed amongst the modeled core nodes according to the calculated total decay power for each node.

Since the radial noding establishes a conservatively high peak rod power (and a conservatively high peak deposit thickness) the choice of axial noding is not critical. Examples of values used for radial core noding is provided in Table E-1, where the number of rods in each node and the relative power at each node are specified for different core types (References E-8 and E-9). **It must be noted that this table is provided for information only and should not be used as a reference for radial core noding in LOCADM calculations without first contacting the plant fuel vendor for applicability regarding a particular core design.**

The debris and chemicals in solution are assumed to be evenly distributed among all core nodes. While it is possible that there could be small variations in concentration of debris chemicals between nodes within the mixing volume, large variations are not thought to be possible since large concentration variations would lead to density differences which would lead to conservative mixing. The possibility of small variations in concentration between nodes is not expected to result in non-conservative predictions of deposit thickness, because other highly conservative assumptions have been made. LOCADM includes conservative predictions of debris dissolution and corrosion product release. All such released material which is transported to fuel cladding surfaces by boiling is assumed to deposit, and it is assumed that there is no competitive deposition in other system locations.

Like the power distribution, the initial crud thickness and the initial zirconium oxide thickness are specified for each node as described in the following section. A core average value is modified by relative thickness for each region and axial location.

Table E-1 Example of Relative Power Distributions for Calculating Node Power					
Four-Loop Westinghouse NSSS					
15x15 Fuel Array			17x17 Fuel Array		
Relative Power	Number of Rods	Percentage of Rods	Relative Power	Number of Rods	Percentage of Rods
1.80	1	0.0025%	1.80	1	0.0020%
1.60	203	0.5156%	1.60	263	0.5162%
1.23	30192	76.6839%	1.23	39072	76.6839%
0.20	8976	22.7979%	0.20	11616	22.7979%
Three-Loop Westinghouse NSSS					
15x15 Fuel Array			17x17 Fuel Array		
Relative Power	Number of Rods	Percentage of Rods	Relative Power	Number of Rods	Percentage of Rods
1.80	1	0.0031%	1.80	1	0.0024%
1.60	203	0.6338%	1.60	263	0.6345%
1.17	26112	81.5287%	1.17	33792	81.5287%
0.20	5712	17.8344%	0.20	7392	17.8344%
Two-Loop Westinghouse NSSS					
14x14 Fuel Array			16x16 Fuel Array		
Relative Power	Number of Rods	Percentage of Rods	Relative Power	Number of Rods	Percentage of Rods
1.80	1	0.0046%	1.80	1	0.0035%
1.60	178	0.8218%	1.60	234	0.8229%
1.19	17184	79.3388%	1.19	22560	79.3388%
0.20	4296	19.8347%	0.20	5640	19.8347%
B&W NSSS					
Relative Power	Number of Rods	Percentage of Rods			
1.79	1	0.0027%			
1.79	207	0.5623%			
1	36608	99.435%			
CE NSSS					
14x14 Fuel Array			16x16 Fuel Array		
Relative Power	Number of Rods	Percentage of Rods	Relative Power	Number of Rods	Percentage of Rods
1.65	1	0.0026%	1.65	1	0.0024%
1.56	175	0.4594%	1.56	235	0.5646%
1.0	37916	99.5380%	1.00	41386	99.4330%

E.8 CALCULATION OF DEPOSITION MASS AND FUEL TEMPERATURE

Deposition of impurities on the fuel after a LOCA may occur by many different mechanisms. These mechanisms include electrostatic attachment of particles, crystallization driven by supersaturation, and boiling deposition. Since the boiling deposition mechanism results in the most rapid deposit growth and forms the most tenacious deposits, the LOCADM model assumes that all deposition occurs through the boiling process if conditions at a core node predict any boiling. All impurities transported into the deposit by boiling are assumed to be deposited at a rate proportional to the steaming rate.

The process of deposit growth during the core boiling phase is illustrated in Figure E-2.

The cladding surface just after the LOCA will start out with both a protective oxide layer and also a pre-existing crud deposit that was formed during normal operation. Both will have some porosity, but the crud deposit will be highly porous, with pore spaces composing about 60 percent of the deposit volume. The large pores are referred to as boiling chimneys and they typically are 2-5 microns in diameter. The smaller pores are sub-micron in size.

The coolant along with impurities will be wicked through the small pores. Boiling does not take place in the small pores, because of the boiling point elevation caused by surface stabilization of the liquid (capillary action). However, at the base of the larger chimneys, the coolant is converted to steam which exits through the top of the chimney into the coolant. Non-volatile species near the saturation limit will precipitate within the boiling deposit since such species cannot be transported into the steam phase, and they concentrate within the pores. High solubility species will not precipitate, and their concentration is limited by back-diffusion into the coolant or transport along the chimney walls. LOCADM calculates the concentration of boric acid, sodium tetraborate, trisodium phosphate and sodium hydroxide in the core as a function of time and provided in a tabular form. Consistent with current licensing basis calculations for PWRs that demonstrate that the boric acid concentration in the core is limited to values below the solubility limit, LOCADM does not precipitate boric acid. The existing plants EPO provide actions that are required to assure boric acid solubility limits are not reached. The same is true for sodium phosphate, sodium borates and sodium hydroxide, which are also highly soluble. This process has been studied extensively as described in References E-10 through E-12.

As the pores fill at the base of the original crud layer with newly formed crystals, the original crud layer will be pushed out, and the total deposit thickness will increase. This process often happens in steps, with crevices forming under the deposit which are quickly refilled by new crystal growth. The growth in deposit thickness will further insulate the cladding surface, so boiling within thick scale will continue even when the bulk coolant temperature falls below the boiling point.

Westinghouse thermodynamic predictions suggested that in the post-LOCA environment, the chemical compounds that deposit on the fuel would include: $\text{Ca}_2\text{B}_2\text{O}_5$, AlOOH , and $\text{CaAl}_2\text{Si}_3\text{O}_{10}(\text{OH})_2$. Calculations by AREVA NP using a thermodynamic equilibrium code (see Appendix F) suggested that $\text{NaAlSi}_3\text{O}_8$, $\text{Ca}_3(\text{BO}_3)_2$, Na_4SiO_4 , $\text{Al}(\text{OH})_3$ and SiO_2 may also precipitate.

Suspended matter such as small particles of calcium phosphate would be drawn into the deposit by the boiling mass flux and retained on or within the deposit. Most of the particles would be deposited in the outer portion of the deposit and would not be bonded as tightly as dissolved material that precipitated

within the deposit. This is one of the reasons why sodium phosphates are often used in boiler water conditioning. However, for the purpose of conservatism, the LOCADM model assumes that all suspended solids that are drawn into the deposit will remain as part of the deposit.

LOCADM makes no distinction between suspended solids and dissolved species. Both are deposited at the fuel rod surface. The density of the deposit is an input to LOCADM as is the thermal conductivity. LOCADM calculates the thickness of the deposit and then the heat transfer resistance using the deposit thermal conductivity. Concentrations of suspended solids are predicted to be low, so there will be no significant effect on the coolant density or thermal conductivity.

The following process is used in LOCADM to determine the quantity of the deposit for each node.

First, the temperature at the zirconium oxide/deposit interface is calculated using

$$T_{o/d} = Q/A * (x_c/k_c + x_l/k_l + 1/h) + T_c \quad (E-7)$$

where:

$T_{o/d}$	=	Temperature at the oxide/deposit interface (K)
T_c	=	temperature of the coolant (K)
Q	=	heat transfer rate (watts) for node
A	=	node area (m ²)
x_c	=	thickness of the original crud layer (m)
x_l	=	thickness of the LOCA scale layer (m)
k_c	=	thermal conductivity of the original crud layer
k_l	=	thermal conductivity of the LOCA scale layer
h	=	heat transfer coefficient for thermal resistance of coolant at boundary layer

The saturation temperature (the boiling point) is then calculated for the coolant in the core node being considered. This is derived from the local pressure, which is simply the user specified pressure in the upper plenum corrected for the pressure exerted by the height of the water in the core.

If the temperature calculated for the oxide/deposit interface is calculated to be above the boiling point, LOCADM assumes that all of the heat flux at the node will go towards boiling coolant. In reality, some of the heat will be transferred by radiation and by conduction coupled to non-boiling convection. The multiple modes of heat transfer in a boiling deposit have been described and modeled in Reference E-20, and ignoring the non-boiling mechanisms increases conservatism.

The fluid in all channels is assumed to be at the same temperature, and this temperature is derived from the plant's licensing basis calculations for LTCC. Flow is not modeled explicitly. Instead, a generic heat transfer coefficient of 400 W/m²-°K (70 BTU/ft²-°F) was assumed for transfer of heat between bulk coolant with the fuel channels and the surface of the deposits since this is a typical heat transfer coefficient for convective flow within natural circulation systems. The channel pressure is the sum of the upper plenum pressure and the pressure exerted by the height of the water column above the user and is obtained from a plant's safety analysis for LTCC. The relative amounts of steam and liquid flow from the reactor mixing volume are calculated by LOCADM. The core input is generalized. The coolant flow

could be coming from the CL, the HL, or from upper plenum injection. Various operational modes are accounted for by varying the rate of flow into the mixing volume and the source of the flow (safety injection or recirculated coolant.) Values for generically applicable mixing volumes have been identified and will be provided to users.

Regarding countercurrent flow limiting effects, the limitations on upper plenum injection flow due to countercurrent stream flow must be calculated outside of LOCADM using RELAP5 or another approved code. However, once the effective flow into the mixing volume is calculated, it can be used as an input to LOCADM.

The mass of each impurity element deposited during a time step is calculated simply by multiplying the steaming rate times the concentration of that species.

$$w_n = Q * dt * C_i / h_{fg} \quad (E-8)$$

where:

w_n	=	deposit mass for time step in node
dt	=	time step = 1 second
h_{fg}	=	standard enthalpy of vaporization (joules/kg)
Q	=	heat transfer rate (watts) for node
C_i	=	concentration of species "i" (kg/m^3)

The thickness added to the LOCA scale is then determined by dividing the mass deposited within the node by the density times the area.

$$dx = w_n / (D * A) \quad (E-9)$$

where:

dx	is the increase in the deposit thickness for the node
D	= density in kg/m^3
A	= area of the node in m^2

If the fuel surface is not boiling, the deposition is assumed to be $1/80^{\text{th}}$ the mass that would have been deposited had all of the heat transfer occurred by boiling. This ratio is based on empirical data for mixed calcium salts under boiling and non-boiling conditions (Reference E-13).

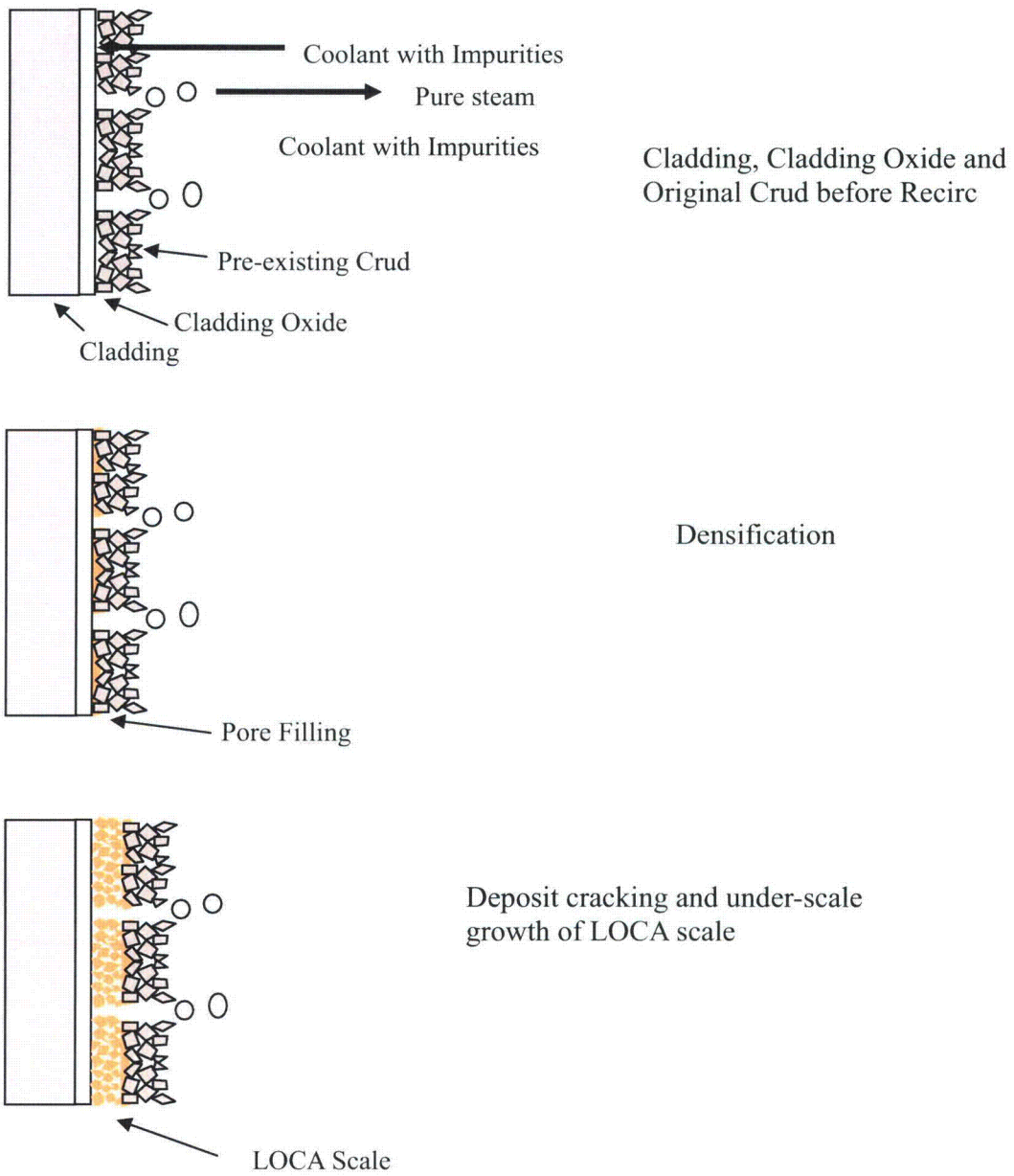


Figure E-2 Deposit Growth Process Assumed by LOCADM When Core is Boiling

For initial fuel oxide values, it is recommended that users input a value consistent with the peak local oxidation allowed by 10 CFR 50.46, which permits oxidation up to 17 percent of the clad wall thickness. For the initial crud deposit thickness, a bounding core average value can be used that produces a peak crud thickness of 140 microns.

The thermal conductivity value for zirconium oxide used in fuel rod design is 1.61 BTU/hr-ft-°F or 2.79 W/m-K (Reference E-16). This value is recommended for LOCADM modeling.

The limiting value for the thermal conductivity of PWR crud is 0.3 BTU/hr-ft-°F or 0.52 W/m-K (Reference E-17). This is also a reasonable value for LOCA scale that is rich in calcium. The thermal conductivity of boiler scale deposits has been measured, and values of 0.29 and 0.55 BTU/hr-ft-°F (0.50 and 0.96 W/m-K) have been reported for calcium-rich deposits (Reference E-18). Thus, a value of 0.3 BTU/h-ft-°F (0.52 W/m-K) is recommended for the LOCA scale thermal conductivity input if calcium is the primary coolant impurity.

The most insulating material that could deposit from post-LOCA coolant impurities would be sodium aluminum silicate. Thermal conductivity values as low as 0.11 BTU/h-ft-°F (0.2 W/m-K) have been reported for sodium aluminum silicate (Reference E-5). The scale in this case was likely a glassy phase with little open porosity, since other sodium aluminum silicate scale (Reference E-6) has possessed a thermal conductivity of 0.7 BTU/h-ft-°F (1.2 W/m-K). It is recommended that a value of 0.11 BTU/hr-ft-°F be used for sodium aluminum silicate scale and for bounding calculations when there is uncertainty in the type of scale that might form.

Densities of 147 to 155 lb/ft³ (2350 to 2640 kg/m³) have been reported for calcium carbonate and calcium hydroxide deposits formed under boiling conditions (Reference E-18). Since calcium, aluminum, and silicon may bond with other RCS chemicals such as phosphate and borate, this number should be reduced significantly to introduce conservatism into the prediction of LOCA scale thickness. Measurements on cross-sectioned calcium sulfate scale have shown (Reference E-10) that the density varies from 12.5 to 106 (200 to 1700 kg/m³) across the thickness of the deposit with an average of 62 lb/ft³ (1000 kg/m³) (Reference E-19). LOCADM requires density to be input in lbm Ca, so the values above should be reduced by the ratio of the calcium atomic weight to the compound molecular weight, about 0.3. A value of 35 lb/ft³ is used as the default for LOCADM.

The values from Reference E-18 are relevant to core deposition after a LOCA in the following respects:

1. Deposits are calcium-rich as would be the case for post-LOCA deposits on the core at many plants.
2. The deposits were formed under boiling conditions.

When selecting a limiting thermal conductivity, a variety of literature sources covering other types of deposits were scanned to select a limiting value for LOCADM (0.1 Btu/(°F⁻¹ ft⁻¹ hr⁻¹).

E.9 VALIDATION OF LOCADM

E.9.1 SKBOR

The SKBOR computer program is part of the Westinghouse methodology for LTCC. For plants with CL injection, SKBOR is used to determine: (1) the time at which ECCS recirculation should be realigned to the RCS HLs to prevent the precipitation of boron in the core; (2) the interval at which cycling between hot and CL injection should be completed, for plants without sufficient simultaneous hot and CL injection; and, (3) the amount of sump dilution at the HL switchover time. For plants with UPI, SKBOR has been used to determine the time at which UPI injection should be established to prevent the precipitation of boric acid in the core, for breaks where the RCS may stabilize above the UPI cut-in pressure.

A typical SKBOR calculation considers two volumes: one representing the effective vessel mixing volume (denoted as the CORE), and one representing the remaining system inventory (denoted as the SUMP). The CORE and SUMP are initially assumed to contain borated liquid at the system-average boron concentration. Vapor generated due to decay heat boiling exits the CORE with a boron concentration of zero. It is assumed to condense fully in containment and is returned to the SUMP as unborated liquid. Borated liquid is added from the SUMP as required to keep the CORE volume full. In this way, the SUMP boron concentration gradually decreases, while the CORE boron concentration increases toward the boric acid solubility limit.

Most of the inputs to SKBOR are used to specify plant-specific parameters such as the component masses and boron concentrations, the effective vessel mixing volume, and the initial core power level. These inputs are generally chosen to maximize the rate at which boron accumulates in the CORE, based on information provided by the utility. The results of the analysis are used to establish the times at which the necessary actions should be initiated, and these times are typically reflected in the FSAR and the EOPs.

The table below shows a comparison between the results for SKBOR and LOCADM.

Table E-2 Comparison of SKBOR and LOCADM Results		
Input Assumption	LOCADM	SKBOR
Core Power	3586.6 MWt	3586.6 MWt
Decay Heat	Appendix K	Appendix K
Liquid Mixing Volume	1050 ft ³	1050 ft ³
Problem Start Time	100 seconds	100 seconds
Initial Sump Boron Concentration	2550 ppm	2550 ppm
SI Subcooling	None	None
Time to Reach 23.53 wt% Boric Acid	5.97 hr	5.96 hr

E.9.2 Discussion

Large scale experiments designed to simulate dissolution and corrosion of containment materials, followed by deposition on the core have not been performed. However, there are ways in which different components of the model can be validated.

Without any heat flux in the core, the model should predict the same dissolution behavior as the chemical effects model in WCAP-16530-NP (Reference E-3). This was found to be true for aluminum and all of the insulation materials.

The LOCADM model should predict the same boron transport behavior as other LOCA codes that have been fully qualified. It was tested against SKBOR, a safety code used to predict boron build-up in the core for a CL break with CL injection. LOCADM predicted that the boric acid concentration would increase to 23.53 weight percent, the HL switchover point, in 7.6 hours while SKBOR version 7 predicted that 8.0 hours would be required. The agreement was considered to be adequate, since the two codes use different standard decay heat curves as a basis for calculation of core boiling. LOCADM used the Appendix K decay heat model. The Appendix K decay heat model is equivalent to the 1971 ANS model multiplied by a factor of 1.2. The 20 percent increase over the best estimate 1971 ANS model insures conservative predictions.

LOCADM should be able to conservatively predict the deposition of any material since deposit-specific chemical reactions were not included in the model. Several laboratory tests on calcium scaling rates with conditions similar to those that would be experienced after a LOCA have been reported in the scientific literature. LOCADM was used to predict deposition rates for the laboratory experiments and the results were found to be conservative in all cases. An example is shown below.

Calcium sulfate was deposited on an electrically heated tube in a laboratory test reported by Brahim et al. (Reference E-19) In the test, a calcium sulfate solution near saturation entered a tube at 80°C (176°F) and was heated causing precipitation on the heat transfer surface. The temperature of the heat transfer surface was monitored with time as the calcium sulfate precipitated. The heat fluxes were high enough to cause boiling within the deposits, according to the author's calculations. The fouling resistance was calculated and plotted.

The agreement between the LOCADM calculations and the Brahim experiment are shown in Figure E-3. The LOCADM deposition rate of $1.69 \times 10^{-4} \text{ m}^2\text{-K/W-hr}$ was equal to the highest deposition rate recorded experimentally. During most of the test, the deposition rate was about 5 times lower than the LOCADM calculation, demonstrating the conservatism in the LOCADM model.

Figure E-3 uses a thermal conductivity of 0.52 W/m-°K assumed for calcium sulfate. The thermal conductivity of the referenced experiment (E-19) was not measured. However, another reference (E-5) states that boiler scale deposits of calcium sulfate range between 0.8 and 2.2 W/m-°K. Thus, the thermal conductivity value used by LOCADM for this comparison was conservative, but not as conservative as the 0.2 W/m-°K which is the recommended value and is the default value in LOCADM. The progressive increasing conservatism shown in the example is most likely due to increasing deposit attrition with increasing thickness due to decreased deposit structural stability rather than any assumptions in heat transfer modeling.

The slab geometry heat transfer model implemented in LOCADM is conservative relative to using a more representative cylindrical model. This is true both for the wire comparison and for applications to fuel cladding. The degree of conservatism is shown in the table below for limiting fuel rod conditions. An increase in the predicted temperature difference across the deposit of 61°F is predicted using a slab geometry model rather than a cylindrical geometry model. While the fuel rods from various fuel designs or vendors may be different, the relationship between the slab and cylindrical model will not change. The slab model will predict conservative results compared to the cylindrical model for any given set of inputs. (Note: The cylindrical and slab heat transfer models can be found in “Mechanical Engineer’s Reference Book,” 12th Edition, Edward H. Smith editor [Butterworth-Heinemann, Oxford] 1994, page 1-41.

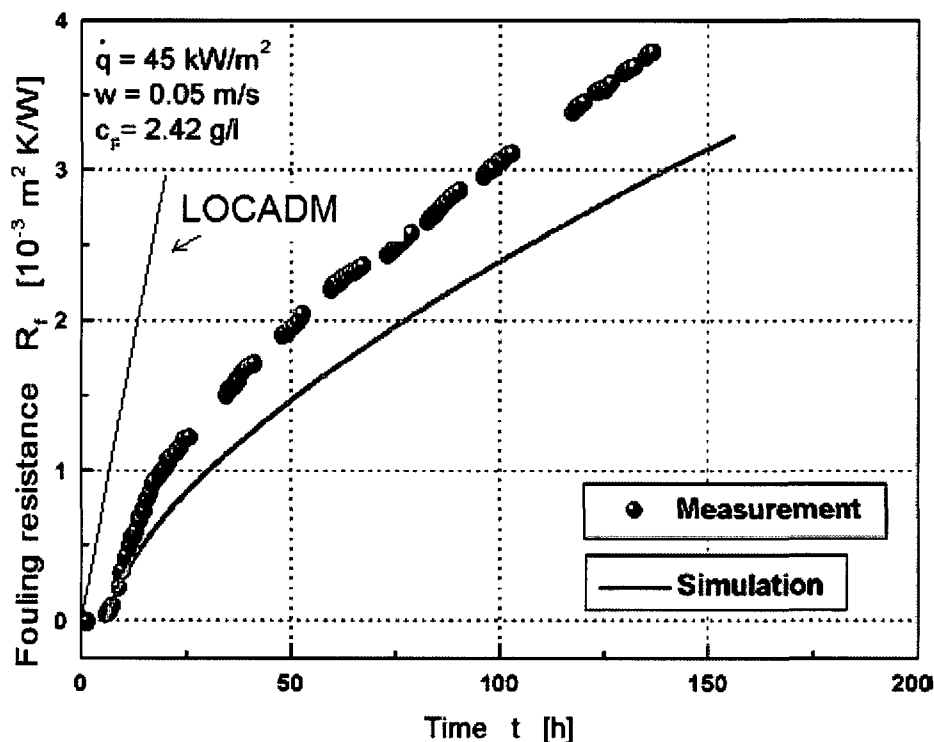


Figure E-3 Experimental Fouling Resistance for Calcium Sulfate Deposition (3) Compared to the LOCADM Calculated Fouling Resistance

The LOCADM model conservatively assumes that all fiber and chemical products that bypass the sump screen will deposit on the fuel cladding (see Section E.9.3.3 for additional details). The assumption that all fiber and chemical products will deposit is a conservative assumption. The amount of conservatism is demonstrated in the plot comparing the deposition predicted by LOCADM over time is shown in Figure E-3.

E.9.3 Additions to Methodology

E.9.3.1 Pre-filled Sump Option

This option provides an alternate method for data entry into LOCADM to pre-fill the sump and reactor rather than requiring LOCADM to track flows to fill the sump and reactor. As previously described, LOCADM considers two modes of plant operation before recirculation of the sump. In Mode 1, the reactor cooling system blows down and the reactor refills via operation of the safety injection system. During Mode 2, the reactor has been refilled, and borated water from the reactor water storage tank continues to be injected into the reactor. Coolant flows from the break during both methods, filling the sump. Mode 2 ends when recirculation from the sump begins.

The LOCADM user has two options for describing flows during LOCA Modes 1 and 2. The first option is to enter an initial RV coolant mass and sump volume, and then completely describe the system flows which then produce a final RV coolant mass and sump volume at the end of Mode 2. The second option is to pre-fill the sump and the reactor and set all flows equal to zero during Modes 1 and 2.

E.9.3.2 Aluminum Release Rate

In Reference E-21, it was stated that the aluminum release rate equation developed in WCAP-16530-NP-A predicts the aluminum concentrations during the initial active corrosion portion of the test. In order to provide more appropriate levels of aluminum release for the LOCADM analysis in the initial days following a LOCA, licensees shall apply a factor of two to the aluminum release as determined by the WCAP-16530-NP spreadsheet, although the total aluminum considered does not need to exceed the total predicted by the WCAP-16530-NP spreadsheet for 30 days. The recommended procedure for modifying the aluminum release rate is described in Reference E-22.

E.9.3.3 Bump-up Factor

LOCADM does not contain an input for debris which bypasses the sump screen and is available for deposition in the core. Only material released from corrosion or dissolution processes is considered. However, some debris fines may bypass the sump screen and enter the core area where it could be deposited.

The quantity of transported fines is expected to be small compared to both the total amount of debris and the amount of debris that dissolves or corrodes. Thus, if the small fibers were included in model predictions, the effect would be small but would vary from plant to plant depending on the screen design and debris mix. A quantitative estimate of the effect of the fiber on deposit thickness and fuel temperature can be accounted for in LOCADM by use of a “bump-up factor” applied to the initial debris inputs. The bump-up factor is set such that total release of chemical products after 30 days is increased by the best estimate of the mass of the fiber that bypasses the sump screen. This allows the bypassed material to be deposited in the same manner as a chemical reaction product.

The recommended procedure for including fiber bypass in the LOCADM deposition calculations is illustrated in Reference E-23.

E.10 EXAMPLE RUN OF LOCADM MODEL

The LOCADM code was run with input conditions simulating a 3188 MW thermal PWR with a high fiberglass debris loading (7000 ft³) and a large quantity of calcium silicate debris (80 ft³). A HL switch-over time of 13 hours was assumed. A value of 0.11 BTU/hr-ft-°F was used for the thermal conductivity of the LOCA scale. The results are shown in Figure E-4 where the maximum scale thickness in the core has been plotted for a 30 day period. The maximum scale thickness was 257 microns (10 mils). The maximum fuel temperature after recirculation was started was 324°F. Thus, LTCC was not compromised.

Table E-3 Time dependent inputs for LOCADM example

Time (sec)	days	Sump pH	Sump Temp. (°F)	Spray Flow from RWST (lbm/s)	Steam or Spray pH	Containment Temp. (°F)	RV Coolant Temp (°F)	Break Flow (lbm/s)	Clean SI Flow into RV (lbm/s)	Clean SI Bypass Flow (lbm/s)	Recirc Flow into RV (lbm/s)	BOP Blowdown Flow (lbm/s)
6	0	6	224	0	9.5	215	225	5660	0	0	0	3500
30	0	6.5	252	0	9.5	255	265	4180	0	0	0	2000
60	0	6.9	238	0	9.5	252	262	3600	90	0	0	1800
120	0	7.25	238	0	9.5	252	262	1000	3200	0	0	0
180	0	7.4	240	0	9.5	251	261	1000	1400	0	0	0
200	0	7.4	241	0	9.5	251	261	1000	190	0	0	0
400	0	7.8	247	0	9.5	253	263	210	310	0	0	0
600	0	7.8	250	0	9.5	255	265	230	330	0	0	0
800	0	7.9	254	1	9.5	257	267	320	400	0	0	0
1000	0	8	256	1	9.5	254	264	400	81	319	0	0
1200	0	8.05	257	1	9.5	252	262	400	77	323	0	0
1400	0	8.15	258	1	9.5	252	262	400	74	326	0	0
1600	0	8.2	259	1	9.5	249	259	400	71	329	0	0
1800	0	8.2	260	1	9.5	248	258	400	68	332	0	0
3200	0	8.2	254	1	9.5	240	250	400	58	342	0	0
4600	0	8.2	246	1	9.5	238	248	400	52	348	0	0
6000	0	8.2	238	0		243	253	400	49	351	0	0
7400	0	8.2	232	0		244	254	400	46	354	0	0
8800	0	8.2	222	0		245	255	400	44	356	0	0
10200	0	8.2	218	0		245	255	400	42	358	0	0
11600	0	8.2	217	0		245	255	400	0	0	40	0
13000	0	8.2	214	0		244	254	400	0	0	39	0
14400	0	8.2	211	0		243	253	400	0	0	38	0
46400	1	8.2	163	0		220	230	400	0	0	27	0
46800	1	8.2	158	0		205	215	400	0	0	200	0
2E+05	2	8.2	156	0		198	208	400	0	0	200	0
3E+05	3	8.2	156	0		193	203	400	0	0	200	0
3E+05	4	8.2	156	0		185	195	400	0	0	200	0
4E+05	5	8.2	156	0		180	190	400	0	0	200	0
9E+05	10	8.2	156	0		161	171	400	0	0	200	0
1E+06	15	8.2	156	0		138	148	400	0	0	200	0
2E+06	20	8.2	156	0		137	147	400	0	0	200	0
2E+06	25	8.2	156	0		135	145	400	0	0	200	0
3E+06	30	8.2	156	0		134	144	400	0	0	200	0

Table E-3 Time dependent input for LOCADM (continued)

Time (sec)	days	NaOH mass flow Spray (lbm/s)	TSP Dissolution Rate (lbm/s)	NaTB Release Rate - Ice or Basket (lbm/s)	Reactor Vessel Liquid Mass (lbm)	Ice Melt Rate (lbm/s)	RV Pressure in Upper Plenum (psia)	Reactor Vessel Steam Flow (lbm/s)
6	0	0	0	0	210000	0	18.85	330.4
30	0	0	0	0	155000	0	38.37	216.7
60	0	2	0	0	110000	0	36.49	178.0
120	0	5	0	0	85000	0	36.49	146.5
180	0	5	0	0	155000	0	35.88	130.7
200	0	5	0	0	162000	0	35.88	126.9
400	0	5	0	0	115000	0	37.11	104.6
600	0	5	0	0	132000	0	38.37	93.5
800	0	5	0	0	142000	0	39.67	86.4
1000	0	5	0	0	143000	0	37.74	81.0
1200	0	5	0	0	143000	0	36.49	76.8
1400	0	5	0	0	143000	0	36.49	73.6
1600	0	5	0	0	143000	0	34.69	70.7
1800	0	5	0	0	143000	0	34.11	68.3
3200	0	5	0	0	143000	0	29.71	57.8
4600	0	0	0	0	143000	0	28.69	52.1
6000	0	0	0	0	143000	0	31.30	48.6
7400	0	0	0	0	143000	0	31.85	45.8
8800	0	0	0	0	143000	0	32.40	43.7
10200	0	0	0	0	143000	0	32.40	41.9
11600	0	0	0	0	143000	0	32.40	40.4
13000	0	0	0	0	143000	0	31.85	39.1
14400	0	0	0	0	143000	0	31.30	38.0
46400	1	0	0	0	143000	0	20.71	26.9
46800	1	0	0	0	143000	0	15.54	26.6
2E+05	2	0	0	0	143000	0	14.70	0.0
3E+05	3	0	0	0	143000	0	14.70	0.0
3E+05	4	0	0	0	143000	0	14.70	0.0
4E+05	5	0	0	0	143000	0	14.70	0.0
9E+05	10	0	0	0	143000	0	14.70	0.0
1E+06	15	0	0	0	143000	0	14.70	0.0
2E+06	20	0	0	0	143000	0	14.70	0.0
2E+06	25	0	0	0	143000	0	14.70	0.0
3E+06	30	0	0	0	143000	0	14.70	0.0

Table E-4 Materials Input for LOCADM example

Class	Material	Amount
Coolant	Recirc Sump Pool Volume (ft3)	
Metallic Aluminum	Aluminum Submerged (sq ft)	799
	Aluminum Submerged (lbm)	179
	Aluminum Not-Submerged (sq ft)	15189
	Aluminum Not-Submerged (lbm)	3406
Calcium Silicate	Cal-Sil Insulation(ft3)	80
	Asbestos Insulation (ft3)	0
	Kaylo Insulation (ft3)	0
	Unibestos Insulation (ft3)	0
E-glass	Fiberglass Insulation (ft3)	7000
	NUKON (ft3)	0
	Temp-Mat (ft3)	0
	Thermal Wrap (ft3)	0
Silica Powder	Microtherm (ft3)	0
	Min-K (ft3)	0
Mineral Wool	Min-Wool (ft3)	0
	Rock Wool (ft3)	0
Aluminum Silicate	Cerablanket (ft3)	0
	FiberFrax Durablanket (ft3)	0
	Kaowool (ft3)	0
	Mat-Ceramic (ft3)	0
	Mineral Fiber (ft3)	0
	PAROC Mineral Wool (ft3)	0
Concrete	Concrete (ft2)	736
Trisodium Phosphate	Trisodium Phosphate Hydrate (lbm)	0
Interam	Interam (ft3)	0
	Initial Sump Liquid Volume (ft3)	20
	Initial Boron Concentration in RCS	800
	Initial Lithium Concentration in RCS	2
	RWST/Accumulator Boron Conc. (ppm)	2500
	NaOH Addition Tank NaOH Conc.	200000

Table E-5. Density values used in LOCADM example

Class	Material	Amount	Density (lb/ft3)	Mass(kg)	Class total (kg)
Coolant	Recirc Sump Pool Volume (ft3)	0	60.957	0.0	0.0
Metallic Aluminum	Aluminum Submerged (sq ft)	799.40		0.0	1626.1
	Aluminum Submerged (lbm)	179.25		81.3	
	Aluminum Not-Submerged (sq ft)	15188.6		0.0	
	Aluminum Not-Submerged (lbm)	3405.75		1544.8	
Calcium Silicate	Cal-Sil Insulation(ft3)	80	14.5	526.2	526.2
	Asbestos Insulation (ft3)	0	14.15	0.0	
	Kaylo Insulation (ft3)	0	14.15	0.0	
	Unibestos Insulation (ft3)	0	14.15	0.0	
E-glass	Fiberglass Insulation (ft3)	7000	2.4	7620.4	7620.4
	NUKON (ft3)	0	4	0.0	
	Temp-Mat (ft3)	0	11.8	0.0	
	Thermal Wrap (ft3)	0	16	0.0	
Silica Powder	Microtherm (ft3)	0	4	0.0	0.0
	Min-K (ft3)	0	4	0.0	
Mineral Wool	Min-Wool (ft3)	0	10	0.0	0.0
	Rock Wool (ft3)	0	10	0.0	
Aluminum Silicate	Cerablanket (ft3)	0	8	0.0	0.0
	FiberFrax Durablanket (ft3)	0	12	0.0	
	Kaowool (ft3)	0	6	0.0	
	Mat-Ceramic (ft3)	0	12	0.0	
	Mineral Fiber (ft3)	0	21	0.0	
	PAROC Mineral Wool (ft3)	0	21	0.0	
Concrete	Concrete (ft2)	736		0.0074027	0.007402688
Interam	Interam (ft3)	0	54	0.0	0.0
	Initial Sump Volume (ft3)	20		554	
	Initial Boron Concentration in RCS	800			
	Initial Lithium Concentration in RCS	2			
	RWST/Accumulator Boron Conc. (ppm)	2,500		5500	
	Calcium Deposit Density			35	
	Aluminum Deposit Density			34	
	Silicon Deposit Density		31		

Table E-6. Core data input

Variable	Units	Value
100% Reactor Power	MW Thermal	3188
Crud Thermal Conductivity	W/m-K	0.52
LOCA Deposit Thermal Conductivity	W/m-K	0.2
Fuel Rod OD	Inches	0.36
Pellet Stack Length	Inches	144
Average Cladding Oxide Thickness	Microns	20
Average Starting Crud Thickness	Microns	30
Number Regions	(200 max)	4
Number of Axial Nodes (up and down each region)	(10 max)	3
Distance from Hotleg Inlet to Top of Pellet Stack	Inches	47

Table E-7. Core axial node definition

Elevation	Relative Power	Relative Oxide Thickness	Relative Crud Thickness
1	0.95	1.5	2.4
2	1.1	0.9	0.3
3	0.95	0.6	0.3

Table E-8 Core radial node definition

Region	Number Rods	Relative Power	Relative Oxide Thickness	Relative Crud Thickness
1	1	1.80	0.8	3.3
2	263	1.60	0.7	2.7
3	39072	1.23	0.8	1.27
4	11616	0.20	1.68	0.05

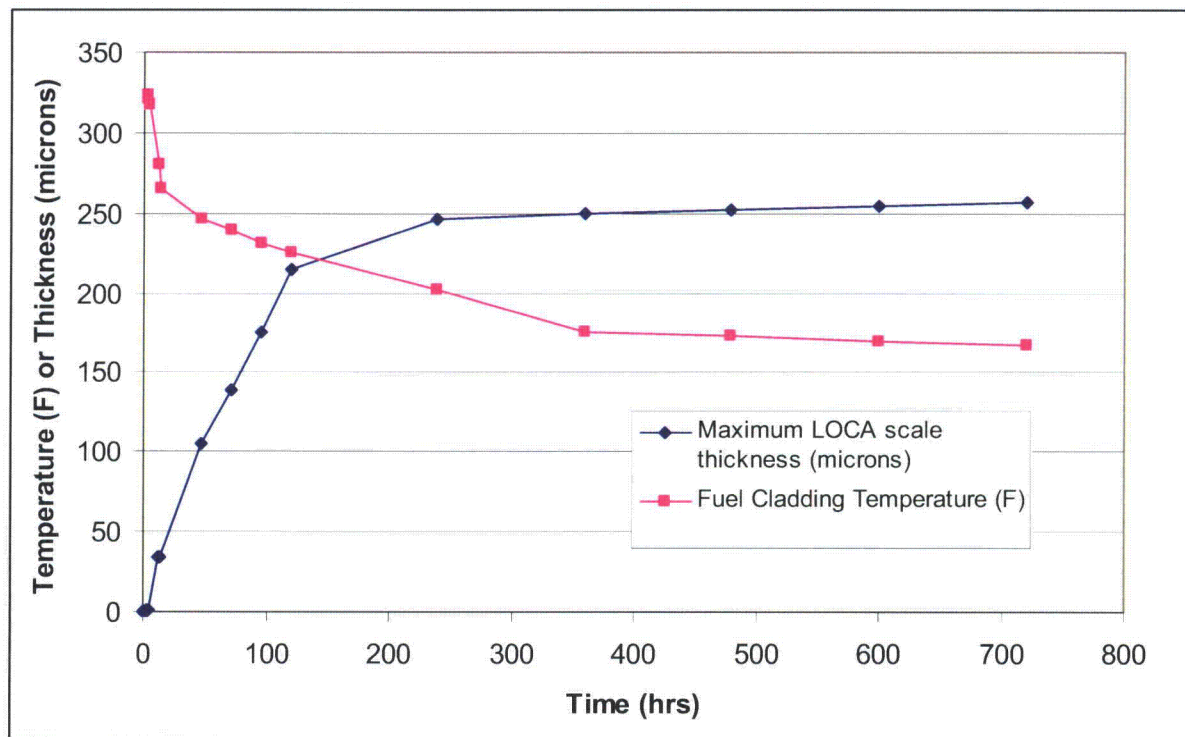


Figure E-4 Maximum Scale Thickness Values for a PWR with High Fiber and Cal-sil Debris

E.11 CONCLUSIONS

The methodology presented here is intended to provide a plant-specific method through use of the LOCADM model to evaluate core deposition, which meets the NRC requirements for predicting post-LOCA deposit formation on the core. Also, it is expected that most plants using this methodology will be able to demonstrate acceptable LTCC in the presence of core deposits. It is anticipated that licensees will use the LOCADM tool to calculate both deposition thickness and cladding temperature.

E.12 REFERENCES

- E-1. Generic Safety Issue 191 (GSI-191), "Assessment of Debris Accumulation on Pressurized Water Reactor (PWR) Sump Performance."
- E-2. NRC Generic Letter 2004-02, "Potential Impact of Debris Blockage on Emergency Recirculation During Design Basis Accidents at Pressurized-Water Reactors," September 13, 2004.
- E-3. WCAP-16530-NP-A, Revision 0, "Evaluation of Post-Accident Chemical Effects in Containment Sump Fluids to Support GSI-191," March 2008.
- E-4. Walton Jensen, "In-Vessel Downstream Effects," GSI-191 Resolution Status Meeting, February 7, 2000, Bethesda, MD.

- E-5. Hans Muller-Steinhagen, "Heat Exchanger Fouling- Mitigation and Cleaning Technologies" (Institution of Chemical Engineers, Rugby, UK, 2000) p. 4.
- E-6. Michael Frasca, "Boiler Water Efficiency Improves with Effective Water Treatment," Energy Matters, May 1999, p. 2.
- E-7. OG-07-419, "Transmittal of LOCADM Software in Support of WCAP-16793-P, 'Evaluation of Long-Term Cooling Associated with Sump Debris Effects' (PA-SEE-0312)," September 2007.
- E-8. LTR-LIS-07-243, "Distribution of Fuel Rod Relative Power for Use in GSI-191 Chemical Deposition Model," April 24, 2007.
- E-9. AREVA Document 51-9051889-001, "Core Power Inputs for GSI-191 Chemical Effects," July 2007.
- E-10. Kovalev, S. A. et al, "Model of Heat Transfer in the Boiling of Liquid at a Porous Surface," Teplofizika Vysokikh Temperatur, Vol. 22, No. 6, 1166-1171, 1984.
- E-11. Uhle, J. L. "Boiling Characteristics of Steam Generator U-Tub Fouling Deposits," PhD Thesis, MIT, February 1997.
- E-12. Bear, J., "Dynamics of Fluids in Porous Media," American Elsevier, New York, 1972.
- E-13. A. Helalizadeh, H. Muller-Steinhagen, M. Jamialahmadi, "Crystallization Fouling of Mixed Salts During Convective Heat Transfer and Sub-Cooled Flow Boiling Conditions," 2003 ECI Conference on Heat Exchanger Fouling and Cleaning: Fundamentals and Applications, Paper 6, Santa Fe, New Mexico.
- E-14. Jayashri N. Iyer, W. J. Leech, E. F. Pulver, S. E. Sidener, Jim McInvale, K. G. Turnage, K. Kargol, J. Deshon, "ZIRLOTM Cladded Fuel Performance in Zinc Environment, Proceedings of the International Conference on Water Chemistry of Nuclear Reactor Systems," San Francisco, October 2004, p. 1704.
- E-15. "Evaluation of Fuel Cladding Corrosion Product Deposits and Circulating Corrosion Products in Pressurized Water Reactors," EPRI, Palo Alto, CA 2004 1009951.
- E-16. WCAP-15063-P-A Rev. 1 with Errata, "Westinghouse Improved Performance Analysis and Design Model," Westinghouse Proprietary Class 2, July 2000.
- E-17. Boron-induced Offset Anomaly (BOA) Risk Assessment Tool, Version 1.0, Product ID #1003211, EPRI, Palo Alto, CA.
- E-18. V.N. Slesarenkoa, V.G. Dobrzanskyb, V.V. Slesarenkoc, "The account of heat exchange features when modelling scale formation at distillation plants," Desalination 152 (2002) 229–236.

- E-19. Fahmi Brahim, Wolfgang Augustin, Matthias Bohnet, "Numerical simulation of the fouling process," *International Journal of Thermal Sciences* 42 (2003) 323-334.
- E-20. P. Cohen, *AIChE Symposium*, Volume 70, Issue 138, pp. 71-80, "Heat and Mass Transfer for Boiling in Porous Deposits with Chimneys," 1974.
- E-21. DC&L
- E-22. OG-08-64, "Transmittal of LTR-SEE-I-08-30, 'Additional Guidance for LOCADM Modification to Aluminum Release' for Westinghouse Topical Report WCAP-16793-NP, 'Evaluation of Long Term Core Cooling Considering Particulate, Fibrous and Chemical Debris in the Recirculating Fluid' (PA-SEE-0312)," February 2008.
- E-23. OG-07-534, "Transmittal of Additional Guidance for Modeling Post-LOCA Core Deposition with LOCADM Document for WCAP-16793-NP (PA-SEE-0312)," December 2007.

APPENDIX F

SUPPORTING SOLUBILITY AND PRECIPITATION CALCULATIONS

F.1 PURPOSE

AREVA NP Inc. has been contracted to provide support to Westinghouse as part of a PWROG program to address potential precipitation of species dissolved in the reactor building sump following a LOCA. The purpose of this calculation is to provide solubility/precipitation calculations of the post-LOCA coolant under sump and core conditions. These calculations were performed to confirm that the model developed in Appendix E identified the major chemical species resulting from the post-LOCA chemical reactions. These calculations are not an alternative method to the LOCADM model described in Appendix E.

F.2 ANALYTICAL METHODOLOGY

The solubility calculations were performed using the OLI Systems, Inc., StreamAnalyzer™ software. StreamAnalyzer has been developed by OLI over 30 years and is used extensively in the petrochemical and the oil and gas industries. The current OLI Databank includes thousands of species, including 79 elements of the periodic table and over 3,000 organic compounds. The recent use of StreamAnalyzer in the nuclear industry includes Version 1.2 being qualified for the high-level waste project by the Center for Nuclear Waste Regulatory Analyses in 2003. The qualification of StreamAnalyzer Version 1.2 for thermodynamic modeling of debris components under post-LOCA sump conditions followed in 2005 and was reported in NUREG/CR-6873.

For this evaluation, the OLI Thermodynamic Framework and the Aqueous Chemistry Model were utilized. These systems provide accurate prediction of multi-component aqueous systems including aqueous liquid, vapor, organic liquid, and multiple solid phases over the general range of 0 to 30 molal, -50 to 300°C, and 0 to 1500 Bar. Computed thermodynamic properties such as pH, ionic strength, enthalpy, density, and osmotic pressure are supplied automatically.

The current OLI SteamAnalyzer database contains thermodynamic information on twenty-two boron species, including various polyborates and borates of calcium, lithium, and sodium. These data were derived, in part, from published solubility data of sodium and boron species over a range of temperatures and pressures (References F-1 and F-2). The code utilizes activity models for the aqueous phase (Bromley-Zematis) and the vapor phase (Soave-Redlich-Kwong) to adjust the equilibrium calculations based on compositional effects, allowing predictions for complex mixed-chemistry environments over a wide range of solute concentrations.

This section is intended to provide verification of the LOCADM model. It is specifically used to identify the most likely precipitate species and to verify the assumption that 100 percent of the dissolved species are available for precipitation due to boiling in the core. The SteamAnalyzer database and calculation framework are sufficiently reliable for the intended purpose.

The results of these calculations are expected to be valid for the chemical species present at the sump and core conditions up to a solute concentration of 50 mole percent. Because OLI is a thermodynamic equilibrium code, other factors (i.e., kinetics, inhibitions of crystal nucleation, etc.) are not considered.

However, these factors, if present, would normally serve to inhibit precipitation. Therefore, the OLI calculation would be expected to be conservative.

F.3 KEY ASSUMPTIONS

The solubility calculations performed for this project utilized the OLI StreamAnalyzer thermodynamic aqueous chemistry model. As a consequence, the following assumptions are implicit in the results:

- System transients and non-equilibrium conditions are not considered. Each phase (solid, liquid, and gas) is assumed to be in thermodynamic equilibrium with the surrounding phases.
- Kinetic reaction rates are not included in the model. As a result, all species that reach thermodynamic solubility are assumed to precipitate to reach equilibrium. In reality, some degree of super-saturation is required to prompt solid nucleation and initiate precipitation. Because these kinetic reactions are not considered, the solubility calculations are expected to be conservative.
- Finally, no species-specific interactions that could potentially influence crystal nucleation and growth are considered. As a result, certain rare reactions that inhibit precipitation are not replicated, thereby making the calculation results conservative.
- Specific reactor conditions like concentration gradients and HL recirculation are not utilized since this calculation is intended to be supporting material for Appendix E. Rather, a conservative final concentration factor of 20 was selected.

Other key inputs for the calculations were taken from customer-supplied inputs and are detailed as part of the calculations.

F.4 INPUTS SUMMARY

As previously stated, Appendix F is intended to determine the reasonability of assumptions within Appendix E, such as percentage and type of precipitate species expected to generate in the core following a LOCA. The data presented here is not a direct input to Appendix E. The masses determined in the OLI simulations are reported for information only.

The solubility calculations were performed for four “Runs” as summarized in Table F-1. The inputs were selected to be reasonably representative of the expected post-LOCA conditions and, as such, are not intended to be bounding of all plants and scenarios. The four cases analyzed include reasonably representative extremes of temperature, solute concentration, and pH (as a function of buffering media) expected for a post-LOCA environment. No scenarios in addition to these were calculated. However, because the LOCADM calculation (Appendix E) assumes 100 percent precipitation of all solutes present in the liquid that is evaporated, and because LOCADM uses conservative values for deposit density and conductivity to bound a range of potential precipitates, there would be no change in the final LOCADM results.

Parameter	Run 1	Run 2	Run 3	Run 4
Sump Temperature	220°F	150°F	220°F	150°F
Fuel Surface Temperature	260°F	212°F	260°F	212°F
Pressure	40 psia	40 psia	40 psia	40 psia
pH @ 25°C	10	10	7	7
Input Ca (ppm)	15	133	15	133
Input Al (ppm)	17	80	17	80
Input Si (ppm)	69	156	69	156
Input H ₃ BO ₃ (ppm)	14,300	14,300	14,300	14,300
Input LiOH (ppm) ⁽²⁾	0.69	0.69	0.69	0.69
Input Oxygen (ppm)	2	4	2	4
Input Hydrogen (ppm)	0.01	0.01	0.01	0.01
pH Modifier	NaOH	NaOH	Na ₂ B ₄ O ₇	Na ₂ B ₄ O ₇
Concentration Factor for Evaporation	20 ⁽¹⁾	1	20 ⁽¹⁾	1
Note:				
1. For the evaporation step, it is necessary to reduce the system overpressure to maintain a boiling point of 260°F as the solution concentrates.				
2. The lithium concentration was entered for completeness. However, the lithium has very little impact on the solution pH and does not significantly affect speciation at such a low concentration. The concentration of sodium is significantly higher and dominates the solution pH and speciation. Therefore, a reduction in the assumed lithium concentration would have a negligible impact on the calculation results.				

In addition to the inputs provided in Table F-1, the mass of the input (sump) stream, the mass of the core feed that is vaporized, and the mass of the residual core liquid is needed to predict the mass of precipitates. These input values were selected based on sump mass, reactor inventory, and steaming information. The stream masses utilized in this evaluation are provided in Table F-2.

Parameter	Run 1	Run 2	Run 3	Run 4
Sump Inventory (kg)	2,200,000	2,200,000	2,200,000	2,200,000
Total Core Feed (kg)	570,000	2,200,000	570,000	2,200,000
Core Residual After Steaming (kg)	145,000	N/A	145,000	N/A

The quantities listed in Table F-2 are water-volume mass inputs to the OLI software evaluation. The 'total core feed' refers to the amount of water transported to the reactor. For Runs 1 and 3, this corresponds to the mass of water steamed off and replaced following the accident (with water only replaced at the rate at which boil-off occurs to maintain conservatism) up until HL switchover. For Runs 2 and 4, solubility during long-term cooling was evaluated, and therefore, it was assumed that the entire sump inventory would be passed through the reactor. These values were determined using the decay heat evaluated from the 1971 ANS model multiplied by a factor of 1.2 and assuming HL switchover would take place after 8 hours (total vapor quantity boiled off determined as 570,000 kg.) The 'core residual after steaming' input refers to the liquid mass in the RV after blowdown and refill. These values were based on typical plant values.

F.5 RESULTS, SUMMARY/CONCLUSION

The following sections summarize the pertinent results for the solubility calculations. These calculations were performed to confirm that the model developed in Appendix E identified the major chemical species resulting from the post-LOCA chemical reactions. These calculations are not an alternative method to the LOCADM model described in Appendix E.

F.5.1 Run 1 Results

Run 1 addresses the time period immediately following a large CL break up until HL switch over (HLSO) is initiated. While HLSO is typically accomplished 6-8 hours after such a break, the sump chemistry is based on the 24-hours corrosion/leaching values for conservatism. This calculation case uses NaOH to adjust the pH of the sump fluid to 10 at 25°C.

Based on the OLI software, approximately 100 percent of the Al and 77 percent of the silicon in the sump are predicted to precipitate as $\text{NaAlSi}_3\text{O}_8$ upon addition of the pH modifier (NaOH). No precipitation of calcium is predicted. No additional precipitation is predicted as the sump liquid is heated to core temperatures.

As the coolant boils in the core, up to a concentration factor of 20, 100 percent of the Si and 81 percent of the Ca in the core inlet fluid is predicted to precipitate as Na_4SiO_4 and $\text{Ca}_3(\text{BO}_3)_2$, respectively. However, no additional precipitation is expected as the residual coolant is allowed to cool to 212°F.

A summary of the steam quantities, precipitation quantities, and the residual solution chemistries are presented in Table F-3.

	Sump (220°F)	Heat to Core Temperature (260°F)	Boil to CF 20	Cool to 212°F
Stream Mass (kg)	2,200,000	570,000	570,000	145,000
Precipitates (kg)	NaAlSi ₃ O ₈ : 361.1	None	Ca ₃ (BO ₃) ₂ : 13.7 Na ₄ SiO ₄ : 59.0 kg	None
Residual Solution Conc. (ppm)	CaO 20.8 LiBO ₂ 1.4 NaB ₅ O ₈ 3,144.3 NaBO ₂ 10,069.9 O ₂ 1.9 SiO ₂ 33.8	CaO 20.8 LiBO ₂ 1.4 NaB ₅ O ₈ 3144.3 NaBO ₂ 10069.9 O ₂ 1.9 SiO ₂ 33.8	CaO 65.1 LiBO ₂ 23.9 NaB ₅ O ₈ 54534.1 NaBO ₂ 165964.0	CaO 65.1 LiBO ₂ 23.9 NaB ₅ O ₈ 54534.1 NaBO ₂ 165964.0
pH	9.2	9.1	10.2	10.4

F.5.2 Run 2 Results

Run 2 addresses the sump and core conditions during long-term cooling following a LOCA. The sump chemistry is based on corrosion/leaching calculations for 30 days following a LOCA. NaOH is used to adjust the sump fluid pH to 10 at 25°C.

Based on the OLI thermodynamic data, approximately 97 percent of the Al and 100 percent of the Si in the sump is predicted to precipitate when the pH modifier (NaOH) is added. No additional precipitation is expected as the coolant is heated to core temperature (212°F), provided that boiling is not occurring in the core.

A summary of the steam quantities, precipitation quantities, and the residual solution chemistries are presented in Table F-4.

	Sump (150°F)	Heat to Core Temperature (212°F)
Stream Mass (kg)	2,200,000	2,200,000
Precipitates (kg)	Al(OH) ₃ : 173.1 NaAlSi ₃ O ₈ : 1,060.7	None
Residual Solution Conc. (ppm)	Al ₂ O ₃ 5.0 CaO 185.0 LiBO ₂ 1.4 NaB ₅ O ₈ 3439.4 NaBO ₂ 9605.2 SiO ₂ 0.1	Al ₂ O ₃ 5.0 CaO 185.0 LiBO ₂ 1.4 NaB ₅ O ₈ 3439.4 NaBO ₂ 9605.2 SiO ₂ 0.1
pH	9.4	9.2

F.5.3 Run 3 Results

Run 3 addresses the time period immediately following a large CL break up until HLSO is initiated. While HLSO is typically accomplished 6-8 hours after such a break, the sump chemistry is based on the 24-hours corrosion/leaching values for conservatism. This calculation case uses $\text{Na}_2\text{B}_4\text{O}_7$ to adjust the sump fluid pH to 7 at 25°C.

Based on the model predictions, approximately 100 percent of the Al and 77 percent of the silicon in the sump are predicted to precipitate as $\text{NaAlSi}_3\text{O}_8$ upon addition of the pH modifier ($\text{Na}_2\text{B}_4\text{O}_7$). No precipitation of calcium is predicted. No additional precipitation is predicted as the sump liquid is heated to core temperatures.

As the coolant boils in the core, up to a concentration factor of 20, 90 percent of the Si in the core inlet fluid is predicted to precipitate as SiO_2 . In the case of silicon, aqueous speciation is primarily governed by pH. For the pH range in question, the predominant aqueous species predicted are $\text{H}_3\text{SiO}_4^{1-}$ and $\text{H}_2\text{SiO}_4^{2-}$. Upon cooling the reactor contents to 212°F, another 40 percent of the remaining silicon inventory is expected to precipitate as SiO_2 . For this case, no precipitation of calcium is predicted.

A summary of the steam quantities, precipitation quantities, and the residual solution chemistries are presented in Table F-5.

	Sump (220°F)		Heat to Core Temperature (260°F)		Boil to CF 20		Cool to 212°F	
Stream Mass (kg)	2,200,000		570,000		570,000		145,000	
Precipitates (kg)	$\text{NaAlSi}_3\text{O}_8$: 363.0		None		SiO_2 : 17.3		SiO_2 : 3.4	
Residual Solution Conc. (ppm)	B(OH)_3	11877.2	B(OH)_3	11877.2	B(OH)_3	196712.0	B(OH)_3	196716.0
	CaO	21.0	CaO	21.0	CaO	347.2	CaO	347.2
	LiBO ₂	1.4	LiBO ₂	1.4	LiBO ₂	23.7	LiBO ₂	23.7
	NaB_5O_8	2742.4	NaB_5O_8	2742.4	NaB_5O_8	45419.9	NaB_5O_8	45420.9
	SiO_2	34.0	SiO_2	34.0	SiO_2	58.4	SiO_2	35.1
pH	7.1		7.1		4.7		4.6	

F.5.4 Run 4 Results

Run 4 addresses the sump and core conditions during long-term cooling following a LOCA. The sump chemistry is based on corrosion/leaching calculations for 30 days following a LOCA. $\text{Na}_2\text{B}_4\text{O}_7$ is used to adjust the sump fluid pH to 7 at 25°C.

Based on the OLI thermodynamic data, approximately 100 percent of the Al and 100 percent of the Si in the sump is predicted to precipitate when the pH modifier ($\text{Na}_2\text{B}_4\text{O}_7$) is added. No additional precipitation is expected as the coolant is heated to core temperature (212°F) provided that boiling is not occurring in the core.

A summary of the steam quantities, precipitation quantities, and the residual solution chemistries are presented in Table F-6.

Table F-6 Calculation Run 4 Results Summary				
	Sump (150°F)		Heat to Core Temperature (212°F)	
Stream Mass (kg)	2,200,000		2,200,000	
Precipitates (kg)	Al(OH) ₃ : 191.0 NaAlSi ₃ O ₈ : 1,066.7		None	
Residual Solution Conc. (ppm)	B(OH) ₃	13353.1	B(OH) ₃	13353.1
	CaO	186.0	CaO	186.0
	LiBO ₂	1.4	LiBO ₂	1.4
	NaB ₅ O ₈	1293.6	NaB ₅ O ₈	1293.6
	SiO ₂	0.1	SiO ₂	0.1
pH	7.1		7.0	

F.6 REFERENCES

- F-1 W.C. Blasdale and C.M. Slansky, "The Solubility Curves of Boric Acid and the Borates of Sodium," J. Am. Chem. Soc. 1939, 61, 917-24.
- F-2 N.P. Nies and R.W. Hulbert, "Solubility Isotherms in the System Sodium Oxide-Boric Oxide-Water, Revised Solubility-Temperature Curves of Boric Acid, Borax, Sodium Pentaborate, and Sodium Metaborate," J. Chem. Eng. Data 1967, 12(3), 303-313.

APPENDIX G

DESCRIPTION OF FUEL ASSEMBLY TESTING

G.1 INTRODUCTION

The PWROG initiated prototypical FA testing to establish limits on the debris mass (particulate, fibrous, and chemical) that could bypass the reactor containment building sump screen and not result in unacceptable head loss that would impede core inlet flow and challenge LTCC. An overall test protocol (Reference G-1) and specific test procedures were developed to ensure that possible thin bed effects were investigated, and debris types and characteristics expected in the RCS were represented. Debris loads used in the test were based on sump screen bypass information provided by licensees.

The effects of differing fuel inlet nozzle designs were also considered in the test program. Both AREVA and Westinghouse have performed testing with their respective fuel inlet nozzles to assure that the results applied to all current fuel designs. Each fuel bundle tested also had prototypical grids above the bottom nozzle debris capturing design features. Thus, the test data obtained from testing takes into account the fuel inlet nozzle, protective filter design features, and spacer grid designs. Descriptions of the fuel components tested, including bottom nozzles and grids, is provided in proprietary submittals describing the testing performed and the results obtained (References G-2 and G-3).

These tests demonstrated that for the debris loads tested, the specified flow rate through the FA mock-up was maintained with acceptable pressure drops such that LTCC is reasonably assured.

G.2 TEST OVERVIEW

A full area, partial height FA equipped with various fuel filters was used for the testing. Each assembly also included a number of spacer grids. Debris laden water was introduced to the bottom of the test region and flowed up through a simulated lower plenum region, through the simulated core support plate, and through the FA. (The flow pattern was reversed for the UPI test.) As debris caught on the FA, the differential pressure was measured across various locations including the bottom nozzle and individual grids as well as across the entire FA. The differential pressure measurements were used to determine an acceptable debris load. The test loop was intended to test the debris capture characteristics of a full-area FA under the debris loading conditions of a postulated LOCA.

The output of this test program is a set of acceptance criteria. The acceptance criteria define maximum debris masses which, if passed through the reactor containment building sump screen, will result in an acceptable pressure drop in the core.

G.2.1 Test Loop Description

AREVA and Westinghouse performed the FA tests at different locations. However, both test facilities took great lengths to ensure conformity between both test loops. The discussion below applies to both facilities.

The Westinghouse test loop for testing the debris capture characteristics of a full area FA is shown in Figure G-1 and a schematic of this test loop is given in Figure G-2. The AREVA test loop is shown in Figure G-3 and a schematic of the loop is shown in Figure G-4. The test loop is composed of four main parts:

- Mixing tank system
- Recirculation system
- Test column
- Computer monitoring system

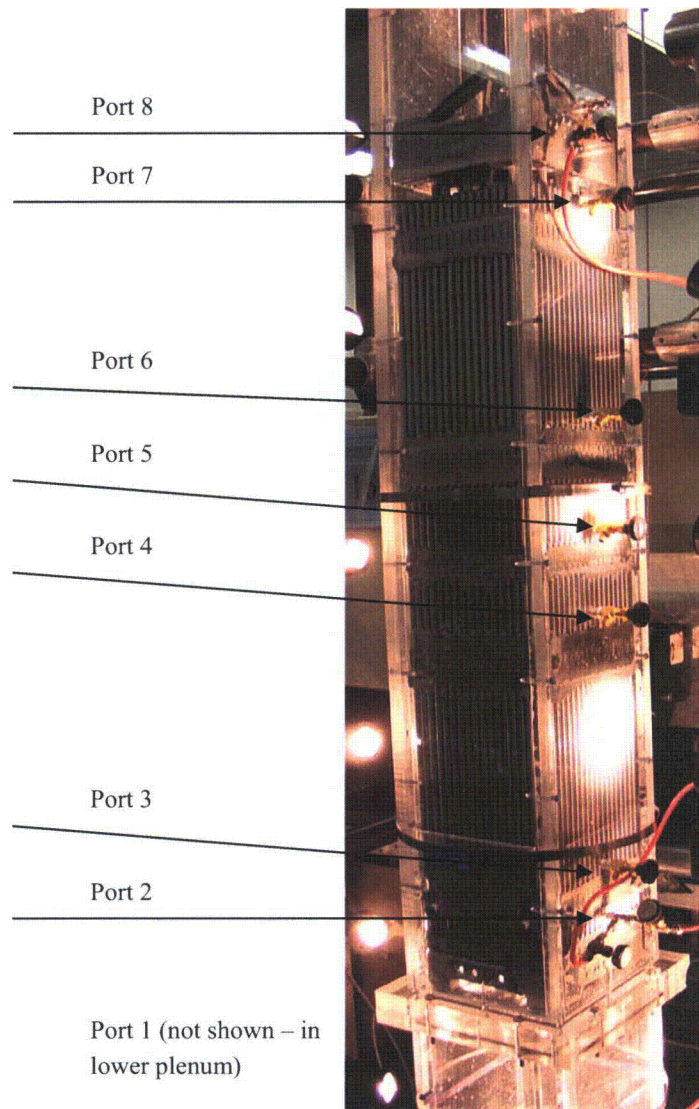


Figure G-1 Westinghouse Fuel Test Vessel

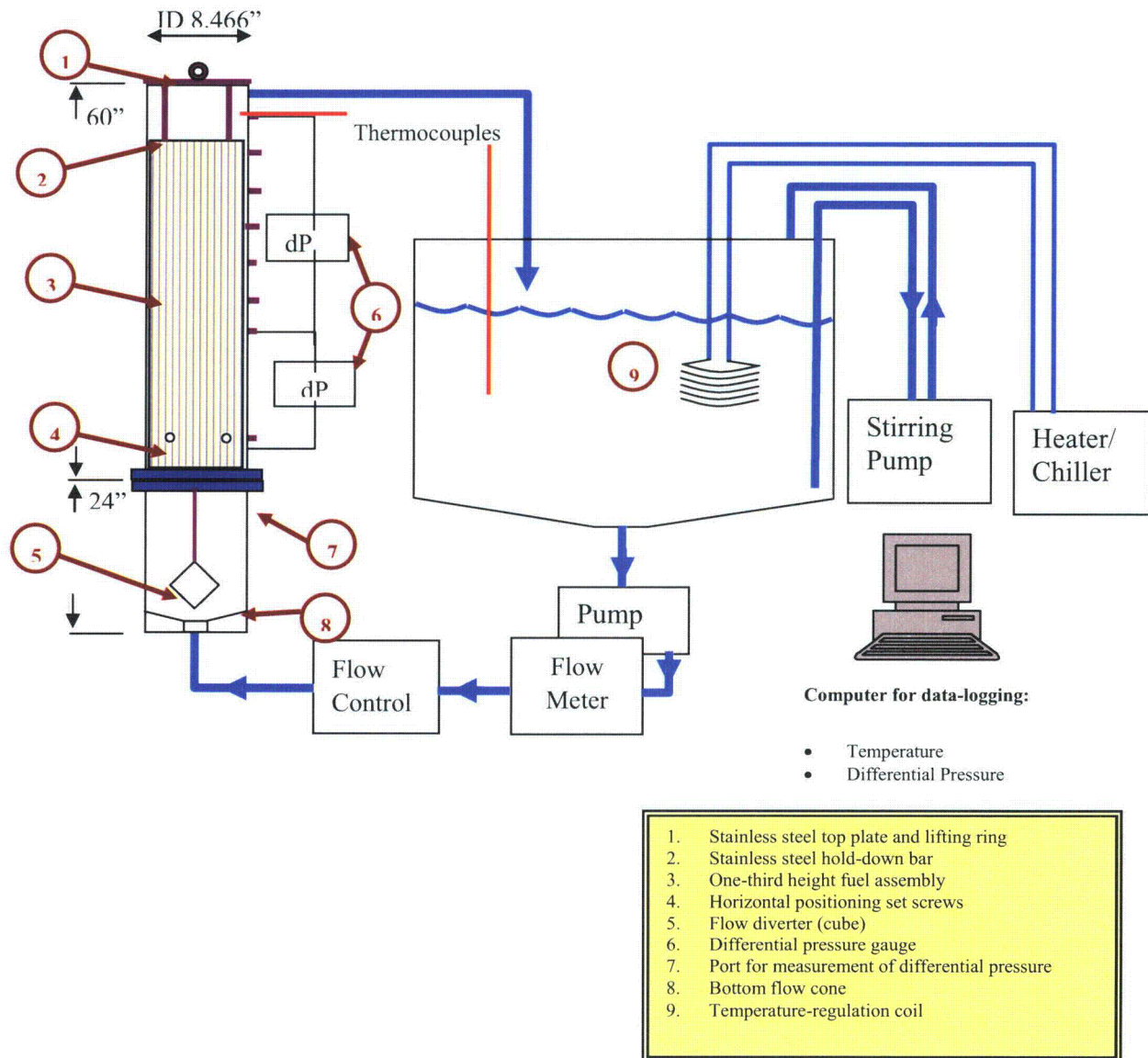


Figure G-2 Schematic of Westinghouse Test Loop

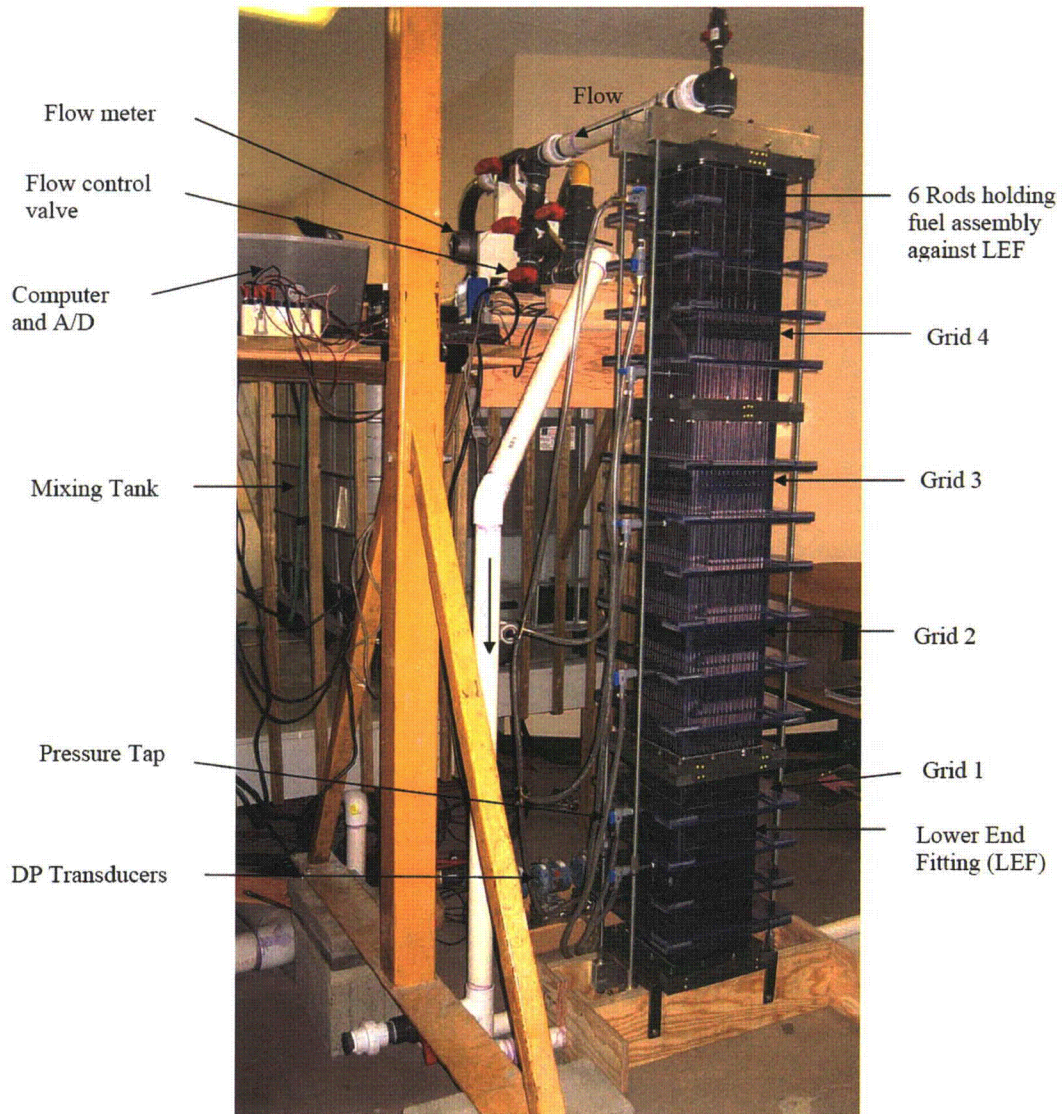


Figure G-3 AREVA Test Loop

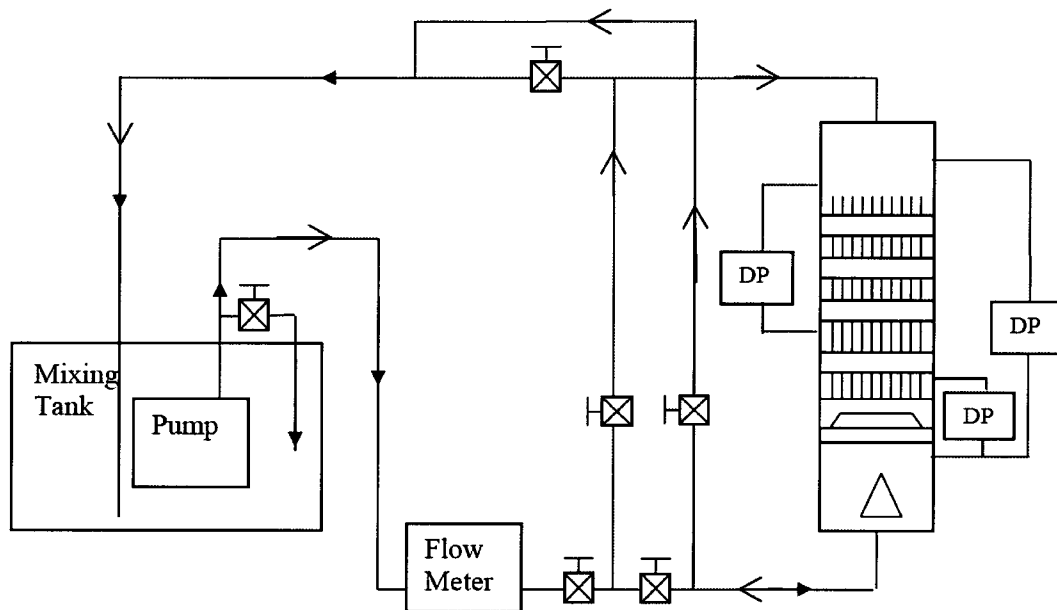


Figure G-4 Schematic of AREVA Test Loop

G.2.2 Mixing Tank System

The mixing tank system includes a plastic tank, a temperature control system, and a mixing system. The mixing tank is where debris can be added during the test. The tank design and mixing system helps preclude the settling and loss of debris on the bottom of the tank. The temperature of the water in the tank is controlled by a heater element and/or by running water at a higher or lower temperature through a heater/chiller. The water temperature can be controlled from a low temperature of approximately 60°F to a high temperature of approximately 100°F, and the temperature of the water is measured continuously in the tank by a submerged thermocouple.

G.2.3 Recirculation System

The recirculation system pumps the water from the tank, through the test column and back into the tank. A pump draws the water out of the bottom of the mixing tank. The recirculation system is continuous duty to accommodate longer tests.

G.2.3.1 Flow Rate

Each test is performed at a specified flow rate to represent a bounding core inlet velocity for breaks in various RCS locations. The following flow rates (on a per assembly basis) were tested:

- Westinghouse and B&W plants:
 - Hot Leg Flow Rates = 44.5 ($\pm 10\%$) gpm
 - Cold Leg Flow Rates = 3.0 ($\pm 10\%$) gpm

- CE plants:
 - Hot Leg Flow Rates = 11 and 6.25 ($\pm 10\%$) gpm
 - Cold Leg Flow Rates = 3.0 ($\pm 10\%$) gpm

The flow rate is maintained during the test. Additional details can be found in Reference G-1.

G.2.3.2 Test Column

The test column contains the FA and simulates the geometry inside of the RV. The test column includes a lower plenum region, a core support plate, the FA, and an upper plenum region. The debris laden water is introduced to the bottom of the lower plenum region. The design of this region is not prototypical of an RV lower plenum. It is designed instead to ensure that the debris remains well-mixed in the fluid flow and precludes any debris settling, thereby ensuring that all debris introduced to the test column will reach the FA. The lower plenum region and the FA are divided by a simulated core support plate. The FA rests directly on this simulated core support plate. The region that contains the FA is made of Plexiglas for viewing during the test. This region is sized to represent the FA pitch for the test assembly that is being tested.

The debris and water enter through the bottom nozzle and flow up through the simulated core support plate. As debris catches on the FA, the differential pressure is measured constantly across the fuel filter as well as across the entire FA. There are extra ports available on the sides of the test column if a measure of the differential pressure across a specific portion of the FA as required.

G.2.4 Computer Monitoring System

The computer monitoring system continuously records the following data:

- Temperature of the water in the mixing tank
- Flow rate
- Differential pressure measurements from ΔP gauges

This data can be recorded at a time interval chosen by the operator.

G.3 DESIGN OF FUEL PROTECTIVE FILTER IN THE TEST

AREVA and Westinghouse performed tests with all relevant fuel filters.

Westinghouse

- 17x17 FA with Westinghouse P-grid
- 16x16 FA with Guardian Grid

The alternate p-grid design was not tested, as previous test results had concluded that the standard p-grid was the limiting design.

While the test fuel assemblies represented the Westinghouse 17x17 and CE 16x16 fuel design, these test results apply to all current Westinghouse fuel designs as discussed in the Westinghouse test report (Reference G-3).

AREVA

- 17x17 FA with AREVA FUELGUARD™
- 17x17 FA with AREVA TRAPPER™ coarse mesh screen
- 17x17 FA with AREVA TRAPPER™ fine mesh screen

While the test FA tested represented AREVA 17x17, Mark-BW fuel design, these test results apply to all current AREVA fuel designs as discussed in the AREVA test report (Reference G-2).

G.4 DEBRIS DISCUSSION

G.4.1 Debris Type and Size Distribution

The debris types that might reach the RCS that were considered included particulate, fiber, chemical precipitates, Calcium Silicate (CalSil), and microporous insulation. Of these debris types, fiber is the “debris of interest.” Therefore, the mass of acceptable fiber was determined by adding it in small increments until an unacceptable pressure drop was determined or a predetermined mass was achieved. The mass of all other debris types were maximized to bound as many operating plants as possible.

The NUKON fiber was used to represent fiber in the RCS. It was sized to match the industry reported average strainer bypass distribution. Each batch was characterized by light microscopy to determine the distribution of the fiber lengths. The actual fiber distributions fall within the allowable limits of the target fiber distribution shown in Table G-1.

Fiber Length	Target	Range
< 500 μm	77%	67–87%
500 – 1000 μm	18 %	8–28%
> 1000 μm	5%	0–15%

Silicon carbide powder with a nominal 9.5 micron particle size was used to simulate particulate debris. The actual particulate size was measured using scanning electron microscopy. This silicon carbide powder is used as a surrogate for the particulate debris in the reactor because of its chemical stability and the fact that the fine particulates collect within a fiber bed and result in conservative head losses. Silicon carbide has a relatively high specific gravity of about 3.2, which would normally cause it to settle out quickly. However, due to the small size of the particles and the test loop design and flow rates, this settling is minimized.

The microporous insulation was represented by Microtherm. The material was supplied in a pulverized form and was then passed through a #7 sieve with a hole size of 0.11 in. The sieving is necessary to remove larger fibers and clumps of material that would not pass through the sump screen. The material was analyzed by scanning electron microscopy to characterize the material. The typical appearance of the Microtherm material used can be seen in Figure G-5.

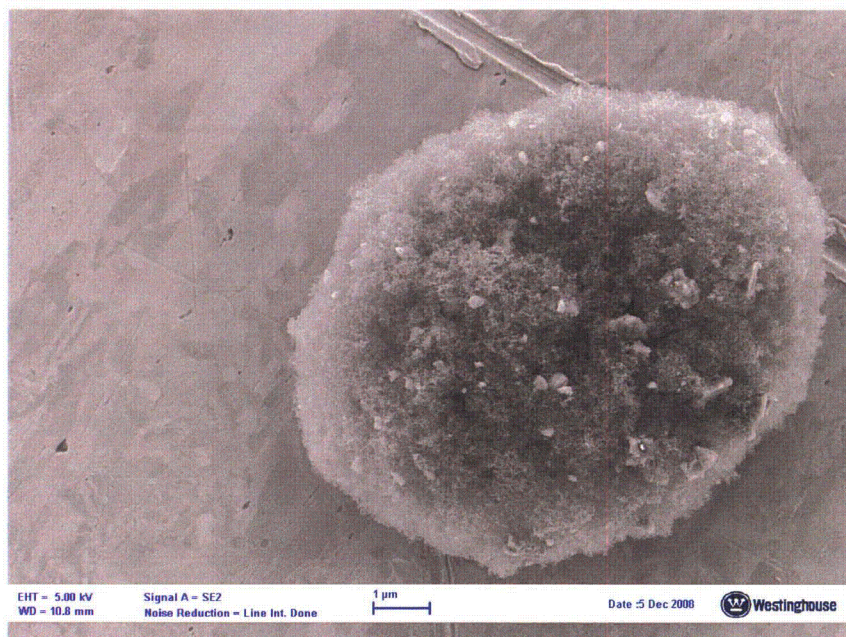


Figure G-5 Microtherm Scan

Calcium silicate insulation was pulverized into a fine powder by a hammer mill and then passed through a #7 sieve with a hole size of 0.11 in. Then the CalSil was analyzed by scanning electron microscopy to characterize the material. The typical appearance of the CalSil material used can be seen in Figure G-6.



Figure G-6 Cal Sil Scan

AlOOH was prepared according to the recipe in WCAP-16530-NP-A (Reference G-4) at a concentration of 11 g/L. The one hour settling volume of the precipitate met the criteria in WCAP-16530-NP-A (Reference G-4).

G.4.2 Order of Debris Addition

For tests that only included particulate, fiber, and chemical, NRC guidance regarding the order of addition was followed. The entire particulate load was added first, followed by fiber in 10 gram increments and then by chemicals in specified increments. For tests that included particulate, fiber, chemical, calcium silicate, and/or microporous material, the order of addition was varied slightly. Like the other tests, the entire particulate load was the first addition. Then, to simulate the initial blast introduction of calcium silicate and/or microporous material, a specified amount of these materials was added, this was followed by fiber additions in 10 gram increments, then the chemical was added and the final additions were calcium silicate and/or microporous material to simulate the slow erosion of these materials during an accident.

G.4.3 Information Related to Debris Test Amounts

The objective of the FA test program was to develop acceptance criteria for debris loads that could be tolerated in the core region and not adversely affect LTCC. The test matrices for the Westinghouse (Table G-2) and AREVA (Table G-3) tests were then developed with this objective in mind.

The Westinghouse test matrix is as follows:

Test No.	Debris Grid Filter Design	Flow Rate (gpm)	Nukon (g)	Particulate (lbm)	Microtherm (lbm)	Cal-sil (lbm)	AIOOH (g)
CIB01	p-grid	44.7 ⁽¹⁾	680.4	14	-	-	66
CIB02	p-grid	44.7 ⁽¹⁾	53	3	-	-	66
CIB03	p-grid	44.7 ⁽¹⁾	53	14	-	-	66
CIB04	p-grid	44.7 ⁽¹⁾	90	3	-	-	66
CIB05	CE Guardian	6.25 ⁽²⁾	53	14	-	-	66
CIB06	p-grid	44.7 ⁽¹⁾	53	14	-	3.20	484
CIB07	p-grid	44.7 ⁽¹⁾	53	14	1.47	1.56	689
CIB08	p-grid	44.7 ⁽¹⁾	200	29	-	-	4180
CIB09	p-grid	3.0 ⁽³⁾	100	29	-	-	4536
CIB10	p-grid	44.7 ⁽¹⁾	200	3	-	-	3386
CIB11	p-grid	17.0 ⁽⁴⁾	200	29	-	-	836

Notes:

1. This flow rate corresponds to the maximum expected flow rate for Westinghouse three- and four-loop plants. It was calculated considering all ECCS pumps available during sump recirculation and is consistent with the guidance provided in Reference 0.
2. This flow rate corresponds to the maximum expected flow rate for CE-designed plants. It was calculated considering all ECCS pumps available during sump recirculation and is consistent with the guidance provided in Reference 0.
3. This flow rate corresponds to the maximum expected core boil-off rate at the time of sump switchover. It was calculated assuming Appendix K decay heat and the earliest time of sump switchover per the guidance provided in Reference 0.
4. This flow rate corresponds to the maximum expected upper injection plenum flow rate for Westinghouse two-loop plants.

The AREVA test matrix is as follows:

Test No.	Bottom Nozzle	Flow Rate (gpm)	Nukon (g)	Particulate (lbm)	Microtherm (lbm)	Cal. Sil. (lbm)	AlOOH (g)
FM-FPC-W-1	Fine Mesh	44.7 ¹	110	29	0	0	4540
FG-PFC-W-2	FUELGUARD	44.7 ¹	150	29	0	0	4540
CM-FPC-W-3	Coarse Mesh	44.7 ¹	150	29	0	0	4540
FG-FPCSC-W-5	FUELGUARD	44.7 ¹	150	29	0	6	4540
FG-FPMC-W-6	FUELGUARD	44.7 ¹	150	29	1.2	0	4540
FG-FPC-CE-7	FUELGUARD	11 ²	150	17.5	0	0	5900
FG-FPC-W-10	FUELGUARD	3 ³	100	29	0	0	4540

Notes:

1. This flow rate corresponds to the maximum expected flow rate for B&W- and Westinghouse-designed plants scaled to a single fuel assembly. It was calculated considering all ECCS pumps available during sump recirculation and produces a velocity at the core inlet of 0.2 ft/s.
2. This flow rate corresponds to the maximum expected flow rate for CE-designed plants scaled to a single fuel assembly. It was calculated considering only high pressure safety injection (HPSI) pumps are available during sump recirculation and produces a velocity at the core inlet of 0.05 ft/s. For CE-designed plants that may continue to use low pressure safety injection (LPSI), the flow rates noted in Note 1 would apply.
3. This flow rate corresponds to the maximum expected core boil-off rate at the time of sump switchover scaled to a single fuel assembly. It was calculated assuming Appendix K decay heat and the earliest time of sump switchover.

G.5 CONCLUSION

The observations and detailed discussions can be found in the proprietary test reports from AREVA and Westinghouse, References G-2 and G-3, respectively.

The purpose of the FA testing described in this section was to justify acceptance criteria for the mass of debris that can reach the RCS and not impede LTCC. These results have been evaluated and are used to determine the debris load acceptance criteria. Based on the test results and the discussions presented in the proprietary test reports, the acceptance criteria in Table G-4 are provided for both AREVA and Westinghouse fuel designs.

These FA tests were performed to define the limits on the mass of debris that may bypass the sump screen and still provide for a sufficient flow pressure drop across the FA such that sufficient flow is provided to assure LTCC requirements are satisfied. Plants that are within the limits of the parameters tested are bounded by the tests and meet the LTCC requirements. Several courses of action have been identified for plants whose debris loads are outside of the limits tested. These actions include, but are not limited to, reduction of debris sources by removing or restraining the affected debris source or plant-specific FA testing.

Table G-4 Acceptance Criteria Debris Limits Based on FA Testing	
Westinghouse fuel designs, AREVA coarse mesh, AREVA FUELGUARD	
Debris Type	Debris Load per FA (lb)
Fiber	< 0.33
Particulate	< 29
Chemical	< 13
Cal-sil	< 6.0
Microporous Insulation	< 3.2

For fuel designs that incorporate the AREVA TRAPPER fine mesh debris filter, the limits in Table G-5 apply:

Table G-5 Acceptance Criteria Debris Limits Based on FA Testing	
AREVA TRAPPER fine mesh	
Debris Type	Debris Load Per Fuel Assembly
Fiber	<0.24 lb
Particulate	<29 lb
Chemical	<13 lb
Cal-sil	<6 lb
Microporous Insulation	<1.2 lb

G.6 REFERENCES

- G-1 LTR-SEE-I-09-34, "Transmittal of PWROG Fuel Assembly Debris Capture and Head Loss Protocol to PWROG Members," March 11, 2009.
- G-2 AREVA Document 51-9102685-000, "GSI-191 FA Test Report for PWROG," March 2009. [Proprietary to AREVA fuel customers.]
- G-3 WCAP-17057-P, "GSI-191 Fuel Assembly Test Report for PWROG," March 2009. [Proprietary to Westinghouse fuel customers.]
- G-4 WCAP-16530-NP-A, "Evaluation of Post-Accident Chemical Effects in Containment Sump Fluids to Support GSI-191," March 2008.

APPENDIX H
RAI SET #1 [ML080220258]

RAI #1

What is the basis for stating blockage of the core will not occur on page xviii? What is the maximum amount of debris that can enter the core and lower plenum and what is the maximum potential blockage from debris at the core inlet and the first spacer grid location?

RESPONSE TO RAI #1

The basis for the statement on page xviii that blockage of the core will not occur is derived from the four (4) bulleted statements on page xvii and the supporting discussion presented in Section 2 of the main body of the report. The conclusion is based on the following:

1. Test data demonstrating sump screen bypass fiber does not completely block flow to a fuel assembly which allows for decay heat to be removed. This is true even for large quantities of fiber and particulate debris as discussed further in RAI #2.
2. Fibrous debris, if it enters the core region, does not tightly adhere to the surface of the fuel cladding as demonstrated by testing reported in NEA/CSNI/R (95)11.
3. A calculation using limiting inputs to the sample problem described in Appendix E and listed on the response to RAI # 6(b), and a conservative deposition model, also described in Appendix E, demonstrated that the calculated deposition thickness would not result in long-term cladding temperatures in excess of the 800°F acceptance basis value.

The maximum amount of debris that can enter the core is based on plant-specific debris generation calculations, the pass-through performance of a plant-specific sump screen design and the scenario considered (flow rate to the sump screen, hot-leg break versus cold-leg break).

Therefore, as noted from the first bullet item on page xvii and Item 1 above, based on available test data of debris collection by a debris-capturing grid at the bottom nozzle of a modeled fuel assembly for an active replacement sump screen as described in the response to RAI #2, no potential blockage that terminates flow into or through the core is expected.

RAI #2

On page 2-3 it is stated that recent observations from testing of a partial-length fuel assembly using plant-specific fibrous and particle debris have confirmed that the NUREG/CR-6224 correlation is quite conservative for application at the core inlet. Please provide a complete description of this test facility, the tests that were performed and the results.

RESPONSE TO RAI #2

Testing has been performed to determine the effects of collection of fibrous debris on the debris capturing grids located at the bottom nozzle of a simulated fuel assembly. The testing was performed at a licensee's replacement sump screen vendor's test facility. The test conditions were for a high-fiber plant and an active sump screen, which provided for a large amount of fibrous debris to bypass the sump screen.

Conditions for the test were:

Screen Design: Active sump screen (plow and blade design)

Core Simulation: Single assembly

Core Flow: 6 gpm from a simulated lower plenum upward into a partial length fuel assembly. This flow rate was determined to be a maximum fuel grid flow rate for the plant. The total maximum core flow rate is 1060 gpm total for this plant under long-term core cooling conditions.

Description of Test LoopFlow Diagram

A schematic of the test loop is shown in Figure 2-1 below. The test article was mounted approximately 12 inches above the bottom of a Lexan test chamber. Flow entered from the bottom of the chamber. An inverted solid circular cone directed flow along the bottom of the chamber to minimize the settling of debris. Flow exited the top of the chamber and returned to the mixing tank. The taps for a differential pressure transmitter were connected to the test chamber above and below the test article. The mixing tank allowed debris to be added to the system near the pump suction.

Instrumentation

The primary purpose of the test program was to measure the head loss across the test article as a function of flow rate and debris load. Appropriately calibrated and ranged differential pressure and flow instruments were used to measure head loss and flow rate for each test. Unless specifically noted to the contrary, the instrument errors were assumed to be independent and the square root of the sum of the squares was used to determine the instrument loop uncertainty. All measurement and display devices were calibrated to NIST traceable standards.

A thermocouple was used to measure the working fluid in the mixing tank.

Test Article Description

The test article consisted of a simulated core support plate, a bottom nozzle, a debris-capturing grid, an intermediate support grid, simulated fuel rods and simulated control rods. Figure 2-2 is a diagram of the test article in the test chamber.

A 1-inch thick simulated core support plate was fastened to the test chamber. The core support plate was sealed to the test chamber walls to prevent flow around the edge of the support plate. The plate supported the weight of the bottom nozzle / fuel filter grid assembly.

The fuel rods were simulated with 3/8" plastic rod. The simulated control rods were sized such that they would extend to the same height as the simulated fuel rods.

The bottom nozzle used in the testing was similar to other debris capturing bottom nozzle designs used in PWRs. The bottom nozzle sat on the simulated core support plate. The test facility provided for a gap between the edge of the debris capturing grid and the side walls of the Lexan test chamber, simulating the gap that would exist between adjacent fuel assemblies¹.

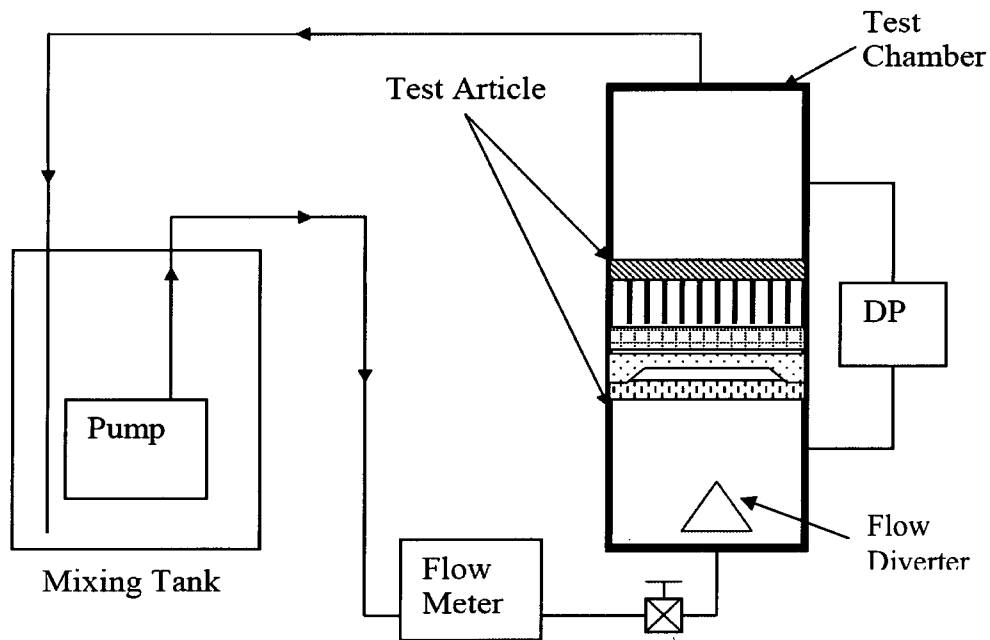


Figure 2-1: Schematic of Fuel Assembly Fibrous Debris Capture Test Loop

¹ Once the normal flow path had collected debris, more of the debris would go into the gap. Even with a gap that was 1.5 times the replacement sump screen strainer hole size, it was observed that this gap between the debris capturing grid and the Lexan sidewalls would collect fiber as well which, in turn, limited the bypass of fiber beyond the debris capturing grid.

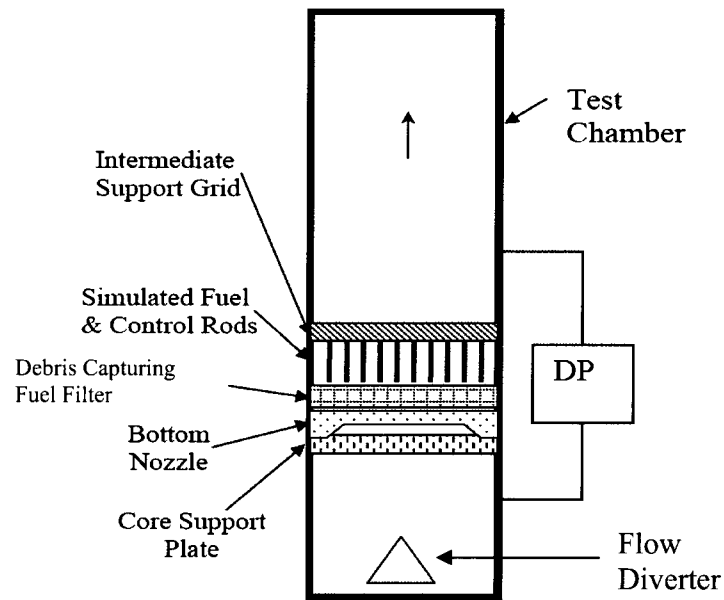


Figure 2-2: Schematic of Test Article in Test Chamber

The fuel rods were located on the bottom nozzle between the fuel rod flow holes by the debris-capturing grid. The tapered ends of the simulated fuel rods were pushed against the bottom nozzle. Control rod simulations were screwed into the control rod holes in the bottom nozzle and sealed these holes. The instrumentation tube hole was also plugged.

The licensee supplied the debris-capturing grid used in the testing. This grid accurately simulated the grid used the plant. The debris-capturing grid was fastened and positioned to the bottom nozzle as would be in the plant. An intermediate support grid was mounted near the top of the simulated fuel rods, and was used in the test primarily to maintain the orientation of the fuel rods.

Description of Debris

A brief description of the debris used in the test is presented in the sections below.

Fibrous Debris

The fibrous debris used in the fuel filter tests was obtained from fiber that bypassed the active sump screen in the bypass testing. The fibrous debris was supplied and shredded by the licensee or selected and approved by the licensee for the bypass tests.

The fiber was dried and weighed prior to use in the fuel filter tests. The fiber was not separated by type for the fuel filter tests.

Particulate Debris

A particulate insulation / dust / dirt mixture was identified by the licensee as appropriate for testing.

Quality Assurance Program

All quality-related activities were performed in accordance with the test performer’s Quality Assurance Program. Quality-related activities were defines to be those which were directly related to the planning, execution and objectives of the test. Supporting activities such as test apparatus design, fabrication and assembly were not controlled by the test performer’s Quality Assurance Program. These activities included fabrication of the tank, platform, and piping. The important information concerning the test facility was documented after fabrication. The test performer’s Quality Assurance Program provides for compliance with the reporting requirements of 10 CFR Part 21. All instrument certifications, instrument calibrations, testing procedures, data reduction procedures and test results are contained in a Design Record File which will be kept on file at the test performer’s offices.

Key Observations from Testing

Key observations from testing were:

- Almost all of the fibrous debris collected at the first grid (Debris Capturing Fuel Filter).
- No significant collection of fiber was observed to be above the first grid.
- The fibrous debris collected at the first grid during testing was not observed to compact or compress.
- Complete “blockage” of the fuel assembly tested was not observed in testing. Coolant flow through the fiber collection at the bottom of the first grid was maintained.
- Fiber debris did not adhere to the grid; the loose fiber mass was observed to drop from the first grid (Debris Capturing Fuel Filter) when flow was stopped and did not transport back to the grid when flow was reinitiated.

Active replacement sump screens are known to maximize debris passed through the screen. Comparing the two right-most columns in Table 2-1, the test results clearly provide conservative amounts of fibrous debris at the inlet to the fuel and, in fact, bound the fiber bypass through passive replacement sump screens for high-fiber plants.

Fibrous Debris Loading from Testing:

Using the debris loading for the single assembly tests described in this RAI response, calculations were performed to extrapolate those debris loadings used in the tests performed for single assembly to the core of the plant. These calculated values were then compared to expected fibrous debris bypass from testing of replacement passive sump screens. This comparison was made to demonstrate the conservatively large volume of fibrous debris that was used in the test. A summary of the inputs used for these calculations and a summary of the results are listed in Table 2-1. Comparing the calculated fibrous debris at the core entrance from the test given in Column C to the maximum expected fibrous bypass for passive replacement sump screen given in Column D, it is concluded that the fibrous debris used in the test bounds that expected from the largest passive replacement sump screen.

Table 2-1: Comparison of Fiber Load Tested to Expected Passive Replacement Strainer Fiber Load

No.	Fibrous Debris Used in Active Strainer Test			(D)
	(A) Mass (One Fuel Assembly)	(B) Volume ⁽¹⁾ (One Fuel Assembly)	(C) Total at Core Entrance ⁽²⁾	Maximum Fibrous Debris at Core Entrance for a Passive Strainer ^(3, 4)
1	0.24 lbm of fiber	0.10 ft ³	21.7 ft ³	16.0 ft ³
2	0.84 lbm of fiber	0.35 ft ³	75.9 ft ³	16.0 ft ³
3	0.96 lbm of fiber	0.40 ft ³	86.8 ft ³	16.0 ft ³

Notes:

- The volume of fibrous debris is calculated by dividing the mass of fiber of a test by 2.4 lbm/ft^3 , which is the density for low density fiberglass as identified in NEI 04-07 and accepted in the associated NRC Safety Evaluation (SE) on that document.
- The debris at the fuel entrance is calculated by multiplying the volume and mass used in a test by the number of fuel assemblies in the plant for which the test was performed (217 fuel assemblies).
- The median size of the replacement sump screen for a U.S. PWR is about $4,400 \text{ ft}^2$. A $16,000 \text{ ft}^2$ value is conservatively representative of the largest replacement sump screen for U.S. PWRs as identified in a presentation made by NEI at a Public Meeting on GSI-191 held February 9, 2006.
- At the Public Meeting on GSI-191 held February 9, 2006, vendors of passive replacement sump screens shared that, based on flume testing using licensee-specific fibrous debris loadings, about 1 ft^3 of fiber bypass is observed per 1000 ft^2 of replacement strainer surface area. The values listed in this column are calculated by multiplying a replacement sump screen surface of $16,000 \text{ ft}^2$ by the ratio of 1 ft^3 of fiber / 1000 ft^2 of replacement sump screen area.

Pressure Drop Measurements from Testing:

Pressure drop measurements were taken during testing performed for the active replacement sump screen. (It is noted that this licensee is no longer pursuing the implementation of an active sump screen.) The conditions under which pressure drop measurements were made, and the corresponding range of values of the measurements, are listed in Table 2-2, given below.

As identified in the fibrous debris loading discussion given earlier in this response, vendors performing testing of passive replacement sump screens have reported that, based on flume testing using licensee-specific fibrous debris loadings, about 1 ft^3 of fiber bypass is observed per 1000 ft^2 of replacement strainer surface area. From Note (4) of Table 1 above, the majority of the replacement sump screens for U.S. PWRs are less than $10,000 \text{ ft}^2$ in surface area. However, a value of $16,000 \text{ ft}^2$ value was selected to conservatively represent the largest replacement sump screen for U.S. PWRs. As described above, with a maximum replacement sump screen area of $16,000 \text{ ft}^2$, no more than about 16 ft^3 of fibrous debris is expected to collect on the core entrance.

From the pressure drop data given in the table below, even with a collection of 21.7 ft^3 of fibrous debris and 1388.8 lb_m of particulate debris at the entrance to the core, a bounding head loss that would be expected is about 10.2 inches of water. The bounding 10.2 inch increase in head loss translates into an increase in pressure drop of about 0.37 psi at the core entrance. Considering the WCOBRA/TRAC calculations of Appendix B that assumed an arbitrary 99.4% reduction in flow area, the bounding head loss increase of 10.2 inches of water are evaluated to not affect long-term core cooling.

Table 2-2: Summary of Head Loss Data for Observation Configuration

Flow Rate (gpm)	Fibrous Debris			Particulate Debris		Measured Head Loss (in_{H_2O})
	Mass - One Assembly	Volume - One Assembly ⁽¹⁾	Volume - At Core Entrance ⁽²⁾	Mass - One Assembly	Mass - At Core Entrance ⁽²⁾	
6	0.04 lb _m	0.017 ft ³	3.62 ft ³	0.0 lb _m	0.0 lb _m	0.4
				0.4 lb _m	86.8 lb _m	0.8
6	0.06 lb _m	0.025 ft ³	5.43 ft ³	0.0 lb _m	0.0 lb _m	1.2
				1.2 lb _m	260.4 lb _m	2.9
6	0.12 lb _m	0.050 ft ³	10.85 ft ³	0.0 lb _m	0.0 lb _m	1.9 – 2.5 ⁽³⁾
				1.6 lb _m	347.2 lb _m	4.5 – 7.0 ⁽³⁾
6	0.24 lb _m	0.100 ft ³	21.7 ft ³	0.0 lb _m	0.0 lb _m	3.8 – 5.8 ⁽³⁾
				6.4 lb _m	1388.8 lb _m	10.2
6	0.36 lb _m	0.150 ft ³	32.55 ft ³	0.0 lb _m	0.0 lb _m	12.9
				16 lb _m	3472 lb _m	38.5
6	0.48 lb _m	0.200 ft ³	43.40 ft ³	0.0 lb _m	0.0 lb _m	0.8 – 16.3 ⁽³⁾
				16 lb _m	3472.0 lb _m	> 60
6	0.96 lb _m	0.400 ft ³	86.80 ft ³	0.0 lb _m	0.0 lb _m	24.1
				6.4 lb _m	1388.8 lb _m	> 60

Notes:

- (1) The volume of fibrous debris is calculated by dividing the mass of fiber of a test by 2.4 lbm/ft³, which is the density for low density fiberglass as identified in NEI 04-07 and accepted in the associated NRC Safety Evaluation (SE) on that document.
- (2) The debris at the fuel entrance is calculated by multiplying the volume and mass used in a test by the number of fuel assemblies in the plant for which the test was performed (217 fuel assemblies).
- (3) Multiple entries indicate more than one (1) test run was made with the fibrous and particulate debris loading identified in the table. The minimum and maximum values of head loss that were recorded are listed in the table.

Applicability of Test Data and Observations to PWRs:

The data and conclusions presented in this response are applicable to all PWRs with passive sump screens for the following reasons;

- The formation of a fiber bed at the core inlet serves as a collector for particulates which, in turn result in an increase in pressure drop across the core inlet. Since active sump screens are known to maximize debris passed through the screen, the data is applicable and bounding for all PWRs with passive sump screens.
- Without a fiber bed, particulates that are lifted into the core are sufficiently small that they will not collect at and block the core entrance (Reference 2-1). Without a fiber bed to capture particulates, there is no impact on the head loss at the core inlet.

Thus, the fiber bed formation and subsequent collection of particulates and the consequential head loss observed in the test and test data described above is both applicable and bounding for all PWRs with passive sump screens

Applicability of NUREG/CR-6224 Correlation:

The NUREG/CR-6224 head loss correlation is not directly applicable to the head loss associated with the collection of fibrous debris on fuel grids. The NUREG/CR-6224 head loss correlation was developed for a different situation than that seen for the collection of fibrous debris on fuel grids. Thus, for the same fibrous and particulate debris loading, the correlation will be overly conservative in predicting the head loss through the fibrous debris bed on a fuel grid.

This position is supported by the following:

- Replacement sump screen testing has shown that, due to the small hole size used for the replacement sump screens, the fibrous debris bypassed through replacement sump screens is much shorter than the fibrous debris that was used in the testing performed to support the development of the NUREG/CR-6224 head loss correlation due to the small hole sizes of the replacement sump screen. The shorter fibers provide for a different fiber bed morphology than what was used for the development of the NUREG/CR-6224 correlation
- The flow in the test was upward with gravity acting to pull the fiber bed down and away from the bottom of the fuel. For the testing performed to support the NUREG/CR-6224 correlation, the fibrous bed was formed on the top of a mesh or perforated screen and the flow downward through the fibrous bed and the screen which tended to compress the fiber bed.
- Similarly, gravity worked on particulates that were caught in the fibrous bed formed in the test tended to pull the fibrous bed apart, whereas, for the testing performed to support the development of the NUREG/CR-6224 head loss correlation, particulates were trapped on top of the fibrous debris bed and gravity, like the flow, worked to compress the fibrous debris bed.
- The NUREG/CR-6224 head loss correlation was developed from data collected using a vertical loop test facility with a small diameter flow channel in which all of the flow was directed downward through a fixed, predetermined debris bed. In a reactor, the flow area is large and the flow patterns sufficiently varied that the uniform directional flow conditions of the NUREG/CR-6224 test do not apply.
- Finally, the NUREG/CR-6224 correlation was developed from test data for velocities ranging from 0.15 ft/sec to 1.5 ft/sec (NUREG/CR-6224, Section 6.4). As shown in Table 1 of the response to RAI #3, the liquid velocities in the core are at or below the bottom range of the velocities used in developing the NUREG/CR correlation. The lower velocities associated with PWRs would not compact a fiber bed to the same degree as those higher velocities used in the testing that supported the development of the NUREG/CR-6224 head loss correlation. Less compaction of a fibrous bed provides for a smaller pressure drop across the bed.

For these reasons, the NUREG/CR-6224 head loss correlation is not directly applicable to the head loss associated with the collection of fibrous debris on fuel grids and, for the same fibrous and particulate debris loading, will be overly conservative in predicting the head loss through the fibrous debris bed on a fuel grid.

REFERENCE FOR RAI #2 RESPONSE:

- 2-1 Andreychek, T. S., "Evaluating Effects of Debris Transport within a PWR Reactor Coolant System during Operation in the Recirculation Mode," Particulate Phenomena and Multiphase Transport, Proceedings of the 4th Miami International Symposium on Multiphase Transport and Particulate Phenomena, 15-17 December 1986, published by Hemisphere Publishing Corporation (1988)

RAI #3

To show that the pressure drop correlation of NUREG/CR-6225 is adequate to evaluate core inlet blockage, please provide a comparison of the materials and flow velocities of the test data used to develop the correlation to those which would be expected at a reactor core inlet during long term cooling. UPI plants should be included in this comparison.

RESPONSE TO RAI #3

The NUREG/CR-6224 head loss correlation is not directly applicable to the head loss associated with the collection of fibrous debris on fuel grids. The NUREG/CR-6224 head loss correlation was developed for a different situation than that seen for the collection of fibrous debris on fuel grids. Thus, for the same fibrous and particulate debris loading, the correlation will be overly conservative in predicting the head loss through the fibrous debris bed at the core inlet.

This position is supported by the following:

- Replacement sump screen testing has shown that, due to the small hole size used for the replacement sump screens, the fibrous debris bypassed through replacement sump screens is much shorter than the fibrous debris that was used in the testing performed to support the development of the NUREG/CR-6224 head loss correlation. The shorter fibers provide for a different fiber bed morphology than what was used for the development of the NUREG/CR-6224 correlation
- The flow in the demonstration test was upward with gravity acting to pull the fiber bed down and away from the bottom of the fuel. For the testing performed to support the NUREG/CR-6224 correlation, the fibrous bed was formed on the top of a mesh or perforated screen and the flow downward through the fibrous bed and the screen which tended to compress the fiber bed.
- Similarly, gravity worked on particulates that were caught in the fibrous bed of the demonstration testing tended to pull the fibrous bed apart, whereas, for the testing performed to support the development of the NUREG/CR-6224 head loss correlation, particulates were trapped on top of the fibrous debris bed and gravity, like the flow, worked to compress the fibrous debris bed.
- The NUREG/CR-6224 head loss correlation was developed from data collected using a vertical loop test facility with a small diameter flow channel in which all of the flow was directed downward through a fixed, predetermined debris bed. In a reactor, the flow area is large and the flow patterns sufficiently varied that the uniform directional flow conditions of the NUREG/CR-6224 test do not apply.
- Finally, the NUREG/CR-6224 correlation was developed from test data for velocities ranging from 0.15 ft/sec to 1.5 ft/sec (NUREG/CR-6224, Section 6.4). As shown in Table 3-1 below, the liquid velocities in the core are at or below the bottom range of the velocities used in developing the NUREG/CR correlation. At lower velocities associated with PWRs, there would be less compaction of any fiber bed.

For these reasons, the NUREG/CR-6224 head loss correlation is not directly applicable to the head loss associated with the collection of fibrous debris at the core inlet and, for the same fibrous and particulate debris loading, will be overly conservative in predicting the head loss through the fibrous debris bed on a fuel grid.

Finally, based on the observations and data presented in the response to RAI #2, core “blockage” is not experienced over the range of conservative fibrous and particulate debris loadings on debris capturing features of current fuel design. These observations and data confirm that the same type of debris bed head loss seen in the tests to develop NUREG/CR-6224 does not form for fuel geometries and orientations.

The table below lists representative velocities that are expected to occur in the core during long-term core cooling when the ECCS is realigned to recirculate coolant from the reactor containment building sump into the cold leg. These velocities were evaluated are prior to initiating hot-leg recirculation.

Table 3-1: Representative Core Velocities at Time of Initiation of Recirculation from the Reactor Containment Building Sump			
NSSS Design	Break Location	ECCS Operation	Core Velocity
B&W, CE and W 3- and 4-loop plants	Cold-leg Break	1 or 2 trains	0.10 ft/sec ⁽¹⁾
	Hot-Leg Break	1 train	0.20 ft/sec ⁽²⁾
		2 train	0.40 ft/sec ⁽²⁾
W 2-loop plants	Cold-Leg Break	Max. UPI flow	0.10 ft/sec ⁽³⁾
	Hot-Leg Break	Max UPI flow	N/A ⁽⁴⁾

Notes:

- (1) Velocity is based on making up for core boil-off. The value listed is considered a maximum core velocity as it is taken at time of ECCS switchover from RWST/BWST injection to recirculation from the sump when the core decay heat is a maximum.
- (2) All ECCS flow is taken to flow through the core.
- (3) Assumes all ECCS flow to the core is through the UPI port.
- (4) For the hot-leg break, the core is deluged by the UPI flow and excess coolant flows out the hot-leg break. While there is recirculation of flow in the core for a hot-leg break in a Westinghouse 2-loop PWR with the UPI flow, a bulk core velocity (such as would be occur with bottom-flooding of a 3-loop or 4-loop PWR) is not meaningful for a 2-loop PWR plant.

RAI #4

On page xvi and xvii, it is stated that 99.4% blockage results in adequate flow to the core to provide cooling. This result is not surprising since the vessel is in a boiling pot condition which will enable the fluid levels to balance under such low flow hydrostatic conditions. However, the injection water contains boric acid. Since the core is boiling, the boric acid will buildup in the core and because the 99.4% of the core inlet is blocked, the higher density boric acid solution in the core will not mix with the lower plenum. The boric acid concentration in the core will increase until precipitation occurs. As such, because the evaluation did not consider the buildup of boric acid, adequate core cooling is not assured and the statements guaranteeing adequate core cooling are unfounded. Evaluations need to be performed to show that with the maximum credible blockage, boric acid precipitation is assured. The evaluation and analysis with COBRA/TRAC performed with 99.4% blockage is meaningless. Furthermore, what is the minimum blockage that enables the boric acid to mix sufficiently with the lower plenum to preclude precipitation? Can the concentrated boric acid mixture combine with the blockage materials at the inlet can prevent flushing of the core following the switch to simultaneous injection? What happens as boric acid settles on top of potential blockages at the inlet to the core of the core and spacer grid locations?

RESPONSE TO RAI #4

The condition of 99.4% blockage scenario was presented as a demonstration case representing extreme conditions where core cooling would still be maintained. As discussed in Section 2.1, significant blockage of the core is not expected even for the most limiting case of a hot leg break and maximum core SI throughput. The limiting scenario for boric acid precipitation is a cold leg break where the core flow is stagnant with only enough core inlet flow to replace core boiloff. A stagnant core region provides the only scenario for which boric acid will accumulate. For this scenario, core inlet SI throughput is an order of magnitude less than the hot leg break case. For a hot leg break, all cold leg injected SI flow is forced through the lower plenum; whereas for a cold leg break, all cold leg injected SI flow in excess of that required to

replace core boiloff spills out the break. Furthermore, since the excess SI flow spills out the break, it would be repeatedly re-filtered through the sump screens. Only high levels of core inlet blockage would have an effect on core region / lower plenum mixing. However, since a high level of core inlet blockage will not occur even for the worst case of maximum core SI throughput (see discussion in Section 2.1), and since for the limiting scenario (i.e. cold leg breaks), the amount of core inlet blockage would be an order of magnitude less than the worst case, lower plenum mixing is justified and licensing basis boric acid control analyses remain valid.

A high level of core inlet blockage will not occur. Therefore no testing to determine the mixing behavior between the core and lower plenum with a blockage at the core inlet has been performed to date.

After the switch to simultaneous injection, SI flow injected into the hot leg will initiate the dilution process for a highly concentrated core. Since the break must be in the cold leg (to get a highly concentrated core), the driving head for the core dilution flow can extend well up into the intact hot legs and SGs. This driving head would force flow through the core and therefore the conditions for boric acid precipitation will not exist.

RAI #5

On page 2-4 it is stated that analyses using WCOBRA/TRAC demonstrated that with even as much as 99.4% of the core blocked, core decay heat was adequately removed.

- a. So that this analysis may be related to a plant specific core blockage condition, please relate the results of the WCOBRA/TRAC analyses for the minimum blockage for which adequate core cooling can still be provided to an equivalent fiber bed using the pressure drop correlation of NUREG/CR-6224.
- b. As debris and chemicals are concentrated within the core by the boiling process, the density of the fluid in the core will increase. This increase in density will act to retard core flow. Provide an evaluation of the effect of increased core density on the results from the WCOBRA/TRAC analysis of core blockage.

RESPONSE TO RAI #5

- a. As noted in the responses to RAI #2 and RAI #3, the pressure drop correlation of NUREG/CR-6224 is not directly applicable to fibrous debris collected at the core inlet for PWRs.

The response to RAI #2 provides observations and data from tests of the collection of bypass debris, both fibrous and particulate, from an active replacement sump screen for a high fiber plant on debris capturing grids for a fuel assembly. The data testing provided in the response to RAI #2 shows that, even if a fiber bed with particulates forms at the bottom of the fuel, coolant will continue to pass through the bed.

Finally, the NUREG/CR-6224 correlation was developed from test data for velocities ranging from 0.15 ft/sec to 1.5 ft/sec (NUREG/CR-6224, Section 6.4). As shown in Table 1 of the response to RAI #3, the liquid velocities in the core are at or below the bottom range of the velocities used in developing the NUREG/CR correlation.

Thus, it is concluded the requested comparison cannot be performed such that it is meaningful to evaluating long-term core cooling.

- b. An increase in the core fluid density due to concentration of debris and chemicals will result in an unstable configuration leading to natural convection flow patterns between the core and the less dense lower plenum, which will limit the density build-up. This was demonstrated in the BACCHUS test results previously provided to the NRC in the following reference:

Entergy Letter to NRC, W3F1-2005-0012, "Supplement to Amendment Request NPF 38 249, Extended Power Uprate, Waterford Steam Electric Station, Unit 3," February 16, 2005.

The effects of an increase in density in the core (and eventually, lower plenum) due to concentrating debris and chemicals would not be expected to affect the main conclusions of the WCOBRA/TRAC study; namely, that core cooling would be expected to be maintained even with significant blockages. This cannot be quantitatively demonstrated by WCOBRA/TRAC, as it is beyond the code's modeling capability. Also, the resulting density would be dependent on a number of plant-specific factors. However, it can be qualitatively supported by responses to recent NRC questions on an Extended Power Uprate application. Actions are taken to initiate core dilution measures prior to reaching the solubility limit of boric acid. In this RAI response, it was shown that a boric acid and water solution that approaches the solubility limit would have a density increase on the order of 10%, based on information provided in EPRI NP-5558. Such an increase would not be expected to offset the available driving head seen in the WCOBRA/TRAC calculations presented in Appendix B. (This density increase did not include any effects of debris in the core. However, build-up of any debris in the core would be expected to be very gradual, and not significant enough to alter this conclusion.)

(RAI #4 commented that the WCOBRA/TRAC study performed with 99% blockage is meaningless. It should be noted that the primary purpose of the calculations summarized and presented in Appendix B was to complement similar studies performed by NRC staff with the RELAP-5 and TRACE codes. Similar modeling assumptions and simplifications were made in the NRC assessments; the results of the NRC studies were presented at a NRC/industry meeting held on August 2, 2006.)

RAI #6

On page 2-7 it is stated that two sample calculations were provided in Section 5 for predicting chemical deposition on fuel cladding.

- a. The staff was only able to find one sample calculation in Section 5 and in Appendix E. Please provide the other sample calculation.
- b. For a plant specific submittal to reference a sample calculation as bounding for that plant, a list of critical input parameters would need to be compared. Please provide a table giving these parameters and the values assumed in the sample calculations.

RESPONSE TO RAI #6

- (a) The text incorrectly identified that two (2) sample calculations were provided in Section 5. Only one was provided. The text will be corrected to reflect that only one (1) sample calculation is presented.
- (b) A table showing the input values for the LOCADM sample calculation has been provided. (See Attachment 1.)

RAI #7

On page 2-12 it is stated that the effect of settled debris in the lower plenum on licensing basis boric acid precipitation analyses is judged to be small and plant-specific evacuations are not required. Please provide evidence that this statement is true for all PWRs or provide criteria that plants should meet to demonstrate that this concern is not an issue in plant specific submittals.

RESPONSE TO RAI #7

Section 9.1 in Reference 7-1 (below) discusses the impact of settled debris on the reactor internals and advises licensees to evaluate the volume of settled debris against the available volume of the lower plenum. The calculation of the amount of

settled debris in the lower plenum would be based on the limiting scenario of a hot leg break and maximum reactor vessel throughput.

Boric acid precipitation is not an issue for a hot leg break since there will be forced flow through the reactor vessel such that boric acid accumulation will not occur. For a hot leg break, the licensees will demonstrate that the volume of debris that settles in the lower plenum is less than the available free volume in the lower plenum and therefore a flow path to the core is assured.

The limiting scenario for boric acid precipitation is a cold leg break where the core is stagnant with only enough core inlet flow to replace core boiloff. For this scenario, lower plenum flow is an order of magnitude less than the hot leg break case where the lower plenum sees maximum throughput. Furthermore, the vast majority of SI flow would go out the break and would be repeatedly re-filtered through the sump screens. Since the volume of settled debris in the lower plenum would be approximately proportional to the flow into the lower plenum, the maximum volume of settled debris in the lower plenum for a cold leg break would be less than one tenth of the available volume of the lower plenum (based on an order of magnitude difference cold leg break and hot leg break core flow).

In response to recent NRC concerns, evaluations have been performed so that there are now few, if any, plants that rely on the total lower plenum volume when calculating core region boric acid buildup. A clarification letter has been sent to licensees advising of the need to consider displaced lower plenum volume on these calculations.

NRC reviewers have requested examples of licensing basis boric acid precipitation analyses under this RAI. The references listed below are examples of licensing basis boric acid precipitation analyses that have been recently submitted to NRC for Westinghouse PWRs:

Plant Type	ADAMS Accession Number
Westinghouse 2-Loop PWR	ML060180262
Westinghouse 3-Loop PWR	ML053290133
Westinghouse 4-Loop PWR	ML072000400

These submittals were made with the appropriate affidavit of withholding, as applicable, and should be handled accordingly.

It should be noted that each plant has a boric acid precipitation strategy as part of their licensing basis. While the methods described in the examples identified in this RAI response may not be exactly the same from plant to plant, the examples are representative of the approach taken throughout the PWR industry with respect to establishing a core mixing volume.

REFERENCE FOR RAI #7 RESPONSE:

- 7-1. WCAP-16406-P, Evaluation of Downstream Sump Debris Effects in Support of GSI-191, June 2005.

RAI #8

On page 2-13 it is stated that for limiting boric acid precipitation scenarios (i.e. relatively stagnant core region) the alternate core flow paths would not see significant blockage since the flow areas are not effective debris traps or filters. Please demonstrate that for such a cooling scenario that boric acid and other dissolved and suspended substances would not accumulate in the core and precipitate.

RESPONSE TO RAI #8

The licensing basis for US PWRs includes analyses that demonstrate boric acid precipitation will not occur for the limiting cold leg break and stagnant core region scenario. Typically the purpose of these analyses is to verify the timeliness of an active or passive core dilution mechanism. Nearly all of these analyses credit alternate flow core flow paths either to support an expanded mixing volume or to provide core dilution. Active or passive core dilution mechanisms will keep boric acid and other dissolved and suspended substance from accumulating in the core. There are no credited alternate flow paths that would have minimum flow restrictions less than the particle size that might pass through the sump screens.

NRC reviewers have requested examples of licensing basis boric acid precipitation analyses under this RAI. The references listed below are examples of licensing basis boric acid precipitation analyses that have been recently submitted to NRC for Westinghouse PWRs:

Plant Type	ADAMS Accession Number
Westinghouse 2-Loop PWR	ML060180262
Westinghouse 3-Loop PWR	ML053290133
Westinghouse 4-Loop PWR	ML072000400

These submittals were made with the appropriate affidavit of withholding, as applicable, and should be handled accordingly.

It should be noted that each plant has a boric acid precipitation strategy as part of their licensing basis. While the methods described in the examples identified in this RAI response may not be exactly the same from plant to plant, the examples are representative of the approach taken throughout the PWR industry with respect to establishing a core mixing volume.

RAI #9

Page 2-15 states that debris buildup on mixing vanes, fuel grids will occur over time. Since the boric acid is also concentrating over time, combination of the debris in vanes and grids over time may form a localized blocked region or regions (containing debris and boric acid) that could cause localized precipitations that could collectively build over time and eventually block large regions of the core. The combination of the debris and the higher concentrate boric acid could form sustained blockages at the vanes and or grids or core inlet. Please explain. Please also discuss the calculations performed to show how the boric acid mixes through the core and lower plenum with debris in the vanes/grids and lower plenum. Current long term cooling analyses assume perfect uniform mixing of the boric acid in the core, lower and upper plenum. Localized gradients that may occur due to the debris/boric acid concentrations could cause local concentrations to exceed the precipitation limit. Since the lower plenum contains cooler injection water plus debris, a higher concentration will be needed in the core to initiate mixing into the lower plenum during the long term. Please demonstrate that the worst plant would not develop boric acid concentrations that approach the precipitation limit with the largest amount of debris. Also, how does high concentrate boric acid (up to 32 wt%) diffuse downward through fibrous and/or debris blockages plus the strainers at the core inlet while the water flows upward to keep the core covered? Please explain.

RESPONSE TO RAI #9

As mentioned previously, there are three considerations that minimize the potential for the postulated blockage of large regions of the core.

1. Ingested debris will not begin to collect until the ECCS enters recirculation phase. Since the core boiloff rate decreases with time, the period of the greatest rate of boric acid accumulation will occur prior to recirculation.
2. For a hot leg break, the scenario for greatest debris accumulation is not a concern. Conversely, for a cold leg break, which is the boric acid precipitation scenario of concern, core flow is stagnant and therefore debris accumulation is minimal. (See response to RAI#7 for additional discussion.)
3. All plants have boric acid precipitation control measures that promote core dilution after a LOCA. These measures typically rely on an operator initiated action, at some specified time, to start core dilution prior to reaching the boric acid solubility limit. These measures will serve to dilute concentrated sump chemical and suspended debris that might accumulate in the core region. Core dilution flow will flush concentrated chemicals and suspended debris out of the vessel and out the break.

With little debris accumulating in the core, at the core inlet, or in the RV lower plenum regions, mixing will continue due to convection, diffusion, local turbulence, and bubble mixing phenomena.

For the stagnant flow conditions of the boric acid precipitation scenario, there will not be sufficient core region, core inlet and lower plenum debris accumulation to invalidate licensing basis boric acid precipitation analyses. When considering the potential for boric acid precipitation after the switch to sump recirculation, the calculations in Appendix F indicate that the sump chemistry is such that boric acid precipitation will not occur, even in high concentrations. For example, Runs 1 and 3 in Appendix F indicate no boric acid precipitates when the sump solution is concentrated to a factor of 20, and then cooled to 212°F.

RAI #10

On page 2-14 in Section 2.7.2 dealing with upper plenum injection at UPI plants, it is stated that for a hot leg break, the coolant flow-through from the cold leg through the core and out the break is sufficiently large to maintain debris introduced by the UPI flow, entrained in the flow and transported it out the break. Please provide justification for this statement. The NRC staff understands that for some UPI plants, cold leg ECCS flow is terminated when sump recirculation begins. Under these conditions core flow would be stagnant and debris will accumulate.

RESPONSE TO RAI #10

The statement in the WCAP is incorrect. The licensing basis for Westinghouse 2-loop PWRs is for the recirculation flow to be provided through the UPI ports and for all cold-leg flow to be secured. This statement in the WCAP will be corrected.

The UPI nozzle for a Westinghouse 2-loop PWR has an inside diameter of about 4 inches. These nozzles are located approximately 180° opposite of each other. Assuming a minimum total UPI flow of 1200 gpm and an equal flow distribution between the two UPI nozzles, the flow rate through each nozzle is 600 gpm or approximately 1.34 ft³/sec. Thus, the minimum velocity of the UPI flow through each UPI nozzle is calculated to be approximately 15.3 ft/sec. At these jet velocities, the upper plenum coolant inventory is not stagnant. Rather, the UPI jet flow, in conjunction with impingement of the jets on upper internals structures, generates turbulent mixing of the UPI flow with the coolant inventory in the upper plenum.

The volume between the top of the active fuel and the bottom of the hot-leg for a Westinghouse 2-loop PWR is about 190 ft³. For a UPI flow of 1200 gpm, the equivalent volumetric flow is about 2.68 ft³/sec. Neglecting any water level above the bottom of the hot-leg, which would be small for a double-ended guillotine hot-leg break, and assuming a constant volume of water in the upper plenum, approximately 71 seconds are required to "turn over" the entire fluid inventory of the upper plenum. This quick turn-over time further supports that the upper plenum is well mixed by the UPI flow.

The turbulent mixing, in turn precludes settle-out of debris in the upper plenum. With the turbulent flow and mixing in the upper plenum precluding debris settle-out in the upper plenum, debris will be carried with the expulsion of UPI flow out the hot-leg break.

RAI #11

On page 2-15 it is stated that complete compaction of debris that might collect at the bottom of the fuel at the debris trapping features will not occur for a UPI plant and that the packing will likely be less than 60 percent. Please provide the flow loss coefficient which would occur for this condition and give guidance as to what maximum loss coefficient would be acceptable.

RESPONSE TO RAI #11

The 60% voiding can be conservatively approximated as a 60% blockage of the core. This would present a bounding or maximum resistance to flow through the debris bed.

The WCOBRA/TRAC evaluations described in Section 6 demonstrate that adequate flow is maintained with a deterministically assigned blockage of 82% to provide for long-term core cooling. Thus, conservatively taking the 60% packing factor to be representative of a 60% blockage, adequate long-term core cooling will be provided for.

RAI #12

On page 2-15 regarding UPI plants, it is stated that if coolant flow is sufficiently restricted through a debris bed that clad temperatures increase to about 15^oF to 20^oF above the coolant temperature, the coolant would begin to boil. The steam formed would be about 40 to 50 times the volume of the water, and would cause the debris bed to be displaced, allowing for coolant to flow and to cool the cladding surface. Please justify that cooling will be maintained for a debris bed blocking the bottom of the core with steam rising through the top. Provide justification that boric acid and chemicals dissolved in the coolant would not increase to an unacceptable concentration under these conditions.

RESPONSE TO RAI #12

Blockage of the core may occur only by debris-laden coolant being provided to the core. The refueling water storage tank (RWST) does not have debris in it. Therefore, during injection of the RWST inventory, no debris is provided to the core for PWRs.

Westinghouse 2-loop plants with upper plenum injection (UPI) do not maintain flow into cold legs once the switchover of the emergency core cooling system (ECCS) from injecting from the RWST to recirculating coolant from the reactor containment building sump is accomplished; the recirculating flow is ducted to the reactor vessel through the UPI penetrations in the reactor upper plenum. For cold leg breaks, coolant is introduced into the reactor vessel from the UPI nozzles and flows down through the core and out the break. If blockage due to the accumulation of debris were to occur, it would occur at the top of the fuel. As was the case with bottom-up flooding of the core, and as demonstrated in the data presented in the response to RAI #2, a complete blockage is not expected because of the short fibers that pass through the sump screen do not provide for a bed formation as demonstrated in the replacement sump screen tests.

The switchover of the ECCS from injecting from the RWST to recirculating coolant from the reactor containment building sump is accomplished by operators taking the actions identified in their plant-specific Emergency Operating Procedures (EOPs). Each of the UPI plants has a licensing basis analysis for addressing boric acid precipitation that has been reviewed and approved by NRC. This same flow that provides for core cooling and boric acid precipitation will dilute the core and keep boron compounds and other chemicals that may be dissolved in the recirculating coolant from accumulating in the core.

As described in the response to RAI #10, for hot leg breaks, the upper plenum will be well mixed in the upper plenum with excess UPI flow exiting out the break. Debris accumulation in the upper plenum and upper fuel region will be minimal since debris will be carried out the break with the excess ECCS flow.

In case of either a hot-leg or a cold-leg break, the formation of a debris bed on the bottom of the fuel is not considered credible.

A representative evaluation of core dilution for a 2-loop PWR was identified and provided in the response to RAI #7 and RAI #8.

The evaluation of effect of chemicals dissolved in the UPI flow for a hot-leg break are performed on a plant-specific basis using the LOCADM calculation tool described in Appendix E of WCAP-16793-NP.

RAI #13

Calculations for cladding heat up behind fuel grids are presented in section 4.1 and Appendix C. The ANSYS code was used in these calculations. Please provide a reference for this computer code and for the review of this computer code by the NRC staff.

RESPONSE TO RAI #13

The ANSYS Mechanical software was used for the cladding heat up behind fuel grid. This software is in common use internationally to solve a wide range of mechanical engineering problems. The use of the thermal analysis capability of the ANSYS Mechanical software for WCAP-16793-NP was in accordance and consistent with standard industry practices for both ANSYS Mechanical software, and other similar engineering problem solving software.

The ANSYS Mechanical software offers a comprehensive product solution for structural linear/nonlinear and dynamics analysis. The product offers a complete set of elements behavior, material models and equation solvers for a wide range of engineering problems. In addition, ANSYS Mechanical offers thermal analysis and coupled-physics capabilities involving acoustic, piezoelectric, thermal-structural and thermal-electric analysis. For the cladding heat up calculations, only the thermal solution capabilities of the ANSYS Mechanical software were used.

As a clarification, by submitting WCAP-16793-NP, the PWR Owners Group is not requesting NRC review the ANSYS Mechanical software. Rather, the PWR Owners Group is requesting that the NRC concur that the software was appropriately used consistent with industry practice and that the results of the analyses are acceptable.

Additional information regarding the ANSYS Mechanical software may be obtained from the following website: www.ansys.com.

RAI #14

The maximum debris thickness that was evaluated using the ANSYS computer code was 50 mills. Is 50 mills the maximum acceptable thickness for debris collection behind a fuel element spacer grid? If not, please provide the acceptance criterion. What would be the thickness of debris if a spacer grid were to become completely filled? Provide an analysis of the resulting peak cladding temperature if the location between a spacer grid and an fuel rod were to become completely filled with debris.

RESPONSE TO RAI #14

The minimum clearance between two adjacent fuel rods, including an allowance for the spacer grid thickness, is greater than 100 mills. Therefore, the 50-mil debris thickness on a single fuel rod is maximum deposition to preclude touching of the deposition of two adjacent fuel rods with the same deposition. The 50 mil thickness is the maximum acceptable deposition thickness before bridging of adjacent fuel rods by debris is predicted to occur.

For current fuel designs, the minimum clearance between the cladding and the spacer grid is about 40 mills; this occurs where the springs and dimples of the grid contact the fuel rod. The maximum clearance between the cladding and the spacer grid occurs along the diagonal of the of a grid cell and is about 110 mills. Thus, if a spacer grid were to become completely filled, the radial thickness of the debris on the outside clad would vary from about 40 mills to about 110 mills about the circumference of a fuel rod.

The example chemical product deposition calculation performed in Appendix E of WCAP-16793-NP was performed with inputs intended to maximize chemical deposition. That deposition calculated for the sample case was less than 30 mills. Thus, although the chemical deposition of fuel is a plant-specific calculation, plants are not expected to calculate deposition thicknesses in excess of 30 mills. Thus, for chemical deposition, the range of cladding heat up calculations behind spacer grids presented in WCAP-16793-NP is bounding.

The formation of a chemical deposition layer followed by the collection of fibrous debris in the remaining open channel will not challenge the cooling of the clad. The response to RAI #15 shows that the effective thermal conductivity of a fibrous debris bed is at least 5 times greater than the minimum thermal conductivity of 0.1 Btu/(hr-ft-°F) used in the cladding heat up calculations. Based on observations from testing of fibrous debris collection on debris capturing grids identified in the response to RAI #2, a complete blockage of a spacer grid with fibrous and particulate debris is not credible. The test data shows that, even under extreme fibrous and particulate debris loads, flow through the resulting debris bed is maintained.

To assess a maximum clad temperature under worst case debris deposition in a single spacer grid/fuel rod configuration, the following assumptions are made:

- A uniform debris layer thickness of 110 mills is assumed on the cladding, and,
- The debris layer is assigned the conservative effective thermal conductivity for a fibrous debris bed recommended in the response to RAI #15 for Debris Thermal Conductivity = 0.1 Btu/(hr-ft-°F).

Under these limiting assumptions, extrapolating the calculated clad temperatures listed in Table 4-3 listed for the effective thermal conductivity $k_{EFF} = 0.1$ Btu/(hr-ft-°F), it is estimated that the maximum clad temperature behind a grid would be less than 738°F. This is an extremely conservative estimate of the clad temperature for the following reasons;

- A conservatively small value of conduction through the debris bed identified in the response to RAI #15 is used,
- The calculation does not account for circumferential heat transfer about the debris bed which would form in the spacer grid between the dimples and springs and the corners of the spacer grid, and,

- Convection of heat by the flow of coolant through the debris bed is neglected. (The ability of coolant to pass through a fibrous and particulate debris bed under PWR flow conditions was demonstrated in the response to RAI #2.)

Therefore, the estimation of an maximum clad temperature of 738°F is a very conservative estimate of the maximum clad temperature if the location between a spacer grid and an fuel rod were to become completely filled with debris.

RAI #15

Section 4.1.4 states that in using the ANSYS code that debris is assumed to have the same thermal properties as crud. A value for thermal conductivity of 0.5 BTU/(hr*ft*deg-F) is recommended and the lowest value of thermal conductivity examined was 0.1 BTU/(hr*ft*deg-F). If a debris bed trapped behind a fuel element spacer grid were composed of fibrous insulation the thermal conductivity would be much lower. Please justify not using a thermal conductivity appropriate for fibrous insulation.

RESPONSE TO RAI #15

NUKON[®] is a low density fiberglass insulation material commonly used in PWR reactor containment buildings. Performance Contracting, Inc. (PCI), the owners of the NUKON[®] product line, were requested to provide information they had regarding the effect of wetting NUKON[®] on the effective thermal conductivity of the insulation. PCI noted that the thermal conductivity of fibrous insulation is a function of the moisture content. Under normal industrial and nuclear applications, NUKON[®] is used on hot piping and components; thus the moisture content is low. PCI stated they had no data for the thermal performance of wetted insulation as, for industrial applications, when insulation becomes wetted it ceases to perform its function and remedial action are taken. The remedial actions are usually removing the source of moisture and either drying or replacing the affected insulation.

Although they did not have data on the effect moisture had on effective thermal conductivity of NUKON[®], based on their experience in both industrial and nuclear applications of NUKON[®], PCI noted that as fiberglass wool becomes wetted, the value of the thermal conductivity of the wetted insulation tends towards the value of water. As the insulation becomes fully saturated, or if there is water flow through the wool, then the effective thermal conductivity takes on a mixed conductive/convective value that is greater than the conductivity of water.

WCAP-16793-NP states that fibrous material on fuel structures with at least a porosity of 40%. As the fibrous debris is collected first on fuel structures (grids) at the core entrance, the fibrous collection will be fully saturated with the voids between fibers filled with water. Furthermore, the fibers are expected to collect on fuel structures (grids) in a random orientation. Assuming the water in the fiber bed is stagnant, a volume-weighted thermal conductivity would appropriately represent a minimum thermal conductivity for a saturated fiber bed.

For a saturated fiber bed with a porosity of 40%, a volume-weighted thermal conductivity is calculated as follows;

Thermal conductivity of water and glass:

$$\text{Water} = 0.40 \text{ Btu}/(\text{hr}\cdot\text{ft}\cdot^{\circ}\text{F})$$

$$\text{Glass} = 0.59 \text{ Btu}/(\text{hr}\cdot\text{ft}\cdot^{\circ}\text{F})$$

Volume Fraction of water and glass in the debris collection:

$$\text{Water} = 0.40$$

$$\text{Glass} = 0.60$$

Effective Thermal Conductivity (k_{EFF})

$$k_{EFF} = 0.4 \times 0.40 \text{ Btu}/(\text{hr-ft-}^\circ\text{F}) + 0.6 \times 0.59 \text{ Btu}/(\text{hr-ft-}^\circ\text{F})$$

$$k_{EFF} = 0.514 \text{ Btu}/(\text{hr-ft-}^\circ\text{F})$$

Thus, assuming the water in the fibrous debris is stagnant, a minimum effective thermal conductivity of the saturated collection of fibrous debris on fuel components is calculated to be 0.514 Btu/(hr-ft-°F). As demonstrated from the test data presented in the response to RAI #2, there is fluid movement through the fiber collected at the entrance to the core. Thus, the actual effective thermal conductivity through the fibrous debris would be greater than the 0.514 Btu/(hr-ft-°F) value.

As stated previously, the thermal conductivity of fibrous insulation is a function of the moisture content in the insulation. In the case where the insulation contacts a boiling surface, it is a function of both the moisture and steam content. A literature search was performed to support the calculation presented above. Reference 15-1 states that the dry thermal conductivity of fiberglass insulation of 0.05 BTU/(hr-ft-°F) doubles (to 0.1 BTU/ft h °F) with only eight percent of its volume filled with water. Reference 15-2 shows that when a mixture of steam and liquid are present, the thermal conductivity will increase by a factor of approximately 12 when the liquid and steam are present in equal amounts in a porous medium. These references support the value of minimum effective thermal conductivity calculated above, and suggest that a thermal conductivity at least as large as 0.6 BTU/(hr-ft-°F) may be used for fiberglass trapped between fuel element and a spacer gird is reasonable since coolant will have access to the fiber.

Thus, based on the information presented above, the WCAP-16793-NP value of 0.1 BTU/(hr-ft-°F) is an appropriately conservative choice for representing a lower bound thermal conductivity for wet fibrous insulation.

REFERENCES FOR RAI #15 RESPONSE:

- 15-1 "Joint Departments of the Army and Air Force, USA, Technical Manual TM 5-852-5/AFR 88-19, Vol. 5, Arctic and Sub-arctic Construction: Utilities." Chapter 12
- 15-2 Ho-Jeen Su and Wilbur Somerton, "Thermal Behavior of Fluid Saturated Porous Media with Phase Changes" Proceedings of the 16th International Thermal Conductivity Conference, November 7-9 Chicago, Published by Plenum Press, New York, page 193-204

RAI #16

Page xvi and Appendix A state that clad temperatures of 800 F are considered acceptable. From a long term cooling perspective, 800 F clad temperatures establish a low rate heat oxidation process similar to the problem that developed at Calvert Cliffs during the late 70's. Clad temperatures were increased to 800 F so that operation for several weeks caused the oxide layer to build on the cladding. Please discuss the impact on long term cooling and the long term build-up of oxide and the potential to approach or even exceed the 17% 10CFR50.46 limit.

RESPONSE TO RAI #16

The core conditions that resulted in the clad oxidation at Calvert Cliffs during the late 1970's would not exist in the core post-LOCA. At-power clad corrosion is driven by temperature, fast neutron flux and thermal feedback through an oxide layer. During long term cooling post-LOCA, the fast neutron flux is negligible and the heat flux is low. Thus, for post-LOCA conditions, only the temperature is directly applicable to corrosion and autoclave data is more representative of the temperature-driven corrosion that would be experienced by cladding. Evaluation of the autoclave data at temperatures at 800° F and below shows only small increases in the corrosion thickness and hydrogen loading compared to the post-LOCA transient conditions immediately following the postulated break and prior to long-term cooling.

Local increases in corrosion due to local hot spots will not impact long term cooling. The impact of corrosion on the clad material properties is small and the heat load continues to decrease with time. The 17% ECR criteria applies to the LOCA

event only. If the local conditions immediately post-LOCA were close to the 17% Equivalent Clad Reacted (ECR) limit (pre-transient corrosion and transient ECR), then the small amount of additional corrosion from a hot spot which resulted in approaching 800° F for 30 days could reach or marginally exceed 17% ECR. However, based on the sample deposition calculation, the conservative core blockage calculations and the parametric clad heat-up calculations presented in WCAP-16793, cladding temperatures approaching 800° F for post-LOCA long-term core cooling are not expected.

Also, the peak ECR region on the rod is not expected to be the same region where a local hot spot would occur. Local hot spots would be expected to occur lower in the core and at or just below a spacer grid. Pre-transient corrosion is suppressed at the spacer grid locations.

In addition, much of the reduction in ductility from high temperature oxidation (> 1832° F) is due to oxygen diffusion ahead of the oxide layer. At temperatures of < 930° F, there is no observation of oxygen diffusion ahead of the oxide layer.

RAI #17

Appendix A states that a peak cladding temperature of 2200 deg F is acceptable for the post-quench, long term evaluation. This limit is inconsistent with previous statements and not supported by the autoclave data. In a telecon on July 26, PWROG representatives acknowledged that this was not the intent - instead, the previously states 800 deg F was the proposed upper limit on local cladding temperature. Please revise the topical report to clarify.

RESPONSE TO RAI #17

The text of WCAP-16793-NP will be amended to clarify that 800°F is the long-term core cooling acceptance basis for cladding temperature by replacing the text in question with the following text:

“Transitioning the ECCS from RWST/BWST injection to recirculation from the reactor containment building sump is addressed under the current licensing basis of PWRs.

Once the transition of the ECCS from RWST/BWST injection to recirculation of coolant from the reactor containment building sump has occurred, there is no interruption (termination) of coolant flow to the core due to system realignments such as initiation of hot leg recirculation. For plants that have a reduction in flow associated with systems realignments, the supplied flow remains above the core boil-off rate and will not result in a reheat of the cladding. Therefore, for long term cooling, the appropriate acceptance basis for clad temperature is 800°F. This acceptance basis is based on long term autoclave testing in clean water up to about 700°F, and steam above that temperature.”

RAI #18

Page A-7 states that the maximum allowable fuel clad temperature for short transients such as hot leg switch over and for localized hot spots is 2200°F during long term cooling. Please provide methodology as to how transient cladding temperatures during hot leg switch over will be calculated. Include processes and phenomena included in the methodology which cause cladding temperatures to increase during hot leg switchover and those which act to mitigate the transient.

RESPONSE TO RAI #18

The reference to hot-leg switch-over as resulting in a heat-up transient for cladding is incorrect. Also, there is no known phenomena that would cause localized hot spots during long term core cooling. The text in the WCAP will be amended as follows:

“During hot-leg switch-over or, for B&W plants, the establishment of a core flushing flow, there is no interruption of coolant to the core. Therefore, there is no clad heat-up transient during this operation.”

RAI #19

The proposed 800 deg F upper limit on local cladding temperature is based on long-term autoclave data and focus solely on the formation of nodular corrosion.

- a. Long-term oxidation tests need to be conducted on pre-hydrated specimens which have previously been exposed to LOCA heat-up and quench conditions.
- b. Post-quench fuel rod damage mechanisms should be identified and dispositioned relative to the proposed 800 deg F limit. Mechanisms include (1) further evolution of post-quench microstructure and its impact on ductility, (2) hydride formation and re-orientation, (3) crack propagation near burst region, (4) cladding creep / ballooning (non-burst rods), and (5) degradation of oxide layer and hydrogen absorption.

The stability of the oxide layer and the tetragonal-to-monoclinic transformation are sensitive to alloying elements, surface finish, and temperature history (due to local stress states within oxide layer). Please address these items with respect to the proposed upper limit and 30 day duration.

RESPONSE TO RAI #19

The autoclave testing was performed to demonstrate that no significant degradation in cladding mechanical properties was expected due to a localized hot spot. The autoclave testing demonstrated that the increase in oxide thickness and hydrogen loading was limited at 800°F. The autoclave test data and a review of literature indicate that susceptibility to localized accelerated corrosion occurred at temperatures greater than 800°F. Therefore no significant degradation in cladding properties would occur due to 30-day exposure at 800°F and there would not be any adverse impact on core coolability. Based on the autoclave results, the data is sufficient to justify 800°F.

RAI #20

Page A-7 gives two examples of when reactor fuel experienced significant damage and a coolable geometry was maintained. One example is operational experience at Three Mile Island. The NRC staff does not believe that the 1979 accident at Three Mile Island Unit 2 resulted in a coolable geometry. The other example given is operational experience at the International PHEBUS-FP Program. Please provide the PHEBUS-FP data referred to and discuss the relationship of this data to local hot spots which might occur during the long term cooling period at PWR following a large LOCA.

RESPONSE TO RAI #20

The reference to the 1979 accident at Three Mile Island Unit 2 will be deleted from the text of Page A-7.

The PHEBUS-FP tests simulated severe accident conditions in order to study fuel degradation and fission product release and transport. As such, they are best considered as a controlled simulation of phenomena experienced as a result of local hot spots that evolve into a damage of the fuel cladding.

The conclusion in this part of Appendix A could be better stated as:

“In the PHEBUS-FP Program a coolable geometry was lost, but eventually restored. The facility was eventually able to be cleaned up with negligible impact to the health and safety of the public.”

The following table lists several ADAMS Accession numbers for PHEBUS-FP presentations made to NRC and the Advisory Committee on Reactor Safeguards. The reference to the PHEBUS-FP tests on Page A-7 was as an example of the coolability of cladding that had damage and cooling of the resulting geometry was achieved.

ADAMS Accession Number	Title	Date
ML031340628	Summary of PHEBU RTF Programme	2000-03-20
ML071240063	Memo to Frank Gillespie, Providing Information on the PHEBUS-FP for ACRS Meeting 543 – June 6-8, 2007	2007-05-04
ML003744641	RES Info Ltr-RIL-0004, “Use of Results from PHEBUS-FP Tests to Validate Severe Accident Codes - 003744641	2000-08-21

As discussed in responses to other RAIs, cladding temperatures of local hot spots, if they occur, are expected to remain below the 800°F acceptance basis identified in Appendix A. At these low temperatures, based on autoclave data, additional clad damage is due to oxidation and hydrogen pickup has been shown to be negligible; no loss of a coolable geometry is expected. Thus, there is no direction relationship of the data PHEBUS-FP program to hot spots that may be expected under acceptance basis of 800°F for long-term core cooling conditions identified in Appendix A.

RAI #21

Section A.4 on page A-5 states that the acceptance basis for boric acid precipitation and chemistry effects of debris will be as follows: A core flushing flow will be established that is sufficient to prevent the calculated maximum boric acid concentration in the core region from exceeding the precipitation limit. Please provide acceptance criteria for other species of chemicals and debris which might be washed into the reactor core during the recirculation process.

RESPONSE TO RAI #21

The acceptance criterion is no rod-to-rod bridging of deposits due to deposit growth and predicted cladding temperature < 800°F after deposition. Both deposit thickness and cladding temperature are predicted by LOCADM using estimates of debris chemicals washed into the core by the recirculation process.

RAI #22

Calculations for cladding heat up between fuel grids are presented in Section 4.2 and Appendix D. The maximum debris thickness evaluated was 50 mills. Is 50 mills the maximum acceptable thickness for debris collection between fuel grids? If not please provide the acceptance criterion.

RESPONSE TO RAI #22

As noted in the response to RAI #14, the minimum clearance between two adjacent fuel rods is greater than 100 mils. Therefore, the 50-mil debris thickness on a single fuel rod is maximum deposition to preclude touching of the deposition of two adjacent fuel rods with the same deposition. The 50 mil thickness is the acceptance basis for maximum deposition.

RAI #23

Methodology for calculating the cladding temperature that would result from post-LOCA crud deposition on the fuel rods is presented in Appendixes C, D, and E. Methodology for calculating crud thickness is only presented in Appendix E. Please describe methodology which licensees would use to calculate crud thickness using Appendixes C and D.

RESPONSE TO RAI #23

The method of calculating depositon thickness is given in Appendix E. For a deposition thickness calculated using Appendix E, Appendixes C and D may be used to evaluate the change in clad temperature for different themal conductivities of the depositon material.

RAI #24

Appendix C is titled Fuel Clad Heat-up Behind Grids, whereas Appendix D is entitled Fuel Clad Heat-up between grids. Please describe the specific treatment of the grids in Appendix C which make these calculations different from the methodology in Appendix D. Section D.7 indicates that if the same inputs were used for the methodology of Appendix D as was used for Appendix C, similar results would be obtained.

RESPONSE TO RAI #24

The calculation results presented in Appendix C included conduction in both the radial and the axial directions of a fuel rod. The calcuations in Appendix D accounted for heat transfer only in the radial direction of a fuel. Both calculations are steady state claculations. Reviewing the calculations, it was observed that there is limited axial heat transfer due to a combination of the clad material being thin and the relatively small thermal conductivity of the clad material. The small amount of heat transfer in the axial direction of the model is the basis for the statement that, for similar inputs, similar results would be expected.

RAI #25

Appendix E describes the LOCADM computer code which calculates dissolution of materials from the containment to the sump water and deposition of the dissolved material on the surfaces of the reactor core. Please discuss how the LOCADM code will be made available to utilities to calculate individual plant responses. Discuss the training that the PWROG will provide to utility personnel to assure the code is being used properly.

RESPONSE TO RAI #25

LOCADM is not a multi-dimensional thermal-hydraulic code that models the reactor with a high level of detail. as is RELAP5, VIPRE, and other similar codes. The "A Short Description of LOCADM" (see Attachment 2) gives a description of how LOCADM works and the essential inputs that are needed. At this time we do not believe that any additional training is required.

RAI #26

The LOCADM computer code performs the evaluations for the concentration of debris and chemicals within the reactor core. An important feature in the concentration evaluation is the volume of water which is available to mix with the concentrating material. Please describe how this mixing volume is calculated. Include assumptions for the liquid fraction

within the core, upper plenum and lower plenum. Compare the assumptions used by LOCADM to those which the NRC staff has accepted in licensing calculations for post-LOCA boric acid concentration. Provide a comparison to the volume of water assumed to be available for mixing by LOCADM with that calculated by WCOBRA/TRAC.

RESPONSE TO RAI #26

LOCADM does not calculate the core mixing volume independently. The reactor vessel volume is an input to LOCADM and it can be set to a value which includes only the volume which is considered to be well-mixed with entering coolant. The guidance provided with LOCADM will recommend generic mixing volume assumptions that are typical of those used in licensing basis calculations for a given plant design. Both AREVA and Westinghouse designed plants will be included. Alternately, the licensees can use the mixing volume used in their licensing basis boric acid precipitation analysis. It should be noted that the results produced by LOCADM are not highly sensitive to the core mixing volume, since virtually all of the coolant impurities entering the core are eventually deposited. For example, when the mixing volume used in the sample problem of 2346 cubic feet was reduced to 1100 cubic feet, the final thickness values for the deposits increased by one percent.

RAI #27

Please provide the decay heat model which is used in LOCADM to determine coolant boil off from the core and justify that the model is conservative for safety analysis.

RESPONSE TO RAI #27

The Appendix K decay heat model was used. The Appendix K decay heat model is equivalent to the 1971 ANS model multiplied by a factor of 1.2. The 20 percent increase over the best estimate 1971 ANS model insures that conservative predictions will be made.

RAI #28

On page E-8 it is stated that the LOCADM computer code can model the core with up to 200 radial nodes and 10 axial nodes. Please provide the criteria which should be utilized in selecting adequate noding detail. Please discuss how local chemical and debris concentrations are determined for the fluid volume adjacent to each of the core nodes.

RESPONSE TO RAI #28

The guidance for radial core noding is given in WCAP-16793, Table E-1, where the number of rods in each node and the relative power at each node are specified for different core types. This guidance is consistent with the criteria for selecting radial noding detail as has been described in WCAP-12945-P-A (Proprietary) Volume I (Revision 2) and Volumes II-V (Revision 1), and WCAP-14747 (Non-Proprietary), "Westinghouse Code Qualification Document for Best Estimate Loss of Coolant Accident Analysis," Bajorek, S. M., et al, 1998. Since the radial noding establishes a conservatively high peak rod power (and a conservatively high peak deposit thickness) the choice of axial noding is not critical.

The debris and chemicals in solution are assumed to be evenly distributed among all core nodes. While it is possible that there could be small variations in concentration of debris chemicals between nodes within the mixing volume, large variations are not thought to be possible since large concentration variations would lead to density differences which would lead to convective mixing. The possibility of small variations in concentration between nodes is not expected to result in non-conservative predictions of deposit thickness, because other highly conservative assumptions have been made. LOCADM includes conservative predictions of debris dissolution and corrosion product release. All such released

material which is transported to fuel cladding surfaces is assumed to deposit, and it is assumed that there is no competitive deposition in other system locations.

RAI #29

Page E-11 states that high solubility species will not precipitate, and their concentration is limited to back-diffusion into the coolant or transport along the chimney walls. Boiling in the core before hot leg recirculation is initiated will act to increase the concentration of the high solubility species. Describe how the LOCADM code tracks the concentration of high solubility species to ensure that the solubility limit is not exceeded.

RESPONSE TO RAI #29

LOCADM calculates the concentration of boric acid, sodium tetraborate, trisodium phosphate and sodium hydroxide in the core as a function of time. The results are output in tabular form.

Consistent with current licensing basis calculations for PWRs that demonstrate that the boric acid concentration in the core is limited to values below the solubility limit, the LOCADM does not precipitate boric acid. The existing Plant's EOP provide actions that are required to assure boric acid solubility limits are not reached. The same is true for sodium phosphate, sodium borates and sodium hydroxide, which are also highly soluble.

RAI #30

Describe the treatment of suspended solids by the LOCADM computer code. Discuss the treatment of these concentrated solids in the core as to the effect core density, core heat transfer and plate out on fuel rods.

RESPONSE TO RAI #30

LOCADM makes no distinction between suspended solids and dissolved species. Both are deposited at the fuel rod surface. The density of the deposit is an input to LOCADM as is the thermal conductivity. LOCADM calculates the thickness of the deposit and then the heat transfer resistance using the deposit thermal conductivity. Concentrations of suspended solids are predicted to be low (see RAI #35 response), so there will be no significant effect on the coolant density or thermal conductivity.

RAI #31

On page E-11 it is stated that the LOCADM computer code assumes that deposition occurs through the boiling process if conditions at a core node predict any boiling. Please discuss and provide the calculational methodology by which coolant channel thermodynamic conditions are determined. Include discussions for hot leg recirculation as well as for cold leg recirculation. The NRC staff understands that for some UPI plants, ECCS flow to the cold legs is terminated during recirculation. For a UPI plant which experiences a hot leg break please provide the methodology by which LOCADM would determine core concentrations for the resultant countercurrent flow which would be relied upon to cool the core during the recirculation period.

RESPONSE TO RAI #31

The attached document "A Short Description of LOCADM" (Attachment 2) gives a concise description of how the thermodynamic conditions are determined in coolant channels.

The fluid in all channels is assumed to be at the same temperature, and this temperature is derived from the plant's licensing basis calculations for long term core cooling. Flow is not modeled explicitly. Instead, a generic heat transfer coefficient of $400 \text{ W/m}^2\text{-}^\circ\text{K}$ ($70 \text{ BTU/ft}^2 \text{ }^\circ\text{F}$) was assumed for transfer of heat between bulk coolant with the fuel channels and the surface of the deposits since this is a typical heat transfer coefficient for convective flow within natural circulation systems. The channel pressure is the sum of the upper plenum pressure and the pressure exerted by the height of the water column above the node. Coolant flow rates into the reactor mixing volume as a function of time must be provided by the user and are obtained from a plant's safety analysis for long term core cooling. The relative amounts of steam and liquid flow out reactor mixing volume are calculated by LOCADM. The core input is generalized. The coolant flow could be coming from the cold leg, the hot leg, or from upper plenum injection. Various operational modes are accounted for by varying the rate of flow into the mixing volume and the source of the flow (safety injection or recirculated coolant.) Values for generically applicable mixing volumes have been identified and will be provided to users.

Regarding CCFL (Countercurrent Flow Limiting) effects, the limitations on upper plenum injection flow due to countercurrent steam flow must be calculated outside of LOCADM using RELAP5 or another approved code. However, once the effective flow into the mixing volume is calculated, it can be input into LOCADM.

RAI #32

On page E-14 it is indicated that the initial fuel oxide thickness to be input to the LOCADM code for the start of the post-LOCA deposition calculation could be based on post operational fuel examinations. The staff does not believe that use of post operational data would be appropriate for fuel which has experienced a LOCA. Please provide methodology by which the post-LOCA oxide thickness will be determined for input to LOCADM. This concern needs to also addressed for the methodology of Appendix C and Appendix D.

RESPONSE TO RAI #32

The post-LOCA oxide thickness recommended for use as input to LOCADM will be revised to be the maximum peak local oxidation layer allowed by 10 CFR 50.46, or 17% of the cladding wall thickness. A lower value can be used on a plant-specific basis with sufficient justification.

For example, considering a volume increase of 1.56 upon oxidation of cladding metal to oxide, a calculation for a typical cladding thickness of 0.0225 inches would be assumed to start with a reduced metal thickness of 0.0187 inches and an oxide layer of 0.006 inches.

The thermal calculations in Appendices C and D are parametric studies to demonstrate margin to the 800° F acceptance basis. The calculations reported in Table 4-3, Table 4-4 and Table 4-5 of WCAP-16793-NP used an initial oxide thickness of 0.004 inches (0.4 mils). Increasing the initial oxide layer from 0.004 inches (0.4 mils) to 0.006 inches (0.6 mils), using the calculated clad temperatures listed in Table 4-3, Table 4-4 and Table 4-5 and assuming a thermal conductivity of 0.1 Btu/(hr-ft-°F) for the oxide, the increased oxide thickness is evaluated to result in an increased clad temperature of no more than 2° F over those reported in the three tables. Even with the increase of 2° F, the calculated clad temperatures reported in the three tables are well below the 800° F acceptance basis temperature. Thus, increasing the initial oxide thickness by 0.002 inches (0.2 mils) has negligible impact on the margin to the 800° F acceptance basis.

RAI #33

On page E-15 a comparison of the results by the LOCADM computer code and the SKBOR computer code are described for a post-LOCA boric acid concentration calculation. Please provide more details of this comparison including core boric acid concentration as a function of time. Provide a reference available to the NRC staff describing the SKBOR computer code and including any review and approval by the NRC staff.

RESPONSE TO RAI #33

SKBOR has not been reviewed or approved by the NRC. This FORTRAN code is essentially an automated hand calculation that calculates the buildup of boric acid in the core as a function of time after a LOCA. It uses the same calculational approach as LOCADM for boron concentration, but the coding was developed independently. A description of SKBOR is provided below, along with a comparison of the outputs from LOCADM and SKBOR as a function of time.

Description of Westinghouse SKBOR Computer Program

The SKBOR computer program is part of the Westinghouse methodology for long-term core cooling. For plants with cold leg injection, SKBOR is used to determine: (1) the time at which ECCS recirculation should be realigned to the RCS hot legs to prevent the precipitation of boron in the core; (2) the interval at which cycling between hot and cold leg injection should be completed, for plants without sufficient simultaneous hot and cold leg injection; and, (3) the amount of sump dilution at the hot leg switchover time. For plants with upper plenum injection (UPI), SKBOR has been used to determine the time at which UPI injection should be established to prevent the precipitation of boric acid in the core, for breaks where the RCS may stabilize above the UPI cut-in pressure.

A typical SKBOR calculation considers two volumes: one representing the effective vessel mixing volume (denoted as the CORE), and one representing the remaining system inventory (denoted as the SUMP). The CORE and SUMP are initially assumed to contain borated liquid at the system-average boron concentration. Vapor generated due to decay heat boiling exits the CORE with a boron concentration of zero; is assumed to condense fully in containment; and, is returned to the SUMP as unborated liquid. Borated liquid is added from the SUMP as required to keep the CORE volume full. In this way, the SUMP boron concentration gradually decreases, while the CORE boron concentration increases toward the boric acid solubility limit.

Most of the inputs to SKBOR are used to specify plant-specific parameters such as the component masses and boron concentrations, the effective vessel mixing volume, and the initial core power level. These inputs are generally chosen to maximize the rate at which boron accumulates in the CORE, based on information provided by the utility. The results of the analysis are used to establish the times at which the necessary actions should be initiated, and these times are typically reflected in the FSAR and the Emergency Operating Procedures.

The table and figure below show a comparison between the results for SKBOR and LOCADM.

Input Assumption	LOCADM	SKBOR
Core Power	3586.6 MWt	3586.6 MWt
Decay Heat	Appendix K	Appendix K
Liquid Mixing Volume	1050 ft ³	1050 ft ³
Problem Start Time	100 seconds	100 seconds
Initial Sump Boron Concentration	2550 ppm	2550 ppm
SI Subcooling	None	None
Time to Reach 23.53 wt% Boric Acid	5.97 hr	5.96 hr

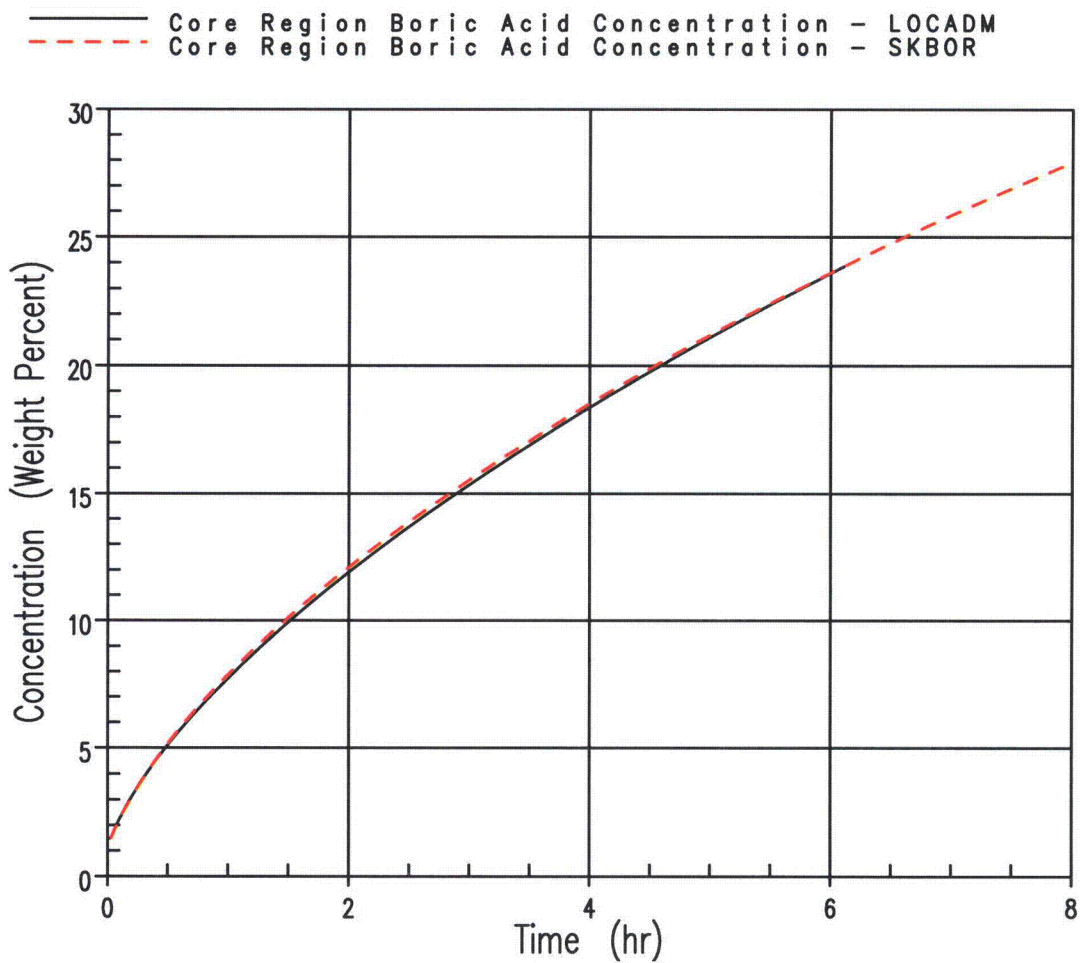


Figure 33-1 Comparison of LOCADM and SKBOR Calculated Core Region Boric Acid Concentration

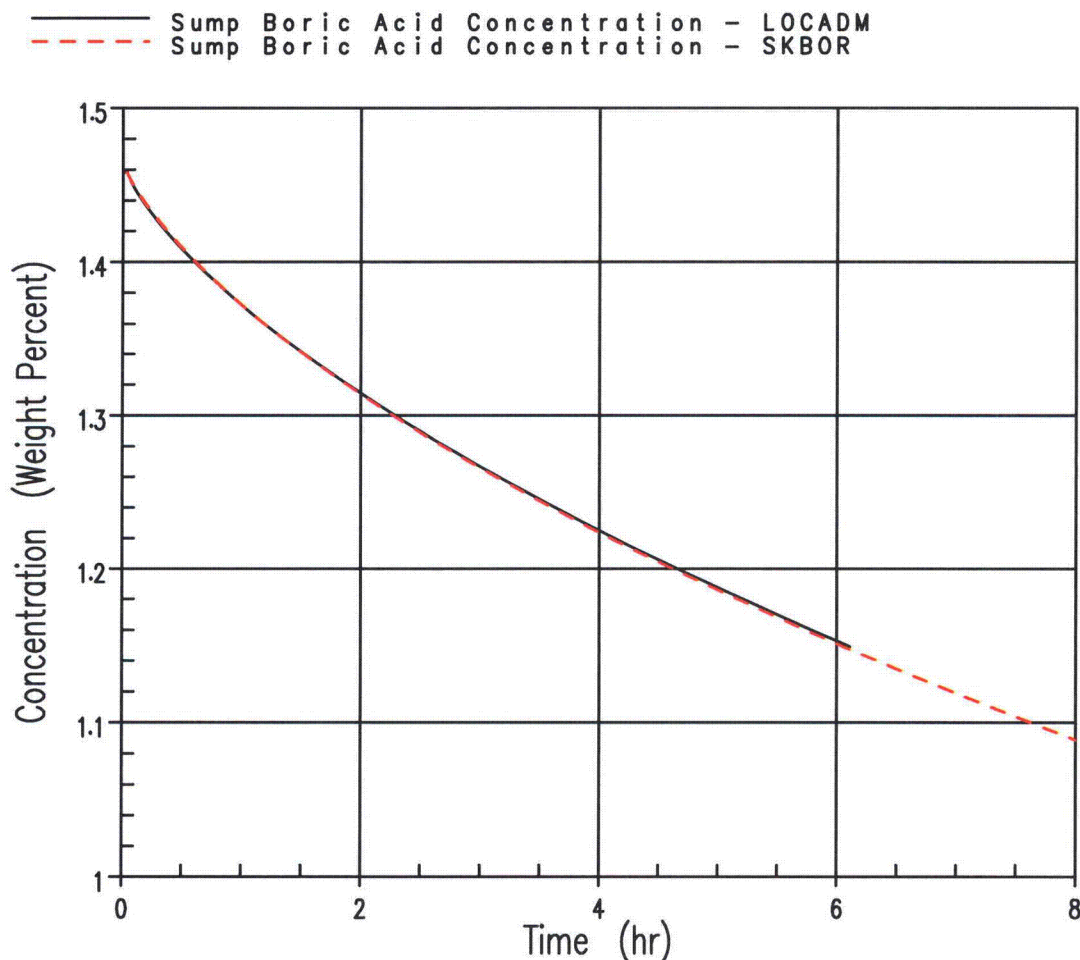


Figure 33-2 Comparison of LOCADM and SKBOR Calculated Containment Sump Boric Acid Concentration

RAI #34

Figure E-3 gives a comparison between an experiment and LOCADM for fouling resistance. The LOCADM results are shown to be conservative. The LOCADM results would be sensitive to the thermal conductivity of calcium sulfate used in the test. Provide a comparison for the thermal conductivity assumed in the LOCADM simulation to experimental values for calcium sulfate. LOCADM is shown to become more conservative as the simulation progressed. Please comment on the effect of the use of slab geometry by LOCADM in modeling heat transfer from a wire as producing this conservatism.

RESPONSE TO RAI #34

A thermal conductivity of 0.52 W/m²K was assumed for calcium sulfate in the LOCADM comparison in Figure E-3. There was no direct measure of thermal conductivity in the referenced experiment (E-19), but another reference, E-5 in WCAP-16793, states that boiler scale deposits of calcium sulfate range between 0.8 and 2.2 W/m²K. Thus, the thermal conductivity value used by LOCADM for this comparison was conservative, but not as conservative as the 0.2 W/m²K which was recommended in WCAP-16793 and is the default value in LOCADM. The progressive increasing

conservatism shown in the example was most likely due to increasing deposit attrition with increasing thickness due to decreased deposit structural stability rather than any assumptions in heat transfer modeling.

RAI #35

Page E-16 describes a sample calculation using LOCADM. A high fiber glass loading of 7000 cubic feet was assumed. Please provide the assumptions regarding transport of this fiberglass into the core including the effect of the sump screen and settling on the containment floor. What fiberglass concentration was assumed in the incoming ECCS flow? Eighty cubic feet of calcium silicate was also assumed to be present. Provide the concentration of calcium silicate assumed in the incoming ECCS flow. Discuss any difference in assumptions for plate out of suspended fiberglass and calcium silicate on the core fuel rods. Compare these assumptions with the PWROG recommendations stated in Section 2.3, Collection of Fibrous Material on Fuel Cladding.

RESPONSE TO RAI #35

In the LOCADM sample calculation, all fiberglass and CaSil were assumed to remain in the sump until they dissolved and only dissolved matter was transported. Any fiber bypassing the sump screen would only collect on the first support grid as indicated in Section 2.3 and would behave no differently than if it was in the sump. Dissolved concentrations are shown as a function of time below:

Time (s)	RV Al (ppm)	Sump Al (ppm)	RV Ca (ppm)	Sump Ca (ppm)	RV Si (ppm)	Sump Si (ppm)
6	0.0	1.0	0.0	1.0	0.0	2.7
30	0.0	1.9	0.0	1.2	0.0	4.3
60	0.0	2.8	0.0	1.4	0.0	5.8
120	0.0	4.0	0.0	1.9	0.0	8.2
180	0.0	5.4	0.0	2.4	0.0	11.3
200	0.0	5.8	0.0	2.5	0.0	12.2
400	0.0	9.5	0.0	4.0	0.0	22.1
600	0.0	13.6	0.0	5.3	0.0	33.2
800	0.0	17.2	0.0	6.3	0.0	42.5
1000	0.0	19.7	0.0	6.9	0.0	49.8
1200	0.0	21.4	0.0	7.3	0.0	55.6
1400	0.0	22.8	0.0	7.7	0.0	60.6
1600	0.0	23.8	0.0	7.9	0.0	65.0
1800	0.0	24.6	0.0	8.1	0.0	68.8
3200	0.0	26.8	0.0	8.7	0.0	79.8
4600	0.0	26.9	0.0	8.8	0.0	79.6
6000	0.0	24.4	0.0	8.6	0.0	76.3
7400	0.0	20.4	0.0	8.5	0.0	72.2
8800	0.0	17.5	0.0	8.3	0.0	67.9
10200	0.0	15.3	0.0	8.1	0.0	63.7
11600	2.5	14.4	1.4	8.4	11.0	63.5
13000	6.4	14.3	3.8	9.0	28.5	66.2
14400	8.9	14.1	5.5	9.5	40.9	68.3
46400	12.9	11.6	13.0	12.4	73.9	67.1
46800	12.6	11.6	12.9	12.5	72.2	67.0
172800	6.7	7.3	21.8	23.7	43.4	47.2
259200	5.7	6.0	28.2	29.8	41.6	43.9
345600	5.8	5.8	38.3	38.4	47.6	47.7
432000	6.1	6.1	46.8	46.9	53.2	53.3
864000	7.3	7.3	69.0	69.0	76.5	76.6
1296000	8.5	8.5	71.5	71.5	75.6	75.7
1728000	9.7	9.7	70.7	70.8	74.8	74.9
2160000	10.9	10.9	70.0	70.1	74.1	74.1
2592000	12.1	12.1	69.4	69.4	73.4	73.4

RAI #36

The Example Run in Appendix Section E.9 states that a high fiberglass loading of 7000 cubic feet was used to determine the thickness of scale which might form on the fuel rods. Section 2.3 indicates that fibrous debris that is carried to the core will not adhere to fuel rod surfaces and therefore will not adversely affect heat transfer. Fibrous material in the core will be concentrated by the boiling process as calculated by LOCADM. Provide a discussion as to the effect on core cooling from high fiber content. What is the maximum loading of fibers which could be concentrated within the core without adversely affecting core heat transfer?

RESPONSE TO RAI #36

The deposition of small fibers that do not dissolve but are small enough to be transported through the sump screen and into the core cannot be ruled out.

The quantity of transported fines is expected to be small compared to both the total amount of debris and the amount of debris that dissolves or corrodes. Thus, if the small fibers were included in model predictions, the effect would be small but would vary from plant to plant depending on the screen design and debris mix. A quantitative estimate of the effect of the fiber on deposit thickness and fuel temperature can be accounted for in LOCADM by use of a "bump-up factor" applied to the initial debris inputs. The method for implementing the bypass bump-up factor is given in the response to RAI#6 in the second set of RAIs.

RAI #37

Appendix F describes AREVA methodology for predicting solubility of containment materials in the containment sump water. Appendix E describes a similar Westinghouse model that is documented in WCAP-16530-NP. Which model should utilities utilize for plant analysis? For a given reactor core how would the results differ in using the two models?

RESPONSE TO RAI #37

Appendix F does not provide an alternative method to the LOCADM model described in Appendix E. The calculations documented in Appendix F were performed to confirm that the model developed in Appendix E identified major chemical species resulting from the post-LOCA chemical reactions.

RAI #38

Please describe StreamAnalyzerVersion 1.2 as it is used to calculate the concentration of post LOCA materials within the core in more detail. How are concentrations determined in the presence of boiling? Are concentration gradients within the core accounted for? How is hot leg recirculation accounted for?

RESPONSE TO RAI #38

(Note: StreamAnalyzer Version 2.0.43 was used for the Appendix F calculation. It was created and is maintained by OLI.)

The concentration of materials in the core was calculated by the following methodology:

- Input concentration of LOCA materials in sump (inputs for different runs are given below)

<u>Input Concentration</u>	<u>Run 1</u>	<u>Run 2</u>	<u>Run 3</u>	<u>Run 4</u>
Ca (ppm)	15	133	15	133
Al (ppm)	17	80	17	80
Si (ppm)	69	156	69	156

- pH adjust the sump solution to the required value using the specified pH additive (NaOH or NaTB).
- Calculate the speciation and solubility at the sump and core temperatures. Calculate the speciation and solubility as water is removed by steaming to a final Concentration Factor of 20.

The OLI software calculates the concentration of solid, dissolved, and gaseous/vapor species based on the solution thermodynamics.

The Appendix F calculations were performed to verify two key assumptions of the Appendix E model: (1) the likely precipitate species and (2) the extent to which Ca, Al, and Si would deposit from solution. Because the Appendix F calculation was not intended as an alternative calculation method to Appendix E, but rather as supporting material, specific reactor conditions like concentration gradients and hot leg recirculation were not utilized. Rather, a conservative final concentration factor of 20 was selected.

RAI #39

What is the significance of the quantities in Table F-2 Steam Masses Utilized in Solubility Calculation? How were they determined? How is the Total Core Feed determined? What is meant by Core Residual After Steaming?

RESPONSE TO RAI #39

The quantities listed in Table 4-2 of Appendix F are water-volume mass inputs to the OLI software evaluation. The 'total core feed' refers to amount of water transported to the reactor. For Runs 1 and 3, this corresponds to the mass of water steamed off and replaced following the accident (with water only replaced at the rate at which boiloff occurs to maintain conservatism) up until hot leg switchover. For Runs 2 and 4, solubility during long-term cooling was evaluated; therefore, it was assumed that the entire sump inventory would be passed through the reactor. These values were determined using the decay heat evaluated from the 1971 ANS model multiplied by a factor of 1.2 and assuming hot leg switchover would take place after 8 hours (total vapor quantity boiled off determined as 570,000 kg). The 'core residual after steaming' input refers to the liquid mass in the reactor vessel after blowdown and refill. These values were based on typical plant values.

Note that these masses are not critical to the final application of Appendix F. The Appendix F calculations were performed to verify two key assumptions of the Appendix E model: (1) the likely precipitate species and (2) the extent to which Ca, Al, and Si would deposit from solution. Therefore, in this respect, the percent deposition figures stated in Appendix F are needed, and the total masses are not critical.

RAI #40

Other inputs in the methodology of Appendix F are described as the sump mass, reactor inventory, and steaming information. Please describe how these qualifies are determined so as to be conservative for reactor safety analysis. For the reactor inventory, discuss how voiding within the reactor vessel and limited circulation in the lower plenum is taken into account in determining the mass of water available to mix with the material being concentrated within the core.

RESPONSE TO RAI #40

The information reported in Appendix F was meant as a supplemental analysis, and not a direct input, to the information reported in Appendix E. The purpose of Appendix F was to determine the reasonability of assumptions within Appendix E, such as percentage and type of precipitate species expected to generate in the core following a LOCA. Appendix F did indicate that the general type and expected percentages of materials that could form in the core were legitimate, as assumed for input into the LOCADM model. The masses determined in the OLI simulations are reported for information only. Appendix E does not use the data from Appendix F as an input to the evaluation. It is a supplemental analysis only.

Because Appendix F was intended for supplemental information only, detailed modeling of the water mass available for mixing was not performed. Rather, a conservative final concentration factor of 20 was utilized in the calculation.

RAI #41

Tables F-5.1 and F-5.3 indicate that chemical precipitates would form in the core for the sample calculations that were performed. Since boiling occurs at the surface of the fuel rods, the staff assumes that is where the chemical precipitates calculated in Appendix F would be located. Please provide a comparison of the deposit thickness calculated by the methodology of Appendix F to that of Appendix E. How will the power peaking in the core be taken into account in determining the Appendix F deposits?

RESPONSE TO RAI #41

As stated in the response to RAI #37, Appendix F does not provide an alternative method to the LOCADM model described in Appendix E. The calculations documented in Appendix F were performed to confirm that the model developed in Appendix E identified major chemical species resulting from the post-LOCA chemical reactions.

RAI #42

It is not clear how a utility will utilize the information in WCAP-16793-NP. Please provide the guidance document that the utilities may utilize to perform specific assessments of (but not limited to) for example :

- 1) maximum debris that enters the core and lower plenum
- 2) debris accumulation in the reactor vessel
- 3) calculation of debris and chemical concentration in the reactor core
- 4) the maximum debris blockage at the core inlet
- 5) the debris that collects on mixing vanes and spacers and the impact on boric acid buildup when the debris and boric acid concentrate combines at these locations
- 6) impact of debris on the long term cooling boric acid precipitation analyses
- 7) the impact of the debris on boric acid buildup for plants with low elevation suction legs if the break is located on the top of the discharge piping

Also, what calculations are performed to show that once the switch to simultaneous injection is made, that the injection can flush the core with boric acid and debris at all collection locations? How would a utility perform this calculation? It is also suggested that a sample calculation be performed for a plant illustrating how one would utilize the information to show acceptable long term cooling ECCS performance following all break sizes. A plant with the largest potential debris source should be selected. The sample analysis should address all calculations covering the multitude of issues discussed in the report.

RESPONSE TO RAI #42

A guidance document for licensees to implement WCAP-16793-NP is being developed.

Plants will be provided a copy of the LOCADM automated hand calculation tool with instructions on what inputs are needed to support the calculations. They will also be provided with a sample problem to confirm that the installation of the automated hand calculation tool on their system did not affect the calculation results obtained from LOCADM.

Plant will need to perform a plant-specific calculation using LOCADM. Using plant-specific inputs, plants will first calculate plant-specific chemical deposition on cladding. As part of the deposition calculation, the cladding temperature will with the deposition loading will also be calculated. Plants will then compare the calculated cladding thickness and cladding temperature against the 50 mil maximum deposition thickness and the 800°F clad temperature acceptance basis. If unacceptable comparisons are obtained, plants will need to reduce the materials contributing to chemical effects by either demonstrating they do not become debris or by eliminating them from containment.

As noted in the responses to RAI #1 and RAI #2, fibrous debris does not block the core. Furthermore, as demonstrated in the sample calculation in Appendix E, precipitates do not block the core. Thus, the arguments WCAP-16793-NP would become part of the plant licensing basis by reference. Further, current licensing basis calculations for core flushing remain intact and are not affected by the evaluations presented in WCAP-16793-NP.

RAI #43

The NRC staff understands that at some plants the equivalent of hot leg recirculation may be obtained using the pressurizer spray. Under these conditions the pressurizer spray nozzles might become clogged with debris. Does the PWROG have guidance on how the occurrence and consequences of such blockage may be evaluated in plant specific evaluations?

RESPONSE TO RAI #43

Given the bore of the pressurizer spray nozzles is 3/8 inches and the size of the holes in the replacement sump screens is on the order of 0.1 inches, blockage of these nozzles is not considered credible.

Guidance on the evaluation of potential for blockage of containment spray nozzles resulting from debris in the sump fluid is given in WCAP-16406-P, "Evaluation of Downstream Sump Debris Effects in Support of GSI-191." This same guidance is applicable to pressurizer spray nozzles. The following statement will be added to WCAP-16793-NP:

"Plants that utilize pressurizer spray nozzles to accomplish core dilution should evaluate the spray nozzles using the guidance given in WCAP-16406-P for containment spray nozzles."

RAI #44

Following a large break LOCA, many of the fuel rods in the core may swell and rupture leaving sharp edges at the rupture locations and a diminished channel flow area. Debris may collect in the restricted channels and at the rough edges at the rupture locations. The PWROG should evaluate the possibility of excessive blockage being produced by the combination of swelling and rupture and debris collection. Such blockage might produce the occurrence of the hot spots above the blockage location. Discuss how the occurrence and magnitude of such hot spots might be evaluated.

RESPONSE TO RAI #44

Cladding rupture is only expected to occur in a limited number of fuel rods in the core, namely, the highest power fuel rods in the highest power assemblies. A realistic, yet still quite conservative, assessment of the extent of cladding rupture during a large break LOCA was recently reported in a paper from Reference 44-1 entitled "Realistic Assessment of Fuel Rod Behavior Under Large-Break LOCA Conditions." Estimates of the extent of rupture throughout the core of a typical Westinghouse 4-loop plant were made by considering peak cladding temperature dependence on rod power, rupture temperature as a function of cladding pressure differential, burnup effects on rod internal pressure, and a core-wide census of rod power and burnup. With this information it was estimated that less than 10% of the core (12 of 193 assemblies) would achieve sufficient cladding temperatures to have cladding rupture. Therefore, wide-spread blockage due to swelling and rupture would not be expected in a large break LOCA scenario.

Any debris that did enter the lower plenum for a cold leg injection plant would have had to navigate the bottom nozzles, any debris capturing devices, and a number of structural/heat transfer enhancement grids before reaching the rupture elevation. Build-up of significant debris at the localized rupture locations of the highest power assemblies prior to hot leg switchover is therefore considered highly unlikely.

A somewhat different response is required for plants with upper plenum injection. Prior studies have shown that, through the reflood portion of the transient, the upper plenum drains into the lower powered portion of the core, while the hotter regions of the core are cooled by a bottom-up reflood. This general flow pattern is expected to continue after core quench, resulting in circulation patterns with downflow from the upper plenum in the low powered regions, and continuing upflow in the high powered regions. With such a flow pattern, the debris would have to navigate the top nozzles of the lower powered assemblies and a number of structural/heat transfer enhancement grids before reaching the rupture locations. (Note that rupture would only be expected for the higher powered assemblies in the hotter regions of the core.) Build-up of significant debris at the localized rupture locations in the highest power fuel assemblies is therefore also considered highly unlikely in plants with upper plenum injection.

REFERENCE FOR RAI #44 RESPONSE:

- 44-1 NUREG/CP-0192, "Proceedings of the Nuclear Fuels Sessions of the 2004 Nuclear Safety Research Conference," 2005.

RAI #45

The mixture of chemicals within the core is postulated to include a mixture of epoxy and non-epoxy paint chips, insulation, ablated structural material, small particles from corrosion of system materials, dissolved corrosion products, buffering agents, boric acid, and lithium hydroxide. This material will be in a high radiation field from release of the fuel rod gap activity as the result of the LOCA and from gamma radiation from the fuel rods. Please describe the chemical and physical changes which may occur within this mixture within the core and the effect on core heat transfer.

RESPONSE TO RAI #45

The modeling which was done assumed that all inorganic impurities entering the core region will either collect at the first grid support (in the case of fiber) or will completely deposit on the fuel. This conservative approach diminishes the importance of impurity chemical or radiochemical reactions since these reactions could not increase the amount of core deposition beyond what was already assumed. Organic coating materials are not expected to experience radiation levels which would cause degradation and subsequent transfer onto heat transfer surfaces.

ATTACHMENT 1
LOCADM SAMPLE INPUTS (REF. RAI # 6(b) RESPONSE)

Table A1-1. Time dependent inputs for LOCADM example

Time (sec)	day s	Sump pH	Sump Temp. (°F)	Spray Flow from RWST (lbm/s)	Steam or Spray pH	Containment Temp. (°F)	RV Coolant Temp (°F)	Break Flow (lbm/s)	Clean SI Flow into RV (lbm/s)	Clean SI Bypass Flow (lbm/s)	Recirc. Flow into RV (lbm/s)	BOP Blowdown Flow (lbm/s)
6	0	6	224	0	9.5	215	225	5660	0	0	0	3500
30	0	6.5	252	0	9.5	255	265	4180	0	0	0	2000
60	0	6.9	238	0	9.5	252	262	3600	90	0	0	1800
120	0	7.25	238	0	9.5	252	262	1000	3200	0	0	0
180	0	7.4	240	0	9.5	251	261	1000	1400	0	0	0
200	0	7.4	241	0	9.5	251	261	1000	190	0	0	0
400	0	7.8	247	0	9.5	253	263	210	310	0	0	0
600	0	7.8	250	0	9.5	255	265	230	330	0	0	0
800	0	7.9	254	1	9.5	257	267	320	400	0	0	0
1000	0	8	256	1	9.5	254	264	400	81	319	0	0
1200	0	8.05	257	1	9.5	252	262	400	77	323	0	0
1400	0	8.15	258	1	9.5	252	262	400	74	326	0	0
1600	0	8.2	259	1	9.5	249	259	400	71	329	0	0
1800	0	8.2	260	1	9.5	248	258	400	68	332	0	0
3200	0	8.2	254	1	9.5	240	250	400	58	342	0	0
4600	0	8.2	246	1	9.5	238	248	400	52	348	0	0
6000	0	8.2	238	0		243	253	400	49	351	0	0
7400	0	8.2	232	0		244	254	400	46	354	0	0
8800	0	8.2	222	0		245	255	400	44	356	0	0
10200	0	8.2	218	0		245	255	400	42	358	0	0
11600	0	8.2	217	0		245	255	400	0	0	40	0
13000	0	8.2	214	0		244	254	400	0	0	39	0
14400	0	8.2	211	0		243	253	400	0	0	38	0
46400	1	8.2	163	0		220	230	400	0	0	27	0
46800	1	8.2	158	0		205	215	400	0	0	200	0
2E+05	2	8.2	156	0		198	208	400	0	0	200	0
3E+05	3	8.2	156	0		193	203	400	0	0	200	0
3E+05	4	8.2	156	0		185	195	400	0	0	200	0
4E+05	5	8.2	156	0		180	190	400	0	0	200	0
9E+05	10	8.2	156	0		161	171	400	0	0	200	0
1E+06	15	8.2	156	0		138	148	400	0	0	200	0
2E+06	20	8.2	156	0		137	147	400	0	0	200	0
2E+06	25	8.2	156	0		135	145	400	0	0	200	0
3E+06	30	8.2	156	0		134	144	400	0	0	200	0

Table A1-2. Time dependent input for LOCADM, page 2.

Time (sec)	days	NaOH mass flow Spray (lbm/s)	TSP Dissolution Rate (lbm/s)	NaTB Release Rate - Ice or Basket (lbm/s)	Reactor Vessel Liquid Mass (lbm)	Ice Melt Rate (lbm/s)	RV Pressure in Upper Plenum (psia)	Reactor Vessel Steam Flow (lbm/s)
6	0	0	0	0	210000	0	18.85	330.4
30	0	0	0	0	155000	0	38.37	216.7
60	0	2	0	0	110000	0	36.49	178.0
120	0	5	0	0	85000	0	36.49	146.5
180	0	5	0	0	155000	0	35.88	130.7
200	0	5	0	0	162000	0	35.88	126.9
400	0	5	0	0	115000	0	37.11	104.6
600	0	5	0	0	132000	0	38.37	93.5
800	0	5	0	0	142000	0	39.67	86.4
1000	0	5	0	0	143000	0	37.74	81.0
1200	0	5	0	0	143000	0	36.49	76.8
1400	0	5	0	0	143000	0	36.49	73.6
1600	0	5	0	0	143000	0	34.69	70.7
1800	0	5	0	0	143000	0	34.11	68.3
3200	0	5	0	0	143000	0	29.71	57.8
4600	0	0	0	0	143000	0	28.69	52.1
6000	0	0	0	0	143000	0	31.30	48.6
7400	0	0	0	0	143000	0	31.85	45.8
8800	0	0	0	0	143000	0	32.40	43.7
10200	0	0	0	0	143000	0	32.40	41.9
11600	0	0	0	0	143000	0	32.40	40.4
13000	0	0	0	0	143000	0	31.85	39.1
14400	0	0	0	0	143000	0	31.30	38.0
46400	1	0	0	0	143000	0	20.71	26.9
46800	1	0	0	0	143000	0	15.54	26.6
2E+05	2	0	0	0	143000	0	14.70	0.0
3E+05	3	0	0	0	143000	0	14.70	0.0
3E+05	4	0	0	0	143000	0	14.70	0.0
4E+05	5	0	0	0	143000	0	14.70	0.0
9E+05	10	0	0	0	143000	0	14.70	0.0
1E+06	15	0	0	0	143000	0	14.70	0.0
2E+06	20	0	0	0	143000	0	14.70	0.0
2E+06	25	0	0	0	143000	0	14.70	0.0
3E+06	30	0	0	0	143000	0	14.70	0.0

Table A1-3. Materials Input for LOCADM example.

Class	Material	Amount
Coolant	Recirc Sump Pool Volume (ft3)	
Metallic Aluminum	Aluminum Submerged (sq ft)	799
	Aluminum Submerged (lbm)	179
	Aluminum Not-Submerged (sq ft)	15189
	Aluminum Not-Submerged (lbm)	3406
Calcium Silicate	CalSil Insulation(ft3)	80
	Asbestos Insulation (ft3)	0
	Kaylo Insulation (ft3)	0
	Unibestos Insulation (ft3)	0
E-glass	Fiberglass Insulation (ft3)	7000
	NUKON (ft3)	0
	Temp-Mat (ft3)	0
	Thermal Wrap (ft3)	0
Silica Powder	Microtherm (ft3)	0
	Min-K (ft3)	0
Mineral Wool	Min-Wool (ft3)	0
	Rock Wool (ft3)	0
Aluminum Silicate	Cerablanket (ft3)	0
	FiberFrax Durablanket (ft3)	0
	Kaowool (ft3)	0
	Mat-Ceramic (ft3)	0
	Mineral Fiber (ft3)	0
	PAROC Mineral Wool (ft3)	0
Concrete	Concrete (ft2)	736
Trisodium Phosphate	Trisodium Phosphate Hydrate (lbm)	0
Interam	Interam (ft3)	0
	Initial Sump Liquid Volume (ft3)	20
	Initial Boron Concentration in RCS	800
	Initial Lithium Concentration in RCS	2
	RWST/Accumulator Boron Conc. (ppm)	2500
	NaOH Addition Tank NaOH Conc.	200000

Table A1-4. Density values used in LOCADM example

Class	Material	Amount	Density (lb/ft ³)	Mass(kg)	Class total (kg)
Coolant	Recirc Sump Pool Volume (ft ³)	0	60.957	0.0	0.0
Metallic Aluminum	Aluminum Submerged (sq ft)	799.40		0.0	1626.1
	Aluminum Submerged (lbm)	179.25		81.3	
	Aluminum Not-Submerged (sq ft)	15188.6		0.0	
	Aluminum Not-Submerged (lbm)	3405.75		1544.8	
Calcium Silicate	CaSiI Insulation(ft ³)	80	14.5	526.2	526.2
	Asbestos Insulation (ft ³)	0	14.15	0.0	
	Kaylo Insulation (ft ³)	0	14.15	0.0	
	Unibestos Insulation (ft ³)	0	14.15	0.0	
E-glass	Fiberglass Insulation (ft ³)	7000	2.4	7620.4	7620.4
	NUKON (ft ³)	0	4	0.0	
	Temp-Mat (ft ³)	0	11.8	0.0	
	Thermal Wrap (ft ³)	0	16	0.0	
Silica Powder	Microtherm (ft ³)	0	4	0.0	0.0
	Min-K (ft ³)	0	4	0.0	
Mineral Wool	Min-Wool (ft ³)	0	10	0.0	0.0
	Rock Wool (ft ³)	0	10	0.0	
Aluminum Silicate	Cerablanket (ft ²)	0	8	0.0	0.0
	FiberFrax Durablanket (ft ³)	0	12	0.0	
	Kaowool (ft ³)	0	6	0.0	
	Mat-Ceramic (ft ³)	0	12	0.0	
	Mineral Fiber (ft ³)	0	21	0.0	
	PAROC Mineral Wool (ft ³)	0	21	0.0	
Concrete	Concrete (ft ²)	736		0.0074027	0.007402688
Interam	Interam (ft ³)	0	54	0.0	0.0
	Initial Sump Volume (ft ³)	20		554	
	Initial Boron Concentration in RCS	800			
	Initial Lithium Concentration in RCS	2			
	RWSI/Accumulator Boron Conc. (ppm)	2,500		5500	
	Calcium Deposit Density		35		
	Aluminum Deposit Density		34		
	Silicon Deposit Density		31		

Table A1-5. Core data input

Variable	Units	Value
100% Reactor Power	MW Thermal	3188
Crud Thermal Conductivity	W/m-K	0.52
LOCA Deposit Thermal Conductivity	W/m-K	0.2
Fuel Rod OD	Inches	0.36
Pellet Stack Length	Inches	144
Average Cladding Oxide Thickness	Microns	20
Average Starting Crud Thickness	Microns	30
Number Regions	(200 max)	4
Number of Axial Nodes (up and down each region)	(10 max)	3
Distance from Hotlet Inlet to Top of Pellet Stack	Inches	47

Table A1-6. Core axial node definition

Elevation	Relative Power	Relative Oxide Thickness	Relative Crud Thickness
1	0.95	1.5	2.4
2	1.1	0.9	0.3
3	0.95	0.6	0.3

Table A1-7 Core radial node definition

Region	Number Rods	Relative Power	Relative Oxide Thickness	Relative Crud Thickness
1	1	1.80	0.8	3.3
2	263	1.60	0.7	2.7
3	39072	1.23	0.8	1.27
4	11616	0.20	1.68	0.05

ATTACHMENT 2
A SHORT DESCRIPTION OF LOCADM

LOCADM is a calculational tool that can be used to conservatively predict the build-up of chemical deposits on fuel cladding after a LOCA. The source of the chemical products is the interaction of the fluid inventory in the reactor containment building sump with debris and other materials exposed to and submerged in the sump fluid or containment spray fluid. LOCADM predicts both the deposit thickness and cladding surface temperature as function of time at a number of core locations or “nodes”. The deposit thickness and maximum surface temperature within the core are listed in the output for each time period so that the user can compare these values to the acceptance basis for long term cooling.

The chemical inputs into LOCADM are the volumes of different debris sources such as fiberglass and calcium silicate (cal-sil) insulation. The surface areas of uncoated concrete, aluminum submerged in the sump, and aluminum exposed to spray are also required. The sump and spray pH are specified as a function of time, as are the inputs of sodium hydroxide, trisodium phosphate, sodium tetraborate, lithium hydroxide and boric acid.

Chemical product transport into the core is assumed to occur by the following process:

1. Containment materials corrode or dissolve forming solvated molecules and ions
2. Some of the dissolved material precipitates, but the precipitates remain in solution as small particles that do not settle
3. The dissolved material and suspended particles pass through the sump screen and into the core during recirculation. For the purpose of adding conservatism, it is assumed that none of the precipitates are retained by the sump screen or any other non-fuel surfaces

Note that the transport of small fibers that do not dissolve but are small enough to be transported through the sump screen and into the core is not considered explicitly in LOCADM. The quantity of transported fines is expected to be small compared to both the total amount of debris and the amount of debris that dissolves or corrodes. Fiber can be accounted for in LOCADM in cases where it is significant by use of a “bump-up factor” applied to the initial debris inputs. The bump-up factor is set such that total mass of deposits on the core after 30 days is increased by the best estimate of the mass of the fiber that bypasses the sump screen.

Coolant flow rates into the reactor mixing volume as a function of time must be provided by the user and are obtained from a plant’s safety analysis for long term core-cooling. The relative amounts of steam and liquid flow out reactor mixing volume are calculated by LOCADM. The core input is generalized. The coolant flow could be coming from the cold leg, the hot leg, or from upper plenum injection. Various operational modes are accounted for by varying the rate of flow into the mixing volume and the source of the flow (safety injection or recirculated coolant.) Values for generically applicable mixing volumes have been identified and will be provided to users. The temperature of the sump and reactor coolant as a function of time must also be entered by the user.

Within the mixing volume, the coolant is assumed to be perfectly mixed. Coolant chemical products entering the reactor are distributed evenly between all core nodes before deposition calculations are performed. The entire mixing volume is also assumed to be at the same temperature. Pressure is determined by the upper plenum pressure and the hydrostatic pressure at different elevations in the core. No attempt was made to model flow within the mixing volume and variations in that flow that might be caused by grids and flow obstructions. Since flow was not modeled, a heat transfer coefficient of $400 \text{ W/m}^2\text{-}^\circ\text{K}$ ($70 \text{ BTU/ft}^2 \text{ }^\circ\text{F}$) was assumed for

transfer of heat between bulk coolant with the fuel channels and the surface of the deposits since this is a typical heat transfer coefficient for convective flow within natural circulation systems.

LOCADM deposits chemical products that are dissolved or suspended in solution throughout the core in proportion to the amount of boiling in each core node. It is assumed that deposition rate is equal to the steaming rate times the chemical product concentration at each node. If there is no boiling, the chemical products are distributed according to heat flux, at an empirically derived rate that is $1/80^{\text{th}}$ of the deposition that would have occurred if all of the heat had gone into the boiling process.

The deposition algorithm does not rely on solubility or any other chemical characteristics of the chemical products to determine the deposition rate. All chemical material that is transported to the fuel surface by boiling is assumed to deposit. LOCADM uses a default deposit thermal conductivity for the deposited material of 0.1 Btu/(hr-ft-°F), which is low enough to bound expected core deposits. Likewise, the default deposit density is low enough (e.g. 35 lbm Ca/ft²) to bound expected deposits including those that incorporate adsorbed boron or boron bonded to chemical product elements. Consistent with current licensing basis calculations for PWRs that demonstrate that the boric acid concentration in the core is limited to values below the solubility limit, the LOCADM does not precipitate boric acid. The same is true for sodium phosphate, sodium borates and sodium hydroxide, which are also highly soluble.

The core noding within LOCADM can be adjusted by the user. WCAP-16793 provides guidance to the LOCADM user for node selection for different types of cores. The node selection recommended in the WCAP provides conservative power distributions with respect to core deposition.

LOCADM runs within Microsoft EXCEL and should be easy to use for those familiar with EXCEL. The first sheet of the workbook instructs the user on how to enter the chemical and flow inputs into worksheets in tabular form. A macro written in Visual Basic for Applications is then run. The macro reads the input, looks for input errors, calculates core conditions in one second intervals, and then outputs the results within the same workbook.

APPENDIX I
RAI SET #2 [ML080220258]

RAI #1

General: - There are several mathematical models used in deriving predicted solubilities, fuel surface temperatures, etc. Please provide a reference for each model used that identifies the corroborating assumptions described in the WCAP and how these models are appropriate for this scenario.

RESPONSE TO RAI #1

Based on a clarification offered by the reviewers, this question was clarified to be the heat transfer calculations documented in WCAP-16793-NP. The following responses clarify the heat transfer codes and models use in the calculations of WCAP-16793-NP.

1. The core blockage / peak clad temperature calculations were performed using the WCOBRA/TRAC code. The code is described in detail in WCAP-12945-P-A, Volume 1, Revision 2, and Volumes 2 through 5, Revision 1. "Code Qualification Document for Best Estimate LOCA Analysis," Bajorek, S.M., et. Al., 1998.
2. The ANSYS code was used to calculation clad heat-up behind grids. ANSYS has been used to support design and analyses previously submitted to NRC. Additional information regarding the ANSYS code may be obtained from the following website: www.ansys.com.

The clad heat-up between grids was calculated using basic heat conduction in cylindrical coordinates using the commercially available software, 'MATHCAD*'. A discussion of heat transfer in cylindrical coordinates can be obtained from an appropriate basic heat transfer text. One example of such a text is "Heat Transmission," by Wm. H. McAdams, McGraw-Hill Book Company (1954).

RAI #2

Page 2-2 - There is a tacit assumption here that the only mechanism for blockage is by single particles bridging across the opening. Operational experience with heat exchangers shows that debris much smaller than the diameter of a tube can build up at the tube mouth, and close down the opening diameter. The deposition mechanism of this smaller debris is via adhesion. For the lower core plate inlet, adhesion may occur due to increased temperature at the surface and the presence of corrosion products which have an irregular surface.

Does the model that is being used account for surface irregularities capturing smaller debris than the span diameter? If not, justify why this could not happen or describe how build up of smaller debris would affect the results?

How long will it take to span the gap if debris build up were to occur from all the particulate passing through the sump screen depositing at the core inlet area?

RESPONSE TO RAI #2

We agree that particles smaller than the gap diameters can build-up to form deposits at the mouths of openings in heat exchangers but it is unlikely that this process could cause a blockage at the lower core plate within 30 days, regardless of the surface roughness of the core plate. Thus, the modeling done in WCAP 16793-NP did not consider preferential build-up of small particle deposits at the lower core plate inlet. The following describes why the formation of this type of deposit was not considered.

Westinghouse and others have studied the build-up of deposits on tube mouths and the mouths of flow passages in tube support plates since such deposits can cause level oscillations and flow instability in steam generators. Such deposits

are observed to grow at the entrance to the passages, and in fewer cases, at the exits. The deposits take the form of thin lips that extend from all sides of the of the flow passages. The deposits are both hard and dense.

There are two predominant deposition mechanisms which explain the broach hole and tube mouth deposition processes (Ref. 2-1). The first is the vena contracta effect. This mechanism is operative when fluid flow is sharply contracted, such as flow through a plate with a hole. The flow separates from the wall following the sharp contraction in the mouth of the restricted passage. In the vena contracta region, there is a low velocity recirculation zone in which particles can deposit. Particle growth and deposit consolidation is accelerated by evaporation of liquid in the vena contracta region due to lowered pressure if the stream is a two-phase liquid/steam mixture. The particles grow and the deposit densifies as fluid is supersaturated with dissolved impurities. The greatest deposition rates are observed in regions where the steam quality is between 30 and 50 percent.

The second mechanism is termed particle trapping. In this case, larger particles such as detached tube scale flakes impact the area at the edge of the flow passage and marginally extend into the flow stream. The particles are cemented to the surface by crystallization growth, and then the newly formed lip is able to create recirculation flow which supports further deposition of large particles that further restrict the flow through the opening.

There are several reasons why these mechanisms would not produce blocking deposits at the inlet to the core which would be sufficient to restrict core cooling.

1. Fluid velocities at the lower core plate are low during recirculation so the vena contracta effect would be minimal. Vena contracta deposition increases with fluid velocity.
2. The flow at the lower core plate will be single phase during recirculation under most circumstances. Thus, vena contracta deposition will be minimized because the two phase flow which accelerates this type of deposition will not be present.
3. The concentration of larger particles that could be deposited via the particle trapping mechanism will be low because of settling and filtration at the sump screen.
4. There is not sufficient time to form such deposits. Several fuel cycles are usually required for flow passages to be closed off in steam generators when the chemistry and thermal hydraulics favor this type of deposition.

Low temperature industrial heat exchanges outside the nuclear industry are also subject to tube sheet fouling. In most cases, the fouling is either due to large debris or biological activity (Ref. 2-2). Neither would be expected in the early stages of a LOCA when flow requirements are high.

REFERENCES FOR RAI #2 RESPONSE:

- 2-1 Helena E. C. Rummens, J. T. Rogers, and C. W. Turner, "The thermal hydraulics of tube support fouling in nuclear Steam Generators" Nuclear Technology 148, 2004, p 268 to 286
- 2-2 Mohammad Abdul-Kareem Al-Sofi, Fouling phenomena in multi stage flash (MSF) distillers, Desalination 126 (1999) 61-76

RAI #3

Page 2-2 - The assumption related to largest particle size that passing into the reactor vessel does not account for particulate agglomeration downstream of the screens, particularly during the temperature drop in the Residual Heat Removal (RHR) heat exchangers. How does the model demonstrate that the particle size (due to agglomeration of micron and sub-micron size precipitates) and temperature decrease (causing subsequent precipitation) will not exceed what is predicted here for particle size?

RESPONSE TO RAI #3

On page 2-2 of WCAP 16793-NP the blockage of the core inlet by particles was being discussed and no modeling of the particle size or deposition was performed. Some agglomeration of particles may occur after the sump screen in the RHR heat exchangers but when the resulting flocs are carried to the core, they will not lead to blockages of the lower core plate and do not need to be considered when modeling core blockages.

The primary reason that the flocs would not block lower core plate passages is that large, freshly formed flocs have little strength (1). It was observed during WCAP-16530-NP bench testing (2) that the freshly formed agglomerates formed after cooling of simulated sump solutions were soft and easily broken apart, that is, they had low shear strength. As such, they could not form a blockage by bridging flow openings in the lower core plate.

Another aspect of flocculation that works against formation of large, hard particles that could form blockages is limited time available for agglomeration in the ECCS before the floc enters the reactor. Flocculation is typically not a rapid process and it typically takes on the order of 10 to 15 minutes to grow particles from the sub-micron size range to the size that could be settled even when water treatment chemicals designed to promote flocculation have been added (3). Thus, there would not be enough time for agglomerates to grow to the 0.1 inch size needed to span flow passages in the lower core plate as the coolant traveled from the RHR heat exchanger and to the reactor vessel. If an agglomerate survived its passage through the core, it would likely settle in the sump or be filtered out at the sump screen before it had a chance to grow larger in a second pass through the RHR.

REFERENCES FOR RAI #3 RESPONSE:

3-1 Arthur T. Hubbard, "Encyclopedia of Surface and Colloid Science" (World Scientific, London) 2002, p. 2218

3-2 WCAP-16530, "Evaluation of Post-Accident Chemical Effects in Containment Sump Fluids to Support GSI-191," February, 2006.

3-3 P. Zhang, H.H. Hahn, E. Hoffmann, "Study on Flocculation Kinetics of Silica Particulate Suspensions" in "Chemical Water and Wastewater Treatment" Hermann H. Hahn, Erhard Hoffmann, Hallivard Odegaard editors., IWA Publishing, London 2004, p. 277

RAI #4

Page 2-3 - Was the partial fuel length assembly pre-conditioned so that the corrosion film on its surface would be representative of that found in a plant in its third fuel cycle? If not, describe how the presence of a representative oxide film could affect the test results.

RESPONSE TO RAI #4

The partial length fuel assembly was not preconditioned to produce a corrosion film that might be representative of that found in a plant during normal operation. The purpose of the test was to specifically evaluate the collection of fibrous debris on debris capturing fuel grids and the consequential head loss of that fiber bed and the particulates collected in that bed when the Emergency Core Cooling System (ECCS) is aligned to recirculate coolant from the reactor containment building sump. As this test facility was a recirculating loop, the use of smooth rods minimized the possible capture of fiber on rod surfaces and maximized the potential for fibrous and particulate debris to be either captured on a second grid or recirculate and be captured on the fiber bed formed at the fuel assembly entrance. Thus, the use of smooth rods was conservative for the purposes of this test.

In the plant, an oxide film may provide sites for the collection of fiber on the cladding surface between support grids. Should this collection occur, it would have negligible affect on the plant for the following reasons;

- From the test observations and data presented in the response to RAI #2 from the first set of RAIs, most of the fibrous debris is captured at the core entrance. Thus, there is only a small amount of fiber that is passed by the support grids at the core entrance and therefore only a small amount of fiber to collect downstream on the cladding surface.
- If the fiber forms a bed, WCAP-16793-NP states that fibrous material on fuel structures with at least a porosity of 40%.
 - Being porous, there would be fluid movement through the fiber bed. This is demonstrated by the data included in the response to RAI #2.
 - The movement of fluid through the porous bed will remove heat from the cladding surface by convection.
- From the response to RAI #15 from the first set of RAI responses, the thermal conductivity of a fibrous bed is conservatively represented as being 0.1 Btu/(hr-ft-°F). This is the same value used to conservatively simulate the thermal conductivity of chemical precipitants on cladding surfaces.
 - The thermal conductivity through glass is about 0.59 Btu/(hr-ft-°F). Explicitly accounting for fiberglass debris in the surface deposition would enhance heat transfer.
 - As noted above, accounting for only conductive heat transfer through a fiber bed conservatively neglects convective heat transfer through the porous bed.

Thus, the collection of fibrous material on an oxide layer would have negligible effect on long-term core cooling clad temperatures.

RAI #5

Page 2-3 - Was the partial length fuel assembly internally heated to the temperature anticipated when debris would come in contact with it? If not, please demonstrate what effect heat at the clad surface will have.

RESPONSE TO RAI #5

The partial length fuel assembly was not heated to the temperature anticipated when debris would come into contact with. The purpose of the test was to specifically evaluate the collection of fibrous debris on debris capturing fuel grids and the consequential head loss of that fiber bed and the particulates collected in that bed when the Emergency Core Cooling System (ECCS) is aligned to recirculate coolant from the reactor containment building sump. As this test facility was a recirculating loop, the use of unheated rods minimized the possible capture of fiber on rod surfaces and maximized the potential for fibrous and particulate debris to be either captured on a second grid or recirculate and be captured on the fiber bed formed at the fuel assembly entrance. Thus, the use of unheated rods was conservative for the purposes of this test.

The WCOBRA/TRAC calculations presented in Section 6 and Appendix B of WCAP-16793-NP demonstrate that a reduction in flow associated with potential core blockage has negligible effect on peak clad temperatures calculated anywhere in the core as shown in Figure 6-5 (and Figure B-20). These two figures are temperature history plots of the calculated peak clad temperature anywhere in the core for two (2) blockage cases; 82% of the core blocked and 99.4% of the core blocked, respectively. The calculated peak clad temperatures anywhere in the core are about 270° F, all other calculated clad temperatures are either equal to or less than the calculated temperatures shown in Figure 6-5 (and Figure B-20). These low temperatures are below the melting point of glass and other materials such as epoxy coatings. Thus, heated clad surfaces will have a negligible effect on attracting or holding debris, either fibrous or particulate, to the clad surface in either the test, or in plants.

RAI #6

Page 2-6, Section 2.3 of the WCAP states that fibrous debris entering the core will not tightly adhere to the surface of fuel cladding. The WCAP further states that adherence of fibrous debris is not plausible and will not adversely affect core cooling. During strainer testing, the staff has observed that fiber coated with chemical precipitate can adhere to surfaces, such as plexiglass walls. Therefore, provide a justification for why is it not plausible that fibers that have precipitate or other chemical products attached can tightly adhere to the surface of fuel cladding? If fibers did adhere to the fuel cladding, how would this affect the deposition model predictions?

RESPONSE TO RAI #6

The deposition of small fibers that do not dissolve but are small enough to be transported through the sump screen and into the core cannot be ruled out.

The quantity of transported fines is expected to be small compared to both the total amount of debris and the amount of debris that dissolves or corrodes. Thus, if the small fibers were included in model predictions, the effect would be small but would vary from plant to plant depending on the screen design and debris mix. A quantitative estimate of the effect of the fiber on deposit thickness and fuel temperature can be accounted for in LOCADM by use of a "bump-up factor" applied to the initial debris inputs. The bump-up factor is set such that total release of chemical products after 30 days is increased by the best estimate of the mass of the fiber that bypasses the sump screen. This allows the bypassed material to be deposited in the same manner as a chemical reaction product.

The recommend procedure for including fiber bypass in the LOCADM deposition calculations is illustrated in the example below where the LOCADM example in WCAP-16793-NP is extended to include fiber bypass

A. Estimate the mass of material bypassing the sump screen.

Example: The sump screen area in the WCAP-16793-NP example plant is 5000 ft². The type of screen used at the plant is known to bypass a maximum of 1 ft³ of fiber for every 1000 ft² of screen area, so the volume bypassed is estimated to be:

$$(1 \text{ ft}^3 \text{ fiber} / 1000 \text{ ft}^2 \text{ screen}) * 5000 \text{ ft}^2 = 5 \text{ ft}^3 \text{ fiber}$$

Then the volume of fiber is converted to mass using the density of fiberglass. NEI 04-07 (Reference 6-1) identifies that the density for low-density fiberglass is approximately 2.4 lbm/ft³. This value is consistent with the density range of 2 to 3 lbm/ft³ identified in NUREG/CR-6808 (Reference 6-2). To maximize the effects of bypassed fiberglass on the LOCADM model, a density of 4 lbm/ft³ is used:

$$5 \text{ ft}^3 \text{ fiber} * 4 \text{ lbm ft}^{-3} = 20 \text{ lbm}$$

Thus, the bypass bump-up factor must be selected so that the chemical product release (aluminum + calcium + silicon) in LOCADM is increased by at least 20 lbm.

Note that the bypass mass can be estimated by other techniques such as the direct measurement of bypassed material mass during screen qualification tests.

B. Calculate the "increase factor" for the chemical products.

Example: LOCADM is run first not accounting for bypass using the plant specific material inputs. The total Ca + Al + Si release is obtained by summing outputs in the "Releases by Material" worksheet of LOCADM (B3:D11). A value of 554.8 kg or 1221 lbs is obtained. The total release after the bypassed matter added is 1221 + 20 lbs or 1241 lbs. Thus, the increase factor is:

$(1241 \text{ lbs}) / 1221 \text{ lbs} = 1.016$ (a 1.6% increase)

C. Adjust the "increase factor" to create the bypass bump-up factor.

If all of the debris material reacts to form chemical products, the increase factor calculated in "B" would be the bypass bump-up factor. However, in cases where the containment materials are not completely dissolved or corroded as is typical, the bypass bump-up factor must be adjusted upward to account for the incomplete reaction. This is a trial and error process. An adequate estimate is usually obtained by doubling the percentage increase in release calculated in "B"

Example:

$1.016 + 0.016 = 1.032$ (the bypass bump-up factor)

D. Increase all material inputs by the bump-up factor rerun LOCADM.

Example:

Class	Material	Amount	
		Before Bump-up	After Bump-up
Coolant	Recirc Sump Pool Volume (ft3)		
Metallic Aluminum	Aluminum Submerged (sq ft)	799	825
	Aluminum Submerged (lbm)	179	185
	Aluminum Not Submerged (sq ft)	15189	15675
	Aluminum Not Submerged (lbm)	3406	3515
Calcium Silicate	CalSil Insulation (ft3)	80	82.56
E-glass	Fiberglass Insulation (ft3)	7000	7224
Concrete	Concrete (ft2)	736	762

RESULTS:

	Before Bump-up	After Bump-up
Released Material (Ca+Al+Si) lbm	1221	1247
Maximum Deposit Thickness (mils)	10.1	10.3
Maximum Temperature (°F)	323.6	323.6

Note that the released material has increased by 26 lbm, six pounds more that the required 20 lbm needed to account for the fiber material. If the amount of the increase was less than 20 lbm, or if the increase was too conservative, the bump-up factor would be adjusted up or down proportional to the undershoot or overshoot, and LOCADM would be rerun after reapplication of the new bump-up factor to the initial masses.

REFERENCES FOR RAI #6 RESPONSE:

- 6-1 NEI 04-07, Revision 0, "Pressurized Water Reactor Sump Performance Evaluation Methodology, Volume 1, Pressurized Water Reactor Sump Performance Evaluation Methodology," December 2004.
- 6-2 NUREG/CR-6808, "Knowledge Base for the Effect of Debris on Pressurized Water Reactor Emergency Core Cooling Sump Performance," U. S. Nuclear Regulatory Commission, February 2003.

RAI #7

Page 2-15 - This section describes the conservative clad heat-up calculations.

- A) Is the 50 mils of solid precipitate described here in addition to the normal layer of fuel corrosion product?
- B) Is this calculation on a clean fuel basis or a fuel surface that has the maximum allowable crud layer (~100 microns)?
- C) Is the 'weighting' factor for the crud and the precipitate the same? Provide a reference for the assumptions made regarding the individual contributions to this term.

RESPONSE TO RAI #7

The text on page 2-15 refers to the calculation summarized in Section 4.2, "Cladding Heatup Between Grids" and the details of those calculations presented in Appendix D, also titled "Cladding Heatup Between Grids." A schematic of the calculation model is given in Figure D-1. The schematic identifies that both an oxide layer and a crud layer are explicitly accounted for in the model used for these calculations and supports the following response.

- A) The 50 mils of solid precipitation described in the last paragraph of Section 2.7, page 2-15, are in addition to both a clad oxide and a crud layer. The thickness of the layer of oxide is identified under the third bullet in Section 4.2.3, "Assumptions" as being 100 microns (4 mils). The basis for this thickness is given on page D-4 as PWR industry experience.

Thus, the 50 mils of solid precipitate thickness is in addition to a layer of fuel corrosion product.

- B) Similar to the response to Item A, above, the calculations were performed assuming a layer of crud. Again, under the third bullet in Section 4.2.3, "Assumptions," 100 microns (4 mils) of crud was assumed for the clad heat-up calculations. The basis for this thickness is given on page D-4 as PWR industry experience.
- C) There is no reference to a "weighting factor" in the description of clad heat-up calculations given on Page 2-15. A thermal conductivity of 1.27 Btu/(hr-ft-°F) was used to represent the oxide layer and a thermal conductivity of 0.30 Btu/(hr-ft-°F) was used to represent and crud layer (see page D-3). These values are representative of industry experience for the oxide, and a value recommended by the Electric Power Research Institute (EPRI) for crud.

RAI #8

Page 5-3 - One of the stated assumptions in this section is, "The non-boiling rate of deposit build-up is proportional to heat flux and is 1/80th of the rate of boiling deposition at the same heat flux". Please provide the technical basis for this assumption. Also provide a copy of reference E-13.

RESPONSE TO RAI #8

The 1/80th factor was empirically derived in reference E-13. This was done by comparing the deposition rate obtained for mixed calcium salts under boiling and non-boiling conditions on a heated surface. The application in the post-LOCA environment is justified since calcium is one of the elements of most concern in fuel deposition. The 1/80th factor also seems reasonable when applied to fuel cladding deposits of different compositions. A review of five PWR fuel crud exams showed an average deposit mass per area ratio of 1/92 between non-boiling and boiling regions of the fuel.

Reference E-13 is available in open literature.

RAI #9

Page 5-3 - The relationship between the WCAP-16530-NP dissolution model and WCAP-16793 deposition model is discussed in Section 5.4.1. Please clarify how the output from the dissolution model is related to the input for the deposition model. In other words, is the mass from the dissolution model equal to the mass input to the deposition model, or is the dissolution mass output reduced by precipitate settling, sump strainer debris bed filtering, etc?

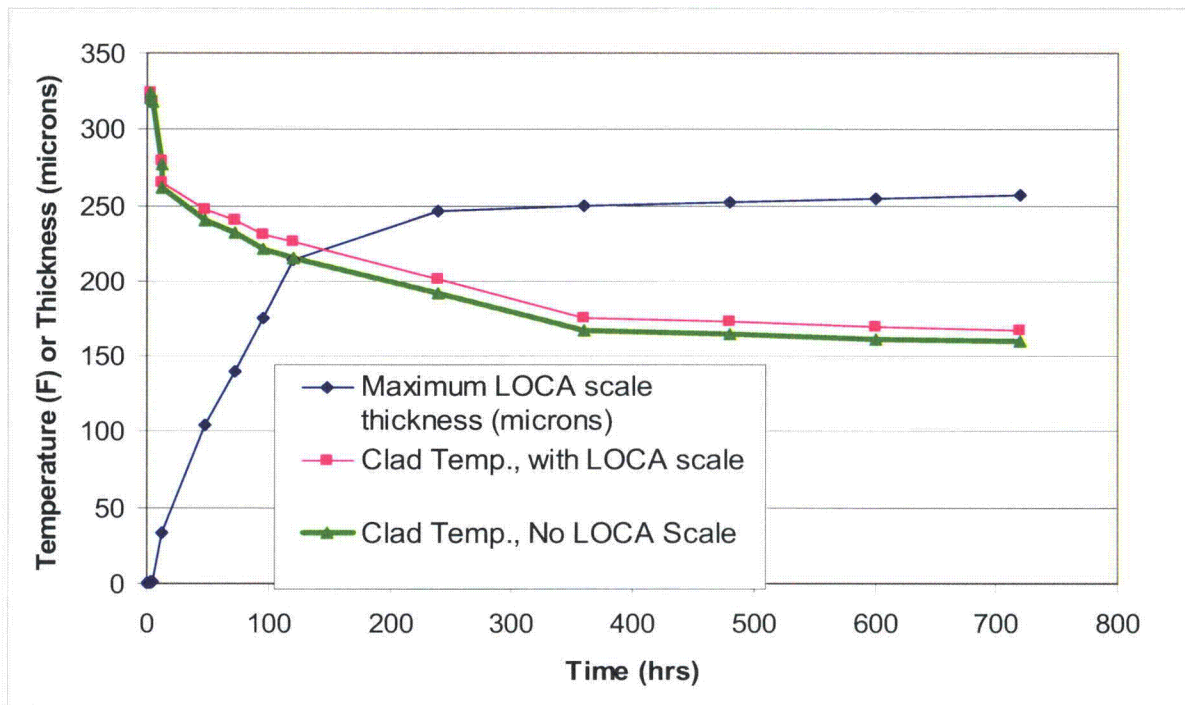
RESPONSE TO RAI #9

Containment materials in non-core locations (in the sump, sump screen, in spray...) release corrosion products into solution at rates determined by the WCAP-16530-NP model. The model takes into account initial amounts of each containment material, temperature, pH, and the concentration of materials released into solution. For the WCAP-16793 LOCADM calculations, it is assumed that once the corrosion products are released, they can only deposit in the core. To establish a high degree of conservatism, no deposition on ex-core surfaces such as the sump screen is allowed. The loss of material to core deposits will increase dissolution of debris outside the reactor, since solution concentrations are lowered.

RAI #10

Page 5-9 - In Figure 5-3, please show what the fuel cladding temperature profile would look like for a case with no debris contamination at the fuel surface?

RESPONSE TO RAI #10



The fuel cladding temperature with no LOCA scale has been plotted above. Other parameters such as core power, initial crud thickness, etc., were the same as in the original WCAP example.

RAI #11

Page 5-9 - Model predictions generally have a confidence level associated with the "calculated" value. The figure here identifies a "maximum" scale thickness. How is this maximum value calculated and does it represent a 50%, 95% or some other confidence level?

RESPONSE TO RAI #11

The scale thickness varies throughout the core and is dependent on the local heat flux and boiling. The maximum scale thickness at each point in time was determined by surveying the thickness predicted at every location, and selecting the largest value.

The confidence interval was not calculated for the maximum scale thickness, but this value is bounding because of the many conservative assumptions that were made in the model. These include conservative chemical product generation rates from the WCAP-16530-NP model, the *highly* conservative assumption that chemical products are not lost on system surfaces outside the core, and the assumption that all material transported to boiling fuel surfaces will deposit.

If refinements are made in the WCAP-16530-NP model to reduce conservatisms, the LOCADM user will have to demonstrate that the results still adequately bound chemical product generation. This will ensure that the deposition calculations are also bounding.

RAI #12

Page C-6 - Please explain the basis for the assumption that the top third of the fuel rod would be covered in debris and not the bottom third. Also demonstrate how this assumption would provide a conservative estimate for (low) heat transfer.

RESPONSE TO RAI #12

The deposition model used in LOCADM assumes deposition of material on the clad is by boiling (page 5-5, Section 5.5, first two paragraphs). For a postulated hot-leg break, all of the coolant flow provided by the emergency core cooling system (ECCS) flows through the core. This flow is in excess of that needed to remove decay heat. For a postulated cold leg break, coolant flow into the core is limited to make-up of boiloff. This limited flow provides for more of the core to be in a boiling heat transfer regime than for a postulated hot-leg break. Thus, for the deposition model assumed by LOCADM, a postulated cold-leg break is the bounding break as it provides for the maximum amount of core to be in boiling and subject to precipitant deposition.

The basis for the assumption that the top one-third of the core is boiling at the time of initiation of recirculation from the containment sump for a postulated cold-leg break is the WCOBRA/TRAC calculations described in Appendix B of WCAP-16793-NP. This assumption is applicable to all PWRs that provide recirculation flow from the bottom of the core.

Consistent with the assumption in the LOCADM code, deposition of material on the clad is by boiling (page 5-5, Section 5.5, first two paragraphs). This is conservative as all deposition was then assumed on only one-third of the cladding. This assumption minimizes the cladding area for deposition which, in turn, maximizes the deposition thickness. The maximization of deposition thickness provides for the calculation of conservatively high clad temperatures.

This deposition assumption, used in concert with the portion of the core calculated to be in boiling from the calculation described in Appendix B, provide for a conservative calculation of cladding temperature. The power shape for the calculation described in Appendix B is skewed to the top of the core (see Figure B-1 of WCAP-16793-NP) which

provides for a relatively high total peak factor ($F_Q = 2.3$). The skewed power shape provides for a conservatively large heat flux along the length of fuel cladding where boiling and deposition is occurring.

Thus, the application of a maximum material deposition, coupled with a maximum fuel rod heat flux, provides for a conservative clad temperature evaluation.

RAI #13

Page C-6 - For modeling purposes it has been assumed that the debris that reaches the fuel rod is evenly distributed over the entire surface. The more likely scenario is that deposits will build up on one spot and continue to grow in the vicinity of the original deposition. Can the modeling be modified to have a non-uniform deposit of debris on the fuel? For example, the curves in Figure C-1 are generated for uniform deposition of debris. What effect would localized debris build up have on the clad peak temperature? Specifically, how much debris would be necessary to exceed clad temperature limits or reduce effective cooling to the fuel assembly due to corrosion product blockage? Demonstrate that the uniform distribution assumption will *not* lead to *non-conservative* heat transfer conclusions.

RESPONSE TO RAI #13

The calculations shown in Appendix C are a parametric study showing a single rod. The calculations were not intended to model the deposition process, only to assess the affect of deposition on clad temperature. The conservative calculation of deposition is performed by the LOCADM calculation aid described in Appendix E. The LOCADM calculation aid accounts for different local rates of deposition based on the local boiling rate and calculates a resulting cladding temperature based on the local chemical deposition on cladding surface. The LOCADM calculations may be performed on a plant-specific basis to account for plant-specific conditions.

However, the affect of non-uniform deposition may be conservatively evaluated from the calculation results already presented in Appendix C. The calculations in Appendix C account for both radial and axial heat transfer behind a grid strap. While the calculated temperature values listed in Table C-7 can be used to evaluate a conservative temperature difference between two adjacent but different deposition thicknesses on the same fuel rod, it is suggested that a more conservative evaluation is derived from the use of the calculations listed in Appendix D. The calculations of Appendix D do not account for axial conduction and therefore allow only heat transfer in the radial direction; this maximizes the calculated clad temperature for any set of inputs used for the calculation. Thus the affect on non-uniform deposition may be conservatively evaluated without modifying the model presented in Appendix C or Appendix D.

For example, assuming a deposition thermal conductivity of 0.1 Btu/(hr-ft-°F), and assuming a deposition thickness of 10 mils, Table D-1 lists a clad temperature of 336°F. For the same conditions, and assuming a deposition thickness of 30 mils Table D-1 lists a clad temperature of 453°F. Thus, assuming a step-change in deposition thickness from 10 mils to 30 mils on a fuel rod, accounting for only radial heat transfer and ignoring axial conduction in the fuel rod, a maximum axial temperature gradient of (453°F - 336°F) or 117°F is conservatively evaluated. This evaluation may be repeated for any of the deposition thicknesses listed in Table D-1.

Thus, a non-uniform deposition due to localized buildup will result in an increase in clad temperature compared to an adjacent location with less deposition.

However, extrapolating the conservative calculated clad temperatures summarized in Table D-1 for a deposition on the fuel cladding having a thermal conductivity of 0.1 Btu/(hr-ft-°F), it is estimated that a deposition thickness in excess of 90 mils would be needed to reach or exceed the 800°F acceptance basis value identified in Section 3 and Appendix A of WCAP-16793-NP.

Thus, the uniform distribution of deposition assumption provides for conservative heat transfer conclusions (it does not lead to non-conservative heat transfer conclusions).

RAI #14

Page C-6 - Show why insulation does not become incorporated into the debris covering the fuel rods. If the debris is insulation based, what would be a realistic heat transfer coefficient for this material? Please provide a reference or technical basis for this value.

RESPONSE TO RAI #14

The response to this RAI is similar to the response to RAI #4 of this set of RAIs.

From the test observations and data presented in the response to RAI #2 from the first set of RAIs, most of the fibrous debris is captured at the core entrance. Thus, there is only a small amount of fiber that is passed by the support grids at the core entrance and therefore only a small amount of fiber to collect downstream of the core entrance on the cladding surface.

If debris is insulation based, it would have negligible affect on the removal of decay heat from the fuel for the following reasons;

- If the fiber forms a bed, WCAP-16793-NP states that fibrous material on fuel structures with at least a porosity of 40%.
 - Being porous, there would be fluid movement through the fiber bed. This is demonstrated by the data included in the response to RAI #2.
 - The movement of fluid through the porous bed will remove heat from the cladding surface by convection.
- From the response to RAI #15 from the first set of RAI responses;
 - The thermal conductivity of a fibrous bed is realistically calculated to be about 0.59 Btu/(hr-ft-°F).
 - The thermal conductivity of a fibrous bed is conservatively represented as being 0.1 Btu/(hr-ft-°F). This is the same value used to conservatively simulate the thermal conductivity of chemical precipitants on cladding surfaces.
 - The thermal conductivity through glass is about 0.59 Btu/(hr-ft-°F). Explicitly accounting for fiberglass debris in the surface deposition would enhance heat transfer from the cladding.
 - As noted above, accounting for only conductive heat transfer through a fiber bed conservatively neglects convective heat transfer through the porous bed.

Also from the response to RAI #15 from the first set of RAIs, the thermal conductivity of fibrous insulation (not individual fibers, but intact fibrous insulation) is a function of the moisture content in the insulation. In the case where the insulation contacts a boiling surface, such as a fuel rod, it is a function of both the moisture and steam content. A literature search was performed to support the calculation presented above. Reference 14-1 states that the dry thermal conductivity of fiberglass insulation of 0.05 BTU/(hr-ft-°F) doubles (to 0.1 BTU/ft h °F) with only eight percent of its volume filled with water. Reference 14-2 shows that when a mixture of steam and liquid are present, the thermal conductivity will increase by a factor of approximately 12 when the liquid and steam are present in equal amounts in a porous medium. These references support the value of minimum effective thermal conductivity of to 0.1 BTU/(hr-ft-°F), and suggest that a thermal conductivity at least as large as 0.6 BTU/(hr-ft-°F) may be used for fibrous debris incorporated into debris that might cover the fuel rods. Thus, based on the information presented above, the WCAP-16793-NP value of 0.1 BTU/(hr-ft-°F) is an appropriately conservative choice for representing a lower bound thermal conductivity for fibrous insulation that may become incorporated into debris covering fuel rods.

Thus, if debris is insulation based, it would have negligible affect on the removal of decay heat from the fuel.

REFERENCES FOR RAI #14 RESPONSE:

- 14-1 "Joint Departments of the Army and Air Force, USA, Technical Manual TM 5-852-5/AFR 88-19, Vol. 5, Arctic and Sub-arctic Construction: Utilities." Chapter 12
- 14-2 Ho-Jeen Su and Wilbur Somerton, "Thermal Behavior of Fluid Saturated Porous Media with Phase Changes" Proceedings of the 16th International Thermal Conductivity Conference, November 7-9 Chicago, Published by Plenum Press, New York, page 193-204

RAI #15

Page C-7 - Regarding Table C-7, identify the change in solubility of sodium aluminosilicate, aluminum hydroxide, and calcium silicate at these temperatures. These compounds and other zeolites that may form have retrograde solubility. What is the rate of build up of these compounds on the fuel clad surface?

RESPONSE TO RAI #15

The calculations presented in Appendix C are a parametric study of the affect of deposition thickness on calculated clad surface temperature behind fuel grids. The sole purpose of the calculations is to parametrically evaluate clad temperature as a function of deposition thickness and deposition thermal conductivity. The calculations did not model, nor did they account for, either the rate of build-up or the solubility of materials (sodium aluminosilicate, aluminum hydroxide, and calcium silicate) or the solubility or change in solubility of these compounds. However, the minimum thermal conductivity used in these calculations, 0.1 Btu/(hr-ft-°F) bounds the thermal conductivity associated with deposition of these compounds. Therefore, the calculation results summarized in Appendices C and D apply to the deposition of these materials on cladding surfaces for the thicknesses considered in the calculations.

The identification and solubility behavior of chemical compounds is discussed in Section 5, "Chemical Precipitation and Subsequent Impact," Appendix E which has the same title as Section 5, and Appendix F, "Supporting Solubility and Precipitation Calculations." The calculations presented in Appendix F support the calculations in Appendix E, including identification of predominant chemical species.

The calculation of deposition rates and total deposition of chemical products on cladding, and the affect of that deposition on cladding temperature, is calculated using the LOCADM tool described in Section 5 and Appendix E. These are plant-specific calculations that use plant-specific inputs to evaluate the chemical products generated and the rate of deposition of those products.

RAI #16

Page D-2 - Deposition of the thickest crud layers on fuel surfaces occurs on the top third of the fuel assemblies. Therefore it seems likely that the heat conduction in the axial direction downward could be significant since there would be decreased cooling water flow.

- A) Describe how axial heat conduction would affect the temperature profile calculated assuming radial heat conduction only; which case provides a conservative bound?
- B) Demonstrate that the assumption made here represents the most conservative case for build up of precipitates in all interstitial sections of the fuel assembly including the top third.

RESPONSE TO RAI #16

- A) The response to this RAI is similar to the response to RAI #13, which also questions the effect of axial conduction on clad temperature. As stated in the response to RAI #13, accounting for axial heat conduction would attenuate (reduce) the calculated clad surface temperatures, particularly near the interface of the clad surface with no deposition and the clad surface with deposition. As the objective of the calculations summarized in Appendix D was to provide conservative and bounding cladding temperatures, neglecting axial conduction in the fuel rod cladding provides for the calculation of maximum clad temperatures. These calculations are conservative and bound all plants.
- B) The calculations presented in Appendix D are a parametric study of clad temperature versus deposition thickness on a fuel rod between grids. The conservatism associated with assuming deposition on only the top 1/3 of the fuel is described in the response to RAI #12. The evaluation of precipitates, the rate of deposition and the total deposition of those precipitates is beyond the scope of this parametric study. The identification and conservative treatment of chemical compounds deposited on cladding surfaces is discussed in WCAP-16793-NP in Section 5, "Chemical Precipitation and Subsequent Impact," and Appendix E which has the same title as Section 5.

The rate of deposition and the total deposition of chemical products on cladding, and the consequential effect of that deposition on cladding temperature, is conservatively calculated using the LOCADM calculation aid described in Section 5 and Appendix E of WCAP-16793-NP. These are plant-specific calculations that use plant-specific inputs to assess chemical products produced and deposition rates based on plant-specific parameters.

RAI #17

Page D-4 - Can you describe what this term "contact resistance" between material layers means and why it represents a conservative assumption for these calculations?

RESPONSE TO RAI #17

The term 'contact resistance' refers to the resistance to the transmission of heat across the boundary of two adjacent solids. This resistance to heat flow is due to gases or vacant spaces between the two solids. A discussion of contact resistance and contact coefficients is given on page 17 of the text, "Heat Transmission," by Wm. H. McAdams, McGraw-Hill Book Company (1954).

The development of the oxide layer and the deposition of the crud layer on the oxide, both which occur at power operations, are gradual and occur over time. The oxide provides nucleation sites for the deposition of the crud and the crud adheres to the outer oxide layer. The thermal conductivity of both the clad oxide layer and the crud already account for the morphology of their formation, including gases or vacant spaces. Since the crud adheres to the outer clad oxide layer by attaching itself to surface irregularities in the oxide layer, including additional surface resistance was evaluated to not be appropriate during long-term core cooling operation.

Similarly, the deposition of the chemical layer on the crud surface is also gradual and occurs over time. The chemical product deposition on and adhesion to the surface of the crud layer is evaluated to be similar to that of the crud onto the clad oxide layer. Considering that a conservatively small thermal conductivity value for the chemical deposition of 0.1 Btu/(hr-ft-°F) is used for the parametric study, the use of a contact resistance is evaluated to be both inappropriate and overly conservative..

RAI #18

Page D-6 - The calculations presented here represent the instantaneous clad surface temperature maxima at 20 minutes into the accident. Although the Fuel Centerline Temperature (FCT) and Clad Surface temperatures will decrease with time after this point, the precipitate masses and thicknesses will continue to increase. Please demonstrate:

- a) What the buildup of precipitate thickness will be over the next 30 days?
- b) How the build up of the precipitates over 30 days affects the fuel clad surface temperature during this time?

RESPONSE TO RAI #18

A) The calculations presented in Appendix D are a parametric study of the affect of deposition thickness on calculated clad surface temperature between fuel grids. The sole purpose of the calculations in Appendix D is to parametrically evaluate maximum clad temperature as a function of a specific deposition thickness and deposition thermal conductivity; not to calculate the time rate of deposition of chemical products on cladding surface. As the purpose of the calculations was to evaluate maximum clad temperatures, not rate of chemical deposition, the calculations of Appendix D did not evaluate lower decay heat rates at various chemical product deposition thicknesses.

The deposition rate and total deposition of chemical products on cladding is conservatively calculated using the LOCADM tool described in Section 5 and Appendix E of WCAP-16793-NP. This calculation is a plant-specific calculation that uses plant inputs to determine the chemical products formed and calculate the rate of deposition and total chemical deposition. The sample calculation in given in Appendix E provides an example of the precipitant thickness over a 30-day period.

B) As noted in the response to item (A) above, the deposition rate and the total deposition of chemical products on cladding over time are conservatively calculated using the LOCADM tool described in Section 5 and Appendix E of WCAP-16793-NP. The LOCADM code also calculates cladding temperature associated with the calculated deposition over the 30 day time period of interest. This calculation is a plant-specific calculation that uses plant inputs to calculate the clad temperature during the 30-day time period of interest, based on plant-specific rate of deposition and total chemical deposition.

RAI #19

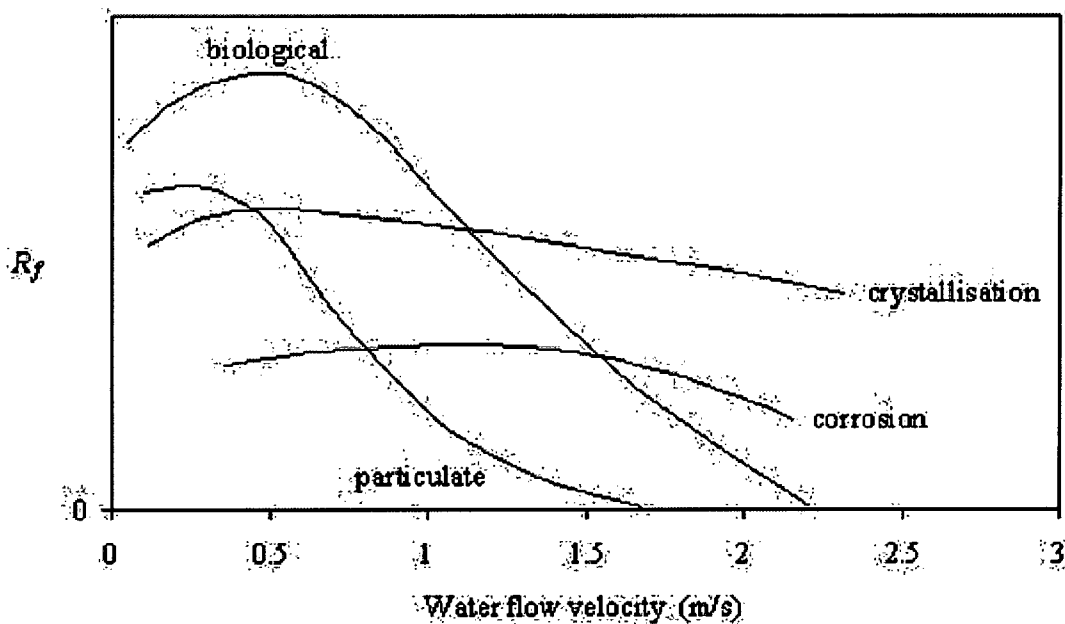
Page E-3 - Can it be shown that precipitate deposition on the residual heat removal heat exchanger surfaces will not lead to reduced flow and heat transfer such that the maximum fuel clad temperature assumption of 800 °F will not be exceeded? The topical report indicates that all debris and precipitate is transferred to the vessel. Please demonstrate that a drop in the heat exchanger flow is not a more conservative assumption based on reduced heat exchanger cooling capability.

RESPONSE TO RAI #19

It is possible that some debris material will be retained on RHR surfaces, either by the mechanism of particle deposition or by crystallization of solids having a “normal” solubility curve, i.e., one in which the solubility increases with temperature. However, it is not expected that such material will foul the RHR heat exchangers beyond the fouling margins that are already maintained to assure Appendix R cool-down requirements are met.

The precipitates and deposits that have formed upon cool-down in the WCAP 16530-NP testing and in subsequent integrated tests at Westinghouse STD have never formed hard deposits on the cooled surfaces which were available. Precipitates had no strength such would be required to block an RHR heat exchanger. When deposits formed on cooler surfaces, they could be easily removed with a paper towel or soft cloth. Flow rates through the RHR heat exchangers

will be high, 2.5 to 5 ft/second or about 1 meter per second. This flow will keep the thickness of such weak deposits to a minimum, since in general, high flow rates minimize particulate deposition (Ref. 19-1). The generalized effect of flow on particulate deposition is shown in the plot below.



The effect of water flow velocity on particulate deposition (from reference 19-1)

Another factor minimizing the chance of flow blockage by deposits is that the RHR pumps can generate a high pressure differential (>300 psi) to remove an obstruction in the unlikely event that one forms.

Another factor the argues against RHR system heat exchanger fouling problems is the short period of time over which the RHR system must operate near peak capacity (a few days). When similar heat exchanger have been run with a highly flawed chemistry which favored deposition of concentrated coolant chemicals (calcium > 300 ppm and alkalinity > 100 ppm), losses in thermal performance of 16% per year were observed (Ref.19-2). This data has been provided in an attached file.

REFERENCES FOR RAI #19 RESPONSE:

- 19-1 S. Pugh, G. F. Hewitt and H. Muller-Steinhagen, "Fouling during the Use of Seawater as Coolant - The Development of a 'User Guide', Paper 3", 2003 ECI Conference on Heat Exchanger Fouling and Cleaning: Fundamentals and Applications, Santa Fe, New Mexico
- 19-2 Loss of Thermal Performance of the Essential Cooling Water (EW) and Emergency Diesel Generator (EDG) Intercooler Heat Exchangers, Palo Verde Report CRDR 2897810, May, 2006

RAI #20

Page E-3

- A) Do any of these assumptions account for increase of deposit mass based on incorporation of boric acid into the deposited material?
- B) Do these calculations include 10% by weight of the boric acid in the precipitate?
- C) Are waters of hydration included in these calculations? If not, please describe the effects of including waters of hydration?

RESPONSE TO RAI #20

The calculations assume an increase in deposit volume (or indirectly, mass) during precipitation due to the incorporation of species such as the waters of hydration or boric acid. However, specific compounds are not assumed. This is done by specifying a deposit density that is sufficiently low to bound possible hydrates and adsorbed species. For instance, for calcium silicate, LOCADM calculates a thickness that is more than three times the amount that would be calculated assuming the theoretical density of 180 lbs/ft³ for calcium silicate (Ref. 20-1). This 3X margin is sufficient to account for waters of hydration, boron adsorption, and porosity.

REFERENCE FOR RAI #20 RESPONSE:

20-1 CRC Handbook of Chemistry and Physics, 55th addition (CRC Press, Cleveland Ohio) 1975, p. B79 entry c178 for alpha calcium metasilicate

RAI #21

Page E-7 - Should there be parentheses around the term (m_x/m_T)?

RESPONSE TO RAI #21

Yes. The parentheses would clarify the order of operation.

RAI #22

Page E-7 - Should there be parentheses around the terms ($C_x \cdot \text{Flowrate} \cdot dt$)?

RESPONSE TO RAI #22

Yes. The parentheses would clarify the order of operation.

RAI #23

Page E-7 - Does the value for h_{fg} only consider the enthalpy of dissolved boric acid or does it include all other dissolved species as well?

RESPONSE TO RAI #23

The standard enthalpy of vaporization for water was used in the LOCADM code. A formula was used to calculate this value as a function of temperature. The function produces a value near 2250 kJ/kg near 212°F. The standard enthalpy of vaporization for water is a good approximation except for the most concentrated boric acid solution, and then the water value will produce conservative results (more steaming than actual).

RAI #24

Page F-3 - Please demonstrate how the calculations performed here provide the appropriate values for solubility. Specifically:

- A) The value of 0.69 ppm is unrealistic for lithium concentration - what happens when this is reduced to 0.2 or less?
- B) Calculate the solubilities when aluminum is 100 ppm at fuel temperature of 260 F.
- C) Calculate the solubilities when the expected concentrations of hydrogen and oxygen that result from radiolysis exist.

RESPONSE TO RAI #24

- A) The lithium concentration was entered for completeness. However, the lithium has very little impact on the solution pH and does not significantly affect speciation at such a low concentration. The concentration of sodium is significantly higher and dominates the solution pH and speciation. Therefore, a reduction in the assumed lithium concentration would have a negligible impact on the calculation results.
- B) If an aluminum concentration of 100 ppm was equilibrated at the fuel temperature of 260 F, the OLI StreamAnalyzer™ code predicts that AlO(OH) would precipitate. However, the calculations in Appendix F were performed to verify the chemical deposition model developed in Appendix E. The Appendix E calculation conservatively assumes that all precipitation occurs in the core region. Since the Appendix E calculation will be used by the licensees to evaluate the chemical effects of debris on the core region, evaluating aluminum concentrations of 100 ppm at 260 °F is unnecessary.
- C) The Appendix F calculation includes representative concentrations for oxygen and hydrogen in the sump liquid. The oxygen and hydrogen are allowed to partition between the liquid and vapor phases as appropriate. Changes in the Oxidation-Reduction Potential (ORP) of the solution, either by oxygen and hydrogen from radiolysis or through other potential radiolysis products (hydrogen peroxide or nitrate), could slightly decrease the solubility of some of the predicted precipitates. However, because the LOCADM calculation (Appendix E) already assumes 100% precipitation of all solutes present in the liquid that is evaporated, there would be no change in the final LOCADM results.

RAI #25

Page E-11 - Section E.7 describes thermodynamic predictions for chemical compounds that would deposit on the fuel. Results are included from Westinghouse thermodynamic predictions and from thermodynamic equilibrium code calculations performed by AREVA NP. The NRC staff has a number of questions related to these thermodynamic predictions:

What is the basis for the Westinghouse thermodynamic predictions?

How are the AREVA and Westinghouse predictions integrated to model the quantity and compounds that form in the vessel? If only one is used indicate why it is more conservative than the other.

Does the model account for the change of $\text{Ca}(\text{BO}_3)_2$ to CaB_2O_5 when the precipitate is in contact with the fuel surface above 180 °F?

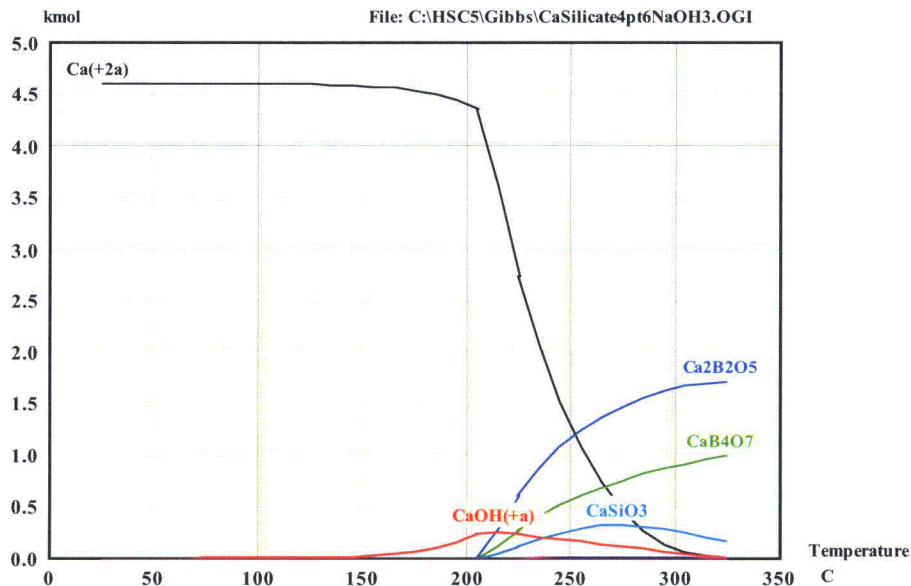
RESPONSE TO RAI #25

The Westinghouse thermodynamic predictions were done using HSC, a thermochemical modeling program from Outokomptu, Inc. Species expected to be in the sump liquid were input into the program which calculated the most stable species using a Gibbs free energy minimization routine. A parameter such as temperature or the amount of sodium hydroxide (pH) was changed, and any changes in solution species or the formation of solid phases was noted. An example is shown below, where the effect of an increase in temperature on dissolved CaSil was explored:

Input species:

Species	Input Amount (kmol)	Species	Input Amount (kmol)
H ₂ O	116640	SiO ₂ (a)	0
BO ₂ (-a)	0	SiO ₄ (-4a)	0
B(OH) ₃ (a)	0	Si(OH) ₄ (a)	0
B(OH) ₄ (-a)	0	Si(OH) ₃ (-a)	0
Ca(+2a)	0	SiO ₂ (OH) ₂ (-2a)	0
Ca(HSiO ₃)(+a)	0	SiO ₃ (OH)(-3a)	0
CaOH(+a)	0	B ₂ O ₃	0
H ₂ (a)	0	CaB ₄ O ₇	0
H(+a)	0.000001	Ca ₂ B ₂ O ₅	0
H ₃ BO ₃ (a)	0	CaO	0
H ₂ BO ₃ (-a)	0	Ca(OH) ₂	0
H ₂ SiO ₃ (a)	0	*2CaO*SiO ₂	0
H ₄ SiO ₄ (a)	0	*3CaO*SiO ₂	0
HSiO ₃ (-a)	0	*3CaO*2SiO ₂	0
H ₂ Si(OH) ₆ (a)	0	CaSiO ₃	4.6
Na(+a)	0	H ₃ BO ₃	485.5
NaHSiO ₃ (a)	0	Na ₂ B ₄ O ₇	0
O ₂ (a)	0	Na ₂ B ₄ O ₇ *10H ₂ O	0
OH(-a)	0.000001	NaOH	3
		Na ₂ O*2SiO ₂	0
		Na ₂ SiO ₃	0
		SiO ₂ (Q)	0

Results: Equilibrium species at different temperatures



Note that CaB_2O_5 is not predicted, but rather $\text{Ca}_2\text{B}_2\text{O}_5$.

The results of the thermodynamic modeling were not integrated into the LOCADM model even though the original intent was to limit deposition based on solubility. The HSC program and the OLI program used by AREVA produced different results and it was concluded that including solubility calculations in deposition predictions would add too much uncertainty to the LOCADM model if either was used in the calculations. Instead, the Westinghouse and AREVA calculations were simply used as guides when selecting deposit densities. Further the StreamAnalyzer OLI predictions were only used to confirm the conservatism of the LOCADM calculations. The OLI StreamAnalyzer was used for the “quantitative” predictions of Appendix F simply because of ease of use and because the predictions for sodium aluminum silicate were more consistent with the WCAP-16530-NP testing. Since results predicted with LOCADM have been confirmed to be conservative, plant specific analyses using either the HSC or OLI StreamAnalyzer software is not planned and is unnecessary.

RAI #26

Page E-14 - Reference E-18 refers to the scale build up and thermal conductivity in a desalination unit. Please provide the reference and show how the thermal conductivity of scale and insulation on the fuel would be comparable to that in the desalination unit.

RESPONSE TO RAI #26

Reference E-18 is available in open literature. This work is relevant to core deposition after a LOCA in the following respects:

1. Deposits were calcium-rich as would be the case for post-LOCA deposits on the core at many plants
2. The deposits were formed under boiling conditions.

When selecting a limiting thermal conductivity, a variety of literature sources covering other types of deposits were scanned to select a limiting value for LOCADM. ($0.1 \text{ btu } ^\circ\text{F}^{-1} \text{ ft}^{-1} \text{ hr}^{-1}$)

RAI #27

Page F-2 - The OLI StreamAnalyzer™ thermodynamic code data bank most probably does not include data from concentrated borated water environments. Therefore, justify why the thermodynamic equilibrium code predictions are reliable for use when modeling a concentrated boron environment in the reactor vessel following a postulated loss-of-coolant-accident (LOCA).

RESPONSE TO RAI #27

The current OLI StreamAnalyzer™ database contains thermodynamic information on twenty-two boron species, including various polyborates and borates of calcium, lithium, and sodium. These data were derived, in part, from published solubility data of sodium and boron species over a range of temperatures and pressures (Ref. 27-1 and 27-2). The code utilizes activity models for the aqueous phase (Bromley-Zematis) and the vapor phase (Soave-Redlich-Kwong) to adjust the equilibrium calculations based on compositional effects, allowing predictions for complex mixed-chemistry environments over a wide range of solute concentrations.

Appendix F was utilized to provide verification of the LOCADM model. It was specifically used to identify the most likely precipitate species and to verify the assumption that 100% of the dissolved species are available for precipitation due to boiling in the core (i.e., negligibly low solubility under core conditions). The StreamAnalyzer™ database and calculation framework are sufficiently reliable for the intended purpose.

The Appendix F calculations verified that the assumption of 100% precipitation, while conservative, is reasonable. In addition, the Appendix F results identified additional precipitation species for consideration when selecting the deposit density and thermal conductivity values used in the LOCADM code. While the OLI database does not include all possible species available for precipitation, it includes a large number of species from the relevant categories (i.e., oxides, hydroxides, aluminum-containing silicates, non-aluminum-containing silicates, and borates). It is unlikely that a precipitated species, not included in the thermodynamic database, would have density and conductivity characteristics significantly different from the conservative values utilized in the LOCADM model.

REFERENCES FOR RAI #27 RESPONSE:

- 27-1 W.C. Blasdale and C.M. Slansky, "The Solubility Curves of Boric Acid and the Borates of Sodium," J. Am. Chem. Soc. 1939, 61, 917-24.
- 27-2 N.P. Nies and R.W. Hulbert, "Solubility Isotherms in the System Sodium Oxide-Boric Oxide-Water, Revised Solubility-Temperature Curves of Boric Acid, Borax, Sodium Pentaborate, and Sodium Metaborate," J. Chem. Eng. Data 1967, 12(3), 303-313.

RAI #28

Page F-3 - Table F-1 provides an input summary for solubility calculations that are intended to be reasonably representative of the expected post-LOCA conditions and not bounding of all plants and scenarios. Was a parametric study performed to evaluate conditions other than the four results summarized in Table F-1? For example, were sensitivity studies performed to assess effects of pH, temperature, and elemental concentrations?

RESPONSE TO RAI #28

Appendix F is not an independent calculation of core precipitation, nor is it intended as an alternative method to Appendix E. Rather, Appendix F is a small sensitivity study intended to verify key assumptions / inputs of Appendix E with regards to solubility and precipitate form. The four cases analyzed include reasonably representative extremes of temperature, solute concentration, and pH (as a function of buffering media) expected for a post-LOCA environment. No scenarios in addition to those reported were calculated. However, because the LOCADM

calculation (Appendix E) assumes 100% precipitation of all solutes present in the liquid that is evaporated, and because LOCADM uses conservative values for deposit density and conductivity to bound a range of potential precipitates, there would be no change in the final LOCADM results.

RAI #29

Page F-4 - Thermodynamic software results from Run 1 are presented in Section F.5.1. Based on the OLI software, approximately 100% of the aluminum and 77% of the silicon in the sump are predicted to form a sodium aluminum silicate precipitate. No additional precipitation is predicted as the sump liquid is heated to core temperatures. Compare the in-vessel deposition results based on this assumption to the results that would be predicted given the same concentrations but assuming no sodium aluminum precipitate formed in the sump.

RESPONSE TO RAI #29

If sodium aluminum silicate precipitation in the sump were excluded from consideration, the equivalent mass would be expected to precipitate in the core. However, the LOCADM model (Appendix E) already assumes that all solute species are available for deposition in the core, and deposition in the sump is excluded. Therefore, changes in the Appendix F assumptions, as described in the question, would not impact the LOCADM results.

RAI #30

Page F-5, Section F.5.3 – There appears to be an assumption here that any silica specie in the RCS will be present at the starting point as SiO_2 . The predominant form of silica in the RCS (RWST and the spent fuel pool) is reactive silica and not SiO_2 .

- A) Does the model assume that SiO_2 precipitates without starting out as $\text{H}_2\text{SiO}_4^{2-}$?
- B) How does the presence of silica as $\text{H}_2\text{SiO}_4^{2-}$ or as $\text{H}_3\text{SiO}_4^{1-}$ affect the potential precipitation of other species such as calcium silicate or sodium aluminum silicate?
- C) Even if SiO_2 were to precipitate it would likely be transformed into $\text{H}_2\text{SiO}_4^{2-}$ rather rapidly. How does this change the predictions of the model?

RESPONSE TO RAI #30

- A) No. The neutral species (which OLI calls the Apparent Molecular Species) were listed for simplicity. However, the actual aqueous, solid, and vapor phase compositions are determined based on the thermodynamic calculation. In the case of silicon, aqueous speciation is primarily governed by pH. For the pH range in question, the predominant aqueous species predicted are $\text{H}_3\text{SiO}_4^{1-}$ and $\text{H}_2\text{SiO}_4^{2-}$.
- B) As stated in the response to Part A, the predominant aqueous species predicted are $\text{H}_3\text{SiO}_4^{1-}$ and $\text{H}_2\text{SiO}_4^{2-}$; therefore, the effect of these species is already included in the calculation results. It should be noted that SiO_2 (trigonal form) is predicted to form only in Case 3. For this case, the low in-core pH during boil-off, which results from the use of NaTB rather than NaOH for pH adjustment, prevents the precipitation of calcium silicate, calcium borate, or sodium silicate. Sodium aluminum silicate is not predicted to deposit due to the precipitation of essentially all of the aluminum in the sump. It should be noted, however, that the final LOCADM model does not consider sump precipitation; all deposition is assumed to occur in core.
- C) As previously discussed, the presence of $\text{H}_3\text{SiO}_4^{1-}$ and $\text{H}_2\text{SiO}_4^{2-}$ are included in the model. Additionally, laboratory analyses of crud taken from operating fuel assemblies have shown the presence of silicon in the absence of significant quantities of sodium, calcium, aluminum, or magnesium. Therefore, it must be concluded

that SiO₂ is stable under reactor conditions, even in the presence of operational radiation fluxes. Finally, the LOCADM model utilizes conservative values of deposit density and thermal conductivity to bound a range of expected precipitates. Therefore, the exact structural form of silica; whether trigonal, amorphous, or partially-substituted metal silicates; is not critical to the results of the LOCADM model.

APPENDIX J
RAI SET #3 [ML090680765]

- 1) WCAP-16793-NP, Appendix B, presents analyses of the effect of core inlet blockage using the WCOBRA/TRAC analysis code. Since the report was prepared additional analyses have been performed to determine the blockage level that would reduce core flow below that necessary to match coolant boil-off. Please provide documentation of the additional analyses that have been performed, including figures, for the integrated core inlet and exit flow, peak cladding temperature, core collapsed liquid level, core exit void fraction, and core pressure drop for the bounding conditions. The results should be presented for each case analyzed up to and including the blockage level for which boiloff is no longer satisfied.

RESPONSE:

Introduction:

Several additional WCOBRA/TRAC (WC/T) analyses were performed in support of WCAP-16793-NP. The WC/T runs were performed at the request of the Advisory Committee for Reactor Safeguards (ACRS) with the purpose of determining the blockage level (either using a reduction in area or increase loss coefficient) that would reduce core flow below that necessary to match coolant boil-off. As requested by this RAI, the documentation includes figures of the integrated core inlet and exit flow, peak cladding temperature, core collapsed liquid level, core exit void fraction, and core pressure drop for the bounding conditions.

Method Discussion & Input:

The WC/T runs made in support of WCAP-16793-NP are described in Reference 1. As stated in the above Introduction Section, in order to assess the blockage level that would reduce core flow below that necessary to match coolant boil-off, modifications were made to the flow area and loss coefficient input values used in the original runs and the calculations repeated.

The base case for the calculation results presented in this RAI response is Case 2, or the more restricted flow area case, from Section 6.0 of Reference 1. The Darcy equation defines pressure drop as being proportional to the form-loss coefficient and inversely proportional to the flow area squared. Using this principle, two separate approaches were taken to determine the blockage level needed to preclude sufficient flow into the core to provide for long-term core cooling. The first approach considered an area reduction while maintaining the form-loss coefficients. The second approach considered form-loss coefficient increases while maintaining the flow area constant.

- For the first approach, the flow area of the hot channel, Channel 13, was reduced. The input value of the hydraulic loss coefficient, C_D , for the other channels into the core, Channels 10, 11, 12 and 13 remained the same as the base case. As discussed on pages 26-27 of Reference 1, for this modeling approach, flow will only enter the core through the hot channel (Channel 13). To maintain the total core flow area, the adjacent channel (Channel 11, representing an "average channel") flow area was increased to offset the change in flow area to Channel 13. This change is needed to preserve the total core flow area; however, no flow will enter the core through Channel 11.
- For the second approach, the loss coefficients were increased in increments until boil-off could not be matched.

Areas Used in Reduced Flow Area Approach:

The flow area values used in the two flow area reduction cases are as listed below.

Channel 13 50% Flow Reduction Case:

$$\text{Channel 13 Flow Area} = 23.76 * (0.50) = 11.88 \text{ in}^2$$

$$\text{Channel 11 Flow Area} = 1782 + 23.76 * (0.50) = 1794. \text{ in}^2$$

Channel 13 80% Flow Reduction Case:

$$\text{Channel 13 Flow Area} = 23.76 * (0.20) = 4.752 \text{ in}^2$$

$$\text{Channel 11 Flow Area} = 1782 + 23.76 * (0.80) = 1801. \text{ in}^2$$

Due to time constraints, the transient run time was reduced from 2400 seconds to 1500 seconds for the calculations that were performed. The transient calculation time of 1500 seconds is sufficient to demonstrate whether the reduction in core flow would be sufficient to match boil-off.

C_D Values used in Increased Loss Coefficient Approach:

In order to determine the blockage level that would reduce core flow below that necessary to match coolant boil-off, the inlet core loss coefficients were increased in increments until boil-off could not be matched. The computer calculations made include uniform loss coefficients of 50,000, 100,000, and 1,000,000. The only changes required for these runs were updates to the variables used to activate the dimensionless loss coefficient ramp logic. For these cases, the C_D input value was changed from 10⁹ to desired C_D value to reduce flow through peripheral channels, the average channels and the hot assembly channel instead of block flow. Also, the feature to allow the C_D value of all core inlet channels to vary as a function of time was enabled.

Three runs were made; C_D = 50,000, C_D = 100,000 and C_D = 1,000,000. The increase in C_D values to the desired values was accomplished over a 30 second time interval. The ramp up started at the time of switchover from injection from the BWST/RWST to recirculation from the sump, transient time t = 1200 seconds and was completed at transient time t = 1230 seconds.

Again, due to time constraints, the transient run time was reduced from 2400 seconds to 1500 seconds for the calculations that were performed. The transient calculation time of 1500 seconds is sufficient to demonstrate whether the reduction in core flow would be sufficient to match boil-off.

Results from Flow Area Reduction Runs:

The first flow reduction run performed reduced the hot channel (Channel 13) flow area by 50%, which yields a total core inlet flow reduction of 99.7% compared to an unblocked core. The requested plots for this case are shown in Figures 1 through 7. Figures 1 and 2 show comparisons of the integrated core inlet flow and the core boil-off rate. As shown, even with the increase in core blockage, the flow that enters the core is still in excess of the boil-off rate. Figure 3 displays the integrated liquid flow at the core exit. The figure illustrates that, although liquid in excess of that needed to keep the core quenched enters the core, every little liquid flow is present at the core exit after the blockage occurs. The Peak Cladding Temperature (PCT) is shown in Figure 4. There are no significant PCT excursions after the core is blocked. Figure 5 displays the collapsed liquid level of the average assembly core channel (Channel 11 of Figure 6.3.4-3 in Reference 1). The figure shows that the collapsed liquid level drops slightly at the time blockage occurs, however, the liquid level continues to increase even after the blockage to the hot channel (Channel 13) is fully implemented at 1230 seconds. The void fraction at the core exit shown in Figure 6 again illustrates that liquid is present at the top of the core which shows the flow that enters the core after blockage occurs is still in excess of the boil-off rate. The core pressure drop is displayed in Figure 7. The figure displays an increased pressure drop of roughly 2 psi as blockage at the core inlet is increased. As the conditions in the Reactor Coolant System (RCS) adjust to increase in core blockage, it is noticed that the core pressure drop fluctuates consistent with the core liquid level.

The next flow reduction run performed reduced the hot channel (Channel 13) flow area by 80%, which yields a total core inlet flow area reduction of 99.9%. The requested plots for this case are shown in Figures 8 through 14. Figures 8 and 9 show comparisons of the integrated core inlet flow and boil-off rate. As shown, with the increase in core blockage, the flow that enters the core can not match the boil-off rate. Since all the liquid entering the core at the inlet is boiled-off, there is no liquid flow at the core exit (as shown in Figure 10). In addition, Figure 11 shows that the PCT increases until the end of the transient once the core liquid level, shown in Figure 12, is reduced to a level that the core becomes unquenched. Continuing with the trend discussed above, the void fraction at the core exit (Figure 13) shows that only vapor is present. The core pressure drop is displayed in Figure 14. The figure displays an increased pressure drop of roughly 4 psi as blockage at the core inlet is increased and the core liquid level begins to stabilize.

These results indicate that a total core inlet area reduction of up to as much as 99.7% will still allow sufficient flow into the core to provide for removal of decay heat and assure long-term core cooling.

Results from Uniform Loss Coefficient Runs:

The first uniform loss coefficient run performed applied a uniform C_D of 50,000 at the core inlet. The requested plots for this case are shown in Figures 15 through 21. Figures 15 and 16 show comparisons of the integrated core inlet flow and boil-off rate. As shown, even with the increase of the loss coefficient at the inlet, the flow that enters the core is still in excess of the boil-off rate. (Note that the integrated mass flow behavior shown between time $t = 1200$ seconds and time $t = 1250$ seconds of Figure 16 is the result of the 30 second ramp-up of the hydraulic loss coefficient, C_D , to 50,000 that is initiated in the calculations at time $t = 1200$ seconds.) Figure 17 displays the integrated liquid flow at the core exit. The figure displays that liquid in excess of that needed to keep the core quenched enters the core and that liquid flow is present at the top of the core even after the increase of the loss coefficient at the inlet. The PCT is shown in Figure 18. There are no significant PCT excursions after the core inlet loss coefficient is increased. Figure 19 displays the collapsed liquid level of the average assembly core channel (Channel 11 of Figure 6.3.4-3 in Reference 1). The figure shows that the collapsed liquid level drops slightly at time blockage occurs, however, the liquid is maintained even after the increase in the loss coefficient at the inlet. The void fraction at the core exit shown in Figure 20 again illustrates that liquid is present at the top of the core which shows the flow that enters the core after the increase of the loss coefficient occurs is still in excess of the boil-off rate. The core pressure drop is displayed in Figure 21. The figure displays an increased pressure drop of roughly 2 psi as blockage at the core inlet is increased. As the conditions in the Reactor Coolant System (RCS) adjust to increase in core blockage, it is noticed that the core pressure drop fluctuates consistent with the core liquid level.

The second uniform loss coefficient run performed applied a uniform C_D of 100,000 at the core inlet. The requested plots for this case are shown in Figures 22 through 28. Figures 22 and 23 show comparisons of the integrated core inlet flow and boil-off rate. As shown, even with the further increase of the loss coefficient at the inlet, the flow that enters the core is still in excess of the boil-off rate. (Note that the integrated mass flow rate of Figure 23 shows a similar behavior as was shown in Figure 16. Again, this is due to the 30 second ramp-up of the hydraulic loss coefficient, C_D , to 100,000 that is initiated in the calculations at time $t = 1200$ seconds, but extends the behavior over a slightly longer period of time.) Figure 24 displays the integrated liquid flow at the core exit. The figure displays that liquid in excess of that needed to keep the core quenched enters the core and that some liquid flow is still present at the top of the core even after the increase of the loss coefficient at the inlet. The PCT is shown in Figure 25. There are no significant PCT excursions after the core inlet loss coefficient is increased. Figure 26 displays the collapsed liquid level of the average assembly core channel (Channel 11 of Figure 6.3.4-3 in Reference 1). The figure shows that the collapsed liquid level drops slightly at time blockage occurs, however, the liquid level recovers even after the increase in the loss coefficient at the inlet. The void fraction at the core exit shown in Figure 27 again illustrates that liquid is present at the top of the core which shows the flow that enters the core after the increase of the loss coefficient occurs is still in excess of the boil-off rate. The core pressure drop is displayed in Figure 28. The figure displays an increased pressure drop of roughly 2 psi as blockage at the core inlet is increased. As the conditions in the Reactor

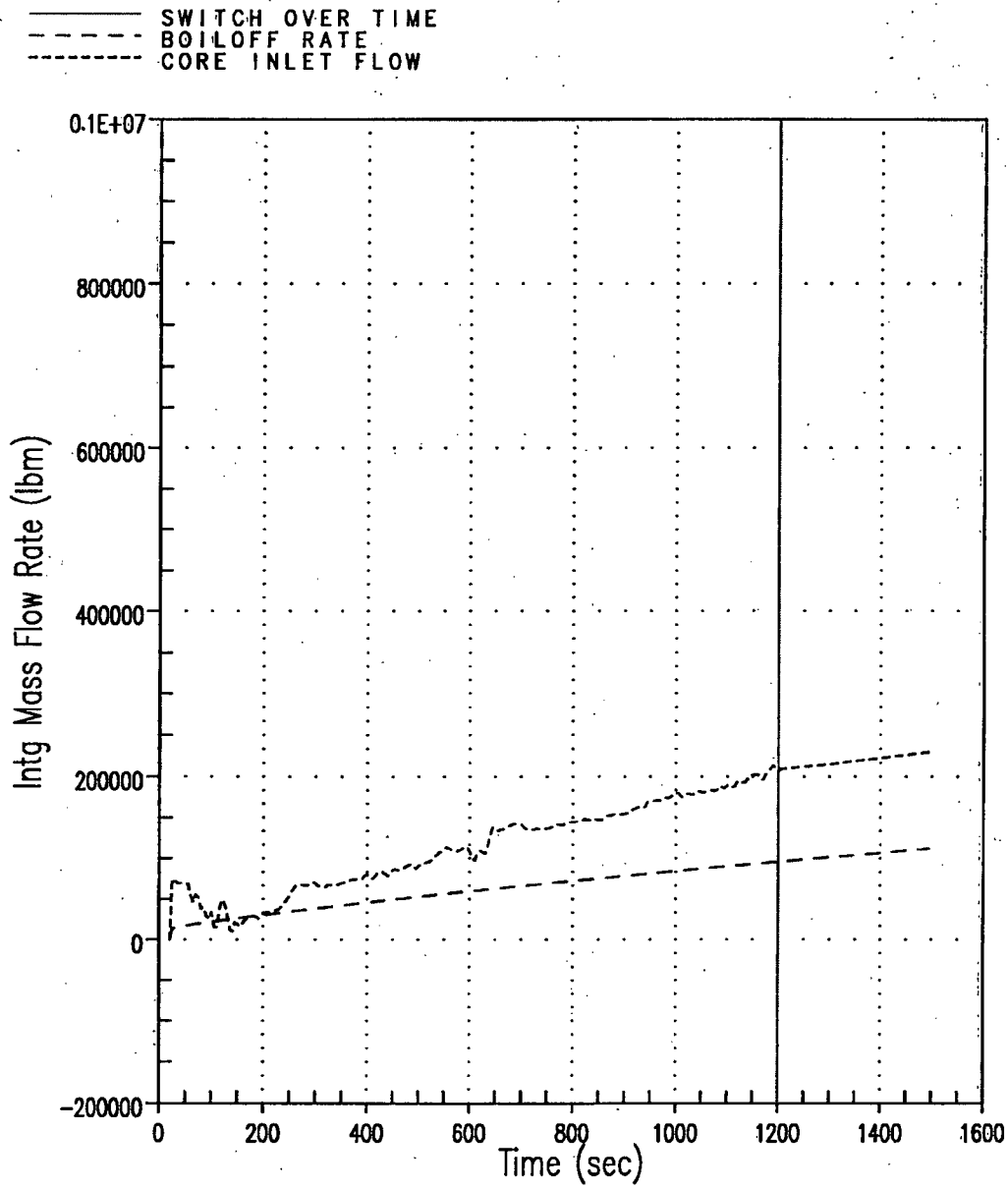
Coolant System (RCS) adjust to increase in core blockage, it is noticed that the core pressure drop fluctuates consistent with the core liquid level.

The next uniform loss coefficient run performed applied a uniform C_D of 1,000,000 at the core inlet. The requested plots for this case are shown in Figures 29 through 35. Figures 29 and 30 show comparisons of the integrated core inlet flow and boil-off rate. As shown, with the increase in core blockage, the flow that enters the core can not match the boil-off rate. Since all the liquid entering the core at the inlet is boiled-off, there is no liquid flow at the core exit (as shown in Figure 31). In addition, it is displayed in Figure 32 that the PCT increases until the end of the transient once the core liquid level, shown in Figure 33, is reduced to a level that the core becomes unquenched. Continuing with the trend discussed above, the void fraction at the core exit (Figure 34) shows that only vapor is present. The core pressure drop is displayed in Figure 35. The figure displays an increased pressure drop of roughly 4 psi as blockage at the core inlet is increased and the core liquid level begins to stabilize.

The results indicate that an increase in the form loss coefficient at the core inlet of up to $CD = 100,000$ for the limiting plant and fuel load design will allow for sufficient flow into the core to remove decay heat and provide for long-term core cooling.

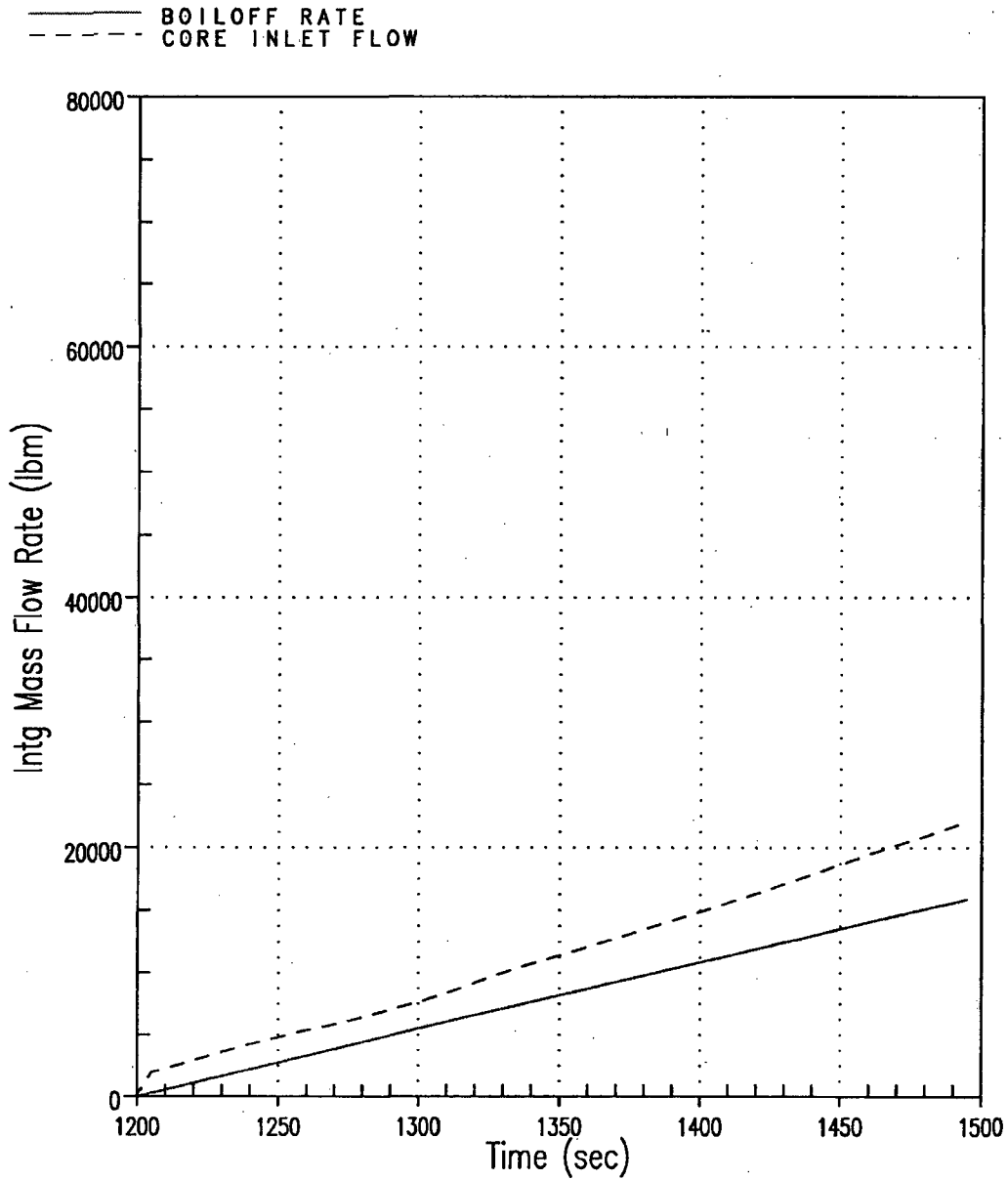
References:

1. WCAP-16793-NP, "Evaluation of Long-Term Cooling Considering Particulate, Fibrous and Chemical Debris in the Recirculating Fluid," May 2007.



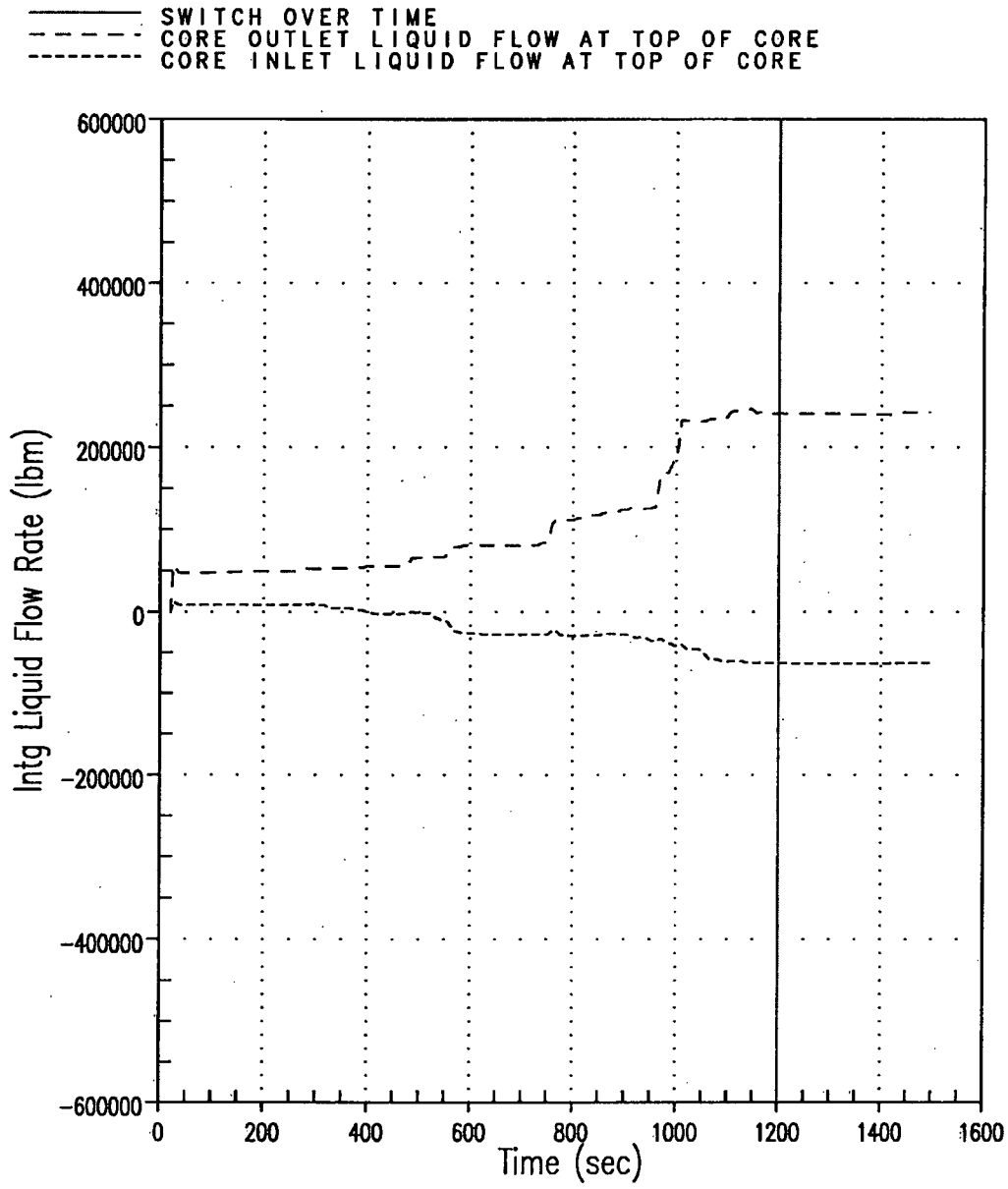
409461908

Figure 1: Integrated Core Flow vs. Core Boil-off for Channel 13 Flow Reduction 50%



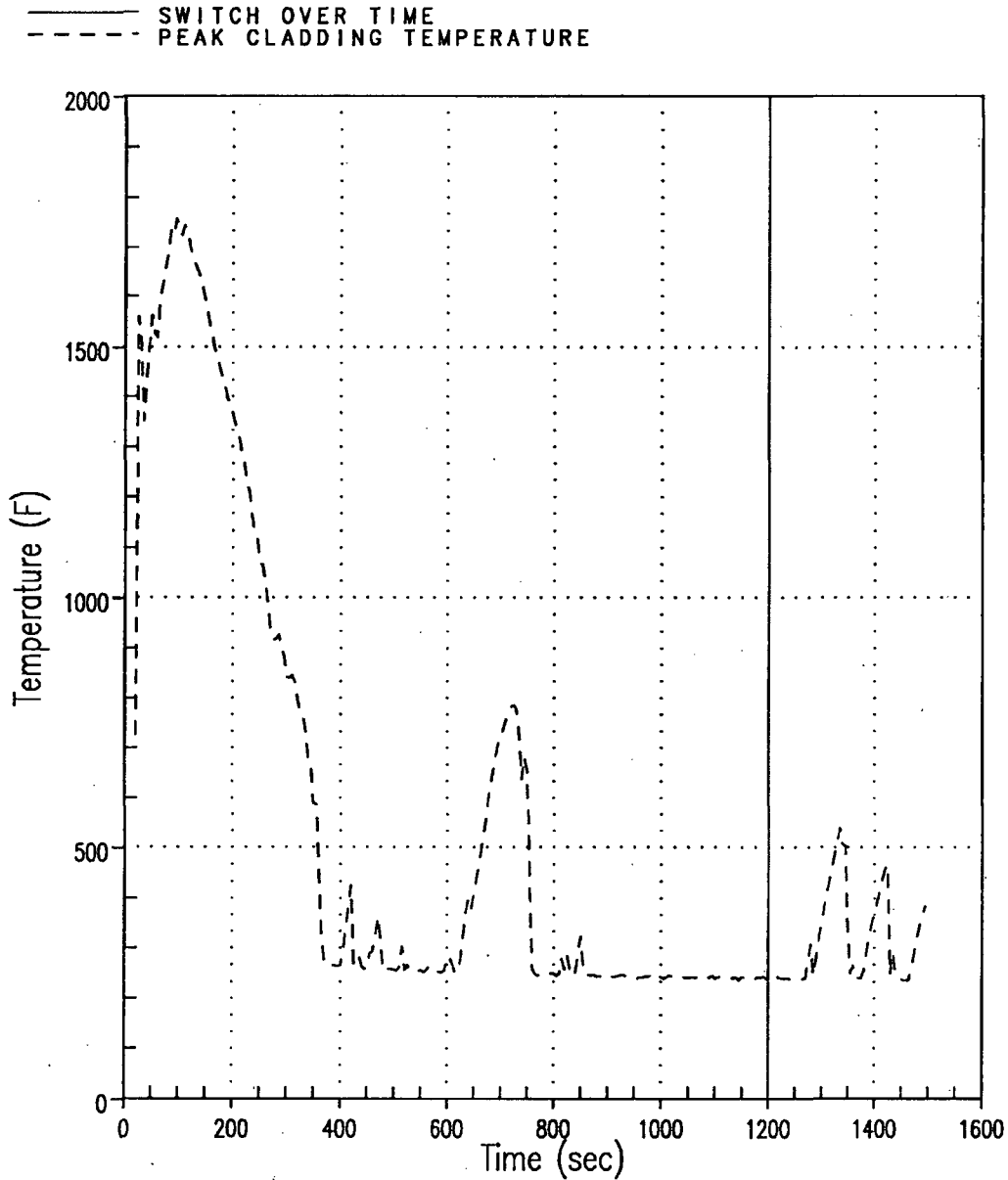
409481908

Figure 2: Integrated Core Flow vs. Core Boil-off for Channel 13 Flow Reduction 50% Case (Shifted Scale)



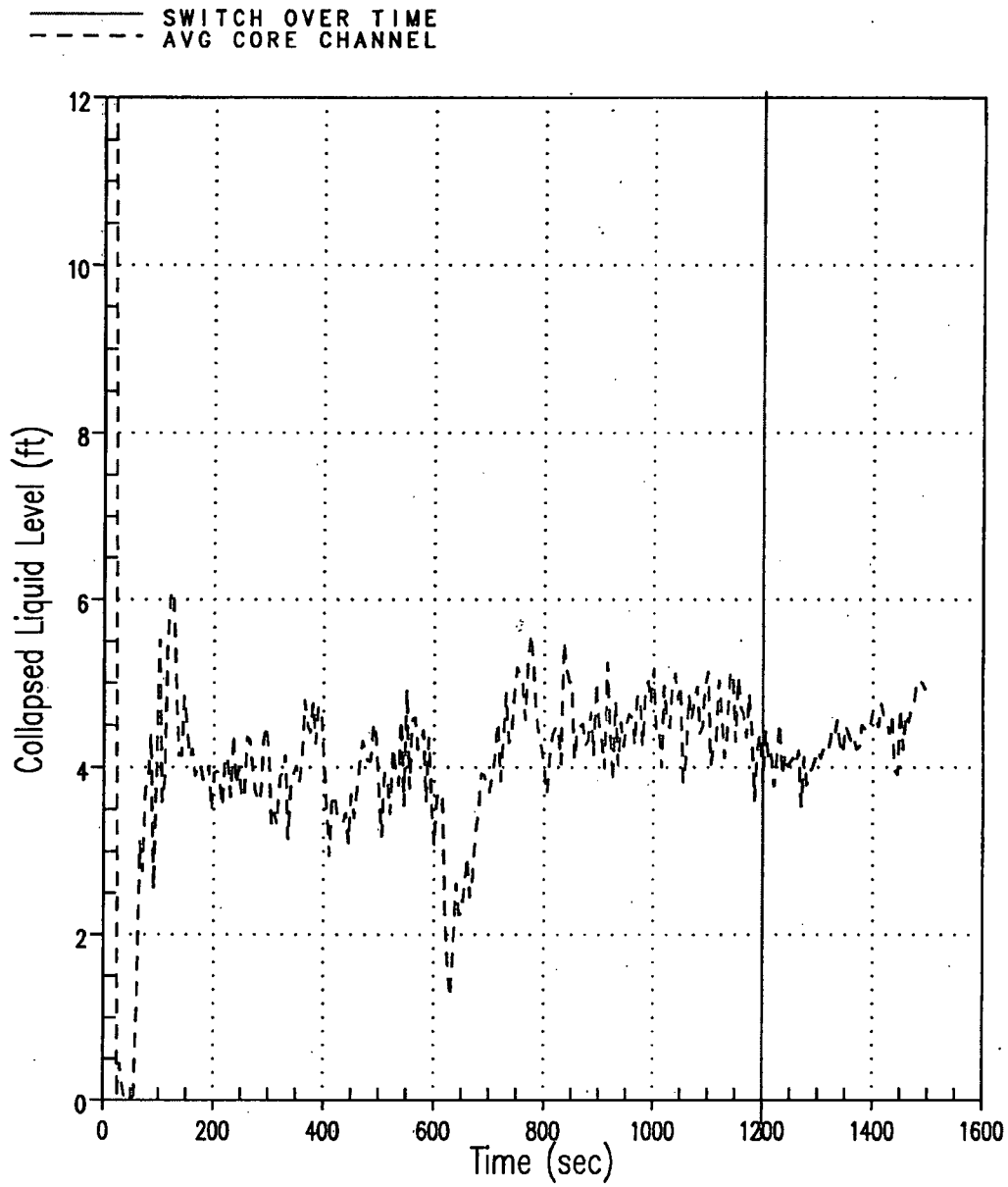
512214912

Figure 3: Total Integrated Liquid Flow at the Top of the Core for Channel 13 Flow Reduction 50% Case (Positive/Outlet flow represents HA, GT, AVG channels; Negative/Inlet flow represent LP channel)



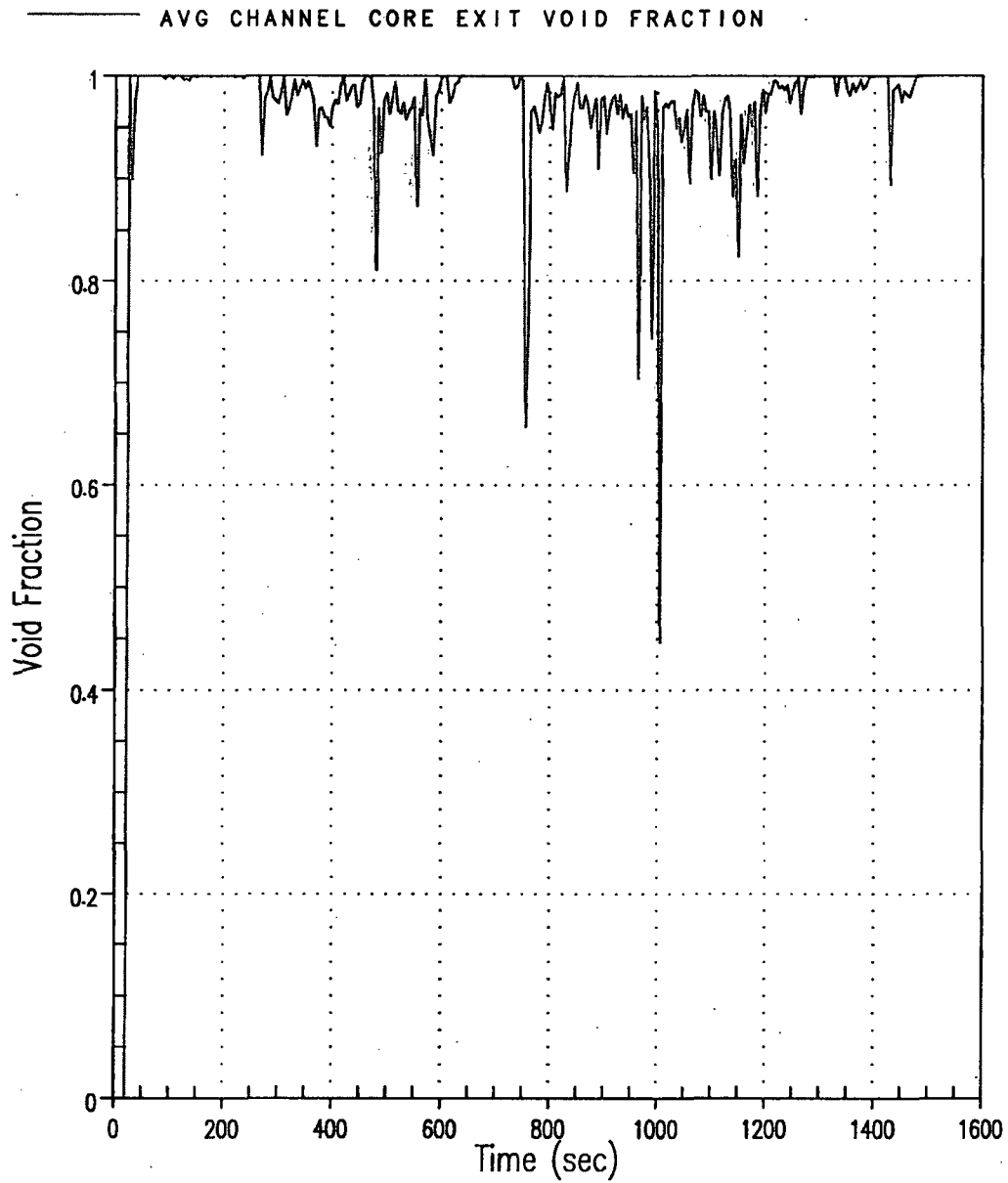
188413088

Figure 4: Hot Rod PCT for Channel 13 Flow Reduction 50% Case



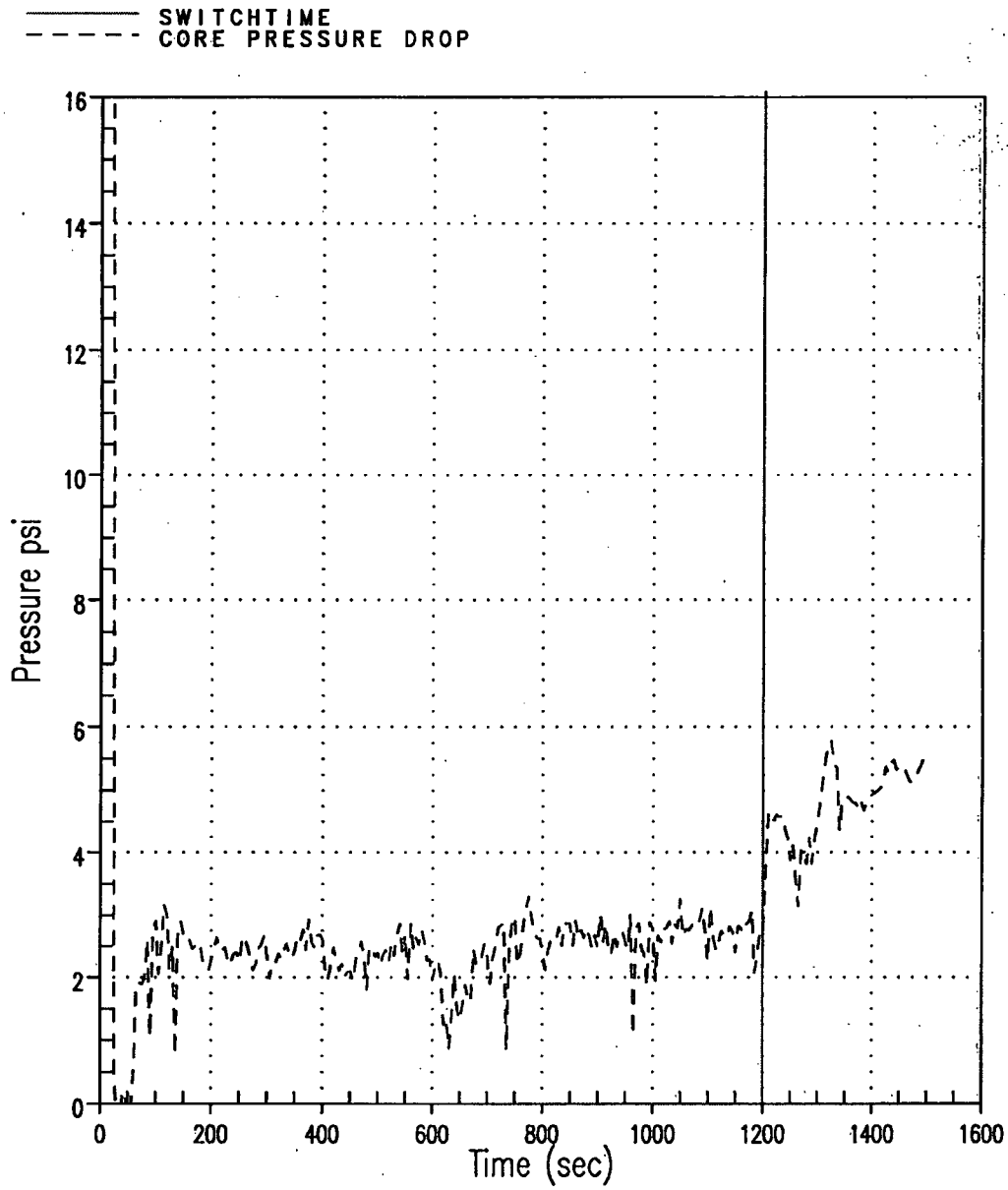
1075481719

Figure 5: Average Core Channel Collapsed Liquid Level for Channel 13 Flow Reduction 50% Case



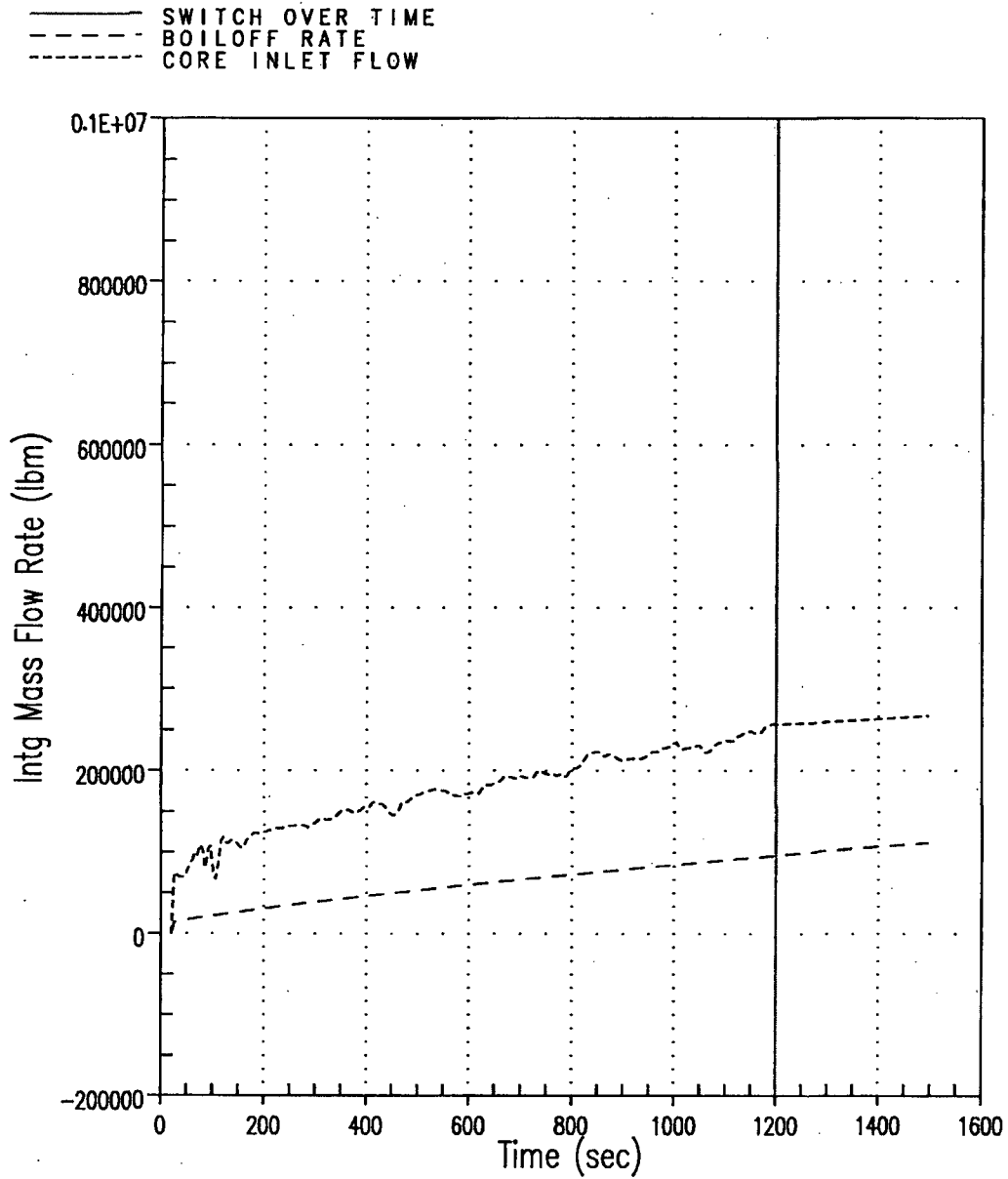
1951861530

Figure 6: Void Fraction at the Exit of the Average Core Channel for Channel 13 Flow Reduction 50% Case



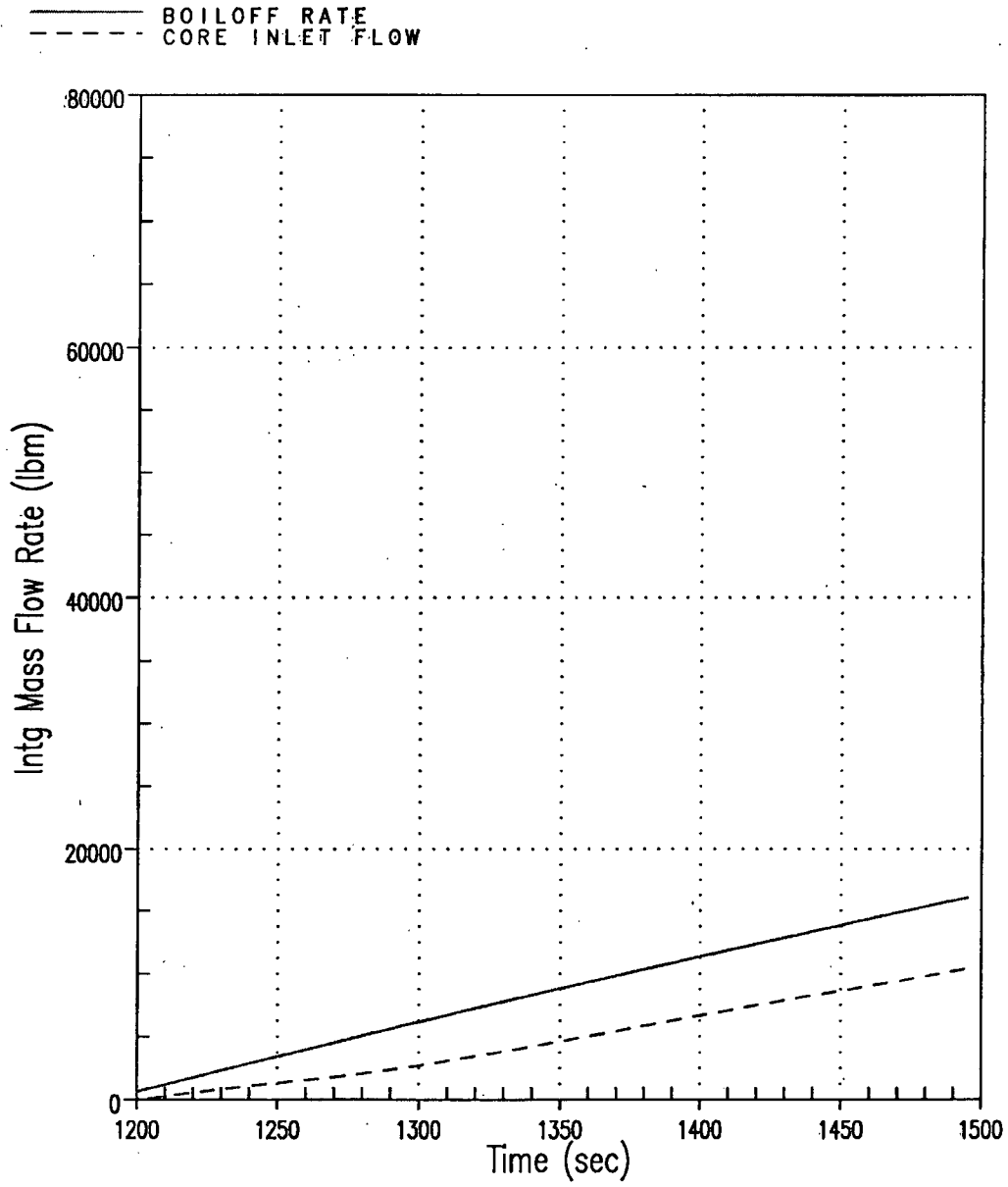
1566789324

Figure 7: Core Pressure Drop for Channel 13 Flow Reduction 50% Case



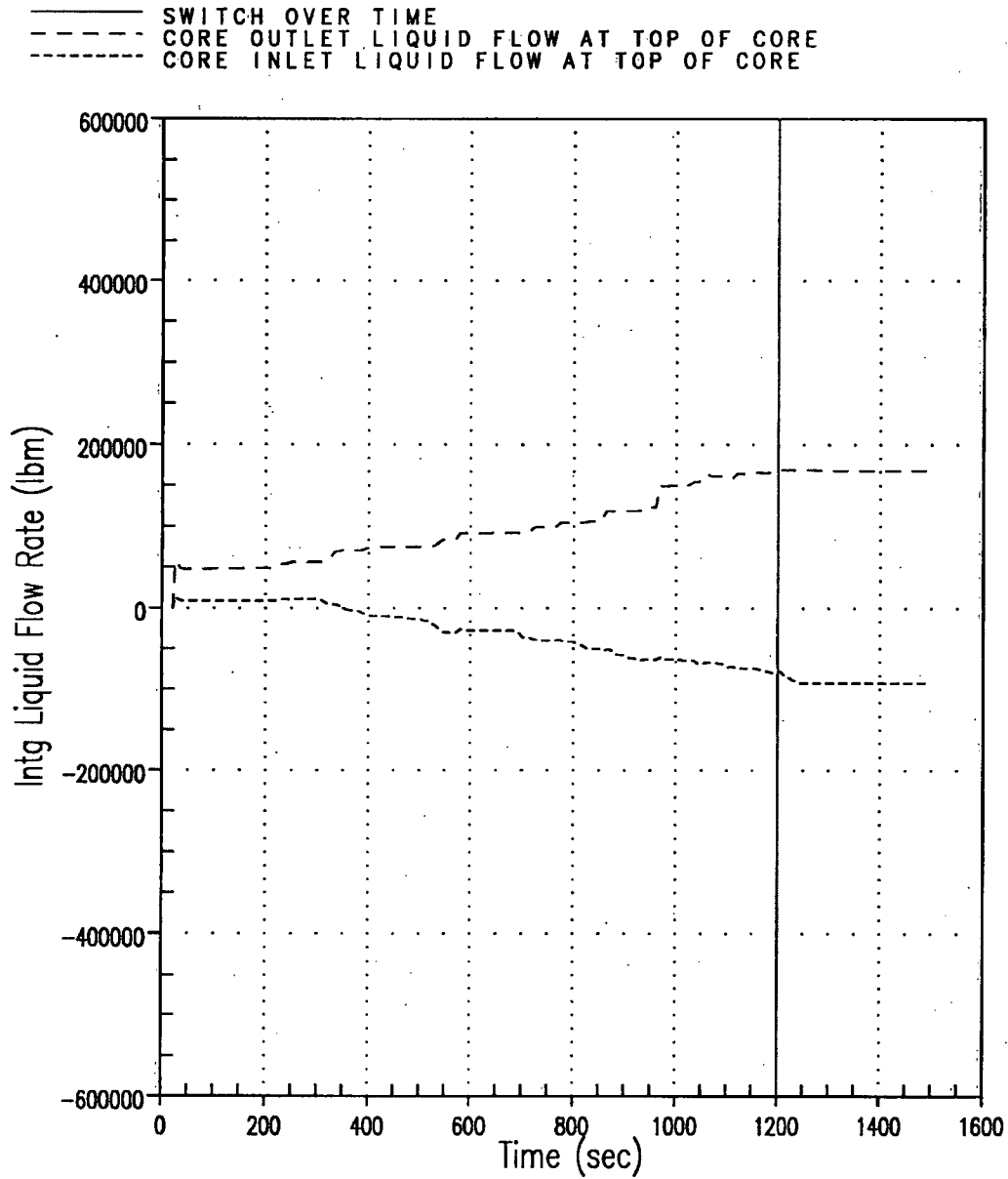
441843533

Figure 8: Integrated Core Flow vs. Core Boil-off for Channel 13 Flow Reduction 80% Case



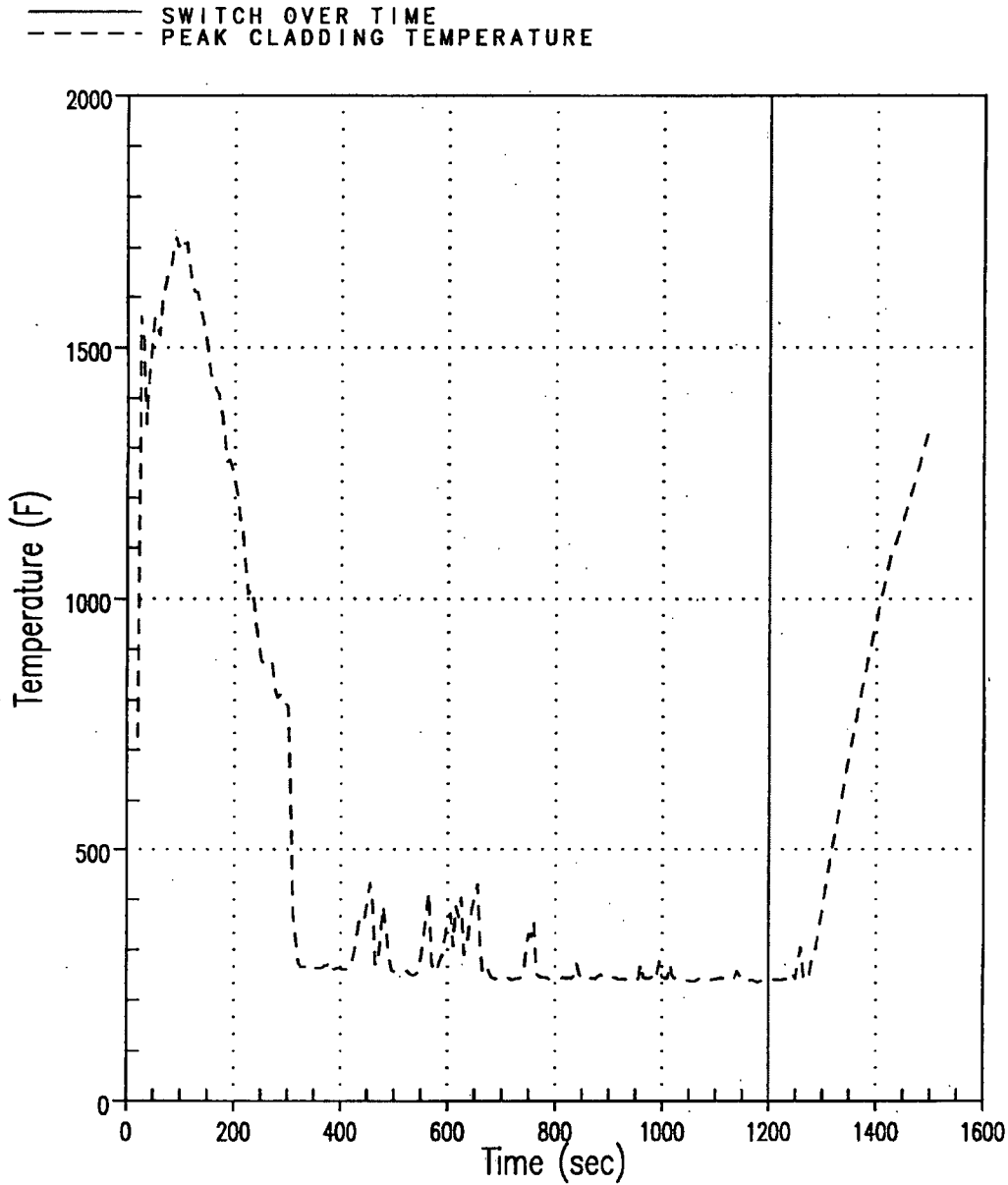
441943533

Figure 9: Integrated Core Flow vs. Core Boil-off for Channel 13 Flow Reduction 80% Case (Shifted Scale)



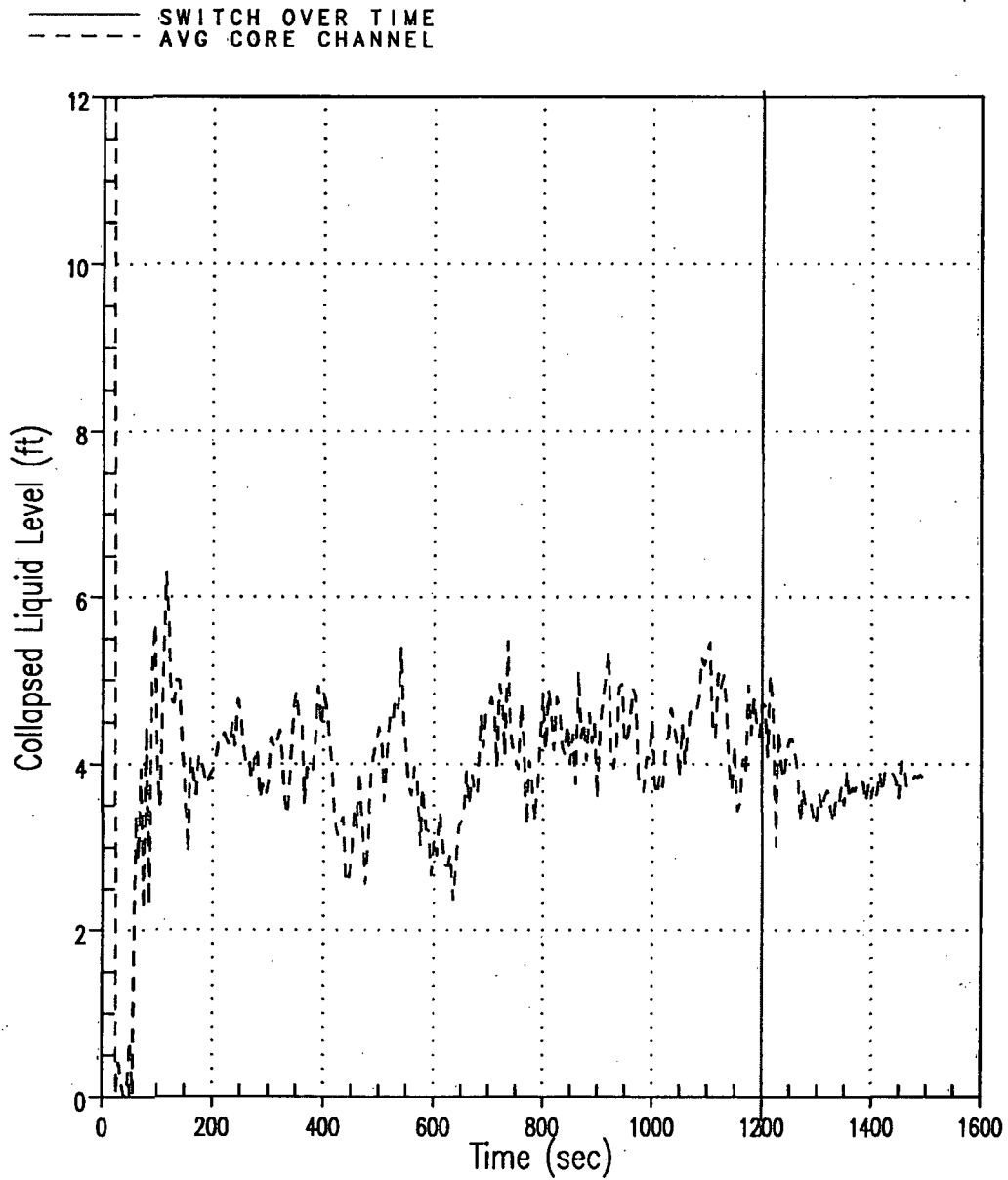
269992098

Figure 10: Total Integrated Liquid Flow at the Top of the Core for Channel 13 Flow Reduction 80% Case (Positive/Outlet flow represents HA, GT, AVG channels; Negative/Inlet flow represent LP channel)



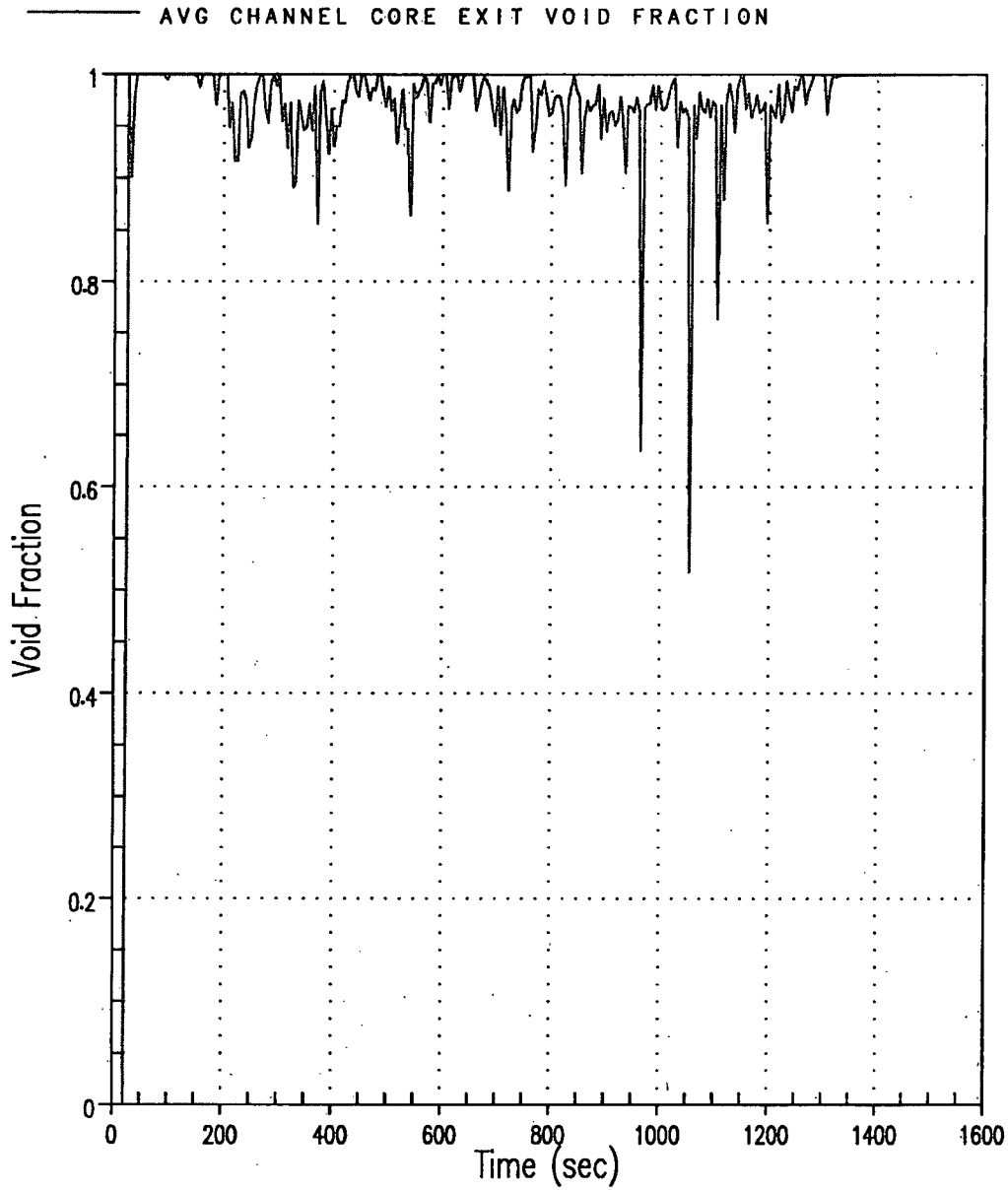
858292612

Figure 11: Hot Rod PCT for Channel 13 Flow Reduction 80% Case



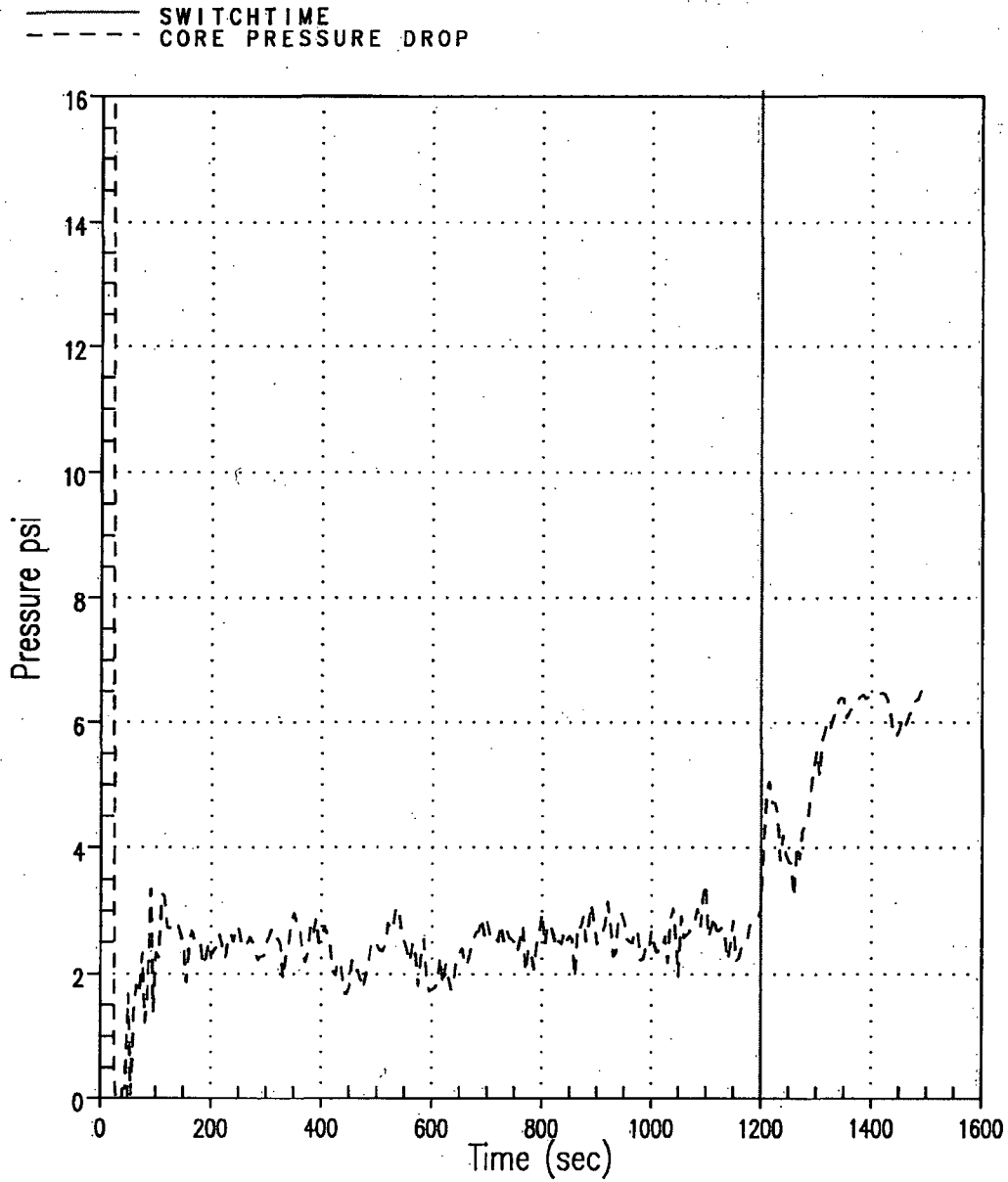
2061668183

Figure 12: Average Core Channel Collapsed Liquid Level for Channel 13 Flow Reduction 80% Case



1088718945

Figure 13: Void Fraction at the Exit of the Average Core Channel for Channel 13 Flow Reduction 80% Case



301250483

Figure 14: Core Pressure Drop for Channel 13 Flow Reduction 80% Case

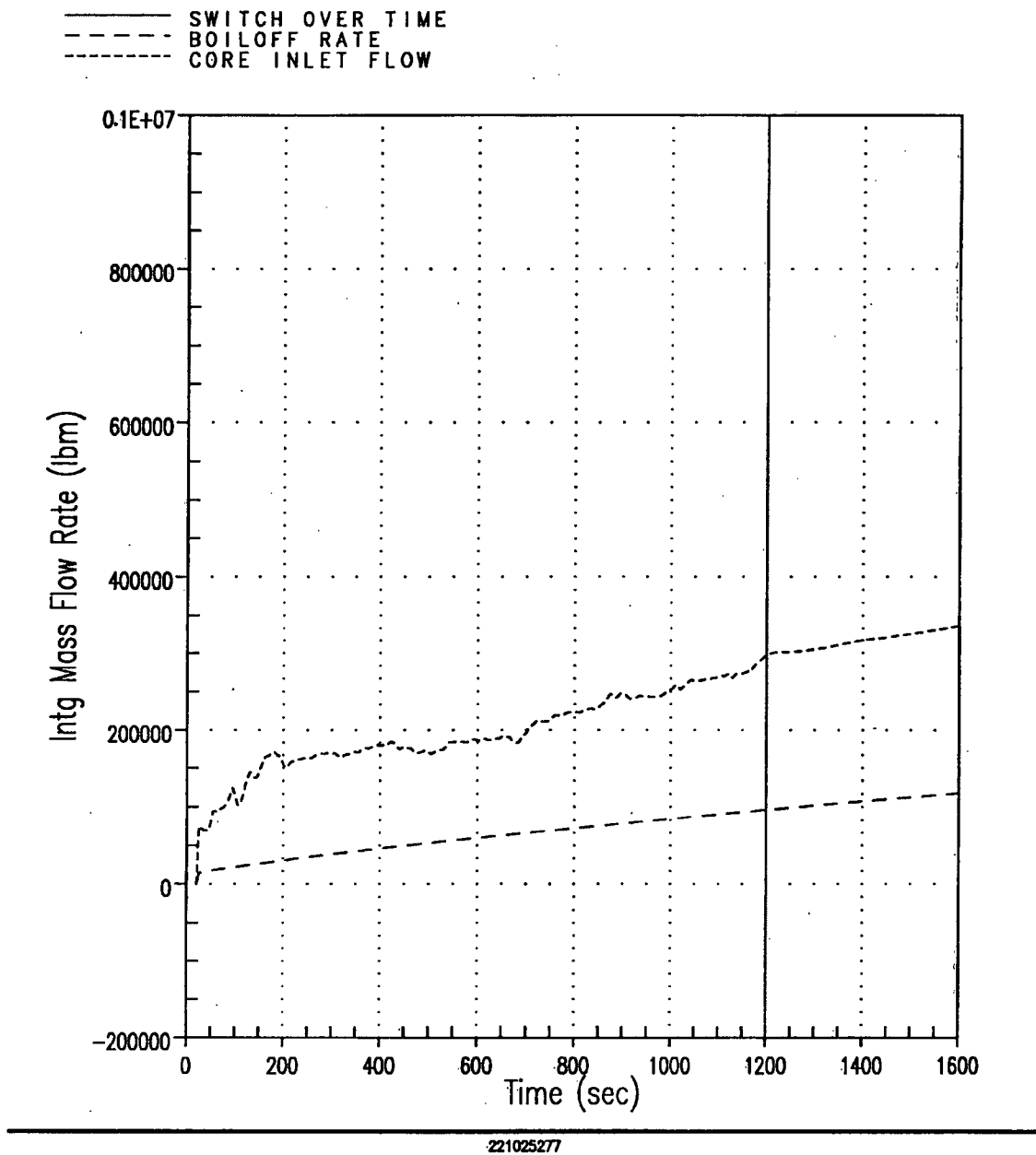
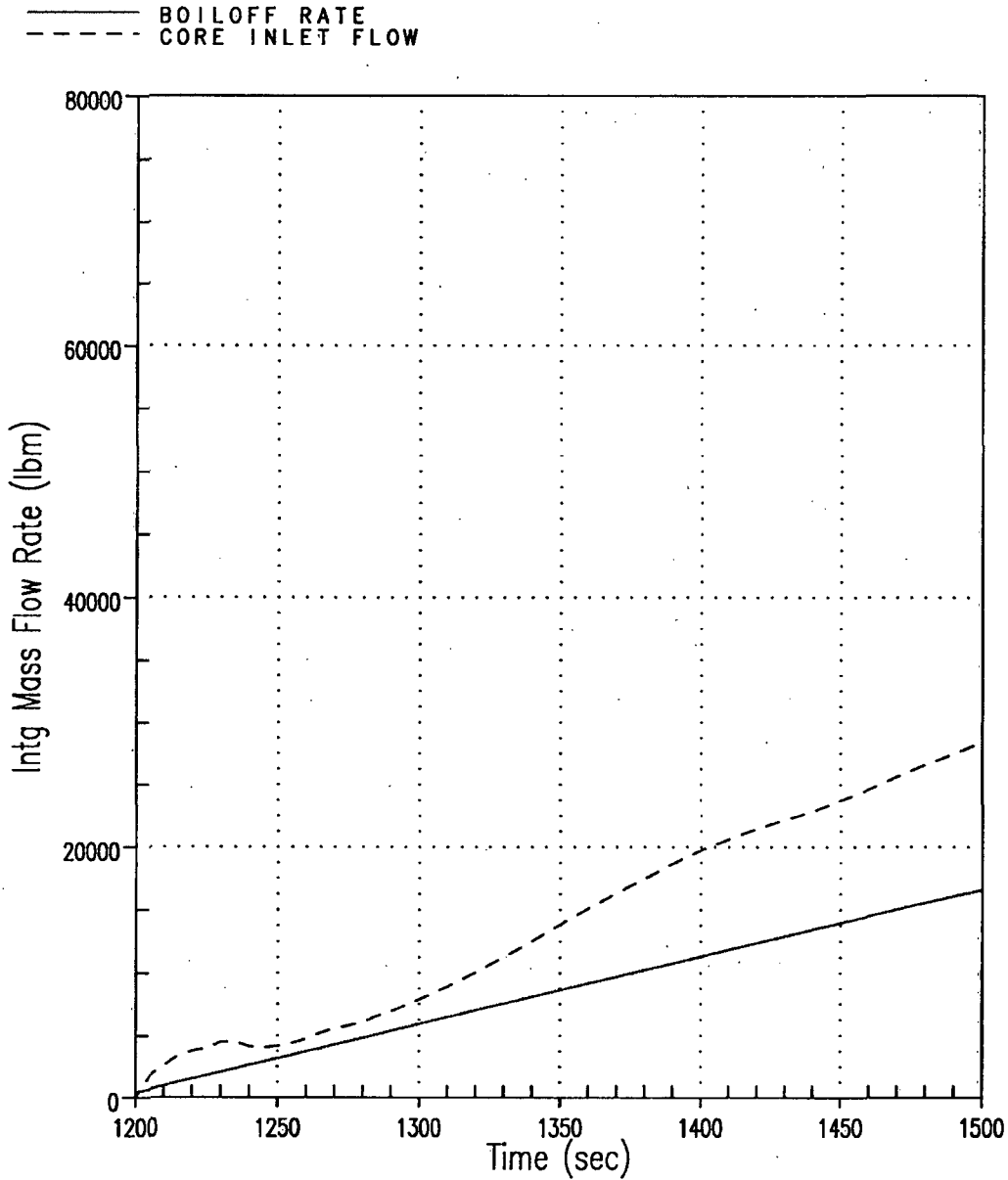
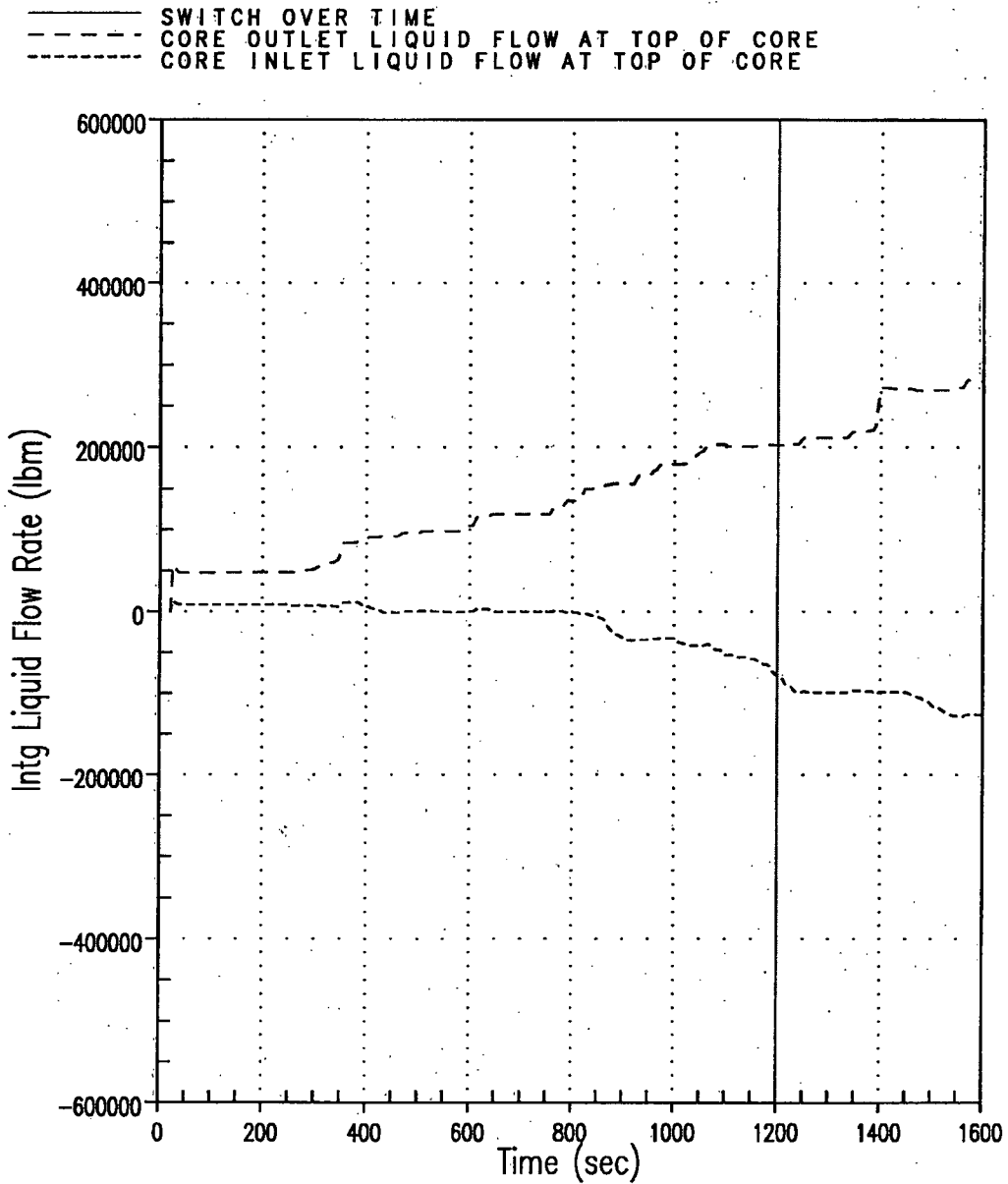


Figure 15: Integrated Core Flow vs. Core Boil-off for Uniform $C_D = 50,000$ Case



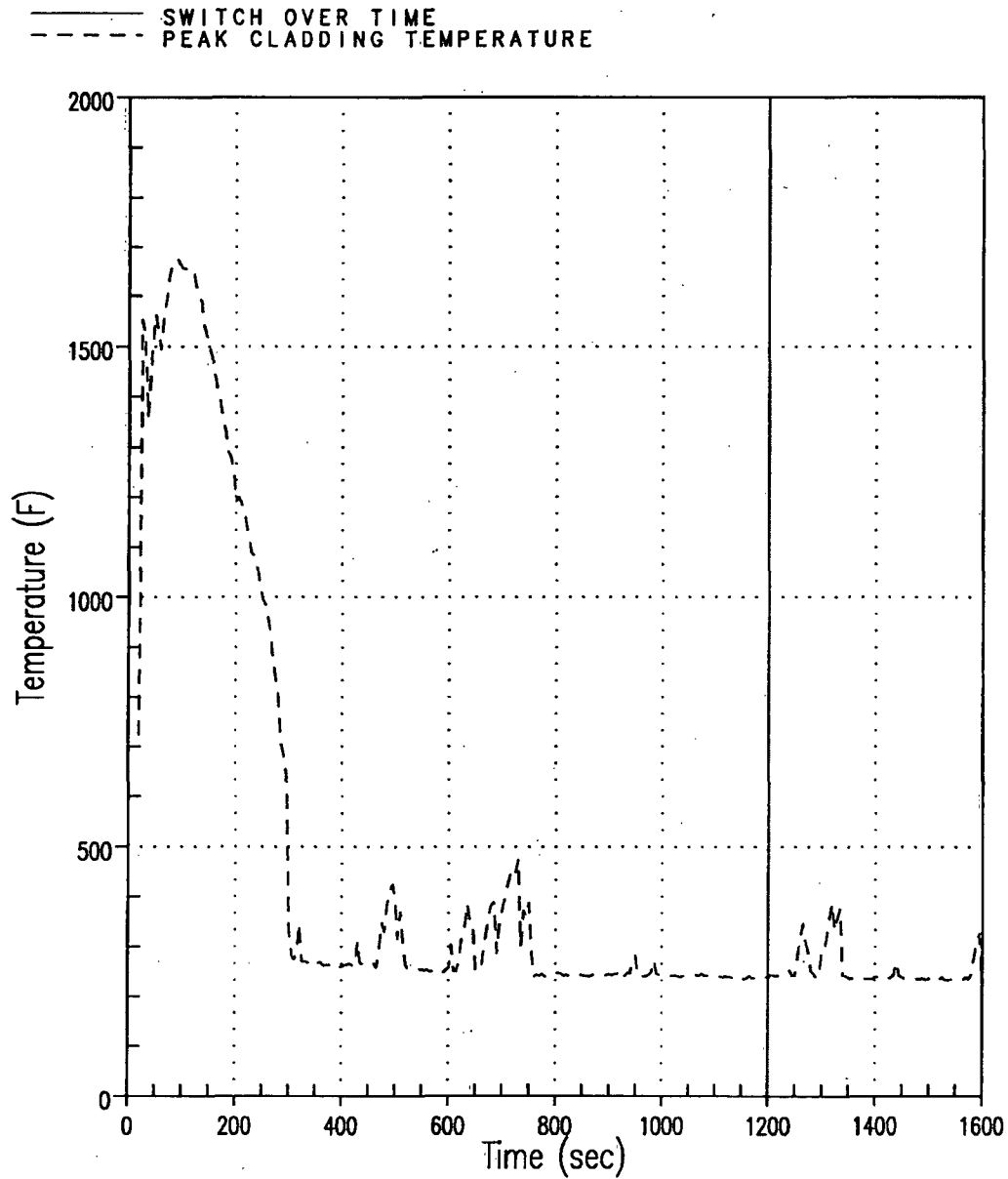
221025277

Figure 16: Integrated Core Flow vs. Core Boil-off for Uniform $C_D = 50,000$ Case (Shifted Scale)



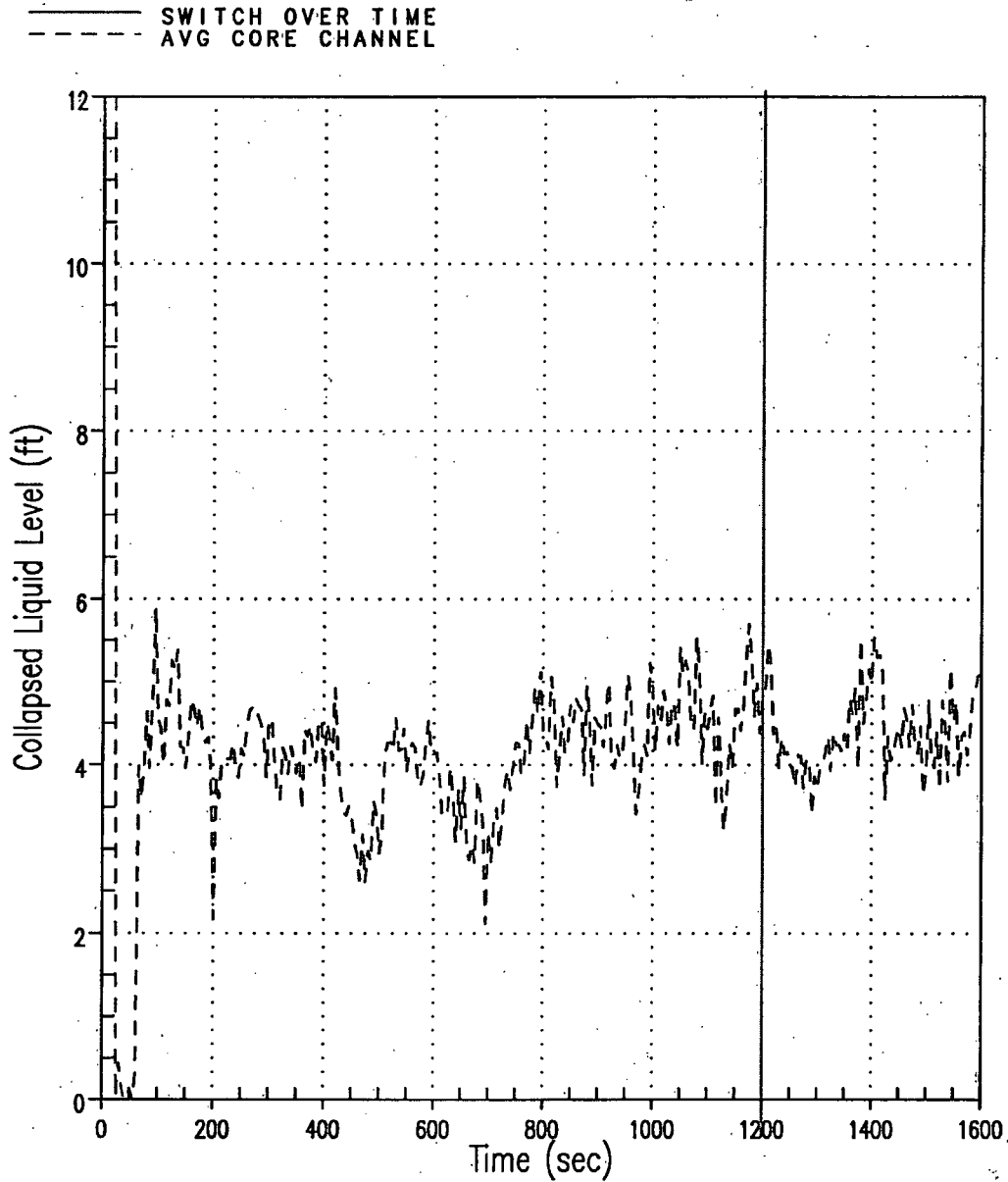
1745042723

Figure 17: Total Integrated Liquid Flow at the Top of the Core for Uniform $C_D = 50,000$ Case (Positive/Outlet flow represents HA, GT, AVG channels; Negative/Inlet flow represent LP channel)



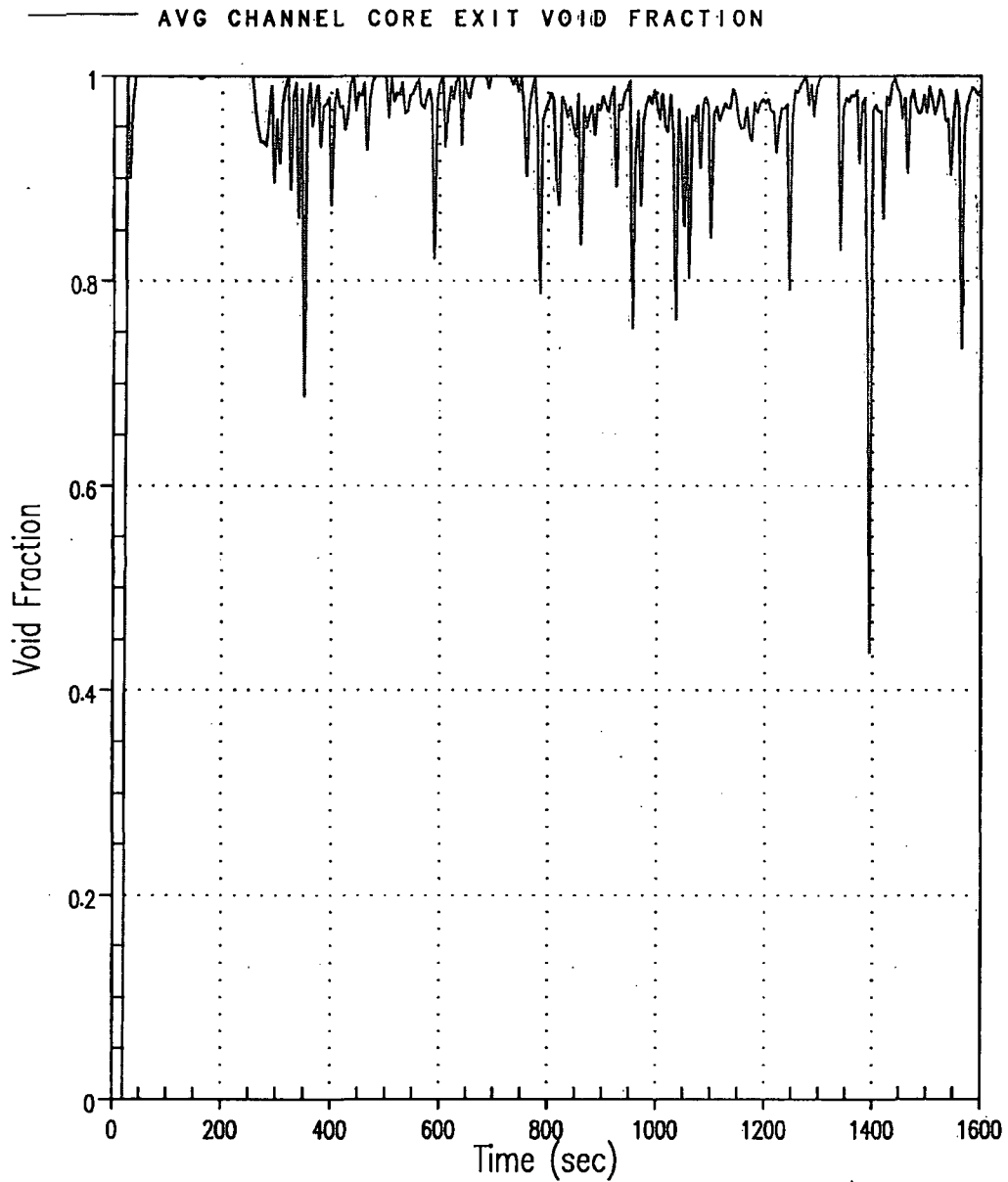
1912580093

Figure 18: Hot Rod PCT for Uniform $C_D = 50,000$ Case



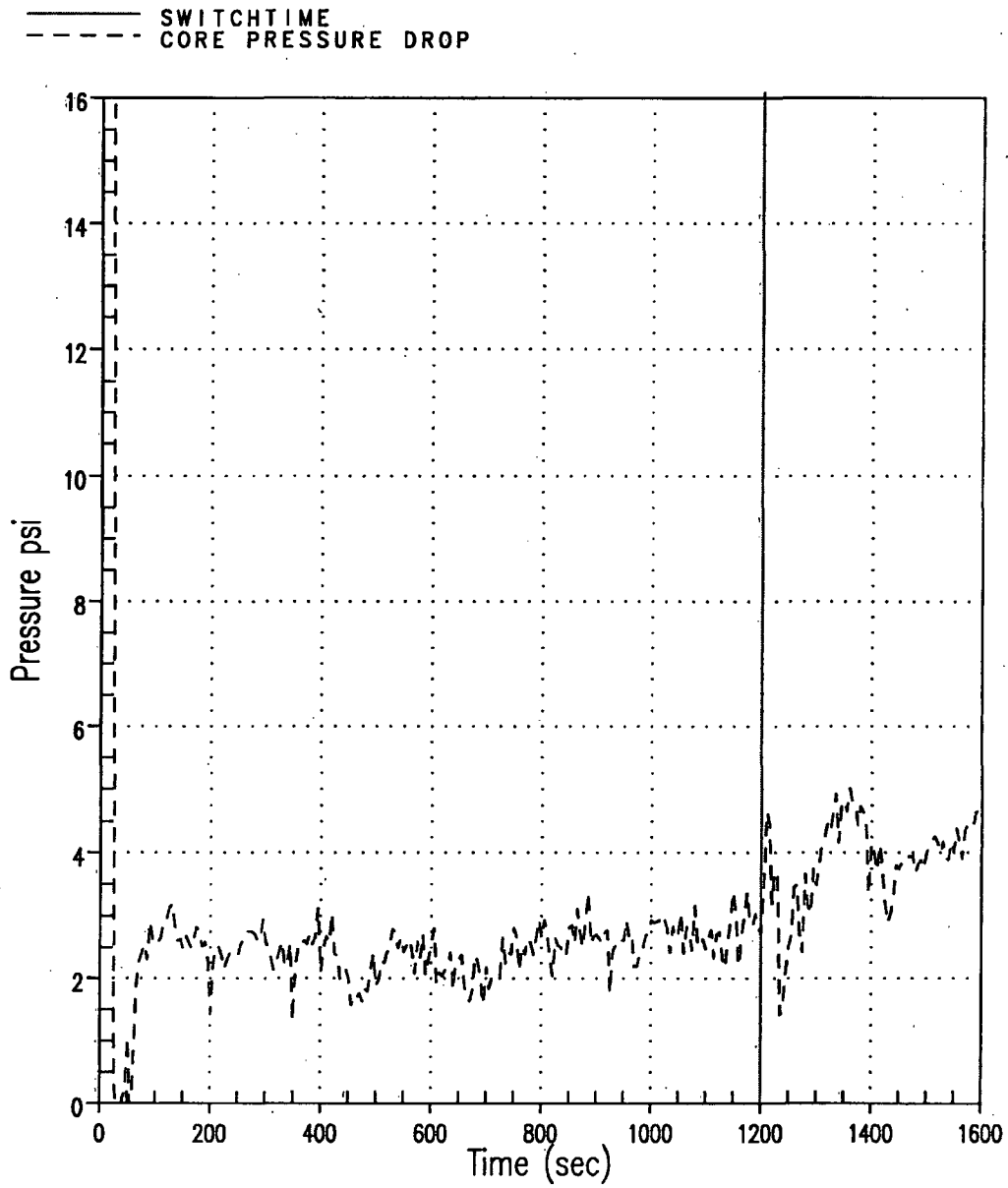
428299048

Figure 19: Average Core Channel Collapsed Liquid Level for Uniform $C_D = 50,000$ Case



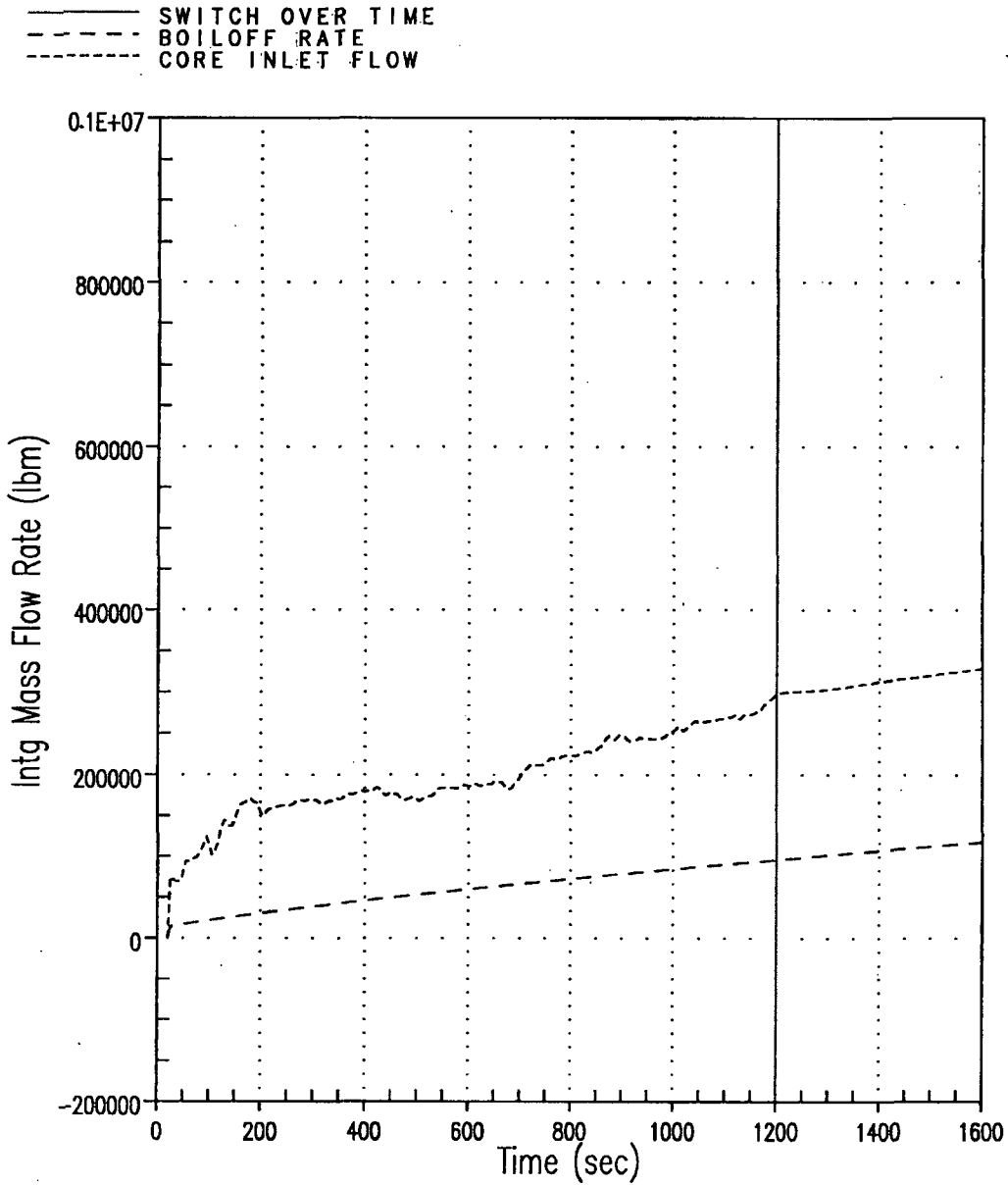
354120919

Figure 20: Void Fraction at the Exit of the Average Core Channel for Uniform $C_D = 50,000$ Case



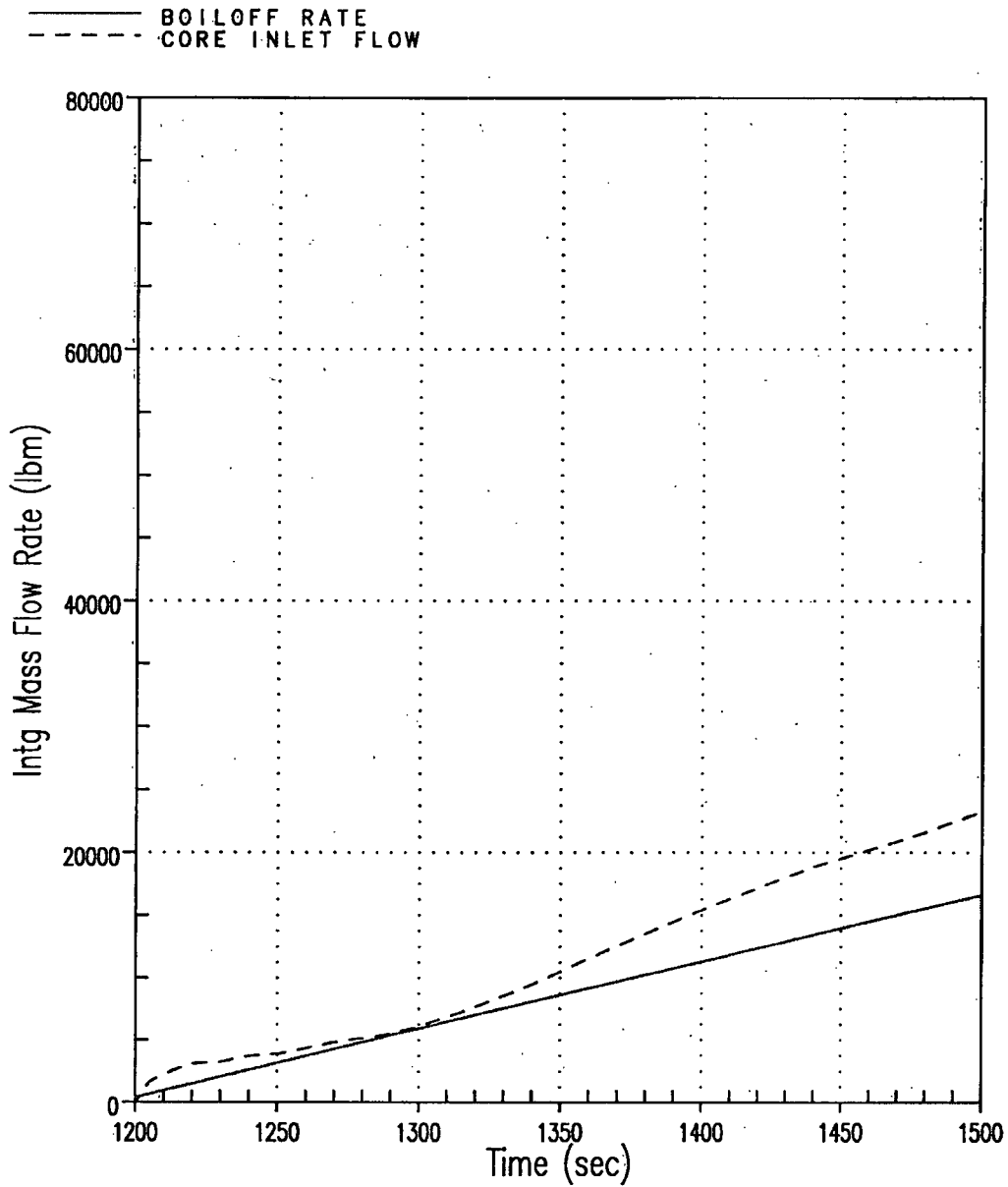
321274172

Figure 21: Core Pressure Drop for Uniform $C_D = 50,000$ Case



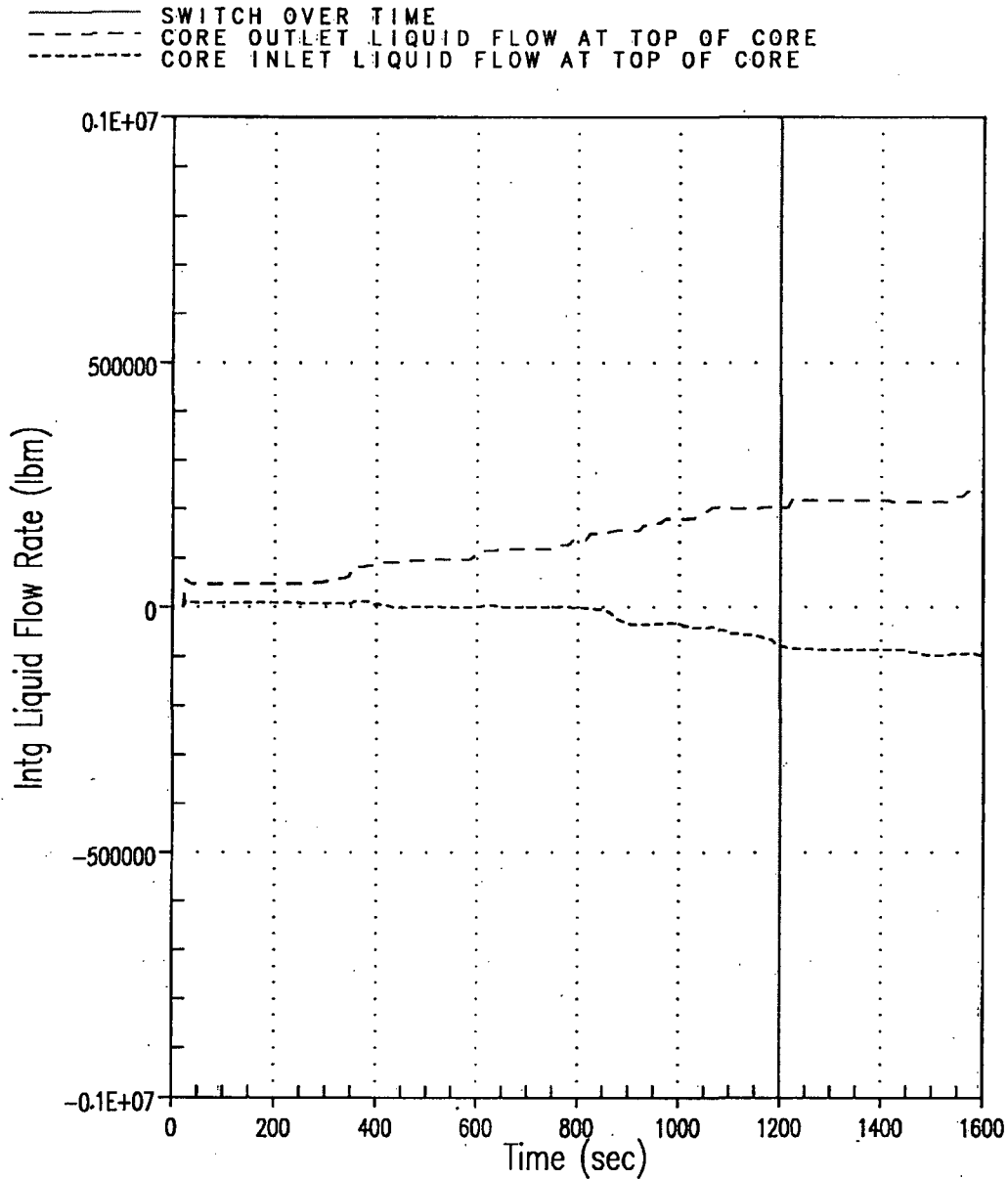
913425722

Figure 22: Integrated Core Flow vs. Core Boil-off for Uniform $C_D = 100,000$ Case



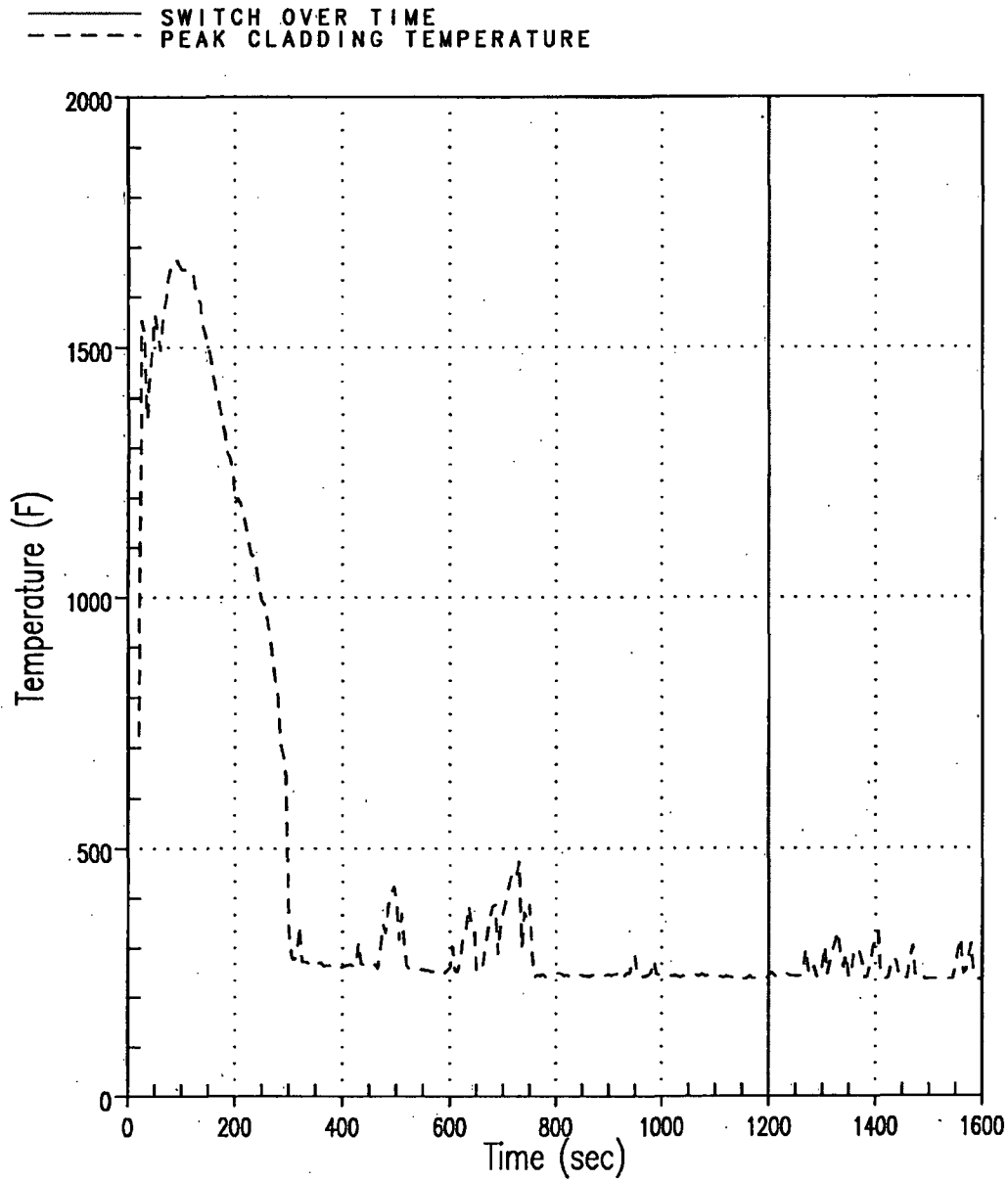
913425722

Figure 23: Integrated Core Flow vs. Core Boil-off for Uniform $C_D = 100,000$ Case (Shifted Scale)



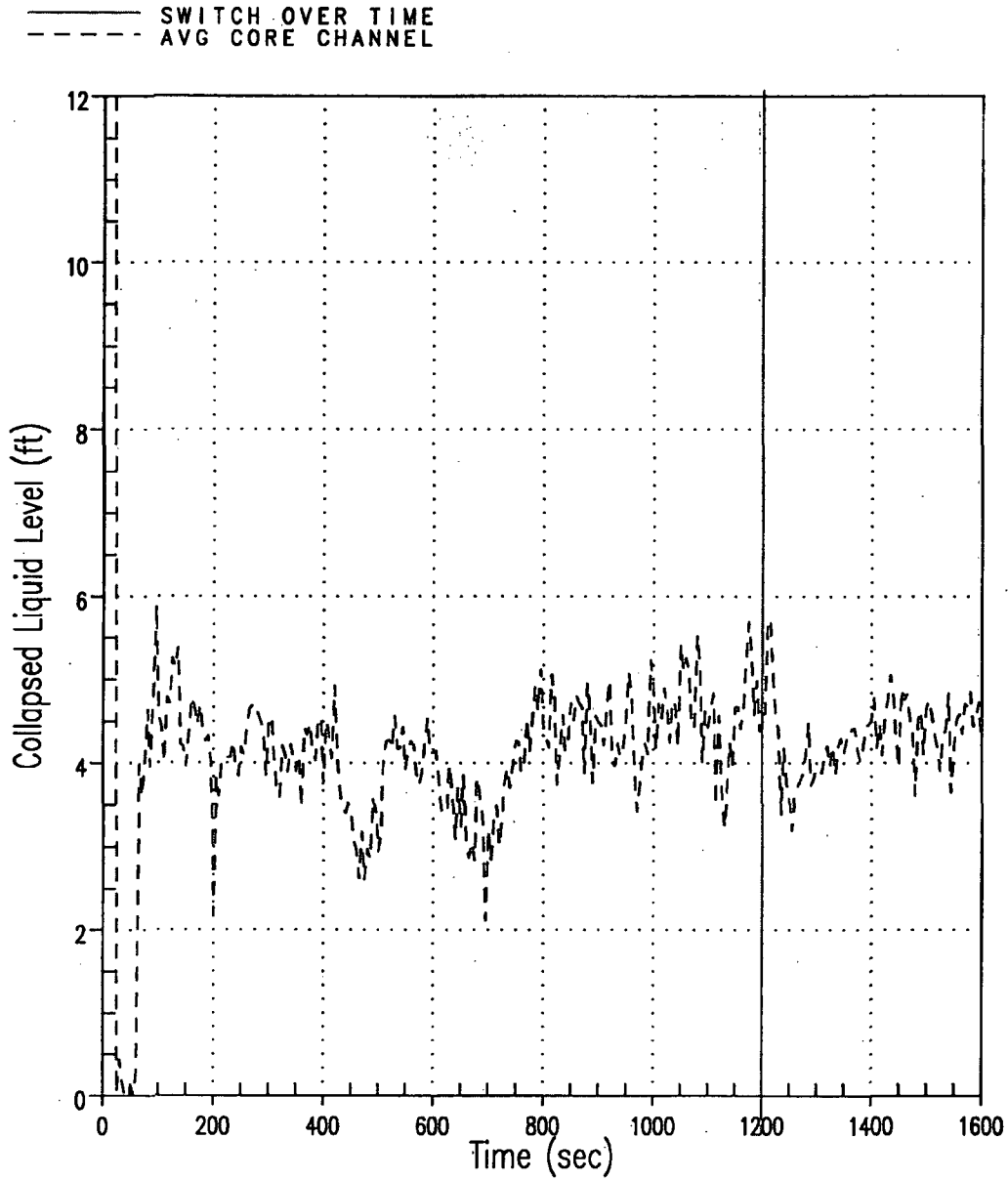
1072306012

Figure 24: Total Integrated Liquid Flow at the Top of the Core for Uniform $C_D = 100,000$ Case (Positive/Outlet flow represents HA, GT, AVG channels; Negative/Inlet flow represent LP channel)



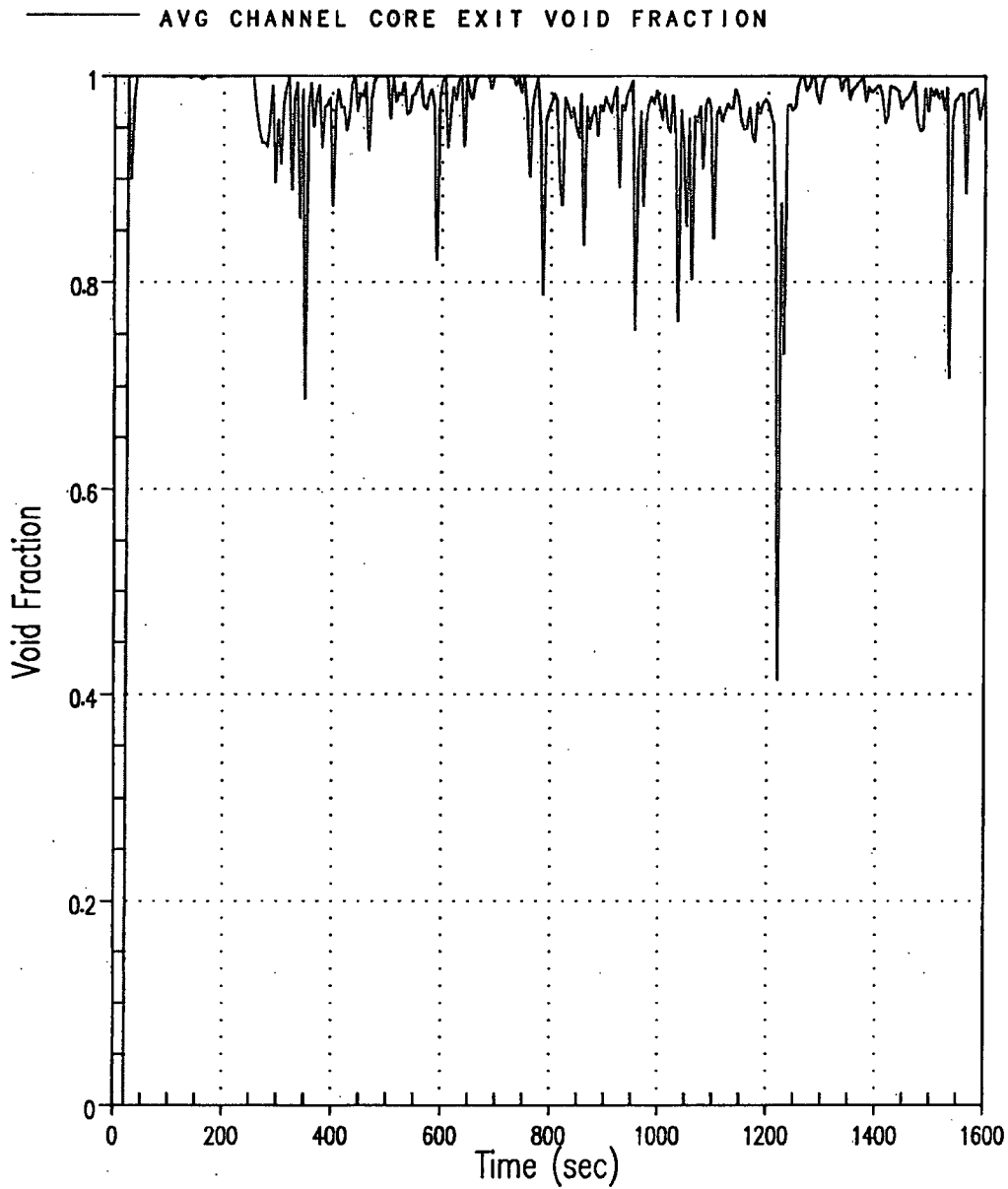
2013607248

Figure 25: Hot Rod PCT for Uniform $C_D = 100,000$ Case



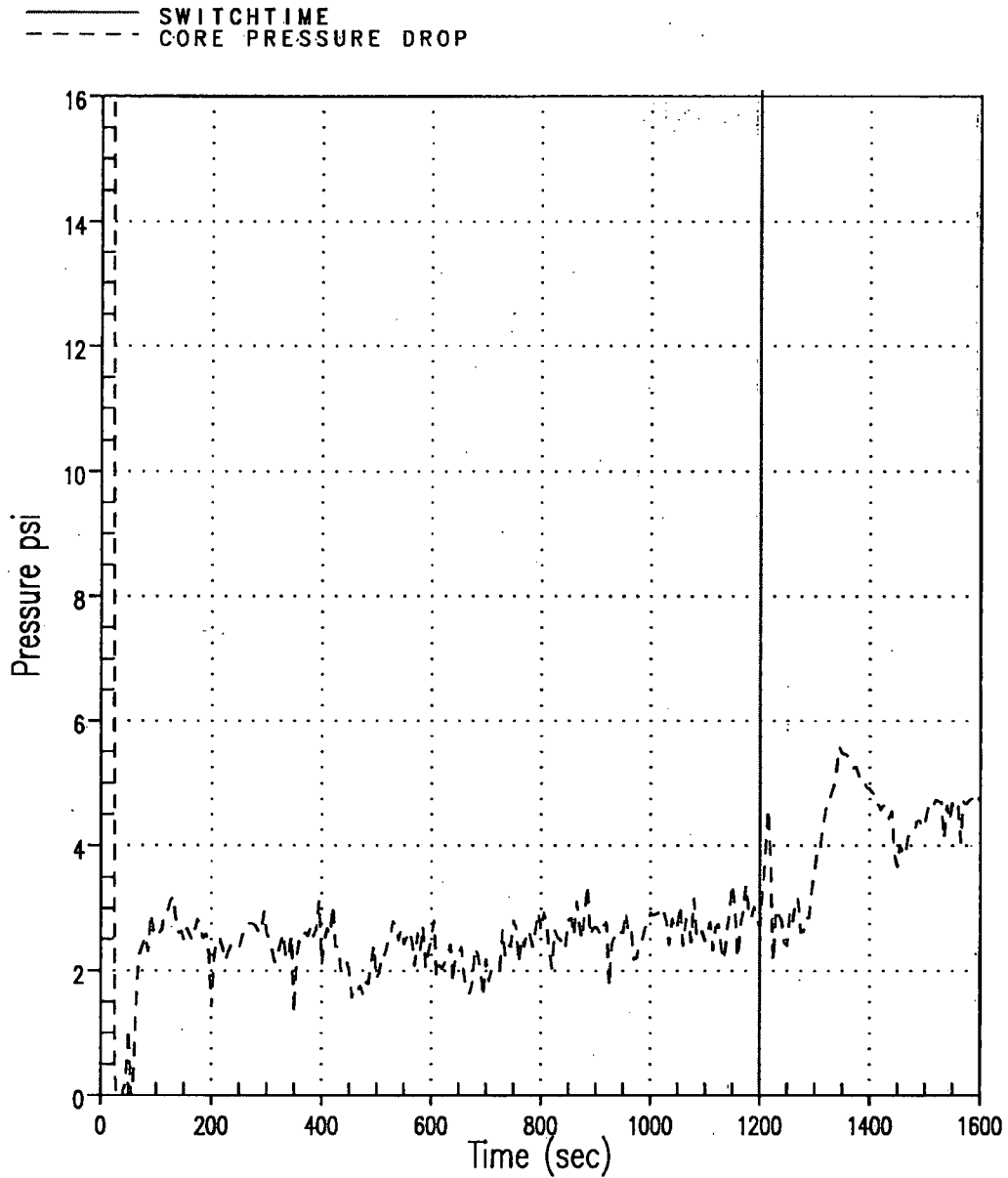
1470404378

Figure 26: Average Core Channel Collapsed Liquid Level for Uniform $C_D = 100,000$ Case



747525079

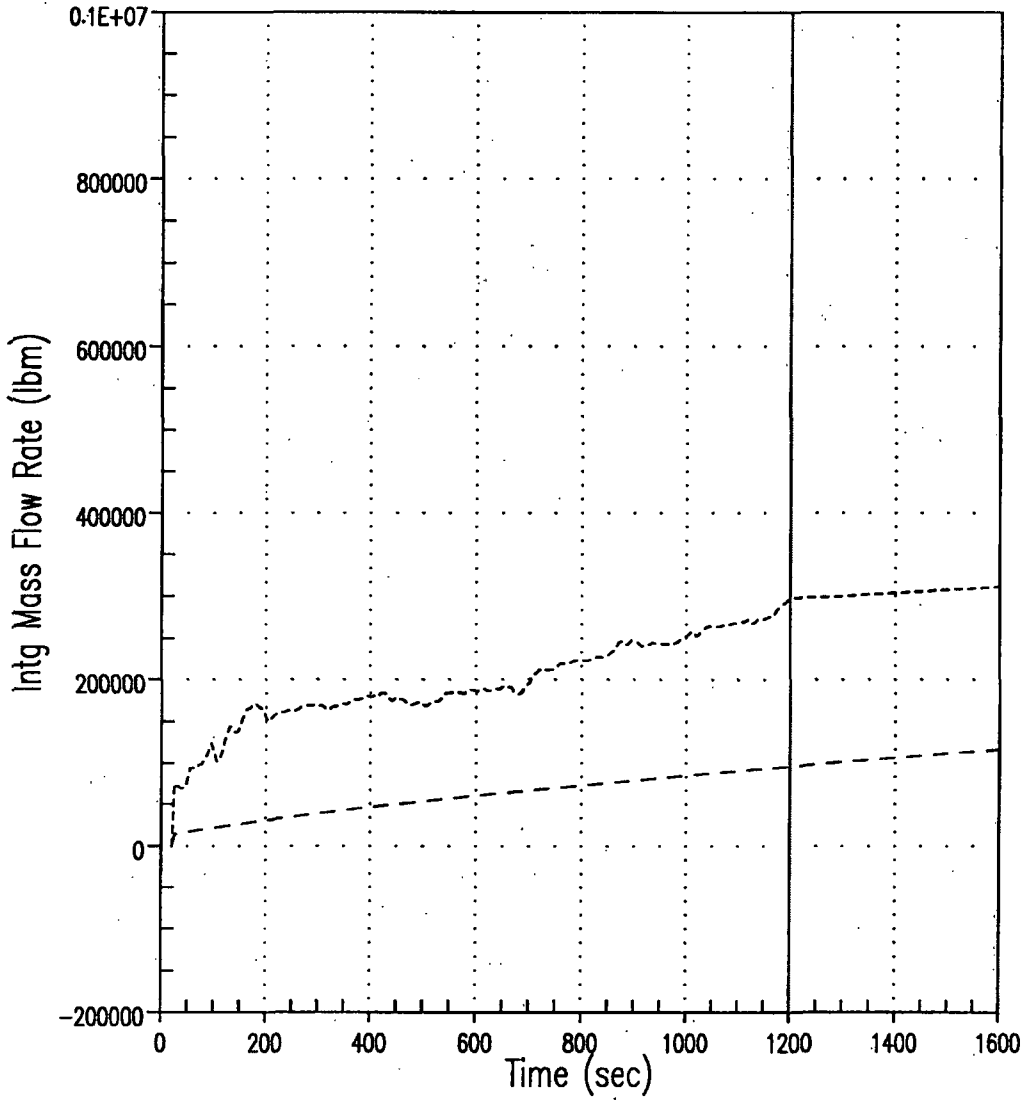
Figure 27: Void Fraction at the Exit of the Average Core Channel for Uniform $C_D = 100,000$ Case



1552950110

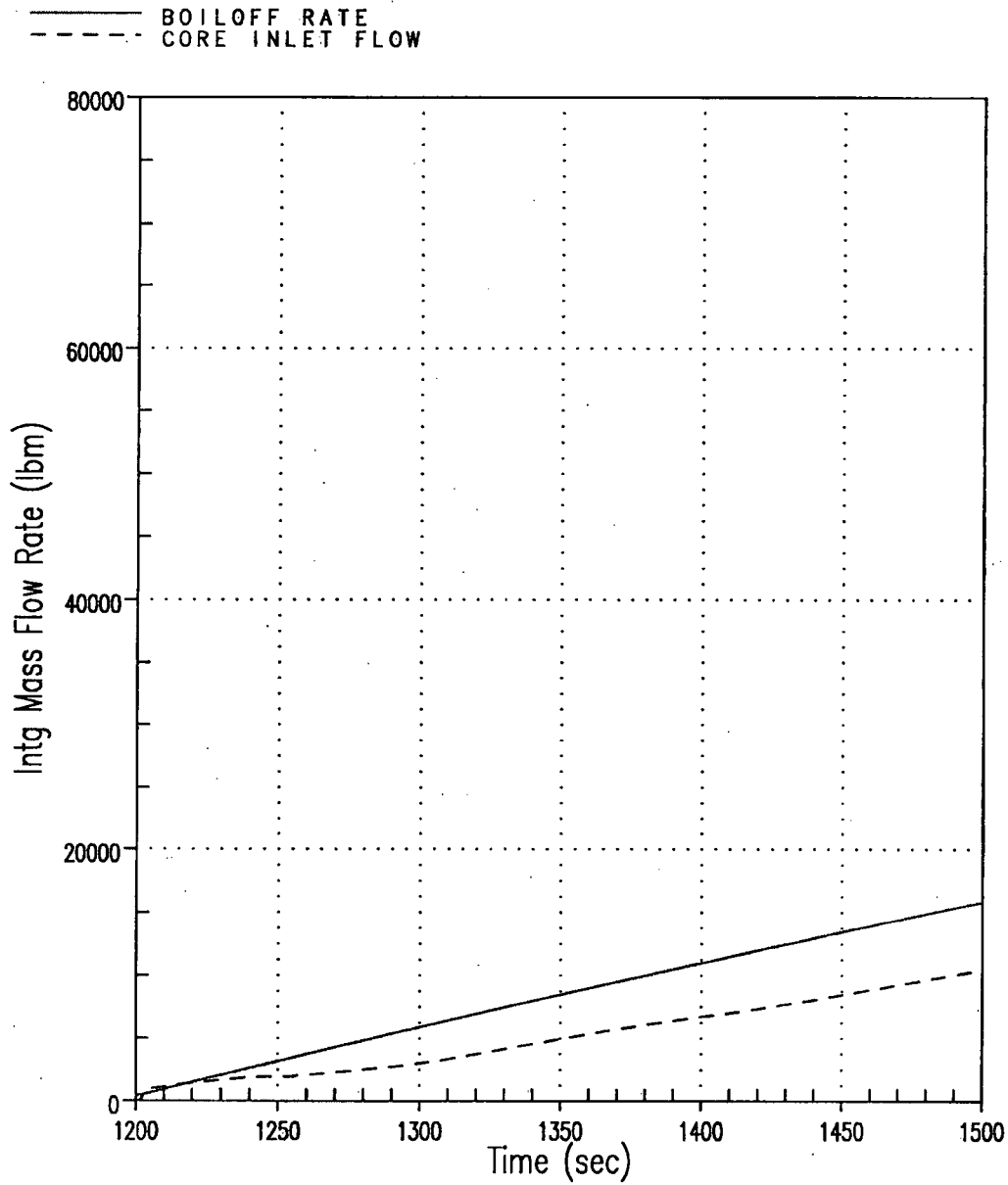
Figure 28: Core Pressure Drop for Uniform $C_D = 100,000$ Case

———— SWITCH OVER TIME
- - - - BOILOFF RATE
- - - - CORE INLET FLOW



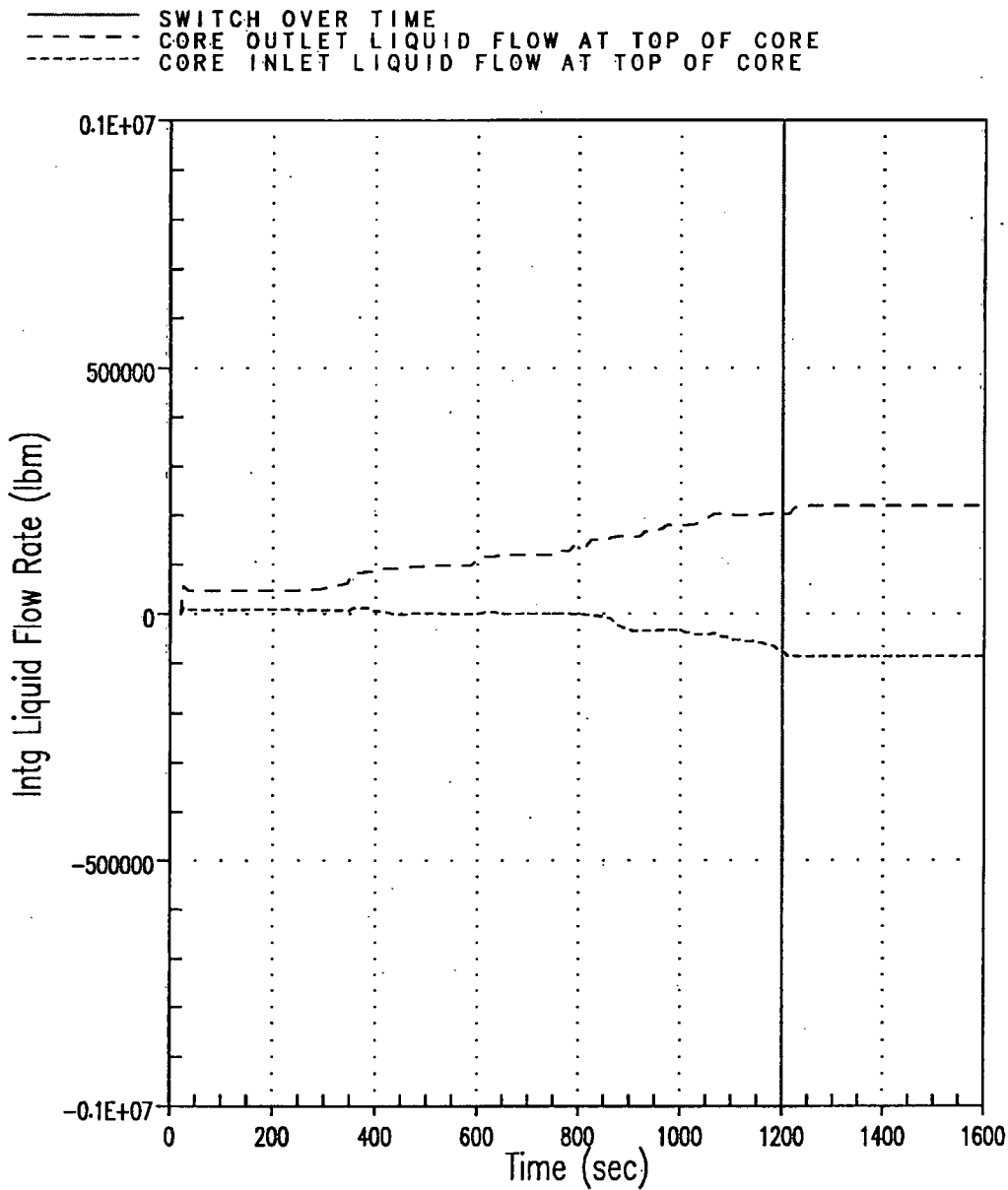
1628827304

Figure 29: Integrated Core Flow vs. Core Boil-off for Uniform $C_D = 1,000,000$ Case



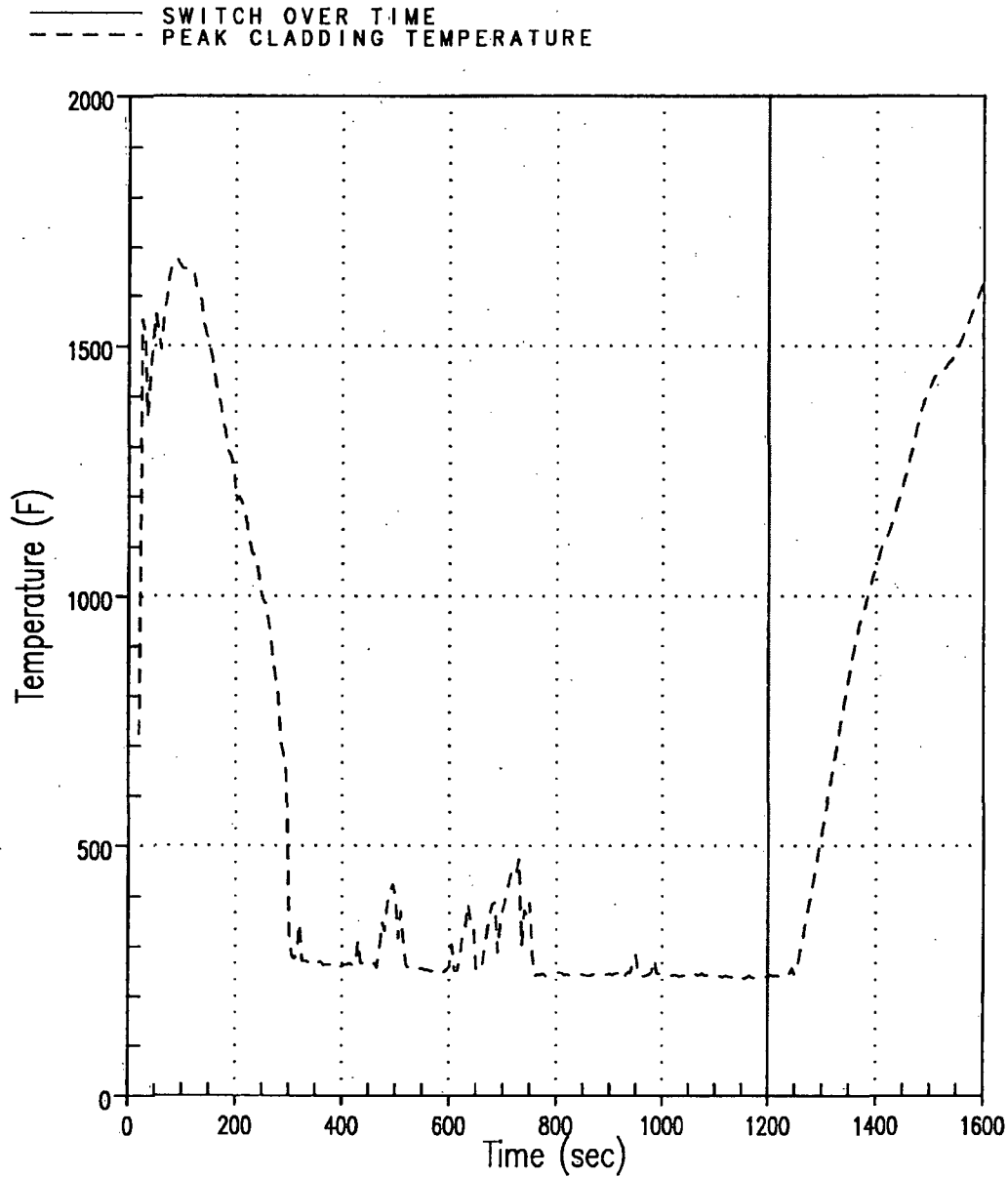
1628827304

Figure 30: Integrated Core Flow vs. Core Boil-off for Uniform $C_D = 1,000,000$ Case (Shifted Scale)



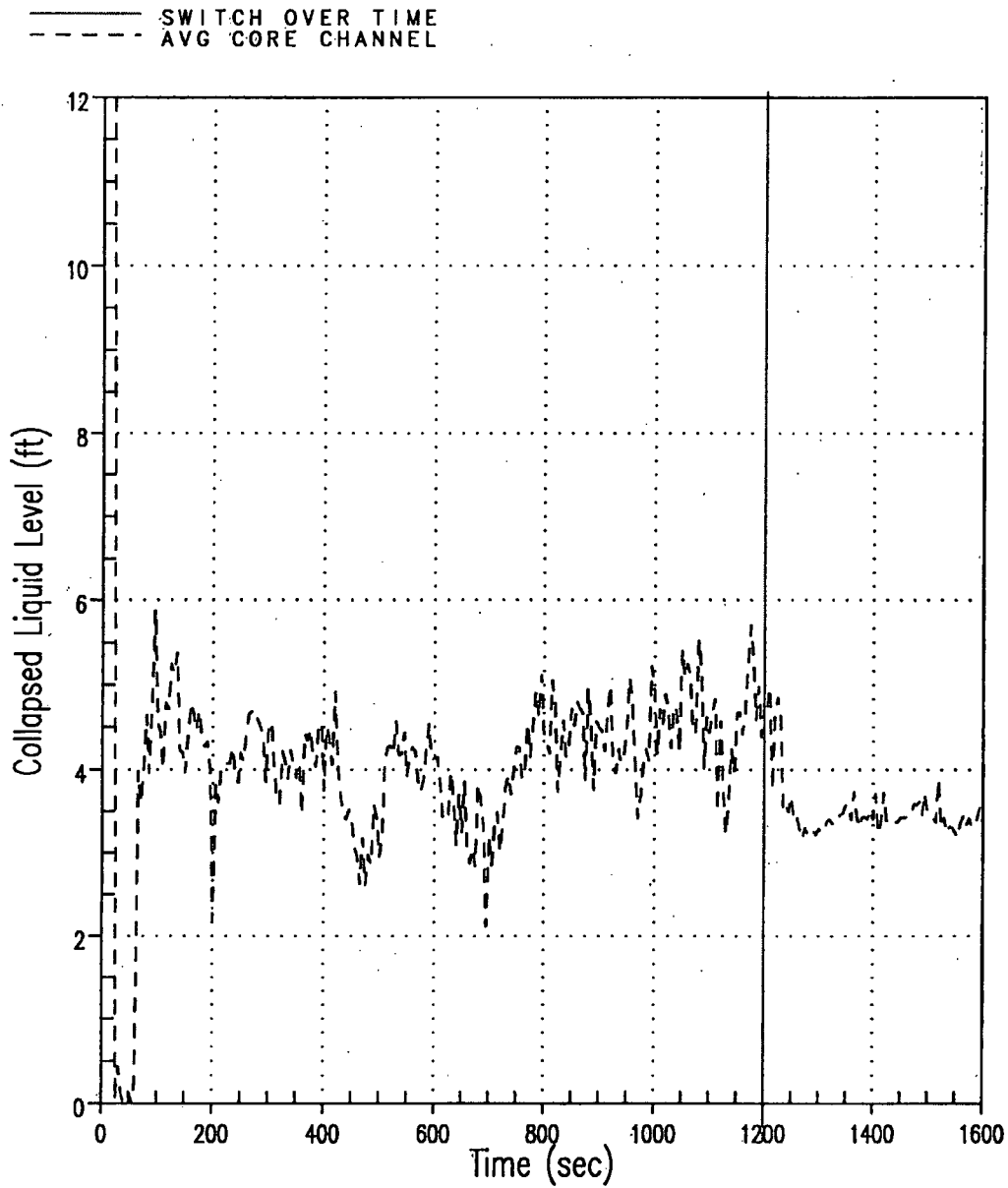
973451785

Figure 31: Total Integrated Liquid Flow at the Top of the Core for Uniform $C_D = 1,000,000$ Case (Positive/Outlet flow represents HA, GT, AVG channels; Negative/Inlet flow represent LP channel)



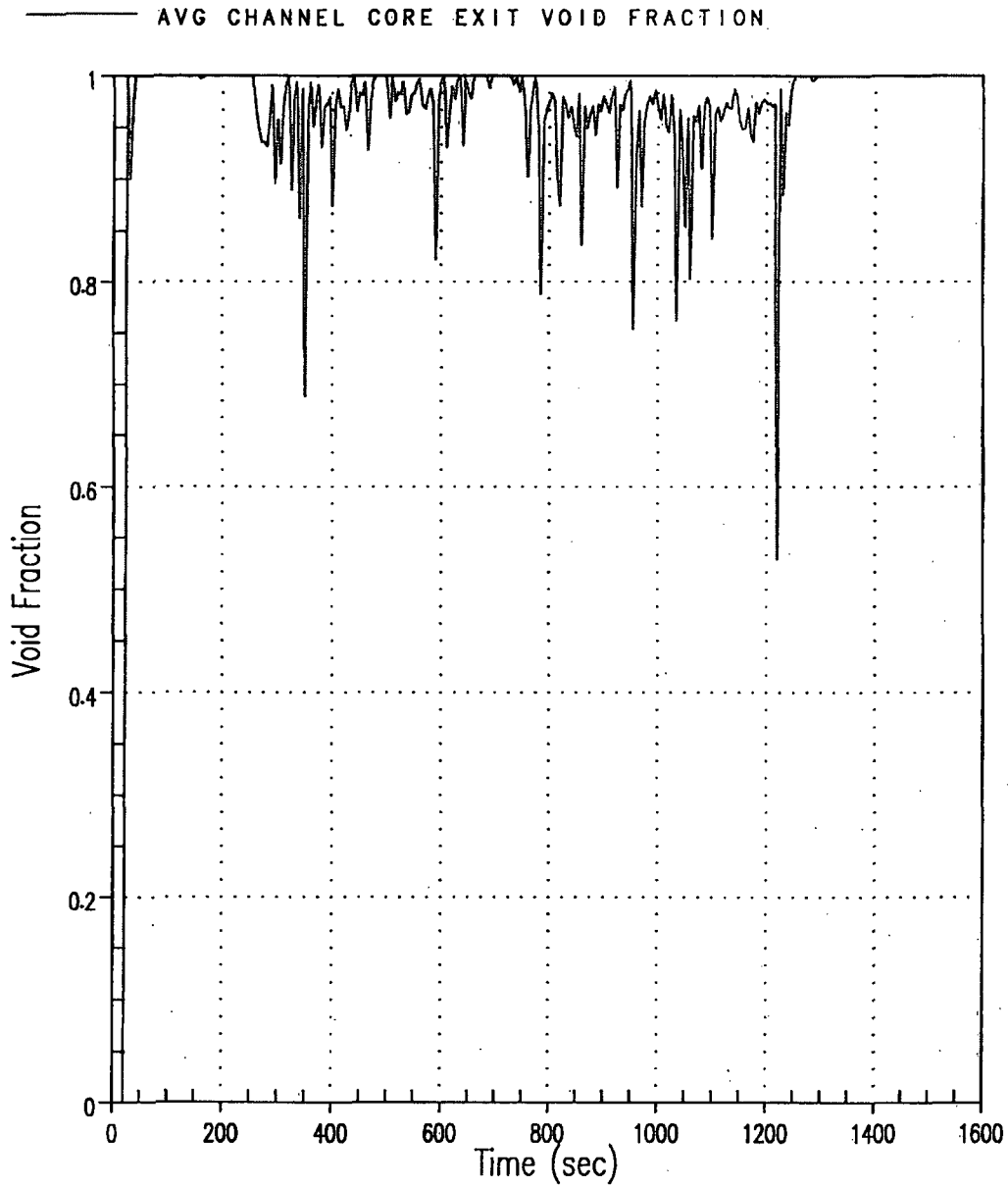
568586943

Figure 32: Hot Rod PCT for Uniform $C_D = 1,000,000$ Case



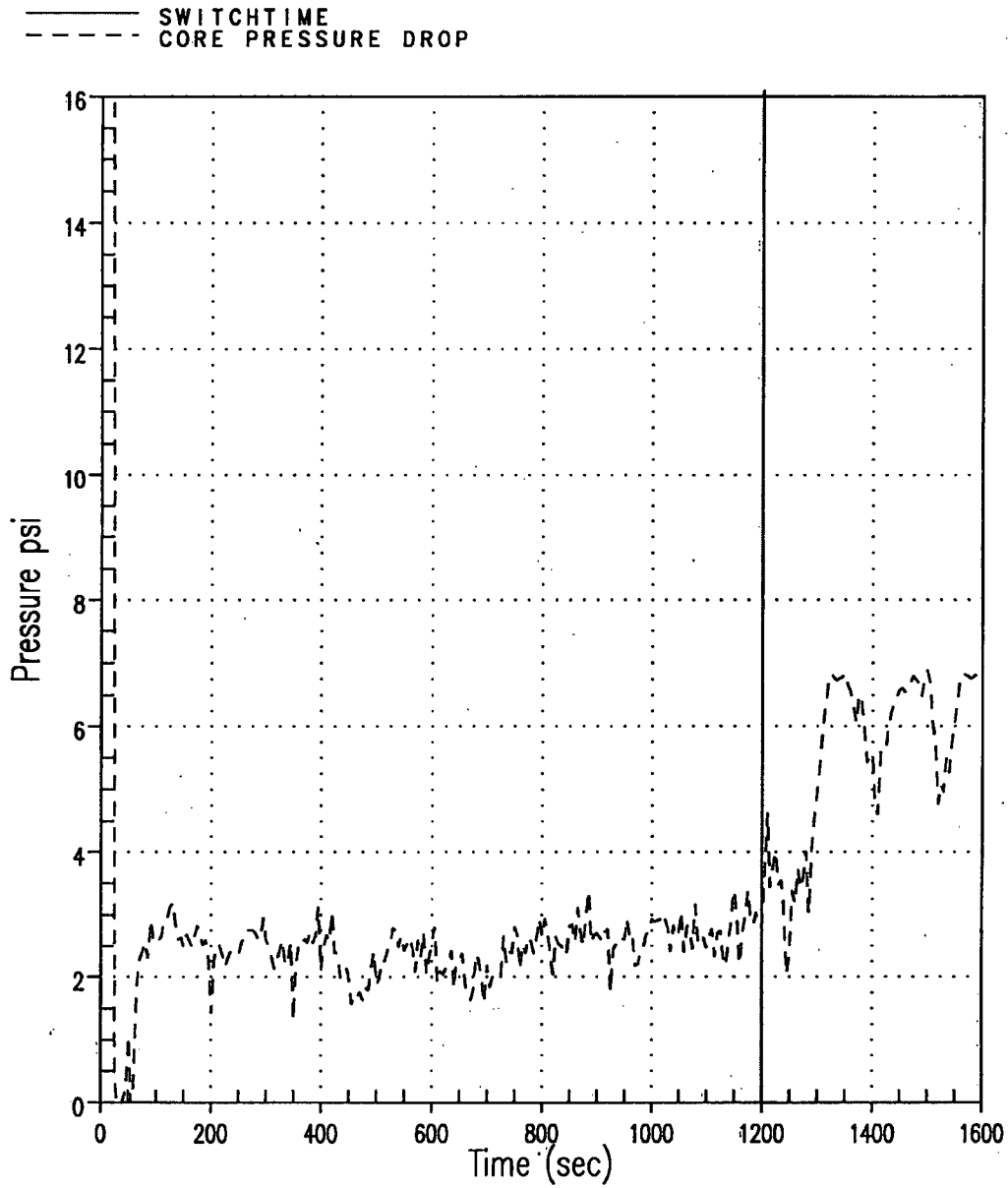
403478450

Figure 33: Average Core Channel Collapsed Liquid Level for Uniform $C_D = 1,000,000$ Case



1414870568

Figure 34: Void Fraction at the Exit of the Average Core Channel for Uniform $C_D = 1,000,000$ Case



1923232683

Figure 35: Core Pressure Drop for Uniform $C_D = 1,000,000$ Case

- 2) Please clarify the WCAP assumptions regarding local blockage due to debris buildup. First, when a debris buildup of 110 mils or 50 mils is assumed at a spacer grid, please describe the assumed circumferential or azimuthal coverage of that debris layer. Given recent test observations, please justify any assumptions of less than full coverage. If the debris buildup bridges fuel rods, state whether the two rod heat sources are simultaneously applied in the analysis. Second, please discuss the same considerations regarding the layer of oxide, crud, and precipitate debris build-up on the fuel rods between spacer grids. Third, tests observed by staff indicate that fiber, particulate, and chemical precipitates can completely fill the grid space between adjacent rods in the first fuel assembly spacer grid. Please describe the effect of this debris build-up on local heating of pins and confirm that this effect is addressed in WCAP 16793-NP local effects analysis.

RESPONSE:

The text of Appendix C, "Fuel Clad Heat-Up Behind Grids," of WCAP-16793-NP describes the model, assumptions and inputs used to calculate the heat-up behind the grids. This calculation was a parametric study to assess the impact of thickness and thermal conductivity of debris and the thickness of the deposition on cladding in the boiling region.

The simulation of debris being applied to the model was accomplished as follows:

1. The space between the clad and the grid was modeled as being filled with debris. This is stated in the fifth bulleted item of Section C.5, "Assumptions." The assumption used in this model was that, "no convection occurs under the grids in the fuel rod assembly." Thus, although the model of Appendix C predates recent testing performed by the PWR Owners Group, modeling the space between the clad and the grid as having no convection is representative of current fuel assembly debris capturing test observations.
2. The deposition on the clad between grids was parametrically evaluated by varying the thickness between 0 mils, or no deposition, and 50 mils, or the maximum deposition considered. The deposition was modeled as occurring between the spacer grids in the fuel model. A deposition thickness of 50 mils on each of two adjacent rods will not fill the gap between rods as the fuel rod spacing is at least 110 mils or greater.

Thus, in all of the parametric calculations, the model did not allow for convective heat transfer from the fuel rod considering blockage within the grid straps, regardless of the thickness of the deposition modeled. Likewise, no convective heat transfer was modeled on the surface of the grid strap.

Conduction through space between the fuel clad outside diameter and the grid strap was, however, modeled. The same thermal conductivity was assigned to this space as was assigned to the deposition thickness between adjacent fuel assemblies.

Due to symmetry and the assumption of adiabatic surfaces along grid straps, modeling adjacent fuel rods in a grid strap was unnecessary. The model accounted for no convection behind adjacent grid straps.

The calculations of Appendix C did not model either an oxide or a crud layer on the fuel. However, the calculations described in Appendix D did consider both 17% oxidation of the fuel and a 100 micron layer of crud on fuel in the span between grids. As described on Page C-8, the temperatures of the model of Appendix D yields temperature predictions between 15°F to 86°F greater than those of the model in Appendix C. The discussion also notes that additional conservatism were used in the calculations presented in Appendix D; the bulk fluid temperature and heat flux used in the calculations of Appendix D are 25°F warmer and 25% higher, respectively, than those used in Appendix C. Thus, even with the additional conservatisms used in the calculations of Appendix D, the peak clad temperature behind a grid will remain well below the 800°F limit defined in Appendix A.

Subsequent to receipt of this RAI, and in response to comments from the Advisory Committee on Reactor Safeguards (ACRS), the PWR Owners Group initiated prototypical fuel assembly (FA) testing to establish limits on the debris mass (particulate, fibrous and chemical) that could bypass the reactor containment building sump screen and not result in unacceptable head loss that would impede core inlet flow and challenge long-term core cooling of the core. An overall test protocol and specific test procedures were developed to ensure that possible thin bed effects were investigated, and debris types and characteristics expected in the RCS were represented. Debris loads used in the test were based on sump screen bypass information provided by licensees. The fuel assemblies used in these tests included intermediate spacer grids. The results of these tests will be integrated into Revision 1 of WCAP-16793-NP as they pertain to debris buildup at the spacer grids.

- 3) For each of the following items, please discuss how the evaluation methods presented in WCAP-16793 will ensure that each plant that uses the methods will not incur unacceptable blockage at the core inlet or within the core (at grid spacers), considering the following:
- The potential for filtering debris beds on horizontal downward facing surfaces at typical core inlet flow rates that have been observed during strainer and fuel inlet blockage testing.
 - Impacts of debris loading (fibrous, particulate, chemical).
 - Impacts of fuel inlet nozzle, protective filter, and spacer grid designs.
 - The potential impact of less than the maximum amount of postulated debris arriving at the core (thin bed). The staff believes that the potential for a fuel inlet thin bed is dependent on the protective filter above the inlet nozzle and the fuel inlet nozzle design, but has no test data to evaluate some of the designs. Filtering debris beds of less than 1/8 inch that have been observed during strainer testing.
 - Impacts of plant-specific flow rates and available head for postulated cold and hot leg breaks.
 - Justification for crediting settling in the lower plenum (if such credit is sought) based on lower plenum geometry, flow rates, and turbulence.

Please include a discussion of how each plant is bounded by the WCAP analyses or how the WCAP prescribed methods will ensure that the plants have adequate guidance to perform a plant-specific evaluation of core inlet blockage. To the extent the WCAP attempts to extrapolate test results from one fuel assembly design to others, please provide the minimum and maximum fuel assembly inlet nozzle opening sizes including obstructions, such as due to spacer grids, for the fuel assembly designs involved. Please also include a description of the geometry of each fuel assembly inlet nozzle design in use, with dimensions, and identify the combinations of first fuel spacer-grid/inlet nozzle designs in use.

RESPONSE:

General Response:

Subsequent to receipt of this RAI, and in response to comments from the Advisory Committee on Reactor Safeguards (ACRS), the PWR Owners Group initiated prototypical fuel assembly (FA) testing to establish limits on the debris mass (particulate, fibrous and chemical) that could bypass the reactor containment building sump screen and not result in unacceptable head loss that would impede core inlet flow and challenge long-term core cooling of the core. An overall test protocol and specific test procedures were developed to ensure that possible thin bed effects were investigated, and debris types and characteristics expected in the RCS were represented. Debris loads used in the test were based on sump screen bypass information provided by licensees. The results of these tests will be integrated into Revision 1 of WCAP-16793-NP.

To use the results of this testing for closure of GSI-191, each plant will compare their plant-specific debris bypass load against the debris masses tested. Plants that have bypass debris loadings that are within the limits of the debris masses tested are bounded by the test. Several courses or actions have been identified for plants whose debris loads are outside of the limits tested. These actions include, but not limited to, reduction of problematic debris sources by removing or restraining the affected debris source or plant-specific fuel assembly testing.

The effects of differing fuel inlet nozzle designs were also considered in the test program. Both AREVA and Westinghouse have performed testing with their respective fuel inlet nozzles. Both vendors tested their various bottom nozzle designs and identified the limiting design (limiting was defined as the design

that provided for the maximum pressure drop at the same flow and debris loading conditions). Each fuel bundle tested also had prototypical grids above the bottom nozzle debris capturing design features. Thus, the test data obtained from testing takes into account the fuel inlet nozzle, protective filter design features, and spacer grid designs. Descriptions of the fuel components tested, including bottom nozzles and grids, will be provided in proprietary submittals describing the testing performed and the results obtained.

Specific Responses to Specific Questions:

- a. The ability of a model fuel assembly to capture fibrous, particulate and chemical surrogate debris has been tested with the objective of defining limits on the mass of debris that may bypass the reactor containment building sump screen and still provide for a sufficient low pressure drop across the model fuel assembly such that sufficient flow is provided to assure long-term core cooling requirements are satisfied. Plants that have bypass debris loadings that are within the limits of the debris masses tested are bounded by the test. Several courses or actions have been identified for plants whose debris loads are outside of the limits tested including, but not limited to, reduction of problematic debris sources by removing or restraining the affected debris source or plant-specific fuel assembly testing.
- b. Testing has been performed to demonstrate and assess the ability of a model fuel assembly to capture fibrous, particulate and chemical surrogate debris. Based on that testing, limits have been defined on the mass of debris that may bypass the reactor containment building sump screen and still provide for a sufficient low pressure drop across the model fuel assembly such that sufficient flow is provided to assure long-term core cooling requirements are satisfied. Plants that have bypass debris loadings that are within the limits of the debris masses tested are bounded by the test. Several courses or actions have been identified for plants whose debris loads are outside of the limits tested including, but not limited to, reduction of problematic debris sources by removing or restraining the affected debris source or plant-specific fuel assembly testing.
- c. The effects of differing fuel inlet nozzle designs have been assessed as both AREVA and Westinghouse have performed testing with their respective fuel inlet nozzles. Both vendors tested their various bottom nozzle designs and identified the limiting design (limiting was defined as the design that provided for the maximum pressure drop at the same flow and debris loading conditions). Both fuel bundles also had prototypical grids above the bottom nozzle debris capturing design features. Thus, the test data obtained from testing takes into account the fuel inlet nozzle, protective filter design features, and spacer grid designs. Plants that have bypass debris loadings that are within the limits of the debris masses tested are bounded by the test. Several courses or actions have been identified for plants whose debris loads are outside of the limits tested including, but not limited to, reduction of problematic debris sources by removing or restraining the affected debris source or plant-specific fuel assembly testing.
- d. Testing was performed using the NRC March 2008 protocol of adding all particulate debris, then beginning to add the fibrous debris in small quantities so as to provide for the formation of a thin bed. Westinghouse performed several tests in this manner, with the NRC staff observing on such test. In all cases, NO thin bed was observed to form, even with very small quantities of fibrous debris. It was concluded by both the PWR Industry and the NRC that a thin bed was not likely to form.
- e. Testing has been performed to define limits on the mass of debris that may bypass the reactor containment building sump screen and still provide for a sufficient low pressure drop across the model fuel assembly such that sufficient flow is provided to assure long-term core cooling requirements are satisfied. Testing used maximum hot-leg flow rates and maximum particulate debris loading, then varied fibrous debris loading to establish a limit on the mass of particulate, fibrous and chemical surrogate debris that could be bypassed by the sump screen and still provide sufficient flow to provide for long-term core cooling. Plants that have bypass debris

loadings that are within the limits of the debris masses tested are bounded by the test. Several courses of actions have been identified for plants whose debris loads are outside of the limits tested including, but not limited to, reduction of problematic debris sources by removing or restraining the affected debris source or plant-specific fuel assembly testing.

Cold leg testing is being planned and the results will be reported in the next revision of WCAP-16793-NP.

- f. Credit for settling in the lower plenum is not being considered as part of the demonstration of long-term core cooling for GSI-191 closure in WCAP-16793-NP (Reference 1). However, credit for settling in the lower plenum may be considered, with appropriate and applicable justification, for other issues associated with the closure of GSI-191.

- 4) Please provide information on potential flow paths that could bypass the fuel inlet to provide cooling in the event the core inlet becomes fully blocked with debris. Specifically, discuss the potential alternate flow paths (e.g., location, number, and sizes) for coolant to reach the core in the event that a complete blockage at the core inlet occurred. If these flow paths are credited for passing water to the core, please justify that they will not become blocked with debris and that they will pass adequate flow to the core to maintain cooling. Please also justify that these bypass flows will not result in problematic debris build up in the core.

RESPONSE:

Subsequent to receipt of this RAI, and in response to comments from the Advisory Committee on Reactor Safeguards (ACRS), the PWR Owners Group initiated prototypical fuel assembly (FA) testing to establish limits on the debris mass (particulate, fibrous and chemical) that could bypass the reactor containment building sump screen and not result in unacceptable head loss that would impede core inlet flow and challenge long-term core cooling of the core. The effects of differing fuel inlet nozzle designs were also considered in the test program. Both AREVA and Westinghouse have performed testing with their respective fuel inlet nozzles. Both vendors tested their various bottom nozzle designs and identified the limiting design (limiting was defined as the design that provided for the maximum pressure drop at the same flow and debris loading conditions). Each fuel bundle tested also had prototypical grids above the bottom nozzle debris capturing design features. Thus, the test data obtained from testing takes into account the fuel inlet nozzle, protective filter design features, and spacer grid designs.

This testing identifies debris loading limits that preclude the core inlet from becoming fully blocked with debris. Thus, if the core debris loading of plants fall within the limits of the debris loads tested, the core inlet will not become fully blocked with debris. Therefore, alternate flow paths are not considered in applying WCAP-16793-NP and are not credited or utilized in establishing acceptable debris loading conditions for long-term core cooling.

Several courses or actions have been identified for plants whose debris loads are outside of the limits tested including, but not limited to, reduction of problematic debris sources by removing or restraining the affected debris source or plant-specific fuel assembly testing.

In the event that a plant should choose to credit alternate flow paths for long-term core cooling, the plant would be expected to identify the number, size, flow capability and potential for blockage of the flow paths they are crediting.

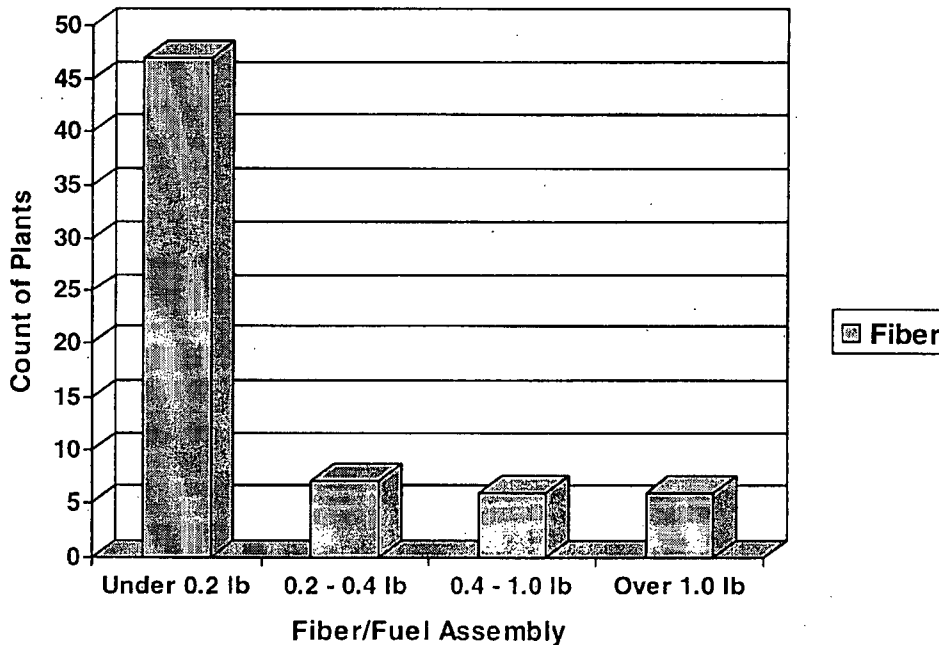
- 5) Please provide data that show the basis for the assumption that fibrous strainer bypass of 1 ft³/1000 ft² of strainer area provides a reasonable estimation of fiber bypass and that use of this number will not affect plant evaluations non-conservatively. Note that some protective fuel filters may be challenged by lower amounts of fiber (i.e. a thin bed) while some may be challenged by higher amounts. Please verify that these data were correlated with the area of the test strainer and that the results were not confounded by extrapolation to strainer areas less than the total of all strainers that may be in service during the event (i.e., strainer bypass estimates should assume all available strainer area is available for bypass).

RESPONSE:

Subsequent to receipt of this RAI, the PWROG initiated prototypical fuel assembly (FA) testing to establish limits on the debris mass (particulate, fibrous and chemical) to establish limits on the debris mass (particulate, fibrous and chemical) that could bypass the reactor containment building sump screen and not result in unacceptable head loss that would impede core inlet flow and challenge long-term core cooling of the core. The results of these tests will be integrated into Revision 1 of WCAP-16793-NP. As part of the effort to invoke this WCAP in the plant licensing basis, each plant will compare their plant-specific debris load against the masses tested. Therefore, the assumption of fibrous strainer bypass of 1 ft³/1000 ft² of strainer area is no longer relevant.

The assumption of fibrous strainer bypass of 1 ft³/1000 ft² of strainer area has been replaced by considering sump screen fiber bypass mass on a per fuel assembly basis. Total sump screen fiber bypass mass has been provided by licensees through a PWR Industry survey. This licensee-provided information was used to determine the amount of fibrous debris used in fuel assembly debris capture testing. The following chart shows the breakdown of bypass fibrous debris on a per fuel assembly basis for all plants that participated in the survey. The figure takes into account the number of fuel assemblies in the core of each plant reporting sump screen bypass values.

Figure 1: Survey Results of PWR Sump Screen Fibrous Debris Bypass



- 6) Please provide the following information for all fuel/core blockage tests that have been sponsored by the PWROG.
- a. flow rates and bases including any variation in the flow rate during testing
 - b. debris types and size distribution for all debris added
 - c. amounts of each type of debris added to each test or subtest
 - d. bases for amounts and sizes of debris added to each test or subtest
 - e. scaling information for debris amounts and test flow rates
 - f. information regarding the prototypicality or conservatism of test facility flow pattern and settlement
 - g. head loss value experienced for each test or subtest including time dependent plots if available
 - h. observations of debris transport and accumulation including any settling with differences noted at different flow rates
 - i. behavior of debris during testing (agglomeration)
 - j. test methodology and setup
 - k. details of debris preparation and introduction
 - l. order and rate of debris addition
 - m. dimensions of fuel inlet test mock-up
 - n. design of fuel protective filter modeled in the test
 - o. photographs as available to assist in understanding the tests theoretical debris bed thickness based on as-manufactured fiber density

RESPONSE:

Introduction:

Subsequent to receipt of this RAI, and in response to comments from the Advisory Committee on Reactor Safeguards (ACRS), the PWR Owners Group initiated prototypical fuel assembly (FA) testing to establish limits on the debris mass (particulate, fibrous and chemical) that could bypass the reactor containment building sump screen and not result in unacceptable head loss that would impede core inlet flow and challenge long-term core cooling of the core. An overall test protocol and specific test procedures were developed to ensure that possible thin bed effects were investigated, and debris types and characteristics expected in the RCS were represented. Debris loads used in the test were based on sump screen bypass information provided by licensees. The results of these tests will be integrated into Revision 1 of WCAP-16793-NP.

The effects of differing fuel inlet nozzle designs were also considered in the test program. Both AREVA and Westinghouse have performed testing with their respective fuel inlet nozzles. Both vendors tested their various bottom nozzle designs and identified the limiting design (limiting was defined as the design that provided for the maximum pressure drop at the same flow and debris loading conditions). Each fuel bundle tested also had prototypical grids above the bottom nozzle debris capturing design features. Thus, the test data obtained from testing takes into account the fuel inlet nozzle, protective filter design features, and spacer grid designs. Descriptions of the fuel components tested, including bottom nozzles and grids, will be provided in proprietary submittals describing the testing performed and the results obtained.

Testing was performed using bounding debris loads and hot leg break flow rates. These tests demonstrated that for the bounding debris loads tested, the hot-leg flow rate through the fuel assembly mock-up was maintained with acceptable pressure drops. The results of these tests will be integrated into Revision 1 of WCAP-16793-NP. To be responsive to this RAI, the following summary is provided.

Test Overview:

A full area, partial height fuel assembly equipped with various fuel filters was used for the testing. Each assembly included a number of intermediate spacer grids including at least one intermediate flow mixing (IFM) grid or equivalent. Debris laden water was introduced to the bottom of the test region and flowed up through a simulated lower plenum region, through the simulated core support plate, and through the fuel assembly. As debris caught on the fuel assembly, the differential pressure was measured across various locations including the bottom nozzle and individual grids as well as across the entire fuel assembly. The differential pressure measurements were used to determine an acceptable debris load. The test loop was intended to test the debris capture characteristics of a full-area fuel assembly under the debris loading conditions of a hypothetical LOCA.

The output of this test program will be a set of acceptance criteria. The acceptance criteria will define maximum debris masses which, if passed through the reactor containment building sump screen, will result in an acceptable pressure drop at the core inlet. For a given plant to demonstrate acceptable long term core cooling, it will need to show that each of the plant specific sump screen bypass masses are bounded by the limits in the acceptance criteria.

Test Loop Description:

This section addresses the following parts of the RAI:

- Description of fuel inlet test mock-up
- Flow rates and bases including any variation in the flow rate during testing
- Information regarding the prototypicality or conservatism of test facility flow pattern and settlement
- Design of fuel protective filter modeled in the test

AREVA and Westinghouse performed the fuel assembly tests at different locations. However, both test facilities took great lengths to ensure conformity between both test loops. The answer below applies to both facilities.

The Westinghouse test loop for testing the debris capture characteristics of a full-width fuel assembly is shown in Figure 1. A schematic of this test loop is given in Figure 2. The AREVA test loop is shown in Figure 3. The schematic of this test loop is shown in Figure 4. The test loop is composed of four main parts:

- Mixing tank system
- Recirculation system
- Test column
- Computer monitoring system

Mixing Tank System:

The mixing tank system includes a plastic tank, a temperature control system, and a mixing system. The mixing tank is where debris can be added during the test. The tank design and mixing system helps

preclude the settling and loss of debris on the bottom of the tank. The temperature of the water in the tank is controlled by either a heater element and/or by running water at a higher or lower temperature through a heater/chiller. The water temperature can be controlled from a low temperature of approximately 60°F to a high temperature of approximately 100°F, and the temperature of the water is measured continuously in the tank by a submerged thermocouple.

Recirculation System:

The recirculation system pumps the water from the tank, through the test column and back into the tank. A pump draws the water out of the bottom of the mixing tank. The recirculation system is continuous duty to accommodate longer tests.

Flow Rate:

Each test is performed at applicable hot-leg approach velocity. The bounding velocities below the core plate are:

- Westinghouse and B&W plants – 0.2 (+ 10%) feet per second.
- CE plants – 0.03 (+ 10%) feet per second (or 0.05 (+ 10%) feet per second for certain plants).

The flow rate is maintained during the test.

Test Column:

The test column contains the fuel assembly and simulates the geometry and many of the conditions that would be experienced inside of the reactor vessel. The test column includes a lower plenum region, a core support plate, the fuel assembly, and an upper plenum region. The debris laden water is introduced to the bottom of the lower plenum region. The design of this region is not prototypical of an RV lower plenum; it is designed instead to ensure that the debris remains well mixed in the fluid flow and precludes any debris settling, thereby ensuring that all debris introduced to the test column will reach the fuel assembly. The lower plenum region and the fuel assembly are divided by a simulated core support plate with 2.75" flow holes. The fuel assembly rests directly on this simulated core support plate. The region that contains the fuel assembly is made of Plexiglas for viewing during the test. This region is sized to represent the fuel assembly pitch for the test assembly that is being tested.

The debris and water enter through the bottom nozzle and flow up through the simulated core support plate. As debris catches on the fuel assembly, the differential pressure is measured constantly across the fuel filter as well as across the entire fuel assembly. There are extra ports available on the sides of the test column if a measure of the differential pressure across a specific portion of the fuel assembly as required.

Computer Monitoring System:

The computer monitoring system continuously records the following data:

- Temperature of the water in the mixing tank
- Flow rate
- Differential pressure measurements from ΔP gauges

This data can be recorded at a time interval chosen by the operator. The computer is also used to check the slope of the ΔP (pressure drop) or flow versus time graphs in order to determine if the curves have reached a point close enough to equilibrium.

Design of Fuel Protective Filter in the Test:

AREVA and Westinghouse performed tests with all relevant fuel filters.

Westinghouse*

- Fuel assembly with Westinghouse P-grid
- Fuel assembly with Guardian Grid

*Note: The alternate p-grid design was not tested as previous test results had concluded that the standard p-grid was the limiting design.

AREVA

- 17x17 fuel assembly with AREVA FUELGUARD™ Grid
- 17x17 fuel assembly with AREVA TRAPPER™ coarse mesh screen
- 17x17 fuel assembly with AREVA TRAPPER™ fine mesh screen

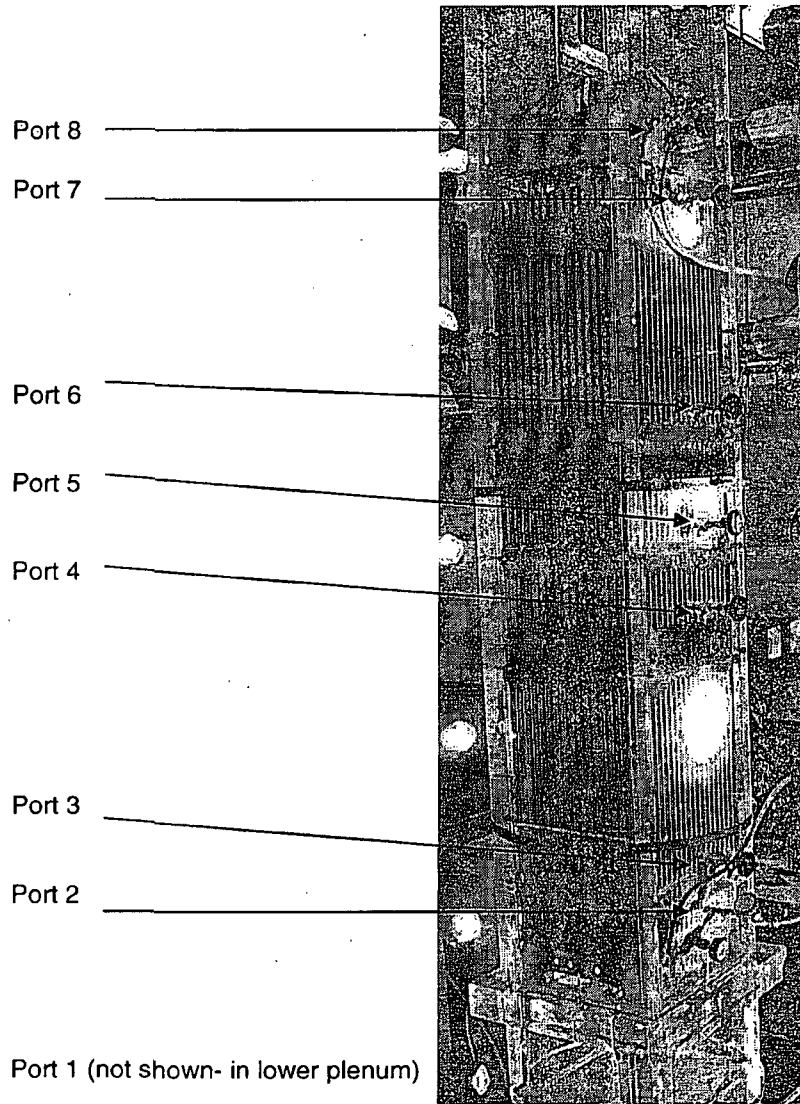


Figure 1: Photograph of the Westinghouse Fuel Test Vessel

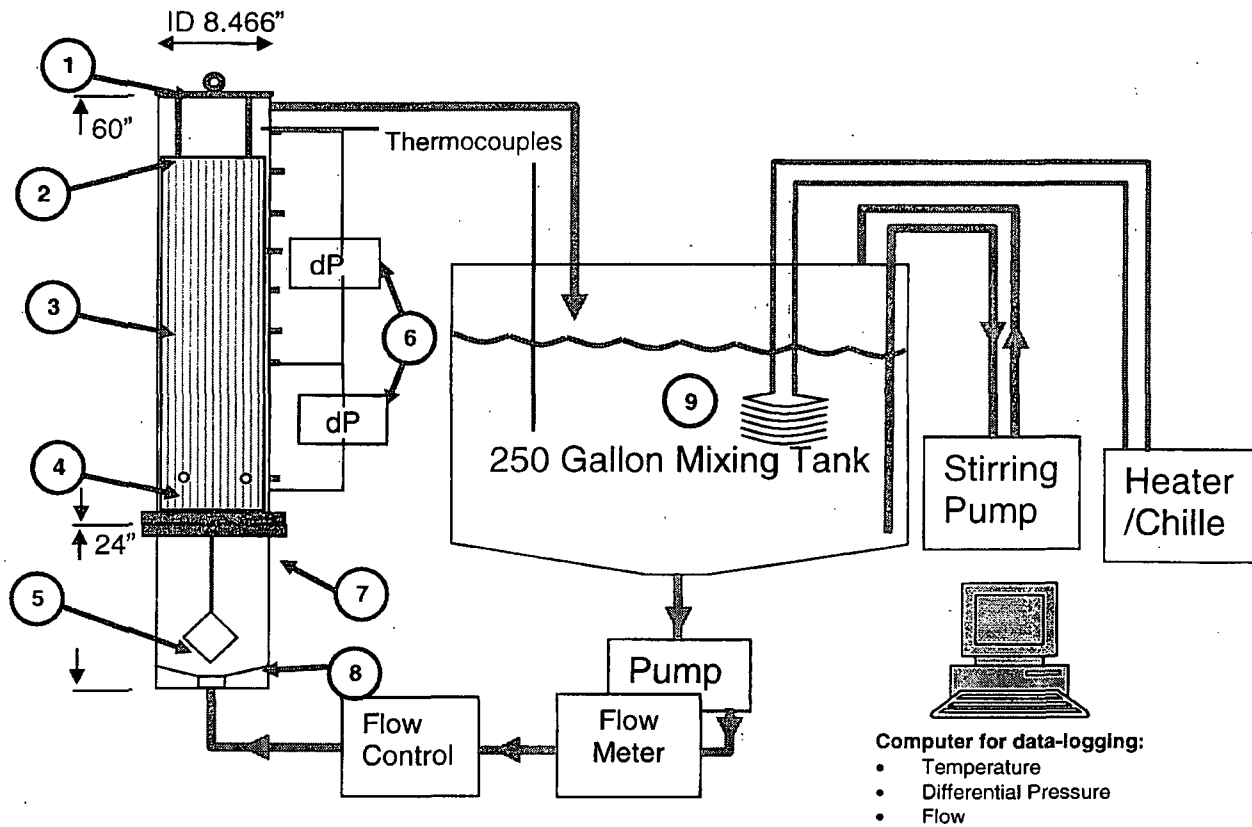


Figure 2: Schematic of the Westinghouse Test Loop

- | | |
|---|---|
| 1 | Stainless steel top plate and lifting ring |
| 2 | Stainless steel hold-down bar |
| 3 | One-third height fuel assembly |
| 4 | Horizontal positioning set screws |
| 5 | Flow diverter (cube) |
| 6 | Differential pressure gauge |
| 7 | Port for measurement of differential pressure |
| 8 | Bottom flow cone |
| 9 | Temperature regulation coil |

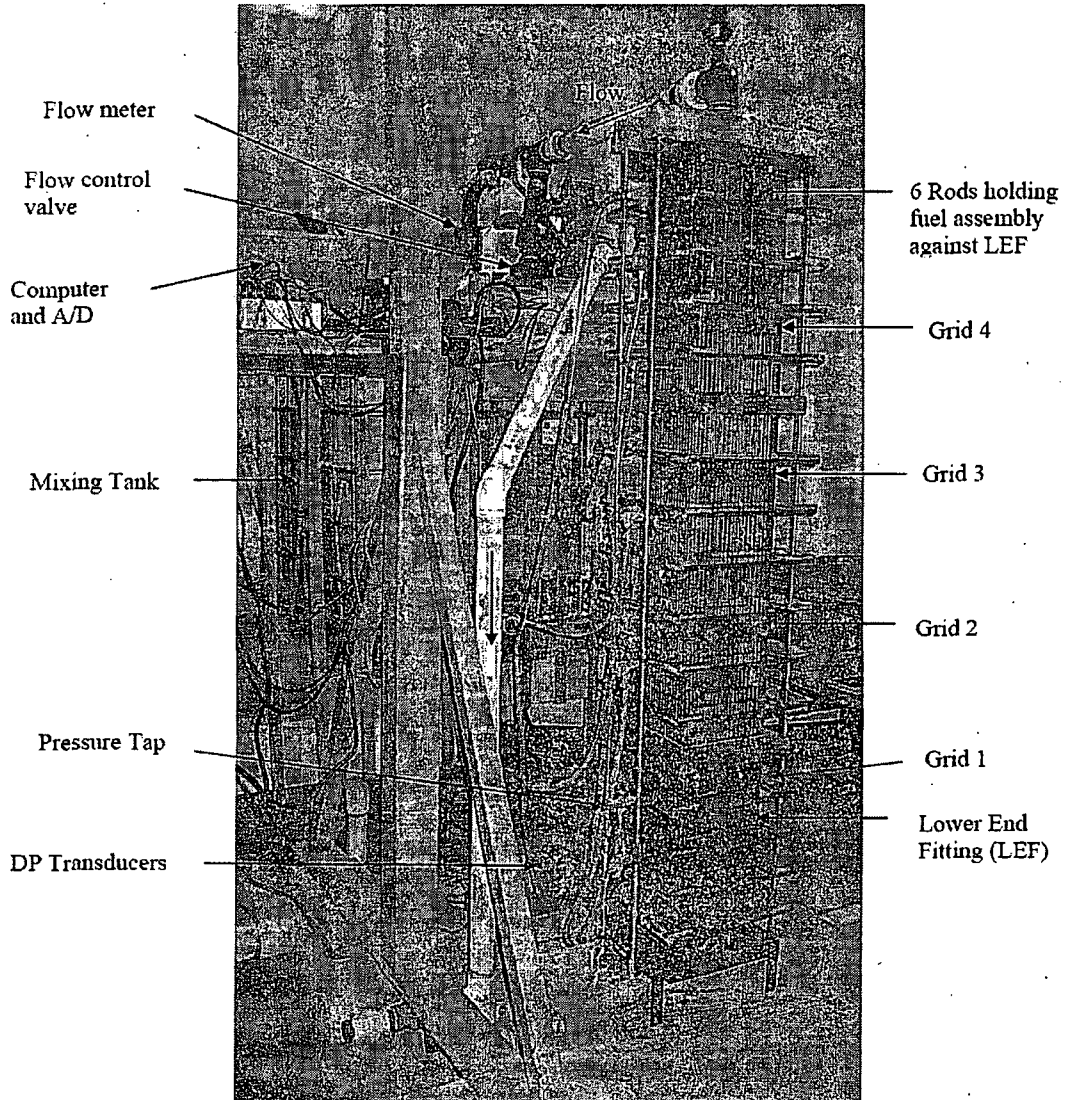


Figure 3: AREVA Test Loop

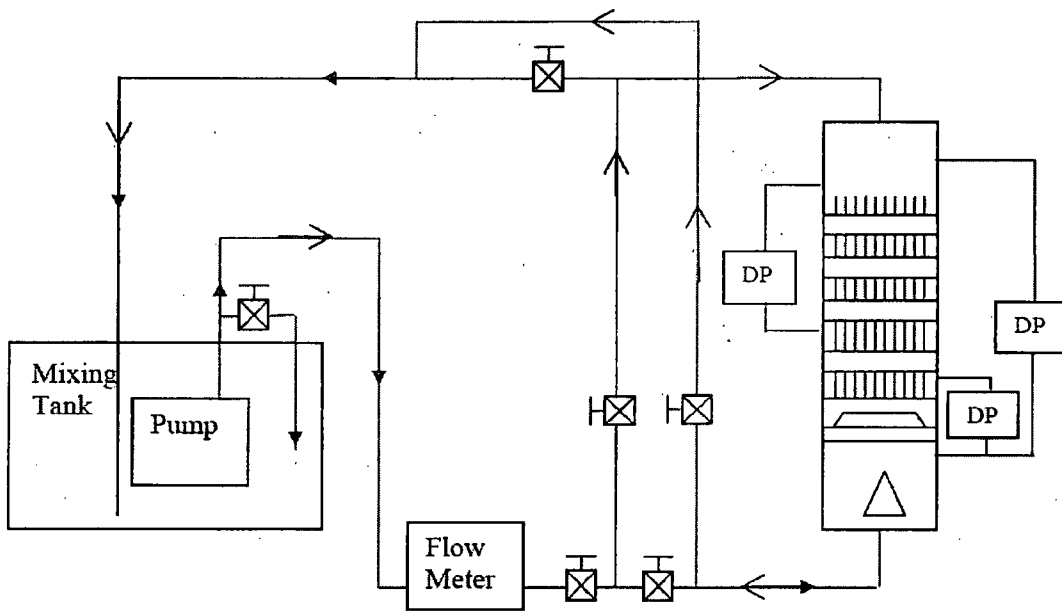


Figure 4: Schematic of AREVA Test Loop

Debris Discussion:

This section addresses the following parts of the RAI:

- Debris types and size distribution for all debris added
- Details of debris preparation and introduction
- Order and rate of debris addition
- Amounts of each type of debris added to each test or subtest
- Bases for amounts and sizes of debris added to each test or subtest
- Scaling information for debris amounts and test flow rates

Debris Type and Size Distribution:

The main debris materials added to the fuel nozzle testing were NUKON™ fiber, silicon carbide, Microtherm, calcium silicate, AlOOH chemical surrogate, and filtered tap water. The NUKON™ fiber was chopped and sized to match the industry reported average strainer bypass distribution per an acceptable procedure. Each batch was characterized by light microscopy to determine the distribution of the fiber lengths. The actual fiber distributions fall within the allowable limits of the target fiber distribution shown in Table 1.

Table 1: Values Specified for Fiber Length

Description	Specified Value	Range
Fiber length < 500µm:	77% + 10%	67%- 87%
500µm < Fiber length < 1000µm:	18% + 10%	8%- 28%
Fiber length > 1000µm:	5% + 10%	0%- 15%

Silicon carbide powder with a nominal 9.5 micron particle size was used to simulate particulate debris. The actual particulate size was measured using scanning electron microscopy. This silicon carbide powder is used as a surrogate for the particulate debris in the reactor because of its chemical stability and the fact that the fine particulates collect within a fiber bed and result in conservative head losses. Silicon carbide has a relatively high specific gravity of about 3.2, which would normally cause it to settle out quickly. However, due to the small size of the particles and the test loop design and flow rates, this settling is minimized.

The microporous insulation, Microtherm, was obtained from Microtherm, Inc. The material was supplied in a pulverized form, and then was passed through a #7 sieve with a hole size of 0.11". The sieving is necessary to remove larger fibers and clumps of material that would not pass through the sump screen. Then the material was analyzed by scanning electron microscopy to characterize the material. The typical appearance of the Microtherm material used can be seen in Figure 5.

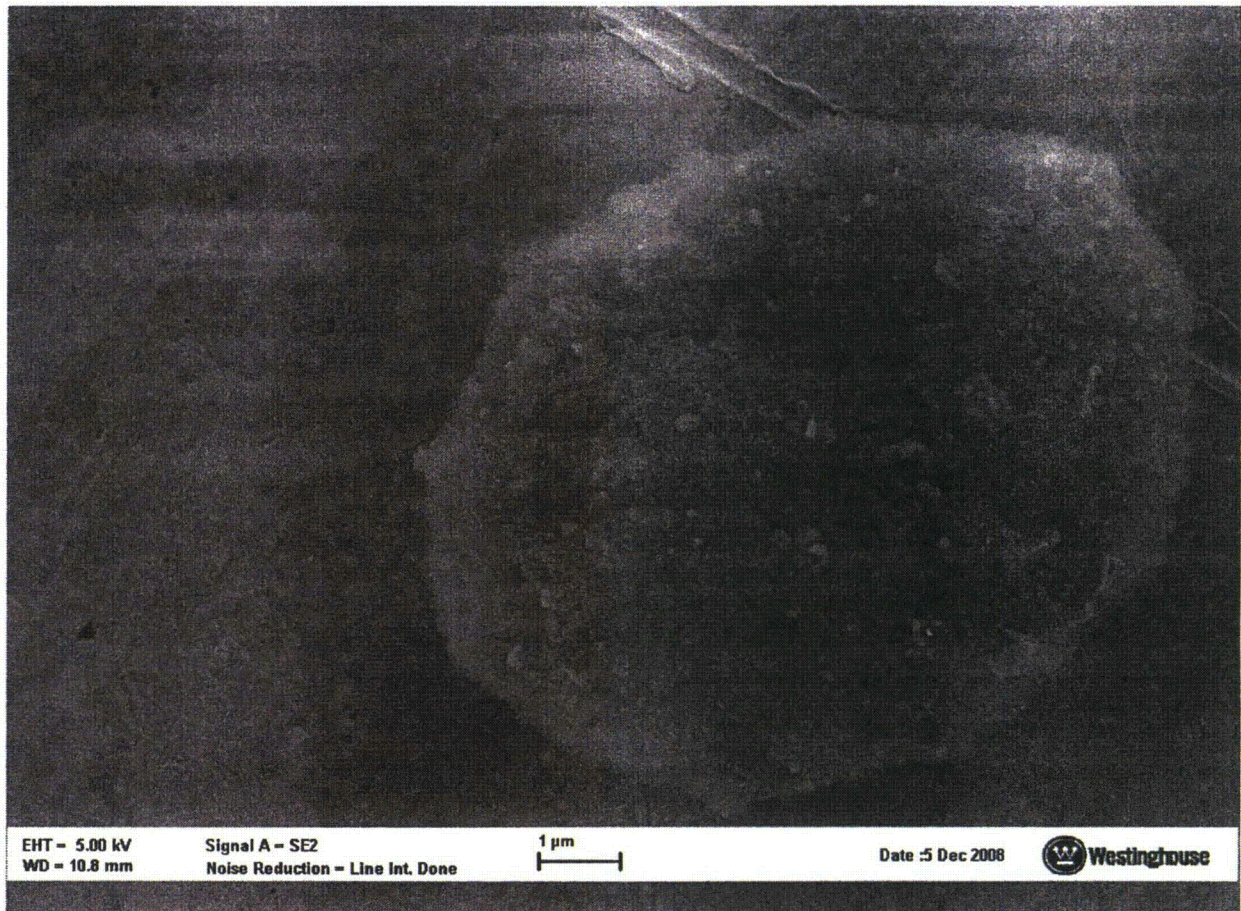


Figure 5: Microtherm Scan

Calcium silicate insulation material, Lot # S15-276, was obtained from Performance Contracting Incorporated (PCI). PCI obtained the material from Industrial Engineering Group and pulverized it into a fine powder by a hammer mill. Upon receipt at Westinghouse Science and Technology Department, the material was passed through a #7 sieve with a hole size of 0.11". Then the CalSil was analyzed by scanning electron microscopy to characterize the material. The typical appearance of the CalSil material used can be seen in Figure 6.

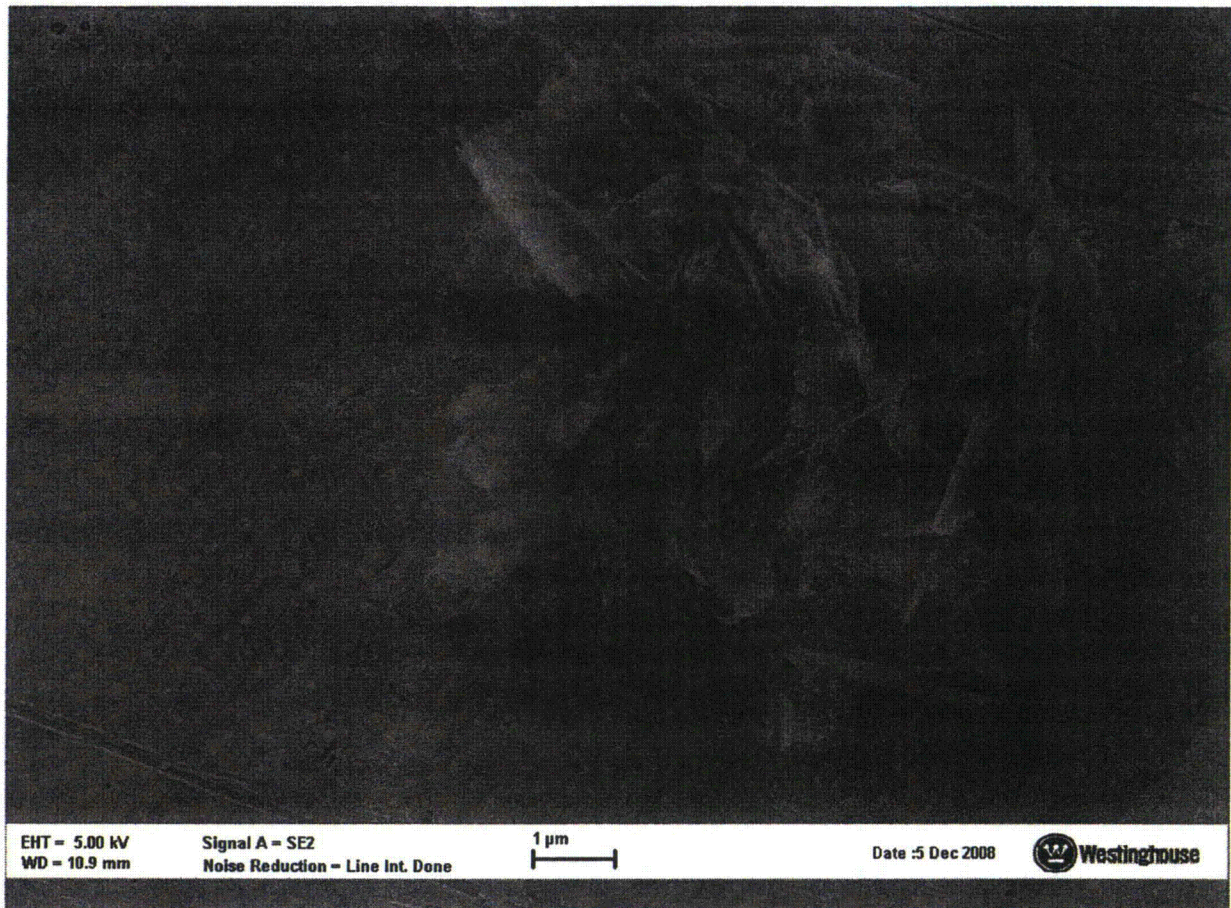


Figure 6: Calcium Silicate Scan

AIOOH was prepared according to the recipe in WCAP-16530-NP-A at a concentration of 11 g/L. The 1 hour settling volume of the precipitate met the criteria in WCAP-16530-NP-A.

Order of Debris Addition:

For tests that only included particulate, fiber and chemical, NRC guidance regarding the order of addition was followed. The entire particulate load was added first, followed by fiber in 10 gram increments and then by chemicals in specified increments. For tests that included particulate, fiber, chemical, calcium silicate and/or microporous material, the order of addition was varied slightly. Like the other tests, the entire particulate load was the first addition, then, to simulate the initial blast introduction of calcium silicate and/or microporous material, a specified amount of these materials were added, this was followed by fiber additions in 10 gram increments, then the chemical was added and the final additions were calcium silicate and/or microporous material to simulate the slow erosion of these materials during an accident.

Method of Debris Introduction:

This is a lengthy and site specific discussion. The method of introduction will be extensively covered in the test report associated with Revision 1 of WCAP-16793-NP.

Rate of Debris Addition:

The initial particulate addition of silicon carbide was introduced in its entirety. The remaining debris types required a wait of two loop turnovers between each addition.

Information Related to Debris Test Amounts:

It was communicated to the PWROG that an acceptance criteria for debris loads was being developed. In order to define debris test loads that were applicable to and bounds, to the extent possible, all PWRs, all plants were asked to provide their downstream debris values.

These values were then divided by the total fuel assemblies of each plant. This provided the test program with per fuel assembly debris values. These values were then used to determine the bounding conditions of the fuel assembly tests.

The amounts of each type of debris added to each test will be published in the next revision of WCAP-16793-NP.

Test Observations:

This section addresses the following parts of the RAIs:

- Head loss value experienced for each test or subtest including time dependent plots if available
- Observations of debris transport and accumulation including any settling with differences noted at different flow rates
- Behavior of debris during testing (agglomeration)
- Photographs as available to assist in understanding the tests theoretical debris bed thickness based on as-manufactured fiber density

These will be discussed in-depth in proprietary test reports that will be submitted to NRC and are associated with Revision 1 of WCAP-16793-NP.

- 7) For hot leg and cold leg breaks, some debris may bypass the fuel inlet because it flows to the containment spray system (CSS) instead of the emergency core cooling system (ECCS). Also, for cold-leg breaks, some flow bypasses the core by flowing out the break. If bypass is credited for a reduction of debris at the core inlet, please provide the basis for the magnitude of the reduction of debris entering the core.

RESPONSE:

Subsequent to receipt of this RAI, and in response to comments from the Advisory Committee on Reactor Safeguards (ACRS), the PWR Owners Group initiated prototypical fuel assembly (FA) testing to establish limits on the debris mass (particulate, fibrous and chemical) that could bypass the reactor containment building sump screen and not result in unacceptable head loss that would impede core inlet flow and challenge long-term core cooling of the core. An overall test protocol and specific test procedures were developed to ensure that possible thin bed effects were investigated, and debris types and characteristics expected in the Reactor Coolant System (RCS) were represented. Debris loads used in the test were based on sump screen bypass information provided by licensees.

The effects of differing fuel inlet nozzle designs were also considered in the test program. Both AREVA and Westinghouse have performed testing with their respective fuel inlet nozzles. Both vendors tested their various bottom nozzle designs and identified the limiting design (limiting was defined as the design that provided for the maximum pressure drop at the same flow and debris loading conditions). Each fuel bundle tested also had prototypical grids above the bottom nozzle debris capturing design features. Thus, the test data obtained from testing takes into account the fuel inlet nozzle, protective filter design features, and spacer grid designs. Descriptions of the fuel components tested, including bottom nozzles and grids, will be provided in proprietary submittals describing the testing performed and the results obtained.

Testing was performed using bounding debris loads and hot leg break flow rates. These tests demonstrated that for the bounding debris loads tested, the hot-leg flow rate through the fuel assembly mock-up was maintained with acceptable pressure drops. No credit was taken in these tests for flow bypassing the core due to operation of the containment spray system. The results of these tests will be integrated into Revision 1 of WCAP-16793-NP.

Following a LOCA, some debris may pass through the sump screens and enter the ECCS system. The ECCS system will deliver fluid and debris to the containment spray (CS) system and to the RCS. For the RCS and core evaluations, it is conservative to assume that all of the debris that passes through the sump screens reaches the RCS. Therefore, the WCAP-16793-NP methodology does not credit debris reduction by considering flow through the CS system.

However, licensees may choose to credit this flow path and reduce the debris that reaches the RCS by considering the following:

- 1) The flow split between what is delivered to the core and what is delivered to the postulated break location (i.e., cold-leg break versus hot-leg break),
- 2) The flow split between what is delivered to containment spray system and what is delivered to the reactor coolant system, and,
- 3) The time frame that the containment spray system is operational.

Of the debris that reaches the RCS, the amount that is transported to the core is dependent on the ECCS injection configuration and break location. ECCS is delivered to the RCS in two locations depending on the plant type. For most PWRs, ECCS is delivered to the cold legs or upper RV downcomer. For Westinghouse 2-loop designs, ECCS is also delivered to the RV upper plenum.

Licensees that may choose to credit partitioning of flow between the core and the break, or the reactor vessel and the containment spray system, would do so on a plant specific basis. These licensees would

develop the technical basis for their crediting a reduction of debris loading ducted to the core based on the flow splits identified above, consistent with expectations for information NRC has identified that they need to evaluate these exceptions to the methods described in WCAP-16793-NP.

- 8) Following a LOCA, thermal energy stored in the thick reactor vessel shell and the reactor vessel baffle/barrel can influence the coolant temperature at the core inlet. For both a hot leg break and a cold leg break, please provide an estimate of the core inlet temperature as a function of time, starting at the onset of ECCS recirculation and ending when an equilibrium reactor vessel metal temperature has been reached. Please discuss how this temperature would affect:
- the solubility of aluminum-based precipitates,
 - the solubility of calcium-based precipitates and,
 - the potential for chemical precipitates to form in the vessel as a result of these phenomena.

RESPONSE:

The thermal energy stored in the thick reactor vessel (RV) shell and the RV baffle/barrel is small, as demonstrated below, and has no more than about a 5°F influence on the coolant temperature from the time it enters the RV until it enters the core inlet. This temperature rise in the RV is small and has results in no more than about a 5% change in solubility of aluminum-based and calcium-based precipitates. This change has no affect on the potential for chemical precipitates to form in the vessel as a result of these phenomena.

The postulated cold-leg break was chosen as this is the bounding case for heat-up of the coolant as it passes by the thick metal components of the RV. The low flow-rates associated with a cold-leg break (matching boil-off) provide the greatest residence time of the fluid next to the metal structures, allowing for the maximum heat-up of the coolant. A postulated hot-leg break, while having a larger velocity, also has a reduced residence time in the RV, minimizing the opportunity for coolant heat-up.

At the time that the Emergency Core Cooling System (ECCS) is realigned to draw suction from the reactor containment building sump from the Borated/Refueling Water Storage Tank (BWST/RWST), the heat transfer process between the thick metal components of the RV and the ECCS fluid in the RV is conduction limited. Under these conditions, there is little increase in temperature of the ECCS fluid as it passes by the thick-metal RV components and enters into the reactor core. The time history plots prepared from the WCOBRA/TRAC calculations reported in WCAP-16793-NP, confirm that this is conduction-limited heat transfer process, and that there is minimal temperature change of the coolant as it enters the RV and flows to the core.

Figure 1, Comparison of Reactor Vessel Metal Temperature at Bottom of Fuel; Outside Diameter versus Inside Diameter, and Figure 2, Comparison of Reactor Vessel Metal Temperature at Top of Fuel; Outside Diameter versus Inside Diameter, are time history plots of the temperature of the inner and outer RV metal nodes of the WCOBRA/TRAC calculations for a postulated cold-leg break. From Figures 1 and 2, it is noted that the temperature of the inner RV metal node at the top and bottom of the core is relatively unchanged over the 300 seconds following switchover from BWST/RWS injection to recirculation from the reactor containment building sump. Over this same time period, the outer RV node is predicted to drop by about 30°F. These figures demonstrate that the heat transfer process is conduction limited.

Figure 3, Comparison of Fluid Temperature at Top and Bottom of Downcomer, shows that there no more than about 5°F temperature gain in the coolant as it passes from the top to the bottom of the downcomer. Likewise, Figure 4, Comparison of Fluid Temperature at Top and Bottom of Baffle, shows a similar behavior. It is noted that the initial 10°F temperature difference diminishes to about a 5°F temperature difference within about 150 seconds of switchover from BWST/RWST injection to recirculation from the reactor containment building sump. Figure 5, Comparison of Fluid Temperature in Lower Plenum to Core Inlet, shows that the coolant at the core entrance is calculated to be generally slightly warmer but within about 5°F of the coolant in the RV lower plenum. Figures 6 and 7, Comparison of Fluid Temperature Between Core Inlet and Inside Baffle, and Comparison of Fluid Temperature Between Core Outlet and Inside Baffle, respectively, shows the calculated fluid temperatures at the core inlet and core outlet to be within less than about 5°F of each other throughout the calculation time period. More importantly, over

the last 100 seconds of the calculation period, comparisons show almost no temperature difference between the fluid in the core and in the baffle.

Based on these comparisons for a postulated cold-leg break, it is concluded that the thermal energy stored in the thick RV shell and the RV baffle/barrel has no more than about a 5°F influence on the coolant temperature from the time it enters the RV until it enters the core inlet for either the cold-leg or hot-leg break scenarios. This conclusion is applicable to all plants, as is demonstrated by considering the Biot number, N_{Bi} , for this scenario. The Biot number is the ratio of surface conductance to internal conduction of a solid;

$$N_{Bi} = \frac{H \times L}{k}$$

where:

- H = Surface heat transfer coefficient
- L = Thickness of the solid
- k = Thermal conductivity of the solid

At the time of initiation of recirculation from the reactor containment building sump, there is no boiling in the downcomer and the convective heat transfer coefficient between the thick metal and the coolant is

dependent upon local flow rate and is evaluated to between less than $3 \frac{Btu}{hr - ft^2 - ^\circ F}$ for a postulated

hot-leg break. The thickness of a reactor vessel is about 8 inches. For evaluating a Biot Number, one-half of the thickness or 4 inches (0.33 ft.) will be used. The thermal conductivity of mild (carbon) steel is

about $28 \frac{Btu}{hr - ft - ^\circ F}$. Thus, the Biot Number for this scenario would be;

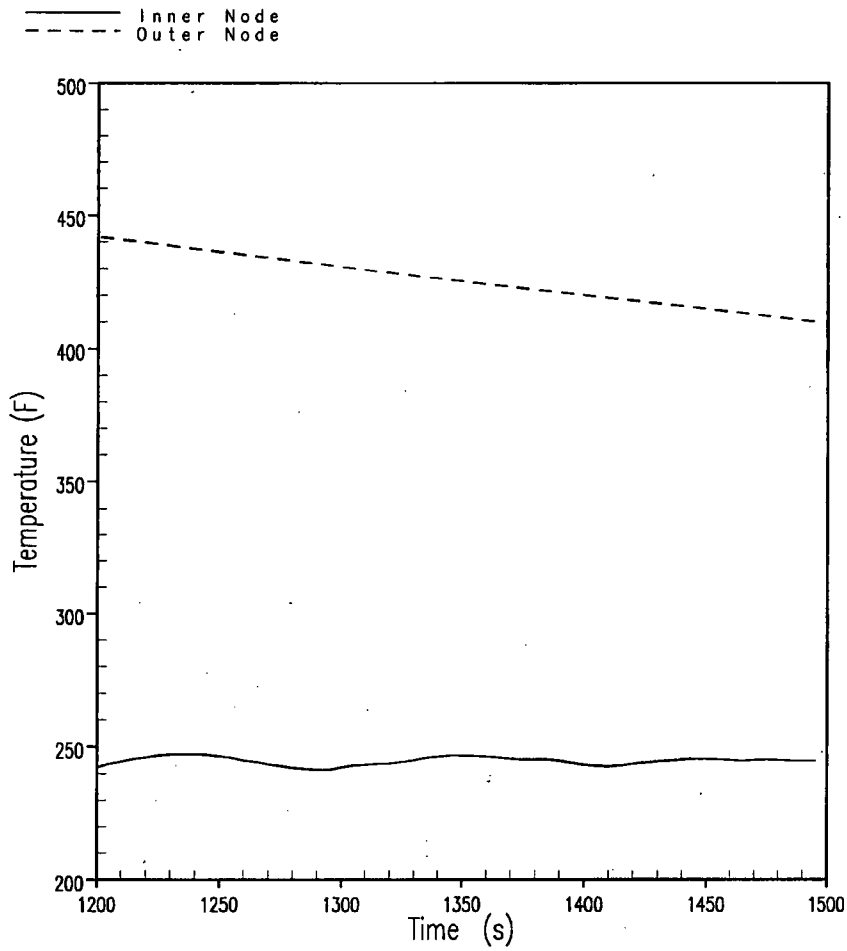
$$N_{Bi} \leq 0.036$$

The above calculation demonstrates that the dominate resistance to heat transfer from the reactor vessel thick metal during recirculation is due to the convective resistance between the reactor vessel surface and the fluid.

The stainless steel cladding on the inside of the reactor vessel was ignored for this evaluation. Stainless steel is about 1/3 as conductive as mild (carbon) steel. Although the cladding is thin, inclusion of this material in the evaluation of a Biot Number would further favor the convection limited process.

The fluid temperature rise of $\leq 5^\circ F$ predicted by WCOBRA/TRAC calculations for a postulated cold-leg break is small in comparison to that needed to change solubility limits and is evaluated to have no affect on the solubility of aluminum-based precipitates, the solubility of calcium-based precipitates and the potential for chemical precipitates to form in the vessel as a result of the release of stored thermal energy from thick-metal components of the RV.

Bottom of Active Fuel Vessel Wall

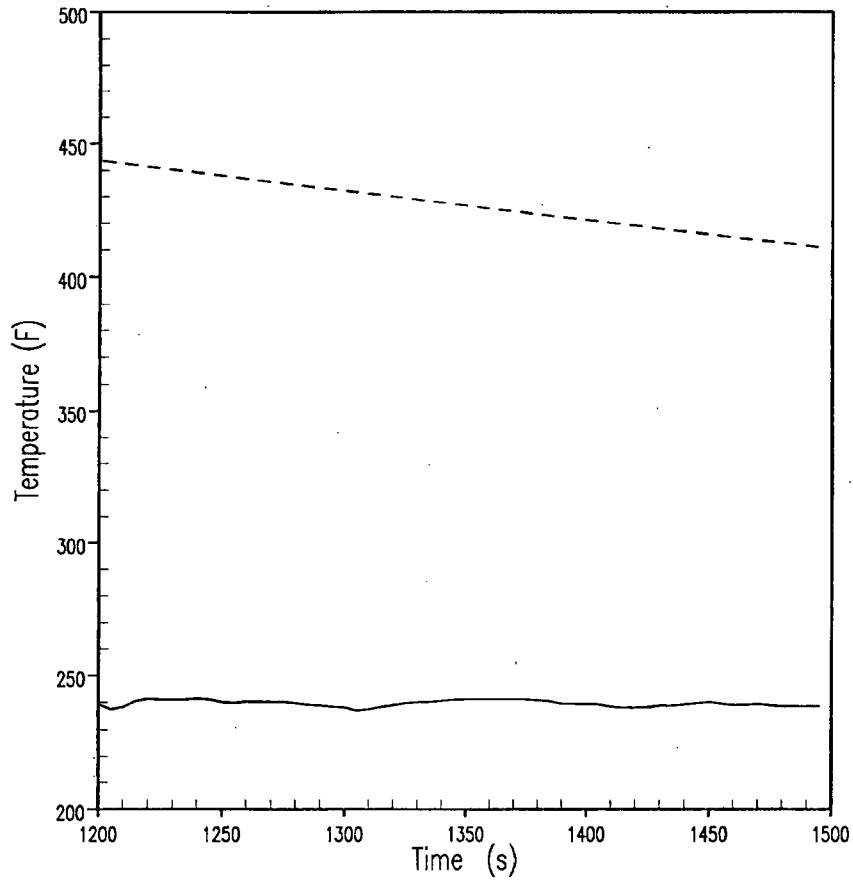


1781435584

Figure 1 Comparison of Reactor Vessel Metal Temperature at Bottom of Fuel; Outside Diameter versus Inside Diameter

Top of Active Fuel Vessel Wall

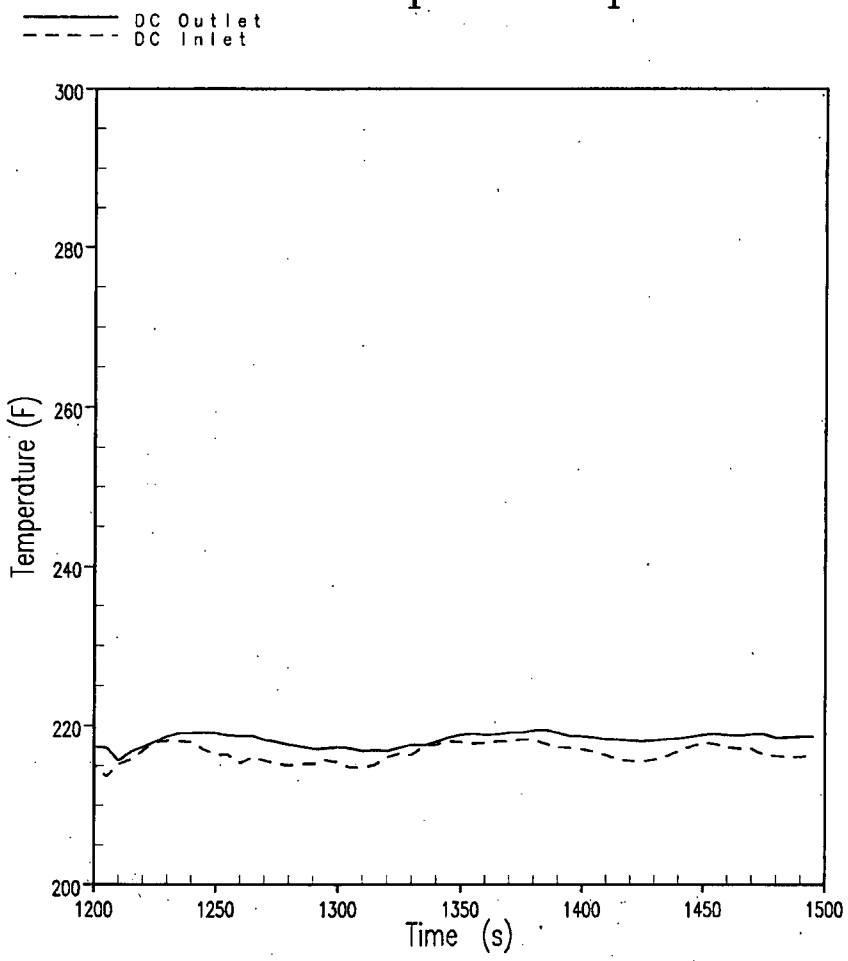
—— Inner Node
- - - - Outer Node



178145584

Figure 2 Comparison of Reactor Vessel Metal Temperature at Top of Fuel; Outside Diameter versus Inside Diameter

Downcomer Liquid Temperature



1761455584

Figure 3 Comparison of Fluid Temperature at Top and Bottom of Downcomer

Baffle Inlet/Outlet Liquid Temperature

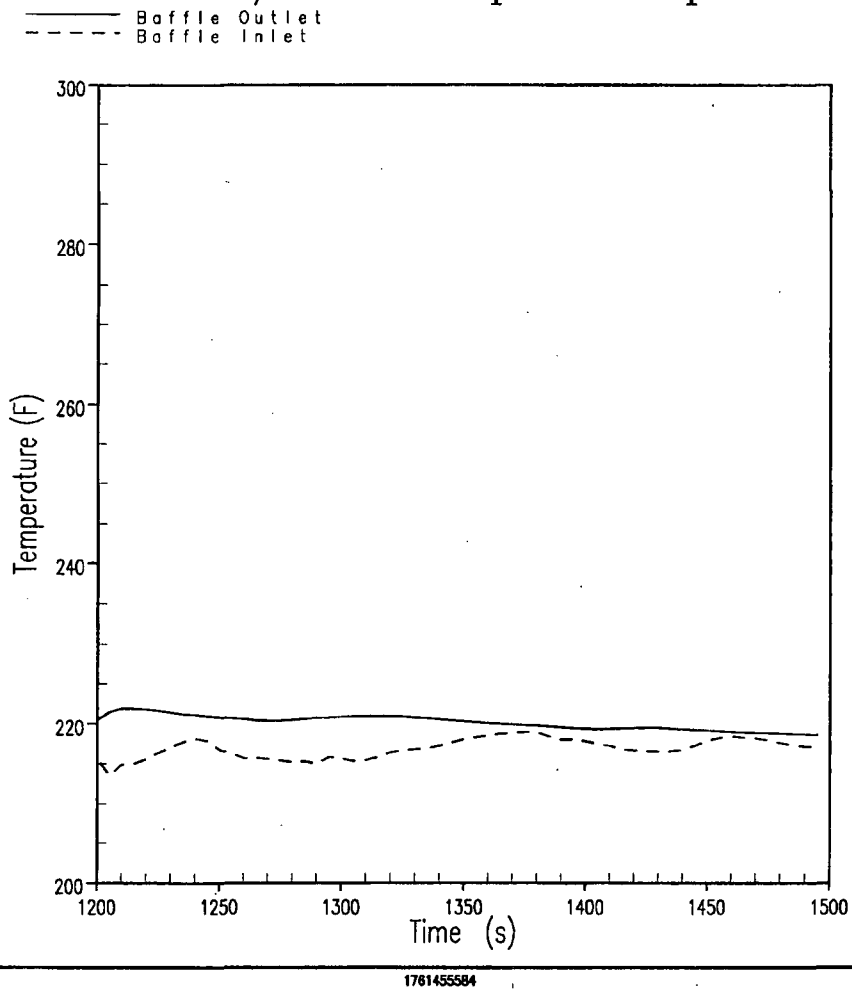
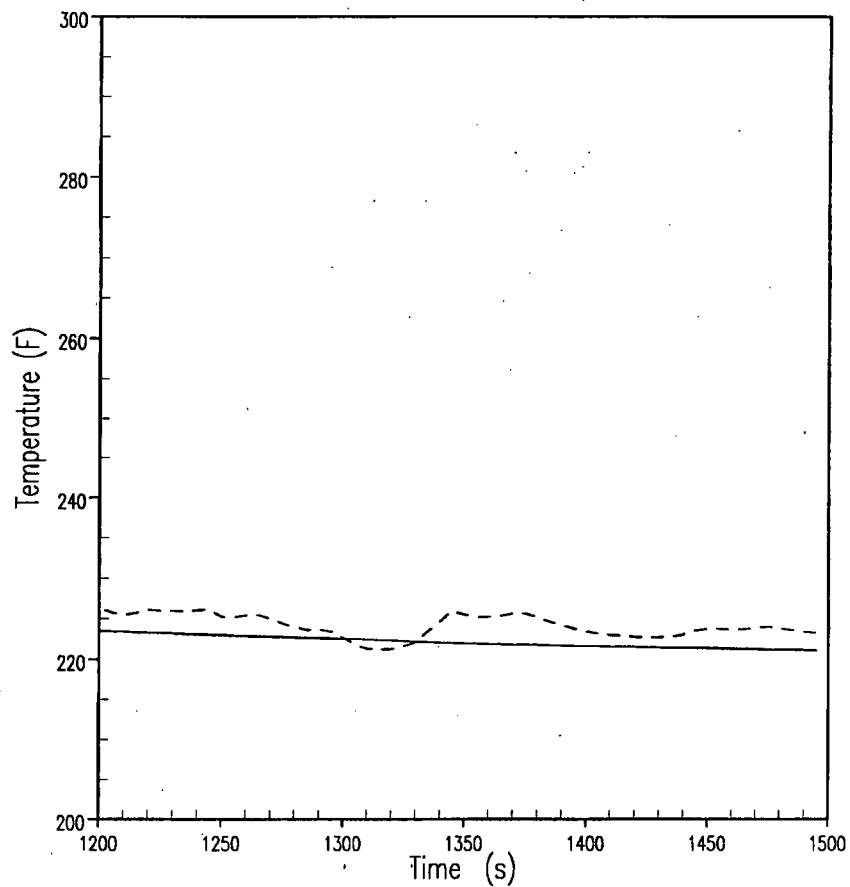


Figure 4 Comparison of Fluid Temperature at Top and Bottom of Baffle

Lower Plenum to Core Liquid Temperature

— Lower Plenum
- - - Bottom of Core



1761455584

Figure 5 Comparison of Fluid Temperature in Lower Plenum to Core Inlet

Core Inlet Elevation Baffel Plate

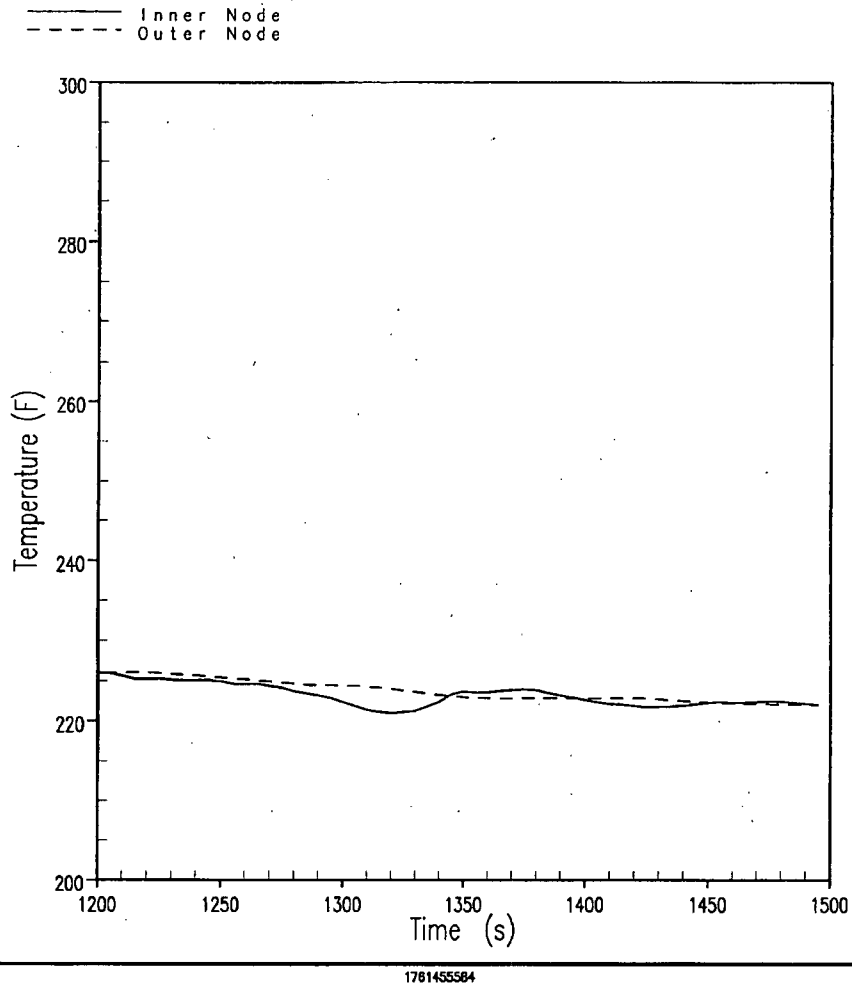
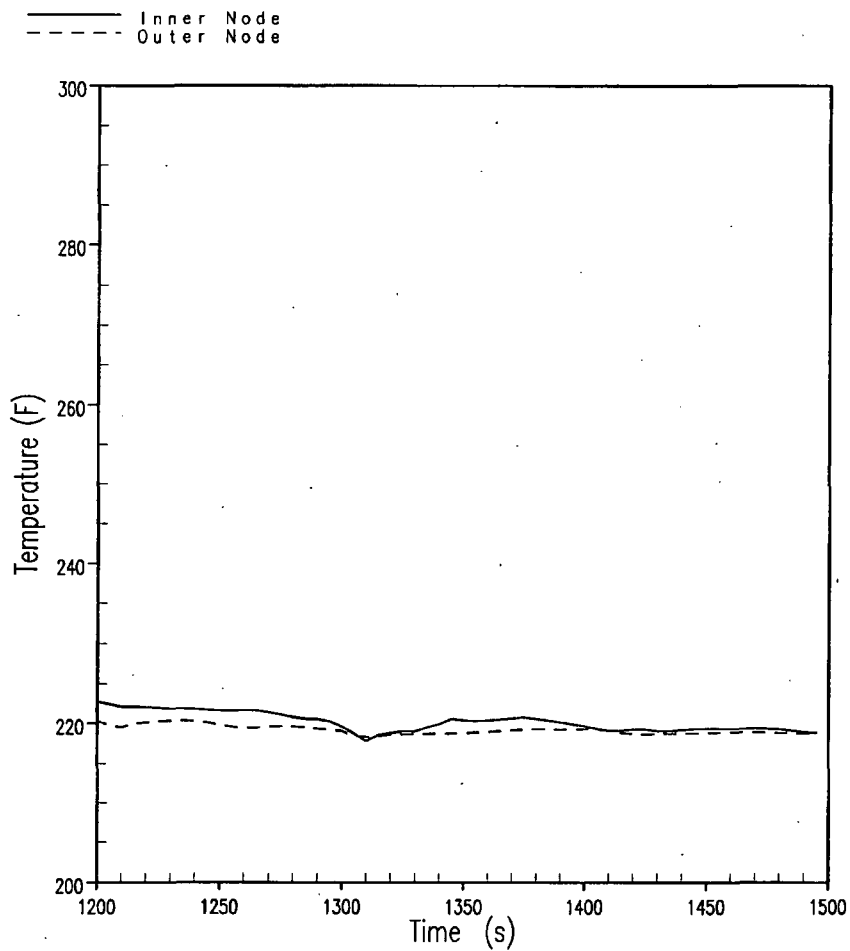


Figure 6 Comparison of Fluid Temperature Between Core Inlet and Inside Baffle

Core Outlet Elevation Baffel Plate



1761455584

Figure 7 Comparison of Fluid Temperature at Core Outlet and Top Baffle

- 9) The topical report does not provide specific guidance to licensees concerning the evaluation of potential chemical effects on a debris bed formed at the core inlet. Various factors can affect potential chemical precipitate interaction with a debris bed on the core inlet. For example, plant-specific amounts of LOCA debris and sump strainer surface area will determine the amount and type of debris materials that bypass the sump strainer. Bypass particulate such as microporous insulation and calcium silicate will influence the filtering properties of a debris bed differently than latent dirt particulate. Elevated temperature can either increase the solubility of precipitates or decrease the solubility of certain precipitates. Please discuss how pressure drop at the core inlet could result from chemical precipitate interaction with a debris bed. Also, please discuss your plans for providing guidance in the WCAP for licensees to evaluate this potential phenomenon.

RESPONSE:

Subsequent to receipt of this RAI, the PWROG began prototypical fuel assembly (FA) testing to establish limits on the debris mass (particulate, fibrous, microporous and chemical) that could be tolerated in the reactor core and the long-term core cooling function continue to be successfully achieved. Debris loads used in the test were based on sump screen bypass information provided by licensees and post-accident chemical precipitate loads based on evaluations using the methods of WCAP-16530-NP-A (Reference 1). The FA testing will be reported in proprietary submittals that will be made in support of Revision 1 of WCAP-16793-NP. The results from these FA tests will be integrated into Revision 1 of WCAP-16793-NP. As part of the effort to invoke this WCAP in the plant licensing basis, each plant will compare their plant-specific debris load against the FA debris masses tested. Revision 1 of WCAP-16793-NP will also include guidance on how that comparison is to be accomplished.

Reference:

1. WCAP-16530-NP-A, "Evaluation of Post-Accident Chemical Effects in Containment Sump Fluids to Support GSI-191," March, 2008.

- 10) In addressing the effects of core inlet blockage on the availability of the lower-plenum mixing volume to delay the onset of boron precipitation, the WCAP states, "In the extreme, core inlet blockage could inhibit mixing between the core region and the lower plenum and would effectively reduce the credited mixing volume contribution of the lower plenum and core baffle region in the analysis of record." The report also states, "Only total or severe core inlet blockage would effectively isolate the lower plenum from the core region." Please provide an analysis of the degree of core isolation and reduction in mixing capability expected for the degree of core blockage created by the quantity of bypassed debris evaluated in the WCAP to be acceptable. Also, please address the effect the density gradients between the liquid in the core and the liquid in the lower plenum may have on localized fluid velocities and the transport of debris to and/or into the core.

RESPONSE:

Subsequent to receipt of this RAI, and in response to comments from the Advisory Committee on Reactor Safeguards (ACRS), the PWR Owners Group initiated prototypical fuel assembly (FA) testing to establish limits on the debris mass (particulate, fibrous and chemical) that could bypass the reactor containment building sump screen and not result in unacceptable head loss that would impede core inlet flow and challenge long-term core cooling of the core. An overall test protocol and specific test procedures were developed to ensure that possible thin bed effects were investigated, and debris types and characteristics expected in the RCS were represented. Debris loads used in the test were based on sump screen bypass information provided by licensees. The results of these tests will be integrated into Revision 1 of WCAP-16793-NP.

The effects of differing fuel inlet nozzle designs were also considered in the test program. Both AREVA and Westinghouse have performed testing with their respective fuel inlet nozzles. Both vendors tested their various bottom nozzle designs and identified the limiting design (limiting was defined as the design that provided for the maximum pressure drop at the same flow and debris loading conditions). Each fuel bundle tested also had prototypical grids above the bottom nozzle debris capturing design features. Thus, the test data obtained from testing takes into account the fuel inlet nozzle, protective filter design features, and spacer grid designs. Descriptions of the fuel components tested, including bottom nozzles and grids, will be provided in proprietary submittals describing the testing performed and the results obtained.

Testing was performed using bounding debris loads and hot leg break flow rates. These tests demonstrated that for the bounding debris loads tested, the hot-leg flow rate through the fuel assembly mock-up was maintained with acceptable pressure drops. The maintenance of core flushing flow with full 30-day debris loads (particulate, fibrous and chemical) precludes boric acid precipitation for hot-leg breaks. Additional details on the possibility of localized blockage following a hot leg are provided in the response to RAI #11, which follows.

For a postulated cold-leg break, the core flow rate is determined by core boil-off, which is on the order of 500 gpm or less at the time of initiation of recirculation from the reactor containment building sump and continually decrease as the time passes. Flow in excess of core boil-off spills from the reactor vessel downcomer and out the cold-leg break and into the reactor containment building sump where it is again recirculated through the sump screen. In this scenario, both the debris loads provided to the core and the core flow rates are considerably lower than for a postulated hot-leg break.

From the fuel assembly testing performed with postulated hot-leg break flows and debris loading conditions, flow through the gaps at the fuel assembly bottom nozzles and gaps at grid straps was observed. These gaps would exist at cold-leg flow rates and continue to provide coolant to remove decay heat. A test using cold-leg break flows and debris loads has been conducted to prove this principle (Note: test will be performed by mid-February 2009.)

In addition, the timing of events should be considered in evaluating boric acid precipitation concerns as described below.

- Following a large LOCA, realignment of the Emergency Core Cooling System (ECCS) and Containment Spray System (CSS) to draw suction from the reactor containment building sump can occur from between about 20 minutes to about 60 minutes after break initiation, depending upon the size of the Borated/Refueling Water Storage Tank (BWST/RWST) and number of ECCS and CSS trains in operation.
- Over a period of time that is determined by plant design the next 1 to 2 hours, again depending upon the number of trains in operation and their pumping capability, the ECCS will recirculate roughly the entire sump volume through the sump screens.
 - For B&W and Westinghouse plants, this duration may range from about 30 minutes to 2 hours, depending upon the number of trains operating and their pumping capacity.
 - For CE plants, this duration may take several hours more.
- For a postulated hot leg LOCA, most of the ECCS flow is through the core. Testing has shown that the core inlet did not totally block at the debris loads representing 30 days of sump recirculation.
- For the postulated cold-leg break:
 - For B&W and Westinghouse plants, approximately 1/5th of the ECCS flow may reach the core inlet.
 - For CE plants, as much as approximately 1/2 of the ECCS flow may reach the core inlet.
- Thus, the debris loading associated with a cold-leg break is a fraction of that of the hot-leg break. Therefore there is less debris at the core inlet for the cold-leg break than for a hot-leg break.
- Hot leg recirculation (from high head/low flow pumps) causes core flow reversal and debris loading at the core inlet is terminated.
- Also, since the hot leg recirculation dilutes the boric acid in the core, the boric acid precipitation concerns are alleviated and the lower plenum mixing volume is no longer needed.

These events, and their timing, further mitigate the concern regarding the impact of debris collection at the core inlet and on grids on potential boric acid precipitation.

Taking the discussion of sequencing and timing of events given above in conjunction with the limits on sump screen bypass set by testing performed to date, the reactor vessel lower plenum would continue to be available as a mixing volume to mitigate for boron precipitation.

With respect to boron precipitation, it is also noted that the Pressurized Water Reactor Owners Group (PWROG) has a program in place to develop a new Post LOCA-Boric Acid Precipitation Analysis Methodology. That program will utilize the same bounding debris loading determine by the fuel-debris testing in considering the effects of debris in the recirculating coolant on boric acid precipitation analysis methodology.

- 11) The WCAP does not include a discussion on boron precipitation associated with a hot-leg break. To address the effect of localized blockage on localized boron precipitation for hot-leg break scenarios, please address the following:
- In the event of localized debris accumulation at the core inlet, has it been demonstrated that adequate flow would travel through or around the debris such that excessive boron build up is prevented? What quantity of boron would be expected to precipitate downstream of the local blockage?
 - Discuss, in terms of boron precipitation, the effects of local blockage on first grid structure above the fuel inlet nozzle.
 - Describe how boric acid control measures would be effective at controlling the potential localized precipitate buildups, as well as controlling general boron precipitation.

If localized boron precipitation were to occur due to local debris accumulation or lack of mixing between the core and the lower plenum, please state and justify the conclusion regarding whether the 800 F peak cladding temperature acceptance criterion would be met.

RESPONSE:

For most Pressurized Water Reactors (PWRs) currently in operation in the US, following a postulated hot leg break, coolant provided by the Emergency Core Cooling System (ECCS) is ducted into the cold legs or upper downcomer and must pass through the core region to reach the break. Some flow may pass through the baffle region, but the majority of the flow will pass through the core. For these plants, the core flow is approximately equivalent to the ECCS flow rate. With the continuous flow through the core, the boric acid concentration does not increase substantially; any concentrated by boiling is continuously flushed upward through the core and out of the break. Consequently, bulk boric acid precipitation following a hot leg break for most PWRs currently in operation in the US is not a concern unless the core inlet becomes nearly completely blocked. As described later in this response, fuel assembly debris capture testing has been recently performed to enable plants compare their plant-specific conditions to those tested with the objective of demonstrating that sufficient flow is maintained to provide for core cooling following a postulated hot-leg break. With continual flow through the core, bulk precipitation of boric acid following a postulated hot leg break will not occur.

Some PWRs introduce coolant directly into the reactor vessel upper plenum using an upper plenum injection (UPI) design. The effect of debris on UPI plants is discussed in Section 2.7.2, "Upper Plenum Injection Plants," of WCAP-16793-NP, Revision 0. In addition, responses to RAI 9, RAI 10, RAI 33 and RAI 44 in the first set of RAIs received from NRC on WCAP-16793-NP address debris collection by and within the core following a postulated hot-leg break. Finally, to address a request from NRC reviewers, the response to RAI 7 from that collection of RAIs also identified a licensing basis boric acid precipitation analysis for a UPI plant. Also, subsequent to receipt of the RAI, the PWR Owners Group initiated prototypical fuel assembly (FA) testing to establish limits on the debris mass (particulate, fibrous and chemical) that could enter the core and not result in unacceptable head loss that would impede core inlet flow and challenge long-term core cooling. This testing addresses the UPI plant configuration.

This RAI implies that localized blockage could induce some localized boric acid precipitation. By way of a response, it is insightful to review the conditions required for boric acid precipitation. In order to concentrate boric acid to the solubility limit, it must concentrate by a factor greater than 20:1 over the typical initial RCS boric acid concentration. This means that in order to concentrate to the precipitation point, the water in an isolated volume in the core would need to be converted to steam and be replaced 20 times. Since the concentrating mechanism is boil-off, the conditions would require that the steam escape the isolated volume without disrupting the isolation barrier and would also require that the makeup flow into the control volume be precisely the same amount as boil-off. If steam flow out of the isolated volume promotes liquid flow out of the volume, or if liquid flow into the volume exceeds boil-off by some degree, the boric acid concentration buildup will cease. Sample calculations (provided in Attachment B) show that the liquid mass flow into the volume of less than 110% boil-off mass flow will be sufficient to

dilute the volume. A completely isolated volume is ruled out as incredible; this would result in overheating of the fuel. Therefore, the sample calculations indicate that the semi-isolated volumes would need only flow communication of 10% above boil-off.

As identified in the first paragraph of this response, subsequent to receipt of this RAI, and in response to comments from the Advisory Committee on Reactor Safeguards (ACRS), the PWR Owners Group initiated prototypical fuel assembly (FA) testing to establish limits on the debris mass (particulate, fibrous and chemical) that could bypass the reactor containment building sump screen and not result in unacceptable head loss that would impede core inlet flow and challenge long-term core cooling of the core. An overall test protocol and specific test procedures were developed to ensure that possible thin bed effects were investigated, and debris types and characteristics expected in the RCS were represented. Debris loads used in the test were based on sump screen bypass information provided by licensees. The results of these tests will be integrated into Revision 1 of WCAP-16793-NP.

The effects of differing fuel inlet nozzle designs were also considered in the test program. Both AREVA and Westinghouse have performed testing with their respective fuel inlet nozzles. Both vendors tested their various bottom nozzle designs and identified the limiting design (limiting was defined as the design that provided for the maximum pressure drop at the same flow and debris loading conditions). Each fuel bundle tested also had prototypical grids above the bottom nozzle debris capturing design features. Thus, the test data obtained from testing takes into account the fuel inlet nozzle, protective filter design features, and spacer grid designs. Descriptions of the fuel components tested, including bottom nozzles and grids, will be provided in proprietary submittals describing the testing performed and the results obtained.

Testing was performed using bounding debris loads and hot leg break flow rates. These tests demonstrated that for the bounding debris loads tested, the hot-leg flow rate through the fuel assembly mock-up was maintained with acceptable pressure drops. The maintenance of core flushing flow with full 30-day debris loads precludes boric acid precipitation for hot-leg breaks. This conclusion is applicable to all Pressurized Water Reactors (PWRs) that introduce their ECCS flow into the reactor coolant system cold legs.

The intent of the test program was, in part, to determine the amount of debris loading passing through the reactor containment building sump screen ("debris bypass") that would impede core flow. To use the results of this test program for closure of GSI-191, each plant will compare their plant-specific debris bypass load against the debris masses that were tested and determined to be acceptable. Plants that have bypass debris loadings that are within the limits of the debris masses tested are bounded by the test; the debris build-up for that plant will not impede core flow below that required to remove core decay heat.

The test FA included a bottom nozzle and a number of intermediate spacer grids. The relationship between blockages at each of these locations and the possibility of localized boric acid precipitation is discussed separately.

1. At the core inlet, the initial results from tests that simulated flow rates following a postulated hot leg break indicate that some debris buildup might occur on the fuel filters. As stated above, the test results showed that the head loss due to the debris buildup is not sufficient to block flow from entering the core. If the fuel filter does not block completely, then continuous flow is assured and no localized precipitation will occur. If the filter blocks completely, gaps between fuel assembly bottom nozzles and the fuel assemblies themselves will allow flow to enter the core region.
2. If a small localized region of the bottom nozzle fuel filter blocks completely, then flow will continue around the blockage through the fuel filter. Due to the core quenching process and the core power shape, boiling near the bottom of the core is lower than at higher elevations. If the region downstream of the blockage becomes starved of flow and begins to boil, then the boil-off will be replaced by the liquid that flowed around the blockage or through the gaps between the fuel assemblies. This liquid inflow will assure that these regions remain well mixed and preclude localized precipitation at the core inlet.

3. The tests also showed that, at the core spacer grids, some debris build up might occur. However, initial test results indicate that the buildup does not preclude flow through the debris bed; the blockage is not complete and the fluid remains well mixed such that localized boric acid precipitation will not occur.
4. However, even if a solid localized blockage occurs, once the flow passes through the gaps between the FA spacer grids or around a small localized blockage, the low pressure region just downstream of the blockage caused by boiling will assure that the flow will mix into these regions, just as at the core inlet. Therefore, continuous flow is assured and no localized precipitation will occur at the spacer grids.

Therefore, for plants that have bypass debris loadings that are within the limits of the debris masses tested are bounded by the test, maintaining coolant flow through the fuel precludes local blockages. This flow also precludes local boric acid precipitation.

The LOCADM methodology considers the deposition of all chemical constituents in the sump fluid onto the fuel rod except the highly soluble chemicals of boron and sodium. The LOCADM methodology includes acceptance criteria specifying that the fuel clad temperatures must stay below 800°F. The ultimate ability of boric acid or sodium borate to insulate the fuel rods is limited since orthoboric acid and sodium borate precipitates have melting points well below 800°F.

ATTACHMENT BHAND CALCULATION - CALCULATION OF MINIMUM RECIRCULATION DILUTION FLOW

Question: For a hot leg break could localized blockage create a localized isolated region that would be sufficiently isolated so as to create the conditions for localized boric acid precipitation?

For a hot leg break the bulk core conditions would be diluted since SI flow in excess of core boil-off would go through the core and out the break.

Conditions for Boric Acid Concentration to Increase to the Precipitation Point

1. There would need to be boiling in the isolated region since boiling is the process by which water is removed, replaced by a boric acid solution, thus increase the boric acid concentration in the isolated volume.
2. Steam would need to escape the control volume with minimal disruption of control volume isolation.
3. The boil-off makeup flow must flow into the control volume with minimal disruption of control volume isolation.
4. Liquid in isolated volume must be evaporated and replaced 20 times before boric acid solubility limit is reached (i.e. from 2500 ppm to 50,000 ppm)

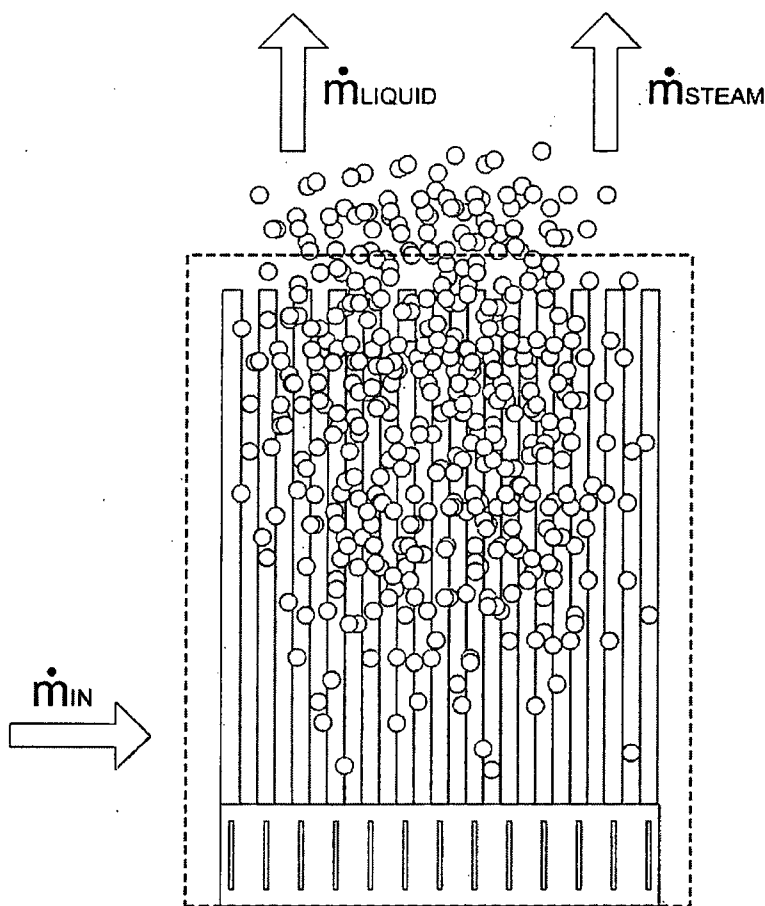
Calculation of the Isolation Efficiency to Permit Boric Acid Concentration to Exceed the Solubility Limit

1. Assume isolation is not perfect (i.e. semi-isolated).
2. Boric Acid Solubility Limit = 29.27 wt. % in control volume.
3. Some liquid in the isolated volume escapes with the steam exiting the isolated region (interfacial drag).
4. Dilution flow into the control volume replaces liquid that goes out of the control volume.
5. Liquid surrounding control volume is at bulk core conditions.

Conclusion: The conditions for isolation sufficient to cause a buildup in boric acid are unlikely. However if a buildup did occur, only a small amount of dilution flow must penetrate the volume to promote or maintain dilution.

Question: If a buildup of boric acid did occur in an isolated volume, how much flow out of (or into) the control volume (as a percentage of the boil-off rate in the semi-isolated volume) is necessary to maintain dilution below the solubility limit?

1. Assume isolation is not perfect (i.e. semi-isolated).
2. Boric Acid Solubility Limit = 29.27 wt. % in control volume.
3. Some liquid in the isolated volume escapes with the steam exiting the isolated region (interfacial drag).
4. Dilution flow into the control volume replaces liquid that goes out of the control volume.
5. Liquid surrounding control volume is at bulk core conditions.



Assumptions;

\dot{m}_{in} = liquid mass entering control volume

\dot{m}_{steam} = boil-off inside the control volume

\dot{m}_{liquid} = liquid leaving the control volume with the steam

\dot{m}_{liquidW} = water in the form of liquid leaving the control volume with the steam

$\dot{m}_{\text{liquidBA}}$ = boric acid in the form of liquid leaving the control volume with the steam

Basic boric acid relationships are as follows:

$$\text{Weight Fraction of Boric Acid} = \text{Boron [ppm]} / 174,840 \quad (a)$$

Using conservation of mass:

$$\dot{m}_{\text{in}} = \dot{m}_{\text{steam}} + \dot{m}_{\text{liquid}} \quad (1)$$

$$\dot{m}_{\text{liquid}} = \dot{m}_{\text{liquidW}} + \dot{m}_{\text{liquidBA}} \quad (2)$$

$$\dot{m}_{\text{in}} = \dot{m}_{\text{inW}} + \dot{m}_{\text{inBA}} \quad (3)$$

Dilution will occur at point where the liquid in (\dot{m}_{in}) is just greater than that needed to keep the core region at the boric acid solubility limit. The equilibrium point would occur when:

$$\dot{m}_{\text{inBA}} = \dot{m}_{\text{liquidBA}} \quad (4)$$

Using (1) and (2):

$$\dot{m}_{\text{in}} = \dot{m}_{\text{steam}} + \dot{m}_{\text{liquidW}} + \dot{m}_{\text{liquidBA}}$$

Then using Equation (4):

$$\dot{m}_{\text{in}} = \dot{m}_{\text{steam}} + \dot{m}_{\text{liquidW}} + \dot{m}_{\text{inBA}} \quad (5)$$

Using the basic relationship (a):

$$\dot{m}_{\text{inBA}} = \dot{m}_{\text{in}} \times \text{PPM}_{\text{CORE}} / 174,840$$

and using Equation (5):

$$\dot{m}_{\text{in}} = \dot{m}_{\text{steam}} + \dot{m}_{\text{liquidW}} + \dot{m}_{\text{in}} \times \text{PPM}_{\text{CORE}} / 174,840 \quad (6)$$

The concentration in the isolated volume will be the boric acid solubility limit, BA_{LIMIT} . Working on \dot{m}_{liquidW} :

$$\dot{m}_{\text{liquidW}} = \dot{m}_{\text{liquid}} \times (1 - \text{BA}_{\text{LIMIT}})$$

Using (1) to eliminate \dot{m}_{liquid}

$$\dot{m}_{\text{liquidW}} = (\dot{m}_{\text{in}} - \dot{m}_{\text{steam}}) \times (1 - \text{BA}_{\text{LIMIT}}) \quad (7)$$

Putting (7) into (6)

$$\dot{m}_{\text{in}} = \dot{m}_{\text{steam}} + (\dot{m}_{\text{in}} - \dot{m}_{\text{steam}}) \times (1 - \text{BA}_{\text{LIMIT}}) + \dot{m}_{\text{in}} \times \text{PPM}_{\text{CORE}} / 174,840$$

Rearranging:

$$\dot{m}_{\text{in}} = \dot{m}_{\text{steam}} + (\dot{m}_{\text{in}} \times (1 - \text{BA}_{\text{LIMIT}}) - \dot{m}_{\text{steam}} + \dot{m}_{\text{steam}} \times \text{BA}_{\text{LIMIT}} + \dot{m}_{\text{in}} \times \text{PPM}_{\text{CORE}} / 174,840)$$

Reducing:

$$\dot{m}_{in} \times [(BA_{LIMIT}) - PPM_{CORE} / 174,840] = BA_{LIMIT} \times \dot{m}_{steam}$$

And finally:

$$\dot{m}_{in} = \dot{m}_{steam} \times [BA_{LIMIT} / (BA_{LIMIT} - PPM_{CORE} / 174,840)]$$

Or:

$$\dot{m}_{in} = R_{dilution-mass} \times \dot{m}_{steam} \text{ where:} \tag{8}$$

$$R_{dilution-mass} = \text{Dilution Ratio} = BA_{LIMIT} / (BA_{LIMIT} - PPM_{CORE} / 174,840) \tag{9}$$

If one considers liquid volumetric flow out of the semi-isolated volume, the ratio of the volume of liquid that must exit with the steam would be as follows.

$$R_{dilution-volume} = (R_{dilution-mass} - 1) \times (\rho_{steam} / \rho_{liquid}) + 1$$

Where:

$$\rho_{steam} = 0.037 \text{ lbms/ft}^3$$

$$\rho_{liquid} = 59 \text{ lbms/ft}^3$$

At the solubility limit of 29.27 wt.% (i.e. $BA_{LIMIT} = 0.2927$), the values for $R_{dilution-mass}$ for $R_{dilution-volume}$ for different core boron concentrations are given in Table 1. Note that for a hot leg break, the core will be continuously diluted and will approximately be at the sump boron concentration.

Table 1			
PPM _{CORE}	Bulk Core (wt.%)	R _{dilution-mass}	R _{dilution-volume}
2500	1.43	1.051	1.000042
3000	172	1.062	1.000039
4000	2.29	1.084	1.000053

Conclusion: If even a small amount of liquid mass escapes the semi-isolated volume with the steam (< 10% above the steaming rate inside the semi-isolated volume), the semi-isolated volume will remain below the boric acid solubility limit. On a volume basis, the volume ratio of the liquid to steam exiting the semi-isolated volume to provide dilution is < .005 %.

- 12) Emergency Operating Procedures typically specify use of hot leg injection at some point in the LOCA recovery period to reverse the core flow and control boron concentration and precipitation. Please identify the time into the accident at which each PWR class of design will employ hot leg injection. Also, discuss the effect of the change in flow distribution on the debris bed that has formed at the core inlet and fuel spacer grids.

RESPONSE:

Action times from analyses of record and identified in plant Emergency Operating Procedures (EOPs) for hot leg injection and/or other actions to prevent boric acid precipitation are discussed in the PWR Owners Group Letter OG-06-200 (Reference1). The action times from Table A-3 of that letter are listed in Table 1 of this RAI response for hot leg injection and/or other actions to prevent boric acid precipitation for all classes of currently operating Pressurized Water Reactors (PWRs).

Subsequent to receipt of this RAI, and in response to comments from the Advisory Committee on Reactor Safeguards (ACRS), the PWR Owners Group initiated prototypical fuel assembly (FA) testing to establish limits on the debris mass (particulate, fibrous and chemical) that could bypass the reactor containment building sump screen and not result in unacceptable head loss that would impede core inlet flow and challenge long-term core cooling of the core. The effects of differing fuel inlet nozzle designs were also considered in the test program. Both AREVA and Westinghouse have performed testing with their respective fuel inlet nozzles. Both vendors tested their various bottom nozzle designs and identified the limiting design (limiting was defined as the design that provided for the maximum pressure drop at the same flow and debris loading conditions). Each fuel bundle tested also had prototypical grids above the bottom nozzle debris capturing design features. Thus, the test data obtained from testing takes into account the fuel inlet nozzle, protective filter design features, and spacer grid designs. Descriptions of the fuel components tested, including bottom nozzles and grids, will be provided in proprietary submittals describing the testing performed and the results obtained.

Testing was performed using bounding debris loads and hot leg break flow rates. These tests demonstrated that for the bounding debris loads tested, the hot-leg flow rate through the fuel assembly mock-up was maintained with acceptable pressure drops. The maintenance of core flushing flow with full 30-day debris loads (particulate, fibrous and chemical) for cold-leg recirculation demonstrates that flow paths through the core remain available. These flow paths would be available from the top of the core to the lower plenum for the lower hot-leg recirculation flow (< 150 gpm).

For a postulated cold-leg break, the core flow rate is determined by core boil-off, which is on the order of 500 gpm or less at the time of initiation of recirculation from the reactor containment building sump and continually decrease as the time passes. Flow in excess of core boil-off spills from the reactor vessel downcomer and out the cold-leg break and into the reactor containment building sump where it is again recirculated through the sump screen. In this scenario, as described in the response to RAI #10, both the debris loads provided to the core and the core flow rates are considerably lower than for a postulated hot-leg break. Thus, similar to the hot-leg break scenario, and considering the lower debris loading for the cold-leg break scenario, flow paths would again be available from the top of the core to the lower plenum for the lower hot-leg recirculation flow (< 150 gpm).

Given the above discussion, the debris collection that has formed at the core inlet and fuel spacer grids is expected to have no effect on the flow distribution in the core during hot-leg recirculation.

It is also noted that the Pressurized Water Reactor Owners Group (PWROG) has a program in place to define, develop and obtain NRC approval of a new Post LOCA-Boric Acid Precipitation Analysis Methodology. That program will utilize the same bounding debris loading determined by the fuel-debris testing, discussed above, that demonstrated that mixing will occur between the core region and the lower plenum.

Reference:

1. PWROG Letter OG-06-200, "Suspension of NRC Approval for Use of Westinghouse Topical Report CENPD-254-P, Post LOCA Long Term Cooling Model, Due to Discovery of Non-Conservative Modeling Assumptions During Calculation Audit, PA-ASC-0290", June 19, 2006. (ML061720175)

Table 1: Time of Initiation of Core Flushing Flow
 From Letter OG-06-200 (ADAMS ML061720175)

Group	No. of Plants	Plant Design	Action Time (hrs) ^[a]
B-1	3	B&W	4.94 – 7.56
B-2	1	B&W	24
C-1	4	CE	3 – 10
C-2	4	CE	3 – 6.5
C-3	2	CE	20
C-4	1	CE	13
C-5	1	CE	6
C-6	1	CE	3
C-7	1	CE	8.5
W-1	24	W	5.5 – 14
W-2	8	W	3 – 6.5
W-3	2	W	3
W-4	2	W	5
W-5	2	W	8
W-6 ^[e]	1	W-UPI	20
W-7	3	W-UPI	NA
W-8	2	W-UPI	14

NOTES TO TABLE 1:

Only those notes applicable to Table 1, above, were taken from Table A-3 of PWROG Letter OG-06-200. There designation associated with the note remains the same as in PWROG Letter OG-06-200.

NA = Not Applicable

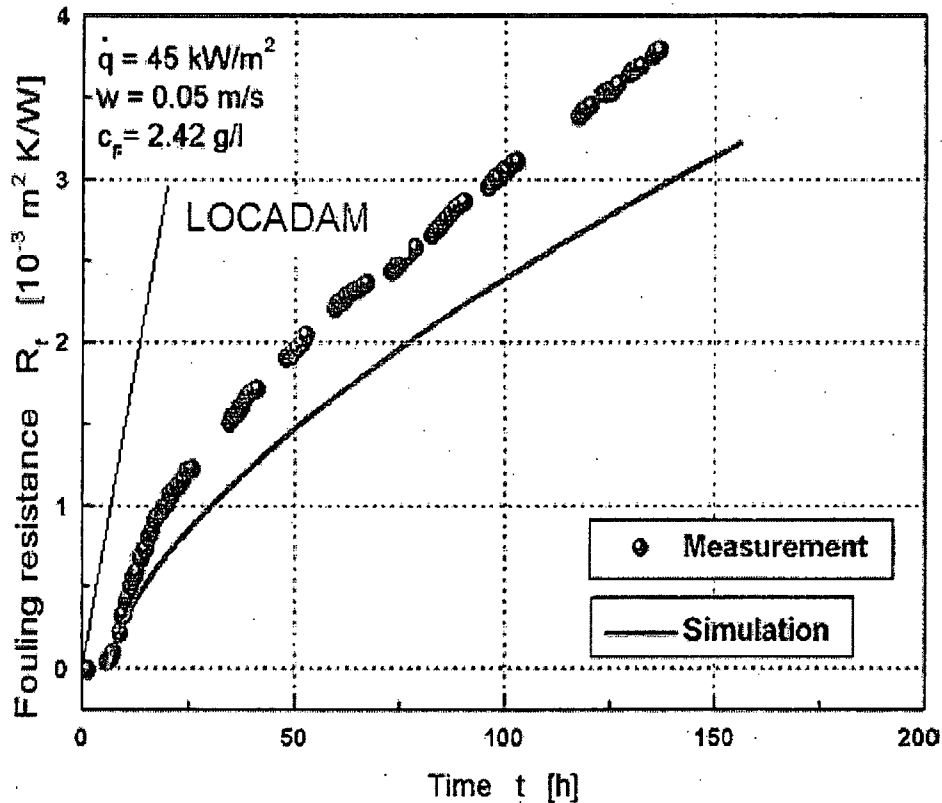
[a] = EOP Action time is latest hot leg switchover time, time to switch to simultaneous injection, or other actions to initiate core dilution.

[e] = For W 2-Loop UPI plants, UPI flow provides flushing flow for cold leg breaks and UPI/core region mixing prevents boric acid precipitation for hot leg breaks

- 13) Part of the LOCADM Model validation involved benchmarking against an experiment in which calcium sulfate solution entered an electrically heated tube and formed deposits on the heat transfer surface, Brahim et al. The heat fluxes were high enough to cause boiling within the deposits, according to the author's calculations. The LOCADM-predicted deposition rate was calculated to be higher than the deposition rate determined experimentally. Please discuss any additional LOCADM validation that has been performed, or will be performed, involving experimentally determined deposition rates to confirm that the amount of deposit predicted by LOCADM is conservative.

RESPONSE:

As described in WCAP-16793-NP, the LOCADM model conservatively assumes that all fiber and chemical products passed by the sump screen and transported to fuel surfaces by boiling will deposit on the fuel cladding. The assumption that all fiber and chemical products will deposit is a conservative assumption. The amount of conservatism is demonstrated in the plot comparing the deposition predicted by LOCADM over time to the experimental data of Brahim et.al. and is shown in the figure below. Considering the amount of conservatism in the LOCADM predictions to the observed test data, no additional LOCADM validation has been or is planned to be performed.



Fahmi Brahim, Wolfgang Augustin, Matthias Bohnet, "Numerical simulation of the fouling process" International Journal of Thermal Sciences 42 (2003) 323-334

- 14) For each plant type and configuration, please provide the driving head available for hot-leg and cold-leg break scenarios to push flow into the core across the core inlet.

RESPONSE:

At the time of sump switchover, the core has been fully recovered and the fluid inventory in the Reactor Coolant System (RCS) is above the top of the core. The core decay heat is being removed by Emergency Core Cooling System (ECCS) injection. The driving head at the core inlet is dependent on the break location.

For postulated cold leg pump discharge (CLPD) breaks, the ECCS from each cold leg runs to the break, ensuring that the downcomer is full to at least the bottom of the cold leg nozzles. The core level is established by the manometric balance between the downcomer liquid level, the core level, and RCS pressure drop through the loops. The core flow is only what is required to make up for core boiling to remove the decay heat. For postulated cold leg breaks, most of the ECCS spills directly out of the break. The situation is similar for cold leg pump suction (CLPS) breaks.

For a break in the hot leg, the ECCS must pass through the core to exit the break. The driving force is the manometric balance between the liquid in the downcomer and core. Should a debris bed begin to build up in the core, the liquid level will begin to build in the cold legs and into the Steam Generators (SGs). As the level begins to rise in the SG tubes, the elevation head to drive the flow through the core increases as well. The driving head reaches its peak when the shortest SG tube has been filled (in the W and CE plant designs) or the SG and hot legs to the spillover elevation have filled (in the B&W plant design) and the flow begins to spill over. Once the ECCS flow reaches the elevation of the shortest tubes, the spillover flow is sufficiently large that no increase in water level to the higher tubes is achieved. This is conservative as it provides for the minimum static head available in the steam generator tubes. The core mixture level will be at least to the hot leg nozzle elevation, and the core flow rate will equal the ECCS flow rate.

Core flow is only possible if the manometric balance between the downcomer side and the core is sufficient to overcome the flow losses in the Reactor Vessel (RV) downcomer, RV lower plenum, core, and loops at the appropriate flow rate.

$$\Delta P_{\text{avail}} = \Delta P_{\text{dz}} - \Delta P_{\text{flow}}$$

where:

$$\Delta P_{\text{avail}} = \text{Available head to drive flow into the core}$$

$$\Delta P_{\text{dz}} = \text{Elevation head between downcomer side and core}$$

$$\Delta P_{\text{flow}} = \text{Flow losses in the RV downcomer, RV lower plenum, core and loops (W \& CE designs) or reactor vessel vent valves (B\&W designs)}$$

The manometric differences are determined considering plant geometry and core void fractions. The flow losses are calculated using the Darcy equation.

For a postulated hot leg break, the value of ΔP_{dz} is evaluated by taking elevation difference between the elevation of the shortest tube in the steam generator (W and CE plant designs) or the hot leg spillover elevation (B&W plant designs) and the elevation the bottom of the inside diameter of the hot leg. For a postulated hot leg break, no voiding in the coolant passing through the core and out the hot leg is assumed at time of initiation of recirculation from the reactor containment building sump. This provides for the evaluation of a minimum driving head for the fleet of PWRs of approximately 13 psid.

The temperature of the SG secondary side inventory may be above the saturation temperature associated with the containment pressure, which could cause boiling the SG and a reduction in the driving head of the water column. The 13 psid value does not account for either density variations in the column that may result due to heating of the water in the steam generator tubes by the warmer SG secondary side inventory, or the pressure increase on the cold leg water column that would result from the generation and venting of steam due to heat transfer from the warmer SG inventory to the coolant in the SG tubes.

The effect of effect of density due to heating of the coolant in the SG tubes on available head is bounded by comparing the density of water at saturated condition to the density of subcooled water. This approach conservatively uses extreme values and ignores density gradients that would be present in the actual system which, if considered, would provide less extreme values. At 1200 seconds, most reactor containment buildings are at a pressure of about 40 psia or less. The sump fluid temperature is at or near saturated conditions; this is about 267°F for 40 psia. Allowing for a conservatively large amount of cooling of the recirculating fluid by heat exchangers in the Emergency Core Cooling (ECC) or Containment Spray (CS) lines, an ECC fluid temperature of 200°F is used for this evaluation. Comparing the density differences at 40 psia for saturated conditions and 200°F water,

$$\Delta H = \frac{58.31 \text{ lb}_m/\text{ft}^3}{60.11 \text{ lb}_m/\text{ft}^3} = 0.97$$

From the equation above, there would be no more than a 3% reduction in available head due to the heating of the water column in the SGs. Using this conservative approach would reduce the approximately 13 psid acceptance criteria to approximately 12.6 psid. It is also observed that, as the containment tends to cool, the difference between the saturation density and the subcooled density (assuming a 60°F temperature difference) decreases. Thus, this density effect diminishes as the containment pressure continues to decrease following the postulated accident. Further, the conservatisms included in this calculation will overcome this small potential variation in results such that it can be ignored. One such conservatism is that the whole water column is uniformly heated to a temperature of 267°F.

Per the Darcy equation, as flow rate increases, the pressure drop will increase. The highest flow rate through the core is achieved with a hot leg break and the minimum driving head for operating plants is approximately 13 psid. As the flow decreases, the pressure drop decreases. The available cold leg driving head for operating plants is approximately 3 psid. Testing for the PWROG used these values as guidelines for the test design.

Specific plant values for the acceptable minimum driving head for operating plants will be included in proprietary data reports that are being prepared for the AREVA and Westinghouse testing.

- 15) The LOCA-DM program used to calculate deposition in the reactor core following a LOCA assumes that species present in the coolant deposit as the water boils away at the hot surface of the fuel cladding. Please discuss how deposition of material with retrograde solubility (e.g., calcium scales) is adequately accounted for by the LOCA-DM model. If applicable, provide results from any experiments (not previously discussed in WCAP-16793-NP) that show deposits predicted by LOCA-DM account for deposition from any mechanism, including retrograde solubility, in a conservative manner.

RESPONSE:

LOCADM looks at two categories of deposit formation on fuel cladding surfaces.

Category 1 deposition is driven by the boiling process. Evaporation at the fuel rod surface draws coolant through a preexisting crud deposit to the surface of the fuel rod. The amount of coolant drawn to the surface is determined by the boiling rate which is determined by a number of factors such as the decay heat flux, the deposit thickness and thermal conductivity, and bulk temperature of the coolant at the location being modeled. LOCADM assumes that any dissolved debris material that is drawn to the cladding surface will precipitate as a solid. The exact mechanism is not addressed since it is conservatively assumed that all of the dissolved debris material deposits. By considering all dissolved material to deposit due to the boiling process conservatively accounts for retrograde solubility.

Category 2 deposition includes all other mechanism by which dissolved material or chemical precipitates could be deposited on the fuel after transport by convection or diffusion. Due to the high level of uncertainties in flow, chemistry, and temperature gradients within the core, an empirical correlation was used to predict Category 2 deposition. This correlation was developed from operational core deposition data during normal operation and included factors for heat flux and impurity concentrations. Like the boiling case, retrograde solubility calculations are not done explicitly, but are included in the empirical correlation.

A sensitivity study was done examining the effect of increasing the Category 2 deposition above the level specified by the empirical correlation. It was discovered that increasing the Category 2 deposition to simulate an increased level of deposition due to retrograde solubility actually decreases the peak deposit thickness and cladding temperature. This occurs because Category 2 deposition mirrors the power profile during normal operation, and deposits are spread over a broad area of the core. This reduces solution concentrations and deposit buildup in the more localized boiling deposits is reduced.

In summary, LOCADM deals with Category 1 deposition in a conservative manner by assuming that all dissolved debris and chemical product are deposited. It deals with Category 2 deposition in a representative manner, and increasing the amount of deposition from retrograde solubility would actually be non-conservative since it would spread deposits out making them thinner and reducing fuel cladding surface temperatures.

No additional experimental data not previously discussed in WCAP-16793-NP are available.